

Functionalization of Benzene and its Derivatives by Coordination to a Tungsten Dearomatization Agent

Katy Blair Wilson
Chattanooga, Tennessee

B.S., Chemical Engineering, Washington and Lee University, 2013

A Dissertation presented to the Graduate Faculty
of the University of Virginia in Candidacy for the Degree of
Doctor of Philosophy

Department of Chemistry

University of Virginia
July 2018

Abstract

Chapter 1 begins with a discussion of the concept of chemical space and the limits of traditional synthetic methods. This is put into the context of medicinal chemistry, with a discussion of important factors for biological activity including the 3D shape of small molecules and the need for new synthetic methods that allow access to non-traditional scaffolds. To this end, dearomatization is proposed as a means to convert planar aromatic compounds into more complex 3D small molecules. The different synthetic approaches to dearomatization are briefly outlined, including enzymatic, photochemical/thermal, and transition-metal mediated dearomatization.

In Chapter 2 the activation of benzene towards electrophilic addition reactions via dihapto-coordination to the $\{\text{TpW}(\text{NO})(\text{PMe}_3)\}$ fragment is investigated. Conditions enabling the stereo- and regioselective addition of a proton and range of nucleophile across an uncoordinated double bond of the benzene ring are described. The ability of the resulting η^2 -1,3-diene complexes to undergo a second electrophilic addition is demonstrated, leading to asymmetric η^2 -allyl complexes. Subsequent addition of a range of nucleophiles is shown to typically occur with a high degree of regiocontrol, depending on the steric and electronic influences of the nucleophiles. Oxidation of these functionalized η^2 -cyclohexene complexes enabled the isolation of a range of 1,2- 1,3- and 1,4-disubstituted cyclohexenes.

In Chapter 3 the effects of an electron-withdrawing group on the organic chemistry of an η^2 -bound benzene ring are explored using the complex $\text{TpW}(\text{NO})(\text{PMe}_3)(\eta^2\text{-PhCF}_3)$. This trifluorotoluene complex is found to undergo a highly regio- and stereoselective 1,2-addition reaction involving protonation of an ortho carbon followed by addition of a carbon

nucleophile. The resulting η^2 -1,3-diene complexes are shown to undergo a second protonation and nucleophilic addition, with the proton and nucleophile adding in a 1,4-fashion, again with a high degree of regio- and stereocontrol. This reactivity pattern established with η^2 -PhCF₃ is compared to the reactivity of η^2 -benzene to highlight the impact of the CF₃ group. In this case, subsequent oxidation of the metal results in the isolation of highly substituted trifluoromethylcyclohexenes with as many as four stereocenters set by the metal.

Chapter 4 continues the investigation of the reactivity of η^2 -PhCF₃, with a focus on the use of amines as nucleophiles. The optimal conditions to allow for the isolation of the reversible amine addition products are described. The successful addition of primary and secondary amines, as well as amines with other functional groups present is demonstrated. Furthermore, the ability to take the resulting dihapto amine diene complexes through a second tandem addition reaction is shown. Additionally, an intramolecular cyclization reaction with an amine complex is described, which leads to the formation of a tetrahydrobenzimidazole ring system.

Chapter 5 outlines the coordination chemistry that has been demonstrated for aniline and its derivatives with the {TpW(NO)(PMe_s)₃} fragment. The stable coordination of *N,N*-dimethylaniline is achieved through in-situ protonation with a relatively weak Brønsted acid. The general reactivity pathways accessible to the η^2 -*N,N*-dimethylanilinium complex are outlined. This cationic complex is shown to be activated towards a second electrophilic addition by the tungsten system, and the resulting dicationic allyl complex is reactive with a broad range of nucleophiles, including relatively weak aromatic nucleophiles, at the para position. Potential influences on the regioselectivity observed for

the η^2 -*N,N*-dimethylanilinium system are discussed and compared to the regioselectivity observed with the η^2 -benzene and η^2 -PhCF₃ systems. New reactivity of the η^2 -*N,N*-dimethylanilinium complex with carbon electrophiles such as Michael acceptors is explored. Additionally, the synthesis of η^2 -*N,N*,4-trimethylanilinium system is described, and the ability of the more sterically hindered aniline system to undergo the expected reactivity pathways is investigated.

In Chapter 6 the coordination of biologically relevant multicyclic nitrogen heterocycles, specifically tetrahydroquinoline derivatives, is shown utilizing the acid trapping method established for the aniline system. The regioselectivity of the initial protonation is discussed and the reactivity of the η^2 -*N*-methyltetrahydroquinolinium system is explored. Coordination of the para-methylquinoline derivative via acid trapping is investigated to determine the effect of the methyl group on the regioselectivity of protonation. The activation of this species towards addition reactions at the uncoordinated double is demonstrated, leading to the synthesis of octahydroquinoline derivatives.

Chapter 7 addresses the issue of chirality in η^2 -dearomatization chemistry and methods to enable absolute stereocontrol in the formation of stereocenters. Starting with the achiral pentaammineosmium system, the challenges and solutions to enable absolute stereocontrol are summarized for the previous dihapto-dearomatization agents. A method for the resolution of the chiral {TpW(NO)(PMe₃)} fragment through protonation of TpW(NO)(PMe₃)(η^2 -1,3-dimethoxybenzene) with a chiral acid is described. The optimization of this procedure, which allows for the recovering of both enantiomers of the metal from the racemic mixture, is discussed. Substitution from enantioenriched TpW(NO)(PMe₃)(η^2 -1,3-dimethoxybenzene) complex to other η^2 -aromatics is shown to

occur with retention of the enantioenrichment of the metal center. Subsequent functionalization of the enantioenriched η^2 -benzene and η^2 -PhCF₃ complexes and oxidation to access the free organics is demonstrated. The successful transfer of chirality from the metal to the cyclohexene organics is confirmed by chiral HPLC, reflecting ee's ranging from 86-99%.

Copyright Information

Chapter 3 is a modified version of a published work and has been reproduced in accordance with Section II.1 of American Chemical Society Journal Publishing Agreement. Proper citation for **Chapter 3** is given. **Chapters 2** and **5** are outlines for upcoming publications. All chapters are presented as individual pieces

Chapter 2:

Katy B. Wilson, Jacob A. Smith, Diane A. Dickie, W. Dean Harman.

Chapter 3:

Wilson, K. B.; Myers, J. T.; Nedzbala, H. S.; Combee, L. A.; Sabat, M.; Harman, W. D., *Journal of the American Chemical Society* **2017**, *139* (33), 11401-11412.

Chapter 5:

Katy B. Wilson, Brianna L. Macleod, Jared A. Pienkos, William H. Myers, W. Dean Harman.

Acknowledgements

I have managed to put off writing these acknowledgements till the night before my final dissertation submission is due. For those of you who know me, I think you would describe this as a perfectly fitting way to end my graduate career in chemistry. But besides my tendency to come in right at the wire, my hesitation to begin writing my acknowledgements stems from my certainty that I will never be able to adequately thank everyone or put into words the countless memories and moments that have built up to this thesis. I, like my father, tend to be an over sharer, and I try to express my feelings openly. With that being said, I hope that I have made clear to all of you at some point how much you mean to me, because you should not have to wait five years to hear how much you are appreciated. However, I think the least that I can do is try to put down on my paper how much I love and appreciate all of you. I have been lucky enough to be surrounded by intelligent, caring, fun people all my life. There have been times along the way when I did not even understand how I could possibly deserve all the love and support that has kept me sane and happy these past five years. So thank you all, I would not have made it here without you.

I want to start by thanking my parents, big Kev and Scarlett. The classic debate of nature vs. nurture does not matter with my parents, because no matter what, I am the most fortunate daughter in the world. If I turn out to be a fraction of the people that my parents are, I will be lucky. And as far as nurture goes, I could not imagine a better childhood and environment to continue to grow up in. My parents were endlessly supportive and loving. From my dad, I learned patience, humor, and the idea of appreciating life everyday. When I was young, he would spend hours with me playing any game I could imagine, typically

involving a ball. He was my first basketball coach and showed unending patience, as he taught me how to shoot on the hoop in our driveway till it got too dark to see. My mom taught me compassion, strength and selfless love. I used to go to her bedroom when I was little, balancing a huge stack of books in my arms and insist that she read all of them to me. She has been a rock in my life, and I think a hug from Scarlett can fix almost anything. Through all of my curiosities and passions (which at one point included collecting rocks), my parents have encouraged me and let me be my weird self, which probably explains a lot about how I turned out. They taught me how to be a good eater, to be open minded and compassionate, and naturally, both being lawyers, they taught me how to argue, a skill that I have found very useful in grad school during the heated debates that often occur over lunch in the Harman lab conference room.

Early on my parents made my education a top priority. They forced me to transfer schools when I was in 6th grade to get a better education. My mom drove me almost 2 hours round trip everyday, because they wanted me to have the best opportunities possible. Naturally, I hated them for this unfair upheaval of my life and cried almost everyday for a year. They ended up being right, which they had an annoying habit of being most times. Their choice led to some of the best years of my life at Baylor, where I was taught, mentored, coached and befriended by many incredible teachers, coaches and friends. Baylor was also where I first discovered my love of chemistry, during Coach Key's sophomore year chemistry class.

When I got older and started making my own important life decisions, like where to go to college or what to actually do with my life, I was met with an unending flow of support from my parents. I first started at the University of Virginia in the Chemical

Engineering Department, and was unhappy and overwhelmed to say the least. But through all of that, I was never afraid about the future, because my parents were always there for me no matter what. They instilled in me hope and always had confidence in me, even when I could not find it in myself. I am realizing as I write that I can't realistically explain all of the reasons/memories why my parents are the most important people in my life. You all have made me the person I am today, and I am still learning from you. I just want to say to you both that I love you and thank you for everything.

To my brother Seth, I want to thank you for making me tough. My brother likes to take credit for my basketball "career", because when I was really young and just getting my feet under me, he tied me to the back of his hot wheels and forced me to run. My brother eventually found less terrifying ways to challenge and encourage me, and I was constantly trying to make him proud. Eventually, in high school we even got to become friends. Some of my best memories are from random nights in our basement watching some dumb movie that my brother found hilarious, or from staying up all night on Black Friday to go to Toys "R" Us with Maximilian, or from all our crazy trips to the beach and D.C. I know that you beat me to the doctorate, but I couldn't be more proud of you. Thank you for training me early on to be tough, thank you for all of your support. I love you brother. I also want to thank my uncle Kent, who travelled all the way to see my thesis defense, and my aunt Dace and uncle Jorgy, my grandparents and the rest of my family. You have all been so supportive, and are always there for me, ready to share a great meal and play some card games. I love you all.

Before I get to my Charlottesville family, I want to quickly acknowledge a couple Professors who I was lucky enough to learn from while I was an undergraduate at

Washington and Lee University. I did not do any chemistry research as an undergraduate, but I found my passion for chemistry when I took organic chemistry my junior year. For most normal people, organic might have been one of their least favorite classes, but I could not get enough of it. I think that was in part due to the puzzle-like aspect of organic chemistry and additionally being taught by Dr. Lisa Alty and Dr. Marcia France. Dr. Alty was perhaps one of the most patient professors I had at W&L. She was incredibly smart and passionate and luckily enough for her students, her passion was teaching. She held office hours and I, along with a couple other students would ask questions for literally hours, and Dr. Alty would stay until we were out of questions. Dr. Marcia France was my other organic Professor and probably one of the most intelligent people I have ever been taught by. She had a profound impact on my chemistry career in many ways. We talked on the phone when I had decided to leave the Chemical Engineering program at UVA, and I wasn't sure what to do with my life. Once I made the switch to the chemistry Ph.D. program at UVA, I was struggling with the overwhelming decision of picking of group, especially from my limited chemical research background. Again she offered me advice, saying that I should go with the decision that would make me happy, to pursue my passion, and follow a path that allowed me to be excited every day when I got up to go to lab. She said it all came down to loving what you do, and I think it was the best advice I ever received, because it led me to the Harman lab.

Although I switched from the Chemical Engineering program at UVA to the Chemistry department, I managed to stay socially connected with the engineers. Luckily for me, one of those engineers, Lauren Russell ended up being my roommate for three years, during which time we established several ridiculous roommate rituals, killed at least one

fish, decorated many Christmas trees, and kicked quite a few kegs. Lauren, thanks for all the great memories, hopefully we can make a couple more before we leave. I also want to thank Nik, another one of my roommates off and on in Charlottesville. We have shared some great times, and you have always been there for a deep conversation, a late night out, or a trip to Maharaja.

I also want to acknowledge Paige Corvino, who impacted my life at W&L and then UVA. For those of you who know Paige, you know how overwhelming friendly and warm she is. I was lucky enough to be close to her for much of my time in grad school. Although she had a limited idea of what I was doing with tungsten and aromatic things, she was always one of my biggest supporters. She is one of the kindest and most humble people I have ever known, and I am fortunate to have many great Charlottesville memories with her. Thank you for everything Paige.

This leads me to the Chemistry Department at UVA. I know that I will not be able to list all of you or all of the memories we have shared over the years, so I apologize for that. The number of people that were at my thesis defense was both humbling and touching, and I felt unbelievably blessed to be able to share my research and feel the support in that room. I believe that the chemistry department at UVA is made up of a special group of people, a rare combination of intelligent, fun, supportive, social and surprisingly... athletic. I have been lucky enough to be in a department with people who share so many of my passions, and have even agreed to play basketball with me before work every week. I want to acknowledge everyone that I every got to play beach volleyball with, my harry potter game night crew, and all the Honey Potter kickball teams. Since I transferred into the chemistry department for the second semester, I was a “half-year” and didn’t really have a

class. But I was quickly adopted into the class below me, as well as the department as a whole. I have had so many great memories from all the department hosted parties, game nights at Eagles Landing, the Halloween parties, and any other chance I got to hangout with you all. Charlie Clark thanks for being my chesties partner. I have enjoyed having you and Eric to watch March Madness with and always willing to play any kind of sport of game. Eric Hunt, I remember the first deep conversation we had at St. Maartens during visitation weekend, where we ended up talking most of the night about our lives and relationships. I have always felt comfortable with you; you are just the type of person that gets me I think. You are not only a fun person to play games or sports with, you're also a great friend and I think we have had some important conversations that I really needed over the years. Thank you for being there for me and for all the great times.

As I am writing these acknowledgements, I have realized how long five years really is. I remember being a first year and looking up to all the older graduate students and cherishing all the times I shared with them. And now as a fifth year, the department has grown so much, but still I'm surrounded by a great, albeit slightly younger group of friends. This inherently leads me to the Machan Lab women, Lauren Lieske and Shelby Hooe, or as Jacob put it, the "organometallic women". I have recently been fortunate enough to get close to Lauren and Shelby, who seem to come as a package deal. They have provided me with much-needed breaks from my thesis, basketball buddies every Thursday, and given me probably more fun memories than I should have from this summer while writing my thesis. Shelby is perhaps the most hard-working person I have met, and after years of wanting to befriend this shy, athletic looking girl who never seemed to leave the chemistry building, I can finally call her a friend. Shelby thanks for your encouragement, for always

being up to take a beer break, and for helping me with my frisbee problems, hopefully soon we'll get to the point of consensual hugs. Moving on to BB, sometimes I can't believe Lauren is only a first year with the amount she has accomplished and the standards that she holds herself to. I find myself wanting to be better, just to keep up with these two intelligent, hard-working, athletic women. Lauren, thank you for the joy you have brought me during this whole process, whether it was your visits to my table, keeping me company on many late nights in the chem building, or providing me with so many fun memories and new experiences when I needed a break. Even though you managed to destroy almost all of my stress balls, you have given me energy and provided me with support in ways that I can't express, so thank you for everything. I can't wait to get back into lab and continue to learn from both of you.

We have finally arrived at the Harman lab, the goofy, fun, patient, brilliant, supportive group of people that I have been surrounded by the past 5 years. I remember when I was trying to decide which lab to join, I saw all the pictures in the hallway outside the Harman lab. The pictures featured a happy assortment of people on camping trips, and playing pool and croquet, and I immediately knew this was the group for me. You might think that this is not a very smart method for choosing a potentially career altering chemical research lab, and you would probably be right most of the time. Of course I found the research interesting, but at that point what did I know? It turns out, I was the luckiest person in the world, because I picked a group where I would become unbelievably happy and I also happened to fall in love with the beautiful and powerful chemistry of dearomatization.

Before I attempt to acknowledge individual members of the lab, I want to say to every member past and present, that I could not ask for a better group of people to work with. I am honestly afraid that I will never be able to find a better work environment, because, in addition to having the best boss, I get to work in a lab where we challenge and support each other without question. Working in the Harman lab is not only intellectually fulfilling, but also just plain fun. I have looked forward to going to work almost every day over the past five years, and I don't think I will ever be able to articulate or even fully appreciate how rare of an experience I have had over my graduate career. Every member of the lab has made me a better chemist; I have benefited from their wisdom, and been enriched (haha) by the personal relationships that I have developed with them over the past five years. I am so fortunate that Dean let me into the lab of lost souls, because I was met with unending patience and guidance, when I knew next to nothing. Thank you to all of my lab mates for sharing the joys of our chemistry. I appreciate everything that you have done for me, and I am forever indebted to all of you.

I think it is appropriate to start by thanking Dean. Dean has impacted my life in so many ways over my graduate career. He has been my mentor, my boss, my role model, my teammate, my teacher and my friend. I could spend a whole paragraph describing each one of these facets of our relationship, but the idea that I am able to have the type of relationship with Dean, which encompasses all of these, speaks to the type of person Dean is. I was lucky enough to find in my adviser someone who not only shared a passion for chemistry, but also basketball, camping, croquet, pool and the importance of a good beer.

I have countless great memories with Dean over the years on camping trips, at the Fall and Spring classics, and at pick-up games in the AFC. Over the past few years, Dean and

I have formed a dysfunctional croquet partnership. As teammates we have shared many devastating losses, as we always managed to fall apart at the end of every croquet game no matter how large our lead is. But these losses have always been accompanied by endless laughter and enjoyment, as we threw jibes at each other and every other team, argued over strategy and the real meaning of “Tennessee rules”. Our chemistry on the basketball court is perhaps better than on the croquet field, unfortunately, most of the time I ended up on the opposite team as Dean and had the task of trying to contain his graceful left-handed hook shot. I was so happy to see in the video that was recently filmed highlighting Dean’s impact at UVA, that there was physical evidence of me scoring a lay-up against Dean. What the video did not show were the innumerable times when Dean humbled me by blocking most of my feeble lay-up attempts.

In addition to his talents on the court, Dean is also a master woodsman and eagle scout. After many years of claiming he could start a one-match fire, and many years of failing (due to a number of excuses), Dean finally proved me wrong. The camping trip has provided the perfect opportunity for Dean to share classic Harman lab stories. My best memories probably stem from my first camping trip when Dean and Bill Myers, our second boss hailing from the University of Richmond, went back and forth around the campfire telling the ridiculous stories from past Harman lab ventures and those who came before us. I felt so lucky to be a new member of this historic chemistry family that welcomed me so quickly and completely. The camping trip and every summer in lab has not been the same since Bill passed in the Fall of 2016, and I wish I had the chance to tell him how much he meant to me and how appreciative I am for the knowledge he shared with me, how generous he was with his time and for sharing the stories of his life.

I started out by thanking Dean for all the memories and fun times that we have shared outside of lab, because I do not really know how to thank him adequately for his role in my life as my advisor. I think “boss” has always been a weird way to describe Dean, and I think mentor and teacher probably are a better representation of how he approaches his relationship with students in his lab. I found my passion for chemistry through the Harman lab research. Once I realized I had an endless amount of things to learn, and one of the most intelligent people I have ever met willing to discuss chemistry with me for hours, I was insatiable. I questioned every statement and began to get a more clear picture of chemistry through Dean’s patient and passionate teaching. As soon as I thought I had a grasp on a subject, Dean would talk about something being in the gas phase or under vacuum, and I was right back to square one. I think that is one of the beauties of chemistry. Each new thing you learn helps to build your understanding and clarify the big picture. Something just clicks into place the more you learn. And then it all comes crashing down when you ask a fundamental question. Then you start all over, building back up your understanding, taking into account this new fact. That process happened over and over for me in graduate school and I expect will continue for the rest of my life. I can’t wait.

Dean has guided me through many projects over the years, some that were complete disasters, and some that had us both so excited that we would work on figuring out 2D NMRs for hours or talk about hypothetical things that would be so cool. Intermixed with my research were also many discussions about basic chemistry concepts, which provided the foundation to really understand and appreciate chemistry. After group meeting one time, I remember Dean agreed to go with the group to Durty Nelly’s and we continued our discussion of entropy for another few hours. It is stories like this that truly highlight how

generous Dean is with his time. It has been one of the privileges of my life that I have had the chance to learn from someone so humble, patient, and brilliant, and to work for someone who I respect so much. I am grateful every single day. Thank you for everything Dean, you have truly changed my life. I still have not figured out what light is, but luckily I have another year with you, so hopefully I'll get there one day.

Moving on to the other Harmanites. I want to thank Kevin Welch. I knew Kevin indirectly before he returned to UVA, through reading his papers from when from he was a graduate student in Dean's lab decades ago. I still hold that Kevin wrote my most utilized Tungsten publication, even though he disagrees about its importance. He has essentially rejoined the Harman lab, and I think provided some much appreciated life and support to all of us. More importantly, Kevin, better know from his time on the trivia team "Kevin and the Spaceys" catapulted us into trivia glory every week at the Tin Whistle trivia night. Thank you for your friendship, wisdom, and humor Kevin.

When I first joined the Harman lab, I was trained by Jared Pienkos. He was actually about to graduate and was working on his thesis, but took the time to train me. Now that I have been through the process of writing a thesis, I cannot imagine having to simultaneously train someone. I think Jared is one of the most humble and patient people I have ever met. I asked him questions that I can't even fathom at this point, like how to use a pipet bulb, and he was nothing but helpful and kindhearted. He always had time to answer my questions, and really set me up to be successful in graduate school. I am sad that we did not overlap for longer in the Harman lab, but thank you for everything you did for me Jared.

I next want to thank the other older members of the Harman lab when I first joined, Ben, Bri, Jeff and Phil. Once I got over my initial shyness and started talking to the rest the

lab, I couldn't get enough. Getting close to a group of diverse, incredible, people who I got to work alongside every day was such a fulfilling experience. I remember looking forward to lunch everyday, because our conversations were so exciting and fun. We have sometimes referred to that year or so as the Golden time in the Harman lab. We would go to Three Knotch'd every Thursday (TKT), cheers our beers and just get to know each other and talk about life. We argued a lot and it was just a great time in my life.

I also want to thank Bri for all that she taught me over the couple years we worked together on tungsten chemistry. I learned a lot from her and I am truly grateful for that. Where do I start with Ben? My relationship with Ben has many different facets. He is my friend and lab mate, my fellow tungsten researcher, the one who got Nichole and me together, and now he also happens to be my best friend's fiancée. Ben has provided a spark in my life and I think everyone's life that he has touched. Fittingly, he is just as selfless and kind as Nichole, and always put others in front of himself. Ben seems to be endlessly enthusiastic and embraces life with excitement and compassion. I have had so many fun times with Ben over the years, and it's hard not to because his enthusiasm is contagious. I could not be happier for him and Nichole; I always knew Ben was intelligent, but once he landed Nichole I knew he was brilliant. You all deserve so much happiness; I am blessed that you have shared your love and friendship with me. Thank you for all you have done for me Ben and for all the memories past and to come.

I think Jeff or Jefé as I like to call him, is the lab member that I will have worked alongside the longest. Jeff brings a life to the lab that is really inexplicable. Whether it's playing Christmas music in the middle of the summer, putting on "It's Friday" every Friday, or initiating random dancing sessions, Jeff has truly made the Harman lab a fun place to

work. In addition to his shenanigans, Jeff is also generous with his time. Whenever I have had a question or been struggling, Jeff drops everything to help me. We have had many lively arguments ranging from important topics of chemistry to ridiculous debates that I can't even begin to describe without sounding crazy. He is always ready to go share a beer, and has provided me with a close friend over the years. I am grateful for your friendship and your support, and I am excited to get to share another year with you Jeff.

Steven Steven Steven. When Ben graduated, I was worried our lab would fall apart, but you have become the selfless lab mate, who really takes care of us in a lot of ways. A couple of weeks ago, I mentioned to Steven that I might need a couple of boxes for moving and asked if he could keep an out for some when they came in from the stock room. I returned to my desk later that day and it was no longer visible due to the stacks of boxes piled up. Steven is the type of person who would help out a friend immediately and without question. Recently, we have become closer outside the lab, whether that was playing video games for hours or having long talks. You were there for me at a time that I was really struggling, and that meant more to me than I can put into words. Thank you for the support and the much needed hugs.

I am not sure where to start with Jacob. Jacob and I became close when he first joined the lab. We shared late night grading sessions, watched True Detective and got into all kinds of shenanigans. It is never a dull moment with Jacob. I remember one of his first summers I got a call that he was stranded somewhere downtown because of car trouble and needed a ride. Shortly after I gave him a ride, Jacob showed up on my doorstep with a 12-pack of tacos from taco bell. Now that is a good friend. Aside from Jacob's entertaining antics in lab, his intelligence and never ending curiosity, has remotivated me in lab and for

that I am grateful. He has made me want to be a better scientist, and I could not have been happier than when he started to work on tungsten chemistry. Justin has been my box-mate for the last few years and I couldn't ask for a better one. Once I got to know Justin better as he opened up to me I found that he was this incredibly smart, passionate person, who not only loves cats, but who also brews exceptional craft beer. I have enjoyed our Durty Nelly's and Three Knotch'd adventures and sharing endless cat photos. Spenser has provided so much life to lab recently and I think has reestablished the Harman lab as social within the department. Since I have gotten to know Spenser, I have learned that he is a loyal friend and has a drive to succeed in lab. His visits to my table while I was working on my thesis always made me happy, even if he was frustrated about things not working, which tends to happen in chemistry. I am excited to be staying another year both to improve my spike ball skills and work alongside him in lab.

Nichole, don't worry I haven't forgotten about you. I just figured since you are an honorary Harman lab member that it would be appropriate to acknowledge you within the Harman lab section. I know we started out a little awkward, which I think is fitting, and we both thought that we didn't like the other because I never really talked when we were in class together. But once we overcame that barrier, with the help of Ben, you quickly became one of the most important people in my life. I knew from the start that you were something special, because you were wearing powersox® in class, which apparently is a creepy thing to notice about someone you don't know. Once I got to know more about you besides your sock preferences, I learned that you are an uncommonly kind person with an old soul. You put everyone else before yourself without question, you are loyal and just ridiculously intelligent and humble. You are also competitive in the best way possible, even

though I refuse to play Dutch Blitz with you anymore. You introduced me to the beauty of zucchini and understand the constant need for How I Met Your Mother quotes. You seem to love me no matter how weird I am or what crazy things I do, and I still question how I have deserved the loyalty and support that you've selflessly given me for so long. We have had so many great memories together and a handful of some not so great ones, but I wouldn't change anything, because everything has brought us closer. We have laughed, and cried, and laughed till we cried. You are the only person I think who could make me intentionally lose a game of Mafia, because I couldn't stand the thought of lying to you. I love you and am grateful to have you in my life, thank you for your unwavering love and support Nichhole.

Alexander Heyer. Alex is the type of person who has always baffled me. The amount of activities, clubs, and academic endeavors he is involved in blows my mind. I get tired just thinking about what he did on a daily basis at UVA. Even more impressively, he did all those things and remained a social, active human being that has a knack for developing close personal relationships with many of those around him. Alex is passionate about life in all aspects. He is compassionate and open-minded and truly an amazing human being. I haven't even touched on how intelligent he is. Once Alex gets going talking about science, it is hard to keep up. I was lucky enough to be one people in lab that Alex would approach to talk about science, and I got to see how his mind works. It was a beautiful thing. Alex's passion for life made him a great lab-mate and there was never a dull moment when Alex was in lab. One summer, he would post a question of the day on the board in lab, and got us discussing all sorts of things, from extremely deep topics to more ridiculous things. I was fortunate to also become close with Alex outside of lab. I had many late night adventures with Alex including dancing in the moonlight at the lake and many times at the Biltmore

and even one random night at a fraternity house. In addition to chemistry, Alex and I share an important love of taco bell, perhaps one of the things I respect most about him. Alex is the type of person who can get me to completely open up, with his way of asking just the right questions, and instilling in me a feeling of trust. We have had many deep conversations over the years that have meant so much to me. Then again we've also had a heated multi-hour discussion on the pros and cons of "The Notebook". Alex, I am so proud of you and I hope you remember me when you become a renowned professor. I know you will succeed and find happiness in so many different aspects of your life at Stanford and I am so happy and excited for you. Thank you for your friendship, I love you.

Phil and Hannah, I have not put off acknowledging you till hours before my thesis is due because I don't appreciate you or don't know what to say. I just don't want to think about how great I have had it with the two of you as my best friends, just to remember that you are both leaving me very soon. Phil for the second time.

Phil. You were the first person I really got close to at UVA. As much as I loved work, and was happy to be in the department, before we became friends I still didn't have that one person to share it with. The person who you can count on at any point to hangout, or go grab a beer, or just be there for you. One of the first conversations I remember having with you was about Seinfeld, as we were doing dishes in the dish room together. I don't really remember how we went from casual conversations in lab, to never running out of things to discuss, but it seemed like the most natural thing in the world. I remember every weekend that it was a given that you would come into town and we would go from there, whether it was going into lab or just sitting in my front yard talking. We shared life stories over games of pool at Rapture or on winding drives around Charlottesville when we both needed a

break. We have had so many adventures and nights I will never forget, from trips to the beach, the lake, and most recently the spontaneous overnight camping in Lexington. I have missed our endless debates and having someone so willing to bet and lose to me almost every time. As much as I say you're the worst, I could not ask for a better friend. You are the most selfless person I know. I don't think I will ever be able to adequately thank you for your constant help whenever I needed it, and all the unbelievable things you have done for me. I have learned so much from you as a scientist, especially when I was just beginning my time in lab. You argued with me and taught me and listened to my crazy ideas. You always had more confidence in me than I ever had in myself. I have been so lucky to share so many memories with you, to work- along side you and learn from you. I would not have made it through graduate school without you. Thank you for your friendship and ceaseless support Phil. I hope you know how much you mean to me and how much I love you.

And finally I've arrived at Hannah Nedzbala. Hannah likes to give me a hard time because at first I told Dean I was not ready to mentor an undergraduate and Hannah was turned away. Fortunately, Dean eventually told me I was getting an undergrad ready or not and Hannah was stuck with me. At first I tried to be a good mentor and keep my weirdness at a minimum around Hannah, but that was a fleeting attempt. The best part was that Hannah seemed to roll with everything and instead of getting scared her off, she quickly became my best friend. Soon after Hannah join, the dynamic changed in the Harman lab, with some people graduating. I was worried that the golden years were over, and instead I still had some of the best times to come. I got to work along-side my best friend and share my passion for the Harman lab chemistry. It really was the dream. We have so many memories from lab, some of this great, like trying to figure out what our handshake in the

box should be, or dance parties and sing alongs. There have been many late nights, which have been made enjoyable by sharing your company in lab. I remember your first benzene prep, that fateful Saturday we spent 14 hours and had gone crazy and back multiple times. The benzene prep ended up having a terrible yield, which was most definitely my fault, but in my mind that memory is still a good one. I think it is truly a special friendship that can turn the most disappointing and potentially terrible experiences into cherished memories.

I was lucky to have a mentee who was not only far more intelligent than I ever was in undergrad, but also endlessly ready to learn and prove herself. Hannah, like myself can be a tad competitive at times, and I have truly grown as a person and a scientist from being challenged by her relentless pursuit of knowledge and the desire to solve problems. Hannah I know you are going to succeed at whatever you choose to do. I promise you that you have made the right choice, and I am so proud of you for everything you have accomplished. You deserve to revel in those accomplishments and try to trust yourself.

Hannah, I didn't know what it meant to have "a person" before I met you, but now you are stuck as mine. I have broken down quite a few times over the past couple months and you have always been there to put me back together. You have been endlessly supportive of me even when I did not deserve it and I could not ask for a better friend. I have some of my best graduate school memories over the past three years with you from Halloween parties, lake trips, snow days, fjord crossings, tubing adventures, and eno hangouts. You have always been the person around whom I can just truly relax and let all my weirdness out. I apologize for that. Thank you for watching countless stupid youtube videos with me and for playing cards with at Three Knotch'd for hours. Thank you for dropping everything when I needed you and for all the little things you have done for me. I

don't know how I could have done this whole graduate school thing without out. I am going to miss you so much. I love you bud.

Table of Contents

Abstract	ii
Copyright Information	vi
Acknowledgements	vii
Table of Contents	xxvi
List of Abbreviations	xxx
List of Figures	xxxiii
List of Schemes	xxxv
List of Tables	xxxix
Chapter 1: Introduction	
1.1 Introduction	2
1.2 Aromaticity	3
1.3 Classical Aromatic Reactivity	4
1.4 Dearomatization	5
1.5 Radical Dearomatization	6
1.6 Photochemical/Thermal Cycloaddition Dearomatization	7
1.7 Enzymatic Dearomatization	8
1.8 Transition Metal Mediated Dearomatization	9
1.8.1 Electron-Deficient Dearomatization Agents	10
1.8.2 Electron-Rich Dearomatization Agents	13
1.9 References	18
Chapter 2: The Tungsten Promoted Dearomatization of Benzene	
2.1 Introduction	24

2.2 Results and Discussion	26
2.3 Conclusions	46
2.4 Experimental	48
2.5 References	86

Chapter 3: Sequential Tandem Addition to a Tungsten–Trifluorotoluene Complex: A Versatile Method for the Preparation of Highly Functionalized Trifluoromethylated Cyclohexenes

3.1 Introduction	88
3.2 Results and Discussion	90
3.2.1 Coordination and Reactivity of α,α,α -Trifluorotoluene	90
3.2.2 Second Tandem Addition to η^2 -1,3-Dienes	93
3.2.3 Substituent Effects on the Dearomatization of Substituted Benzenes	99
3.2.4 Comparison of η^2 -Benzene and η^2 -PhCF ₃ Reactivity	101
3.2.5 CF ₃ -Substituted Cyclohexene Synthesis	108
3.3 Conclusions	109
3.4 Experimental	110
3.5 References	136

Chapter 4: The Isolation and Elaboration of Reversible Amine Additions to Dihapto-Trifluorotoluene

4.1 Introduction	140
4.2 Results and Discussion	141
4.2.1 Amine Addition to η^2 -TFT	141
4.2.2 Exploring Further Reactivity of Amine Addition η^2 -Dienes	145
4.3 Conclusions	161
4.4 Experimental	163

4.5 References	177
----------------	-----

Chapter 5: Tungsten Dearomatization of Aniline Derivatives

5.1 Introduction	180
------------------	-----

5.2 Results and Discussion	180
----------------------------	-----

5.2.1 Previous Investigations into the Coordination and Reactivity of η^2 -Aniline	180
---	-----

5.2.2 New Reactivity of η^2 -Anilinium Derivatives	187
---	-----

5.2.3 η^2 -Anilinium Complexes as Precursors to Cyclohexenes	194
---	-----

5.2.4 The Synthesis and Reactivity of η^2 - <i>N,N</i> ,4-trimethylanilinium	196
---	-----

5.3 Conclusion	206
----------------	-----

5.4 Experimental	208
------------------	-----

5.5 References	218
----------------	-----

Chapter 6: Tungsten Dearomatization of Tetrahydroquinoline Derivatives

6.1 Introduction	221
------------------	-----

6.2 Results and Discussion	223
----------------------------	-----

6.2.1 Coordination and Reactivity of <i>N</i> -methyl-1,2,3,4-tetrahydroquinoline	223
---	-----

6.2.2 Coordination and Reactivity of <i>N</i> ,6-dimethyl-1,2,3,4-tetrahydroquinoline	228
---	-----

6.2.3 Reduction of Iminium and Isolation of Octahydroquinoline Organics	234
---	-----

6.3 Conclusions	237
-----------------	-----

6.4 Experimental	239
------------------	-----

6.5 References	252
----------------	-----

Chapter 7: The Development and Application of an Enantioenriched Tungsten Dearomatization Agent

7.1 Introduction	255
------------------	-----

7.2 Results and Discussion	259
----------------------------	-----

7.2.1 Enantioenrichment through Protonation with a Chiral Acid	259
7.2.2 Optimization of Tungsten Enantioenrichment Procedure	262
7.2.3 η^2 -1,3-Dimethoxybenzene as Synthetic Precursor	269
7.2.4 Synthesis of Enantioenriched Organic Compounds	270
7.3 Conclusions	273
7.4 Experimental	275
7.5 References	281
Concluding Remarks	283
Appendix	290

List of Abbreviations

aq	Aqueous
br	Broad
CAN	Ceric ammonium nitrate
Cdr	Coordination diastereomer ratio
COSY	Correlation Spectroscopy
CV	Cyclic voltammetry
DBU	1,8-Diazabicyclo[5.4.0]undec-7-ene
DCM	Dichloromethane
DDQ	2,3-dichloro-5,6-dicyanoquinone
DFT	Density functional theory
DiPAT	Diisopropylammonium triflate
DMA	<i>N,N</i> -Dimethylacetamide
DMAP	4-Dimethylaminopyridine
DME	1,2-Dimethoxyethane
DMF	<i>N,N</i> -Dimethylformamide
DMSO	Dimethyl sulfoxide
DPhAT	Diphenylammonium triflate
EA	Elemental analysis
EDG	Electron donating group
ee	Enantiomeric excess
Et ₃ N	Triethylamine
Et ₂ O	Diethylether

EtOAc	Ethyl Acetate
EVK	Ethyl vinyl ketone
EWG	Electron withdrawing group
HATR	Horizontal Attenuated Total Reflectance
HMBC	Heteronuclear Multiple Bond Coherence Spectroscopy
HRMS	High Resolution Mass Spectroscopy
HSQC	Heteronuclear Single Quantum Correlation Spectroscopy
Hz	Hertz
IR	Infrared
KHMDS	Potassium bis(trimethylsilyl)amide
L	Ancillary ligand
LAH/LiAlH ₄	Lithium Aluminium Hydride
LiDMM	Lithium dimethyl malonate
mCPBA	m-Chloroperbenzoic acid
MeCN	Acetonitrile
MeIm	N-Methylimidazole
MMTP	1-methoxy-2-methyl-1-trimethylsiloxypropene
MTAD	4-Phenyl-1,2,4-triazoline-3,5-dione
MVK	Methyl vinyl ketone
NBS	N-Bromosuccinimide
NCS	N-Chlorosuccinimide
NHE	Normal Hydrogen Electrode
NMR	Nuclear Magnetic Resonance

NOE	Nuclear Overhauser Effect
NOESY	Nuclear Overhauser Effect Spectroscopy
NOPF ₆	Nitrosonium hexafluorophosphate
ORTEP	Oak Ridge Thermal Ellipsoid Program
OTf	Trifluoromethanesulfonate or triflate
PMe ₃	Trimethylphosphine
Ppm	Parts Per Million
Pz	Tp pyrazole ring
TBAH	Tetrabutylammonium hexafluorophosphate
TFT	α,α,α -Trifluorotoluene
THF	Tetrahydrofuran
TLC	Thin layer chromatography
TMS	Tetramethylsilane
Tp	Hydridotris(pyrazolyl)borate
UV	Ultraviolet

List of Figures

Figure 1.1. Dearomatization of benzene	3
Figure 1.2. Resonance stabilization of benzene	4
Figure 1.3. Electron-rich and electron-deficient transition metal dearomatization	10
Figure 1.4. Dihapto-coordination of benzene to a π -basic metal	13
Figure 1.5. Group 6 dearomatization agents	16
Figure 2.1. Synthesis of functionalized cyclohexenes	26
Figure 2.2. Key NOE interactions and crystal structure of 6A	30
Figure 2.3. ^1H NMR spectra of allyl complexes 12 (top), 13 (bottom), and 14 (middle)	34
Figure 2.4. ^{31}P NMR monitoring of addition reactions to 1	35
Figure 2.5. Crystal structure of compound 29A	39
Figure 2.6. Crystal structure of compound 30	42
Figure 3.1. Crystal structure of compound 54	91
Figure 3.2. Crystal structures of compounds 60 (left) and 61 (right)	95
Figure 3.3. Crystal structure of lactam complex 67'	98
Figure 3.4. ^1H NMR comparison of 13 (top) and 75 (bottom)	105
Figure 3.5. ^1H NMR comparison of 12 (top) and 59 (bottom)	107
Figure 4.1. Preliminary results for successful amine addition to 53	144
Figure 4.2. In situ ^1H NMR of allyl 83	147
Figure 4.3. Crystal structure of complex 90	152
Figure 4.4. ^1H -NMR overlay of 85 (top) and 91 (bottom)	153
Figure 4.5. Proposed structure of complex 91 (triflate counterion omitted)	154
Figure 4.6. Crystal structure of complex 91 (triflate counterion omitted)	155

Figure 4.7. Lewis acid induced nitrosyl bending	157
Figure 4.8. ¹ H NMR spectra showing the formation of 91 with and without Et ₃ N	159
Figure 5.1. Comparison of allyl complexes from 1 , 52 , and 96A (triflate omitted)	186
Figure 5.2. Retrosynthetic analysis of bile acid target	200
Figure 5.3. ¹ H NMR assignments of 104	204
Figure 6.1. Alkaloid natural products	221
Figure 6.2. Functionalization of tetrahydroquinoline and indoline cores	222
Figure 6.3. Crystal structure of complex 114	234
Figure 7.1. Matched and mismatched diastereomers of Re-(<i>R</i>)- α -pinene complex	256
Figure 7.2. ³¹ P NMR of (<i>S</i>)- β -pinene test	268
Figure 7.3. Synthesis of enantioenriched cyclohexenes from η^2 -benzene	273

List of Schemes

Scheme 1.1. Electrophilic aromatic substitution reactions	5
Scheme 1.2. Radical dearomatization of benzene	6
Scheme 1.3. Thermal/photochemical dearomatization of benzene	8
Scheme 1.4. Enzymatic dearomatization of benzene	9
Scheme 1.5. {Cr(CO) ₃ } dearomatization of benzene	11
Scheme 1.6. {Mn(CO) ₃ } ⁺ dearomatization of benzene	12
Scheme 1.7. Os(II) promoted dearomatization of benzene	14
Scheme 1.8. Activation of TpRe(CO)(MeIm)(η^2 -benzene) towards cycloaddition	15
Scheme 2.1. Activation of benzene with the tungsten dearomatization agent	25
Scheme 2.2. Protonation of 1 with diphenylammonium triflate	27
Scheme 2.3. Formation of minor addition product to 1	30
Scheme 2.4. Tandem electrophilic/nucleophilic addition to η^2 -1,3-dienes	32
Scheme 2.5. Redox promoted diene isomerization	41
Scheme 2.6. Diene isomerization of 6A	41
Scheme 2.7. Isolation of functionalized cyclohexenes	45
Scheme 3.1. General reaction trends for dihapto-coordinated arene complexes	88
Scheme 3.2. Dihapto-coordination of benzene with an EWG	89
Scheme 3.3. Synthesis and protonation of η^2 -PhCF ₃	90
Scheme 3.4. Nucleophilic addition to 53	92
Scheme 3.5. Protonation and reactivity of 55	94
Scheme 3.6. Second protonation-nucleophilic addition gives trisubstituted cyclohexenes	96
Scheme 3.7. Intramolecular cyclization reaction forming lactam products	97

Scheme 3.8. Regiocontrol in cyclohexene formation from 54 and 56	99
Scheme 3.9. Reactivity pattern for η^2 -benzene and η^2 -PhCF ₃	103
Scheme 3.10. Impact of CF ₃ group on allyl complexes	104
Scheme 3.11. Addition of a proton and NaCN to 10A and 57	106
Scheme 3.12. Addition of a proton and LiDMM to 6A and 55	108
Scheme 4.1. Reactivity pattern for η^2 -PhCF ₃	140
Scheme 4.2. Range of nucleophiles for addition to 53	141
Scheme 4.3. Conditions for amine addition to η^2 -TFT	142
Scheme 4.4. Reaction pathways for protonation and nucleophilic addition to 78	146
Scheme 4.5. Addition of anionic nucleophiles to 78	148
Scheme 4.6. Addition of amine nucleophiles to 78	149
Scheme 4.7. Proposed intramolecular cyclization of 78	151
Scheme 4.8. MMTP addition to 78	152
Scheme 4.9. MMTP addition to 12	156
Scheme 4.10. Proposed mechanism for formation of 91 with bent nitrosyl	158
Scheme 4.11. Expanding the synthesis of tetrahydrobenzimidazoles	161
Scheme 5.1. Dihapto-coordination of aniline	180
Scheme 5.2. In situ protonation of η^2 - <i>N,N</i> -dimethylaniline	181
Scheme 5.3. Protonation comparison of η^2 -benzene and η^2 - <i>N,N</i> -dimethylaniline	183
Scheme 5.4. Reactivity of η^2 - <i>N,N</i> -dimethylanilinium	184
Scheme 5.5. Electrophilic addition at the para position of 96A	186
Scheme 5.6. Addition of methyl triflate to 96A	188
Scheme 5.7. Proposed reaction pathways for 97	189

Scheme 5.8. Reactivity of η^2 - <i>N,N</i> -dimethylanilinium with Michael acceptors	190
Scheme 5.9. Intramolecular cyclization with 96A and MVK	191
Scheme 5.10. Proposed reaction pathways for 98	193
Scheme 5.11. η^2 -Anilinium as precursor for functionalized cyclohexenes	195
Scheme 5.12. In situ acid trapping of <i>N,N</i> ,4-trimethylaniline	196
Scheme 5.13. Tandem electrophilic/nucleophilic addition to 99A	198
Scheme 5.14. Addition of Michael acceptors to 99A	199
Scheme 5.15. Oxidation and hydrolysis of 101	201
Scheme 5.16. Intramolecular cyclizations with η^2 -anisolium	202
Scheme 5.17. Intramolecular cyclization reactions of 101 and 102	203
Scheme 5.18. In situ iminium reduction with 104	205
Scheme 5.19. Proposed reaction pathways for 104 and 105	206
Scheme 6.1. Coordination and reactivity of <i>N</i> -ethylindoline	223
Scheme 6.2. Coordination of <i>N</i> -methyltetrahydroquinoline	225
Scheme 6.3. Michael additions to 106A	226
Scheme 6.4. In situ protonation of <i>N</i> ,6-dimethyl-1,2,3,4-tetrahydroquinoline	228
Scheme 6.5. Tandem electrophilic/nucleophilic addition to 108B	229
Scheme 6.6. Electrophilic fluorination of 108B	231
Scheme 6.7. Second tandem addition to fluorinated quinoline complex	232
Scheme 6.8. Simmons-Smith cyclopropanation of 108B	234
Scheme 6.9. Iminium reduction and octahydroquinoline organic isolation	235
Scheme 7.1. Resolution of TpRe(CO)(MeIm)(η^2 -benzene)	257
Scheme 7.2. Synthesis of racemic organics with W(0) and Mo(0)	258

Scheme 7.3. Synthesis of enantioenriched tungsten benzene complex	260
Scheme 7.4. β -Pinene test for determination of enantioenrichment	262
Scheme 7.5. Precipitation of 1:1 diastereomeric salts out of EtOAc	263
Scheme 7.6. Isolation of enriched (<i>R</i>)-117 and (<i>S</i>)-117	267
Scheme 7.7. Substitution reactions from (<i>R</i>)-117	270
Scheme 7.8. Synthesis of enantioenriched trifluoromethylated cyclohexenes	272

List of Tables

Table 2.1. Tandem electrophilic/nucleophilic addition to 1	29
Table 2.2. Nucleophilic addition reactions to 10A	37
Table 2.3. Nucleophilic additions to 6A and 11A	40
Table 2.4. Nucleophilic addition reactions to 30	44
Table 7.1. Effect of stir time on resolution of (R,R)-118	265

Chapter 1

Introduction

1.1 Introduction

As the efficiency of identifying promising pharmaceutical leads has increased with the use of high throughput bioassays and small-molecule libraries, innovative synthetic methods are sought to keep up with the synthetic challenges of medicinal chemistry and facilitate the stereocontrolled synthesis of novel molecular scaffolds.^{1,2} Traditionally, these types of high throughput bioassays have focused on maximizing the quantity of compounds tested, with less focus on the topological diversity of the library.^{1,3} With the emphasis on the quantity of small molecules, those that make up medicinal chemistry libraries tend to be compounds that are relatively easy to access by traditional synthetic methods.⁴ Among these methods include C-C coupling reactions between aromatic molecules, as well as S_NAr reactions, with the result that overall, the types of compounds tested are predominantly “flat” molecules.^{4,5} This is in contrast to the structural complexity observed in biologically active natural products, which often contain many stereocenters and have long been the targets of synthetic chemists. In a report on the importance of complexity in drug molecule candidates, Lovering et. al. found that both the presence of chiral centers and the fraction of sp^3 hybridized carbons have a significant correlation to the success of compounds in drug development.^{5,6} The unique molecular shape provided by more complex 3-dimensional small molecules is thought to be important for specificity in terms of favorable receptor-ligand interactions.^{1,7,8}

In a recent report, Brown et. al. attributed the deficiency in the structural diversity of many medicinal chemistry libraries to the scarcity of new synthetic methods, citing that none of the most used methods were discovered in the last 20 years.⁴ Overutilization of some synthetic methods leads to an abundance of certain molecular shapes and limits the

efficacy of the screening of these compound libraries. In the last decade, the area of diversity-oriented synthesis has developed with the goal of synthesizing a diverse range of complex molecules, with similar structural features to natural products.^{5,8-11} This type of synthetic approach enables the exploration of new chemical space, expands the diversity of compound libraries, and increases the efficacy in SAR studies.¹¹ To this end, new synthetic methods are sought to rapidly access novel molecular scaffolds and address the increasing demand for synthetic innovation in drug discovery chemistry.^{3,4,12}

Dearomatization provides a powerful synthetic methodology that facilitates the rapid and atom efficient transformation of planar aromatic compounds into more complex alicyclic systems (Figure 1.1). Aromatics are attractive starting materials for synthetic chemists due to their abundance, low cost, and cyclic structure with multiple sites of unsaturation available for functionalization. However, the inherent stability of aromatic systems renders this class of compounds unreactive towards addition reactions under most conditions.

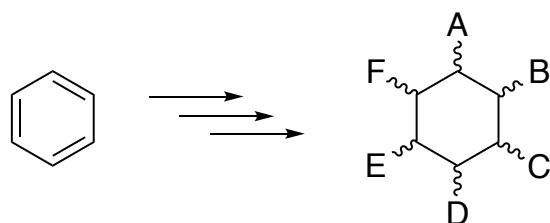


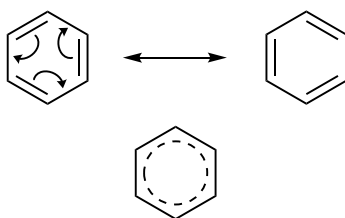
Figure 1.1: Dearomatization of benzene

1.2 Aromaticity

Aromatic compounds are classified by Hückel's rule, which states that for a compound to be aromatic, it must have a cyclic array of $4n + 2 \pi$ electrons.¹³ Figure 1.2

shows the resonance structures of the classic aromatic compound benzene, which results in a delocalized, stabilized π -system. The observed stability of these aromatic compounds however cannot fully be attributed to the conjugated π -system. One classic demonstration of aromatic stability is shown through a comparison of the $\Delta H_{\text{Hydrogenation}}$ between cyclohexene, 1,3-cyclohexadiene, and benzene. The difference between the predicted $\Delta H_{\text{Hydrogenation}}$ for benzene and the observed $\Delta H_{\text{Hydrogenation}}$ was calculated to be ~ 36 kcal/mol, with this energy difference attributed to aromatic stabilization.¹⁴

aromatic resonance stabilization



$4n + 2 \pi$ electrons

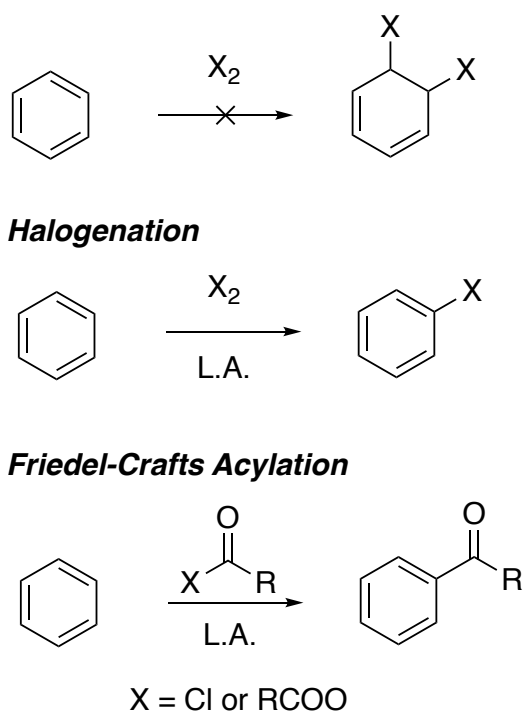
Figure 1.2: Resonance stabilization of benzene

1.3 Classical Aromatic Reactivity

The stability of aromatic compounds has a powerful influence on their reactivity. Typically, relatively harsh conditions are required to facilitate reactions. Furthermore, in contrast to the reactivity of free alkenes, the traditional reactions accessible to aromatics are substitution reactions rather than addition reactions, with a driving force to restore aromaticity in the product (Scheme 1.1). Classic examples of these electrophilic aromatic substitution (EAS) reactions include Friedel-Crafts acylation, Friedel-Crafts alkylation, halogenation, nitration, and sulfonylation (Scheme 1.1). Another group of frequently utilized reaction of aromatics are palladium-catalyzed cross-coupling reactions, such as the

Suzuki-Miyaura cross-coupling reaction, which results in C-C bond formation between aryl groups.^{15,16} Although these EAS and cross-coupling reactions are powerful synthetic tools, neither leads to the formation of new stereocenters in the aromatic ring, and aromaticity is maintained in the products.

Scheme 1.1: Electrophilic aromatic substitution reactions



1.4 Dearomatization

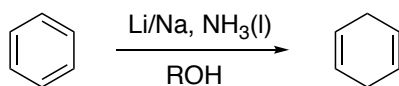
Although aromatics typically undergo reactions with retention of aromaticity, a broad range of dearomatization methods have been explored, which break the aromaticity and give access to alicyclic systems. Dearomatization methods include photochemical/thermal, radical, enzymatic, as well as transition-metal mediated dearomatization.

1.5 Radical Dearomatization

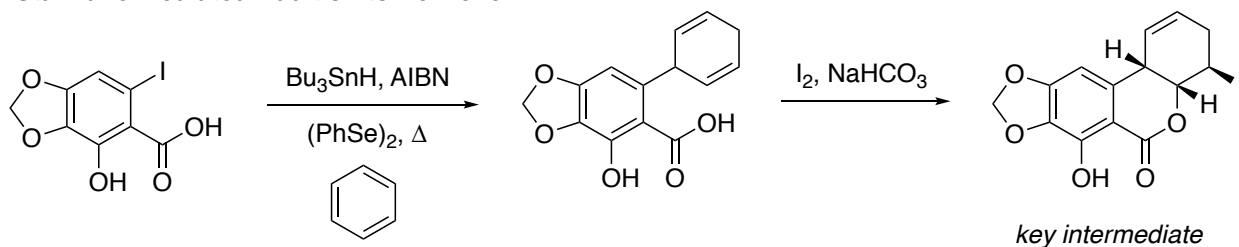
One of the classic dearomatization methods used by synthetic chemists is the Birch reduction, which gives access to alicyclic compounds through a radical mechanism.¹⁷ This methodology requires the use of Na or Li metal in liquid ammonia and a protic solvent, and typically results in the formation of 1,4-dienes (Scheme 1.2, top). Although this method is sometimes limited by functional group tolerance, it provides a powerful tool to disrupt aromaticity and has been used to access many synthetic targets including natural products.¹⁷ Another dearomatization method that has been demonstrated with benzene involves a stannane-mediated radical addition of aryl iodides to benzene, assisted by catalytic benzeneselenol. This method leads to 1,4-dienes that can undergo intramolecular cyclizations with an ortho-substituted aryl ring (Scheme 1.2, bottom). This dearomatization approach has been employed to synthesize phenanthridinone derivatives, including a key intermediate in Danishefsky's synthesis of (\pm)-pancratistatin.¹⁸

Scheme 1.2: Radical dearomatization of benzene

Birch Reduction

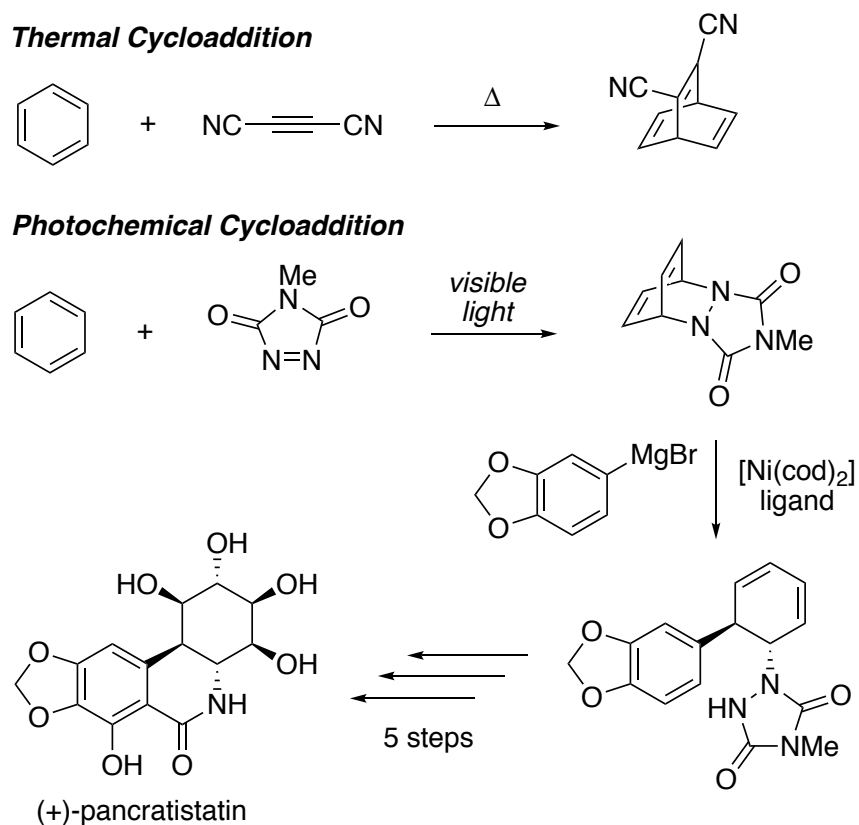


Stannane-Mediated Addition to Benzene



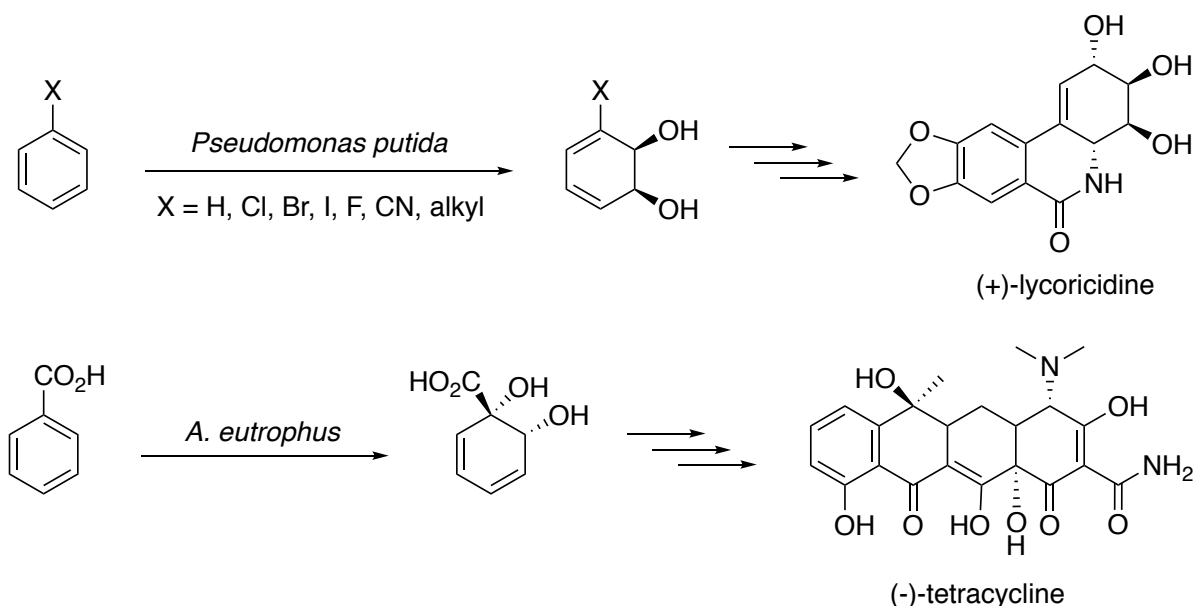
1.6 Photochemical/Thermal Cycloaddition Dearomatization

Although the benzene ring contains a diene group primed for a thermal [4+2] cycloaddition, few examples have been reported for this type of cycloaddition with benzene due to the stability of the aromatic π -system. To enact this cycloaddition requires elevated temperatures and activated dienes, as shown in Scheme 1.3 with the Diels-Alder reaction of benzene with dicyanoacetylene.¹⁹ More success has been reported for the photochemical activation of benzenes towards cycloadditions with alkenes. These reactions typically lead to ortho, meta, or para photocycloaddition products with the aromaticity broken.²⁰⁻²³ Recently, the Sarlah group reported an elegant synthesis of (+)-pancratistatins stemming from a key dearomative photoaddition to benzene.²⁴ In the initial step, benzene undergoes a light-promoted para-cycloaddition with 4-phenyl-1,2,4-triazoline-3,5-dione (MTAD) (Scheme 1.3). Coordination of the resulting cycloadduct to a Ni-catalyst with chiral bidentate ligands results in a catalytic and enantioselective trans-carboamination. After decomplexation, the resulting desymmetrized diene was taken on to (+)-pancratistatins in 5 steps with an er = 98:2.²⁴

Scheme 1.3: Thermal/photochemical dearomatization of benzene

1.7 Enzymatic Dearomatization

Enzymatic dearomatization has been utilized by synthetic chemists as a convenient means of accessing chiral diol dienes from aromatic compounds.²⁵⁻²⁸ The hydroxylated dienes that result from this dearomatization step have been used as key precursors for the enantioselective synthesis of a range of natural products. Hudlickey and coworkers have reported the synthesis of natural products including (+)-lycoricidine, (+)-kifunensine (19), and L-threosphingosine, through the microbial dihydroxylation of substituted benzenes using *Pseudomonas putida*. (Scheme 1.4, top).^{29,30} Additionally, Myers et. al. employed this methodology with the bacterial dioxygenase, *Alcaligenes eutrophus*, to synthesize 6-deoxytetracycline antibiotics from benzoic acid (Scheme 1.4, bottom).²⁶

Scheme 1.4: Enzymatic dearomatization of benzene

1.8 Transition Metal Mediated Dearomatization

Transition metal mediated dearomatization is another widely researched area within the field of dearomatization chemistry.³¹ The coordination of aromatics to transition metals has been shown to have a powerful effect on the reactivity of the aromatic.³² Within this methodology, variations in the metal complex and its electron density impact both the coordination mode of the aromatic and its subsequent. Electron deficient metal systems coordinate aromatic ligands in an η^6 fashion and activate the aromatic towards nucleophilic addition (Figure 1.3, left).³² In contrast, electron rich metal systems coordinate aromatics through only two carbons (η^2) and activate them towards electrophilic addition reactions at an uncoordinated position on the dearomatized ring (Figure 1.3, right).³²⁻³⁴

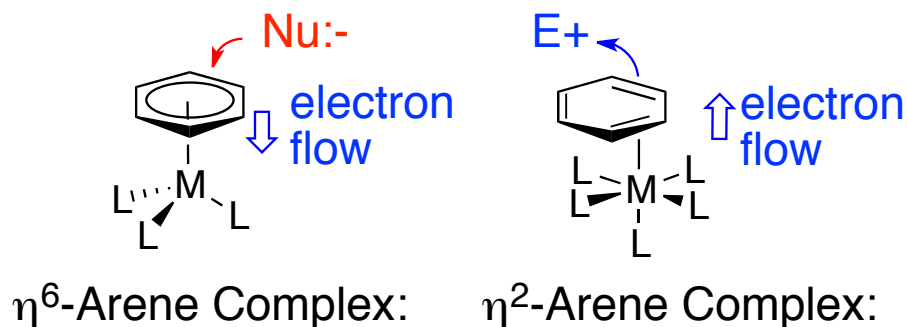


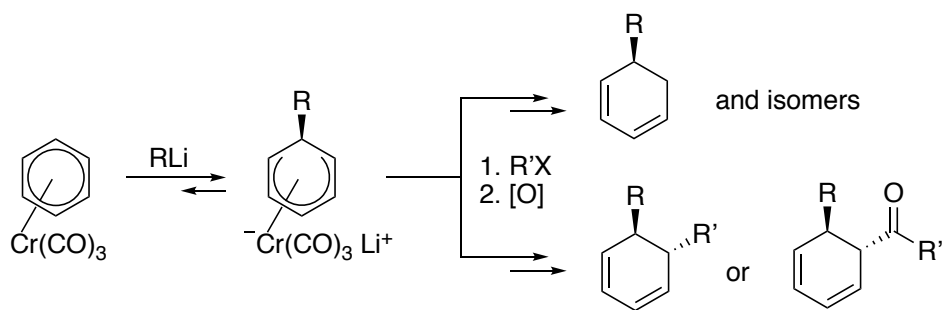
Figure 1.3: Electron-rich and electron-deficient transition metal dearomatization

1.8.1 Electron-Deficient Dearomatization Agents

Electron-deficient dearomatization chemistry has been demonstrated with metal systems such as $\{\text{Cr}(\text{CO})_3\}$ and $\{\text{Mn}(\text{CO})_3\}^+$.^{32,35-37} The η^6 -coordination of aromatics to these π -acidic metal complexes renders the aromatic ligand reactive towards nucleophilic addition, rather than the typical reactivity with electrophiles. The activation of $(\eta^6\text{-arene})\text{Cr}(\text{CO})_3$ systems towards addition with a range of nucleophiles has been demonstrated, giving access to substituted aromatics where aromaticity is restored in the isolated product.^{38,39} Arenes coordinated to the $\{\text{Cr}(\text{CO})_3\}$ system have also been transformed into alicyclic products via the sequential addition of a nucleophile and an electrophile.⁴⁰ The addition of the nucleophile occurs stereoselectively anti to the metal center. The electrophile then attacks the metal center, and is delivered endo to the cyclohexadienyl ligand, giving a trans relationship between substituents on the cyclohexadiene organic (Scheme 1.5). This dearomatization pathway has been demonstrated with nucleophiles including organo lithium compounds, sulfur stabilized carbanions, and in some cases nitrile stabilized carbanions and ester enolates. At reduced temperatures the resulting anionic cyclohexadienyl complexes react with electrophiles

(proton or C-electrophile) to give trans disubstituted cyclohexadiene products (Scheme 1.5).^{31,40} In most cases, CO insertion occurs giving the trans addition of a ketone and nucleophile across one of the double bonds. When propargyl bromide is used as the electrophile, no CO insertion product is observed.

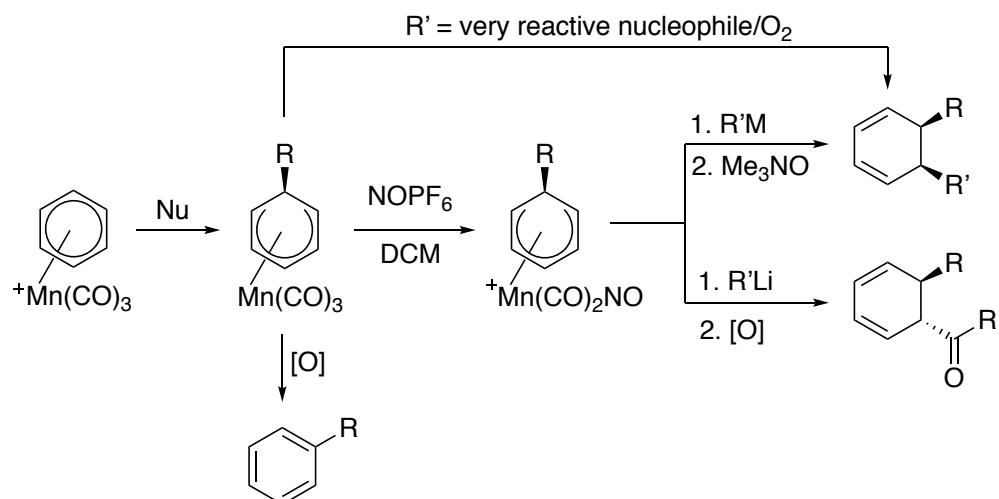
Scheme 1.5: $\{\text{Cr}(\text{CO})_3\}$ dearomatization of benzene



$\text{RLi} = \text{MeLi}, \text{PhLi}, \text{CH}_2\text{CHLi}, \text{NCCH}_2\text{Li}, \text{ect}$

$\text{R}'\text{X} = \text{prim. and sec. alkyl iodides, prim. alkyl bromides, mesylates, triflates allyl- benzyl- and propargyl bromides}$

Cationic $[(\eta^6\text{-arene})\text{Mn}(\text{CO})_3]^+$ complexes are also activated towards a nucleophilic addition reaction at the coordinated aromatic; however, the increased π -acidity of the manganese complex compared to the chromium system expands the range of reagents accessible for the initial nucleophilic addition. Successful nucleophiles demonstrated with $[(\eta^6\text{-arene})\text{Mn}(\text{CO})_3]^+$ complexes include Grignard reagents, ketone enolates, malonates, and hydrides (LiAlH_4).³² Unfortunately, the resulting neutral $\text{Mn}(\text{CO})_3(\text{cyclohexadienyl})$ complexes are not reactive towards a subsequent electrophilic addition. Decomplexation of the cyclohexadienyl ligands typically results in rearomatization (Scheme 1.6).

Scheme 1.6: $\{\text{Mn}(\text{CO})_3\}^+$ dearomatization of benzene

In contrast to the $\{\text{Cr}(\text{CO})_3\}$ system, $[(\eta^6\text{-arene})\text{Mn}(\text{CO})_3]^+$ complexes can undergo two sequential nucleophilic additions, via two different reaction pathways (Scheme 1.6).³² One pathway utilizes a very reactive second nucleophile, which leads to cis-substituted cyclohexadienes, with the second nucleophile also adding anti to the metal system. The other pathway involves the substitution of a CO ligand for a NO^+ ligand, resulting in a cationic complex that is more reactive towards a second nucleophilic addition. This cationic species can react with a second nucleophile at the cyclohexadienyl ligand to give to a cis-disubstituted cyclohexadiene product (Scheme 1.6). Depending on the identity of the second nucleophile, the addition to the cyclohexadienyl ligand can be preempted by CO insertion to give a trans-disubstituted cyclohexadiene product (Scheme 1.6).³²

The application of these electron-deficient dearomatization agents towards asymmetric synthesis has also been reported.³² A variety of methods have been investigated including the use of chiral auxiliaries, chiral nucleophiles and chiral ligands.

These methods have facilitated the synthesis of enantioenriched organics with the $\{\text{Cr}(\text{CO})_3\}$ and $\{\text{Mn}(\text{CO})_3\}^+$ systems.^{32,41}

1.8.2 Electron-Rich Dearomatization Agents

The other branch of transition metal-mediated dearomatization chemistry employs π -basic d^6 18 e^- complexes, which coordinate the aromatic ligand through only two carbons (η^2).^{32,33} This type of coordination is stabilized by the back-donation of electron density from a filled $d\pi$ metal orbital into an anti-bonding orbital of the aromatic system (Figure 1.4). Dihapto-dearomatization differs from the electron deficient hexahapto dearomatization chemistry in that dearomatization occurs upon coordination to the metal, instead of in a subsequent reaction. Support for the dearomatization of benzene upon coordination is provided through crystal structure data, which reflects a lengthening of the coordinated bonds and a shortening of the uncoordinated alkenes, such that the previously aromatic ring resembles a diene (Figure 1.4).⁴² The donation of electron density into the disrupted π -system of the dearomatized ligand activates it towards electrophilic addition and cycloaddition reactions. After the initial electrophilic addition, the resulting allyl complex is typically reactive towards a nucleophilic addition.

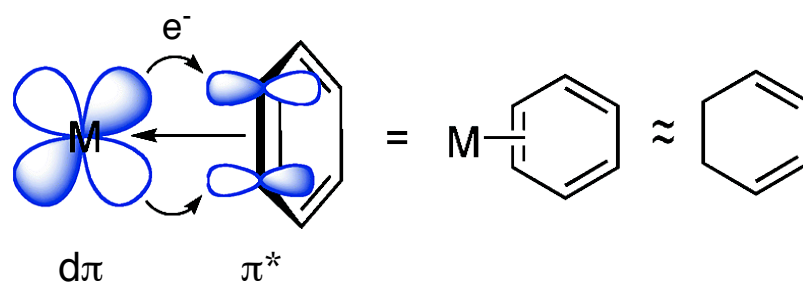
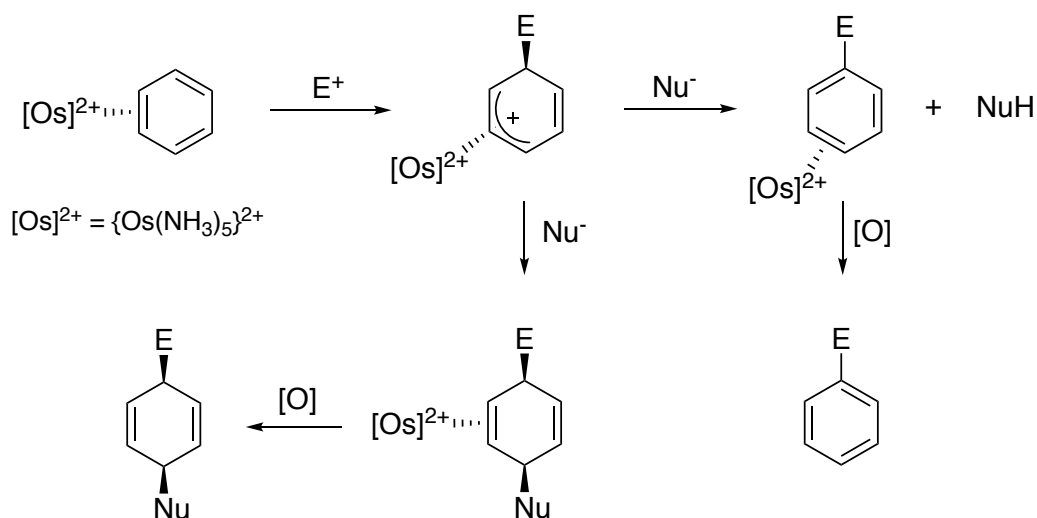


Figure 1.4: Dihapto-coordination of benzene to a π -basic metal

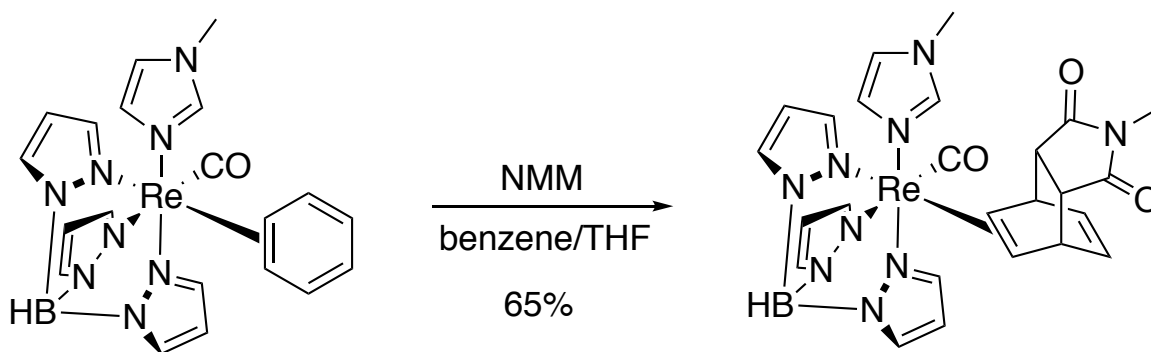
This coordination chemistry was first discovered with the pentaammineosmium(II) system, which was found to coordinate benzene in a dihapto fashion.⁴³ Efforts to expand this type of coordination to other metal systems resulted in the development of the dearomatization agents $\{\text{TpRe}(\text{CO})(\text{L})\}$, $\{\text{TpMo}(\text{NO})(\text{L})\}$, and $\{\text{TpW}(\text{NO})(\text{L})\}$.^{33,42,44-46} The achiral Os(II) system coordinates a range of aromatics including benzene, aniline, anisole, phenol, naphthalene, and pyrroles⁴⁷⁻⁵¹ Coordination of these aromatics facilitates a range of novel electrophilic addition and cycloaddition pathways.^{33,52-56} The dearomatization pathways established with the $[\text{Os}(\text{NH}_3)_5(\eta^2\text{-benzene})]^{2+}$ complex are shown in Scheme 1.7. Benzene was found to undergo an addition reaction with carbon electrophiles, including Michael acceptors and acetals, followed by a nucleophilic addition reaction with masked enolates and alkyl lithium compounds.⁵⁷ In some cases, deprotonation of the allylic species preceded addition. However, the successful addition yields disubstituted 1,4-cyclohexadiene products with a cis stereochemical relationship.

Scheme 1.7: Os(II) promoted dearomatization of benzene



The cost and achiral nature of the $\{\text{Os}(\text{NH}_3)_5\}^{2+}$ system triggered the investigation into alternative metal complexes. Through these investigations the metal d^5/d^6 reduction potential was identified as a key factor in the development of a viable alternative. After much research, it was found that a reduction potential of ~ 0.00 V (NHE) was required to coordinate aromatics in the desired dihapto-fashion.^{33,58} This work resulted in the $\{\text{TpRe}(\text{CO})(\text{L})\}$ dearomatization agent, with an increased π -basicity compared to the osmium system, and with chirality established at the metal center (Scheme 1.8, left). When $\text{L} =$ methyl imidazole (MeIm), the Re(I) system was able to coordinate a similar range of aromatics to the Os(II) system and was even able to coordinate heteroaromatics such as pyridine derivatives.³³ The dearomatization of benzene with the Re(I) system facilitates a Diels-Alder reaction with NMM giving a bicyclo[2.2.2]octene core (Scheme 1.8).⁵⁹ The Re(I) dearomatization agent also activates benzene towards tandem electrophilic/nucleophilic addition reactions similar to those shown for $[\text{Os}(\text{NH}_3)_5(\eta^2\text{-benzene})]^{2+}$ in Scheme 1.7.⁶⁰ The more π -basic $\{\text{TpRe}(\text{CO})(\text{MeIm})\}$ fragment gave higher yields for these transformation compared to osmium, furnishing cis-disubstituted 1,4-cyclohexadiene products.

Scheme 1.8: Activation of $\text{TpRe}(\text{CO})(\text{MeIm})(\eta^2\text{-benzene})$ towards cycloaddition



Issues with the synthesis and scalability of $\{\text{TpRe}(\text{CO})(\text{MeIm})\}$ drove the development of the currently studied group 6 $\text{W}(0)$ and $\text{Mo}(0)$ dearomatization agents. The knowledge gained of the importance of the d^5/d^6 reduction potential in the development of the rhenium dearomatization agent allowed the more rapid synthesis of the $\{\text{TpW}(\text{NO})(\text{PMe}_3)\}$ and $\{\text{TpMo}(\text{NO})(\text{L})\}$ ($\text{L} = \text{MeIm}, \text{NH}_3$) dearomatization agents. The increased electron density of the $\text{W}(0)$ and $\text{Mo}(0)$ metals necessitated a substitution of the CO ligand for an even more π -acidic NO^+ ligand to maintain the proper reduction potential to stabilize the dihapto-coordination of aromatics.³³ The $\{\text{TpW}(\text{NO})(\text{PMe}_3)\}$ fragment is the most π -basic of the four dearomatization agents, and has been shown to coordinate a wide range of aromatics including benzene, arenes, heterocycles, and polycyclic aromatic hydrocarbons.^{33,46,61} Until recently, the range of aromatics that can be coordinated to the $\text{Mo}(0)$ system was limited, potentially due to increased substitution rates of the second row metal. However, our group recently reported the isolation of the $\text{TpMo}(\text{NO})(4\text{-DMAP})(\eta^2\text{-benzene})$ and $\text{TpMo}(\text{NO})(4\text{-DMAP})(\eta^2\text{-PhCF}_3)$ complexes, where the ancillary ligand has been switched from MeIm to 4-dimethylaminopyridine (4-DMAP).⁶²

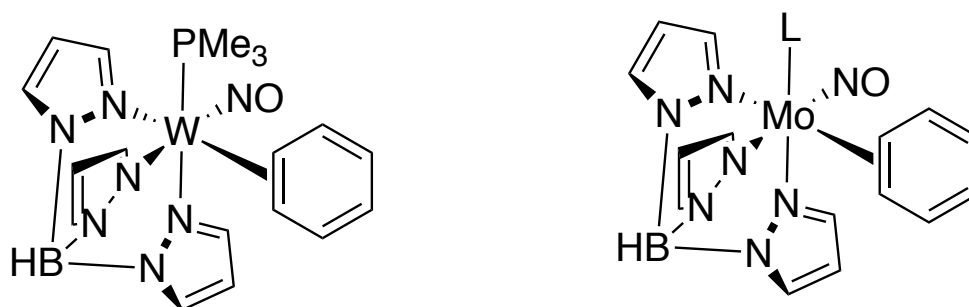


Figure 1.5: Group 6 dearomatization agents

The dearomatization chemistry of benzenes with the $\{\text{TpW}(\text{NO})(\text{PMe}_3)\}$ system will be the focus of this dissertation. Previous work from our group on the coordination and reactivity of classes of aromatics will be compared to the recently explored chemistry of $[\text{W}]-(\eta^2\text{-benzene})$ (Chapter 2), and $[\text{W}]-(\eta^2\text{-PhCF}_3)$ (Chapter 3 & Chapter 4). Much of the novel chemistry with the tungsten system has involved the coordination of nitrogen containing aromatics, such as aniline, pyridine, and more complex bicyclic systems.^{63,64} Chapters 5 and 6 explore the coordination chemistry of anilines and more complex bicyclic heterocycles. In the exploration of the tungsten dearomatization chemistry, ^{31}P NMR plays a key role, as the PMe_3 ancillary ligand provides a convenient spectroscopic handle for monitoring reactions. Furthermore, the $^{183}\text{W}\text{-}^{31}\text{P}$ coupling constant provides valuable information on the coordination mode of aromatics and can be used to help identify the type of complexes that are observed.⁶¹ Further discussion of this feature will be included in the body of the thesis.

The application of these electron-rich dearomatization agents towards asymmetric synthesis will be discussed in Chapter 7. All four of the π -basic dearomatization agents have now been used successfully in asymmetric dearomatization reactions. The methods and limitations for enantioenriched synthesis of these systems will be outlined in Chapter 7. The development and application of the enantioenriched $\{\text{TpW}(\text{NO})(\text{PMe}_3)\}$ system will also be described in Chapter 7.

1.9 References

- (1) Reymond, J.-L.; Awale, M. *ACS Chemical Neuroscience* **2012**, *3*, 649.
- (2) Vitaku, E.; Smith, D. T.; Njardarson, J. T. *Journal of Medicinal Chemistry* **2014**, *57*, 10257.
- (3) Blakemore, D. C.; Castro, L.; Churcher, I.; Rees, D. C.; Thomas, A. W.; Wilson, D. M.; Wood, A. *Nature Chemistry* **2018**, *10*, 383.
- (4) Brown, D. G.; Boström, J. *Journal of Medicinal Chemistry* **2016**, *59*, 4443.
- (5) Lovering, F.; Bikker, J.; Humblet, C. *Journal of Medicinal Chemistry* **2009**, *52*, 6752.
- (6) Ishikawa, M.; Hashimoto, Y. *Journal of Medicinal Chemistry* **2011**, *54*, 1539.
- (7) Yang, Y.; Chen, H.; Nilsson, I.; Muresan, S.; Engkvist, O. *Journal of Medicinal Chemistry* **2010**, *53*, 7709.
- (8) Arya, P.; Joseph, R.; Gan, Z.; Rakic, B. *Chemistry & Biology* **2005**, *12*, 163.
- (9) Burke Martin, D.; Schreiber Stuart, L. *Angewandte Chemie International Edition* **2003**, *43*, 46.
- (10) Schreiber, S. L. *Science* **2000**, *287*, 1964.
- (11) Tan, D. S. *Nature Chemical Biology* **2005**, *1*, 74.
- (12) Marson, C. M. *Chemical Society Reviews* **2011**, *40*, 5514.
- (13) Schleyer, P. v. R. *Chem. Rev.* **2001**, *101*, 1115.
- (14) Good, W. D.; Smith, N. K. *Journal of Chemical & Engineering Data* **1969**, *14*, 102.
- (15) Miyaura, N.; Suzuki, A. *Chem. Rev.* **1995**, *95*, 2457.
- (16) Hartwig John, F. *Angewandte Chemie International Edition* **1998**, *37*, 2046.

- (17) Hook, J. M.; Mander, L. N. *Natural Product Reports* **1986**, *3*, 35.
- (18) Crich, D.; Krishnamurthy, V. *Tetrahedron* **2006**, *62*, 6830.
- (19) Ciganek, E. *Tetrahedron Letts.* **1967**, *34*, 3321.
- (20) Wender, P. A.; Siggel, L.; Nuss, J. M. In *[3+2] and [5+2] Arene-Alkene Photocycloadditions in Comprehensive Organic Synthesis*; Trost, B. M., Fleming, I., Paquette, L. A., Eds.; Pergamon: Oxford, 1991; Vol. 5, p 645.
- (21) Remy, R.; Bochet, C. G. *Chem. Rev.* **2016**, *116*, 9816.
- (22) Hamrock, S. J.; Sheridan, R. S. *J. Am. Chem. Soc.* **1989**, *111*, 9247.
- (23) Southgate, E. H.; Pospech, J.; Fu, J.; Holycross, D. R.; Sarlah, D. *Nature Chemistry* **2016**, *8*, 922.
- (24) Hernandez, L. W.; Pospech, J.; Klöckner, U.; Bingham, T. W.; Sarlah, D. *J. Am. Chem. Soc.* **2017**, *139*, 15656.
- (25) Carless, H. A. J.; Malik, S. S. *Tetrahedron: Asymmetry* **1992**, *3*, 1135.
- (26) Charest, M. G.; Lerner, C. D.; Brubaker, J. D.; Siegel, D. R.; Myers, A. G. *Science* **2005**, *308*, 395.
- (27) Hudlicky, T.; Olivo, H. F. *J. Am. Chem. Soc.* **1992**, *114*, 9694.
- (28) Hudlicky, T. *Chem. Rev.* **1996**, *96*, 3.
- (29) Hudlicky, T. *Pure & Appl. Chem.* **1994**, *66*, 2067.
- (30) T. Hudlicky, J. W. R. *Synlett* **2009**, *5*, 685.
- (31) Kündig, E. P. *Transition Metal Arene Complexes in Organic Synthesis and Catalysis*; Springer: Berlin, 2004; Vol. 7.
- (32) Pape, A. R.; Kaliappan, K. P.; Kündig, E. P. *Chem. Rev.* **2000**, *100*, 2917.
- (33) Keane, J. M.; Harman, W. D. *Organometallics* **2005**, *24*, 1786.

- (34) Harman, W. D.; Lay, P. A. In *Advances in Inorganic Chemistry*; Sykes, A. G., Ed.; Academic Press, Inc.: San Diego, 1991; Vol. 37, p 219.
- (35) Kündig, E. P.; Fabritius, C.-H.; Grossheimann, G.; Romanens, P.; Butenschon, H.; Wey, H. G. *Organometallics* **2004**, *23*, 3741.
- (36) Kündig, E. P. *Pure Appl. Chem.* **2004**, *76*, 689.
- (37) Semmelhack, M. F. In *Comprehensive Organometallic Chemistry II*; Abel, E. W., Stone, F. G. A., Wilkinson, G., Eds.; Pergamon: Oxford, 1995; Vol. 12, p 979.
- (38) Semmelhack, M. F.; Hall, H. T.; Farina, R.; Yoshifuji, M.; Clark, G.; Bargar, T.; Hirotsu, K.; Clardy, J. *J. Am. Chem. Soc.* **1979**, *101*, 3535.
- (39) Semmelhack, M. F.; Clark, G. R.; Farina, R.; Saeman, M. *J. Am. Chem. Soc., Commun.* **1979**, *101*, 217.
- (40) Kündig, E. P.; Cunningham Allan, F.; Paglia, P.; Simmons Dana, P.; Bernardinelli, G. *Helvetica Chimica Acta* **1990**, *73*, 386.
- (41) Amurrio, D.; Kahn, K.; Kündig, E. P. *J. Org. Chem.* **1996**, *61*, 2258.
- (42) Meiere, S. H.; Brooks, B. C.; Gunnoe, T. B.; Sabat, M.; Harman, W. D. *Organometallics* **2001**, *20*, 1038.
- (43) Harman, W. D.; Taube, H. *J. Am. Chem. Soc.* **1987**, *109*, 1883.
- (44) Meiere, S. H.; Brooks, B. C.; Gunnoe, T. B.; Carrig, E. H.; Sabat, M.; Harman, W. D. *Organometallics* **2001**, *20*, 3661.
- (45) Mocella, C. J.; Delafuente, D. A.; Keane, J. M.; Warner, G. R.; Friedman, L. A.; Sabat, M.; Harman, W. D. *Organometallics* **2004**, *23*, 3772.
- (46) Graham, P.; Meiere, S. H.; Sabat, M.; Harman, W. D. *Organometallics* **2003**, *22*, 4364.

- (47) Kolis, S. P.; Gonzalez, J.; Bright, L. M.; Harman, W. D. *Organometallics* **1996**, *15*, 245.
- (48) Cordone, R.; Harman, W. D.; Taube, H. *J. Am. Chem. Soc.* **1989**, *111*, 5969.
- (49) Myers, W. H.; Koontz, J. I.; Harman, W. D. *J. Am. Chem. Soc.* **1992**, *114*, 5684.
- (50) Kopach, M. E.; Harman, W. D. *J. Am. Chem. Soc.* **1994**, *116*, 6581.
- (51) Kolis, S. P.; Kopach, M. E.; Liu, R.; Harman, W. D. *J. Org. Chem.* **1997**, *62*, 130.
- (52) Gonzalez, J.; Koontz, J. I.; Myers, W. H.; Hodges, L. M.; Sabat, M.; Nilsson, K. R.; Neely, L. K.; Harman, W. D. *J. Am. Chem. Soc.* **1995**, *117*, 3405.
- (53) Hodges, L. M.; Gonzalez, J.; Koontz, J. I.; Myers, W. H.; Harman, W. D. *J. Org. Chem.* **1995**, *60*, 2125.
- (54) Kopach, M. E.; Harman, W. D. *J. Org. Chem.* **1994**, *59*, 6506.
- (55) Winemiller, W. D.; Kopach, M. E.; Harman, W. D. *J. Am. Chem. Soc.* **1997**, *119*, 2096.
- (56) Harman, W. D. *Chem. Rev.* **1997**, *97*, 1953.
- (57) Ding, F.; Kopach, M. E.; Sabat, M.; Harman, W. D. *J. Am. Chem. Soc.* **2002**, *124*, 13080.
- (58) Brooks, B. C.; Gunnoe, T. B.; Harman, W. D. *Coord. Chem. Rev.* **2000**, *3*.
- (59) Chordia, M. D.; Smith, P. L.; Meiere, S. H.; Sabat, M.; Harman, W. D. *J. Am. Chem. Soc.* **2001**, *123*, 10756.
- (60) Ding, F.; Harman, W. D. *J. Am. Chem. Soc.* **2004**, *126*, 13752.
- (61) Welch, K. D.; Harrison, D. P.; Lis, E. C.; Liu, W.; Salomon, R. J.; Harman, W. D.; Myers, W. H. *Organometallics* **2007**, *26*, 2791.

- (62) Myers, J. T.; Smith, J. A.; Dakermanji, S. J.; Wilde, J. H.; Wilson, K. B.; Shivokevich, P. J.; Harman, W. D. *J. Am. Chem. Soc.* **2017**, *139*, 11392.
- (63) Harrison, D. P.; Harman, W. D. *Aldrichimica Acta* **2012**, *45*, 45.
- (64) Liebov, B. K.; Harman, W. D. *Chem. Rev.* **2017**, *117*, 13721.

Chapter 2

The Tungsten Promoted Dearomatization of Benzene

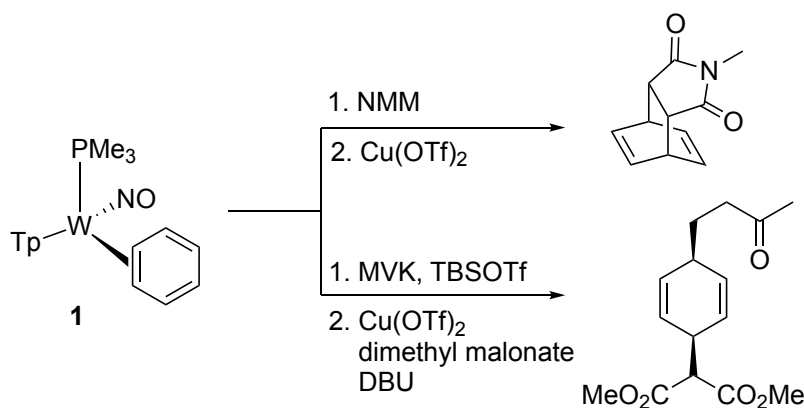
2.1 Introduction

Many different methods for the activation of benzene have been investigated as a means to access a diverse range of cyclic small molecules from a convenient and abundant source (see Chapter 1). Traditionally, benzene undergoes electrophilic aromatic substitution reactions; however, dearomatization methods enable organic transformations that are common with alkene bonds and lead to more complex molecules where aromaticity is broken. The ability of transition metals to promote this type of dearomatization with benzenes has been exploited from two different perspectives. Electron-deficient metal systems, such as $\{\text{Cr}(\text{CO})_3\}$ and $\{\text{Mn}(\text{CO})_3\}^+$, coordinate arenes in an η^6 -fashion and activate them towards nucleophilic addition.¹⁻³ This chemistry has been employed with benzene to access trans-5,6-disubstituted 1,3-cyclohexadienes and cis-5,6-disubstituted 1,3-cyclohexadienes.³ In contrast, electron-rich metal fragments such as $\{\text{Os}(\text{NH}_3)_5\}$ and $\{\text{TpRe}(\text{CO})(\text{L})\}$, coordinate benzene through only two carbons (η^2) and activate the aromatic towards electrophilic addition. In this case, electron-rich dearomatization of benzene gives 1,4-addition reactions with a carbon electrophile followed by a nucleophile, resulting in *cis*-3,6-disubstituted 1,4-cyclohexadienes.

Although the electron-rich $\text{TpW}(\text{NO})(\text{PMe}_3)(\eta^2\text{-benzene})$ complex was first reported almost 15 years ago⁴, the instability of the η^2 -benzene complex under acidic conditions has limited the ability to enact organic transformations. The reactions demonstrated with the tungsten benzene complex have been limited to a Diels-Alder reaction with *N*-methylmaleimide (NMM) and a tandem addition reaction with a carbon electrophile and an enolate.^{4,5} In the case of the tandem addition, the nucleophilic addition could not be accomplished while the metal was still coordinated and instead the complex was oxidized

and reacted with the nucleophile in situ to furnish the organic cyclohexadiene in a 12% yield. Both reactions lead to a η^2 -1,4-diene complex, with an uncoordinated double bond that is no longer in coordination with the metal and thus not activated towards a second addition reaction by the metal.

Scheme 2.1: Activation of benzene with the tungsten dearomatization agent



Recent findings have led us to explore further reactivity available to the $\text{TpW}(\text{NO})(\text{PMe}_3)(\eta^2\text{-benzene})$ system. We proposed that we could effect two sequential addition reactions across the two uncoordinated double bonds of the benzene ring, and in this process generate multiple asymmetric centers from the flat aromatic ligand (Figure 2.1). This method would be complementary to the Diels-Alder reaction, as a means for facile access to functionalized cyclohexene synthetic building blocks for novel small molecule synthesis. The η^2 -benzene complex also provides a unique opportunity to gain insight into the inherent control of the asymmetric tungsten fragment, without the coinciding influence of substituents on the benzene ring. Thus, the ability of the tungsten dearomatization agent, $\{\text{TpW}(\text{NO})(\text{PMe}_3)\}$, to activate a dihapto-coordinated benzene ring towards addition reactions was investigated.

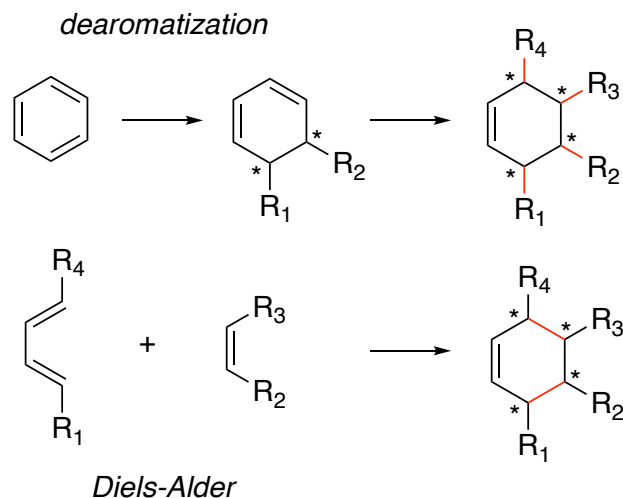


Figure 2.1: Synthesis of functionalized cyclohexenes

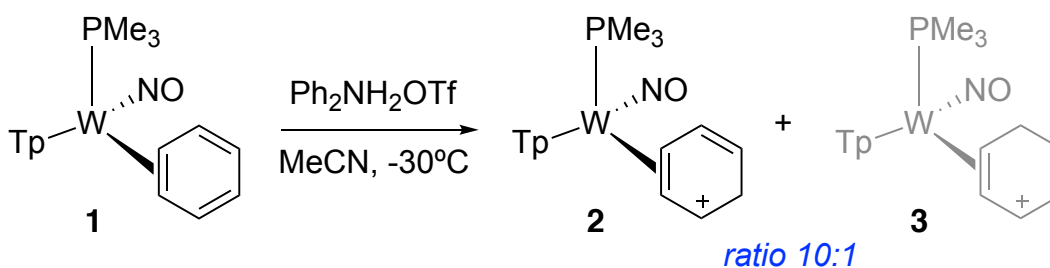
2.2 Results and Discussion

Recently, we have demonstrated the regio- and stereoselective protonation of $\text{TpW}(\text{NO})(\text{PMe}_3)(\eta^2\text{-benzene})$ with a mild Brønsted acid (diphenylammonium triflate (DPhAT)) at reduced temperatures (-30°C) resulting in predominately the allyl complex **2** (Scheme 2.2). Upon warming in the presence of acid, the tungsten complex undergoes an uncontrolled decomposition pathway that leads to the formation of the fully saturated allyl complex. In contrast to traditional symmetric η^3 -allyl complexes, our asymmetric metal fragment causes an asymmetric allyl (allyl distortion), which more accurately can be described as an η^2 -alkene with an adjacent metal stabilized carbocation.⁶ In the two observed allyls the positive charge is localized distal to the PMe_3 ligand, which is consistent with previous reports from our group about the preferential overlap of the asymmetric metal HOMO with a ligand based LUMO with the positive charge distal to the PMe_3 ("down").⁶ These assignments were determined by full 2D NMR analysis (NOESY, COSY, HMQC, HMBC). Key features leading to the identification of **2** include a NOE correlation

between an allyl proton at 6.93 ppm and a proton on a pyrazole ring of the Tp ligand trans to the PMe_3 ligand. This allyl proton also exhibited NOE and COSY interactions with an adjacent methylene group. Furthermore, an alkene resonance was observed at 6.17 ppm with an NOE interaction with the PMe_3 ligand.

DFT studies were conducted for all the possible allyl complexes using the B3LYP method with a “hybrid” basis set with the LANL2DZ pseudopotential and basis set on W and 6-31G(d) on all other atoms. **2** and **3** were the two lowest energy complexes, differing only by ~ 0.12 kcal/mol with a slight preference for **3**. 2D NMR data of this product mixture revealed that complexes **2** and **3** are in dynamic equilibrium, based on an exchange of signals in the NOESY spectrum. The experimentally observed thermodynamic ratio of 10:1 favoring **2** reflects an error in our DFT calculations of ~ 1.3 kcal/mol. The stereoselectivity of the protonation was determined by conducting an experiment with d^2 -DPhAT. 2D NMR of the resulting allyl enabled the confirmation of a stereoselective syn deuteration (protonation).

Scheme 2.2: Protonation of **1** with diphenylammonium triflate



The selective protonation of **1** at reduced temperatures was promising in terms of ultimately enabling the controlled dearomatization of benzene. Thus the ability to do a selective tandem electrophilic/nucleophilic addition across one of the double bonds of η^2 -

benzene was investigated. For these experiments, the electrophilic source was a proton, typically delivered from diphenylammonium triflate (DPhAT). A range of nucleophiles were screened including amines, phosphines, protected enolates, aromatics, methoxide, cyanide, and alkylating agents. The temperature, solvent, and concentration were varied to optimize selectivity and yield, and the results of these experiments are summarized in Table 2.1. In most cases, **1** was protonated at reduced temperature (-30°C to -60°C), and the resulting allylic species **2** was reacted in situ with a nucleophile. In some cases, experiments were monitored by ³¹P NMR to rapidly determine the product ratio and optimize conditions. The yield and product ratios listed are for isolated products, except when the addition complex was too unstable to isolate.

Experimentally, we observed a high degree of regiocontrol, with the proton and nucleophile adding selectively across the uncoordinated double bond distal to the PMe₃ ligand. Additionally, coordination to the bulky tungsten system enforces the incoming nucleophile to stereoselectively add *anti* to the metal center. The products of these reactions were identified using 2D NMR analysis (COSY, NOESY, HSQC, and HMBC), in addition to IR and cyclic voltammetry. Key NOE interactions between the modified aromatic ligand and the rest of the ligand set were used to assign stereochemistry (Figure 2.2). Spectroscopic features consistent for all major products include an alkene proton resonance at ~6.5 ppm that exhibits an NOE correlation with the PMe₃ ligand, and an allylic methine resonance with an NOE correlation to a proton on the Tp ligand (on the pyrazole ring trans to the PMe₃). X-ray analysis of a single crystal of **6A** provides confirmation of the proposed η²-1,3-diene product (Figure 2.2).

Table 2.1: Tandem electrophilic/nucleophilic addition to **1**

Nucleophile	Temp. (°C)	Product A	Product B	A:B	Yield (%)
H ₂ NMe	-30			96:4	59
PMe ₃	-30			97:3	70
	-60			99:1	66
	-30			80:20	42*
	-60			92:8	27*
	-30			50:50	18*
TBAOH/MeOH	-30			95:5	N/A
NaCN	-30			96:4	61
	-30			92:8	33
	-60			97:3	70

*minor amount of **1** present in sample

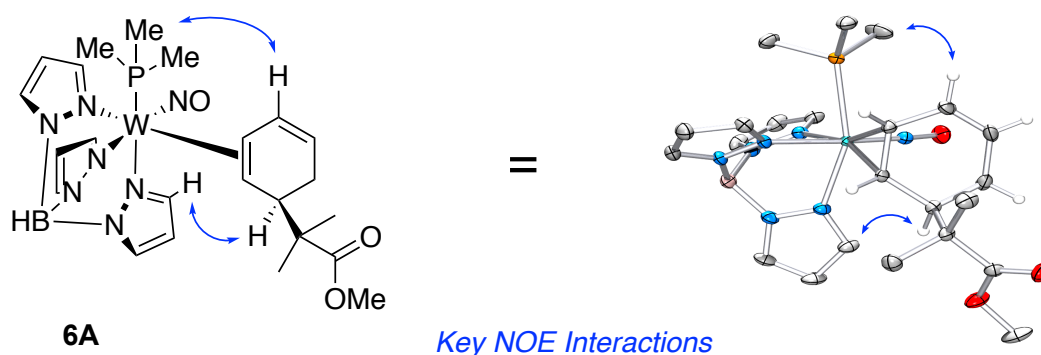
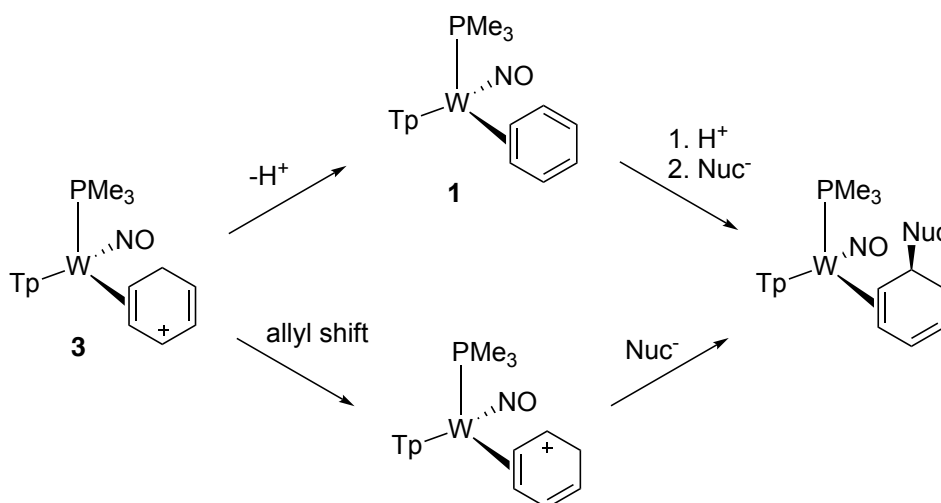


Figure 2.2: Key NOE interactions and crystal structure of **6A**

In instances where an appreciable amount of a minor product was observed, the complex was identified as a coordination diastereomer of the major product. Interestingly, this product does not result from nucleophilic addition at the carbocation of the minor allylic species **3**. To explain the formation of the minor product, we propose two possible mechanisms (Scheme 2.3). The minor allyl could be deprotonated and then reprotonated at a different position on the ring prior to nucleophilic addition (Scheme 2.3, top). Conversely, **3** could undergo an allyl shift where the tungsten moves one position over on the ring, giving an allyl with the positive charge localized proximal to the PMe_3 (Scheme 2.3, bottom). Nucleophilic addition to this allyl would result in the observed minor product.

Scheme 2.3: Formation of minor addition product to **1**

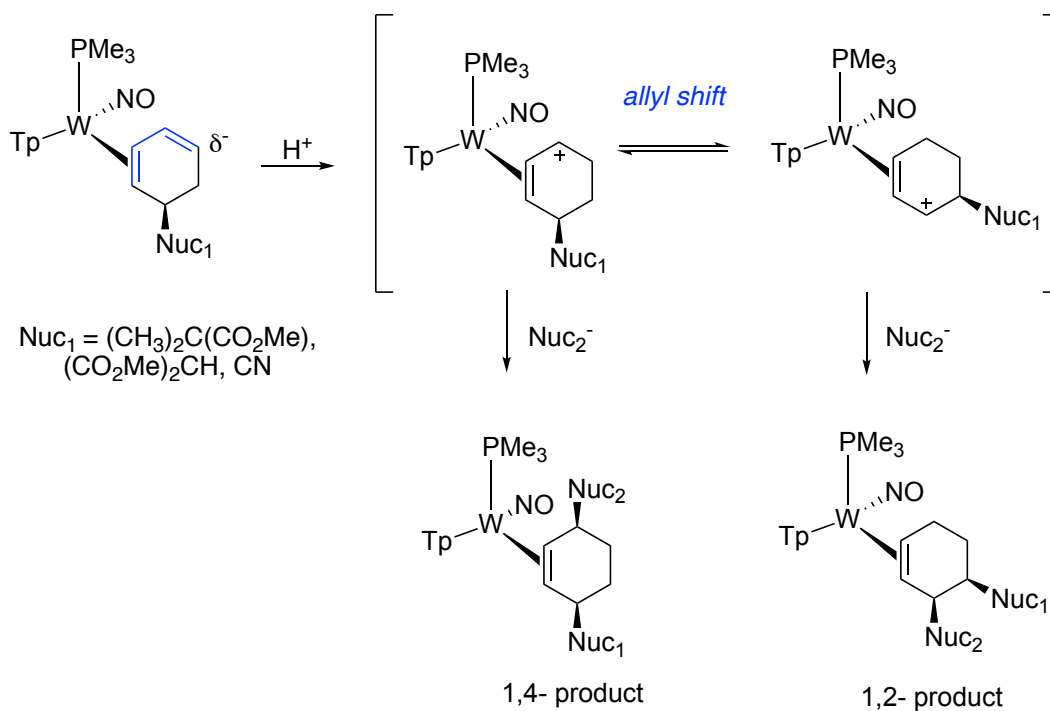


A greater amount of the minor diene complex was observed with the addition of relatively weak aromatic nucleophiles (*N*-methylindole and pyrrole). This reduced regioselectivity was also accompanied by the regeneration of **1**. The diminished selectivity could be a result of the decreased rate of nucleophilic addition allowing for one of the alternative reaction pathways to occur. These nucleophiles could also be functioning as bases to facilitate the top reaction pathway shown in Scheme 2.3. In the case of *N*-methylindole, the product selectivity was improved from 80:20 to 92:8, by reducing the temperature from -30°C to -60°C. Attempts to increase the selectivity of the pyrrole addition by reducing the temperature resulted in no reaction and recovery of **1**. The ability to use stronger nucleophilic alkylating agents, such as MeMgBr and ZnEt₂ was also investigated. In these experiments the isolated allylic complex **2** was treated with the alkylating agent at reduced temperatures (-30°C to -60°C) in dried THF. ¹H NMR data of the product mixture showed minor amounts of the desired products; however, decomposition or deprotonation of the allyl to reform η²-benzene predominated.

The regioselective 1,2-addition across an uncoordinated double bond of **1** results in η²-1,3-diene products, which are susceptible to further tungsten-promoted addition reactions at the remaining uncoordinated double bond. We elected to explore the reactivity of η²-1,3-diene complexes **6A**, **10A**, and **11A**, due to their varying steric and electronic profiles and the “irreversibility” of the first nucleophile. Protonation of these η²-1,3-diene complexes would be expected to occur at the terminal carbon of the uncoordinated diene, resulting in an asymmetric allyl species with the positive charge localized proximal to the PMe₃ (Scheme 2.4). We propose that two distinct allylic species exist in equilibrium, with a low kinetic barrier between the tungsten coordinating to either terminus of the allyl.

Addition of a nucleophile results in the formation of a 1,4-product, a 1,2-product, or a mixture of products depending on which allylic species reacts.

Scheme 2.4: Tandem electrophilic/nucleophilic addition to η^2 -1,3-dienes



The two distinct allyl species differ based on which two carbons are coordinated and where the positive charge is localized. We propose that stabilizing or destabilizing effects on the positive charge affect both the distortion of the allyl and which asymmetric allyl species is favored. Identification and analysis of the favored allyl complex can help rationalize subsequent regioselectivity of nucleophilic additions, as observed with the initial addition reaction to **1**. The allyl complexes were isolated by protonation of the diene complexes **6A**, **10A**, and **11A** with triflic acid (HOTf) in acetonitrile. The corresponding allylic species **12**, **13**, and **14** were precipitated from Et₂O. In each case a single allyl complex was observed; however, the distortion of the allylic species, as determined by ¹H

NMR resonances of the π -allylic protons, varied drastically depending on the identity of the first nucleophile (Figure 2.3). For example, **12** and **14** appear to be very distorted allyls, with the positive charge localized distal to the PMe_3 . The distortion is reflected in the chemical shifts of the allyl protons, with the proton where the positive charge is shown having a signal at ~ 6.3 ppm and the proton at the other terminus of the allyl shifted 2 ppm further upfield ~ 4.3 ppm (Figure 2.3).

Harrison and co-workers from our lab previously published work that focused on hyperdistorted allyl complexes of tungsten, with similar ^1H NMR shifts to those of the benzene system explored herein. These similarities between the distortion of the allyl are further supported by crystal structure data. The W-C bond lengths of the two carbons coordinated to the tungsten were typically $\sim 2.3\text{\AA}$, whereas the third allyl carbon (localized carbocation) was $\sim 2.6\text{\AA}$ from the tungsten center. For **12** and **14**, the distortion of the allyls is consistent with what we expected, with the tungsten fragment favoring the positive charge distal to the PMe_3 . Furthermore, the alkyl substituents on **12** and **14** stabilize the adjacent carbocation. In contrast, **13** (Figure 2.3, bottom), is much less distorted than **12** and **14**, with the terminal protons of the allyl within 0.5 ppm of each other. This allyl complex provides insight into the contrasting effects of the tungsten stabilization of the positive charge down, and the cyanide withdrawing group destabilization of an adjacent carbocation.

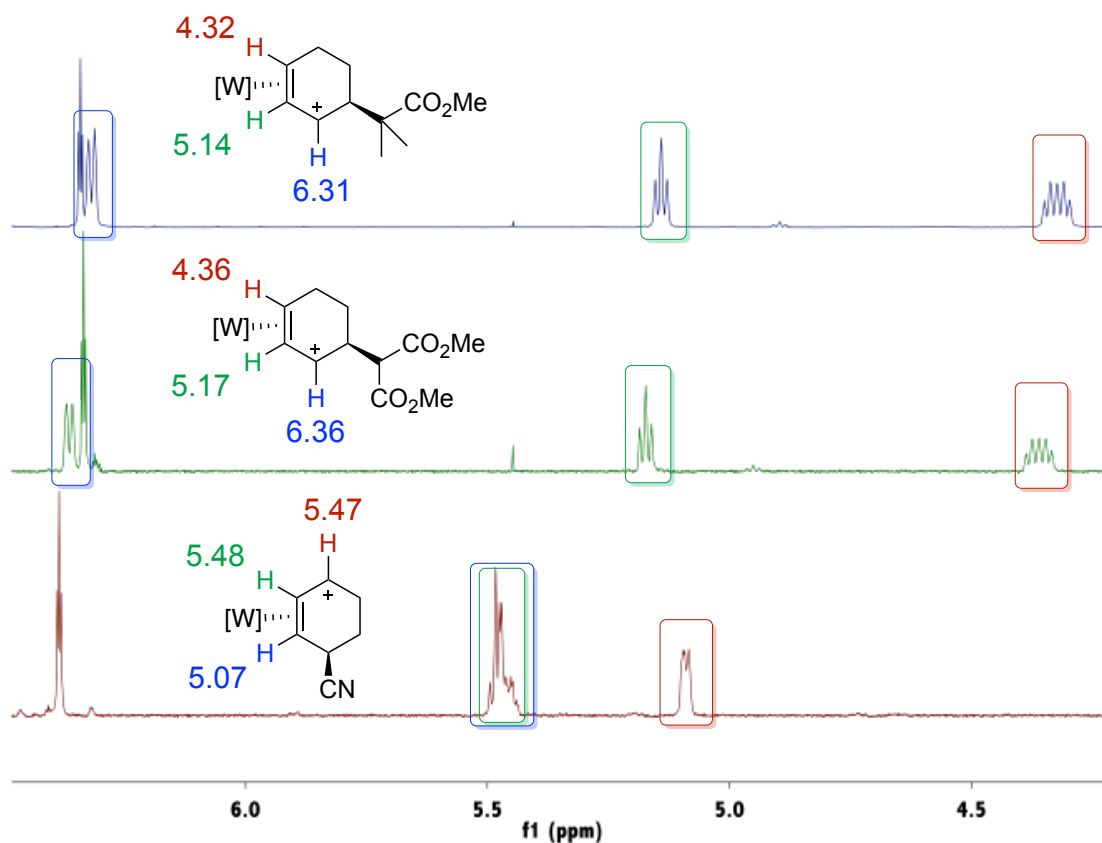


Figure 2.3: ^1H NMR spectra of allyl complexes **12** (top), **13** (bottom), and **14** (middle)

To investigate the reactivity of **6A**, **10A**, and **11A**, each η^2 -1,3-diene complex was treated with acid followed by a nucleophile. The nucleophiles screened for this second addition reaction include methylamine, 1-methoxy-2-methyl-1-trimethylsilyloxypropene (MMTP), NaCN, dimethylmalonate (LiDMM), and MeMgBr. The reactions were monitored by ^1H or ^{31}P NMR to determine the product ratio. ^{31}P NMR is a convenient technique to monitor reactions with the $\{\text{TpW}(\text{NO})(\text{PMe}_3)\}$ system because deuterated solvents are not needed. Furthermore, 14% of naturally occurring tungsten is the NMR active isotope ^{183}W with a spin of $\frac{1}{2}$. The number of tungsten complexes can be easily monitored by ^{31}P NMR, with 14% of the signal split into a doublet by ^{183}W , which we refer to as the tungsten

satellites. Our group has found that the ^{183}W - ^{31}P coupling constant gives information about the type of complex present, including the coordination mode of the ligand of interest.⁷ In general, a ^{183}W - ^{31}P coupling constant of 366 to 415 Hz reflects a 6-coordinate complex. Dihapto-coordinated complexes typically have a coupling constant between 255 and 314 Hz, and 7-coordinate complexes typically fall between 100 and 212 Hz. To illustrate the power of this tool, Figure 2.4 shows an overlay of the ^{31}P NMR spectra starting from η^2 -benzene (top) and going through each addition reaction (protonation and nucleophilic addition, vide infra), with an internal standard for reference. The coupling constant is the largest for the η^2 -benzene, and the lowest for the allylic species (Figure 2.4).

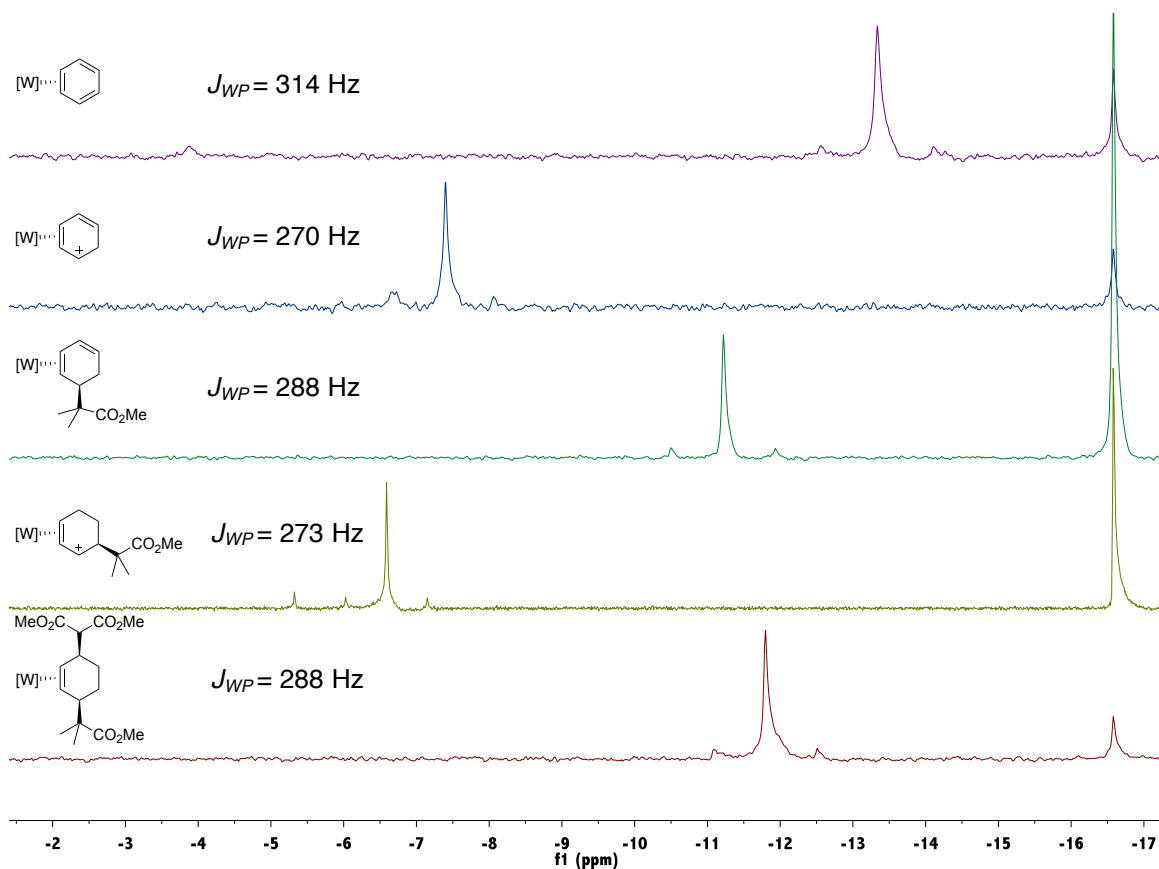


Figure 2.4: ^{31}P NMR monitoring of addition reactions to **1**

The results for the second tandem addition reaction to **10A** are shown in Table 2.2. The addition reactions were carried out in acetonitrile at -30°C to reduce competing deprotonation of the allyl and optimize selectivity. Experiments conducted at room temperature were also successful for some of the addition reactions. The addition of a proton and a nucleophile to **10A** selectively formed a 1,4-product (>10:1) with masked enolates (MMTP and LiDMM) and methylamine. These products result from the nucleophile adding to the allyl that is observed in situ, with the positive charge localized proximal to the PMe₃. Furthermore, the 1,4-arrangement of nucleophiles avoids unfavorable steric interactions present when the nucleophiles are directly next to each other in 1,2-products. For the addition reaction attempted with a Grignard reagent, the isolated allyl complex **13** was used instead of generating the allyl in situ with acid. The subsequent addition of MeMgBr to **13** resulted in a 3:1 ratio of the products (1,4:1,2) in addition to the regeneration of **10A** (60%). Regioselectivity was also reduced when NaCN was used as the second nucleophile, giving a ~2.5:1 ratio of products favoring the 1,4-complex. The reduced regioselectivity for these cases could be a result of increased reactivity of the nucleophiles or potentially the smaller steric profiles of these nucleophiles, which could lessen the preference for 1,4-products due to unfavorable steric interactions.

Table 2.2: Nucleophilic addition reactions to **10A**

Nuc ₁	Nuc ₂	Product A	Product B	A:B	Yield (%)
NaCN	H ₂ NMe			93:7	59
NaCN				97:1 ^a	80
NaCN	NaCN			64:27 ^b	N/A
NaCN				97:3	80
NaCN	MeMgBr*			30:10 ^c	N/A

^aremaining 2% is SM (**10A**). ^bremaining 9% is undetermined product. ^cremaining 60% is SM

In contrast, as shown in Table 2.3, additions to **11A** resulted in 1,2-products with high selectivity for both the primary amine and NaCN. The addition of methyl amine resulted in an intramolecular cyclization reaction, giving the lactam product **20B**, and is

consistent with chemistry observed with the $\text{TpW}(\text{NO})(\text{PMe}_3)(\eta^2\text{-PhCF}_3)$ system (Chapter 3).⁸ The formation of 1,2-products is consistent with the nucleophile selectively adding to the carbocation of the distorted allyl that is observed in solution. Conversely, addition of the relatively bulky protected enolate (LiDMM) changed the selectivity and gave the 1,4-product **23A**. This change in regiochemistry could result from unfavorable steric interactions between the first nucleophile and the bulky incoming nucleophile in the formation of the 1,2-product. The TMS masked enolate MMTP was unreactive with the allylic species. Attempts to cleave the TMS group with iodide and fluoride and activate the enolate towards addition were unsuccessful. Addition of MeMgBr favored the 1,4-product **24A** (90:10). This reaction demonstrates a selective carbon-carbon bond formation, where the nucleophile preferentially reacts with the carbocation and leaves the ester groups intact.

The reactivity of diene complex **6A** under the same set of conditions was similar to **11A**, except the slightly bulkier steric profile of **6A** favored the formation of 1,4-products in all cases. For example, when **6A** is reacted with NaCN, the 1,4-product **27A** is favored by 3:1; however, NaCN addition to **11A** gives almost exclusively the 1,2-product (>20:1). In the case of the MeMgBr addition, single crystal structure determination of **29A** reflects the 1,4-product with syn relative stereochemistry, and verifies the successful addition of the methyl group without disturbance of the ester functionality (Figure 2.5).

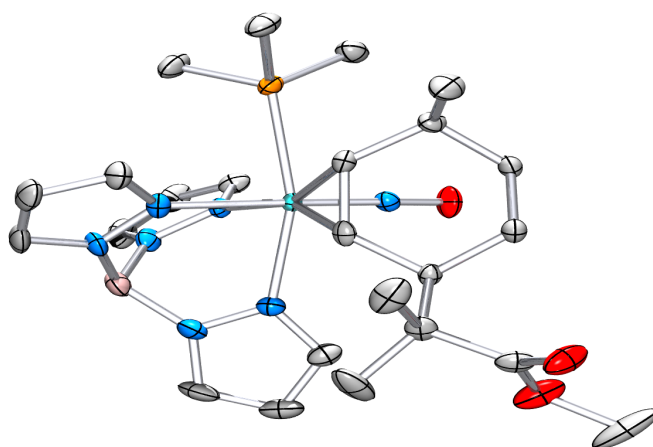
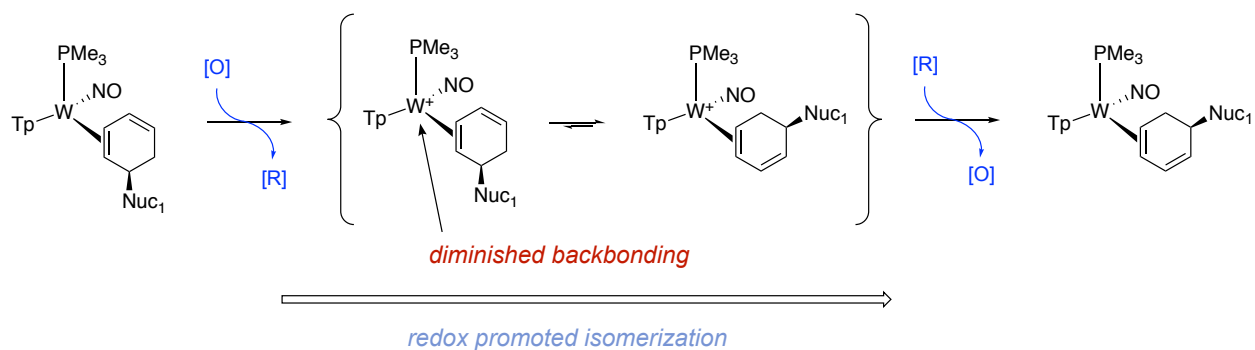


Figure 2.5: Crystal structure of compound **29A**

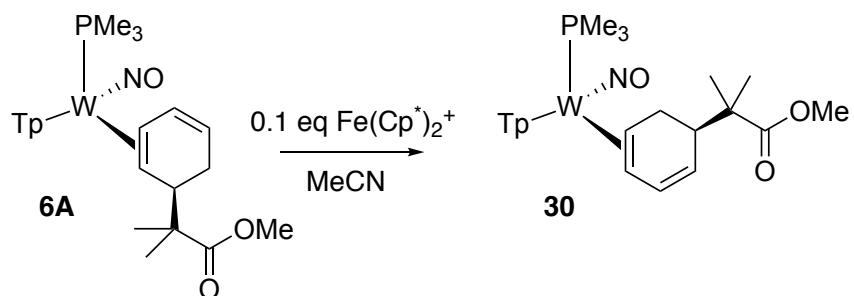
In the instances where the 1,4-product is formed from **6A** and **11A**, we propose that this selectivity is made possible by invoking Curtin-Hammett conditions. As previously discussed, we believe that there is a low kinetic barrier between the two allyl species, allowing for their rapid interconversion. In cases where the reaction of the nucleophile with the allyl that is observed in solution is slow, if the rate of the nucleophilic addition to the unobserved allyl is fast, the rapid interconversion of the two allyls could allow for a kinetically controlled selective formation of the 1,4-product.

Table 2.3: Nucleophilic additions to **6A** and **11A**

Nuc ₁	Nuc ₂	Product A	Product B	A:B	Yield (%)
	H ₂ NMe			6:94	74
				NR	N/A
	NaCN			3:97	73
				96:4	70
	MeMgBr*			90:10	55
	H ₂ NMe			95:5	71
				NR	N/A
	NaCN			76:24	N/A
				100:0	79
	MeMgBr*			96:4	54

Scheme 2.5: Redox promoted diene isomerization

Recently, our group reported the use of a redox catalyst to increase the rate of a ligand substitution reaction with the {TpMo(NO)(DMAP)} system.⁹ Further investigations into the possible applications of this redox catalysis led us to propose a redox promoted isomerization pathway (Scheme 2.5) to access a different type of η^2 -diene. We theorized that upon oxidation, the diminished electron density of the W(I) system and coinciding reduced ability to back-donate would transiently weaken the tungsten alkene bond and enable an intramolecular alkene bond movement. The isomerized diene complex can then be reduced back to W(0), giving the overall catalytic diene isomerization.

Scheme 2.6: Diene isomerization of **6A**

Experimentally, we found that stirring **6A** with 0.1 equivalent of a mild oxidant ($[\text{Fe}(\text{Cp}^*)_2]\text{Tf}_2\text{N}$) resulted in almost complete conversion to **30** within 15 min (by ^1H NMR), with an isolated yield of 87% (Scheme 2.6). The initial identification of **30** was accomplished using 2D NMR analysis. Specifically, an alkene proton resonance exhibited an NOE correlation with a Tp proton trans to the PMe_3 . This led us to believe that the uncoordinated alkene bond was distal to the PMe_3 . Furthermore, the methylene protons had NOE correlations to the PMe_3 . Another characteristic feature of this new type of diene is the collapse of the splitting pattern for the terminal uncoordinated alkene proton. This indicated the loss of coupling with an adjacent proton, which is consistent with the nucleophile being adjacent to the alkene. In addition to 2D NMR analysis, single-crystal molecular structure determination of **30** provided confirmation of the successful isomerization (Figure 2.6).

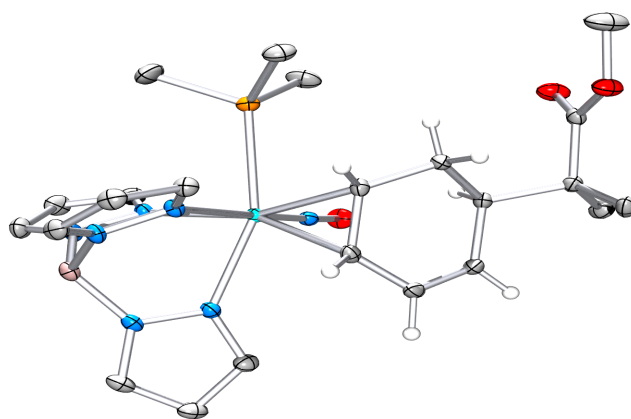


Figure 2.6: Crystal structure of compound **30**

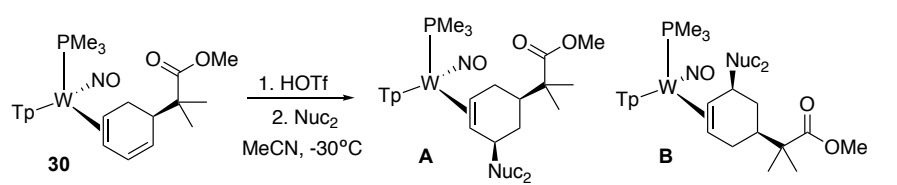
Interestingly, this proposed redox catalyzed isomerization can be accomplished with relatively weak oxidants. Complex **6A** has a $\text{W(I)}/\text{W(0)}$ reduction potential of 0.54 V ($E_{\text{p,a}}$ vs. NHE), whereas the permethylferrocenium salt has a $\text{Fe(III)}/\text{Fe(II)}$ $E_{1/2} = 0.0$ V vs.

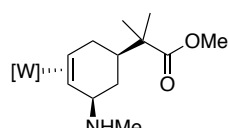
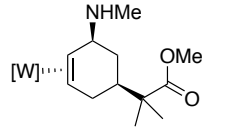
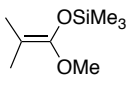
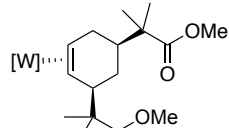
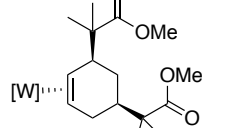
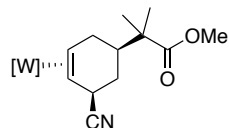
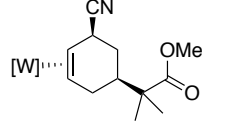
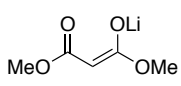
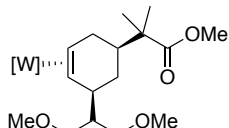
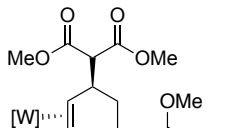
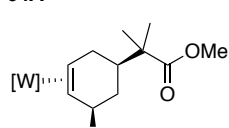
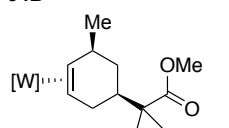
NHE. Additionally, we discovered that stirring a solution of **6A** in air also facilitates this diene isomerization. At this point in time, we are unsure of the mechanism for this isomerization and what causes the reduction of the transient $W(I)$ complex to complete the catalytic cycle. The focus of the work in this case was to implement this type of catalysis to access new dihapto-dienes and explore new reactivity patterns. To this end, this type of isomerization was also attempted with **10A** and **11A**. Treating **10A** with varying oxidants predominately resulted in starting material. Isomerization of **11A** was more promising, in that conversion to the isomerized diene was observed, but we believe that the extent of isomerization is limited by the thermodynamic ratios: In the case of **6A**, we propose that isomerization to **30** is possible because of the thermodynamic preference for **30** over **6A**. In contrast, isomerization of **11A** stops at a 1.2:1 ratio, only slightly favoring the isomerized form. Using more catalyst, as well as using a stronger oxidant, did not change the ratio of products.

The ability to controllably form complex **30** provided the opportunity to expand the range of substitution patterns accessed from the η^2 -benzene complex. The reactivity of **30** was explored with the same range of nucleophiles previously used, and the results are summarized in Table 2.4. In this instance, the two proposed products both have a 1,3-substitution pattern, and would give enantiomers upon removal from the metal. Thus, regiocontrol is paramount for the synthesis of organics as single enantiomers (Chapter 7). Our investigation of the reactivity of **30** resulted in stereo- and regioselective addition reactions with a primary amine, masked enolates, and NaCN. These reactions give 1,3-products where the nucleophile adds distal to the PMe_3 ligand (>95:5). Experiments using MeMgBr as the nucleophile resulted in good regioselectivity (17:1) for the addition

products, but also led to deprotonation (10%) and regeneration of **30**. The reactivity of **30** provides further insight into the regio- and stereocontrol afforded by the asymmetric tungsten complex, due to the decreased steric and electronic influence of the initial nucleophile. With less impact from the first substituent, we observe increased regiocontrol for the addition of the second nucleophile.

Table 2.4: Nucleophilic addition reactions to **30**

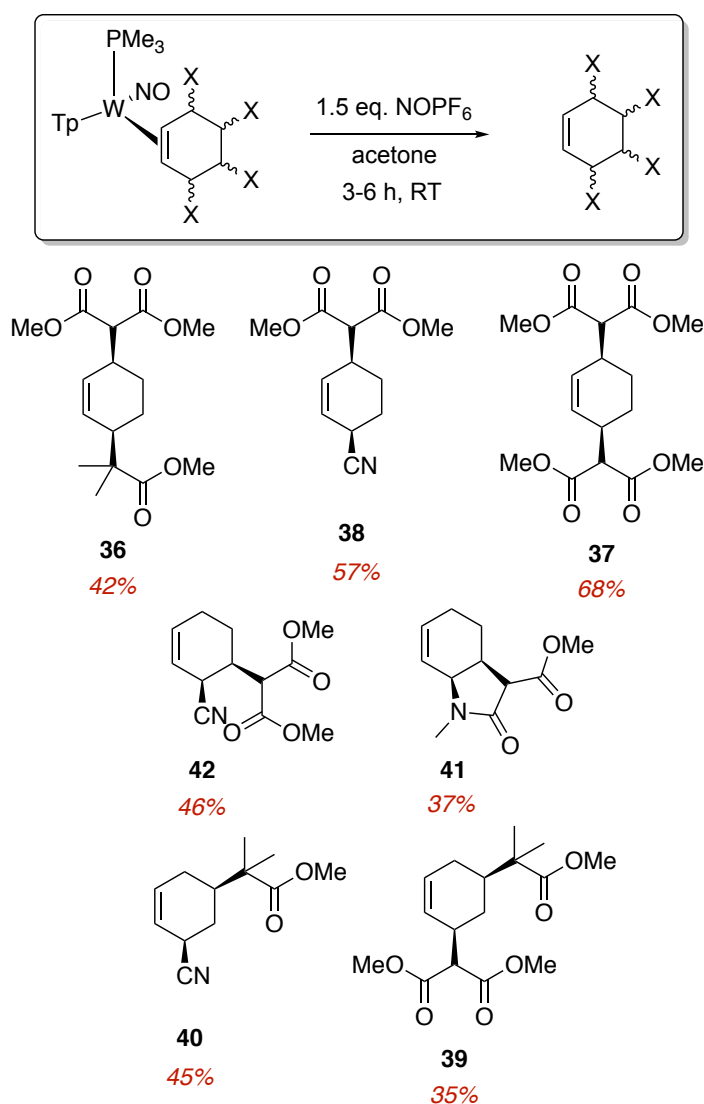


Nucleophile	Product A	Product B	A:B	Yield (%)
H ₂ NMe	 31A	 31B	97:3	56
	 32A	 32B	99:1	87
NaCN	 33A	 33B	95:5	79
	 34A	 34B	96:4	75
MeMgBr*	 35A	 35B	85:5*	35*

*the remaining 10% of the reaction mixture is complex **30**

Ultimately, these sequential additions to dihapto-benzene provide access to a variety of functionalized cyclohexenes with 1,4-, 1,2-, and 1,3-substitution patterns. Oxidation of the tungsten complex with over one equivalent of an one electron oxidant reduces the strength of the π -back bonding interaction and enables the isolation of the free cyclohexene derivatives. The oxidant that was found to work the best was NOPF₆. This process was demonstrated with a range of transformed organic ligands (Scheme 2.7) in modest yields, ranging from 35%-68%. Purification of the cyclohexenes was achieved with a chromatographic work-up using silica gel preparatory plates.

Scheme 2.7: Isolation of functionalized cyclohexenes



2.3 Conclusions

Recently, we discovered the regioselective protonation of $\text{TpW}(\text{NO})(\text{PMe}_3)(\eta^2\text{-benzene})$ with a mild Brønsted acid at reduced temperatures. Addition of a nucleophile to the allylic species results in the selective formation of $\eta^2\text{-1,3-diene}$ complexes, with the metal still in conjugation to the uncoordinated double bond. In the case of benzene, with no substituents on the ring to influence the regioselectivity of addition reactions, the powerful influence of the asymmetric tungsten fragment is demonstrated by the formation of one major allyl complex (>10:1) upon protonation. In situ addition of a nucleophile to the asymmetric benzenium complex leads to 1,3-diene products with the nucleophile adding selectively *anti* to the metal. This 1,2-addition reaction was demonstrated with a range of nucleophiles, including protected enolates, amines, cyanide, methoxide, and phosphines.

Furthermore, the $\eta^2\text{-1,3-diene}$ products are susceptible to further tungsten-promoted addition reactions at the uncoordinated double bond. The activation of the diene complexes was exploited for the synthesis of a range of disubstituted cyclohexenes with 1,2-, 1,3- and 1,4-substitution patterns. In most cases the second tandem addition reaction was accomplished with a high degree of regio- and stereocontrol. The selectivity of the second addition was affected by the steric and electronic influences of the first nucleophile, the metal, as well as the incoming nucleophile. Overall, these reactions represent the first examples of $\eta^2\text{-dearomatization}$ of benzene where a total of four metal-controlled addition reactions were realized. Additionally, this dearomatization chemistry provides a new synthetic route to quickly build up structural and functional complexity from a simple benzene ring. Complementary methods for transforming aromatic compounds into alicyclic structures have been developed with $\{\text{Cr}(\text{CO})_3\}$ and $\{\text{Mn}(\text{CO})_3\}^+$ to give disubstituted 1,3-

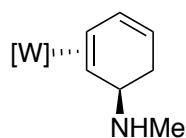
cyclohexadienes.³ The Sarlah group recently reported the conversion of benzene into (+)-pancratistatins through photocatalyzed dearomatization.¹⁰ Additionally, enzymatic dearomatization of benzene facilitates the stereocontrolled synthesis of dihydroxylated 1,3-cyclohexadienes, which provides useful chiral scaffolds for further elaboration. The Hudlicky group has employed this type of methodology to synthesize a range of natural products from convenient aromatic precursors.^{11,12}

2.4 Experimental

General Methods: NMR spectra were obtained on 500, 600 or 800 MHz spectrometers. Chemical shifts are referenced to tetramethylsilane (TMS) utilizing residual ^1H or ^{13}C signals of the deuterated solvents as internal standards. Phosphorus NMR signals are referenced to 85% H_3PO_4 (δ 0.00) using a triphenyl phosphate external standard (δ -16.58). Chemical shifts are reported in ppm and coupling constants (J) are reported in hertz (Hz). Infrared Spectra (IR) were recorded on a spectrometer as a glaze on a diamond anvil ATR assembly, with peaks reported in cm^{-1} . Electrochemical experiments were performed under a nitrogen atmosphere. Most cyclic voltammetric data were recorded at ambient temperature at 100 mV/s, unless otherwise noted, with a standard three electrode cell from +1.8 V to -1.8 V with a platinum working electrode, *N,N*-dimethylacetamide (DMA) or acetonitrile solvent, and tetrabutylammonium hexafluorophosphate (TBAH) electrolyte (~ 1.0 M). All potentials are reported versus the normal hydrogen electrode (NHE) using cobaltocenium hexafluorophosphate ($E_{1/2} = -0.78$ V, -1.75 V) or ferrocene ($E_{1/2} = 0.55$ V) as an internal standard. Peak separation of all reversible couples was less than 100 mV. All synthetic reactions were performed in a glovebox under a dry nitrogen atmosphere unless otherwise noted. All solvents were purged with nitrogen prior to use. Deuterated solvents were used as received from Cambridge Isotopes. When possible, pyrazole (Pz) protons of the (trispyrazolyl) borate (Tp) ligand were uniquely assigned (e.g., "PzB3") using two-dimensional NMR data (see Figure S1). If unambiguous assignments were not possible, Tp protons were labeled as "Pz3/5 or Pz4". All J values for Pz protons are 2 (± 0.4) Hz. BH peaks (around 4-5 ppm) in the ^1H NMR spectra are not assigned due to their quadrupole broadening; however, confirmation of the BH group is provided by IR

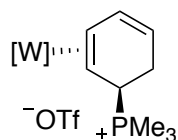
fritted disc and washed with Et₂O (2 x 20 mL, -30°C). The collected product was then desiccated for 2 h yielding **2** and **3** (1.63 g, 2.24 mmol, 86% yield) in a 10:1 ratio.

IR: $\nu(\text{BH}) = 2520 \text{ cm}^{-1}$, $\nu(\text{NO}) = 1637 \text{ cm}^{-1}$. **Complex 2** (major): ³¹P NMR (CD₃CN, δ): -7.44 ($J_{\text{WP}} = 274$). ¹H NMR (CD₃CN, δ , 0°C): 8.33(d, 1H, Pz3B/5B), 8.03 (d, 1H, PzA3), 8.02 (d, 1H, PzC5), 7.97 (d, 1H, PzC3), 7.94 (d, 1H, PzB3/B5), 7.80 (d, 1H, PzA5), 6.93 (d, 1H, H1), 6.54 (t, 1H, PzC4), 6.49 (t, 1H, PzB4), 6.31 (t, 1H, PzA4) 6.17 (m, 1H, H4), 5.04 (m, 1H, H5), 4.91 (t, $J = 7.2$, 1H, H2), 4.24 (m, 1H, H3), 4.16 (d, $J = 28.3$, 1H, H6x), 3.99 (d, $J = 28.3$, 1H, H6y), 1.18 (d, $J = 9.8$, 9H, PMe₃). ¹³C NMR (CD₃CN, δ , 0°C): 147.9 (PzA3), 146.7 (PzC5), 145.7 (C1), 143.0 (Pz3/5), 139.4 (Pz3/5), 139.3 (2C, Pz3/5), 126.1 (C4), 119.5 (C5), 109.2 (PzB4), 108.7 (PzC4), 107.8 (PzA4), 95.1 (C2), 64.5 (C3), 30.7 (C6), 13.1 (d, $J = 34.2$, PMe₃). **Complex 3** (minor): ¹H NMR (CD₃CN, δ , 0°C): 8.31 (d, 1H, Pz3/5), 8.11 (d, 1H, Pz3/5), 8.01 (d, 1H, Pz3/5), 7.92 (d, 1H, PzC3), 7.81 (d, 1H, Pz3/5), 6.55 (buried, 1H, H6), 6.52 (t, 1H, Pz4), 6.34 (m, 2H, Pz4 & H1), 5.89 (m, 1H, H5), 4.71 (t, $J = 7.5$, 1H, H2), 4.65 (m, 1H, H3), 4.34 (d, $J = 25.8$, 1H, H4x), 3.36 (d, $J = 25.8$, 1H, H4y), 1.11 (buried, 9H, PMe₃).



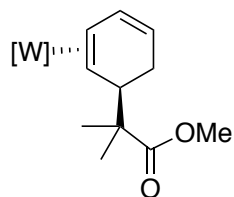
Compound 4A. Diphenylammonium triflate (121 mg, 0.379 mmol) was dissolved in acetonitrile (2.4 mL, -30°C). This solution was added to a 4-dram vial containing **1** (200 mg, 0.344 mmol) with stirring, resulting in a homogeneous golden solution, which was allowed to sit for 15 min at -30°C. 2M H₂NMe/THF (2.0 mL, 4.0 mmol, -30°C) was then added to the reaction vial with stirring and allowed to sit at -30°C for 19 h. While the reaction was still cold, 1M tBuOK in *tert*-butanol (1.0 mL, 1.0 mmol) was added, and then the reaction was

evaporated *in vacuo*. The film was redissolved in minimal THF then added to stirring pentane (30 mL, -30°C). The resulting pale solid was collected on a 15 mL fine porosity fritted disc, washed with H₂O (3 x 4 mL), and pentane (3 x 5 mL) then desiccated overnight, yielding **4A** (125 mg, 0.204 mmol, 59% yield). CV (DMAc) $E_{p,a} = +0.39$ V (NHE). IR: $\nu(\text{BH}) = 2485$ cm⁻¹, $\nu(\text{NO}) = 1548$ cm⁻¹. ³¹P NMR (CD₃CN, δ): -11.63 ($J_{\text{WP}} = 286$). ¹H NMR (CD₃CN, δ): 8.04 (d, 1H, PzB3), 7.99 (d, 1H, PzA3), 7.85 (d, 1H, PzB5), 7.84 (d, 1H, PzC5), 7.76 (d, 1H, PzA5), 7.42 (d, 1H, PzC3), 6.47 (ddd, $J = 8.9, 5.0, 3.2$, 1H, H2), 6.35 (t, 1H, PzB4), 6.27 (overlapping triplets, 2H, PzA4 & PzC4), 4.86 (ddd, $J = 8.9, 6.5, 2.1$, 1H, H1), 3.34 (m, 1H, H5), 2.85 (ddd, $J = 13.4, 10.1, 5.0$, 1H, H3), 2.70 (dm, $J = 16.6$, 1H, H6x), 2.28 (s, 3H, NMe), 2.17 (dd, $J = 16.6, 6.5$, 1H, H6y), 1.28 (dm, $J = 10.1$, 1H, H4), 1.22 (d, $J = 8.5$, 9H, PMe₃). ¹³C NMR (CD₃CN, δ): 144.4 (PzB3), 143.1 (PzA3), 141.8 (PzC3), 137.8 (PzC5), 137.2 (PzB5), 136.9 (PzA5), 132.4 (C2), 117.0 (C1), 107.3 (PzB4), 107.1 (PzC4), 106.8 (PzA4), 59.2 (C4), 58.8 (C5), 50.4 (d, $J = 9.5$, C3), 34.7 (NMe), 28.7 (C6), 13.9 (d, $J = 28.6$, PMe₃).



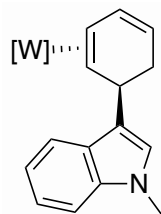
Compound 5A. Diphenylammonium triflate (58 mg, 0.18 mmol) was dissolved in acetonitrile (1 mL, -30°C). This solution was added to a 4-dram vial containing **1** (100 mg, 0.172 mmol) with stirring, resulting in a homogeneous golden solution, which was allowed to sit for 15 min at -30°C. Trimethylphosphine (130 mg, 1.71 mmol, -30°C) was then added to the reaction vial with stirring, and the solution was allowed to sit at -30°C for 17 h. The reaction solution was added to stirring Et₂O (15 mL), and the resulting solid was collected

on a 15 mL fine porosity fritted disc, washed with Et₂O (2 x 5 mL), and pentane (1 x 5 mL) then desiccated overnight, yielding **5A** (94 mg, 0.12 mmol, 70% yield). CV (MeCN) $E_{p,a} = +0.72$ V (NHE). IR: $\nu(\text{BH}) = 2488$ cm⁻¹, $\nu(\text{NO}) = 1550$ cm⁻¹. ³¹P NMR (CD₃CN, δ): 36.33, -11.66 ($J_{\text{WP}} = 279$). ¹H NMR (CD₃CN, δ): 8.05 (d, 1H, PzB3), 7.93 (d, 1H, PzA3), 7.88 (d, 1H, PzB5), 7.87 (d, 1H, PzC5), 7.81 (d, 1H, PzA5), 7.50 (d, 1H, PzC3), 6.55 (ddd, $J = 9.5, 5.2, 3.1$, 1H, H2), 6.38 (t, 1H, PzB4), 6.32 (t, 1H, PzA4), 6.31 (t, 1H, PzC4), 4.99 (ddd, $J = 9.5, 6.6, 1.9$, 1H, H1), 3.41 (m, 1H, H5), 3.01 (ddd, $J = 42.8, 18.1, 8.0$, 1H, H6x), 2.95 (m, 1H, H3), 2.20 (m, 1H, H6y), 1.72 (d, $J = 13.7$, 9H, PMe₃), 1.18 (d, $J = 8.8$, 9H, PMe₃), 1.05 (m, 1H, H4). ¹³C NMR (CD₃CN, δ): 144.3 (PzB3), 142.3 (PzA3/PzC3), 142.2 (PzA3/PzC3), 138.1 (PzC5), 137.5 (PzA5/PzB5), 137.4 (PzA5/PzB5), 134.2 (C2), 115.3 (C1), 107.6 (PzB4), 107.3 (PzA4/PzC4), 107.2 (PzA4/PzC4), 49.5 (d, $J = 11.0$, C3), 48.5 (m, C4), 34.4 (d, $J = 38.2$, C5), 22.9 (C6), 13.5 (d, $J = 29.3$, PMe₃), 8.4 (d, $J = 51.4$, PMe₃).

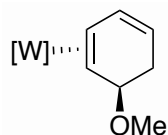


Compound 6A. Diphenylammoniumtriflate (DPhAT, 293 mg, 0.918 mmol) and propionitrile (5 mL) were added to a screw top test tube and cooled to -55°C for 20 min, then this solution was added to a separate screw top test tube charged with **1** (500 mg, 0.860 mmol) and a stir pea. The resulting orange solution was allowed to sit at -55°C for 20 min. Methyl trimethylsilyl dimethylketene acetal (MTDA, 1.90 mL, 9.35 mmol) was added to a separate screw top test tube charged with a stir pea and also cooled to -55°C for 20 min. The reaction solution was then added to the MTDA with stirring and was left at -55°C

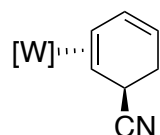
for 15 h then warmed to -30°C for 1 h. The golden reaction solution was quenched with Et_3N (0.50 mL, 3.59 mmol). A 60 mL medium porosity fritted disc was filled $\frac{3}{4}$ full of silica gel and set in Et_2O . The reaction solution was loaded on the column and a pale yellow band was eluted with 125 mL of Et_2O . The filtrate was evaporated *in vacuo*, then redissolved in minimal THF and added to 30 mL stirring pentane. The resulting pale yellow solid was collected on a 15 mL fine porosity fritted disc, washed with pentane (3 x 3 mL) and desiccated overnight, yielding **6A** (390 mg, 0.571 mmol, 66% yield). CV (DMAc) $E_{\text{p,a}} = +0.45$ V (NHE). IR: $\nu(\text{BH}) = 2485 \text{ cm}^{-1}$, $\nu(\text{CO}) = 1719 \text{ cm}^{-1}$, $\nu(\text{NO}) = 1546 \text{ cm}^{-1}$. Anal. Calc'd for $\text{C}_{23}\text{H}_{35}\text{BN}_7\text{O}_3\text{PW}$: C, 40.43; H, 5.16; N, 14.35. Found: C, 40.18; H, 5.00; N, 14.13. ^{31}P NMR (CD_3CN , δ): -11.22 ($J_{\text{WP}} = 288$). ^1H NMR (CD_3CN , δ): 8.10 (d, 1H, PzA3), 8.03 (d, 1H, PzB3), 7.83 (m, 2H, PzB5 & PzC5), 7.77 (d, 1H, PzA5), 7.47 (d, 1H, PzC3), 6.38 (ddd, $J = 9.0, 4.9, 3.3$, 1H, H2), 6.34 (t, 1H, PzB4), 6.29 (t, 1H, PzA4), 6.27 (t, 1H, PzC4), 4.92 (ddd, $J = 9.0, 6.4, 2.2$, 1H, H1), 3.25 (s, 3H, H9), 3.24 (buried, 1H, H5), 2.90 (m, 1H, H3), 2.72 (ddm, $J = 17.7, 9.0$, 1H, H6x), 1.86 (dd, $J = 17.7, 6.4$, 1H, H6y), 1.25 (s, 3H, H10), 1.20 (d, $J = 8.5$, 9H, PMe_3), 1.11 (s, 3H, H11), 0.86 (d, $J = 10.1$, 1H, H4). ^{13}C NMR (CD_3CN , δ): 179.9 (C8), 144.3 (PzB3), 142.3 (PzA3), 141.9 (PzC3), 137.8 (PzC5), 137.1 (2C, PzA5 & PzB5), 131.9 (C2), 118.7 (C1), 107.3 (PzB4), 107.0 (PzC4), 106.5 (PzA4), 53.5 (C4), 52.3 (C7), 51.8 (d, $J = 9.6$, C3), 51.4 (C9), 43.5 (C5), 24.5 (C6), 23.5 (C10), 23.0 (C11), 13.8 (d, $J = 28.6$, PMe_3).



Compound 7A. Diphenylammoniumtriflate (DPhAT, 60 mg, 0.19 mmol) and proprionitrile (1 mL) were added to a screw top test tube and cooled to -60°C for 30 min, then this solution was added to a separate screw top test tube containing **1** (100 mg, 0.172 mmol) with stirring. The resulting orange solution was allowed to sit at -60°C for 20 min. *N*-Methylindole (338 mg, 2.58 mmol) was added to a separate screw top test tube and also cooled to -60°C for 20 min before being added to the reaction solution with stirring. The reaction was left at -60°C for 48 h then Et_3N (75 mg, 0.74 mmol) was added. A 30 mL medium porosity fritted disc was filled $\frac{3}{4}$ full of silica gel and set in Et_2O . The reaction solution was loaded on the column and a pale yellow band was eluted with 50 mL of Et_2O . The filtrate was evaporated *in vacuo*, then redissolved in minimal DCM and added to stirring pentane (15 mL, -30°C). The resulting pale yellow solid was collected on a 15 mL fine porosity fritted disc, washed with pentane (3 x 3 mL) and desiccated overnight, yielding **7A** (33 mg, 0.046 mmol, 27% yield). ^1H NMR (CD_3CN , δ): 8.30 (d, 1H, Pz3/5), 8.08 (d, 1H, Pz3/5), 7.86 (d, 1H, Pz3/5), 7.82 (d, 1H, Pz3/5), 7.80 (d, 1H, Pz3/5), 7.44 (d, 1H, Pz3/5), 7.42 (d, $J = 7.9$, 1H, Ar-H), 7.26 (d, $J = 8.1$, 1H, Ar-H), 7.21 (s, 1H, Ar-H), 7.08 (m, 1H, Ar-H), 6.90 (m, 1H, Ar-H), 6.53 (m, 1H, H2), 6.37 (t, 1H, Pz4), 6.34 (t, 1H, Pz4), 6.22 (t, 1H, Pz4), 4.95 (m, 1H, H1), 4.27 (d, $J = 7.3$, 1H, H5), 3.70 (s, 3H, NMe), 3.04 (dd, $J = 16.5, 7.5$, 1H, H6x), 2.99 (m, 1H, H3), 2.17 (dd, $J = 16.5, 6.5$, 1H, H6y), 1.36 (bd, $J = 10.3$, 1H, H4), 1.26 (d, $J = 8.5$, 9H, PMe_3).

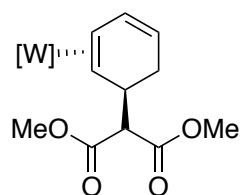


Compound 9A. Diphenylammonium triflate (31 mg, 0.097 mmol) was dissolved in acetonitrile (0.7 mL, -30°C). This solution was added to a 4-dram vial containing **1** (50 mg, 0.086 mmol) with stirring, resulting in a homogeneous golden solution, which was allowed to sit for 20 min at -30°C. 1M Bu₄OH/MeOH (0.3 mL, 0.3 mmol, -30°C) was then added to the reaction vial with stirring and allowed to sit at -30°C for 24 h. The reaction solution was then evaporated *in vacuo* to dryness, and the resulting solid, **9A** was dissolved in CD₃CN for NMR data. ¹H NMR (CD₃CN, δ): 8.03 (d, 1H, PzB3), 7.95 (d, 1H, PzA3), 7.85 (d, 1H, PzB5), 7.84 (d, 1H, PzC5), 7.75 (d, 1H, PzA5), 7.45 (d, 1H, PzC3), 6.46 (m, 1H, H2), 6.35 (t, 1H, PzB4), 6.27 (overlapping triplets, 2H, PzA4 & PzC4), 4.86 (ddd, *J* = 9.2, 6.2, 2.0, 1H, H1), 4.18 (m, 1H, H5), 3.19 (s, 3H, OMe), 2.87 (m, 1H, H3), 2.77 (dm, *J* = 17.4, 1H, H6x), 2.30 (dd, *J* = 17.4, 6.2, 1H, H6y), 1.24 (m, 1H, H4), 1.20 (d, *J* = 8.5, 9H, PMe₃).



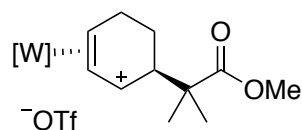
Compound 10A. Diphenylammonium triflate (289 mg, 0.905 mmol) was dissolved in acetonitrile (6 mL, -30°C). This solution was added to a 4-dram vial containing **1** (500 mg, 0.860 mmol) with stirring, resulting in a homogeneous golden solution, which was allowed to sit for 15 min at -30°C. In a separate 4-dram vial, NaCN (257 mg, 5.24 mmol) and MeOH (4 mL, -30°C) were combined and allowed to cool to -30°C for 15 min. The NaCN solution was then added to the reaction vial with stirring and allowed to sit at -30°C for 24 h at

which point a solid had precipitated. The reaction was allowed to warm to room temperature, and then the yellow solid was collected on a 15 mL fine porosity fritted disc, washed with H₂O (2 x 5 mL), MeOH (-30°C, 0.5 mL), and pentane (2 x 4 mL) then desiccated overnight, yielding **10A** (320 mg, 0.526 mmol, 61% yield). CV (DMAc) $E_{p,a} = +0.70$ V (NHE). IR: $\nu(\text{BH}) = 2487$ cm⁻¹, $\nu(\text{CN}) = 2224$ cm⁻¹, $\nu(\text{NO}) = 1557$ cm⁻¹. Anal. Calc'd for C₁₉H₂₆BN₈OPW·H₂O: C, 36.45; H, 4.51; N, 17.90. Found: C, 36.24; H, 4.18; N, 17.52. ³¹P NMR (d⁶-acetone, δ): -11.06 ($J_{\text{WP}} = 282$). ¹H NMR (d⁶-acetone, δ): 8.12 (d, 1H, PzB3), 7.96 (m, 2H, PzB5 & PzC5), 7.95 (d, 1H, PzA3), 7.85 (d, 1H, PzA5), 7.61 (d, 1H, PzC3), 6.57 (m, 1H, H2), 6.40 (t, 1H, PzB4), 6.35 (t, 1H, PzC4), 6.33 (t, 1H, PzA4), 4.98 (m, 1H, H1), 3.74 (dm, $J = 7.0$, 1H, H5), 2.96 (m, 1H, H3), 2.82 (dm, $J = 16.6$, 1H, H6x), 2.10 (dd, $J = 16.6$, 6.5, 1H, H6y), 1.32 (buried, 1H, H4), 1.31 (d, $J = 8.6$, 9H, PMe₃). ¹³C NMR (d⁶-acetone, δ): 144.4 (PzB3), 142.4 (PzA3), 141.8 (PzC3), 137.8 (PzC5), 137.3 (PzB5), 136.8 (PzA5), 132.7 (C2), 128.2 (CN), 115.4 (C1), 107.2 (Pz4), 107.1 (Pz4), 106.9 (Pz4), 55.9 (d, $J = 2.5$, C4), 48.5 (d, $J = 11.0$, C3), 29.5 (C5), 27.4 (C6), 13.7 (d, $J = 28.6$, PMe₃).

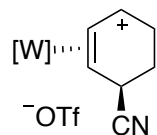


Compound 11A. Diphenylammoniumtriflate (DPhAT, 289 mg, 0.905 mmol) and propionitrile (10 mL) were added to a screw top test tube and cooled to -60°C for 20 min, then added to a separate screw top test tube charged with **1** (500 mg, 0.860 mmol) and a stir pea. The resulting orange solution was allowed to sit at -60°C for 20 min. LiDMM (582 mg, 4.21 mmol), propionitrile (0.5 mL), THF (1.5 mL), and a stir pea were added to a

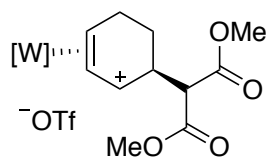
separate screw top test tube and cooled to -60°C for 20 min. The reaction solution with added to the test tube with LiDMM with stirring and left at -60°C for 20 h. A 150 mL coarse porosity fritted disc was filled $\frac{3}{4}$ full of silica gel and set in Et_2O . The reaction solution was loaded on the column and a pale yellow band was eluted with 150 mL of Et_2O . The filtrate was evaporated *in vacuo*, then redissolved in minimal THF and added to 30 mL stirring pentane. The resulting pale yellow solid was collected on a 15 mL fine porosity fritted disc, washed with pentane (3 x 5 mL) and desiccated, yielding **11A** (431 mg, 0.604 mmol, 70% yield). CV (DMAc) $E_{p,a} = +0.48$ V (NHE). IR: $\nu(\text{BH}) = 2487$ cm^{-1} , $\nu(\text{CO}) = 1750$ & 1727 cm^{-1} , $\nu(\text{NO}) = 1551$ cm^{-1} . Anal. Calc'd for $2\text{C}_{23}\text{H}_{33}\text{BN}_7\text{O}_5\text{PW}\cdot\text{H}_2\text{O}$: C, 38.25; H, 4.75; N, 13.58. Found: C, 37.90; H, 4.67; N, 13.26. ^{31}P NMR (CD_3CN , δ): -11.40 ($J_{\text{WP}} = 284$). ^1H NMR (CD_3CN , δ): 8.04 (d, 1H, PzB3), 7.99 (d, 1H, PzA3), 7.86 (d, 1H, PzB5), 7.84 (d, 1H, PzC5), 7.77 (d, 1H, PzA5), 7.35 (d, 1H, PzC3), 6.48 (m, 1H, H2), 6.36 (t, 1H, PzB4), 6.32 (t, 1H, PzA4), 6.25 (t, 1H, PzC4), 4.84 (ddd, $J = 8.9, 6.6, 1.9$, 1H, H1), 3.72 (d, $J = 10.3$, 1H, H7), 3.66 (s, 3H, H9), 3.41 (s, 3H, H11), 3.28 (m, 1H, H5), 2.85 (ddd, $J = 14.2, 10.1, 5.1$, 1H, H3), 2.72 (dm, $J = 17.0$, 1H, H6x), 1.70 (dd, $J = 17.0, 6.6$, 1H, H6y), 1.20 (d, $J = 8.6$, 9H, PMe_3), 0.86 (d, $J = 10.1$, 1H, H4). ^{13}C NMR (CD_3CN , δ): 171.1 (C8), 170.8 (C10), 144.3 (PzB3), 142.9 (PzA3), 141.6 (PzC3), 137.9 (PzC5), 137.3 (PzB5), 137.0 (PzA5), 132.5 (C2), 116.4 (C1), 107.4 (PzB4), 107.1 (PzC4), 106.8 (PzA4), 60.5 (C7), 57.3 (C4), 52.7 (C9), 52.3 (C11), 49.9 (d, $J = 10.3$, C3), 38.6 (C5), 27.1 (C6), 13.7 (d, $J = 28.7$, PMe_3).



Compound 12. To a 4-dram vial charged with a stir pea were added **6A** (100 mg, 0.146 mmol) followed by DCM (0.4 mL, -30°C) and a 1M solution of HOTf in acetonitrile (0.29 mL, 0.29 mmol, -30°C), resulting in a homogeneous golden-orange solution, which was allowed to sit for 20 min at -30°C. The reaction solution was added to stirring Et₂O (20 mL), forming a precipitate, which oiled. The solution was decanted off, and the oil was redissolved in minimal DCM and added to Et₂O (20 mL). The resulting yellow solid was collected on a 15 mL fine porosity fritted disc, washed with Et₂O (2 x 5 mL) and pentane (5 mL), then desiccated overnight, yielding **12** (89 mg, 0.11 mmol, 75% yield). CV (MeCN) $E_{p,a} = +1.87$ V, $E_{p,c} = -0.94$ V (NHE). IR: $\nu(\text{BH}) = 2524$ cm⁻¹, $\nu(\text{CO}) = 1717$ cm⁻¹, $\nu(\text{NO}) = 1636$ cm⁻¹. Anal. Calc'd for 4C₂₄H₃₆BF₃N₇O₆PSW•CH₂Cl₂: C, 34.09; H, 4.31; N, 11.47. Found: C, 34.03; H, 4.22; N, 11.50. ³¹P NMR (CD₃CN, δ): -6.58 ($J_{\text{WP}} = 273$). ¹H NMR (CD₃CN, δ): 8.39 (d, 1H, PzB3), 8.05 (d, 1H, PzA3), 8.00 (d, 1H, PzC5), 7.95 (d, 1H, PzC3), 7.93 (d, 1H, PzB5), 7.79 (d, 1H, PzA5), 6.54 (t, 1H, PzC4), 6.51 (t, 1H, PzB4), 6.33 (t, 1H, PzA4), 6.31 (d, $J = 7.7$, 1H, H1), 5.14 (tm, $J = 7.4$, 1H, H2), 4.32 (m, 1H, H3), 3.74 (s, 3H, H9), 3.61 (m, 1H, H6), 3.14 (m, 1H, H4x), 2.37 (m, 1H, H4y), 1.55 (m, 1H, H5x), 1.32 (s, 6H, H10 & H11), 1.16 (d, $J = 9.9$, 9H, PMe₃), 1.07 (m, 1H, H5y). ¹³C NMR (CD₃CN, δ): 178.7 (C8), 149.0 (PzA3), 146.4 (PzB3), 143.1 (PzC3), 139.7 (Pz5), 139.6 (2C, Pz5 & C1), 139.4 (Pz5), 109.5 (PzB4), 109.1 (PzC4), 108.1 (PzA4), 104.4 (d, $J = 4.0$, C2), 68.7 (d, $J = 13.2$, C3), 52.9 (C9), 48.1 (C7), 43.6 (C6), 26.3 (d, $J = 3.7$, C4), 24.1 (C10/C11), 22.1 (C5), 21.0 (C10/C11), 13.2 (d, $J = 33.1$, PMe₃).

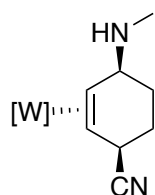


Compound 13. To a 4-dram vial charged with a stir pea were added **10A** (250 mg, 0.411 mmol) followed by DCM (0.7 mL, -30°C) and a 1M solution of HOTf in acetonitrile (0.62 mL, 0.62 mmol, -30°C), resulting in a homogeneous golden-orange solution, which was allowed to stir for 15 min at room temperature. The reaction solution was added drop wise to stirring Et₂O (40 mL, -30°C). The resulting yellow solid was collected on a 15 mL fine porosity fritted disc, washed with Et₂O (2 x 5 mL) and pentane (5 mL), then desiccated for 3 h, yielding **13** (288 mg, 0.380 mmol, 92% yield). ¹H NMR (CD₃CN, δ): 8.34 (d, 1H, PzB3), 8.04 (d, 1H, PzA3), 8.03 (d, 1H, PzB5/PzC5), 7.99 (d, 1H, PzB5/PzC5), 7.90 (d, 1H, PzC3), 7.86 (d, 1H, PzA5), 6.53 (t, 2H, PzB4 & PzC4), 6.38 (t, 1H, PzA4), 5.48 (m, 2H, H1 & H2), 5.08 (m, 1H, H3), 4.17 (m, 1H, H4), 3.23 (dm, *J* = 17.2, 1H, H6x), 2.56 (m, 1H, H6y), 1.98 (m, 1H, H5x), 1.62 (m, 1H, H5y), 1.15 (d, *J* = 9.9, 9H, PMe₃).



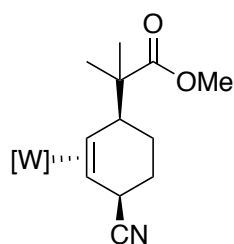
Compound 14. To a 4-dram vial charged with a stir pea were added **11A** (248 mg, 0.348 mmol) followed by DCM (0.7 mL, -30°C) and a 1M solution of HOTf in acetonitrile (0.52 mL, 0.52 mmol, -30°C), resulting in a homogeneous golden-orange solution, which was allowed to stir for 15 min at room temperature. The reaction solution was added drop wise to stirring Et₂O (40 mL, -30°C). The resulting yellow solid was collected on a 15 mL fine porosity fritted disc, washed with Et₂O (2 x 5 mL) and pentane (5 mL), then desiccated for

3 h, yielding **14** (270 mg, 0.313 mmol, 90% yield). $^1\text{H NMR}$ (CD_3CN , δ): 8.46 (d, 1H, Pz3/5), 8.41 (d, 1H, Pz3/5), 8.01 (d, 1H, Pz3/5), 7.95 (overlapping d, 2H, Pz3/5), 7.80 (d, 1H, Pz3/5), 6.54 (t, 1H, Pz4), 6.53 (t, 1H, Pz4), 6.36 (d, $J = 7.4$, 1H, H1), 6.33 (t, 1H, Pz4), 5.17 (t, $J = 7.4$, 1H, H2), 4.36 (m, 1H, H3), 3.90 (m, 1H, H6), 3.77 (s, 6H, H9 & H11), 3.76 (d, $J = 7.9$, 1H, H7), 3.10 (m, 1H, H4x), 2.38 (m, 1H, H4y), 1.58 (m, 1H, H5x), 1.16 (d, $J = 9.9$, 9H, PMe_3), 1.09 (m, 1H, H5y).



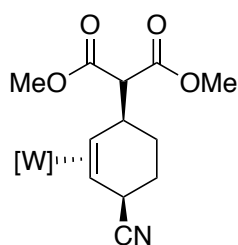
Compound 15A. To a 4-dram vial charged with a stir pea were added **10A** (40 mg, 0.066 mmol) followed by acetonitrile (0.7 mL, -30°C) and a 1M solution of HOTf in acetonitrile (0.14 mL, 0.14 mmol, -30°C), resulting in a homogeneous golden solution, which was allowed to sit for 15 min at -30°C . 2M $\text{H}_2\text{NMe}/\text{THF}$ (0.33 mL, 0.66 mmol, -30°C) was added to the reaction with stirring, and then the solution was allowed to sit at -30°C for 21 h. While the reaction was still cold, 1M tBuOK in *tert*-butanol (0.26 mL, 0.26 mmol) was added, and then the reaction was evaporated *in vacuo*. The film was redissolved in minimal THF and added to stirring pentane (15 mL, -30°C). The resulting pale solid was collected on a 15 mL fine porosity fritted disc, washed with H_2O (2 x 5 mL), pentane (3 x 4 mL) and desiccated overnight, yielding **15A** (25 mg, 0.039 mmol, 59% yield). CV (DMAc) $E_{\text{p,a}} = +0.54$ V (NHE). IR: $\nu(\text{BH}) = 2488 \text{ cm}^{-1}$, $\nu(\text{CN}) = 2229 \text{ cm}^{-1}$, $\nu(\text{NO}) = 1540 \text{ cm}^{-1}$. $^{31}\text{P NMR}$ (CD_3CN , δ): -9.50 ($J_{\text{WP}} = 286$). $^1\text{H NMR}$ (CD_3CN , δ): 8.10 (d, 1H, PzA3), 8.02 (d, 1H, PzB3), 7.87 (d, 1H, PzB5), 7.84 (d, 1H, PzC5), 7.80 (d, 1H, PzA5), 7.41 (d, 1H, PzC3), 6.37 (t, 1H, PzB4), 6.30 (t,

1H, PzA4), 6.26 (t, 1H, PzC4), 4.00 (m, 1H, H1), 3.56 (t, $J = 4.3$, 1H, H4), 2.43 (s, 3H, NMe), 2.24 (t, $J = 11.6$, 1H, H3), 1.86 (m, 1H, H6x), 1.79 (m, 2H, H5x & H6y), 1.64 (m, 1H, H5y), 1.15 (d, $J = 8.5$, 9H, PMe₃), 1.14 (buried, 1H, H2). ¹³C NMR (CD₃CN, δ): 144.4 (PzB3), 142.7 (PzA3), 141.8 (PzC3), 138.1 (PzC5), 137.6 (PzA5), 137.5 (PzB5), 128.0 (CN), 107.7 (PzB4), 107.2 (PzC4), 106.8 (PzA4), 59.9 (C4), 57.4 (d, $J = 11.0$, C3), 51.5 (C2), 34.4 (NMe), 31.9 (C1), 25.5 (C5), 24.3 (C6), 13.4 (d, $J = 28.6$, PMe₃).



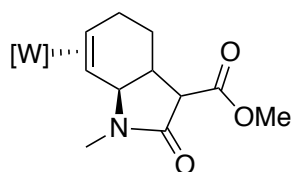
Compound 16A. To a 4-dram vial charged with a stir pea were added **10A** (30 mg, 0.049 mmol) followed by DCM (0.3 mL, -30°C) and a 1M solution of HOTf in acetonitrile (0.10 mL, 0.10 mmol, -30°C), resulting in a homogeneous golden solution, which was allowed to sit for 10 min at -30°C. Methyl trimethylsilyl dimethylketene acetal (104 mg, 0.597 mmol, -30°C) was added to the reaction vial with stirring and allowed to sit at -30°C for 16 h. The reaction was stirred at room temperature for 20 min, and then Et₃N (40 mg, 0.40 mmol) was added. The reaction solution was diluted with DCM (20 mL) and washed with H₂O (20 mL), and then the organic layer was dried over MgSO₄ and evaporated *in vacuo*. The film was redissolved in minimal THF and added to stirring pentane (10 mL, -30°C). The resulting pale solid was collected on a 15 mL fine porosity fritted disc, washed with pentane (3 x 3 mL, -30°C) and desiccated overnight, yielding **16A** (28 mg, 0.039 mmol, 80% yield). CV (DMAc) $E_{p,a} = +0.55$ V (NHE). IR: $\nu(\text{BH}) = 2488$ cm⁻¹, $\nu(\text{CN}) = 2227$ cm⁻¹, $\nu(\text{CO}) =$

1719 cm^{-1} , $\nu(\text{NO}) = 1548 \text{ cm}^{-1}$. ^{31}P NMR (CD_3CN , δ): -11.93 ($J_{\text{WP}} = 297$). ^1H NMR (CD_3CN , δ): 8.21 (d, 1H, PzA3), 8.08 (d, 1H, PzB3), 7.87 (overlapping d, 2H, PzB5 & PzC5), 7.79 (d, 1H, PzA5), 7.51 (d, 1H, PzC3), 6.37 (t, 1H, PzB4), 6.31 (overlapping t, 2H, PzA4 & PzC4), 4.49 (t, $J = 8.7$, 1H, H4), 3.68 (s, 3H, H9), 3.01 (m, 1H, H1), 2.46 (dd, $J = 11.2, 8.3$, 1H, H2), 1.91 (m, 1H, H5x), 1.84 (m, 1H, H6x), 1.81 (m, 1H, H5y), 1.61 (m, 1H, H6y), 1.53 (s, 3H, H10), 1.51 (s, 3H, H11), 1.47 (dt, $J = 11.2, 2.4$, 1H, H3), 1.12 (d, $J = 8.6$, 9H, PMe_3). ^{13}C NMR (CD_3CN , δ): 179.8 (C8), 144.8 (PzB3), 142.7 (PzC3), 142.4 (PzA3), 138.4 (PzC5), 137.7 (PzA5/PzB5), 137.5 (PzA5/PzB5), 128.5 (CN), 107.5 (Pz4), 107.1 (Pz4), 106.8 (Pz4), 55.1 (d, $J = 11.0$, C2), 52.3 (C9), 51.7 (C7), 50.9 (C3), 44.7 (C1), 29.4 (C4), 26.9 (C10), 25.1 (C11), 23.9 (C5), 22.7 (C6), 13.7 (d, $J = 28.7$, PMe_3).



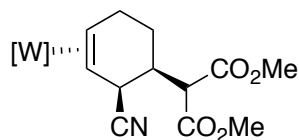
Compound 18A. To a 4-dram vial charged with a stir pea were added **10A** (50 mg, 0.082 mmol) followed by acetonitrile (1 mL, -30°C) and a 1M solution of HOTf in acetonitrile (0.17 mL, 0.17 mmol, -30°C), resulting in a homogeneous golden solution, which was allowed to sit for 20 min at -30°C . LiDMM (68 mg, 0.49 mmol) was added to the reaction vial with stirring, and the reaction was allowed to sit at -30°C for 17 h. The reaction was then diluted with Et_2O (20 mL) and washed with H_2O (20 mL). The organic layer was dried over MgSO_4 and evaporated *in vacuo*. The film was redissolved in minimal THF and added to stirring pentane (20 mL, -30°C). The resulting pale solid was collected on a 15 mL fine

porosity fritted disc, washed with pentane (2 x 3 mL, -30°C) and desiccated overnight, yielding **18A** (49 mg, 0.066 mmol, 80% yield). CV (DMAc) $E_{p,a} = +0.64$ V (NHE). IR: $\nu(\text{BH}) = 2489$ cm^{-1} , $\nu(\text{CN}) = 2229$ cm^{-1} , $\nu(\text{CO}) = 1748$ & 1728 cm^{-1} , $\nu(\text{NO}) = 1547$ cm^{-1} . Anal. Calc'd for $7\text{C}_{24}\text{H}_{34}\text{BN}_8\text{O}_5\text{PW}\cdot\text{pentane}$: C, 39.55; H, 4.80; N, 14.93. Found: C, 39.47; H, 4.62; N, 14.70. ^{31}P NMR (CD_3CN , δ): -11.39 ($J_{\text{WP}} = 288$). ^1H NMR (CD_3CN , δ): 8.11 (d, 1H, PzA3), 8.06 (d, 1H, PzB3), 7.86 (d, 1H, PzB5), 7.85 (d, 1H, PzC5), 7.79 (d, 1H, PzA5), 7.27 (d, 1H, PzC3), 6.37 (t, 1H, PzB4), 6.30 (t, 1H, PzA4), 6.29 (t, 1H, PzC4), 4.25 (m, 1H, H4), 4.00 (d, $J = 8.5$, 1H, H7), 3.76 (overlapping s, 6H, H9 & H11), 3.53 (dm, $J = 8.5$, 1H, H1), 2.24 (t, $J = 10.6$, 1H, H2), 1.88 (m, 2H, H5x & H6x), 1.77 (m, 1H, H5y), 1.59 (m, 1H, H6y), 1.24 (dt, $J = 11.3, 2.5$, 1H, H3), 1.17 (d, $J = 8.5$, 9H, PMe_3). ^{13}C NMR (CD_3CN , δ): 171.0 (C8/C10), 170.6 (C8/C10), 144.8 (PzB3), 142.7 (PzA3), 142.0 (PzC3), 138.3 (PzC5), 137.7 (PzA5/PzB5), 137.6 (PzA5/PzB5), 128.1 (CN), 107.6 (PzB4), 107.3 (PzC4), 106.9 (PzA4), 61.5 (C7), 54.0 (d, $J = 11.7$, C2), 53.1 (C9/C11), 53.0 (C9/C11), 50.2 (C3), 39.0 (C1), 30.2 (C4), 23.9 (C5/C6), 23.8 (C5/C6), 13.8 (d, $J = 28.6$, PMe_3).



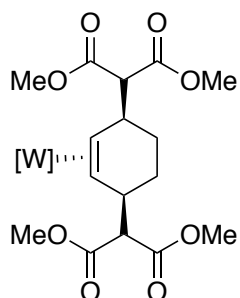
Compound 20B. To a 4-dram vial charged with a stir pea were added **11A** (74 mg, 0.10 mmol) followed by acetonitrile (1 mL, -30°C) and a 1M solution of HOTf in acetonitrile (0.21 mL, 0.21 mmol, -30°C), resulting in a homogeneous golden solution, which was allowed to sit for 10 min at -30°C. 2M $\text{H}_2\text{NMe}/\text{THF}$ (0.8 mL, 0.16 mmol, -30°C) was added to the reaction vial with stirring and allowed to sit at -30°C for 20 h. The reaction was then

allowed to warm to room temperature for 20 min, and then the reaction was diluted with DCM (30 mL) and washed with H₂O (30 mL). The aqueous layer was back extracted with DCM (30 mL), and then the combined organic layers were dried over MgSO₄ and evaporated *in vacuo*. The film was redissolved in minimal THF and added to stirring pentane (15 mL, -30°C). The resulting pale solid was collected on a 15 mL fine porosity fritted disc, washed with pentane (3 x 4 mL, -30°C) and desiccated overnight, yielding **20B** (53 mg, 0.074 mmol, 74% yield). CV (DMAc) $E_{p,a} = +0.51$ V (NHE). IR: $\nu(\text{BH}) = 2487$ cm⁻¹, $\nu(\text{CO}) = 1733$ & 1678 cm⁻¹, $\nu(\text{NO}) = 1539$ cm⁻¹. Anal. Calc'd for 4C₂₃H₃₄BN₈O₄PW•pentane: C, 39.89; H, 5.11; N, 15.35. Found: C, 39.90; H, 4.92; N, 15.39. ³¹P NMR (CD₃CN, δ): -8.70 ($J_{\text{WP}} = 290$). ¹H NMR (CD₃CN, δ): 8.22 (d, 1H, PzA3), 8.05 (d, 1H, PzB3), 7.86 (d, 1H, PzB5), 7.84 (d, 1H, PzC5), 7.82 (d, 1H, PzA5), 7.42 (d, 1H, PzC3), 6.37 (t, 1H, PzB4), 6.31 (t, 1H, PzA4), 6.26 (t, 1H, PzC4), 4.90 (d, $J = 7.1$, 1H, H7a), 3.71 (s, 3H, OMe), 3.44 (m, 1H, H5x), 3.40 (d, $J = 7.8$, 1H, H3), 2.76 (m, 1H, H3a), 2.66 (m, 1H, H6), 2.57 (m, 1H, H5y), 2.48 (s, 3H, NMe), 1.97 (m, 1H, H4x), 1.38 (dq, $J = 13.7, 5.5$, 1H, H4y), 1.13 (d, $J = 8.4$, 9H, PMe₃), 1.01 (dd, $J = 11.3, 1.6$, 1H, H7). ¹³C NMR (CD₃CN, δ): 172.3 (C2), 170.4 (COOMe), 144.3 (PzB3), 142.9 (PzA3), 142.0 (PzC3), 138.0 (PzC5), 137.8 (PzA5), 137.3 (PzB5), 107.5 (PzB4), 107.2 (PzC4), 106.7 (PzA4), 62.0 (C7a), 53.3 (C3), 52.8 (OMe), 51.5 (d, $J = 11.8$, C6), 49.5 (C7), 37.7 (C3a), 27.8 (NMe), 26.6 (C5), 24.0 (C4), 13.4 (d, $J = 28.7$, PMe₃).



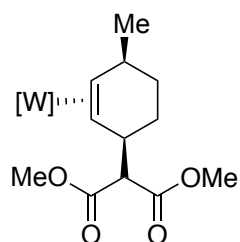
Compound 22B. To a 4-dram vial charged with a stir pea were added **11A** (50 mg, 0.070 mmol) followed by acetonitrile (1 mL, -30°C) and a 1M solution of HOTf in acetonitrile

(0.11 mL, 0.11 mmol, -30°C), resulting in a homogeneous golden solution, which was allowed to sit for 20 min at -30°C. NaCN (21 mg, 0.43 mmol) and MeOH (1 mL, -30°C) were added to a separate 4-dram vial and cooled to -30°C for 20 min. The NaCN/MeOH solution was then added to the reaction vial with stirring, and it was allowed to sit at -30°C for 16 h. The reaction was then diluted with Et₂O (20 mL) and washed with H₂O (20 mL). The aqueous layer was back extracted with Et₂O (20 mL), and then the combined organic layers were dried over MgSO₄ and evaporated *in vacuo*. The film was redissolved in minimal THF and added to stirring pentane (15 mL, -30°C). The resulting pale solid was collected on a 15 mL fine porosity fritted disc, washed with pentane (2 x 3 mL, -30°C) and desiccated overnight, yielding **22B** (38 mg, 0.051 mmol, 73% yield). CV (DMAc) $E_{p,a} = +0.62$ V (NHE). IR: $\nu(\text{BH}) = 2488$ cm⁻¹, $\nu(\text{CN}) = 2220$ cm⁻¹, $\nu(\text{CO}) = 1750$ & 1731 cm⁻¹, $\nu(\text{NO}) = 1549$ cm⁻¹. Anal. Calc'd for 3C₂₄H₃₄BN₈O₅PW•THF: C, 39.81; H, 4.84; N, 14.66. Found: C, 39.39; H, 4.75; N, 14.23. ³¹P NMR (CD₃CN, δ): -10.55 ($J_{\text{WP}} = 285$). ¹H NMR (CD₃CN, δ): 8.02 (d, 1H, PzB3), 8.00 (d, 1H, PzA3), 7.86 (d, 1H, PzB5), 7.82 (overlapping d, 2H, PzA5 & PzC5), 7.32 (d, 1H, PzC3), 6.37 (t, 1H, PzB4), 6.34 (t, 1H, PzA4), 6.27 (t, 1H, PzC4), 3.93 (bs, 1H, H2), 3.77 (s, 3H, H9), 3.71 (s, 3H, H11), 3.47 (d, $J = 11.3$, 1H, H7), 2.94 (m, 1H, H5x), 2.80 (m, 3H, H1, H4 & H5y), 1.44 (m, 1H, H6x), 1.41 (m, 1H, H6y), 1.20 (d, $J = 8.5$, 9H, PMe₃), 1.02 (d, $J = 10.9$, 1H, H3). ¹³C NMR (CD₃CN, δ): 169.6 (2C, C8 & C10), 144.4 (PzB3), 143.7 (PzA3), 141.5 (PzC3), 137.7 (Pz5), 137.6 (2C, Pz5), 126.4 (C12), 107.6 (Pz4), 107.4 (2C, Pz4), 57.5 (C7), 55.6 (C3), 53.4 (C9), 53.2 (C11), 45.5 (d, $J = 11.8$, C4), 35.4 (C2), 35.0 (C1), 28.1 (C5), 26.6 (C6), 13.9 (d, $J = 28.7$, PMe₃).



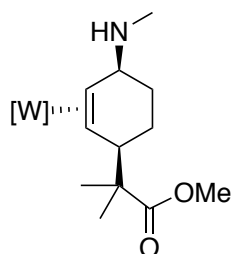
Compound 23A. To a 4-dram vial charged with a stir pea were added **14** (123 mg, 0.142 mmol) followed by acetonitrile (1 mL, -30°C) and a 1M solution of HOTf in acetonitrile (0.14 mL, 0.14 mmol, -30°C), resulting in a homogeneous golden solution. LiDMM (100 mg, 0.724 mmol) was added to the reaction vial with stirring, and the reaction was allowed to sit at -30°C for 3 h. The reaction was then stirred at room temperature for 22 h and completion of the reaction was confirmed by ³¹P NMR. The reaction was diluted with Et₂O (30 mL) and washed with H₂O (30 mL). The aqueous layer was back extracted with Et₂O (30 mL), and then the combined organic layers were dried over MgSO₄ and evaporated *in vacuo*. The film was redissolved in minimal THF and added to stirring pentane (15 mL, -30°C). The resulting pale solid was collected on a 15 mL fine porosity fritted disc, washed with pentane (1 x 4 mL, -30°C) and desiccated overnight, yielding **23A** (85 mg, 0.10 mmol, 70% yield). CV (DMAc) $E_{p,a} = +0.43$ V (NHE). IR: $\nu(\text{BH}) = 2487$ cm⁻¹, $\nu(\text{CO}) = 1749$ & 1729 cm⁻¹, $\nu(\text{NO}) = 1549$ cm⁻¹. Anal. Calc'd for C₂₈H₄₁BN₇O₉PW: C, 39.79; H, 4.89; N, 11.60. Found: C, 39.53; H, 4.75; N, 11.32. ³¹P NMR (CD₃CN, δ): -11.35 ($J_{\text{WP}} = 292$). ¹H NMR (CD₃CN, δ): 8.11 (d, 1H, PzA3), 8.05 (d, 1H, PzB3), 7.85 (d, 1H, PzC5), 7.82 (d, 1H, PzB5), 7.79 (d, 1H, PzA5), 7.23 (d, 1H, PzC3), 6.34 (t, 1H, PzB4), 6.28 (t, 2H, PzA4 & PzC4), 4.14 (d, $J = 9.5$, 1H, H7), 4.01 (m, 1H, H4), 3.75 (s, 3H, H9), 3.74 (s, 3H, H11), 3.62 (s, 3H, H14), 3.59 (s, 3H, H16), 3.47 (d, $J = 5.8$, 1H, H12), 3.42 (m, 1H, H1), 2.25 (t, $J = 10.6$, 1H, H2), 1.92 (m, 1H,

H6x), 1.85 (m, 1H, H5x), 1.47 (m, 2H, H5y & H6y), 1.18 (d, $J = 8.4$, 9H, PMe_3), 0.85 (dt, $J = 11.3$, 2.1, 1H, H3). ^{13}C NMR (CD_3CN , δ): 171.3 (C8), 170.8 (C10), 170.4 (C15), 170.3 (C13), 144.7 (PzB3), 141.9 (2C, PzA3 & PzC3), 138.2 (PzC5), 137.8 (PzA5), 137.3 (PzB5), 107.3 (PzB4), 107.2 (PzC4), 106.8 (PzA4), 61.5 (C7), 60.9 (C12), 56.5 (d, $J = 11.0$, C2), 52.9 (C9), 52.8 (C11), 52.7 (C16), 52.5 (C14), 52.1 (C3), 40.0 (C1), 39.1 (C4), 23.3 (C6), 20.7 (C5), 13.9 (d, $J = 27.9$, PMe_3).



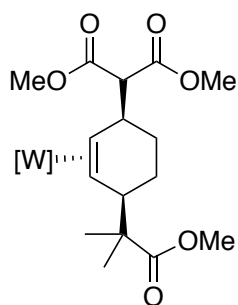
Compound 24A. To a 4-dram vial charged with a stir pea were added **14** (50 mg, 0.058 mmol) followed by THF (0.5 mL, -30°C). A 3M $\text{MeMgBr}/\text{Et}_2\text{O}$ solution (0.11 mL, 0.33 mmol, -30°C) was added dropwise to the reaction vial with stirring. The reaction was allowed to sit at -30°C for 12 h, then quenched with saturated aqueous NH_4Cl , diluted with H_2O (30 mL) and extracted with Et_2O (2 x 30 mL). The combined organic layers were washing with H_2O (20 mL), then dried over MgSO_4 and evaporated *in vacuo*. The film was redissolved in minimal THF and added to stirring pentane (10 mL, -30°C). The resulting pale solid was collected on a 15 mL fine porosity fritted disc, washed with pentane (2 x 2 mL, -30°C) and desiccated overnight, yielding **24A** (23 mg, 0.032 mmol, 55% yield). CV (DMAc) $E_{p,a} = +0.39$ V (NHE). IR: $\nu(\text{BH}) = 2484\text{ cm}^{-1}$, $\nu(\text{CO}) = 1752$ & 1727 cm^{-1} , $\nu(\text{NO}) = 1536\text{ cm}^{-1}$. ^{31}P NMR (CD_3CN , δ): -8.41 ($J_{\text{WP}} = 292$). ^1H NMR (CD_3CN , δ): 8.10 (d, 1H, PzA3), 8.00 (d, 1H, PzB3), 7.83 (overlapping d, 2H, PzB5 & PzC5), 7.81 (d, 1H, PzA5), 7.37 (d, 1H, PzC3), 6.34 (t, 1H,

PzB4), 6.28 (t, 1H, PzA4), 6.25 (t, 1H, PzC4), 3.73 (m, 1H, H1), 3.56 (s, 3H, OMe), 3.55 (s, 3H, OMe), 3.31 (d, $J = 5.4$, 1H, H1'), 2.92 (m, 1H, H4), 2.41 (t, $J = 12.1$, 1H, H3), 1.96 (m, 1H, H5x), 1.76 (m, 1H, H6x), 1.48 (m, 1H, H6y), 1.41 (d, $J = 6.9$, 3H, Me), 1.31 (m, 1H, H5y), 1.13 (d, $J = 8.3$, 9H, PMe₃), 0.82 (dm, $J = 11.5$, 1H, H2). ¹³C NMR (CD₃CN, δ): 170.7 (CO), 170.1 (CO), 144.1 (PzB3), 142.1 (PzA3), 141.6 (PzC3), 137.8 (Pz5), 137.7 (Pz5), 137.1 (Pz5), 107.4 (PzB4), 107.1 (PzC4), 106.7 (PzA4), 60.8 (d, $J = 10.3$, C3), 60.7 (C1'), 53.9 (C2), 52.6 (OMe), 52.2 (OMe), 41.0 (C1), 34.3 (C4), 29.3 (C5), 28.2 (Me), 22.1 (C6), 13.6 (d, $J = 27.9$, PMe₃).



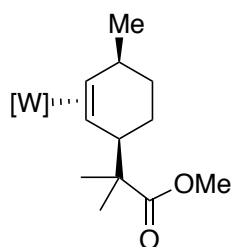
Compound 25A. To a 4-dram vial charged with a stir pea were added **6A** (50 mg, 0.073 mmol) followed by acetonitrile (0.8 mL, -30°C) and a 1M solution of HOTf in acetonitrile (0.15 mL, 0.15 mmol, -30°C), resulting in a homogeneous golden solution, which was allowed to sit for 20 min at -30°C. 2M H₂NMe/THF (0.55 mL, 1.1 mmol, -30°C) was added to the reaction with stirring, and then the solution was allowed to sit at -30°C for 21 h. While the reaction was still cold, 1M tBuOK in *tert*-butanol (0.25 mL, 0.25 mmol) was added, and then the reaction was evaporated *in vacuo*. The film was redissolved in minimal THF then added to stirring pentane (20 mL). The resulting pale solid was collected on a 15 mL fine porosity fritted disc, washed with H₂O (2 x 3 mL), pentane (3 x 3 mL) and desiccated overnight, yielding **25A** (37 mg, 0.052 mmol, 71% yield). CV (DMAc) $E_{p,a} = +0.29$ V (NHE). IR: $\nu(\text{BH}) = 2483$ cm⁻¹, $\nu(\text{CO}) = 1719$ cm⁻¹, $\nu(\text{NO}) = 1537$ cm⁻¹. ³¹P NMR (CD₃CN, δ): -9.39

($J_{WP} = 286$). $^1\text{H NMR}$ (CD_3CN , δ): 8.00 (d, 1H, PzA3), 7.96 (d, 1H, PzB3), 7.83 (d, 1H, PzC5), 7.79 (overlapping d, 2H, PzA5 & PzB5), 7.40 (d, 1H, PzC3), 6.31 (t, 1H, PzB4), 6.27 (t, 1H, PzC4), 6.26 (t, 1H, PzA4), 3.45 (m, 4H, H4 & H9), 3.18 (m, 1H, H1), 2.58 (dd, $J = 14.3, 12.0$, 1H, H3), 2.41 (s, 3H, NMe), 1.84 (tt, $J = 13.7, 3.3$, 1H, H5x), 1.57 (dm, $J = 13.7$, 1H, H5y), 1.49 (m, 1H, H6x), 1.18 (d, $J = 8.3$, 9H, PMe_3), 1.16 (buried, 1H, H6y), 0.88 (s, 3H, H10), 0.79 (dt, $J = 11.8, 1.5$, 1H, H2), 0.63 (s, 3H, H11). $^{13}\text{C NMR}$ (CD_3CN , δ): 179.5 (C8), 143.8 (PzB3), 143.5 (PzA3), 141.3 (PzC3), 137.9 (PzA5), 137.5 (PzC5), 137.0 (PzB5), 107.1 (2C, PzB4 & PzC4), 106.6 (PzA4), 60.3 (C4), 59.5 (d, $J = 10.3$, C3), 52.9 (C2), 51.7 (C9), 49.8 (C7), 44.0 (C1), 34.6 (NMe), 24.0 (C11), 22.6 (C5), 20.6 (C10), 20.3 (C6), 13.4 (d, $J = 27.9$, PMe_3).



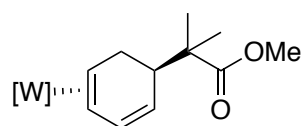
Compound 28A. To a 4-dram vial charged with a stir pea was added **6A** (50 mg, 0.073 mmol) followed by acetonitrile (0.8 mL) and a 1M solution of HOTf in acetonitrile (0.15 mL, 0.15 mmol), resulting in a homogeneous golden solution, which was allowed to stir for 5 min. LiDMM (60 mg, 0.43 mmol) was added to the reaction vial, and the solution was stirred for 30 min. The reaction solution was diluted with DCM (20 mL) and washed with H_2O (20 mL). The aqueous layer was back extracted with DCM (20 mL), and then the combined organic layers were dried over MgSO_4 and evaporated *in vacuo*. The film was redissolved in minimal DCM and added to stirring pentane (10 mL, -30°C). The resulting

pale solid was collected on a 15 mL fine porosity fritted disc, washed with pentane (2 x 3 mL, -30°C) and desiccated overnight, yielding **28A** (37 mg, 0.045 mmol, 62% yield). CV (DMAc) $E_{p,a} = +0.34$ V (NHE). IR: $\nu(\text{BH}) = 2484$ cm^{-1} , $\nu(\text{CO}) = 1751$ & 1723 cm^{-1} , $\nu(\text{NO}) = 1541$ cm^{-1} . Anal. Calc'd for $\text{C}_{28}\text{H}_{43}\text{BN}_7\text{O}_7\text{PW}\cdot\text{H}_2\text{O}$: C, 40.36; H, 5.44; N, 11.77. Found: C, 40.25; H, 5.15; N, 11.45. ^{31}P NMR (CD_3CN , δ): -11.80 ($J_{\text{WP}} = 287$). ^1H NMR (CD_3CN , δ): 8.01 (d, 1H, PzA3), 7.97 (d, 1H, PzB3), 7.85 (d, 1H, PzC5), 7.79 (d, 1H, PzA5), 7.77 (d, 1H, PzB5), 7.25 (d, 1H, PzC3), 6.31 (t, 1H, PzC4), 6.28 (t, 1H, PzB4), 6.25 (t, 1H, PzA4), 3.91 (d, $J = 10.3$, 1H, H7), 3.78 (s, 3H, H9), 3.71 (s, 3H, H11), 3.49 (s, 3H, H14), 3.42 (m, 1H, H4), 3.38 (dm, $J = 10.3$, 1H, H1), 2.46 (t, $J = 11.7$, 1H, H2), 2.18 (tt, $J = 14.2$, 4.0, 1H, H6x), 1.38 (m, 1H, H5x), 1.29 (m, 1H, H5y), 1.22 (m, 1H, H6y), 1.17 (d, $J = 8.3$, 9H, PMe_3), 0.90 (buried, 1H, H3), 0.89 (s, 3H, H15), 0.71 (s, 3H, H16). ^{13}C NMR (CD_3CN , δ): 179.1 (C13), 171.3 (C9), 170.7 (C11), 144.3 (PzB3), 143.5 (PzA3), 141.5 (PzC3), 138.4 (PzA5), 137.8 (PzC5), 137.2 (PzB5), 107.3 (PzC4), 107.0 (PzB4), 106.6 (PzA4), 61.8 (C7), 55.9 (d, $J = 10.3$, C2), 52.9 (2C, C9 & C11), 51.9 (C14), 51.0 (C3), 50.1 (C12), 42.2 (C4), 39.9 (C1), 24.0 (C16), 23.2 (C6), 20.8 (C15), 20.2 (C5), 13.7 (d, $J = 27.9$, PMe_3).



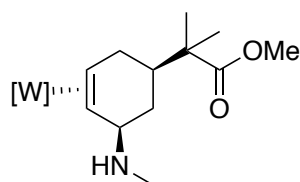
Compound 29A. To a 4-dram vial charged with a stir pea were added **12** (35 mg, 0.042 mmol) followed by THF (1 mL, -30°C), and then a 3M $\text{MeMgBr}/\text{Et}_2\text{O}$ solution (0.07 mL, 0.21 mmol, -30°C) was added dropwise to the reaction vial with stirring. The reaction was

allowed to sit at -30°C for 21 h, then quenched with saturated aqueous NH_4Cl (5 mL), diluted with H_2O (20 mL) and extracted with Et_2O (2 x 20 mL). The combined organic layers were dried over MgSO_4 and evaporated *in vacuo*. The film was redissolved in minimal THF and added to stirring pentane (10 mL, -30°C). The resulting pale solid was collected on a 15 mL fine porosity fritted disc, washed with pentane (3 x 3 mL, -30°C) and desiccated overnight, yielding **29A** (16 mg, 0.023 mmol, 54% yield). CV (DMAc) $E_{\text{p,a}} = +0.28$ V (NHE). IR: $\nu(\text{BH}) = 2480\text{ cm}^{-1}$, $\nu(\text{CO}) = 1719\text{ cm}^{-1}$, $\nu(\text{NO}) = 1541\text{ cm}^{-1}$. ^{31}P NMR (CD_3CN , δ): -8.24 ($J_{\text{WP}} = 283$). ^1H NMR (CD_3CN , δ): 8.01 (d, 1H, PzA3), 7.95 (d, 1H, PzB3), 7.83 (d, 1H, PzC5), 7.79 (d, 1H, PzA5), 7.78 (d, 1H, PzB5), 7.40 (d, 1H, PzC3), 6.30 (t, 1H, PzB4), 6.27 (t, 1H, PzC4), 6.26 (t, 1H, PzA4), 3.47 (s, 3H, H10), 3.22 (m, 1H, H1), 2.85 (m, 1H, H4), 2.69 (dd, $J = 14.8, 11.7$, 1H, H3), 2.13 (m, 1H, H5x), 1.44 (m, 1H, H6x), 1.37 (d, $J = 7.0$, 3H, H7), 1.21 (m, 1H, H6y), 1.19 (m, 1H, H5y), 1.16 (d, $J = 8.1$, 9H, PMe_3), 0.88 (s, 3H, H11), 0.81 (dt, $J = 11.7, 1.5$, 1H, H2), 0.62 (s, 3H, H12). ^{13}C NMR (CD_3CN , δ): 179.4 (C9), 143.8 (PzB3), 143.5 (PzA3), 141.3 (PzC3), 138.0 (PzA5), 137.4 (PzC5), 137.0 (PzB5), 107.1 (2C, PzB4 & PzC4), 106.6 (PzA4), 61.0 (d, $J = 10.0$, C3), 52.9 (C2), 51.7 (C10), 49.8 (C8), 43.7 (C1), 34.1 (C4), 27.6 (2C, C5 & C7), 23.8 (C12), 20.7 (C6), 20.4 (C11), 13.6 (d, $J = 27.9$, PMe_3).



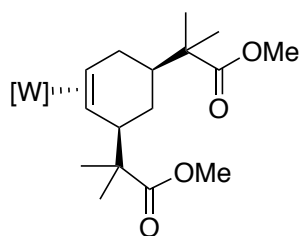
Compound 30. To a 4-dram vial charged with a stir pea were added **6A** (200 mg, 0.293 mmol), $[\text{Fe}(\text{Cp}^*)_2]\text{Tf}_2\text{N}$ (18 mg, 0.030 mmol) and acetonitrile (2 mL), which resulted in a homogeneous pale green solution. After stirring 1 min, precipitate started to form, and the

mixture was stirred for 3 h. The pale yellow solid was collected on a 15 mL fine porosity fritted disc, washed with acetonitrile (1 x 0.4 mL, -30°C), and pentane (2 x 4 mL, -30°C), then desiccated overnight, yielding **30** (175 mg, 0.256 mmol, 87% yield). CV (DMAc) $E_{p,a} = +0.48$ V (NHE). IR: $\nu(\text{BH}) = 2485$ cm^{-1} , $\nu(\text{CO}) = 1721$ cm^{-1} , $\nu(\text{NO}) = 1548$ cm^{-1} . Anal. Calc'd for $4\text{C}_{23}\text{H}_{35}\text{BN}_7\text{O}_3\text{PW}\cdot\text{CH}_2\text{Cl}_2$: C, 39.64; H, 5.08; N, 13.92. Found: C, 39.66; H, 5.09; N, 14.03. ^{31}P NMR (d^6 -acetone, δ): -9.45 ($J_{\text{WP}} = 293$). ^1H NMR (d^6 -acetone, δ): 8.15 (d, 1H, PzA3), 8.06 (d, 1H, PzB3), 7.86 (d, 1H, PzB5), 7.82 (d, 1H, PzC5), 7.72 (d, 1H, PzA5), 7.46 (d, 1H, PzC3), 6.69 (ddd, $J = 9.8, 5.6, 2.9$, 1H, H2), 6.37 (t, 1H, PzB4), 6.26 (t, 1H, PzA4), 6.24 (t, 1H, PzC4), 4.90 (d, $J = 9.8$, 1H, H1), 3.63 (s, 3H, H9), 3.34 (td, $J = 13.2, 4.8$, 1H, H5x), 2.81 (m, 1H, H6), 2.64 (m, 1H, H4), 2.45 (dd, $J = 13.2, 6.6$, 1H, H5y), 1.48 (dd, $J = 10.0, 5.6$, 1H, H3), 1.22 (s, 3H, H10), 1.21 (d, $J = 8.4$, 9H, PMe_3), 1.11 (s, 3H, H11). ^{13}C NMR (d^6 -acetone, δ): 178.7 (C8), 145.0 (PzA3), 144.4 (PzB3), 141.6 (PzC3), 137.6 (PzC5), 136.8 (PzB5), 136.0 (PzA5), 135.8 (C2), 117.9 (C1), 107.1 (PzB4), 106.6 (PzC4), 106.3 (PzA4), 55.3 (d, $J = 12.5$, C4), 51.6 (C9), 50.5 (C3), 45.6 (C7), 41.1 (C6), 32.7 (C5), 24.8 (C10), 21.3 (C11), 13.2 (d, $J = 28.0$, PMe_3).



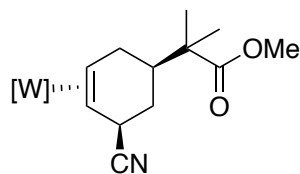
Compound 31A. To a 4-dram vial charged with a stir pea were added **30** (60 mg, 0.088 mmol) followed by acetonitrile (0.7 mL, -30°C) and a 1M solution of HOTf in acetonitrile (0.14 mL, 0.14 mmol, -30°C), resulting in a homogeneous golden solution, which was allowed to sit for 15 min at -30°C. 2M $\text{H}_2\text{NMe}/\text{THF}$ (0.45 mL, 0.90 mmol, -30°C) was added to the reaction with stirring, and then the solution was allowed to sit at -30°C for 6 h. While

the reaction was still cold, 1M tBuOK in *tert*-butanol (0.35 mL, 0.35 mmol) was added, and then the reaction was evaporated *in vacuo*. The film was redissolved in minimal Et₂O then added to stirring pentane (10 mL). The resulting pale solid was collected on a 15 mL fine porosity fritted disc, washed with pentane (2 x 3 mL) and desiccated overnight, yielding **31A** (35 mg, 0.049 mmol, 56% yield). CV (DMAc) $E_{p,a} = +0.32$ V (NHE). IR: $\nu(\text{BH}) = 2482$ cm⁻¹, $\nu(\text{CO}) = 1720$ cm⁻¹, $\nu(\text{NO}) = 1535$ cm⁻¹. ³¹P NMR (CD₃CN, δ): -7.86 ($J_{\text{WP}} = 294$). ¹H NMR (CD₃CN, δ): 8.20 (d, 1H, PzA3), 8.04 (d, 1H, PzB3), 7.85 (d, 1H, PzB5), 7.80 (d, 1H, PzC5), 7.75 (d, 1H, PzA5), 7.37 (d, 1H, PzC3), 6.37 (t, 1H, PzB4), 6.25 (t, 1H, PzA4), 6.22 (t, 1H, PzC4), 3.87 (m, 1H, H5), 3.61 (s, 3H, H9), 3.30 (m, 1H, H2x), 2.71 (m, 1H, H3), 2.62 (dd, $J = 13.5, 4.6$, 1H, H2y), 2.38 (d, $J = 6.5$, 3H, NMe), 2.12 (tdd, $J = 12.3, 4.6, 2.0$, 1H, H1), 2.00 (dm, $J = 11.3$, 1H, H6x), 1.18 (s, 3H, H10), 1.13 (s, 3H, H11), 1.12 (d, $J = 8.2$, 9H, PMe₃), 0.85 (dt, $J = 11.5, 2.4$, 1H, H4), 0.64 (m, 1H, H6y). ¹³C NMR (CD₃CN, δ): 179.3 (C8), 144.1 (PzB3), 142.9 (PzA3), 141.6 (PzC3), 137.8 (PzC5), 137.1 (PzA5/PzB5), 136.9 (PzA5/PzB5), 107.4 (PzB4), 106.9 (PzC4), 106.4 (PzA4), 64.2 (C5), 59.3 (C4), 54.3 (d, $J = 11.0$, C3), 51.9 (C9), 46.3 (C7), 40.4 (C1), 35.2 (C6), 33.8 (2C, C2 & NMe), 23.4 (C10), 22.3 (C11), 13.4 (d, $J = 28.3$, PMe₃).



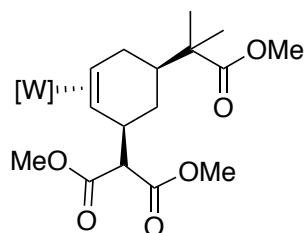
Compound 32A. To a 4-dram vial charged with a stir pea were added **30H** (50 mg, 0.060 mmol) followed by DCM (0.4 mL, -30°C), and then methyl trimethylsilyl dimethylketene acetal (107 mg, 0.614 mmol, -30°C) was added to the reaction vial with stirring. The

reaction was stirred at room temperature for 15 min, and then Et₃N (30 mg, 0.30 mmol) was added. The reaction solution was diluted with DCM (20 mL) and washed with H₂O (20 mL). The aqueous layer was back extracted with DCM (20 mL), and then the combined organic layers were dried over MgSO₄ and evaporated *in vacuo*. The film was redissolved in minimal DCM and added to stirring pentane (10 mL, -30°C). The resulting pale solid was collected on a 15 mL fine porosity fritted disc, washed with pentane (3 x 3 mL, -30°C) and desiccated overnight, yielding **32A** (41 mg, 0.052 mmol, 87% yield). CV (DMAc) $E_{p,a} = +0.28$ V (NHE). IR: $\nu(\text{BH}) = 2483 \text{ cm}^{-1}$, $\nu(\text{CO}) = 1721 \text{ cm}^{-1}$, $\nu(\text{NO}) = 1544 \text{ cm}^{-1}$. Anal. Calc'd for C₂₈H₄₅BN₇O₅PW•CH₂Cl₂: C, 40.02; H, 5.44; N, 11.27. Found: C, 40.31; H, 5.45; N, 11.03. ³¹P NMR (CD₃CN, δ): -8.60 ($J_{\text{WP}} = 289$). ¹H NMR (CD₃CN, δ): 8.02 (d, 1H, PzA3), 7.96 (d, 1H, PzB3), 7.83 (d, 1H, PzC5), 7.79 (overlapping d, 2H, PzA5 & PzB5), 7.36 (d, 1H, PzC3), 6.30 (t, 1H, PzB4), 6.26 (overlapping t, 2H, PzA4 & PzC4), 3.59 (s, 3H, H14), 3.48 (s, 3H, H9), 3.24 (dd, $J = 11.3, 6.0$, 1H, H1), 3.15 (td, $J = 12.7, 6.0$, 1H, H4x), 3.03 (ddd, $J = 15.5, 11.7, 5.9$, 1H, H3), 2.66 (dm, $J = 13.2$, 1H, H4y), 2.28 (tdd, $J = 12.4, 3.5, 2.2$, 1H, H5), 1.29 (m, 1H, H6x), 1.18 (d, $J = 8.2$, 9H, PMe₃), 1.12 (s, 6H, H15 & H16), 0.92 (m, 1H, H6y), 0.86 (s, 3H, H11), 0.82 (dt, $J = 11.7, 1.6$, 1H, H2), 0.62 (s, 3H, H10). ¹³C NMR (CD₃CN, δ): 179.4 (C8), 179.1 (C13), 143.8 (PzB3), 143.6 (PzA3), 141.2 (PzC3), 137.9 (PzC5), 137.5 (PzA5), 137.0 (PzB5), 107.1 (2C, PzB4 & PzC4), 106.6 (PzA4), 54.3 (d, $J = 10.3$, C3), 53.2 (C2), 51.7 (2C, C9 & C14), 49.7 (C7), 46.4 (C12), 46.1 (C1), 39.9 (C5), 33.6 (C4), 30.0 (C6), 24.2 (C10), 23.4 (C15/C16), 22.6 (C15/C16), 20.2 (C11), 13.5 (d, $J = 27.9$, PMe₃).



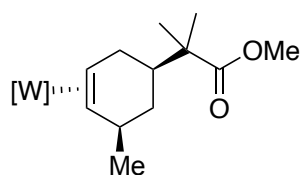
Compound 33A. To a 4-dram vial charged with a stir pea were added **30** (50 mg, 0.073 mmol) followed by acetonitrile (0.6 mL, -30°C) and a 1M solution of HOTf in acetonitrile (0.15 mL, 0.15 mmol, -30°C), resulting in a homogeneous golden solution, which was allowed to sit for 15 min at -30°C. NaCN (23 mg, 0.47 mmol) and MeOH (0.6 mL, -30°C) were added to a separate 4-dram vial and cooled to -30°C for 15 min. The NaCN/MeOH solution was then added to the reaction vial with stirring, and it was allowed to sit at -30°C for 2 h. The reaction solution was diluted with Et₂O (20 mL) and washed with H₂O (20 mL). The aqueous layer was back extracted with DCM (15 mL), and then the combined organic layers were dried over MgSO₄ and evaporated *in vacuo*. The film was redissolved in minimal THF and added to stirring pentane (15 mL, -30°C). The resulting pale solid was collected on a 15 mL fine porosity fritted disc, washed with pentane (2 x 5 mL, -30°C) and desiccated overnight, yielding **33A** (41 mg, 0.058 mmol, 79% yield). CV (DMAc) $E_{p,a} = +0.56$ V (NHE). IR: $\nu(\text{BH}) = 2486 \text{ cm}^{-1}$, $\nu(\text{CN}) = 2230 \text{ cm}^{-1}$, $\nu(\text{CO}) = 1721 \text{ cm}^{-1}$, $\nu(\text{NO}) = 1545 \text{ cm}^{-1}$. Anal. Calc'd for C₂₄H₃₆BN₈O₃PW: C, 40.59; H, 5.11; N, 15.78. Found: C, 40.63; H, 5.03; N, 15.57. ³¹P NMR (CD₃CN, δ): -8.34 ($J_{\text{WP}} = 289$). ¹H NMR (CD₃CN, δ): 8.23 (d, 1H, PzA3), 8.04 (d, 1H, PzB3), 7.87 (d, 1H, PzB5), 7.84 (d, 1H, PzC5), 7.79 (d, 1H, PzA5), 7.38 (d, 1H, PzC3), 6.39 (t, 1H, PzB4), 6.32 (t, 1H, PzA4), 6.26 (t, 1H, PzC4), 4.05 (dt, $J = 12.0, 4.4$, 1H, H5), 3.63 (s, 3H, H9), 3.32 (ddd, $J = 13.7, 12.0, 7.0$, 1H, H2x), 2.66 (m, 2H, H2y & H3), 2.12 (tm, $J = 12.0$, 1H, H1), 2.01 (dm, $J = 12.0$, 1H, H6x), 1.36 (q, $J = 12.0$, 1H, H6y), 1.25 (dm, $J = 11.8$, 1H, H4), 1.19 (s, 3H, H10), 1.15 (s, 3H, H11), 1.13 (d, $J = 8.4$, 9H, PMe₃). ¹³C NMR (CD₃CN, δ):

178.7 (C8), 144.4 (PzB3), 143.1 (PzA3), 141.7 (PzC3), 138.1 (PzC5), 137.5 (PzB5), 137.4 (PzA5), 127.3 (CN), 107.7 (PzB4), 107.1 (PzC4), 106.7 (PzA4), 52.4 (d, $J = 11.8$, C3), 52.1 (C9), 51.6 (C4), 46.2 (C7), 41.5 (C1), 33.2 (C5), 32.8 (C6), 32.3 (C2), 23.2 (C10), 22.1 (C11), 13.3 (d, $J = 28.7$, PMe_3).



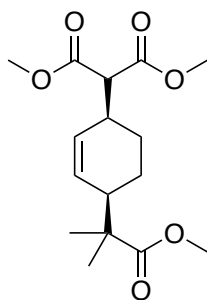
Compound 34A. To a 4-dram vial charged with a stir pea were added **30** (40 mg, 0.059 mmol) followed by acetonitrile (1 mL, -30°C) and a 1M solution of HOTf in acetonitrile (0.09 mL, 0.09 mmol, -30°C), resulting in a homogeneous golden solution, which was allowed to sit for 15 min at -30°C . LiDMM (40 mg, 0.29 mmol) was added to the reaction vial with stirring, and the reaction was allowed to sit at -30°C for 1 h. The reaction solution was diluted with Et_2O (30 mL) and washed with H_2O (20 mL). The aqueous layer was back extracted with DCM (15 mL), and then the combined organic layers were dried over MgSO_4 and evaporated *in vacuo*. The film was redissolved in minimal THF and added to stirring pentane (15 mL, -30°C). The resulting pale solid was collected on a 15 mL fine porosity fritted disc, washed with pentane (3 x 3 mL, -30°C) and desiccated overnight, yielding **34A** (36 mg, 0.044 mmol, 75% yield). CV (DMAc) $E_{p,a} = +0.35$ V (NHE). IR: $\nu(\text{BH}) = 2486$ cm^{-1} , $\nu(\text{CO}) = 1750$ & 1722 cm^{-1} , $\nu(\text{NO}) = 1541$ cm^{-1} . Anal. Calc'd for $\text{C}_{28}\text{H}_{43}\text{BN}_7\text{O}_7\text{PW}$: C, 41.25; H, 5.32; N, 12.03. Found: C, 41.21; H, 5.31; N, 11.77. ^{31}P NMR (CD_3CN , δ): -8.08 ($J_{\text{WP}} = 292$). ^1H

NMR (CD₃CN, δ): 8.09 (d, 1H, PzA3), 8.01 (d, 1H, PzB3), 7.83 (overlapping d, 2H, PzB5 & PzC5), 7.81 (d, 1H, PzA5), 7.34 (d, 1H, PzC3), 6.35 (t, 1H, PzB4), 6.27 (t, 1H, PzA4), 6.25 (t, 1H, PzC4), 3.74 (m, 1H, H1), 3.64 (s, 3H, H9), 3.61 (s, 3H, H14), 3.53 (s, 3H, H11), 3.30 (d, $J = 4.3$, 1H, H7), 3.28 (buried, 1H, H4x), 2.75 (m, 1H, H3), 2.68 (dd, $J = 13.5, 4.0$, 1H, H4y), 2.18 (tm, $J = 12.2$, 1H, H5), 1.58 (dm, $J = 11.7$, 1H, H6x), 1.29 (q, $J = 12.0$, 1H, H6y), 1.15 (s, 3H, H15), 1.14 (d, $J = 8.1$, 9H, PMe₃), 1.12 (s, 3H, H16), 0.89 (m, 1H, H2). ¹³C NMR (CD₃CN, δ): 179.1 (C13), 170.7 (C8), 170.0 (C10), 144.2 (PzB3), 142.1 (PzA3), 141.5 (PzC3), 137.9 (PzC5), 137.7 (PzA5), 137.1 (PzB5), 107.4 (PzB4), 107.1 (PzC4), 106.8 (PzA4), 60.1 (C7), 54.2 (d, $J = 11.0$, C3), 53.7 (C2), 52.8 (C9), 52.2 (C11), 51.9 (C14), 46.3 (C12), 43.0 (C1), 41.9 (C5), 33.5 (C4), 30.5 (C6), 23.0 (C15), 22.6 (C16), 13.4 (d, $J = 28.1$, PMe₃).



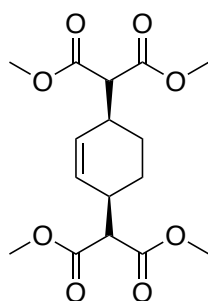
Compound 35A. To a 4-dram vial charged with a stir pea were added **30H** (50 mg, 0.060 mmol) followed by THF (1.5 mL, -30°C). A 3M MeMgBr/Et₂O solution (0.08 mL, 0.24 mmol, -30°C) was added dropwise to the reaction vial with stirring. The reaction was allowed to sit at -30°C for 22 h, then quenched with saturated aqueous NH₄Cl, diluted with H₂O (25 mL) and extracted with Et₂O (2 x 25 mL). The combined organic layers were dried over MgSO₄ and evaporated *in vacuo* to a film. A 15 mL fine porosity fritted disc was filled ³/₄ full of silica gel and set in Et₂O. The film was redissolved in minimal DCM and loaded on the column, and a pale yellow band was eluted with 40 mL of Et₂O. The filtrate was evaporated *in vacuo*, then redissolved in minimal DCM and added to stirring pentane (10 mL, -30°C).

The resulting pale solid was collected on a 15 mL fine porosity fritted disc, washed with pentane (2 x 2 mL, -30°C) and desiccated overnight, yielding **35A** (15 mg, 0.021 mmol, 35% yield). CV (DMAc) $E_{p,a} = +0.33$ V (NHE). IR: $\nu(\text{BH}) = 2483$ cm^{-1} , $\nu(\text{CO}) = 1720$ cm^{-1} , $\nu(\text{NO}) = 1541$ cm^{-1} . ^{31}P NMR (d^6 -acetone, δ): -7.05 ($J_{\text{WP}} = 293$). ^1H NMR (d^6 -acetone, δ): 8.23 (d, 1H, PzA3), 8.07 (d, 1H, PzB3), 7.90 (overlapping d, 2H, Pz5), 7.81 (d, 1H, Pz5), 7.49 (d, 1H, PzC3), 6.38 (t, 1H, PzB4), 6.28 (t, 1H, PzA4/PzC4), 6.27 (t, 1H, PzA4/PzC4), 3.61 (s, 3H, OMe), 3.29 (m, 1H, H2x), 3.16 (m, 1H, H5), 2.80 (m, 1H, H3), 2.73 (dd, $J = 13.0, 4.5$, 1H, H2y), 2.30 (tdd, $J = 12.2, 4.5, 2.0$, 1H, H1), 1.64 (dm, $J = 11.6$, 1H, H6x), 1.20 (d, $J = 8.2$, 9H, PMe_3), 1.19 (s, 3H, Me), 1.14 (s, 3H, Me), 1.00 (d, $J = 6.9$, 3H, H5'Me), 0.95 (dt, $J = 11.4, 2.5$, 1H, H4), 0.72 (q, $J = 11.9$, 1H, H6y). ^{13}C NMR (d^6 -acetone, δ): 178.5 (CO), 143.9 (PzB3), 142.3 (PzA3), 141.4 (PzC3), 137.4 (Pz5), 136.7 (Pz5), 136.6 (Pz5), 107.0 (PzB4), 106.7 (PzC4), 105.9 (PzA4), 59.2 (C4), 54.9 (d, $J = 11.0$, C3), 51.4 (OMe), 46.1 (C1'), 42.2 (C1), 38.7 (C6), 37.0 (C5), 33.9 (C2), 28.1 (C5'), 23.6 (Me), 22.6 (Me), 13.4 (d, $J = 27.2$, PMe_3).



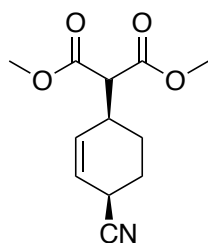
Compound 36. Outside of the glovebox, NOPF_6 (27 mg, 0.15 mmol) was added to a 4-dram vial charged with a stir pea. In a separate 4-dram vial, 28A (83 mg, 0.10 mmol) was dissolved in acetone (1.75 mL) and then added to the vial with NOPF_6 while stirring, resulting in an immediate color change from pale yellow to golden brown. The reaction

solution was stirred for 6 h and then evaporated *in vacuo* to dryness. The film was redissolved in minimal DCM, and then this solution was added to stirring hexanes (20 mL). The resulting precipitate was collected on a 15 mL medium porosity fritted disc and washed with hexanes (2 x 5 mL). The filtrate was evaporated *in vacuo*, and the resulting oil was loaded onto a 250 μm silica preparatory plate with DCM (3 x 0.3 mL) and eluted with 30% EtOAc/hexanes (HPLC grade, 200 mL). A KMnO_4 active band at $R_f = 0.63\text{--}0.74$ was collected and sonicated in EtOAc (HPLC grade, 25 mL) for 15 min. The silica was filtered off on a 30 mL fine porosity fritted disc and washed with EtOAc (HPLC grade, 2 x 15 mL). The filtrate was evaporated *in vacuo*, yielding **36** (13 mg, 0.042 mmol, 42% yield). IR: $\nu(\text{CO}) = 1755 \text{ \& } 1729 \text{ cm}^{-1}$. ^1H NMR (d^6 -acetone, δ): 5.70 (dm, $J = 10.4$, 1H, H2), 5.62 (dm, $J = 10.4$, 1H, H3), 3.70 (s, 3H, OMe), 3.69 (s, 3H, OMe), 3.64 (s, 3H, OMe), 3.34 (d, $J = 10.2$, 1H, H1'), 2.80 (m, 1H, H1), 2.44 (m, 1H, H4), 1.70 (m, 1H, H6x), 1.60 (m, 1H, H6y), 1.54 (m, 1H, H5x), 1.38 (m, 1H, H5y), 1.13 (s, 3H, Me), 1.10 (s, 3H, Me). ^{13}C NMR (d^6 -acetone, δ): 177.9 (CO), 169.2 (CO), 169.1, (CO), 131.1 (C3), 130.0 (C2), 56.9 (C1'), 52.6 (2C, OMe), 51.9 (OMe), 45.7 (C4'), 43.6 (C4), 34.4 (C1), 25.9 (C6), 22.4 (2C, Me), 20.7 (C5).



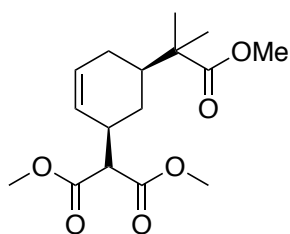
Compound 37. Outside of the glovebox, NOPF_6 (25 mg, 0.14 mmol) was added to a 4-dram vial charged with a stir pea. In a separate 4-dram vial, **23A** (80 mg, 0.095 mmol) was

dissolved in acetone (1.5 mL) and then added to the vial with NOPF₆ while stirring, resulting in an immediate color change from pale yellow to golden brown. The reaction solution was stirred for 3.5 h and then evaporated *in vacuo* to dryness. The film was redissolved in minimal DCM, and then this solution was added to stirring hexanes (20 mL). The resulting precipitate was collected on a 15 mL fine porosity fritted disc and washed with hexanes (2 x 5 mL). The filtrate was evaporated *in vacuo*, and the resulting oil was loaded onto a 250 μm silica preparatory plate with DCM (3 x 0.3 mL) and eluted with 30% EtOAc/hexanes (HPLC grade, 200 mL). A KMnO₄ active band at R_f = 0.40–0.52 was collected and sonicated in EtOAc (HPLC grade, 40 mL) for 20 min. The silica was filtered off on a 30 mL fine porosity fritted disc and washed with EtOAc (HPLC grade, 2 x 15 mL). The filtrate was evaporated *in vacuo*, yielding **37** (22 mg, 0.065 mmol, 68% yield). IR: ν(CO) = 1749 & 1729 cm⁻¹. ¹H NMR (d⁶-acetone, δ): 5.68 (bs, 2H, H2 & H3), 3.70 (bs, 12H, OMe), 3.39 (d, J = 9.2, 2H, H1' & H4'), 2.83 (m, 2H, H1 & H4), 1.71 (m, 2H, H5x & H6x), 1.54 (m, 2H, H5y & H6y). ¹³C NMR (d⁶-acetone, δ): 169.2 (2C, CO), 169.1 (2C, CO), 130.6 (2C, C2 & C3), 56.7 (2C, C1' & C4'), 52.6 (4C, OMe), 35.4 (2C, C1 & C4), 24.2 (2C, C5 & C6).



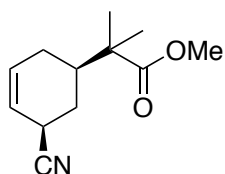
Compound 38. Outside of the glovebox, NOPF₆ (43 mg, 0.25 mmol) was added to a 4-dram vial charged with a stir pea. In a separate 4-dram vial, **18A** (120 mg, 0.162 mmol) was dissolved in acetone (3 mL) and then added to the vial with NOPF₆ while stirring, resulting

in an immediate color change from pale yellow to golden brown. The reaction solution was stirred for 3 h and then evaporated *in vacuo* to dryness. Minimal DCM was added to the vial, and then this solution was added to stirring pentane (20 mL). The resulting precipitate was collected on a 15 mL fine porosity fritted disc and washed with pentane (2 x 10 mL). The filtrate was evaporated *in vacuo*, and the resulting oil was loaded onto a 250 μ m silica preparatory plate with DCM (3 x 0.3 mL) and eluted with 30% EtOAc/hexanes (HPLC grade, 200 mL). A KMnO_4 active band at $R_f = 0.43\text{--}0.57$ was collected and sonicated in EtOAc (HPLC grade, 25 mL) for 20 min. The silica was filtered off on a 30 mL medium porosity fritted disc and washed with EtOAc (HPLC grade, 2 x 20 mL). The filtrate was evaporated *in vacuo*, yielding **38** (21.9 mg, 0.092 mmol, 57% yield). IR: $\nu(\text{CN}) = 2238\text{ cm}^{-1}$, $\nu(\text{CO}) = 1747\text{ \& } 1731\text{ cm}^{-1}$. $^1\text{H NMR}$ (d^6 -acetone, δ): 5.86 (dm, $J = 10.1$, 1H, H2), 5.77 (dddd, $J = 10.1, 4.4, 2.4, 1.0$, 1H, H3), 3.72 (s, 6H, OMe), 3.46 (d, $J = 8.4$, 1H, H1'), 3.44 (m, 1H, H4), 2.89 (m, 1H, H1), 2.01 (m, 1H, H5x), 1.94 (m, 1H, H5y), 1.89 (m, 1H, H6x), 1.63 (m, 1H, H6y). $^{13}\text{C NMR}$ (d^6 -acetone, δ): 169.1 (CO), 169.0 (CO), 133.1 (C2), 124.0 (C3), 121.5 (CN), 56.3 (C1'), 52.7 (2C, OMe), 35.6 (C1), 26.5 (C4), 25.7 (C5), 24.2 (C6).



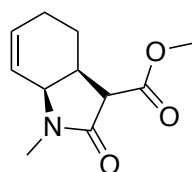
Compound 39. Outside of the glovebox, NOPF_6 (24 mg, 0.14 mmol) was added to a 4-dram vial charged with a stir pea. In a separate 4-dram vial, **34A** (75 mg, 0.092 mmol) was dissolved in acetone (1.7 mL) and then added to the vial with NOPF_6 while stirring,

resulting in an immediate color change from pale yellow to golden brown. The reaction solution was stirred for 4 h and then evaporated *in vacuo* to dryness. The film was redissolved in minimal DCM, and then this solution was added to stirring hexanes (20 mL). The resulting precipitate was collected on a 15 mL medium porosity fritted disc and washed with hexanes (2 x 5 mL). The filtrate was evaporated *in vacuo*, and the resulting oil was loaded onto a 250 μm silica preparatory plate with DCM (3 x 0.3 mL) and eluted with 25% EtOAc/hexanes (HPLC grade, 200 mL). A KMnO_4 active band at $R_f = 0.55\text{--}0.64$ was collected and sonicated in EtOAc (HPLC grade, 25 mL) for 20 min. The silica was filtered off on a 30 mL fine porosity fritted disc and washed with EtOAc (HPLC grade, 2 x 15 mL). The filtrate was evaporated *in vacuo*, yielding **39** (10 mg, 0.032 mmol, 35% yield). IR: $\nu(\text{CO}) = 1754 \text{ \& } 1728 \text{ cm}^{-1}$. ^1H NMR (d^6 -acetone, δ): 5.73 (dm, $J = 10.0$, 1H, H3), 5.51 (d, $J = 10.0$, 1H, H2), 3.69 (s, 6H, OMe), 3.63 (s, 3H, OMe), 3.29 (d, $J = 8.4$, 1H, H1'), 2.88 (m, 1H, H1), 1.95 (m, 1H, H5), 1.93 (m, 1H, H4x), 1.83 (m, 1H, H4y), 1.72 (dm, $J = 12.2$, 1H, H6x), 1.12 (s, 3H, Me), 1.10 (s, 3H, Me), 1.09 (buried, 1H, H6y). ^{13}C NMR (d^6 -acetone, δ): 177.9 (CO), 169.2 (2C, CO), 129.0 (C3), 128.5 (C2), 57.2 (C1'), 52.5 (2C, OMe), 51.8 (OMe), 45.7 (C5'), 42.3 (C5), 38.2 (C1), 29.5 (C6), 27.2 (C4), 22.3 (Me), 22.0 (Me).



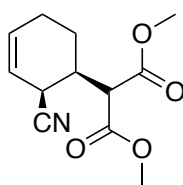
Compound 40. 33A (25 mg, 0.035 mmol) and durene (5 mg, 0.04 mmol) were dissolved in d^6 -acetone (1 mL), and then a ^1H NMR spectrum was taken. Outside of the glovebox, the reaction solution was then added to a vial containing NOPF_6 (10 mg, 0.57), with stirring.

After 20 min, a ^1H NMR spectrum was taken to determine the NMR yield (45% yield). IR: $\nu(\text{CN}) = 2239\text{ cm}^{-1}$, $\nu(\text{CO}) = 1726\text{ cm}^{-1}$. ^1H NMR (d^6 -acetone, δ): 5.92 (m, 1H, H3), 5.61 (d, $J = 9.8$, 1H, H4), 3.65 (s, 3H, OMe), 3.53 (m, 1H, H5), 2.13 (m, 1H, H6x), 1.98 (m, 1H, H2x), 1.91 (m, 2H, H1 & H2y), 1.46 (q, $J = 12.1$ 1H, H6y), 1.17 (s, 3H, Me), 1.14 (s, 3H, Me). ^{13}C NMR (d^6 -acetone, δ): 177.5 (CO), 131.2 (C3), 122.3 (C4), 122.1 (CN), 52.0 (OMe), 45.5 (C1'), 41.1 (C1), 29.2 (C6), 29.1 (C5), 26.5 (C2), 22.2 (Me), 22.1 (Me).



Compound 41. Outside of the glovebox, NOPF_6 (23 mg, 0.13 mmol) was added to a 4-dram vial charged with a stir pea. In a separate 4-dram vial, **20B** (62 mg, 0.087 mmol) was dissolved in acetone (1.5 mL) and then added to the vial with NOPF_6 while stirring, resulting in an immediate color change from pale yellow to golden brown. The reaction solution was stirred for 5 h and then evaporated *in vacuo* to dryness. Minimal DCM was added to the vial, and then this solution was added to stirring hexanes/ Et_2O (19 mL/1 mL). The resulting precipitate was collected on a 30 mL fine porosity fritted disc and washed with hexane/ Et_2O (8/2 mL) and hexanes (10 mL). The filtrate was evaporated *in vacuo*, and the resulting oil was loaded onto a 250 μm silica preparatory plate with DCM (3×0.3 mL) and eluted with 70% EtOAc /hexanes (HPLC grade, 200 mL). A KMnO_4 active band at $R_f = 0.40$ – 0.60 was collected and sonicated in EtOAc (HPLC grade, 30 mL) for 20 min. The silica was filtered off on a 30 mL fine porosity fritted disc and washed with EtOAc (HPLC grade, 2×20 mL). The filtrate was evaporated *in vacuo*, yielding **41** (6.6 mg, 0.032 mmol, 37%

yield). IR: $\nu(\text{CO}) = 1735$ & 1686 cm^{-1} . ^1H NMR (d^6 -acetone, δ): 5.99 (dm, $J = 10.2$, 1H, H6), 5.89 (dm, $J = 10.2$, 1H, H7), 4.05 (m, 1H, H7a), 3.69 (s, 3H, OMe), 3.17 (d, $J = 7.7$, 1H, H3), 2.85 (m, 1H, H3a), 2.81 (s, 3H, NMe), 2.14 (m, 1H, H5x), 2.06 (m, 1H, H5y), 1.80 (m, 1H, H4x), 1.58 (m, 1H, H4y). ^{13}C NMR (d^6 -acetone, δ): 171.1 (CO), 169.0 (CO), 131.7 (C6), 124.2 (C7), 56.3 (C7a), 52.6 (C3), 52.4 (OMe), 36.6 (C3a), 27.8 (NMe), 23.7 (C4), 22.2 (C5).



Compound 42. Outside of the glovebox, NOPF_6 (15 mg, 0.086 mmol) was added to a 4-dram vial charged with a stir pea. In a separate 4-dram vial, **22B** (42 mg, 0.057 mmol) was dissolved in acetone (1 mL) and then added to the vial with NOPF_6 while stirring, resulting in an immediate color change from pale yellow to golden brown. The reaction solution was stirred for 3.5 h and then evaporated *in vacuo* to dryness. Minimal DCM was added to the vial, and then this solution was added to stirring hexanes (20 mL). The resulting precipitate was collected on a 15 mL fine porosity fritted disc and washed with hexanes (2 x 5 mL). The filtrate was evaporated *in vacuo*, and the resulting oil was loaded onto a 250 μm silica preparatory plate with DCM (3 x 0.3 mL) and eluted with 25% EtOAc/hexanes (HPLC grade, 200 mL). A KMnO_4 active band at $R_f = 0.37$ – 0.46 was collected and sonicated in EtOAc (HPLC grade, 25 mL) for 20 min. The silica was filtered off on a 30 mL fine porosity fritted disc and washed with EtOAc (HPLC grade, 2 x 15 mL). The filtrate was evaporated *in vacuo*, yielding **42** (6.2 mg, 0.026 mmol, 46% yield). IR: $\nu(\text{CN}) = 2233$ cm^{-1} , $\nu(\text{CO}) = 1750$ & 1733 cm^{-1} . ^1H NMR (d^6 -acetone, δ): 5.99 (m, 1H, H4), 5.74 (m, 1H, H3), 3.76 (s, 3H, OMe),

3.75 (s, 3H, OMe), 3.61 (m, 1H, H2), 3.50 (d, $J = 11.1$, 1H, H1'), 2.47 (m, 1H, H1), 2.23 (m, 1H, H5x), 2.18 (m, 1H, H5y), 1.73 (m, 1H, H6x), 1.53 (m, 1H, H6y). ^{13}C NMR (d^6 -acetone, δ): 168.7 (CO), 168.5 (CO), 132.2 (C4), 121.5 (C3), 119.0 (CN), 56.2 (C1'), 53.1 (OMe), 53.0 (OMe), 36.4 (C1), 30.5 (C2), 25.7 (C5), 23.8 (C6).

2.5 References

- (1) Pape, A. R.; Kaliappan, K. P.; Kündig, E. P. *Chem. Rev.* **2000**, *100*, 2917.
- (2) Semmelhack, M. F. In *Comprehensive Organometallic Chemistry II*; Abel, E. W., Stone, F. G. A., Wilkinson, G., Eds.; Pergamon: Oxford, 1995; Vol. 12, p 979.
- (3) Pape, A. R.; Kaliappan, K. P.; Kündig, E. P. *Chem. Rev.* **2000**, *100*, 2917.
- (4) Graham, P.; Meiere, S. H.; Sabat, M.; Harman, W. D. *Organometallics* **2003**, *22*, 4364.
- (5) Ding, F.; Harman, W. D. *J. Am. Chem. Soc.* **2004**, *126*, 13752.
- (6) Harrison, D. P.; Nichols-Nielander, A. C.; Zottig, V. E.; Strausberg, L.; Salomon, R. J.; Trindle, C. O.; Sabat, M.; Gunnoe, T. B.; Iovan, D. A.; Myers, W. H.; Harman, W. D. *Organometallics* **2011**, *30*, 2587.
- (7) Welch, K. D.; Harrison, D. P.; Lis, E. C.; Liu, W.; Salomon, R. J.; Harman, W. D.; Myers, W. H. *Organometallics* **2007**, *26*, 2791.
- (8) Wilson, K. B.; Myers, J. T.; Nedzbala, H. S.; Combee, L. A.; Sabat, M.; Harman, W. D. *J. Am. Chem. Soc.* **2017**, *139*, 11401.
- (9) Shivokevich, P. J.; Myers, J. T.; Smith, J. A.; Pienkos, J. A.; Dakermanji, S. J.; Pert, E. K.; Welch, K. D.; Trindle, C. O.; Harman, W. D. *Organometallics* **2018**.
- (10) Hernandez, L. W.; Pospesch, J.; Klöckner, U.; Bingham, T. W.; Sarlah, D. *J. Am. Chem. Soc.* **2017**, *139*, 15656.
- (11) Hudlicky, T. *Pure & Appl. Chem.* **1994**, *66*, 2067.
- (12) Hudlicky, T.; Olivo, H. F. *J. Am. Chem. Soc.* **1992**, *114*, 9694.

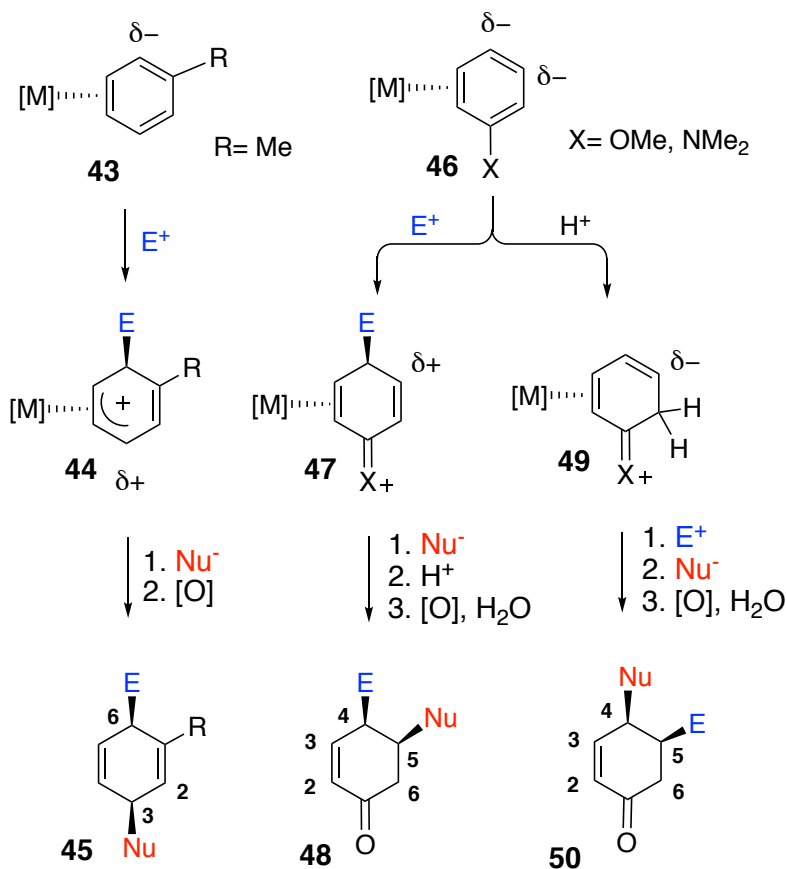
Chapter 3

Sequential Tandem Addition to a Tungsten–Trifluorotoluene Complex: A Versatile Method for the Preparation of Highly Functionalized Trifluoromethylated Cyclohexenes

3.1 Introduction

In Chapters 1 and 2 a variety of dearomatization methods were reviewed for the elaboration of benzene into more complex chiral compounds. In particular, the coordination of benzene to a transition metal has been shown to have a profound effect on its reactivity.¹⁻⁴ Dihapto-coordination of benzene to π -basic complexes has facilitated cycloaddition reactions, as well as the synthesis of 1,4-disubstituted cyclohexadienes and disubstituted cyclohexenes (Chapter 2).⁵⁻⁸ When the η^2 -benzene ligand bears a substituent however, regiochemistry issues arise regarding the site of metal coordination and location of the addition reactions (Scheme 3.1).

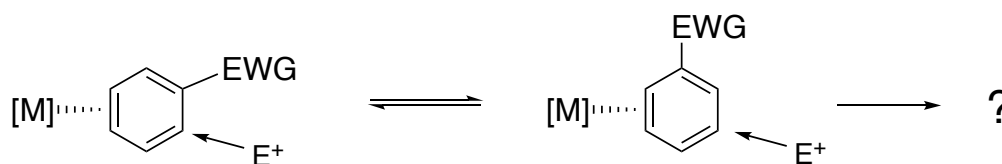
Scheme 3.1: General reaction trends for dihapto-coordinated arene complexes



For example, the methyl group of toluene directs the metal to coordinate in a dihapto fashion to the meta and para carbons (**43**). In this position, the metal effects a selective 1,4-electrophile/nucleophile addition sequence that results in *cis*-3,6-dialkylated 1,4-cyclohexadienes upon liberation from the metal (**45**).^{8,9} In contrast, when a π -donor substituent is utilized the metal coordination is directed to the ortho and meta carbons (**46**). In this configuration, the electrophile-nucleophile reaction sequence leads selectively to *cis*-4,5-disubstituted cyclohexenones (**48**).^{10,11} Alternatively, ortho protonation can occur, generating an arenium complex (**49**) that also can undergo a tandem electrophile/nucleophile reaction sequence, but with *reversed* regiochemistry (**50**).¹²⁻¹⁴

The question arises--*how would an electron-withdrawing group (EWG) influence the regiochemistry of an η^2 -arene tandem addition?* (Scheme 3.2):

Scheme 3.2: Dihapto-coordination of benzene with an EWG



Unfortunately, while an EWG stabilizes the metal-arene back-bonding interaction by lowering the π^* orbitals of the arene,¹⁵ most functional groups that are considered electron-withdrawing have π bonds that compete with η^2 -aromatic coordination (*e.g.*, amides, esters, nitriles).^{16,17} However, an α,α,α -trifluorotoluene (TFT) complex seemed ideal for exploring the fundamental reactivity pattern of an η^2 -benzene bearing an EWG, due to the absence of π bonds in the CF_3 group that could compete with coordination of the ring. Thus, we embarked on a study to determine how an EWG can influence the organic

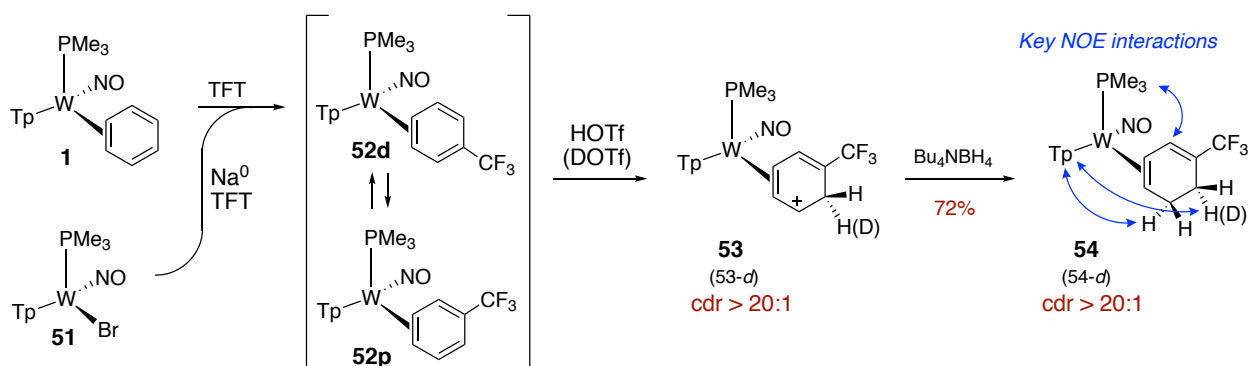
chemistry of a dihapto-coordinated benzene using $\text{TpW}(\text{NO})(\text{PMe}_3)(\eta^2\text{-PhCF}_3)^{15}$ as our model.

3.2 Results and Discussion

3.2.1 Coordination and Reactivity of α,α,α -Trifluorotoluene

The trifluorotoluene complex $\text{TpW}(\text{NO})(\text{PMe}_3)(\eta^2\text{-PhCF}_3)$ (**52**) can be prepared directly through reduction of the $\text{W}(\text{I})$ -bromide precursor **51**,¹⁸ or by ligand exchange from other arene complexes, such as the benzene complex (**1**) (Scheme 3.3). **52** exists in solution as a 1.2:1 ratio of coordination diastereomers (*cdr*; **52d**:**52p**), differing by which face of the prochiral arene is coordinated.¹⁵ Despite this low initial stereoselectivity, upon protonation with triflic acid (in CD_3CN), a single new species (**53**) is observed in solution by ^1H NMR at 20°C (*cdr* > 20:1). Spectroscopic features for the protonated organic ligand include a diastereotopic methylene group at 4.12 and 3.98 ppm, a single (organic) alkene resonance at 7.01 ppm, and three π -allylic protons at 6.95, 5.07, and 4.28 ppm. These signals suggest the formation of an η^2 -arenium species, as shown for **53** in Scheme 3.3.¹⁹

Scheme 3.3: Synthesis and protonation of $\eta^2\text{-PhCF}_3$



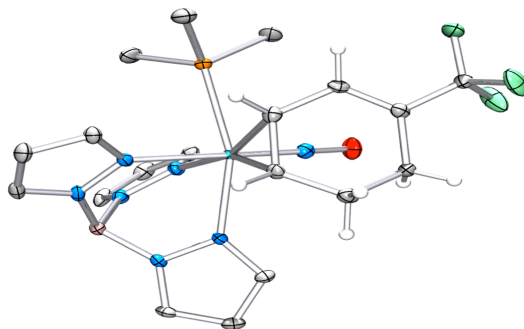
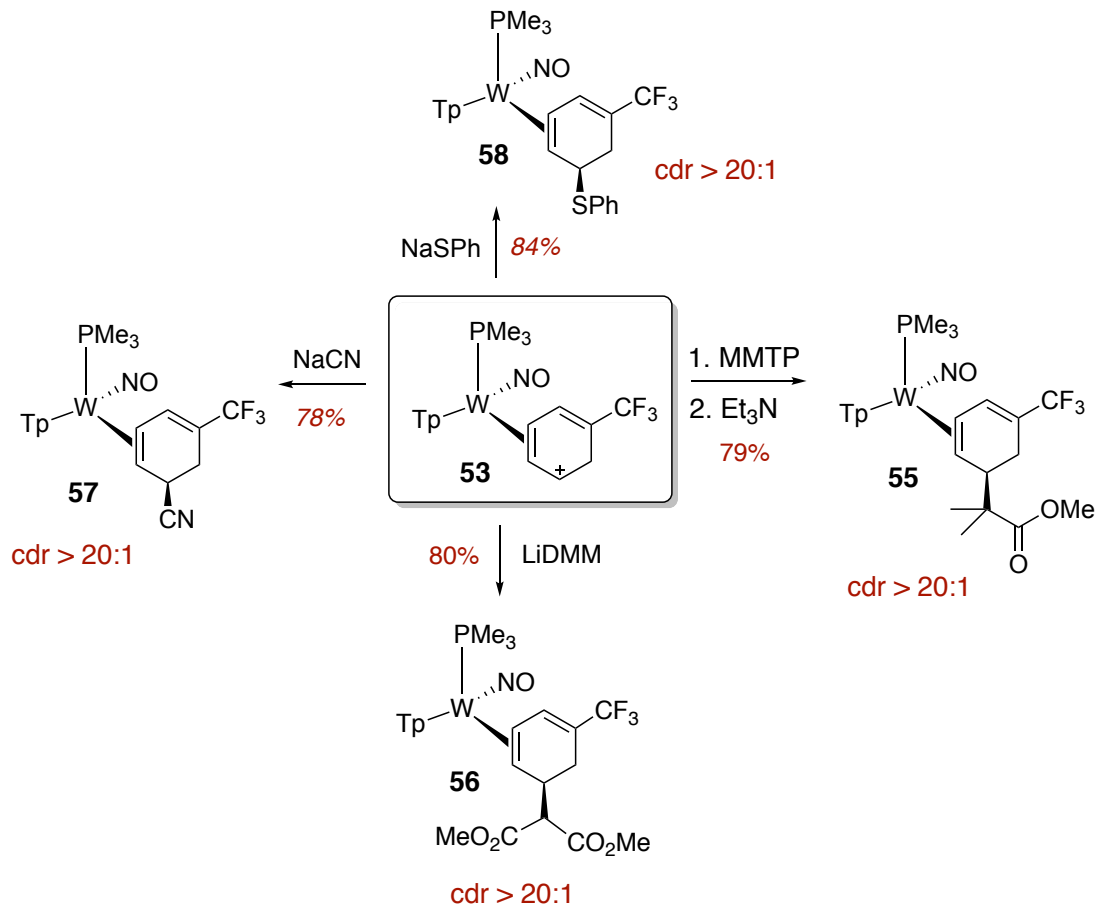


Figure 3.1: Crystal structure of compound **54**

In order to determine whether the initial protonation occurs stereoselectively, an isotopic labeling experiment was performed using DOTf instead of HOTf. ^1H NMR data of the arenium resulting from the addition of a deuterium (**53-d**) showed the disappearance of the methylene proton signal at 3.98 ppm. To confirm the stereochemistry of this selective deuteration, a hydride source was added to the solution of **53-d** and to that of the proteo-variation (**53**), allowing isolation of stable complexes (**54**, **54-d**). 2D NMR, IR, and electrochemical data confirm that **54** is the 1-trifluoromethyl-1,3-cyclohexadiene complex shown in Scheme 3.3, with the tungsten bound to C3 and C4. Further, NOE correlations (blue; Scheme 3.3) between the methylene groups of **54** and a proton from the Tp ligand (on the pyrazole trans to the PMe_3 ligand) were used to assign the four methylene protons of **54**. A comparison of this data with that for **54-d** suggests that protonation (deuteration) of **52** occurs selectively *syn* to the metal, which was also observed with the protonation of the η^2 -benzene complex (Chapter 2). Single crystal structure determination of **54** provided further support for the proposed η^2 -1,3-diene (Figure 3.1).

Scheme 3.4: Nucleophilic addition to **53**

Further reactivity of the TFT complex was investigated by treating a solution of **52** with triflic acid at -30°C followed by the protected ester enolate 1-methoxy-2-methyl-1-trimethylsilyloxypropene (MMTP). After the reaction was complete, it was quenched with Et₃N, and the product was purified using a silica plug yielding the 1,3-diene complex **55** (79%, Scheme 3.4). In a similar manner, lithiated dimethyl malonate (LiDMM) was used as the nucleophile to give complex **56** (80%). We were able to expand this range of nucleophiles to include cyanides (NaCN), which gives another C-C bond forming reaction, as well as heteroatom nucleophiles including sulfur nucleophiles (NaSPh), leading to η²-1,3-diene complexes **57** and **58** (Scheme 3.4). Complexes **57** and **58** conveniently either

spontaneously precipitate out of acetonitrile, or precipitation can be induced by adding H₂O to the reaction solution, giving yields of 78% and 84% respectively. For all five 1,3-diene complexes (**54-58**), careful inspection of NMR data revealed exceedingly high regio- and diastereocontrol (>20:1 selectivity) for these 1,2-additions. All complexes display similar characteristic features including an alkene proton signal around ~6.5-7.3 ppm. Additionally, the IR spectrum of complex **73** features a $\nu(\text{CN})$ stretch at 2225 cm⁻¹ supporting the successful addition of the cyano group.

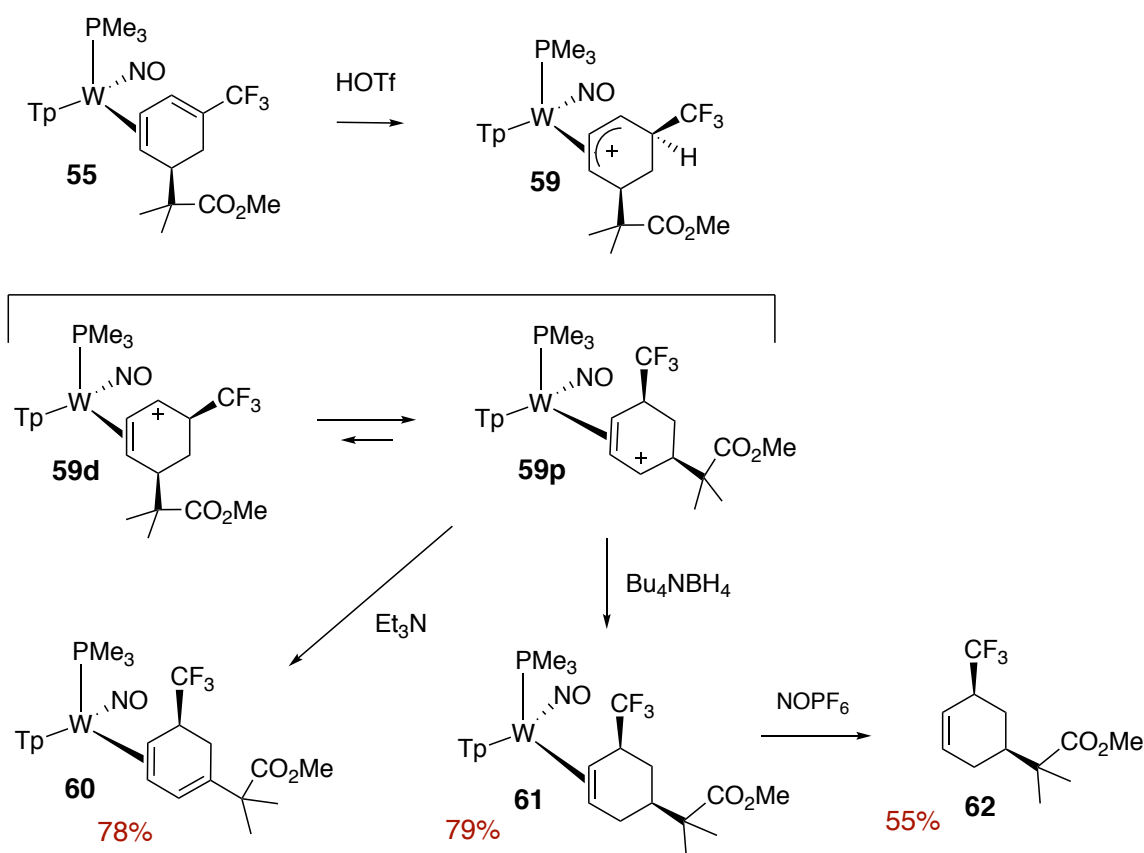
3.2.2 Second Tandem Addition to η^2 -1,3-Dienes

As previously mentioned, alkylated benzene complexes of rhenium and osmium undergo tandem addition reactions to give 1,4-diene products (**45**)⁸ (Scheme 3.1). Prior to decomplexation, the remaining double bond is isolated from the influence of the metal, both in an electronic and in a steric sense. In contrast, complexes **54-58** maintain the π -donating effects of the tungsten (i.e., back-bonding) in conjugation with the uncoordinated alkene linkage. Therefore, our next goal was to explore some of the metal-promoted chemical reactivity of the η^2 -1,3-diene ligands in **54-58**.

These compounds appear structurally similar to the η^2 -arenium **49** (Scheme 3.1), and true to expectation protonation of **55** results in a new η^2 -allyl species (**59**, Scheme 3.5). Notably, this allyl results from protonation of the terminal diene carbon, even though this carbon is bonded directly to the electron-withdrawing CF₃ group. Multinuclear NMR data (³¹P, ¹H, ¹⁹F) support this assertion: ³¹P-¹⁸³W coupling decreases from 281 to 265 Hz, consistent with other TpW(NO)(PMe₃) π -allyl complexes,¹⁹ and proton and fluorine data show a 7.6 Hz coupling constant between the CF₃ fluorines and their vicinal hydrogen.²⁰

Earlier studies of $\{\text{TpW}(\text{NO})(\text{PMe}_3)\}$ allyl complexes indicate that the allyl (**59**) is best considered as an equilibrium of two *dihapto-coordinated* isomers,¹⁹ (**59p**, **59d**). In this case, the dominant species (**59p**) likely has the carbocation away from the CF_3 group (Scheme 3.5). This was supported by a detailed 2D NMR analysis, which revealed that the terminal allyl proton distal to the PMe_3 ligand is considerably more deshielded (~ 1.7 ppm) than the other, indicating the localization of the positive charge at that position.

Scheme 3.5: Protonation and reactivity of **55**



Consistent with this notion are the following two additional observations: treatment of **59** with base does not return the initial diene complex **55**, but rather forms its isomer **60**, in which the alkyl fragment, rather than the CF_3 group, is now at a terminal carbon of

the diene. Secondly, treatment of **59** with tetrabutylammonium borohydride results in the formation of the 3-(trifluoromethyl)cyclohexene complex **61** exclusively, giving an overall “1,4-addition” product. Of course, these observations could simply reflect a greater reactivity of **59p** compared to **59d**, but NMR data support the notion of **59p** as the dominant species in solution (*vide supra*).

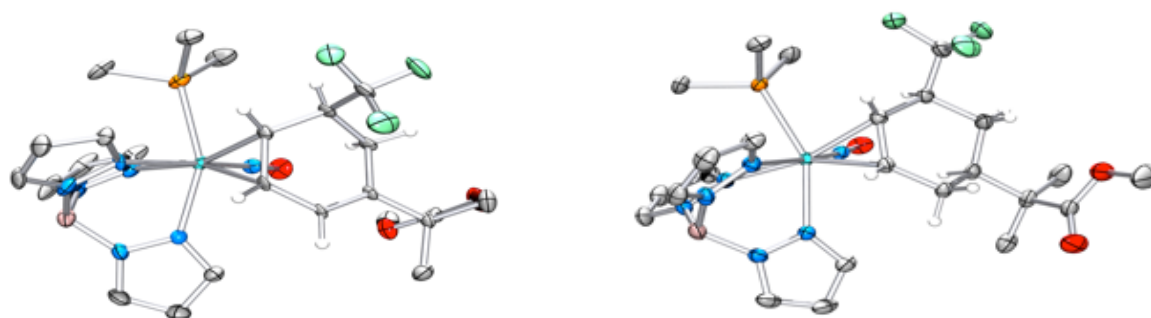
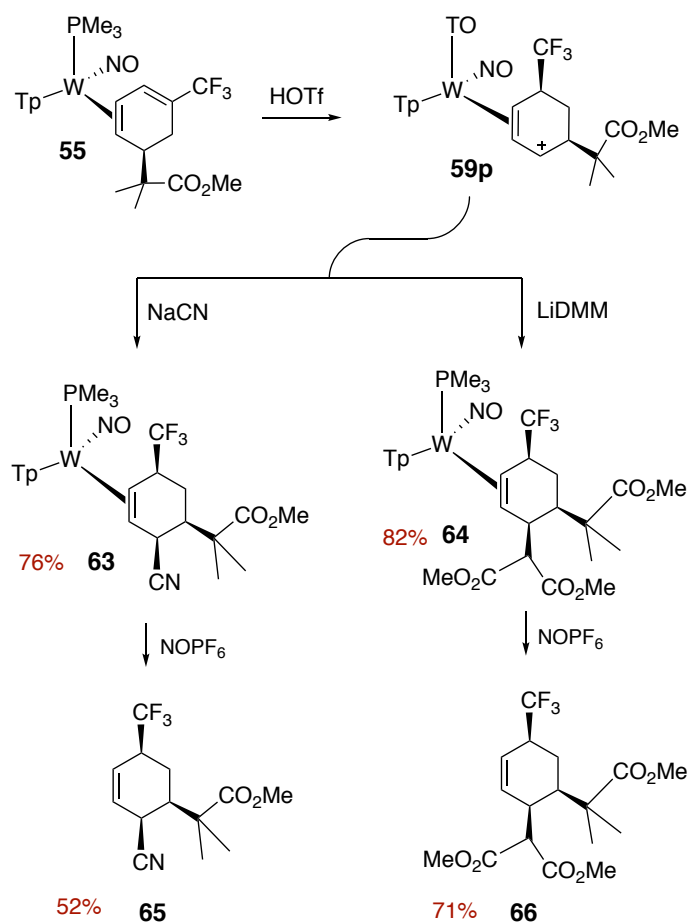


Figure 3.2: Crystal structures of compounds **60** (left) and **61** (right)

X-ray single-crystal molecular structure determinations of both η^2 -diene complex **60** and cyclohexene complex **61** confirm these assignments (Figure 3.2) and indicate that protonation of the CF_3 -substituted diene again occurs *syn* to the metal. We note that one possible explanation of this stereochemistry would be that a hydride is first formed by protonation of the tungsten, which is then transferred to the endo face of the arene. A similar mechanism has been proposed for an η^6 -arene complex of $\text{Mo}(0)$ by Ashby et al.²¹ Alternatively, the protonation could occur directly on the diene, but under thermodynamic control, such that the CF_3 group can extend away from the metal complex. Addition reactions of allyl **59** can also be effected with carbon nucleophiles: reaction of **59** with cyanide (NaCN), or DMM (LiDMM) results in cyclohexene complexes (**63**, **64**) analogous to **61** that feature three new stereocenters in the carbocycle (Scheme 3.6). Full 2D NMR

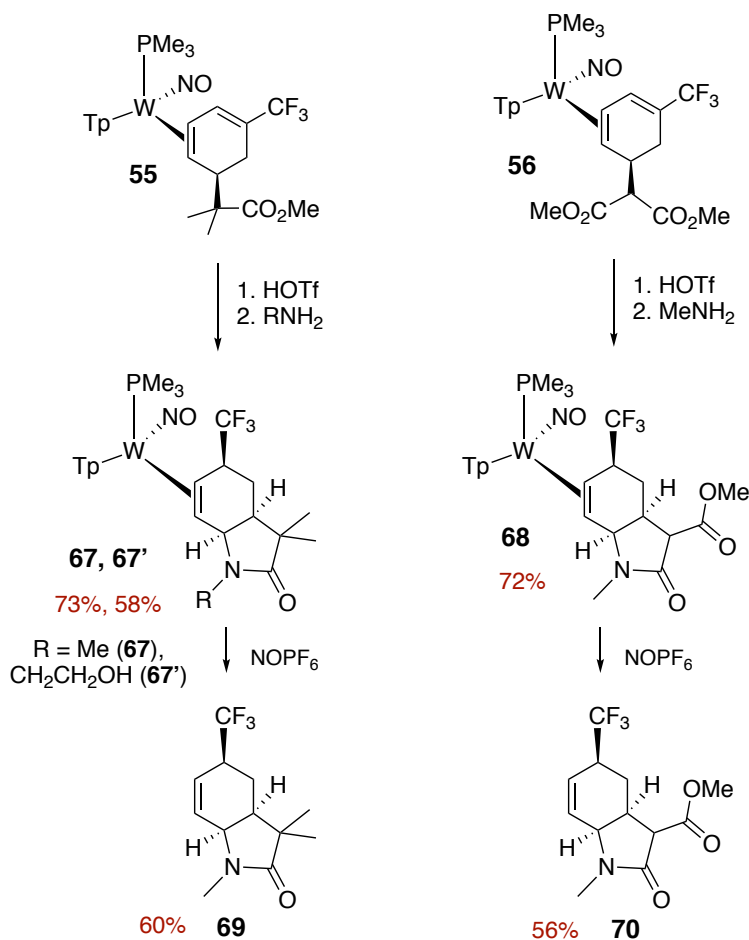
analysis indicates that the final nucleophilic addition in the synthesis of trisubstituted cyclohexenes **63** and **64** is to the carbon para to the CF₃ group, and that this addition occurs on the ring face *anti* to metal coordination. As before, these complexes are prepared as single diastereomers (dr > 20:1). The functionalized cyclohexene ligands of **61**, **63** and **64** (**62**, **65** and **66**, respectively) were subsequently liberated from the metal via an oxidation with NOPF₆, and were isolated using silica preparatory plates in 55%, 52%, and 71% yields respectively (Scheme 3.5 & 3.6).

Scheme 3.6: Second protonation-nucleophilic addition gives trisubstituted cyclohexenes



Interestingly, when complex **55** was treated with HOTf followed by a primary amine (MeNH₂), the product formed could be controlled by changing the concentration of base. At low concentrations, deprotonation occurs, forming the diene complex **60** (vide supra); however, at higher concentration a lactamization occurs with the amine and ester groups, forming complex **67** (Scheme 3.7). To probe the functional group tolerance of this intramolecular lactam formation reaction, ethanolamine was used as the amine source, which resulted in the successful formation of **67'**. X-ray single-crystal molecular structure determination of **67'** shows the cis-fused ring juncture of the lactam (Figure 3.3), with the newly formed 5-membered ring oriented away from the metal center.

Scheme 3.7: Intramolecular cyclization reaction forming lactam products



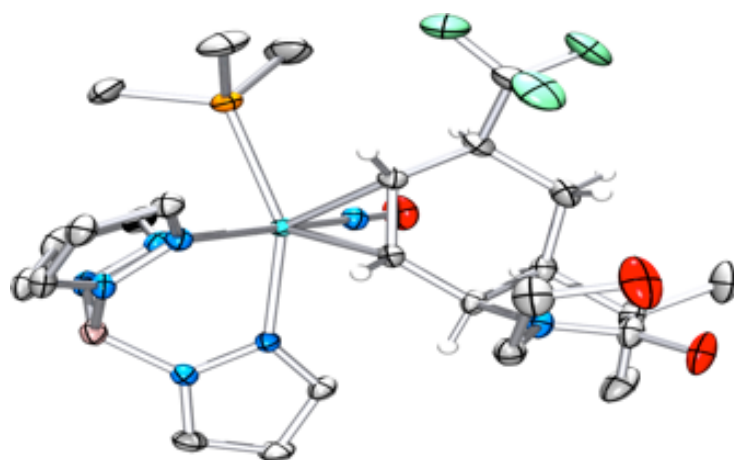


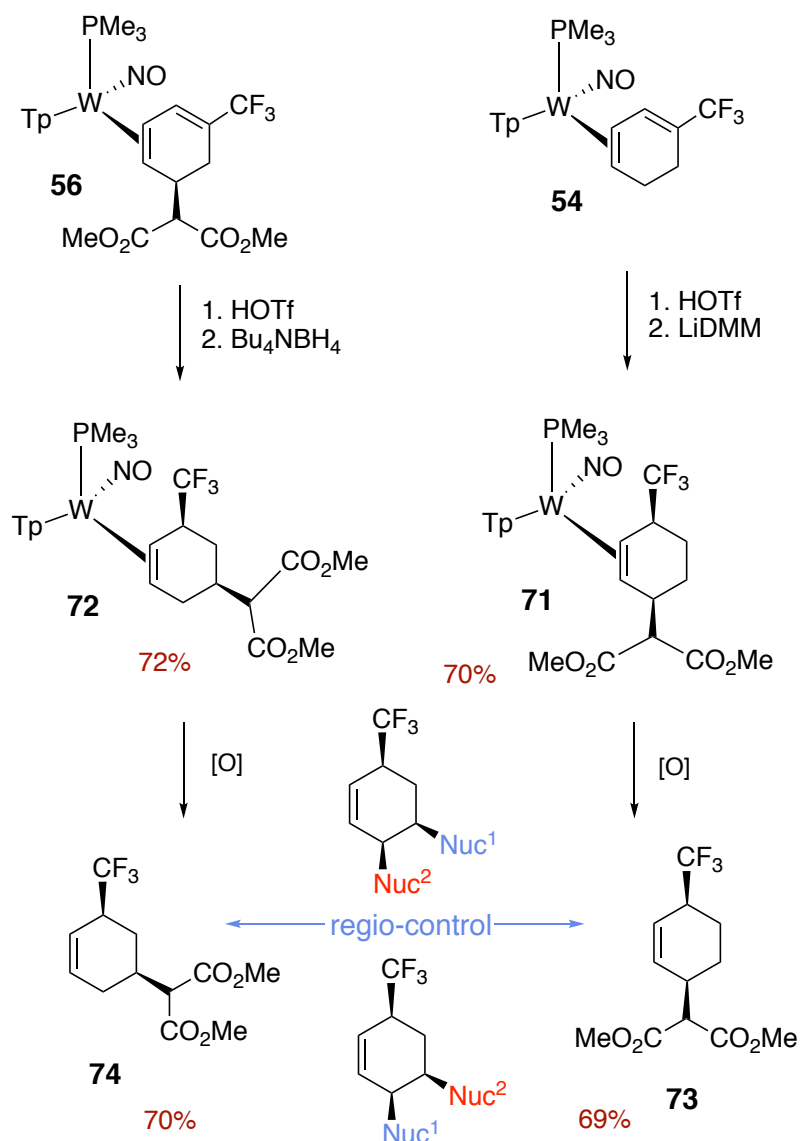
Figure 3.3: Crystal structure of lactam complex **67'**

The intramolecular lactam formation reaction was also attempted starting with the malonate diene **56**, which undergoes a similar cyclization reaction to yield the lactam **68**. The desired product can be formed selectively, without conversion of the second ester to an amide, by conducting the reaction at -30°C and minimizing the time spent at room temperature prior to workup. However, if the reaction is allowed to sit at room temperature with excess base, the second ester group begins to convert to an amide. For **67**, **67'**, and **68**, lactam formation occurs stereoselectively, with a cis-fused-ring juncture. Isolation of the organic lactam products was achieved by oxidation of the corresponding complexes **67** and **68** with NOPF_6 followed by chromatographic purification of the lactams, **69** (60%) and **70** (56%).

Finally, in an effort to demonstrate the regiochemical versatility of the trifluorotoluene system, the η^2 -diene complexes **54** and **56** were subjected to a second protonation followed by addition of dimethylmalonate (LiDMM) or a hydride (tetrabutylammonium borohydride). The resulting cyclohexene isomers **71** and **72** were then subjected to oxidation, liberating the 3,6-dialkylcyclohexene product **73**, and the 3,5-dialkylated counterpart **74** (Scheme 3.8). We note that these cyclohexene isomers of

differing substitution patterns can be selectively generated simply by adjusting the reaction sequence.

Scheme 3.8: Regiocontrol in cyclohexene formation from **54** and **56**



3.2.3 Substituent Effects on the Dearomatization of Substituted Benzenes

The observations in this study reveal that the CF₃ group enables a highly selective tandem addition of an electrophile (proton) and nucleophile to the ortho and meta carbons of the arene, respectively. This selectivity is in stark contrast to the reaction patterns and

stereochemistry observed with other types of arene substituents, or with other π -basic metal complexes that bind benzenes in an η^2 -fashion. Returning to Scheme 3.1, toluene (**43**, R = CH₃) forms a complex with either osmium or rhenium ([M] = [Os(NH₃)₅]²⁺ or [TpRe(CO)(MeIm)]), that consists of two constitutional isomers.⁸ The metal coordinates either *2,3- η^2* or *3,4- η^2* (shown), with the two isomers in dynamic equilibrium at ambient temperature. However, the addition of a proton or carbon electrophile (E⁺) is highly regioselective: addition to an ortho carbon results in development of a partial positive charge at the ipso carbon, as well as the unbound meta carbon (Scheme 3.1; **44**). Subsequent nucleophilic addition occurs to the latter carbon, resulting in a highly regio- and stereoselective overall 1,4-addition sequence (Scheme 3.1; electrophiles include a proton, acetals and Michael acceptors, and nucleophiles include enolates, and aryl lithiums).⁸ With Re(I) or Os(II), this reaction sequence has led to *cis*-3,6-disubstituted 1,4-cyclohexadienes (**45**).^{8,9} In the case of the tungsten dearomatization agent {TpW(NO)(PMe₃)}, attempts to carry out electrophilic addition reactions (e.g., protonation) with alkylated benzenes have been largely unsuccessful, owing to the oxidative decomposition of the metal.⁸ In comparison to the osmium and rhenium chemistry above, lithiated carbanions add to the complex Cr(CO)₃(η^6 -toluene) to give a mixture of ortho and meta products.²²

When the substituent is a π -donor group (X in Scheme 3.1) such as an aniline or anisole, the *2,3- η^2* isomer dominates (**46**),^{11,12,23-27} and carbon electrophiles (E⁺) add to the para carbon (C4). Subsequent nucleophilic addition to **47** at the uncoordinated meta carbon (C5) results in an overall vicinal addition to the cyclohexane ring, and this reaction sequence has led to *cis*-4,5-disubstituted cyclohex-2-enones (**48**) for {Os(NH₃)₅}²⁺,

{TpRe(CO)(MeIm)}, and {TpW(NO)(PMe₃)}.^{10,11} By comparison, anisole and aniline ligands also undergo regioselective nucleophilic addition at the meta carbon in Cr(CO)₃ complexes.²⁸

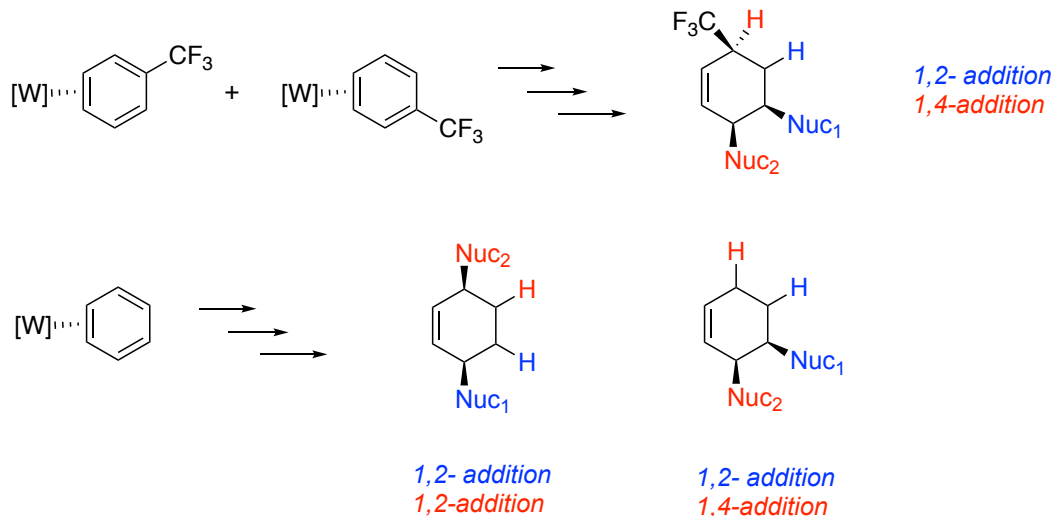
When M = {TpW(NO)(PMe₃)}, protonation of anilines provide 6*H*-anilinium complexes (**49**), which remarkably, can undergo an *additional electrophilic addition*, this time at the meta carbon (C5). Such action can be followed by a nucleophilic addition to the para carbon (C4).¹²⁻¹⁴ Subsequent oxidative decomplexation leads to *cis*-4,5-disubstituted cyclohex-2-enones (**50**) with a *complementary functionality* to that of **48** (Scheme 3.1). None of these scenarios effects a tandem addition across the ortho and meta carbons and, of particular note, none allow for the adjacent installation of two nucleophiles, such as is observed herein with CF₃Ph. This unique reactivity pattern results from the regiochemistry afforded by the CF₃Ph ligand. The initial 1,2-addition reaction at the ortho and meta carbons results in 1,3-diene complexes that can undergo a second tandem addition reaction. Upon protonation, the distortion of the allyl results in a selective 1,4-addition, which allows the installation of two adjacent nucleophiles. Notably, this coordination chemistry enables four stereoselective addition reactions in only two steps, starting from the simple aromatic ligand. Additionally, the resulting organic products can be synthesized in enantioenriched forms (see Chapter 7).

3.2.4 Comparison of η^2 -Benzene and η^2 -PhCF₃ Reactivity

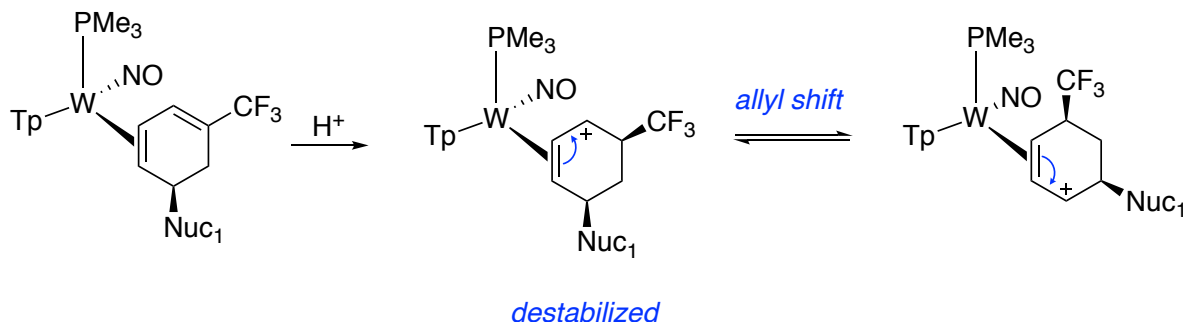
Until recently, we were not able to compare this EWG chemistry to the parent TpW(NO)(PMe₃)(η^2 -benzene) complex, because an oxidative decomposition pathway proceeded any desired reaction. However, optimized low-temperature conditions were recently exploited to tap into benzene chemistry, as discussed in Chapter 2. These advances

enabled us to better understand and distinguish the effects of the EWG vs. the asymmetric metal itself. Because the benzene ring lacks any substituents that could affect the subsequent selectivity of the first addition reaction, it provides a convenient control to compare with the $\text{TpW}(\text{NO})(\text{PMe}_3)(\eta^2\text{-PhCF}_3)$ complex.

Chapter 2 described the reactivity pattern observed with **1**, where initially there are no substituents to affect the regiochemistry of the first addition reaction. However, the identity of the initial nucleophile was shown to affect the regioselectivity of the second tandem electrophilic/nucleophilic reaction. The general reaction scheme established for **1** is shown in Scheme 3.9, as compared to the reactivity scheme shown for **52** as discussed in this chapter. The initial protonation of **1** and **52** occurs at the same position of the ring, giving allyl complexes with the positive charge localized distal to the PMe_3 . In the case of **1**, this protonation is directed by the metal; however, in the case of **52**, the asymmetric metal *and* the CF_3 group *both* influence the site of protonation. We propose that protonation at the alkene carbon that bears the CF_3 group would be less likely, leading to the selective protonation of the other uncoordinated alkene. For both **1** and **52** subsequent addition of a nucleophile results in a regio- and stereoselective 1,2-addition reaction, where the nucleophile adds to the allyl observed in solution.

Scheme 3.9: Reactivity pattern for η^2 -benzene and η^2 -PhCF₃

The first tandem addition reaction to **1** and **52** were accomplished with a similar range of nucleophiles to give η^2 -1,3-diene complexes. In Chapter 2, the regioselectivity of the second tandem electrophilic/reaction was investigated and discussed in terms of the influence of the first nucleophile. The steric and electronic features of the first nucleophile impact both the distortion of the allyl complex resulting from protonation, and the regioselectivity of the nucleophilic addition. Keeping these discussions in mind, the selectivity that was observed with **52** can be more clearly understood and discussed, taking into consideration the impact of the CF₃ group. Protonation of a generic TFT η^2 -1,3-diene complex would theoretically result in an allyl complex with the positive charge localized proximal to the PMe₃; however, we propose that a low kinetic barrier enables the tungsten metal to shift to either terminus of the allyl to give an η^2 -complex with a metal stabilized carbocation (Scheme 3.10).¹⁹ The electron withdrawing nature of the CF₃ group destabilizes the allyl with the positive charge localized adjacent to the CF₃, favoring the allyl complex with the positive charge distal to the PMe₃.

Scheme 3.10: Impact of CF₃ group on allyl complexes

The influence of the metal, first nucleophile, and CF₃ group can be analyzed by comparing the allyl complexes of certain corresponding η^2 -1,3-diene complexes. Figure 3.4 shows the ¹H NMR spectra of the allyl complexes (**13** and **75**) that result from protonation of **10A** and **57** respectively. As discussed in Chapter 2, the ¹H NMR peaks for the two protons at either terminus of the allyl complex **13** (5.07 and 5.47 ppm) differ by less than 0.5 ppm, reflecting an allyl species with little distortion. We proposed that the lack of distortion is due to the conflicting influences of the metal favoring the positive charge down, and the electron withdrawing cyano group destabilizing an adjacent positive charge. In contrast, the additional influence of the CF₃ group present in **75** results in a higher degree of distortion, with the positive charge localized distal to the PMe₃. 2D NMR analysis of **75** enabled the assignment of the allylic resonances, with the most downfield peak (6.02 ppm) having an NOE correlation with a Tp pyrazole proton trans to the PMe₃. The signal for the proton at the other terminus of the allyl has an NOE correlation with the PMe₃ ligand, and is ~1.5 ppm further upfield. These assignments support a distorted allyl with the positive charge localized down, and shows that the combined influence of the CF₃ group and the metal outweigh the influence of the cyano group.

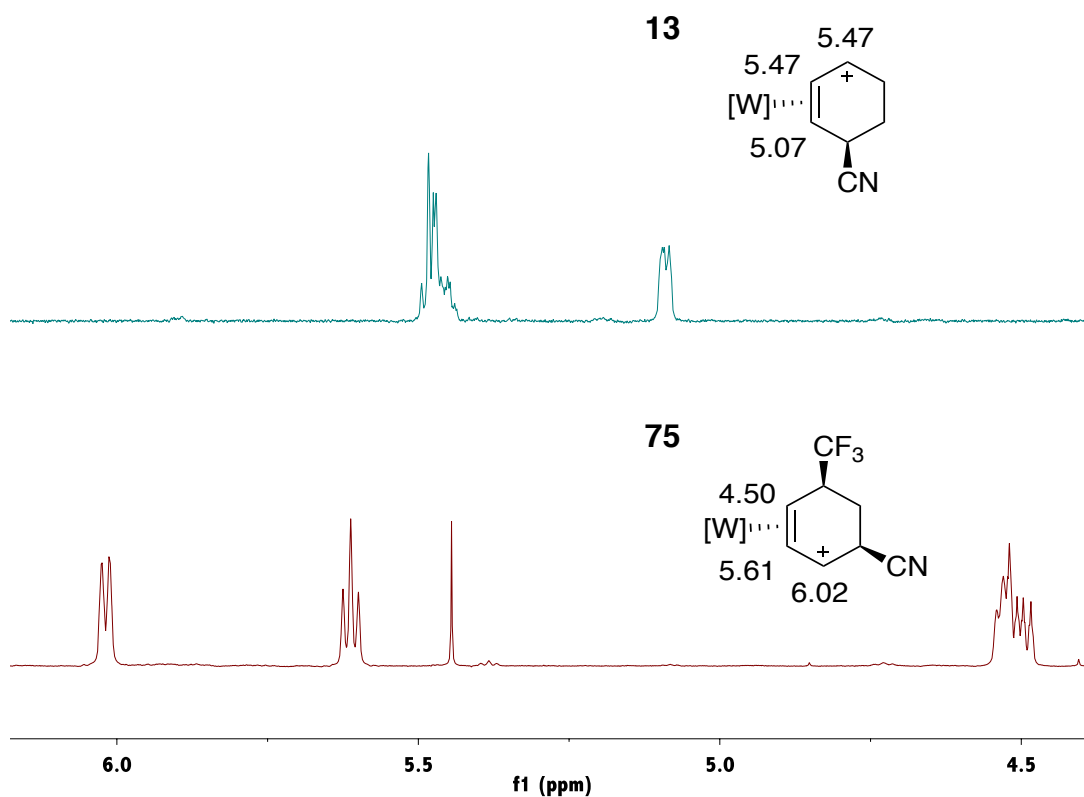
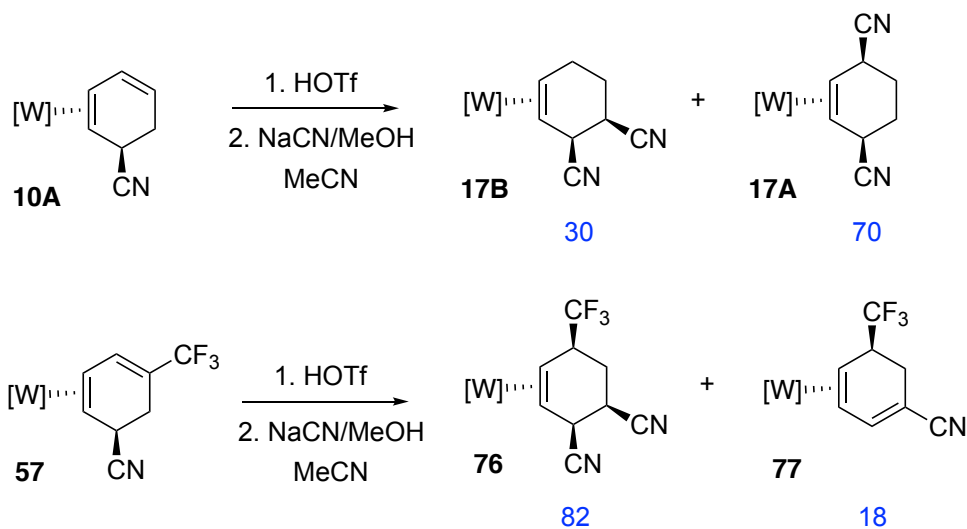


Figure 3.4: ^1H NMR comparison of **13** (top) and **75** (bottom)

The nucleophilic addition of NaCN to **13** and **75** provides further insight into the impact of the CF_3 group. As previously discussed, CN^- addition to **10A** gives a mix of products **17A** and **17B**, favoring the 1,4-substituted product (70:30, Scheme 3.11). The major product results from the nucleophile adding to the allyl that is observed in solution. In contrast, CN^- addition to the TFT allyl (**75**) predominantly gives complex **76**, with a 1,2 relationship between the two nucleophiles. In the minor product observed, CN^- acts as a base, giving the diene **77** instead of adding as a nucleophile adjacent to the CF_3 group. In this case, the presence of the CF_3 group completely changes the regioselectivity of nucleophilic addition, giving a 1,2-substitution pattern.

Scheme 3.11: Addition of a proton and NaCN to **10A** and **57**

Another telling reaction highlights the steric influence of the CF₃ group as well. Protonation of **6A** and **55** gives allyl complexes **12** and **59** (¹H NMR spectra of both allyl complexes are shown in Figure 3.5). In both cases, only one allyl species is observed, and both are similarly distorted, with the positive charge localized distal to the PMe₃ reflected by downfield shifts of the allylic proton signals (6.31 ppm and 6.14 ppm, respectively). These allyls were reacted in situ with LiDMM, a relatively bulky protected enolate (Scheme 3.12). Addition to **6A** gave exclusively the 1,4-substituted product **28A**, resulting from the nucleophile adding to the allyl that is not observed in solution. We attribute this selectivity to an unfavorable steric interaction between the first nucleophile and the incoming nucleophile at the adjacent position, which results in the selective addition para to the initial nucleophile. In contrast, LiDMM addition to **55** gives exclusively product **64B**, with the nucleophilic adding to the carbocation of the allyl observed in solution. This outcome illustrates the steric influence of the CF₃, which alters the regioselectivity and allows for the selective installation of two bulky nucleophiles adjacent two each other. This result is

reflective of the general trend that η^2 -1,3-dienes from the benzene complex (**1**) typically lead to 1,4-substituted products, while the η^2 -1,3-dienes from the TFT complex (**52**) lead to a 1,2-arrangement of the nucleophiles.

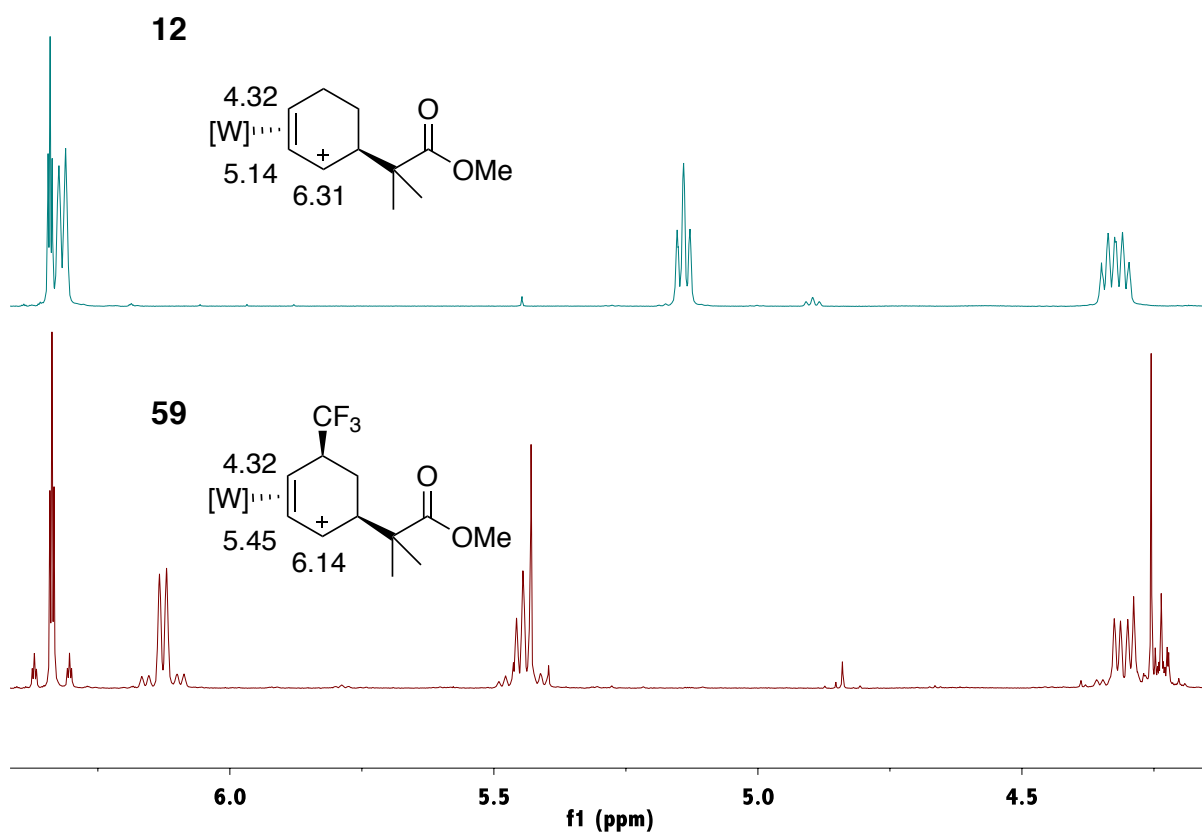
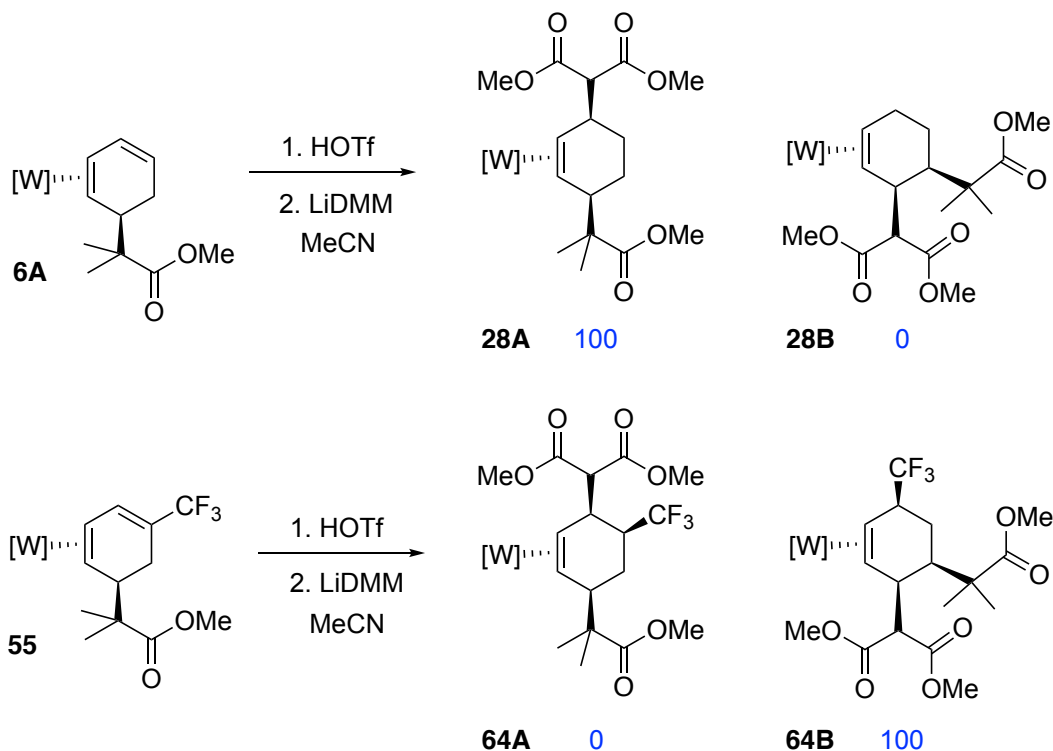


Figure 3.5: ¹H NMR comparison of **12** (top) and **59** (bottom)

Scheme 3.12: Addition of a proton and LiDMM to **6A** and **55**

3.2.5 CF₃-Substituted Cyclohexene Synthesis

The importance of trifluoromethyl groups in pharmaceuticals and agrochemicals has long been appreciated because of their increased hydrolytic, oxidative, metabolic and thermal stability, as well as increased bioavailability. While a multitude of methods are now available for installing CF₃ substituents,²⁹⁻³² few approaches have been described that generate CF₃-substituted cyclohexanes or cyclohexenes from aromatic precursors.²⁰ Hydrogenation of aromatics is a viable method,²⁰ but the present study appears to be the first report describing the synthesis of an alicyclic product from a metal-promoted addition to a CF₃-substituted arene, regardless of hapticity. The Cr(CO)₃(η⁶-PhCF₃) complex has been reported to undergo nucleophilic addition with a carbanion, which after oxidation

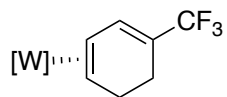
yields substituted arenes (33%) as a 3:7 mix of meta and para isomers, along with polyalkylated products.²² Additionally, an example has been reported for Ru²⁺ in which a nucleophile adds para to the CF₃ group,³³ but no organics were isolated. Cr(CO)₃(η⁶-arene) complexes with other withdrawing groups can lead to 5,6-trans-disubstituted cyclohexadienes, with the nucleophile preferentially adding ortho to the withdrawing group.^{34,35} Finally, Ritter et al. has shown that oxygen nucleophiles add selectively to the ortho position of trifluorotoluene, when coordinated as an η⁶ ligand to Ir(III).³⁶

3.3 Conclusions

The coordination of {TpW(NO)(PMe₃)} to trifluorotoluene dramatically enhances the basicity of the arene. Protonation occurs ortho to the CF₃ group, and the resulting arenium can undergo reactions with a range of nucleophiles to generate η²-1,3-diene complexes. These conjugated systems are susceptible to a second tandem addition sequence, resulting in trisubstituted cyclohexenes that can be oxidatively removed from the metal. Virtually all the reactions explored show exceptional regio- and stereochemical selectivity, typically resulting in a single detectible isomer. Efforts to extend this study to a broader range of reagents will be discussed in Chapter 4. Additionally, investigations into the chemistry of aromatics substituted with other types of EWGs, as well as fluorinated aromatic substrates with multiple substituents are under way.

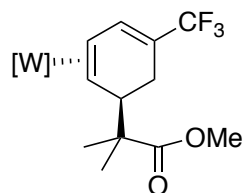
3.4 Experimental

General Methods: NMR spectra were obtained on 500, 600 or 800 MHz spectrometers. Chemical shifts are referenced to tetramethylsilane (TMS) utilizing residual ^1H or ^{13}C signals of the deuterated solvents as internal standards. Phosphorus NMR signals are referenced to 85% H_3PO_4 (δ 0.00) using a triphenyl phosphate external standard (δ -16.58). Chemical shifts are reported in ppm and coupling constants (J) are reported in hertz (Hz). Infrared Spectra (IR) were recorded on a spectrometer as a glaze on a diamond anvil ATR assembly, with peaks reported in cm^{-1} . Electrochemical experiments were performed under a nitrogen atmosphere. Most cyclic voltammetric data were recorded at ambient temperature at 100 mV/s, unless otherwise noted, with a standard three electrode cell from +1.8 V to -1.8 V with a platinum working electrode, *N,N*-dimethylacetamide (DMA) solvent, and tetrabutylammonium hexafluorophosphate (TBAH) electrolyte (~1.0 M). All potentials are reported versus the normal hydrogen electrode (NHE) using cobaltocenium hexafluorophosphate ($E_{1/2} = -0.78$ V, -1.75 V) or ferrocene ($E_{1/2} = 0.55$ V) as an internal standard. Peak separation of all reversible couples was less than 100 mV. All synthetic reactions were performed in a glovebox under a dry nitrogen atmosphere unless otherwise noted. All solvents were purged with nitrogen prior to use. Deuterated solvents were used as received from Cambridge Isotopes. When possible, pyrazole (Pz) protons of the (trispyrazolyl) borate (Tp) ligand were uniquely assigned (e.g., "PzB3") using two-dimensional NMR data (see Figure S1). If unambiguous assignments were not possible, Tp protons were labeled as "Pz3/5 or Pz4". All J values for Pz protons are 2 (± 0.4) Hz. BH peaks (around 4-5 ppm) in the ^1H -NMR spectra are not assigned due to their quadrupole broadening; however, confirmation of the BH group is provided by IR data (around 2500



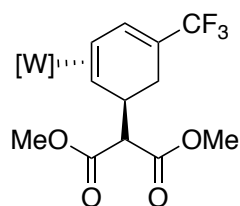
Compound 54. To a 4-dram vial charged with a stir pea were added **52** (500 mg, 0.770 mmol) followed by acetonitrile (5 mL, -30°C) and a 1M solution of HOTf in acetonitrile (0.81 mL, 0.81 mmol, -30°C), resulting in a homogeneous golden solution, which was allowed to sit for 20 min at -30°C. In a separate 4-dram vial, tetrabutylammonium borohydride (590 mg, 2.29 mmol) and acetonitrile (5 mL, -30°C) were combined and allowed to cool to -30°C for 15 min. The hydride solution was then added to the reaction vial with stirring and allowed to sit at -30°C for 22 h. The reaction was allowed to warm to room temperature and then removed from the glovebox. Precipitation was induced by adding H₂O (10 mL) and the pale yellow solid was collected on a 15 mL fine porosity fritted disc, washed with acetonitrile (0.7 mL) and pentane (5 mL) then desiccated overnight, yielding **54** (362 mg, 0.555 mmol, 72% yield). CV (DMAc) $E_{p,a} = +0.70$ V (NHE). IR: $\nu(\text{BH}) = 2488$ cm⁻¹, $\nu(\text{NO}) = 1556$ cm⁻¹. Anal. Calc'd for 3C₁₉H₂₆BF₃N₇OPW• acetonitrile: C, 35.53; H, 4.09; N, 15.45. Found: C, 35.67; H, 4.09; N, 15.36. ³¹P NMR (d⁶-acetone, δ): -12.04 ($J_{\text{WP}} = 278$). ¹H NMR (d⁶-acetone, δ): 8.11 (d, 1H, PzB3), 8.01 (d, 1H, PzA3), 7.95 (t, 2H, PzB5 & PzC5), 7.83 (d, 1H, PzA5), 7.59 (d, 1H, PzC3), 7.18 (m, 1H, H2), 6.39 (t, 1H, PzB4), 6.33 (t, 1H, PzC4), 6.32 (t, 1H, PzA4), 3.36 (m, 1H, H5x), 2.88 (m, 1H, H3), 2.78 (m, 1H, H5y), 2.56 (m, 1H, H6x), 1.96 (dd, $J = 16.2, 5.7$, 1H, H6y), 1.34 (buried, 1H, H4), 1.31 (d, $J = 8.5$, 9H, PMe₃). ¹³C NMR (d⁶-acetone, δ): 144.2 (PzB3), 142.5 (PzA3), 141.7 (PzC3), 137.7 (PzC5), 137.1 (PzB5), 136.9 (m, C2), 136.6 (PzA5), 126.6 (q, $J = 268.8$, CF₃), 118.6 (q, $J = 29.6$, C1),

107.2 (PzB4), 107.0 (PzC4), 106.6 (PzA4), 55.9 (C4), 47.8 (d, $J = 9.6$, C3), 26.9 (C5), 21.6 (C6), 13.8 (d, $J = 28.3$, PMe₃).



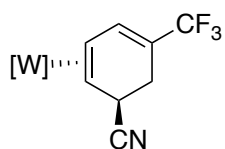
Compound 55. To a 4-dram vial were added **52** (1.00 g, 1.54 mmol) followed by acetonitrile (7.5 mL, -30°C), resulting in a homogeneous golden solution, which was kept at -30°C. After 15 min, a 1M solution of HOTf in acetonitrile (2.9 mL, 2.9 mmol, -30°C) was added, resulting in a homogeneous dark golden/red solution, which was allowed to sit for 15 min at -30°C. To this solution was added 1-methoxy-2-methyl-1-(trimethylsiloxy)propene (MMTP, 1.45 mL, 7.14 mmol, -30°C). After 17 h at -30°C, Et₃N was added to the reaction solution (2.00 mL, 14.3 mmol). A 150 mL medium porosity fritted disc was filled $\frac{3}{4}$ full of silica and set in 1:1 benzene/Et₂O. The reaction solution was loaded on the column and a pale yellow band was eluted with 120 mL of Et₂O. The filtrate was evaporated down *in vacuo*, then redissolved in minimal DCM and added to 50 mL stirring hexanes. The resulting pale yellow solid was collected on a 30 mL fine porosity fritted disc, washed with hexanes (2 x 10 mL) and desiccated overnight, yielding **55** (0.919 g, 1.22 mmol, 79% yield). CV (DMAc) $E_{p,a} = +0.69$ V (NHE). IR: $\nu(\text{BH}) = 2490$ cm⁻¹, $\nu(\text{CO}) = 1723$ cm⁻¹, $\nu(\text{NO}) = 1562$ cm⁻¹. Anal. Calc'd for C₂₄H₃₄BF₃N₇O₃PW: C, 38.37; H, 4.56; N, 13.05. Found: C, 38.19; H, 4.60; N, 12.79. ³¹P NMR (d⁶-acetone, δ): -12.07 ($J_{\text{WP}} = 281$). ¹H NMR (d⁶-acetone, δ): 8.12 (m, 2H, PzA3 & PzB3), 7.95 (d, 1H, Pz5), 7.94 (d, 1H, Pz5), 7.85 (d, 1H, Pz5), 7.68 (d, 1H, PzC3), 7.12 (bs, 1H, H2), 6.40 (t, 1H, Pz4), 6.35 (t, 1H, Pz4), 6.34 (t, 1H,

Pz4), 3.49 (d, $J = 8.4$, 1H, H5), 3.28 (s, 3H, H9), 2.93 (m, 1H, H3), 2.84 (m, 1H, H6x), 2.01 (d, $J = 17.4$, 1H, H6y), 1.28 (d, $J = 8.5$, 9H, PMe₃), 1.26 (s, 3H, H10), 1.10 (s, 3H, H11), 1.05 (d, $J = 9.7$, 1H, H4). ¹³C NMR (d⁶-acetone, δ): 178.9 (C8), 144.4 (Pz3), 142.3 (Pz3), 142.1 (Pz3), 137.9 (Pz5), 137.2 (Pz5), 137.1 (Pz5), 136.7 (m, C2), 126.7 (q, $J = 269$, CF₃), 117.3 (q, $J = 29.0$, C1), 107.4 (Pz4), 107.2 (Pz4), 106.5 (Pz4), 54.0 (C4), 52.3 (C7), 51.4 (C9), 49.2 (d, $J = 9.4$, C3), 43.2 (C5), 23.5 (C10), 22.6 (C11), 22.0 (C6), 13.9 (d, $J = 28.6$, PMe₃).



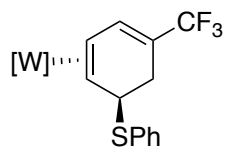
Compound 56. To a 4-dram vial were added **52** (500 mg, 0.770 mmol), acetonitrile (2.5 mL, -30°C) and a 1M solution of HOTf in acetonitrile (1.62 mL, 1.62 mmol, -30°C), resulting in a homogeneous yellow solution. The reaction solution was then added to a second 4-dram vial containing LiDMM (638 mg, 4.62 mmol) and acetonitrile (2 mL, -30°C). The first vial was rinsed with acetonitrile (0.5 mL, -30°C) and added to the reaction. The cloudy yellow mixture was allowed to react at -30°C for 19 h, at which point it had turned green. A 60 mL medium porosity fritted disc was filled $\frac{3}{4}$ full of silica and set in Et₂O. The reaction solution was loaded on the column and a pale yellow band was eluted with 50 mL of Et₂O. The filtrate was evaporated down *in vacuo*, then redissolved in minimal DCM and added to 30 mL stirring pentane. The resulting pale yellow solid was collected on a 15 mL fine porosity fritted disc, washed with pentane (2 x 5 mL) and desiccated overnight, yielding **56** (481 mg, 0.616 mmol, 80% yield). CV (DMAc) $E_{p,a} = +0.79$ V (NHE). IR: $\nu(\text{BH}) = 2486$ cm⁻¹, $\nu(\text{CO}) = 1750$ & 1728 cm⁻¹, $\nu(\text{NO}) = 1559$ cm⁻¹. Anal. Calc'd for

5C₂₄H₃₂BF₃N₇O₅PW•pentane: C, 37.74; H, 4.36; N, 12.32. Found: C, 37.50; H, 4.24; N, 11.99. ³¹P NMR (d⁶-acetone, δ): -11.99 (*J*_{WP} = 278). ¹H NMR (d⁶-acetone, δ): 8.14 (d, 1H, PzB3), 8.04 (d, 1H, PzA3), 7.97 (d, 1H, PzB5), 7.95 (d, 1H, PzC5), 7.83 (d, 1H, PzA5), 7.57 (d, 1H, PzC3), 7.21 (bs, 1H, H2), 6.41 (t, 1H, PzB4), 6.36 (t, 1H, PzA4), 6.33 (t, 1H, PzC4), 3.67 (s, 3H, H9), 3.59 (s, 1H, H7), 3.58 (buried, 1H, H5), 3.40 (s, 3H, H11), 2.89 (m, 2H, H3 & H6x), 1.95 (d, *J* = 17.3, 1H, H6y), 1.29 (d, *J* = 8.6, 9H, PMe₃), 1.13 (d, *J* = 9.6, 1H, H4). ¹³C NMR (d⁶-acetone, δ): 170.4 (C8), 169.8 (C10), 144.3 (PzB3), 142.7 (PzA3), 141.7 (PzC3), 137.9 (PzC5), 137.2 (PzB5), 136.9 (m, C2), 136.8 (PzA5), 126.3 (q, *J* = 269.1, CF₃), 115.6 (q, *J* = 30.0, C1), 107.4 (PzC4), 107.1 (PzB4), 106.7 (PzA4), 60.7 (C7), 57.8 (C4), 52.3 (C9), 51.9 (C11), 47.0 (d, *J* = 9.9, C3), 38.0 (C5), 25.0 (C6), 13.6 (d, *J* = 28.6, PMe₃).



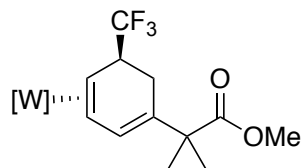
Compound 57. To a 4-dram vial charged with a stir pea were added **52** (100 mg, 0.154 mmol) followed by acetonitrile (0.5 mL, -30°C) and a 1M solution of HOTf in acetonitrile (0.23 mL, 0.23 mmol, -30°C), resulting in a homogeneous golden solution, which was allowed to sit for 15 min at -30°C. In a separate 4-dram vial, NaCN (40 mg, 0.82 mmol) and MeOH (0.5 mL, -30°C) were combined and allowed to cool to -30°C for 15 min. The reaction solution was then added to the vial with NaCN while stirring. The initial vial was rinsed with MeOH (0.4 mL, -30°C) and this was added to the reaction solution. The reaction was then left at -30°C for 16 h at which point a yellow solid had precipitated. The reaction was allowed to stir at room temperature for 5 min, then further precipitation was induced by adding H₂O (0.5 mL). The pale yellow solid was collected on a 15 mL fine porosity fritted

disc, washed with H₂O (3 mL) and pentane (3 x 3 mL) then desiccated overnight, yielding **57** (82 mg, 0.12 mmol, 78% yield). CV (DMAc) $E_{p,a} = +0.94$ V (NHE). IR: $\nu(\text{BH}) = 2490$ cm⁻¹, $\nu(\text{CN}) = 2225$ cm⁻¹, $\nu(\text{NO}) = 1572$ cm⁻¹. ³¹P NMR (d⁶-acetone, δ): -11.84 ($J_{\text{WP}} = 276$). ¹H NMR (CD₃CN, δ): 8.05 (d, 1H, PzB3), 7.88 (t, 2H, PzB5 & PzC5), 7.81 (d, 1H, PzA3), 7.80 (d, 1H, PzA5), 7.48 (d, 1H, PzC3), 7.33 (m, 1H, H2), 6.38 (t, 1H, PzB4), 6.32 (overlapping t, 2H, PzA4 & PzC4), 3.83 (dm, $J = 6.8$, 1H, H5), 2.91 (m, 1H, H3), 2.77 (dm, $J = 16.6$, 1H, H6x), 2.31 (d, $J = 16.6$, 1H, H6y), 1.42 (dm, $J = 9.6$, 1H, H4), 1.23 (d, $J = 8.8$, 9H, PMe₃). ¹³C NMR (CD₃CN, δ): 144.5 (PzB3), 142.6 (PzA3), 142.0 (PzC3), 138.2 (PzC5), 137.8 (PzB5), 137.7 (m, C2), 137.3 (PzA5), 127.7 (CN), 126.1 (q, $J = 268.7$, CF₃), 115.0 (q, $J = 30.3$, C1), 107.7 (PzB4), 107.4 (PzA4/PzC4), 107.2 (PzA4/PzC4), 56.7 (C4), 46.0 (d, $J = 10.3$, C3), 29.5 (C5), 25.6 (C6), 13.6 (d, $J = 29.6$, PMe₃).



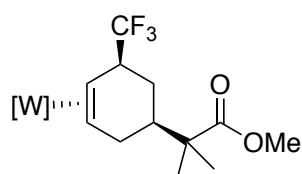
Compound 58. To a 4-dram vial charged with a stir pea were added **52** (100 mg, 0.154 mmol) followed by acetonitrile (1 mL, -30°C) and a 1M solution of HOTf in acetonitrile (0.32 mL, 0.32 mmol, -30°C), resulting in a homogeneous golden solution, which was allowed to sit for 15 min at -30°C. NaSPh (114 mg, 0.863 mmol) was added with stirring, and then the heterogeneous reaction was allowed to sit at -30°C for 22 h. Further precipitation was induced by adding H₂O (3 mL). The pale yellow solid was collected on a 15 mL fine porosity fritted disc, washed with H₂O (2 mL) and pentane (2 x 3 mL) then desiccated overnight, yielding **58** (96 mg, 0.13 mmol, 84% yield). ¹H NMR (d⁶-acetone, δ): 8.10 (d, 1H, Pz3/5), 8.06 (d, 1H, Pz3/5), 8.01 (d, 1H, Pz3/5), 7.98 (d, 1H, Pz3/5), 7.91 (d, $J =$

7.7, 2H, Ar-H), 7.87 (d, 1H, Pz3/5), 7.67 (buried, 1H, Ar-H), 7.66 (d, 1H, Pz3/5), 7.55 (t, $J = 7.7$, 2H, Ar-H), 6.73 (bs, 1H, H2), 6.41 (t, 1H, Pz4), 6.40 (t, 1H, Pz4), 6.36 (t, 1H, Pz4), 4.38 (d, $J = 7.8$, 1H, H5), 2.97 (dd, $J = 18.2, 7.3$, 1H, H6x), 2.71 (m, 2H, H3 & H6y), 1.82 (d, $J = 9.2$, 1H, H4), 1.24 (d, $J = 8.7$, 9H, PMe₃).



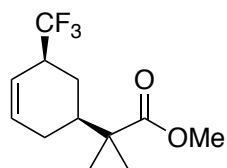
Compound 60. To a 4-dram vial were added **55** (100 mg, 0.133 mmol) followed by acetonitrile (2 mL, -30°C), resulting in a heterogeneous mixture. A 1M solution of HOTf in acetonitrile (0.27 mL, 0.27 mmol, -30°C) was then added, resulting in a homogeneous yellow solution, which was allowed to sit for 17 h at -30°C. The reaction solution was allowed to warm to room temperature over 1 h, then Et₃N (67 mg, 0.67 mmol) was added, and the reaction was stirred for 28 h. Completion of the reaction was checked by ³¹P NMR, then the yellow solution was removed from the glovebox, diluted with DCM (20 mL) and washed with H₂O (15 mL). The aqueous layer was back-extracted with DCM (2 x 20 mL), then the combined organic layers were dried over MgSO₄ and evaporated *in vacuo*. The film was redissolved in minimal DCM and added to stirring hexanes (15 mL). The resulting yellow solid was collected on a 15 mL fine porosity fritted disc and desiccated overnight, yielding **60** (78 mg, 0.10 mmol, 78% yield). CV (DMAc) $E_{p,a} = +0.59$ V (NHE). IR: $\nu(\text{BH}) = 2489$ cm⁻¹, $\nu(\text{CO}) = 1715$ cm⁻¹, $\nu(\text{NO}) = 1505$ cm⁻¹. Anal. Calc'd for C₂₄H₃₄BF₃N₇O₃PW•H₂O: C, 37.48; H, 4.72; N, 12.75. Found: C, 37.24; H, 4.56; N, 12.76. ³¹P NMR (CD₃CN, δ): -11.44 ($J_{\text{WP}} = 279$). ¹H NMR (d⁶-acetone, δ): 8.19 (d, 1H, PzA3), 8.08 (d, 1H, PzB3), 7.96 (m, 2H,

PzB5 & PzC5), 7.82 (d, 1H, PzA5), 7.58 (d, 1H, PzC3), 6.49 (dd, $J = 6.2, 3.0$, 1H, H4), 6.40 (t, 1H, PzB4), 6.33 (t, 1H, PzC4), 6.31 (t, 1H, PzA4), 3.57 (s, 3H, H9), 3.47 (m, 1H, H1), 2.89 (ddd, $J = 17.5, 8.2, 2.6$, 1H, H6x), 2.65 (m, 1H, H2), 2.24 (dt, $J = 17.5, 1.4$, 1H, H6y), 1.53 (ddd, $J = 9.8, 6.3, 1.6$, 1H, H3), 1.34 (s, 3H, H10), 1.34 (s, 3H, H11), 1.28 (d, $J = 8.3$, 9H, PMe_3). ^{13}C NMR (d^6 -acetone, δ): 177.9 (C8), 145.0 (PzA3), 144.0 (PzB3), 141.6 (PzC3), 137.8 (PzC5), 137.1 (PzB5), 136.4 (PzA5), 132.5 (q, $J = 283.5$, CF_3), 128.5 (C4), 127.9 (C5), 107.2 (PzB4), 107.0 (PzC4), 106.4 (PzA4), 51.8 (C9), 51.0 (C3), 49.8 (d, $J = 13.2$, C2), 47.3 (C7), 45.6 (q, $J = 23.4$, C1) 25.9 (C10), 25.0 (C11), 23.1 (C6), 12.8 (d, $J = 28.3$, PMe_3).



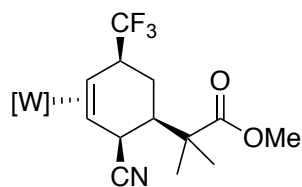
Compound 61. To a 4-dram vial were added **55** (135 mg, 0.180 mmol) followed by acetonitrile (1 mL, -30°C), resulting in a heterogeneous mixture. In a separate 4-dram vial charged with a stir bar, tetrabutylammoniumborohydride (374 mg, 1.45 mmol) was dissolved in acetonitrile (1 mL, -30°C). Both vials were cooled to -30°C for 15 min. Then a 1M solution of HOTf in acetonitrile (0.20 mL, 0.20 mmol, -30°C) was added to the vial with complex, resulting in a homogeneous yellow solution, which was allowed to sit for 10 min at -30°C . This yellow solution was added to the Bu_4NBH_4 /acetonitrile solution while stirring, resulting in a homogenous blue solution. The first vial was rinsed with acetonitrile (0.7 mL, -30°C) and added to the reaction solution. The reaction was left for 15 h at -30°C . The pale yellow mixture was removed from the glovebox and further precipitation was induced by adding H_2O (15 mL). The resulting pale yellow solid was collected on a 15 mL

fine porosity fritted disc, washed with H₂O (1 mL), acetonitrile (0.5 mL), and pentane (2 mL) and desiccated overnight, yielding **61** (107 mg, 0.141 mmol, 79% yield). CV (DMAc) $E_{p,a} = +0.54$ V (NHE). IR: $\nu(\text{BH}) = 2484$ cm⁻¹, $\nu(\text{CO}) = 1721$ cm⁻¹, $\nu(\text{NO}) = 1547$ cm⁻¹. Anal. Calc'd for 2C₂₄H₃₆BF₃N₇O₃PW•3DCM: C, 34.78; H, 4.46; N, 11.13. Found: C, 34.47; H, 4.31; N, 11.43. ³¹P NMR (d⁶-acetone, δ): -11.85 ($J_{\text{WP}} = 279$). ¹H NMR (d⁶-acetone, δ): 8.12 (d, 1H, PzB3), 7.93 (m, 2H, PzB5 & PzC5), 7.82 (d, 1H, PzA3/PzA5), 7.81 (d, 1H, PzA3/PzA5), 7.41 (d, 1H, PzC3), 6.39 (t, 1H, PzB4), 6.31 (t, 1H, PzC4), 6.30 (t, 1H, PzA4), 3.68 (s, 3H, H9), 3.54 (m, 1H, H1), 3.00 (td, $J = 13.7, 4.0$, 1H, H4x), 2.79 (m, 1H, H2), 2.35 (m, 1H, H5), 2.20 (d, $J = 13.7$, 1H, H4y), 1.92 (m, 1H, H6x), 1.30 (m, 1H, H6y), 1.23 (d, $J = 8.3$, 9H, PMe₃), 1.21 (s, 3H, H10), 1.15 (s, 3H, H11), 1.07 (d, $J = 11.3$, 1H, H3). ¹³C NMR (d⁶-acetone, δ): 178.6 (C8), 144.4 (PzA3), 144.3 (PzB3), 141.6 (PzC3), 137.5 (Pz5), 137.1 (Pz5), 136.9 (Pz5), 132.6 (q, $J = 280.0$, CF₃), 107.1 (Pz4), 107.0 (Pz4), 106.5 (Pz4), 55.4 (C3), 51.7 (C9), 46.3 (C7), 43.5 (q, $J = 24.1$, C1), 42.8 (d, $J = 13.2$, C2), 38.6 (C5), 28.1 (C4), 24.6 (C10), 24.4 (m, C6), 20.5 (C11), 13.2 (d, $J = 28.0$, PMe₃).



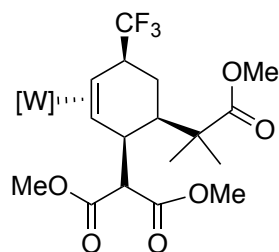
Compound 62. (Outside of glovebox) To a 4-dram vial charged with stir pea was added NOPF₆ (39 mg, 0.22 mmol). In a separate 4-dram vial, **61** (108 mg, 0.143 mmol) and acetone (2 mL) were combined then added to the vial with NOPF₆ while stirring, resulting in an immediate color change from pale yellow to brown. The first vial was rinsed with acetone (1 mL), and this was added to reaction vial. The reaction mixture was stirred for 21

h, at which point it had turned into a golden heterogeneous mixture, and was then evaporated *in vacuo* almost to dryness. DCM (1 mL) was added to the vial and then this solution was added to stirring pentane (20 mL). The resulting cloudy mixture was filtered over a 15 mL fine porosity fritted disc and washed with pentane (5 mL). The clear filtrate was evaporated *in vacuo* and the resulting oil was loaded onto a 250 μm silica preparatory plate with DCM (3 x 0.3 mL) and eluted with 10% EtOAc/hexanes (HPLC grade, 200 mL). A KMnO_4 active band at R_f 0.61-0.84 was collected and sonicated in EtOAc (HPLC grade, 35 mL) for 15 min. The silica was filtered off on a 30 mL fine porosity fritted disc and washed with EtOAc (HPLC grade, 2 x 15 mL) and hexanes (HPLC grade, 10 mL). The filtrate was evaporated *in vacuo* yielding **62** (20 mg, 0.078 mmol, 55% yield). IR: $\nu(\text{CO}) = 1728 \text{ cm}^{-1}$. Anal. Calc'd for $\text{C}_{12}\text{H}_{17}\text{F}_3\text{O}_2$: C, 57.59; H, 6.85. Found: C, 57.69; H, 6.84. ^1H NMR (d^6 -acetone, δ): 5.99 (m, 1H, H3), 5.60 (dm, $J = 10.1$, 1H, H4), 3.65 (s, 3H, OMe), 3.12 (m, 1H, H5), 2.00 (m, 2H, H1 & H2x), 1.92 (m, 2H, H2y & H6x), 1.27 (q, $J = 12.1$, 1H, H6y), 1.18 (s, 3H, H1'Me), 1.14 (s, 3H, H1'Me). ^{13}C NMR (d^6 -acetone, δ): 177.7 (CO), 132.6 (C3), 128.4 (q, $J = 278.5$, CF_3), 120.9 (q, $J = 3.8$, C4), 52.0 (OMe), 45.5 (C1'), 42.7 (q, $J = 26.7$, C5), 40.8 (C1), 27.0 (C2), 24.5 (q, $J = 2.9$, C6), 22.2 (2C, C1'Me₂).



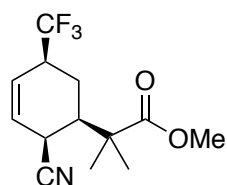
Compound 63. To a 4-dram vial were added **55** (150 mg, 0.200 mmol) followed by acetonitrile (2 mL, -30°C), resulting in a heterogeneous mixture that was allowed to sit for 15 min at -30°C . A 1M solution of HOTf in acetonitrile (0.22 mL, 0.22 mmol, -30°C) was then

added, resulting in a homogeneous yellow solution, which was allowed to sit for 10 min at -30°C. NaCN (20 mg, 0.41 mmol) and MeOH (1.2 mL) were added to a separate 4-dram vial charged with a stir bar. The reaction solution was added to the NaCN/MeOH with stirring, which resulted in a homogenous yellow solution that was allowed to sit at -30°C for 15 h. The reaction, which had spontaneously precipitated out a pale yellow solid, was allowed to warm to room temperature over 3 h and then the yellow solid was collected on a 15 mL fine porosity fritted disc and desiccated overnight, yielding **63** (118 mg, 0.152 mmol, 76% yield). CV (DMAc) $E_{p,a} = +0.80$ V (NHE). IR: $\nu(\text{BH}) = 2484$ cm^{-1} , $\nu(\text{CN}) = 2222$ cm^{-1} , $\nu(\text{CO}) = 1723$ cm^{-1} , $\nu(\text{NO}) = 1559$ cm^{-1} . Anal. Calc'd for $\text{C}_{25}\text{H}_{35}\text{BF}_3\text{N}_8\text{O}_3\text{PW}$: C, 38.58; H, 4.53; N, 14.40. Found: C, 38.42; H, 4.60; N, 14.23. ^{31}P NMR (CDCl_3 , δ): -12.73 ($J_{\text{WP}} = 278$). ^1H NMR (CDCl_3 , δ): 8.03 (d, 1H, PzB3), 7.73 (d, 1H, PzA3), 7.73 (d, 1H, PzC5), 7.71 (d, 1H, PzB5), 7.63 (d, 1H, PzA5), 7.15 (d, 1H, PzC3), 6.29 (t, 1H, PzB4), 6.24 (t, 1H, PzC4), 6.23 (t, 1H, PzA4), 3.79 (m, 1H, H1), 3.73 (s, 3H, H9), 3.53 (bs, 1H, H4), 2.75 (m, 1H, H2), 2.47 (dm, $J = 12.8$, 1H, H5), 1.88 (ddm, $J = 13.2, 6.5$, 1H, H6x), 1.75 (q, $J = 13.2$, 1H, H6y), 1.39 (s, 3H, H11), 1.38 (s, 3H, H10), 1.34 (d, $J = 11.4$, 1H, H3), 1.19 (d, $J = 8.5$, 9H, PMe_3). ^{13}C NMR (CDCl_3 , δ): 177.5 (C8), 144.1 (PzB3), 143.4 (PzA3), 140.7 (PzC3), 136.7 (Pz5), 136.6 (Pz5), 136.5 (Pz5), 130.5 (q, $J = 279.0$, CF_3), 126.4 (C12), 106.6 (Pz4), 106.3 (Pz4), 106.3 (Pz4), 59.2 (C3) 51.9 (C9), 45.2 (C7), 42.5 (m, C1), 39.1 (m, C2), 38.8 (C5), 31.5 (C4), 25.0 (C10), 23.3 (m, C6), 21.5 (C11), 13.6 (d, $J = 29.4$, PMe_3).



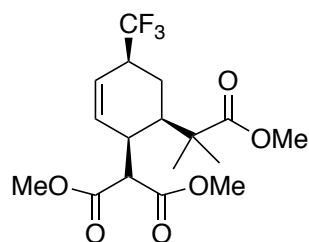
Compound 64. To a 4-dram vial were added **55** (100 mg, 0.133 mmol) followed by acetonitrile (1.5 mL, -30°C), resulting in a heterogeneous mixture. A 1M solution of HOTf in acetonitrile (0.27 mL, 0.27 mmol, -30°C) was then added, resulting in a homogeneous yellow solution, which was allowed to sit for 20 min at -30°C. The reaction solution was then added to a 4-dram vial containing LiDMM (111 mg, 0.800 mmol) and allowed to react at -30°C for 22 h. The reaction was allowed to warm to room temperature then Et₃N (0.13 mL, 0.93 mmol) was added. The pale yellow solution was removed from the glovebox, diluted with DCM (40 mL) and washed with H₂O (20 mL). The aqueous layer was back-extracted with DCM (20 mL), then the combined organic layers were dried over MgSO₄ and evaporated *in vacuo*. The film was redissolved in minimal DCM and added to stirring pentane (20 mL). The resulting pale solid was collected on a 15 mL fine porosity fritted disc, washed with pentane (3 mL) and desiccated overnight, yielding **64** (97 mg, 0.11 mmol, 82% yield). CV (DMAc) $E_{p,a} = +0.54$ V (NHE). IR: $\nu(\text{BH}) = 2483$ cm⁻¹, $\nu(\text{CO}) = 1749$ & 1718 cm⁻¹, $\nu(\text{NO}) = 1544$ cm⁻¹. Anal. Calc'd for 2C₂₉H₄₂BF₃N₇O₇PW•DCM: C, 38.27; H, 4.68; N, 10.59. Found: C, 38.12; H, 4.73; N, 10.59. ³¹P NMR (d⁶-acetone, δ): -12.02 ($J_{\text{WP}} = 279$). ¹H NMR (d⁶-acetone, δ): 8.09 (d, 1H, PzB3), 7.95 (d, 1H, PzA3), 7.92 (m, 2H, PzB5 & PzC5), 7.80 (d, 1H, PzA5), 7.24 (d, 1H, PzC3), 6.36 (t, 1H, PzB4), 6.31 (overlapping triplets, 2H, PzA4 & PzC4), 4.03 (d, $J = 2.6$, 1H, H12), 3.74 (bs, 2H, H1 & H4), 3.69 (s, 3H, H9), 3.62 (s, 3H, H14), 3.25 (s, 3H, H16), 2.79 (m, 1H, H2), 2.55 (m, 1H, H5), 1.69 (ddm, $J = 12.7, 6.1$, 1H, H6x), 1.62

(q, $J = 12.7$, 1H, H6y), 1.35 (s, 3H, H10), 1.27 (s, 3H, H11), 1.17 (d, $J = 8.4$, 9H, PMe_3), 1.11 (d, $J = 11.6$, 1H, H3). ^{13}C NMR (d^6 -acetone, δ): 178.4 (C8), 170.6 (2C, C13 & C15), 144.9 (PzB3), 144.5 (PzA3), 141.7 (PzC3), 137.5 (PzC5), 137.2 (2C, PzA5 & PzB5), 131.8 (q, $J = 279.5$, CF_3), 107.0 (Pz4), 106.9 (Pz4), 106.4 (Pz4), 59.8 (C3) 56.2 (C12), 52.2 (C9), 52.1 (C14), 52.0 (C16), 45.5 (C7), 43.7 (q, $J = 24.8$, C1), 42.5 (C5), 40.9 (d, $J = 12.6$, C2), 38.4 (C4), 27.9 (C10), 23.2 (C11), 22.4 (m, C6), 13.5 (d, $J = 28.5$, PMe_3).



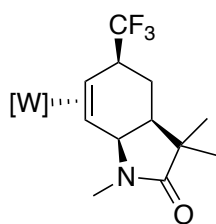
Compound 65. (Outside of glovebox) To a 4-dram vial charged with a stir pea were added NOPF_6 (42 mg, 0.24 mmol) followed by **63** (118 mg, 0.152 mmol). Acetone (4 mL) was added to the vial while stirring, resulting in an immediate color change from pale yellow to brown. The reaction solution was stirred for 4 h, at which point it had turned back to a golden color, and then evaporated *in vacuo* to ~ 0.5 mL. DCM (0.5 mL) was added to the vial and then this solution was added to stirring pentane (20 mL). The resulting cloudy mixture was filtered over a 30 mL fine porosity fritted disc and the precipitate was washed with pentane (5 mL). The filtrate was evaporated *in vacuo* and the resulting oil was loaded onto a 250 μm silica preparatory plate with DCM (3 x 0.3 mL) and eluted with 25% EtOAc/hexanes (HPLC grade, 200 mL). A KMnO_4 active band at R_f 0.36-0.59 was collected and sonicated in EtOAc (HPLC grade, 25 mL) for 20 min. The silica was filtered off on a 30 mL medium porosity fritted disc and washed with EtOAc (HPLC grade, 2 x 20 mL). The filtrate was evaporated *in vacuo* yielding **65** (22 mg, 0.079 mmol, 52% yield). IR: $\nu(\text{CN}) =$

2236, $\nu(\text{CO}) = 1726 \text{ cm}^{-1}$. Anal. Calc'd for $\text{C}_{13}\text{H}_{16}\text{F}_3\text{NO}_2$: C, 56.72; H, 5.86; N, 5.09. Found: C, 57.00; H, 6.05; N, 4.90. ^1H NMR (d^6 -acetone, δ): 6.12 (ddd, $J = 9.8, 5.8, 2.7$, 1H, H3), 5.91 (dm, $J = 9.8$, 1H, H4), 3.69 (s, 3H, OMe), 3.61 (m, 1H, H2), 3.34 (m, 1H, H5), 2.23 (ddd, $J = 12.8, 4.4, 1.8$, 1H, H1), 2.13 (ddq, $J = 13.2, 5.8, 1.6$, 1H, H6x), 1.72 (m, 1H, H6y), 1.35 (s, 6H, H1'Me₂). ^{13}C NMR (d^6 -acetone, δ): 176.9 (CO), 128.8 (C3), 127.8 (q, $J = 278.4$, CF₃), 125.1 (q, $J = 3.7$, C4), 119.2 (CN), 52.3 (OMe), 45.3 (C1'), 43.0 (q, $J = 27.3$, C5), 42.4 (C1), 28.5 (C2), 23.0 (C1'Me), 22.8 (C1'Me), 22.2 (q, $J = 2.9$, C6).



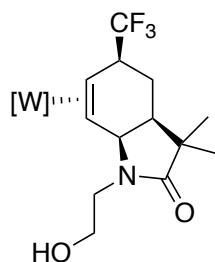
Compound 66. (Outside of glovebox) To a 4-dram vial charged with a stir pea was added NOPF_6 (29 mg, 0.17 mmol). In a separate 4-dram vial, **64** (97 mg, 0.11 mmol) was dissolved in acetone (1.5 mL) and added to the vial with NOPF_6 while stirring, resulting in an immediate color change from pale yellow to brown. The first vial was rinsed with acetone (0.5 mL), and this was added to the reaction vial. The reaction solution was stirred for 2 h, at which point it had turned back to a golden color, and was then evaporated *in vacuo* to dryness. DCM (1.3 mL) was added to the vial and then this solution was added to stirring hexanes (20 mL). The resulting cloudy mixture was filtered over a 15 mL fine porosity fritted disc and washed with hexanes (5 mL). The clear filtrate was evaporated *in vacuo* and the resulting oil was loaded onto a 250 μm silica preparatory plate with DCM (3 x 0.3 mL) and eluted with 20% EtOAc/hexanes (HPLC grade, 200 mL). A KMnO_4 active band at R_f 0.43-0.63 was collected and sonicated in EtOAc (HPLC grade, 25 mL) for 15 min. The silica

was filtered off on a 30 mL medium porosity fritted disc and washed with EtOAc (HPLC grade, 2 x 20 mL). The filtrate was evaporated *in vacuo* yielding **66** (32 mg, 0.078 mmol, 71% yield). IR: $\nu(\text{CO}) = 1730 \text{ cm}^{-1}$. Anal. Calc'd for $\text{C}_{19}\text{H}_{31}\text{F}_3\text{O}_6$: C, 53.68; H, 6.10. Found: C, 53.54; H, 6.11. ^1H NMR (d^6 -acetone, δ): 6.04 (ddd, $J = 10.2, 5.5, 2.6$, 1H, H2), 5.67 (dq, $J = 10.2, 1.6$, 1H, H3), 3.88 (d, $J = 2.4$, 1H, H1'), 3.72 (s, 3H, OMe), 3.67 (s, 3H, OMe), 3.60 (s, 3H, OMe), 3.20 (m, 1H, H1), 3.13 (m, 1H, H4), 2.07 (ddd, $J = 13.2, 5.0, 1.9$, 1H, H6), 2.01 (ddq, $J = 13.1, 5.9, 1.6$, 1H, H5x), 1.62 (td, $J = 13.1, 11.6$, 1H, H5y), 1.29 (s, 3H, H6'Me), 1.28 (s, 3H, H6'Me). ^{13}C NMR (d^6 -acetone, δ): 177.7 (CO), 170.0 (CO), 169.5 (CO), 134.0 (C2), 128.1 (q, $J = 278.4$, CF_3), 122.2 (q, $J = 3.7$, C3), 53.0 (OMe), 52.3 (2C, OMe & OMe), 51.7 (C1'), 45.6 (C6), 44.9 (C6'), 43.3 (q, $J = 27.2$, C4), 36.3 (C1), 25.8 (C6'Me), 23.8 (C6'Me), 20.3 (q, $J = 3.0$, C5).



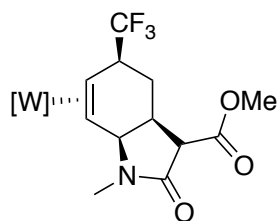
Compound 67. To a 4-dram vial were added **55** (110 mg, 0.146 mmol) followed by acetonitrile (1.1 mL, -30°C), resulting in a heterogeneous mixture. A 1M solution of HOTf in acetonitrile (0.30 mL, 0.30 mmol, -30°C) was then added, resulting in a homogeneous yellow solution, which was allowed to sit for 30 min at -30°C . 2M $\text{H}_2\text{NMe}/\text{THF}$ (1.47 mL, 2.94 mmol, -30°C) was added to the reaction solution, which was left for 20 h at -30°C . The reaction was then allowed to warm to room temperature and left for 19 h, until a single peak was observed by ^{31}P NMR, indicating that the reaction was complete. The pale yellow solution was then removed from the glovebox, diluted with DCM (40 mL) and washed with H_2O (1x 40 mL, 1x 20 mL). The aqueous layer was back-extracted with DCM (2 x 20 mL),

then the combined organic layers were washed with brine (20 mL), dried over MgSO_4 , and evaporated *in vacuo*. The film was redissolved in minimal DCM and added to stirring pentane (20 mL). The resulting pale solid was collected on a 15 mL fine porosity fritted disc, washed with pentane (3 mL) and desiccated overnight, yielding **67** (80 mg, 0.11 mmol, 73% yield). CV (DMAc) $E_{p,a} = +0.64$ V (NHE). IR: $\nu(\text{BH}) = 2488$ cm^{-1} , $\nu(\text{CO}) = 1674$ cm^{-1} , $\nu(\text{NO}) = 1553$ cm^{-1} . Anal. Calc'd for $\text{C}_{24}\text{H}_{35}\text{BF}_3\text{N}_8\text{O}_2\text{PW}\cdot\text{DCM}$: C, 35.95; H, 4.47; N, 13.42. Found: C, 35.56; H, 4.36; N, 13.51. ^{31}P NMR (d^6 -acetone, δ): -11.35 ($J_{\text{WP}} = 284$). ^1H NMR (d^6 -acetone, δ): 8.14 (d, 1H, PzB3), 8.01 (d, 1H, PzC5), 7.96 (d, 1H, PzB5), 7.94 (d, 1H, PzA3), 7.88 (d, 1H, PzA5), 7.56 (d, 1H, PzC3), 6.40 (t, 1H, PzB4), 6.39 (t, 1H, PzC4), 6.32 (t, 1H, PzA4), 4.70 (d, $J = 4.8$, 1H, H4), 3.52 (m, 1H, H1), 2.78 (tq, $J = 11.0$, 3.3, 1H, H2), 2.46 (s, 3H, H12), 2.24 (dt, $J = 11.4$, 5.1, 1H, H5), 1.75 (dt, $J = 13.1$, 5.7, 1H, H6x), 1.28 (m, 2H, H3 & H6y), 1.20 (d, $J = 8.5$, 9H, PMe_3), 1.15 (s, 3H, H10), 1.06 (s, 3H, H11). ^{13}C NMR (d^6 -acetone, δ): 178.9 (C8), 144.9 (PzB3), 143.6 (PzA3), 142.2 (PzC3), 138.0 (2C, PzA5 & PzC5), 137.5 (PzB5), 132.0 (q, $J = 280.1$, CF_3), 107.3 (PzB4), 107.2 (PzC4), 106.7 (PzA4), 59.2 (C4), 49.4 (C3), 45.0 (C7), 43.2 (d, $J = 13.4$, C2), 42.7 (q, $J = 24.2$, C1), 40.8 (C5), 27.4 (C12), 24.4 (C10), 22.8 (m, C6), 19.9 (C11), 13.6 (d, $J = 29.2$, PMe_3).



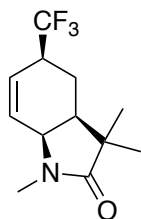
Compound 67'. To a 4-dram vial were added **55** (200 mg, 0.266 mmol) followed by acetonitrile (3 mL, -30°C), resulting in a heterogeneous mixture. A 1M solution of HOTf in

acetonitrile (0.54 mL, 0.54 mmol, -30°C) was then added, resulting in a homogeneous yellow solution, which was allowed to sit for 20 min at -30°C. Ethanolamine (349 mg, 5.71 mmol) was added to the reaction solution, which was left for 16 h at -30°C. The reaction was then allowed to warm to room temperature and left for 4 h, until ^{31}P NMR indicated that the reaction was complete. The pale yellow solution was removed from the glovebox, evaporated *in vacuo* to half volume, then H_2O (15 mL) was added to induce precipitation. The resulting pale yellow solid was collected on a 15 mL fine porosity fritted disc, washed with H_2O (2 mL), acetonitrile (0.5 mL), and pentane (2 mL) and desiccated overnight, yielding **67'** (120 mg, 0.154 mmol, 58% yield). CV (DMAc) $E_{\text{p,a}} = +0.65$ V (NHE). IR: $\nu(\text{BH}) = 2481$ cm^{-1} , $\nu(\text{CO}) = 1659$ cm^{-1} , $\nu(\text{NO}) = 1552$ cm^{-1} . Anal. Calc'd for $\text{C}_{25}\text{H}_{37}\text{BF}_3\text{N}_8\text{O}_3\text{PW}\cdot\text{H}_2\text{O}$: C, 37.62; H, 4.92; N, 14.04 Found: C, 37.52; H, 4.57; N, 13.83. ^{31}P NMR (d^6 -acetone, δ): -11.68 ($J_{\text{WP}} = 282$). ^1H NMR (d^6 -acetone, δ): 8.13 (d, 1H, PzB3), 8.01 (d, 1H, PzC5), 7.95 (d, 1H, PzB5), 7.90 (d, 1H, PzA3), 7.87 (d, 1H, PzA5), 7.55 (d, 1H, PzC3), 6.39 (t, 1H, PzB4), 6.38 (t, 1H, PzC4), 6.32 (t, 1H, PzA4), 4.82 (d, $J = 4.6$, 1H, H4), 3.55 (m, 1H, H1), 3.22 (m, 3H, H12x & H13), 3.06 (m, 1H, H12y), 2.77 (m, 1H, H2), 2.26 (dt, $J = 11.6, 5.1$, 1H, H5), 1.73 (dt, $J = 13.0, 5.5$, 1H, H6x), 1.29 (m, 1H, H6y), 1.25 (d, $J = 10.8$, 1H, H3), 1.20 (d, $J = 8.5$, 9H, PMe_3), 1.18 (s, 3H, H10), 1.06 (s, 3H, H11). ^{13}C NMR (d^6 -acetone, δ): 180.2 (C8), 144.9 (PzB3), 143.6 (PzA3), 142.2 (PzC3), 138.0 (2C, PzA5 & PzC5), 137.5 (PzB5), 132.0 (q, $J = 279.4$, CF_3), 107.3 (PzB4/PzC4), 107.2 (PzB4/PzC4), 106.8 (PzA4), 60.8 (C13), 58.1 (C4), 49.6 (C3), 45.0 (C7), 43.4 (C12), 42.9 (m, C2), 42.5 (m, C1), 40.9 (C5), 24.4 (C10), 22.8 (C6), 19.8 (C11), 13.5 (d, $J = 29.4$, PMe_3).



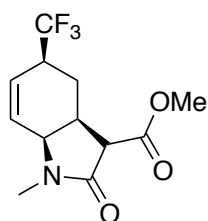
Compound 68. To a 4-dram vial was added **56** (100 mg, 0.128 mmol) followed by acetonitrile (1.6 mL, -30°C), resulting in a heterogeneous pale yellow mixture. A 1M solution of HOTf in acetonitrile (0.27 mL, 0.27 mmol, -30°C) was then added, resulting in a homogeneous yellow solution, which was allowed to sit for 20 min at -30°C. 2M H₂NMe/THF (1.28 mL, 2.56 mmol, -30°C) was added to the reaction solution, which was left for 20 h at -30°C. The reaction solution was allowed to warm to room temperature for 5 min and checked by ³¹P NMR, which showed the presence of a single product. The solution was then removed from the glovebox, diluted with DCM (40 mL) and washed with H₂O (40 mL). The aqueous layer was back-extracted with DCM (20 mL), then the combined organic layers were dried over MgSO₄ and evaporated *in vacuo*. The film was redissolved in minimal DCM and added to stirring pentane (20 mL). The resulting pale solid was collected on a 15 mL fine porosity fritted disc, washed with pentane (2 mL) and desiccated overnight, yielding **68** (72 mg, 0.093 mmol, 72% yield). CV (DMAc) $E_{p,a} = +0.70$ V (NHE). IR: $\nu(\text{BH}) = 2489$ cm⁻¹, $\nu(\text{CO}) = 1731$ & 1683 cm⁻¹, $\nu(\text{NO}) = 1554$ cm⁻¹. Anal. Calc'd for 3C₂₄H₃₃BF₃N₈O₄PW•Et₂O: C, 37.80; H, 4.55; N, 13.92. Found: C, 37.44; H, 4.40; N, 13.84. ³¹P NMR (d⁶-acetone, δ): -11.06 ($J_{\text{WP}} = 281$). ¹H NMR (d⁶-acetone, δ): 8.16 (d, 1H, PzB3), 8.08 (d, 1H, PzA3), 8.02 (d, 1H, PzC5), 7.98 (d, 1H, PzB5), 7.89 (d, 1H, PzA5), 7.63 (d, 1H, PzC3), 6.42 (t, 1H, PzB4), 6.39 (t, 1H, PzC4), 6.35 (t, 1H, PzA4), 4.94 (dt, $J = 6.6, 1.6$, 1H, H4), 3.71 (s, 3H, H11), 3.52 (m, 1H, H1), 3.09 (d, $J = 2.4$, 1H, H7), 2.95 (m, 1H, H5), 2.66 (m, 1H, H2), 2.57 (s, 3H, H12), 2.27 (dt, $J = 14.9, 8.0$, 1H, H6x), 1.46 (dt, $J = 14.9, 5.9$, 1H, H6y), 1.32 (d, $J = 11.0$,

¹H, H3), 1.21 (d, *J* = 8.5, 9H, PMe₃). ¹³C NMR (d⁶-acetone, δ): 171.8 (C10), 169.3 (C8), 144.5 (PzB3), 144.0 (PzA3), 142.1 (PzC3), 138.1 (Pz5), 137.8 (Pz5), 137.4 (Pz5), 132.2 (q, *J* = 280.9, CF₃), 107.4 (Pz4), 107.3 (Pz4), 106.7 (Pz4), 61.3 (C4), 58.8 (C7), 52.4 (C11), 48.3 (C3), 43.5 (m, C2), 42.1 (m, C1), 32.6 (C5), 27.5 (C12), 24.8 (C6), 13.0 (d, *J* = 28.9, PMe₃).



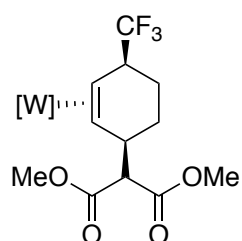
Compound 69. (Outside of glovebox) To a 4-dram vial charged with a stir pea was added NOPF₆ (22 mg, 0.12 mmol). In a separate 4-dram vial, **67** (60 mg, 0.080 mmol) was dissolved in acetone (0.7 mL) and added to the vial with NOPF₆ while stirring, resulting in an immediate color change from pale yellow to brown. The first vial was rinsed with acetone (0.3 mL), and this was added to the reaction vial. The reaction solution was stirred for 4 h, at which point it had turned back to a golden color, and was then evaporated *in vacuo* to dryness. DCM (1 mL) was added to the vial and then this solution was added to stirring pentane (15 mL). The resulting cloudy mixture was filtered over a 15 mL fine porosity fritted disc and washed with Et₂O (1 mL) and pentane (2 mL). The clear/pale yellow filtrate was evaporated *in vacuo* and the resulting oil was loaded onto a 250 μm silica preparatory plate with DCM (3 x 0.3 mL) and eluted with 25% EtOAc/hexanes (HPLC grade, 200 mL). A KMnO₄ active band at R_f 0.065-0.210 was collected and sonicated in EtOAc (HPLC grade, 25 mL) for 15 min. The silica was filtered off on a 30 mL fine porosity fritted disc and washed with EtOAc (HPLC grade, 2 x 20 mL). The filtrate was evaporated *in vacuo* yielding **69** (12 mg, 0.048 mmol, 60% yield). IR: ν(CO) = 1682 cm⁻¹. Anal. Calc'd for

$10C_{12}H_{16}F_3NO \cdot H_2O$: C, 57.87; H, 6.56; N, 5.62. Found: C, 57.85; H, 6.71; N, 5.40. 1H NMR (d^6 -acetone, δ): 6.30 (dt, $J = 10.2, 3.4$ 1H, H7), 6.04 (dq, $J = 10.2, 1.5$, 1H, H6), 4.00 (m, 1H, H7a), 3.10 (m, 1H, H5), 2.76 (s, 3H, NMe), 2.18 (ddd, $J = 13.5, 5.6, 4.3$, 1H, H3a), 1.92 (dtd, $J = 12.3, 4.3, 1.4$, 1H, H4x), 1.16 (q, $J = 12.3$, 1H, H4y), 1.10 (s, 3H, C3Me), 1.06 (s, 3H, C3Me). ^{13}C NMR (d^6 -acetone, δ): 177.8 (C2), 128.7 (C7), 128.2 (q, $J = 278.4$, CF_3), 126.9 (q, $J = 3.7$, C6), 53.2 (C7a), 44.0 (C3), 41.8 (C3a), 41.4 (q, $J = 27.1$, C5), 27.3 (NMe), 24.8 (C3Me), 21.9 (q, $J = 3.0$, C4), 19.3 (C3Me).



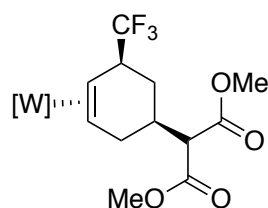
Compound 70. (Outside of glovebox) $NOPF_6$ (23 mg, 0.13 mmol) was added to a 4-dram vial charged with a stir pea. In a separate 4-dram vial **68** (72 mg, 0.092 mmol) was dissolved in acetone (2 mL) and then added to the vial with $NOPF_6$ while stirring, resulting in an immediate color change from pale yellow to golden brown. The reaction solution was stirred for 4 h and then evaporated *in vacuo* to dryness. Minimal DCM was added to the vial and then this solution was added to stirring pentane/ Et_2O (19/1 mL). The resulting precipitate was collected on a 30 mL fine porosity fritted disc and washed with Et_2O (5 mL) and pentane (5 mL). The filtrate was evaporated *in vacuo* and the resulting oil was loaded onto a 250 μm silica preparatory plate with DCM (3 x 0.3 mL) and eluted with 70% $EtOAc$ /hexanes (HPLC grade, 200 mL). A $KMnO_4$ active band at R_f 0.30-0.58 was collected and sonicated in $EtOAc$ (HPLC grade, 25 mL) for 15 min. The silica was filtered off on a 30 mL fine porosity fritted disc and washed with $EtOAc$ (HPLC grade, 2 x 20 mL). The filtrate was evaporated *in vacuo* yielding **70** (14 mg, 0.051 mmol, 55% yield). IR: $\nu(CO) = 1737$ &

1694 cm^{-1} . Anal. Calc'd for $\text{C}_{12}\text{H}_{14}\text{F}_3\text{NO}_3$: C, 51.99; H, 5.09; N, 5.05. Found: C, 51.82; H, 5.18; N, 5.13. ^1H NMR (d^6 -acetone, δ): 6.29 (dt, $J = 10.3$, 3.3 1H, H7), 6.08 (dm, $J = 10.3$, 1H, H6), 4.16 (m, 1H, H7a), 3.68 (s, 3H, OMe), 3.23 (m, 1H, H5), 3.13 (bs, 1H, H3), 2.83 (buried, 1H, H3a), 2.82 (s, 3H, NMe), 2.08 (dtd, $J = 12.6$, 4.5, 1.4, 1H, H4x), 1.36 (q, $J = 12.6$, 1H, H4y). ^{13}C NMR (d^6 -acetone, δ): 170.6 (CO_2Me), 168.6 (C2), 128.1 (C7), 128.0 (q, $J = 278.2$, CF_3), 127.1 (q, $J = 3.6$, C6), 56.1 (C3), 55.5 (C7a), 52.6 (OMe), 40.7 (q, $J = 27.3$, C5), 35.0 (C3a), 27.6 (NMe), 25.1 (q, $J = 2.6$, C4).



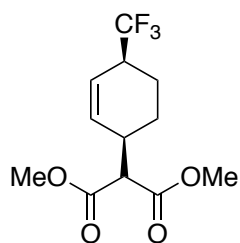
Compound 71. To a 4-dram vial were added **54** (100 mg, 0.154 mmol) followed by d^6 -acetone (2.5 mL), resulting in a heterogeneous mixture. A 1M solution of HOTf in acetonitrile (0.31 mL, 0.31 mmol, -30°C) was then added, resulting in a homogeneous yellow solution, which was allowed to sit for 22 h at room temperature. LiDMM (124 mg, 0.898 mmol) was added to a 4-dram vial charged with a stir pea, and then the reaction solution was added while stirring. The homogeneous yellow solution was allowed to react for 1 h then removed from the glovebox, diluted with DCM (40 mL) and washed with H_2O (40 mL). The aqueous layer was back-extracted with DCM (40 mL), then the combined organic layers were dried over MgSO_4 and evaporated *in vacuo*. The film was redissolved in minimal DCM and added to stirring pentane (25 mL). The resulting solid was collected on a 15 mL fine porosity fritted disc, washed with pentane (3 mL) and desiccated, yielding **71** (84 mg, 0.11 mmol, 70% yield). CV (DMAc) $E_{p,a} = +0.57$ V (NHE). IR: $\nu(\text{BH}) = 2488$ cm^{-1} ,

$\nu(\text{CO}) = 1728 \text{ cm}^{-1}$, $\nu(\text{NO}) = 1550 \text{ cm}^{-1}$. Anal. Calc'd for $4\text{C}_{24}\text{H}_{34}\text{BF}_3\text{N}_7\text{O}_5\text{PW}\cdot\text{acetone}$: C, 37.27; H, 4.49; N, 12.29. Found: C, 37.41; H, 4.52; N, 12.22. ^{31}P NMR (d^6 -acetone, δ): -11.11 ($J_{\text{WP}} = 284$). ^1H NMR (d^6 -acetone, δ): 8.11 (bt, 1H, PzA3), 8.10 (d, 1H, PzB3), 7.97 (d, 1H, PzC5), 7.94 (d, 1H, PzB5), 7.88 (d, 1H, PzA5), 7.52 (d, 1H, PzC3), 6.39 (t, 1H, PzB4), 6.35 (t, 1H, PzC4), 6.30 (t, 1H, PzA4), 3.94 (bm, 1H, H4), 3.57 (s, 3H, H9), 3.55 (s, 3H, H11), 3.49 (m, 1H, H1), 3.33 (d, $J = 5.2$, 1H, H7), 2.60 (m, 1H, H2), 2.12 (m, 1H, H6x), 1.81 (m, 1H, H6y), 1.73 (m, 2H, H5), 1.19 (d, $J = 8.3$, 9H, PMe_3), 1.04 (d, $J = 11.5$, 1H, H3). ^{13}C NMR (d^6 -acetone, δ): 170.1 (C10), 169.5 (C8), 144.2 (PzB3), 142.0 (PzA3), 141.7 (PzC3), 137.8 (2C, PzA5 & PzC5), 137.2 (PzB5), 132.9 (q, $J = 283.0$, CF_3), 107.3 (PzB4), 107.1 (PzC4), 106.4 (PzA4), 60.5 (C7), 53.7 (C3), 52.2 (C9/C11), 51.8 (C9/C11), 46.7 (d, $J = 10.8$, C2), 43.7 (q, $J = 22.7$, C1), 39.2 (C4), 22.2 (C5), 21.0 (C6), 13.1 (d, $J = 28.5$, PMe_3).



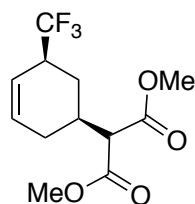
Compound 72. To a 4-dram vial were added **56** (42 mg, 0.054 mmol) followed by acetonitrile (0.7 mL, -30°C), resulting in a heterogeneous mixture. In a separate 4-dram vial charged with a stir pea, tetrabutylammonium borohydride (109 mg, 0.425 mmol) was dissolved in acetonitrile (0.3 mL, -30°C). Both vials were cooled to -30°C for 15 min. Then a 1M solution of HOTf in acetonitrile (0.06 mL, 0.06 mmol, -30°C) was added to the vial with complex, resulting in a homogeneous yellow solution, which was allowed to sit for 15 min at -30°C . This yellow solution was added to the $\text{Bu}_4\text{NBH}_4/\text{acetonitrile}$ solution while stirring, resulting in a homogenous blue solution. The first vial was rinsed with acetonitrile (0.2 mL, -30°C) and added to the reaction solution. The reaction was left for 18 h at -30°C .

The pale yellow solution was removed from the glovebox and precipitation was induced by adding H₂O (5 mL). The resulting pale yellow solid was collected on a 15 mL fine porosity fritted disc, washed with H₂O (1 mL), acetonitrile (0.4 mL), and pentane (1 mL) and desiccated overnight, yielding **72** (30 mg, 0.039 mmol, 72% yield). CV (DMAc) $E_{p,a} = +0.52$ V (NHE). IR: $\nu(\text{BH}) = 2494$ cm⁻¹, $\nu(\text{CO}) = 1755$ & 1731 cm⁻¹, $\nu(\text{NO}) = 1553$ cm⁻¹. Anal. Calc'd for C₂₄H₃₄BF₃N₇O₅PW•DCM: C, 34.59; H, 4.18; N, 11.29. Found: C, 34.38; H, 4.18; N, 11.56. ³¹P NMR (d⁶-acetone, δ): -11.72 ($J_{\text{WP}} = 282$). ¹H NMR (d⁶-acetone, δ): 8.11 (d, 1H, PzB3), 8.02 (d, 1H, PzA3), 7.94 (t, 2H, PzB5 & PzC5), 7.80 (d, 1H, PzA5), 7.40 (d, 1H, PzC3), 6.38 (t, 1H, PzB4), 6.32 (t, 1H, PzC4), 6.28 (t, 1H, PzA4), 3.72 (s, 3H, H9), 3.69 (s, 3H, H11), 3.62 (m, 1H, H1), 3.31 (d, $J = 8.6$, 1H, H7), 2.92 (td, $J = 13.5, 4.3$, 1H, H4x), 2.80 (m, 1H, H2), 2.76 (m, 1H, H5), 2.57 (d, $J = 13.5$, 1H, H4y), 1.99 (m, 1H, H6x), 1.31 (m, 1H, H6y), 1.22 (d, $J = 8.3$, 9H, PMe₃), 1.04 (buried, 1H, H3). ¹³C NMR (d⁶-acetone, δ): 169.9 (C8), 169.7 (C10), 144.9 (PzA3), 144.5 (PzB3), 141.6 (PzC3), 137.5 (PzC5), 137.2 (PzB5), 136.9 (PzA5), 132.4 (q, $J = 279.8$, CF₃), 107.1 (PzB4), 107.0 (PzC4), 106.5 (PzA4), 59.0 (C7), 54.8 (C3), 52.3 (2C, C9 & C11), 42.8 (q, $J = 25.3$, C1), 41.7 (d, $J = 13.1$, C2), 31.8 (C5), 31.2 (C4), 28.4 (m, C6), 13.3 (d, $J = 28.5$, PMe₃).



Compound 73. (Outside of glovebox) NOPF₆ (23 mg, 0.13 mmol) was added to a 4-dram vial charged with a stir pea. In a separate 4-dram vial **71** (74 mg, 0.094 mmol) was dissolved in acetone (1.5 mL) and then added to the vial with NOPF₆ while stirring,

resulting in an immediate color change from golden to golden brown. The vial was rinsed with acetone (0.5 mL) and this was also added to the reaction solution. The reaction was stirred for 5 h and then evaporated *in vacuo* to dryness. Minimal DCM was added to the vial and then this solution was added to stirring pentane (25 mL). The resulting precipitate was collected on a 30 mL fine porosity fritted disc and washed with pentane (10 mL). The clear filtrate was evaporated *in vacuo* and the resulting oil was loaded onto a 250 μm silica preparatory plate with DCM (3 x 0.3 mL) and eluted with 15% EtOAc/hexanes (HPLC grade, 200 mL). A KMnO_4 active band at R_f 0.35-0.5 was collected and sonicated in EtOAc (HPLC grade, 25 mL) for 15 min. The silica was filtered off on a 30 mL fine porosity fritted disc and washed with EtOAc (HPLC grade, 2 x 20 mL). The filtrate was evaporated *in vacuo* yielding **73** (18 mg, 0.065 mmol, 69% yield). IR: $\nu(\text{CO}) = 1753$ & 1735 cm^{-1} . Anal. Calc'd for $3\text{C}_{12}\text{H}_{15}\text{F}_3\text{O}_4 \cdot \text{acetone}$: C, 52.12; H, 5.72. Found: C, 52.33; H, 5.64. ^1H NMR (d^6 -acetone, δ): 5.97 (dt, $J = 10.3, 2.7$, 1H, H2), 5.73 (dm, $J = 10.3$, 1H, H3), 3.71 (s, 3H, OMe), 3.70 (s, 3H, OMe), 3.41 (d, $J = 9.1$, 1H, H1'), 3.01 (m, 1H, H4), 2.88 (m, 1H, H1), 1.87 (m, 1H, H5x), 1.79 (m, 2H, H5y & H6x), 1.62 (m, 1H, H6y). ^{13}C NMR (d^6 -acetone, δ): 169.1 (CO), 169.0 (CO), 134.4 (C2), 128.3 (q, $J = 278.8$, CF_3), 122.9 (q, $J = 3.7$, C3), 56.5 (C1'), 52.7 (OMe), 52.6 (OMe), 39.5 (q, $J = 27.1$, C4), 34.8 (C1), 23.8 (C6), 20.0 (q, $J = 2.6$, C5).



Compound 74. (Outside of glovebox) In a 4-dram vial charged with a stir pea, **72** (54 mg, 0.068 mmol) and acetone (0.8 mL) were combined. NOPF_6 (18 mg, 0.10 mmol) was

weighed out in a separate 4-dram vial, dissolved in acetone (0.8 mL) and then added to the vial with complex while stirring, resulting in an immediate color change from pale yellow to brown. The reaction solution was stirred for 2 h and then evaporated *in vacuo* to dryness. Minimal DCM was added to the vial and then this solution was added to stirring pentane (20 mL). The resulting golden precipitate was collected on a 30 mL fine porosity fritted disc and washed with pentane (5 mL). The clear filtrate was evaporated *in vacuo* and the resulting oil was loaded onto a 250 μm silica preparatory plate with DCM (3 x 0.3 mL) and eluted with 10% EtOAc/hexanes (HPLC grade, 200 mL). A KMnO_4 active band at R_f 0.25-0.43 was collected and sonicated in EtOAc (HPLC grade, 25 mL) for 15 min. The silica was filtered off on a 30 mL fine porosity fritted disc and washed with EtOAc (HPLC grade, 2 x 20 mL). The filtrate was evaporated *in vacuo* yielding **74** (13 mg, 0.047 mmol, 69% yield). IR: $\nu(\text{CO}) = 1752$ & 1733 cm^{-1} . Anal. Calc'd for $3\text{C}_{12}\text{H}_{15}\text{F}_3\text{O}_4 \cdot \text{ethylacetate}$: C, 51.72; H, 5.75. Found: C, 51.95; H, 5.52. ^1H NMR (d^6 -acetone, δ): 5.98 (m, 1H, H3), 5.63 (dm, $J = 10.2$, 1H, H4), 3.72 (s, 3H, OMe), 3.71 (s, 3H, OMe), 3.48 (d, $J = 8.1$, 1H, H1'), 3.19 (m, 1H, H5), 2.38 (m, 1H, H1), 2.17 (dm, $J = 17.8$, 1H, H2x), 2.04 (m, buried, 1H, H6x), 1.98 (m, 1H, H2y), 1.44 (q, $J = 12.2$, 1H, H6y). ^{13}C NMR (d^6 -acetone, δ): 169.2 (2C, CO), 131.9 (C3), 128.3 (q, $J = 278.2$, CF_3), 121.0 (q, $J = 3.7$, C4), 57.1 (C1'), 52.6 (2C, OMe), 42.0 (q, $J = 27.2$, C5), 33.6 (C1), 29.2 (C2), 26.6 (q, $J = 3.0$, C6).

3.5 References

- (1) Collman, J. P.; Hegedus, L. S.; Norton, J. R.; Finke, R. G. *Principles and Applications of Organotransition Metal Chemistry*; 2nd ed.; University Science Books: Mill Valley, 1987.
- (2) Kündig, E. P. *Transition Metal Arene Complexes in Organic Synthesis and Catalysis*; Springer: Berlin, 2004; Vol. 7.
- (3) Keane, J. M.; Harman, W. D. *Organometallics* **2005**, *24*, 1786.
- (4) Harman, W. D. *Chem. Rev.* **1997**, *97*, 1953.
- (5) Chordia, M. D.; Smith, P. L.; Meiere, S. H.; Sabat, M.; Harman, W. D. *J. Am. Chem. Soc.* **2001**, *123*, 10756.
- (6) Ding, F.; Kopach, M. E.; Sabat, M.; Harman, W. D. *J. Am. Chem. Soc.* **2002**, *124*, 13080.
- (7) Graham, P.; Meiere, S. H.; Sabat, M.; Harman, W. D. *Organometallics* **2003**, *22*, 4364.
- (8) Ding, F.; Harman, W. D. *J. Am. Chem. Soc.* **2004**, *126*, 13752.
- (9) Winemiller, M. D.; Kopach, M. E.; Harman, W. D. *J. Am. Chem. Soc.* **1997**, *119*, 2096.
- (10) Kolis, S. P.; E., K. M.; Liu, R.; Harman, W. D. *J. Am. Chem. Soc.* **1998**, *120*, 6205.
- (11) Lis, E. C.; Salomon, R. J.; Sabat, M.; Myers, W. H.; Harman, W. D. *J. Am. Chem. Soc.* **2008**, *130*, 12472.
- (12) Salomon, R. J.; Todd, M. A.; Sabat, M.; Myers, W. H.; Harman, W. D. *Organometallics* **2010**, *29*, 707.

- (13) Pienkos, J. A.; Zottig, V. E.; Iovan, D. A.; Li, M.; Harrison, D. P.; Sabat, M.; Salomon, R. J.; Strausberg, L.; Teran, V. A.; Myers, W. H.; Harman, W. D. *Organometallics* **2013**, *32*, 691.
- (14) MacLeod, B. L.; Pienkos, J. A.; Myers, J. T.; Sabat, M.; Myers, W. H.; Harman, W. D. *Organometallics* **2014**, *33*, 6286.
- (15) Liu, W.; Welch, K.; Trindle, C. O.; Sabat, M.; Myers, W. H.; Harman, W. D. *Organometallics* **2007**, *26*, 2589.
- (16) Graham, P. M.; Mocella, C. J.; Sabat, M.; Harman, W. D. *Organometallics* **2005**, *24*, 911.
- (17) Lis, E. C.; Delafuente, D. A.; Lin, Y.; Mocella, C. J.; Todd, M. A.; Liu, W.; Sabat, M.; Myers, W. H.; Harman, W. D. *Organometallics* **2006**, *25*, 5051.
- (18) Welch, K. D.; Harrison, D. P.; Lis, E. C.; Liu, W.; Salomon, R. J.; Harman, W. D.; Myers, W. H. *Organometallics* **2007**, *26*, 2791.
- (19) Harrison, D. P.; Nichols-Nielander, A. C.; Zottig, V. E.; Strausberg, L.; Salomon, R. J.; Trindle, C. O.; Sabat, M.; Gunnoe, T. B.; Iovan, D. A.; Myers, W. H.; Harman, W. D. *Organometallics* **2011**, *30*, 2587.
- (20) Kitching, W.; Olszowy, H. A.; Drew, G. M.; Adcock, W. J. *J. Org. Chem.* **1982**, *47*, 5153.
- (21) Kowalski, A. S.; Ashby, M. T. *J. Am. Chem. Soc.* **1995**, *117*, 12639.
- (22) Semmelhack, M. F.; Clark, G. R.; Farina, R.; Saeman, M. *J. Am. Chem. Soc., Commun.* **1979**, *101*, 217.
- (23) Harman, W. D.; Taube, H. *J. Am. Chem. Soc.* **1990**, *112*, 2261.
- (24) Kolis, S. P.; Kopach, M. E.; Liu, R.; Harman, W. D. *J. Org. Chem.* **1997**, *62*, 130.

- (25) Kopach, M. E.; Gonzalez, J.; Harman, W. D. *J. Am. Chem. Soc.* **1991**, *113*, 8972.
- (26) Smith, P. L.; Keane, J. M.; Shankman, S. E.; Chordia, M. D.; Harman, W. D. *J. Am. Chem. Soc.* **2004**, *126*, 15543.
- (27) Kolis, S. P.; Gonzalez, J.; Bright, L. M.; Harman, W. D. *Organometallics* **1996**, *15*, 245.
- (28) Semmelhack, M. F.; Harrison, J. J.; Thebtaranonth, Y. *J. Org. Chem.* **1979**, *44*, 3275.
- (29) He, Z.; Tan, P.; Hu, J. *Organic Letters* **2016**, *18*, 72.
- (30) Cho, E. J.; Senecal, T. D.; Kinzel, T.; Zhang, Y.; Watson, D. A.; Buchwald, S. L. *Science* **2010**, *328*, 1679.
- (31) Prakash, G. K. S.; Yudin, A. K. *Chem. Rev.* **1997**, *97*, 757.
- (32) Furuya, T.; Kamlet, A. S.; Ritter, T. *Nature* **2011**, *473*, 470.
- (33) Phillips, A. D.; Zava, O.; Scopelitti, R.; Nazarov, A. A.; Dyson, P. J. *Organometallics* **2010**, *29*, 417.
- (34) Kundig, E. P.; Ripa, A.; Liu, R.; Bernardinelli, G. *J. Org. Chem.* **1994**, *59*, 4773.
- (35) Pape, A. R.; Kaliappan, K. P.; Kundig, E. P. *Chem. Rev.* **2000**, *100*, 2917.
- (36) D'Amato, E. M.; Neumann, C. N.; Ritter, T. *Organometallics* **2015**, *34*, 4626.

Chapter 4

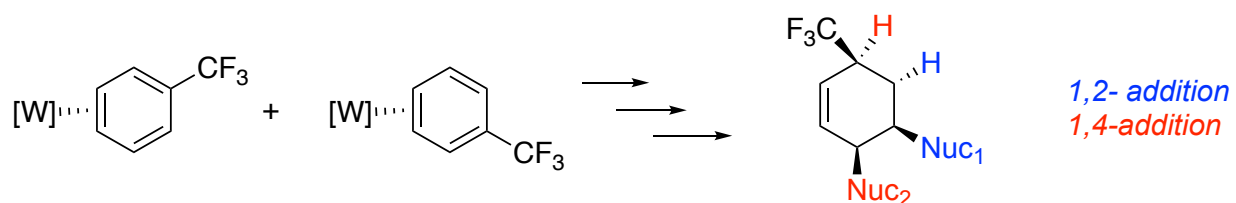
The Isolation and Elaboration of Reversible Amine

Additions to Dihapto-Trifluorotoluene

4.1 Introduction

Chapter 3 presented the initial investigation into the dihapto-dearomatization chemistry of a benzene substituted with an EWG (CF_3), and established a regio- and stereo-selective reactivity pattern to access trisubstituted trifluoromethyl cyclohexenes (Scheme 4.1).¹ The initial electrophilic/nucleophilic addition reaction across an uncoordinated double bond of the TFT ligand was demonstrated with a proton as the electrophile and two protected enolates (MMTP and LiDMM), NaCN, NaSPh, and a hydride source (Bu_4NBH_4) as the nucleophiles. This chapter focuses on expanding the range of nucleophiles that can be successfully added to the allylic species (**53**), specifically to include a range of primary and secondary amines as nucleophiles. In a recent report, Wood et al. highlighted a few important synthetic challenges that the drug development and synthetic methodology fields face, including late stage tolerance of amines and unprotected polar groups. Other synthetic challenges include the incorporation of fluorine into small molecules, and methodology development to either synthesize or modify aliphatic nitrogen heterocycles.²⁻⁴ With this in mind, we chose to next concentrate on incorporating amines as nucleophiles, due to the wide variety of substitution patterns and functional groups that they provide. The ability to further elaborate the amine dienes to cyclohexenes is also discussed, including the addition of a second amine nucleophile.

Scheme 4.1: Reactivity pattern for $\eta^2\text{-PhCF}_3$

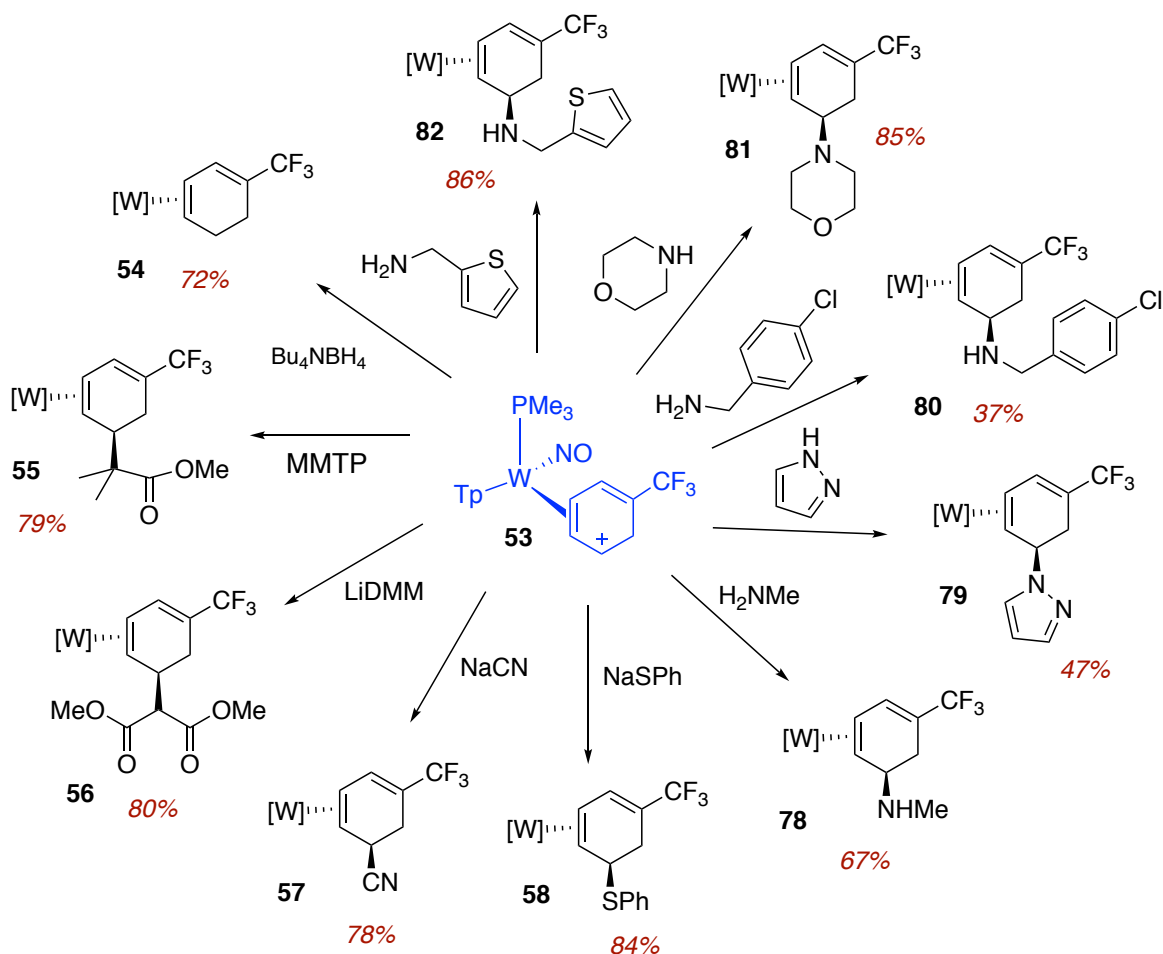


4.2 Results and Discussion

4.2.1 Amine Addition to η^2 -TFT

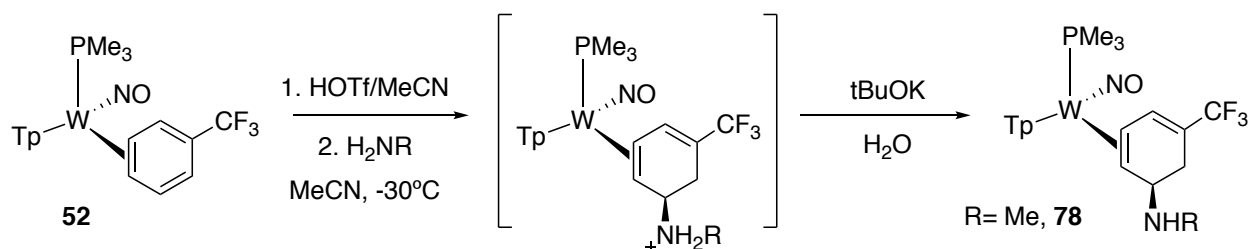
Protonation of **52** at -30°C with HOTf leveled in acetonitrile forms a single allyl complex **53**, with the positive charge localized distal to the PMe_3 ligand. In Chapter 3, the successful in situ reaction of **53** was demonstrated with a range of nucleophiles leading to η^2 -1,3-diene complexes **54-58** (Scheme 4.2). Once the reactivity of **52** was better understood, we endeavored to effect a hydroamination reaction across one of the uncoordinated double bonds of the TFT ligand.

Scheme 4.2: Range of nucleophiles for addition to **53**



Previously our group reported the ability to add a proton followed by a range of amines to the cationic η^2 -*N*-ethylindolinium complex.⁵ In this case, the reaction proceeds at room temperature and can be isolated via a basic extraction. Effecting the overall addition of an amine across one of the uncoordinated alkenes of the neutral η^2 -TFT complex proved to be more challenging, with the amine addition prone to elimination at room temperature, reforming the starting material. In initial experiments using a primary amine (methylamine), the reaction appeared to go to completion, as evidenced by in situ low temperature ¹H NMR. However, warming the reaction solution to room temperature caused the reversal of the addition. Furthermore, any attempt to isolate the tandem addition product resulted in predominately regeneration of **52** as well. To address these issues, the reaction solution was quenched while still at reduced temperatures (-30°C) with a relatively strong base (tBuOK), as shown in Scheme 4.3. We proposed that the base quench would neutralize the ammonium to a neutral amine, which is a worse leaving group. The reaction was then evaporated to dryness, and a ¹H NMR revealed the successful formation of the desired amine addition (**78**). Key features of the diene complex include the characteristic alkene peak at 7.18 ppm, and a methyl singlet at 2.32 ppm that was identified as the methylamine group.

Scheme 4.3: Conditions for amine addition to η^2 -TFT



Although this result was promising, we sought a procedure to isolate the complex as a purified solid. The initial work-up procedure, following the low temperature base quench, was a basic extraction, similar to the procedure reported for the successful addition of amines to η^2 -*N*-ethylindolinium.⁵ However, when a solid was isolated via precipitation after the extraction, a large amount of starting material was observed, indicating that the amine addition was still reversing during the basic aqueous work-up procedure. To circumvent this issue, we sought conditions that minimized the time spent in solution at room temperature following the base quench. Ultimately, we found that after the reaction was quenched with base, the drop-wise addition of H₂O induced the precipitation of a solid. This procedure is optimal in that the excess amine and base are left in the H₂O, and a pure form of the complex precipitates out. However, these precipitation conditions proved to be troublesome at times. If too much H₂O is added, the mixture can become biphasic, the precipitate can turn into an oil, or precipitation never fully occurs and a cloudy colloid forms instead. Additionally, if the precipitation does not occur quickly, the time the complex spends in solution stirring with H₂O causes the regeneration of starting material. Furthermore, if too little base is added the isolated solid is predominantly the initial η^2 -TFT complex (**52**).

Continued optimization of these conditions resulted in the successful isolation of the amine addition products **78-82** (Scheme 4.2). It was found that the amount of base (4 equivalents) and concentration of **52** in acetonitrile (100 mg/1 mL) were key to successfully isolate the addition products. Additional amines have been screened and also showed successful addition, but have not yet been fully optimized (Figure 4.1). In addition to primary alkyl amines, primary amines with other functional groups have been shown to

selectively form the desired amine addition diene. This includes amines with other nucleophilic and/or basic groups such as ethanolamine, as well as benzylic amines, and amines containing aromatic heterocycles (pyridine, furan, thiophene). The addition of cyclic secondary amines, including aromatic (pyrazole) and alkyl amines (morpholine and piperidine) was also successful, giving complexes **79** and **81** (Scheme 4.2 and Figure 4.1). The ability to add a range of amines with functional group tolerance, including cyclic amines with increased steric bulk, is particularly exciting given the prevalence and importance of nitrogen heterocycles in pharmaceuticals. Recently, Njardarson et. al. conducted a study on the presence of nitrogen heterocycles in unique small-molecule drugs and reported that 59% contain a nitrogen heterocycle.^{2,3} They also listed the most common nitrogen heterocycles found in pharmaceuticals, citing piperidine and pyridine as the two most prevalent. So far, we have demonstrated the ability to incorporate these type of desirable functional groups through the stereo- and regioselective addition of an amine to an activated aromatic, including TFT and some initial success with benzene (Chapter 2).

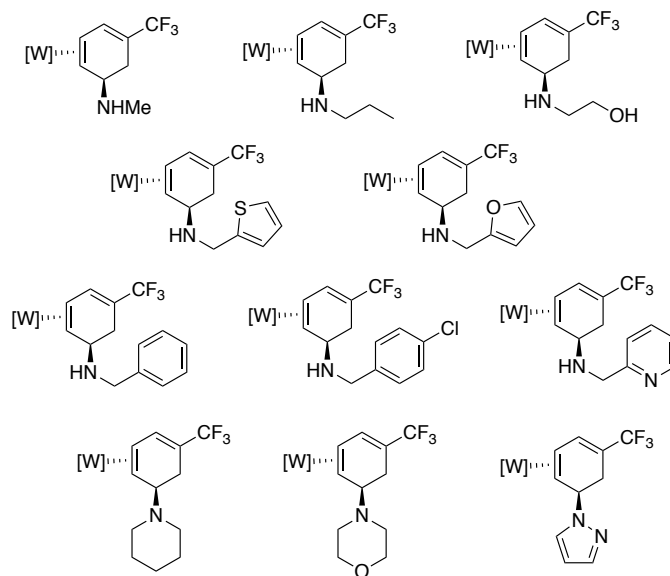
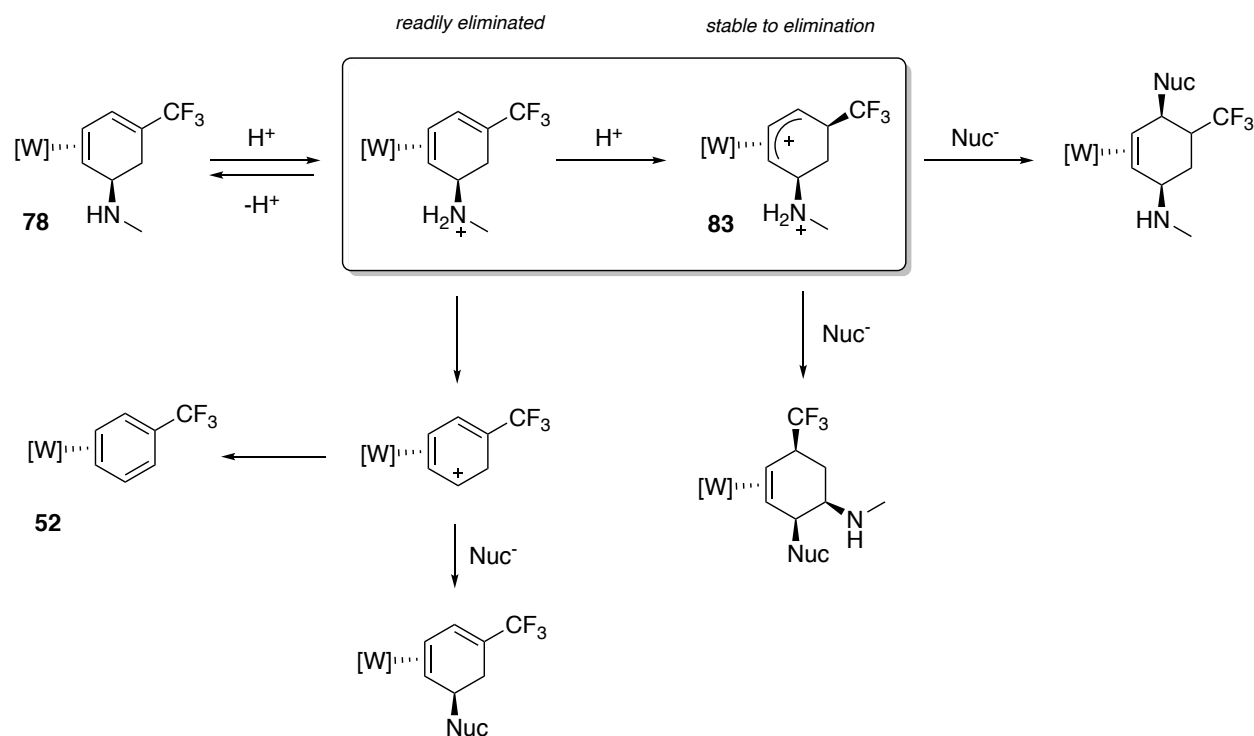


Figure 4.1: Preliminary results for successful amine addition to **53**

4.2.2 Exploring Further Reactivity of Amine Addition η^2 -Dienes

The overall addition of a proton and an amine across a double bond of η^2 -TFT was accomplished by finding conditions to enable the rapid isolation of the unstable η^2 -1,3-diene complexes in their more stable solid forms. As outlined in Chapter 2 and 3, these η^2 -1,3-diene complexes have a π -system still in conjugation with the metal, and are therefore activated towards a second electrophilic addition. Thus, we set out to investigate the reactivity of these delicate dienes, and whether they can go through a second addition reaction while keeping the initial amine substituent intact.

Addition of an acid followed by a nucleophile could potentially result in a number of different pathways, which are outlined in Scheme 4.4. We theorized that protonation of the lone pair on the amine nitrogen would occur the fastest. Furthermore, depending on the acid concentration/equivalents, we could have a mixture of the complex with just the amine protonated and the doubly protonated complex with both the amine and the diene protonated (**83**). If only the amine is protonated, the reaction sequence could lead to a few different outcomes. Elimination could occur, causing the regeneration of the neutral η^2 -TFT complex, or the amine could be deprotonated to regenerate starting material. Alternatively, the incoming nucleophile could replace the protonated amine in an S_N1 -type reaction.

Scheme 4.4: Reaction pathways for protonation and nucleophilic addition to **78**

In order to avoid the pathways that would lead to formation of **52** or **78**, excess acid was used (>2 eq) to ensure protonation of the amine and the diene. Additionally, most reactions were run at reduced temperatures (-30°C), as we have seen in the past that addition reactions seem to be favored over elimination reactions at low temperatures. We postulated that the use of excess acid at cold temperatures would allow for protonation of the amine and the diene, making the amine less likely to fall off. In the doubly protonated form, addition of a nucleophile could potentially result in at least two different products (Scheme 4.4), depending on where the nucleophile preferentially adds.

To support the formation of the doubly protonated complex **83**, the protonation of **78** with 2 equivalents of HOTf was monitored in situ by ^1H NMR in CD_3CN . The NMR spectrum revealed a single complex with signature allyl proton signals (5.87, 5.55 and 4.94

ppm). Additionally, two diastereotopic N-H protons were observed, and the signal for the nitrogen methyl group was split into a triplet, supporting the formation of **83** in situ (Figure 4.2). It is interesting to note that the allyl is much less distorted than we might expect with an electron-donating group; however, this can be explained by the positive charge on the amine, which would destabilize an adjacent carbocation. The signals for the two terminal protons of the allyl are ~ 0.6 ppm apart, making **83** the least distorted allyl that has been observed with the TFT system, and is reflective of the opposing impacts of the CF_3 and $^+\text{NH}_2\text{R}_2$ groups. For comparison, the ^1H NMR shifts of the terminal allyl protons of the cyanide complex **74** of TFT differ by 1.5 ppm, with the carbocation localized distal to the PMe_3 .

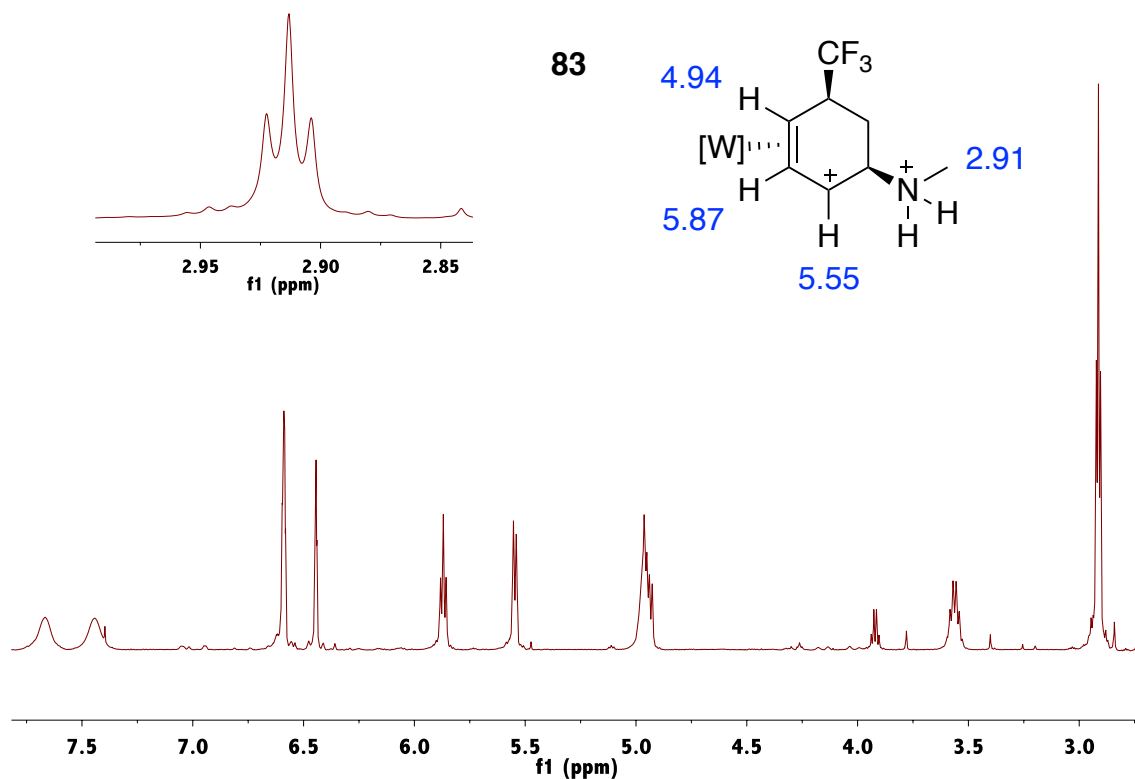
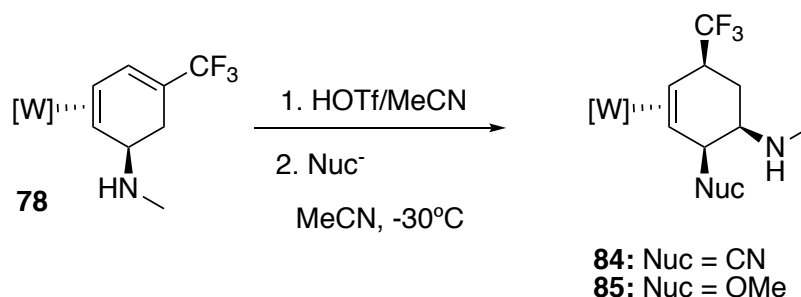


Figure 4.2: In situ ^1H NMR of allyl **83**

Protonation of **78** at -30°C followed by addition of anionic nucleophiles NaCN or $\text{Bu}_4\text{NOH}/\text{MeOH}$, resulted in the formation of **84** and **85**, respectively (Scheme 4.5). This reactivity is consistent with the reaction pattern observed with previous TFT diene complexes (Chapter 3), installing two nucleophiles adjacent to each other. These reactions do not need to be quenched with base, as was necessary with the first amine addition. This could be due to the presence of excess anionic nucleophile, which could also serve as a base and deprotonate the ammonium. It is unclear what occurs first, addition of the nucleophile to the allyl or deprotonation of the ammonium; however, the result is the regioselective addition of the second nucleophile.

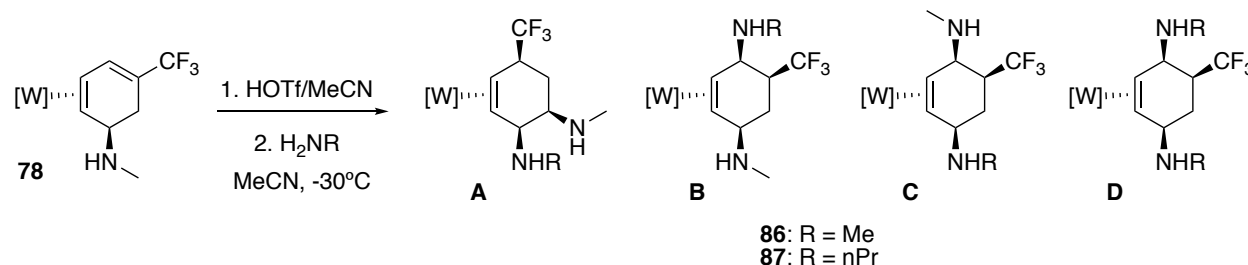
Scheme 4.5: Addition of anionic nucleophiles to **78**



We then attempted to add an amine as the second nucleophile, with the aim of further diversifying the functionalized cyclohexenes that can be accessed with these pharmaceutically important substituents. **78** was treated with acid and excess methylamine at -30°C and left for 24 h, then evaporated to dryness without quenching with base. Contrary to expectation, the only product observed was **86B/C**, which gives a new substitution pattern for the TFT system (Scheme 4.6). However, since both amine groups were identical, we were unable to tell if this product was a result of the second addition

reaction occurring in a 1,2-fashion or if there was some type intramolecular migration of the initial amine. To probe this mechanism, the reaction was repeated with propylamine as the second nucleophile. Two products were observed by ^1H NMR in a $\sim 2:1$ ratio, and 2D NMR allowed us to assign the major complex as **87C**. One of the key features of **87C** is a methine proton at 3.84 ppm with a NOE correlation to the PMe_3 ligand. This methine proton also has a NOE correlation with a singlet at 2.69 ppm integrating for three protons, which we identified as the methyl group on the amine. An HMBC correlation between the methine proton at 3.84 ppm and the methylamine carbon at ~ 32 ppm is also observed. Additionally, a methine proton at 4.00 ppm exhibits a NOE correlation with a proton on the pyrazole ring trans to the PMe_3 ligand. This methine is linked to the adjacent propyl amine group through a NOE correlation to a CH_2 group at 2.87 ppm. The propyl group is easily identified by ^1H NMR due to the characteristic triplet at 0.94 ppm representing the methyl group. The formation of this product implies some type of intramolecular rearrangement of the initial methylamine group (*vide infra*). The minor product has similar characteristic peaks and 2D NMR correlations, which are consistent with a 1,4-relationship between the amine groups on the ring. We tentatively assigned the minor product as **87D**, which has the two propylamine groups para to each other, but overlapping signals in the NMR spectrum complicate the assignment and further analysis is needed to support this.

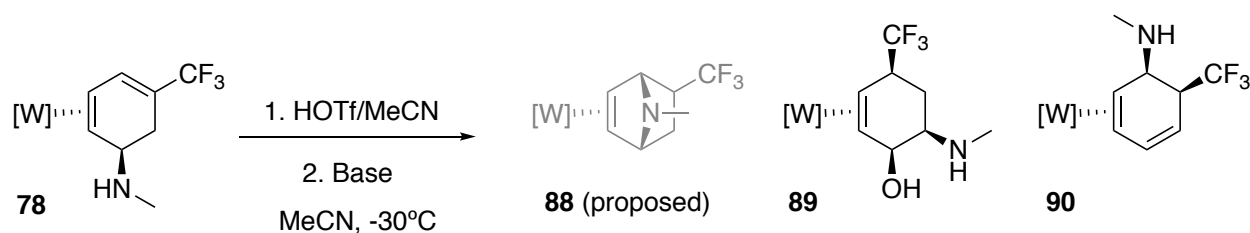
Scheme 4.6: Addition of amine nucleophiles to **78**



In order to test whether the product selectivity could be altered based on the reaction conditions, an experiment was conducted with propylamine as the second nucleophile; however, this time the reaction was quenched with tBuOK at -30°C before being evaporated to dryness. The ^1H NMR of this experiment revealed the formation of a single product, **87A**, giving the overall addition of the two amines at adjacent positions on the cyclohexene ring. This type of reactivity was more consistent with the previously established reactivity of TFT dienes (Chapter 3) and what was seen with the anionic nucleophiles (Scheme 4.5). Preliminary results show that this reaction can be achieved using a range of amines for the first and second nucleophile, and the 1,2-type product can be selectively formed if the reaction is quenched with base at reduced temperature.

When the second tandem addition reaction is not quenched with strong base, we believe that the amine nucleophiles have the potential to transiently fall off or migrate, leading to new types of products. Based off of these interesting results, we began to investigate the ability to promote an intramolecular cyclization reaction with the amine nitrogen with the hope of forming the 7-azabicyclo[2.2.1]heptene system seen in **88** (Scheme 4.7). This type of *N*-bridged alicyclic compound became an important synthetic target in the 1990s when the alkaloid natural product, epibatidine was discovered and found to be a powerful analgesic.^{6,7} Previously, our group reported the synthesis of epibatidine derivatives via the $\{\text{Os}(\text{NH}_3)_5\}^{2+}$ promoted dipolar cycloaddition of pyrroles.^{8,9} We sought to access a similar 7-azabicyclo[2.2.1]heptene core via activation with the $\{\text{TpW}(\text{NO})(\text{PMe}_3)\}$ fragment.

Scheme 4.7: Proposed intramolecular cyclization of **78**



We hypothesized that we could effect an intramolecular cyclization, with the amine closing on the carbocation of the allyl to give **88**, by treating **78** with acid then base at -30°C . Bases that were tested include Et_3N , DBU, $t\text{BuOK}$, OH^- , KHDMS, and n -butyl lithium. The temperature was also varied, and reduced to as low as -78°C . Most experiments resulted in decomposition, regeneration of starting material, or formation of **52**. In a few cases there was a potentially promising product; however, it was ultimately identified as the hydroxide addition product **89**. In some cases, an η^2 -1,3-diene complex that was not starting material was also observed. When **89** was allowed to sit in solution and monitored by ^1H NMR, it slowly converted to this 1,3-diene complex. 2D NMR analysis led to the identification of the new diene as an isomer of **78**, where the methylamine has migrated to a position adjacent to the CF_3 group (**90**). An alkene proton signal with an NOE interaction with a Tp proton trans to the PMe_3 ligand supports this assignment. Although we believed the amine to have migrated to the previously allylic position, this was a point of uncertainty in the assignment. Slow evaporation of solvent allowed for the formation of a single crystal suitable for X-ray diffraction. The crystal structure, shown in Figure 4.3, confirmed our proposed assignment of **90**. In complexes **78** and **89** the methylamine group is two carbons away from the CF_3 group; however, the crystal structure confirms the new position of the amine adjacent to the CF_3 . Although we have yet to find conditions to isolate the cyclized

complex **88**, this structure supports the proposed intramolecular movement of the amine group that has been invoked to explain the formation of the amine complexes **86C** and **87C**.

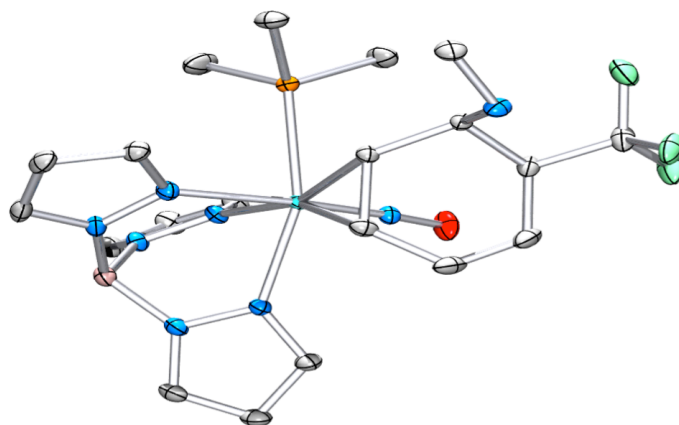
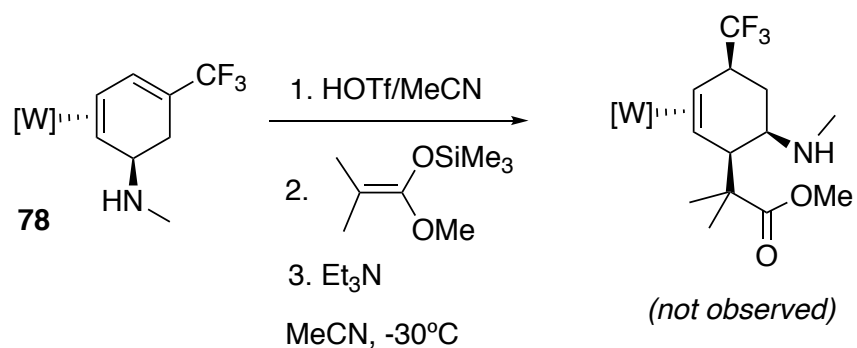


Figure 4.3: Crystal structure of complex **90**

One of the other nucleophiles that we attempted to add to **78** was the masked enolate MMTP. **78** was protonated with 2 equivalents of HOTf in MeCN at -30°C , then excess MMTP was added, and the reaction was left for 16 h (Scheme 4.8). The reaction solution was quenched with excess Et_3N and evaporated down. The ^1H NMR spectrum of the concentrated reaction solution revealed a single complex, but with none of the typical features expected for a successful addition product or for starting material.

Scheme 4.8: MMTP addition to **78**



The ^1H NMR spectrum of the complex lacked upfield methyl singlets for the two methyl groups of MMTP, indicating that the enolate had not been incorporated into the product. Additionally, the complex exhibited two downfield signals at 5.62 and 4.39 ppm that coupled strongly to each other ($J = 12.5$ Hz). The downfield shift and the large coupling constant of these proton signals were different from the typical peaks observed in TFT addition products. Figure 4.4 shows an overlay of the ^1H NMR spectra of the methoxide addition product (**85**) and the unidentified product. In order to explain the large coupling constant between the two downfield protons in the mystery complex, we proposed that a bicyclic system had formed. This could act to constrain the ring such that the dihedral angle between the two protons would be close to 0° , causing the increased coupling constant.

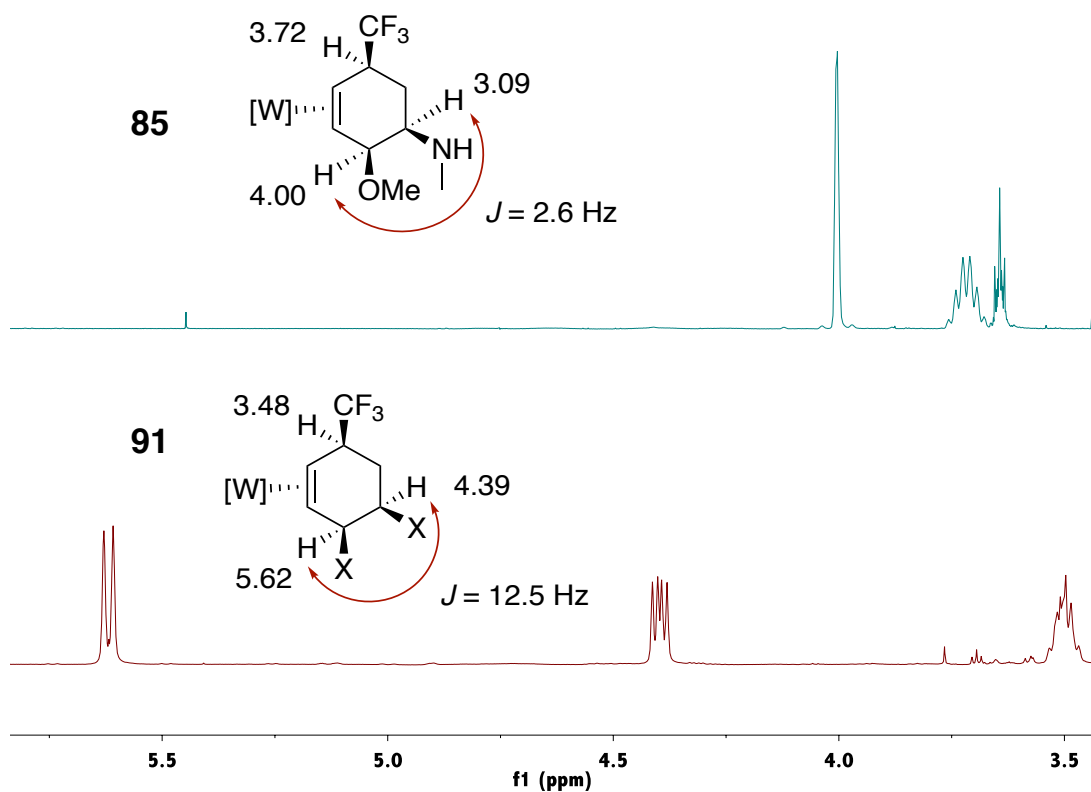


Figure 4.4: ^1H NMR overlay of **85** (top) and **91** (bottom)

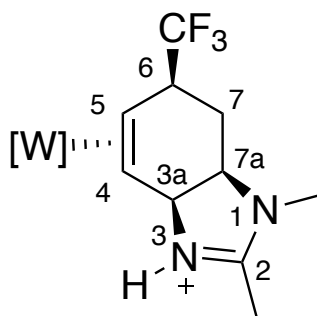


Figure 4.5: Proposed structure of complex **91** (triflate counterion omitted)

Full 2D NMR analysis (COSY, NOESY, HSQC, and HMBC) led to the identification of **91** as the bicyclic complex shown in Figure 4.5, with a benzimidazole type core. One of the key features that led to this conclusion was the observation that two methyl singlets (3.19 and 2.34 ppm) had an HMBC correlation with the same quaternary carbon at 165.6 ppm (C2 in Figure 4.5). Although the reaction was quenched with Et₃N, the isolated complex is still in a protonated form, which is consistent with the increased basicity of the amidine. The ¹H NMR spectrum features an N-H proton signal, which has an NOE correlation with a pyrazole Tp proton that is trans to the PMe₃. The formation of this bicyclic system is believed to be a result of the acetonitrile solvent adding as the nucleophile. This type of reaction is similar to the organic Ritter reaction, where a nitrile adds to a carbocation generated in situ. Similar reactivity was observed previously with the [W]-η²-N-ethylindolinium complex, but with a hydroxy group instead of an amine, leading to a cyclic imidate.⁵ In this case, we propose a mechanism involving the intramolecular cyclization of the amine with the added nitrile group. Gratifyingly, single crystal X-ray structure determination confirmed the proposed bicyclic system (Figure 4.6). Additionally, the cis-fused ring juncture in the crystal structure exhibits a dihedral angle close to 0° between the

two bridgehead protons, which supports our original hypothesis about the increased coupling constant due to angle constraints.

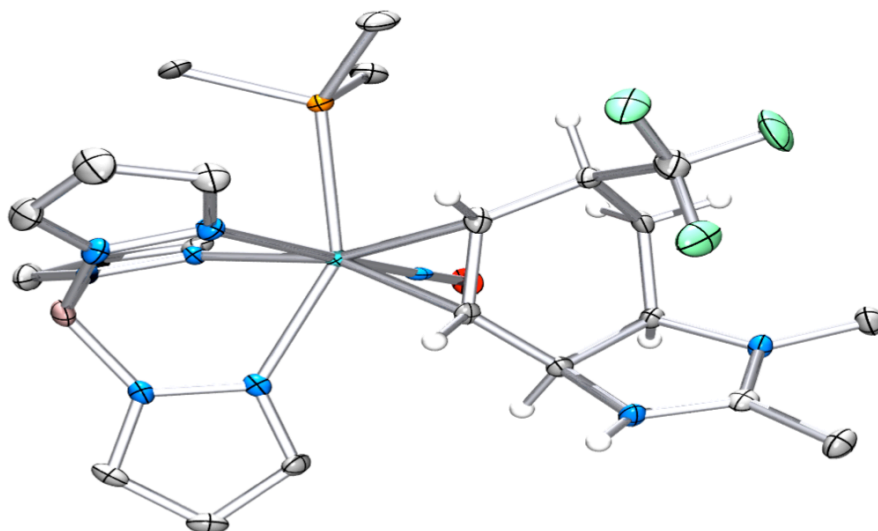


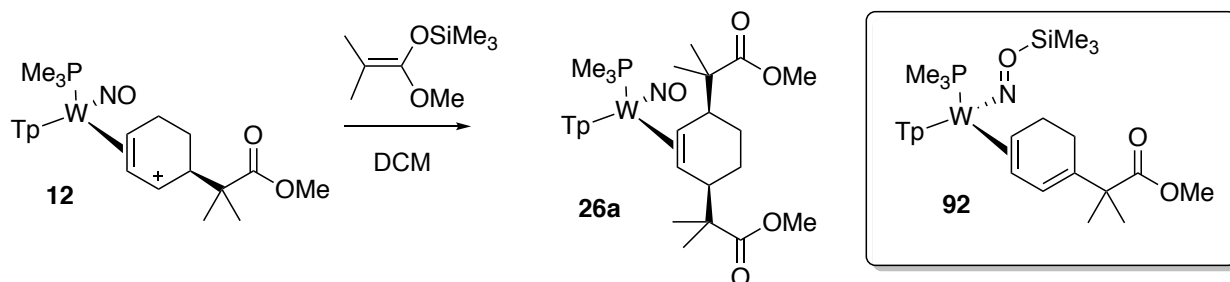
Figure 4.6: Crystal structure of complex **91** (triflate counterion omitted)

Once the structure of **91** was confirmed, we sought to optimize the reaction and try to elucidate the mechanism. Typically, we would not expect acetonitrile to be reactive enough as a nucleophile to add to the allylic species. Since MMTP was not incorporated into the product, subsequent experiments were run without the addition of the masked enolate. Unfortunately, in the absence of MMTP no product formation was observed. However, when the initial reaction conditions were reproduced with excess MMTP, **91** was cleanly formed and isolated via a precipitation from Et₂O in a 66% yield.

Until recently, the potential role of the trimethylsilyl (TMS) protected enolate (MMTP) was not well understood. During the exploration of η^2 -benzene chemistry (Chapter 2), MMTP was reacted with the allyl **12**. The reaction was monitored in situ by ¹H

and ^{31}P NMR, which initially showed no reaction. Over time multiple complexes were observed, and the major complex was tentatively identified as the 1,3-diene complex **92** (Scheme 4.9), based on a comparison to the TFT analogue, **60** discussed in Chapter 3. The key feature of this complex is a single uncoordinated alkene proton resonance. A crystal of **92** was grown, and the corresponding X-ray structure supported our assignment of the 1,3-diene complex. Unexpectedly, the crystal structure also revealed that a TMS group had coordinated to the nitrosyl ligand, causing the NO^+ to convert to a bent formation. Unfortunately, disorder in the crystal precluded complete structure determination; however, the coordination of the TMS group to the nitrosyl ligand was able to be observed.

Scheme 4.9: MMTP addition to **12**



Coordination to the nitrosyl ligand has been reported previously by our group with the $\text{TpW}(\text{NO})(\text{PMe}_3)(\eta^2\text{-cyclopentene})$ and $\text{TpW}(\text{NO})(\text{PMe}_3)(\eta^2\text{-acetone})$ complexes.¹⁰ Treatment of both complexes with MeOTf resulted in the methylation of the nitrosyl. The modification of the nitrosyl ligand causes an increase in the nitrosyl stretching frequency by $\sim 100\text{ cm}^{-1}$ and an increase in the $E_{1/2}$ by $\sim 800\text{ mV}$, reflecting a more electron-deficient metal center. The methylation was proposed to occur at the nitrogen of the NO ligand based on NOE correlations. However, the crystal structure of **92**, which shows the TMS group bound terminally through the oxygen, potentially provides insight into how

electrophilic reagents interact (reversibly or irreversibly) with the nitrosyl ligand. In the literature, there have been two recent reports on Lewis acid coordination to nitrosyl ligands and the subsequent effect on reactivity of the metal complex. Berke et. al. reported the Lewis acid triggered bending of nitrosyl ligands in rhenium complexes (Figure 4.7, top).¹¹ In this case, the Lewis acid acts as a co-catalyst, and coordination to the NO ligand serves to further activate the rhenium catalyst towards alkene hydrogenation. In a related paper, Legzdins et. al. reported Lewis acid coordination to the nitrosyl ligand of Mo(0) and W(0) complexes.¹² The modulation of the nitrosyl ligand induced by a Lewis acid results in an intramolecular orthometalation of one of the $\text{Ph}_2\text{PCH}_2\text{CH}_2\text{PPh}_2$ ligands (Figure 4.7, bottom).

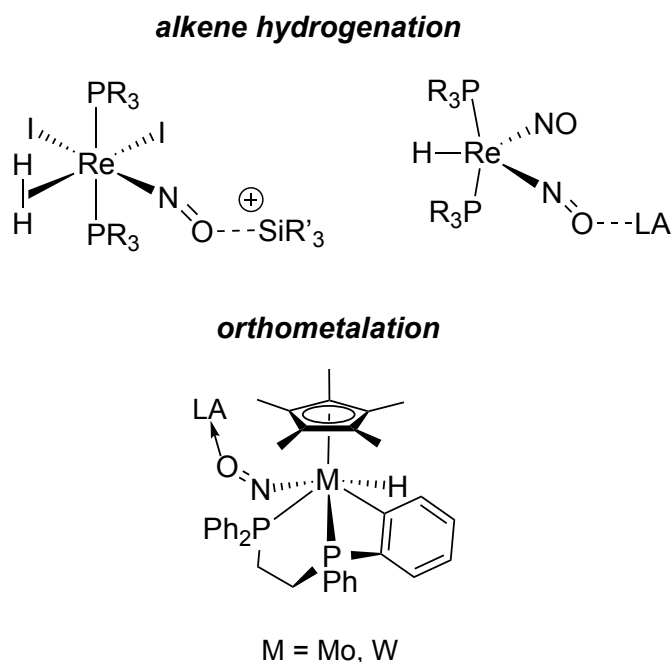
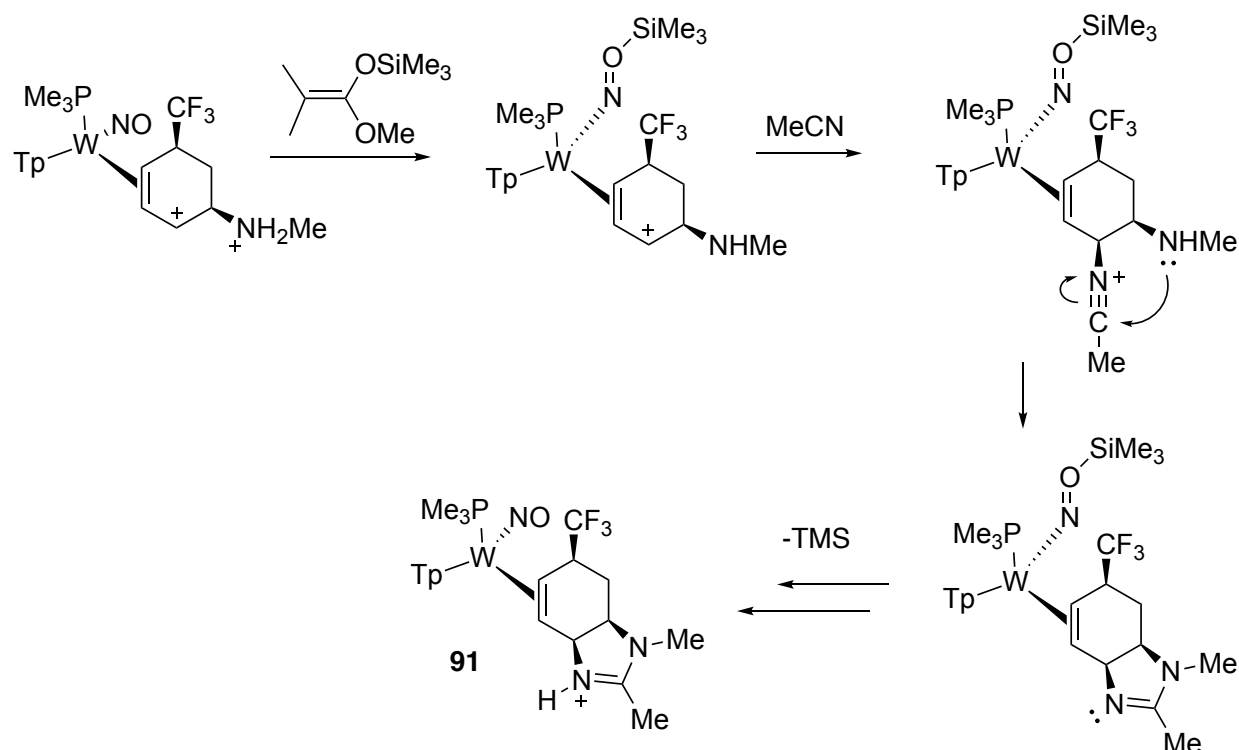


Figure 4.7: Lewis acid induced nitrosyl bending

With these reports in mind, we began to consider the role that Lewis acid coordination could play in the reactivity of dihapto-coordinated ligands. Specifically, we

proposed that the necessity of MMTP for the successful formation of **91** could be due to the generation of a TMS group from the MMTP. As discussed previously, acetonitrile would typically not be considered a strong enough nucleophile to add to our allyl complex. However, in situ coordination of the TMS group to the nitrosyl would reduce the electron density of the metal center, which would theoretically increase the reactivity of the allyl and enable the addition of weaker nucleophiles. Scheme 4.10 outlines a proposed mechanism for the formation of **91** taking into account the effect of the TMS group.

Scheme 4.10: Proposed mechanism for formation of **91** with bent nitrosyl



The proposed role of the TMS group in this case is a reversible modulator of the electron density and thus reactivity of the tungsten complex. To support this type of mechanism, several experiments were conducted to probe the role of the TMS group in the

reversible modulation of the reactivity of the tungsten system. In the initial experiment where formation of **91** was observed, the reaction was quenched with Et₃N. A subsequent experiment was run without the addition of Et₃N to determine whether the base was necessary for the reaction to go forward. The reaction conducted without base was evaporated down and a ¹H NMR was taken in d⁶-acetone (Figure 4.8, bottom).

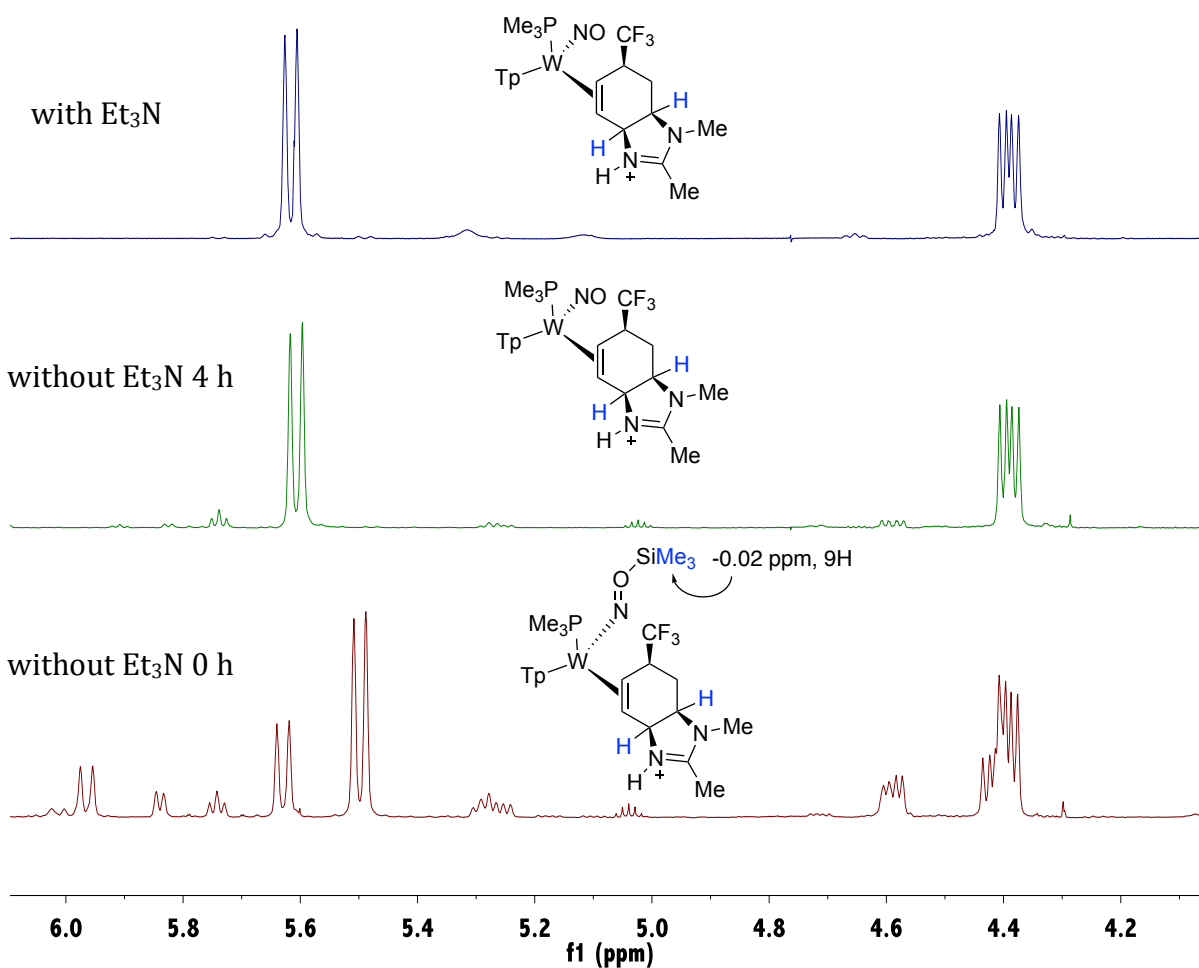


Figure 4.8: ¹H NMR spectra showing the formation of **91** with and without Et₃N

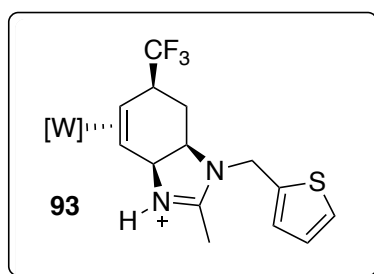
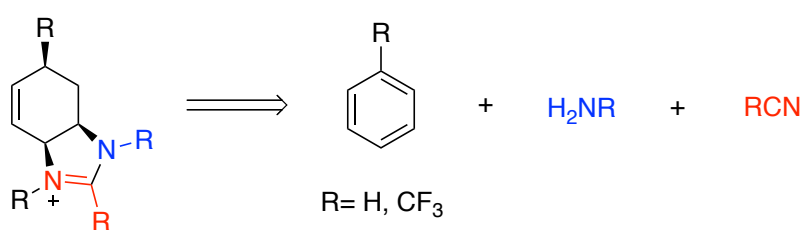
Peaks consistent with the formation of a cyclized product were observed; however, multiple products were present. The proton signals of the major product in the bottom spectrum exhibited similar splitting patterns to the desired complex **91** (Figure 4.8, top),

but had slightly different chemical shifts. Interestingly, we identified a singlet at -0.02 ppm that integrated to 9H relative to the major complex, which would be consistent with the 3 methyls of the TMS group. The solution was left at room temperature for 4 h, then another ^1H NMR spectrum was taken (Figure 4.8, middle). After sitting at room temperature the mixture had converted to a single complex that was identified as **91**, with identical shifts to those observed in the presence of Et_3N . A comparison of the bottom two spectra revealed that the singlet at -0.02 ppm present at the first time point decreased in tandem with the major product first observed. These observations are consistent with the reversible coordination of a TMS group, which can fall off of the nitrosyl ligand when in solution with acetone at room temperature. When the reaction is quenched with Et_3N , the base could more rapidly remove the TMS group, which is not observed in the isolated product **91** (or crystal structure).

These recent observations and crystal structure data have allowed us to better understand the necessary reaction conditions and propose a possible mechanism for the formation of **91**. This cyclization reaction has the potential to be expanded, such that at least three different positions on the benzimidazole ring could be systematically diversified. A variety of analogs could be synthesized by changing the starting aromatic, the primary amine, and the nitrile (Scheme 4.11). Preliminary experiments show that the same type of cyclization can occur when a more complicated primary amine is used as the first nucleophile, as illustrated with complex **82**. Reaction of **82** under the conditions outlined for **91** leads to the formation of **93**, which exhibits the characteristic bridgehead proton peaks of the desired product (Scheme 4.11). The rapid and stereocontrolled elaboration of a simple aromatic into tetrahydrobenzimidazole derivatives is an exciting synthetic

transformation because of the prevalence of the benzimidazole core in pharmaceuticals. Njardarson and coworkers recently cited benzimidazole as the 15th most common nitrogen heterocycle in FDA approved pharmaceuticals.³ This methodology not only provides access to a saturated form of this core structure with high regio- and stereocontrol, but also provides the opportunity to access a diverse range of derivatives.

Scheme 4.11: Expanding the synthesis of tetrahydrobenzimidazoles



4.3 Conclusions

The range of nucleophiles accessible for the first tandem electrophilic/nucleophilic addition to η^2 -TFT was expanded to incorporate a variety of primary and secondary amines, including cyclic amines and amines decorated with additional functional groups. Further functionalization of these amine dienes was investigated to understand how the reversible nature of the first nucleophilic addition affects the second tandem addition reaction. In most cases, the second addition to these TFT complexes resulted in the adjacent installation of nucleophiles. This was accomplished with an amine as the second

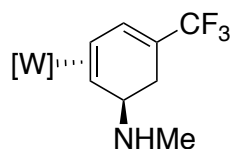
nucleophile by quenching the reaction with base at low temperature. Conversely, if the reaction is not quenched with base, the favored product has a 1,4- relationship between the amines, possibly due to an intramolecular migration of the amine. Unexpectedly, protonating the methylamine diene **78** in the presence of MMTP and acetonitrile resulted in the addition of acetonitrile as the nucleophile. A proposed intramolecular cyclization with the amine substituent led to the formation of a cis-fused bicyclic system with a tetrahydrobenzimidazole core. In our initial investigation into the mechanism of this reaction, we believe that the coordination of a TMS group to the nitrosyl ligand modulates the electron density of the allyl complex and further activates it towards nucleophilic addition. Further investigations into this mechanism and efforts to expand the scope of the reaction are underway.

4.4 Experimental

General Methods: NMR spectra were obtained on 500, 600 or 800 MHz spectrometers. Chemical shifts are referenced to tetramethylsilane (TMS) utilizing residual ^1H or ^{13}C signals of the deuterated solvents as internal standards. Phosphorus NMR signals are referenced to 85% H_3PO_4 (δ 0.00) using a triphenyl phosphate external standard (δ -16.58). Chemical shifts are reported in ppm and coupling constants (J) are reported in hertz (Hz). Infrared Spectra (IR) were recorded on a spectrometer as a glaze on a diamond anvil ATR assembly, with peaks reported in cm^{-1} . Electrochemical experiments were performed under a nitrogen atmosphere. Most cyclic voltammetric data were recorded at ambient temperature at 100 mV/s, unless otherwise noted, with a standard three electrode cell from +1.8 V to -1.8 V with a platinum working electrode, *N,N*-dimethylacetamide (DMA) solvent, and tetrabutylammonium hexafluorophosphate (TBAH) electrolyte (~1.0 M). All potentials are reported versus the normal hydrogen electrode (NHE) using cobaltocenium hexafluorophosphate ($E_{1/2} = -0.78$ V, -1.75 V) or ferrocene ($E_{1/2} = 0.55$ V) as an internal standard. Peak separation of all reversible couples was less than 100 mV. All synthetic reactions were performed in a glovebox under a dry nitrogen atmosphere unless otherwise noted. All solvents were purged with nitrogen prior to use. Deuterated solvents were used as received from Cambridge Isotopes. When possible, pyrazole (Pz) protons of the (trispyrazolyl) borate (Tp) ligand were uniquely assigned (e.g., "PzB3") using two-dimensional NMR data (see Figure S1). If unambiguous assignments were not possible, Tp protons were labeled as "Pz3/5 or Pz4". All J values for Pz protons are 2 (± 0.4) Hz. BH peaks (around 4-5 ppm) in the ^1H -NMR spectra are not assigned due to their quadrupole broadening; however, confirmation of the BH group is provided by IR data (around 2500

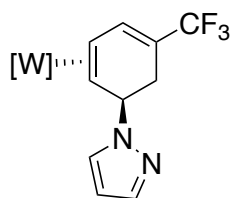
cm⁻¹). Compound **52** was prepared according to a previous literature procedure.¹³ Synthesis and characterization of compounds **54-58** is shown in Chapter 3.

Complex Characterization



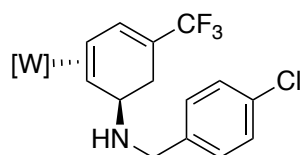
Compound 78. To a 4-dram vial charged with a stir pea were added **52** (500 mg, 0.770 mmol) followed by acetonitrile (2 mL, -30°C) and a 1M solution of HOTf in acetonitrile (1.54 mL, 1.54 mmol, -30°C), resulting in a homogeneous golden solution, which was allowed to sit for 15 min at -30°C. 2M H₂NMe/THF (3.85 mL, 7.70 mmol, -30°C) was then added to the reaction vial with stirring and allowed to sit at -30°C for 2.5 h. While the reaction was still cold, 1M tBuOK in *tert*-butanol (3.1 mL, 3.1 mmol) was added, and then the reaction solution was put back in the freezer at -30°C for 15 min. The reaction was then transferred to a filter flask and evaporated *in vacuo* to ~half volume. Precipitation was then induced by adding H₂O (20 mL), and the resulting pale yellow solid was collected on a 15 mL fine porosity fritted disc, washed with H₂O (1 mL), acetonitrile (1 mL), and pentane (2 x 5 mL) then desiccated overnight, yielding **78** (350 mg, 0.515 mmol, 67% yield). CV (DMAc) $E_{p,a} = +0.70$ V (NHE). IR: $\nu(\text{BH}) = 2487$ cm⁻¹, $\nu(\text{NO}) = 1565$ cm⁻¹. Anal. Calc'd for C₂₀H₂₉BF₃N₃OPW: C, 35.32; H, 4.30; N, 16.48. Found: C, 35.59; H, 4.21; N, 16.20. ³¹P NMR (d⁶-DMSO, δ): -11.10 ($J_{\text{WP}} = 279$). ¹H NMR (CD₃CN, δ): 8.05 (d, 1H, PzB3), 7.98 (d, 1H, PzA3), 7.86 (t, 2H, PzB5 & PzC5), 7.77 (d, 1H, PzA5), 7.44 (d, 1H, PzC3), 7.18 (m, 1H, H2), 6.37 (t,

1H, PzB4), 6.29 (overlapping t, 2H, PzA4 & PzC4), 3.52 (dm, $J = 5.3$, 1H, H5), 2.81 (m, 1H, H3), 2.71 (dm, $J = 16.5$, 1H, H6x), 2.33 (buried, 1H, H6y), 2.32 (s, 3H, NMe), 1.36 (dm, $J = 9.7$, 1H, H4), 1.22 (d, $J = 8.6$, 9H, PMe₃). ¹³C NMR (CD₃CN, δ): 144.5 (PzB3), 143.2 (PzA3), 141.9 (PzC3), 138.0 (PzC5), 137.4 (PzB5), 137.1 (PzA5), 136.8 (m, C2), 126.8 (q, $J = 268.6$, CF₃), 115.8 (q, $J = 29.5$, C1), 107.5 (Pz4), 107.2 (Pz4), 106.9 (Pz4), 60.2 (C4), 58.3 (C5), 47.6 (d, $J = 9.6$, C3), 34.7 (NMe), 26.1 (C6), 13.8 (d, $J = 29.0$, PMe₃).



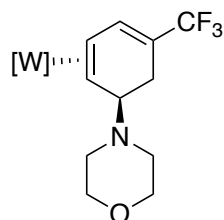
Compound 79. To a 4-dram vial charged with a stir pea were added **52** (50 mg, 0.077 mmol) followed by acetonitrile (0.5 mL, -30°C) and a 1M solution of HOTf in acetonitrile (0.12 mL, 0.12 mmol, -30°C), resulting in a homogeneous golden solution, which was allowed to sit for 15 min at -30°C. Pyrazole (79 mg, 1.2 mmol) was added with stirring, and then the reaction solution was allowed to sit at -30°C for 18 h. While the reaction was still cold, 1M tBuOK in *tert*-butanol (0.31 mL, 0.31 mmol) was added, and then the reaction solution was put back in the freezer at -30°C for 3 h. Precipitation was then induced by adding H₂O (5 mL) to the reaction solution with stirring, and the resulting pale yellow solid was collected on a 15 mL fine porosity fritted disc, washed with H₂O (1 mL), acetonitrile (0.5 mL), and pentane (2 x 3 mL) then desiccated overnight, yielding **79** (26 mg, 0.036 mmol, 47% yield). CV (DMAc) $E_{p,a} = +0.92$ V (NHE). IR: $\nu(\text{BH}) = 2489$ cm⁻¹, $\nu(\text{NO}) = 1572$ cm⁻¹. ³¹P NMR (d⁶-acetone, δ): -11.81 ($J_{\text{WP}} = 278$). ¹H NMR (d⁶-acetone, δ): 8.17 (d, 1H, PzB3), 8.13 (d, 1H, PzA3), 7.99 (d, 1H, PzB5), 7.98 (d, 1H, PzC5), 7.89 (d, $J = 2.2$, 1H, H5'),

7.86 (d, 1H, PzA5), 7.73 (d, 1H, PzC3), 7.32 (m, 1H, H2), 7.31 (d, $J = 1.8$, 1H, H3'), 6.44 (t, 1H, PzB4), 6.38 (t, 1H, PzA4), 6.34 (t, 1H, PzC4), 6.09 (t, $J = 2.0$, 1H, H4'), 5.62 (m, 1H, H5), 3.20 (m, 1H, H3), 3.19 (m, 1H, H6x), 2.53 (d, $J = 17.0$, 1H, H6y), 1.52 (dm, $J = 9.6$, 1H, H4), 1.36 (d, $J = 8.7$, 9H, PMe₃). ¹³C NMR (d⁶-acetone, δ): 144.7 (PzB3), 142.8 (PzA3), 142.0 (PzC3), 138.1 (C3'), 138.0 (PzC5), 137.5 (PzB5), 137.1 (PzA5), 136.9 (m, C2), 127.5 (C5'), 126.2 (q, $J = 268.9$, CF₃), 115.6 (q, $J = 29.9$, C1), 107.5 (PzB4), 107.2 (PzC4), 107.0 (PzA4), 104.7 (C4'), 61.8 (C5), 56.8 (d, $J = 2.2$, C4), 47.7 (d, $J = 10.3$, C3), 28.7 (C6), 13.7 (d, $J = 29.3$, PMe₃).



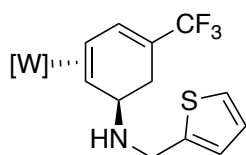
Compound 80. To a 4-dram vial charged with a stir pea were added **52** (100 mg, 0.154 mmol) followed by acetonitrile (1 mL, -30°C) and a 1M solution of HOTf in acetonitrile (0.23 mL, 0.23 mmol, -30°C), resulting in a homogeneous golden solution, which was allowed to sit for 20 min at -30°C. 4-Chlorobenzylamine (370 mg, 2.61 mmol, -30°C) was added with stirring, and then the reaction solution was allowed to sit at -30°C for 19 h. While the reaction was still cold, 1M tBuOK in *tert*-butanol (0.62 mL, 0.62 mmol) was added, and then the reaction solution was put back in the freezer at -30°C for 10 min. The reaction was diluted with H₂O (10 mL), and extracted with Et₂O (10 mL). The organic layer was then evaporated *in vacuo*. The film was redissolved in minimal THF and added to stirring pentane (20 mL), which resulted in an oil. The liquid was decanted off, and the oil was redissolved in THF and added to pentane (20 mL). The resulting pale yellow solid was collected on a 15 mL fine porosity fritted disc, washed with pentane (2 x 5 mL) then

desiccated overnight, yielding **80** (45 mg, 0.057 mmol, 37% yield). IR: $\nu(\text{BH}) = 2487 \text{ cm}^{-1}$, $\nu(\text{NO}) = 1561 \text{ cm}^{-1}$. Anal. Calc'd for $\text{C}_{26}\text{H}_{32}\text{BClF}_3\text{N}_8\text{OPW}$: C, 39.50; H, 4.08; N, 14.17. Found: C, 39.00; H, 3.89; N, 13.86. ^1H NMR (d^6 -acetone, δ): 8.12 (d, 1H, Pz3/5), 7.97 (d, 1H, Pz3/5), 7.95 (d, 1H, Pz3/5), 7.89 (d, 1H, Pz3/5), 7.82 (d, 1H, Pz3/5), 7.61 (d, 1H, Pz3/5), 7.31 (d, $J = 8.4$, 2H, Ar-H), 7.25 (d, $J = 8.4$, 2H, Ar-H), 7.22 (m, 1H, H2), 6.40 (t, 1H, Pz4), 6.35 (t, 1H, Pz4), 6.25 (t, 1H, Pz4), 3.82 (d, $J = 13.6$, 1H, H7x), 3.78 (d, $J = 13.6$, 1H, H7x), 3.77 (buried, 1H, H5), 2.87 (m, 2H, H3 & H6x), 2.45 (d, $J = 16.5$, 1H, H6y), 1.55 (d, $J = 9.6$, 1H, H4), 1.30 (d, $J = 8.5$, 9H, PMe_3). ^{13}C NMR (d^6 -acetone, δ): 144.4 (Pz3), 142.8 (Pz3), 142.0 (Pz3), 141.8 (Ar-C), 137.8 (Pz5), 137.2 (Pz5), 136.8 (m, C2), 136.7 (Pz5), 132.2 (Ar-C), 130.6 (2C, Ar-C), 128.8 (2C, Ar-C), 126.6 (q, $J = 268.7$, CF_3), 115.7 (q, $J = 29.6$, C1), 107.3 (Pz4), 107.1 (Pz4), 106.5 (Pz4), 60.5 (C4), 55.9 (C5/C5'), 51.4 (C5/C5'), 47.4 (d, $J = 9.6$, C3), 26.4 (C6), 13.8 (d, $J = 28.6$, PMe_3).



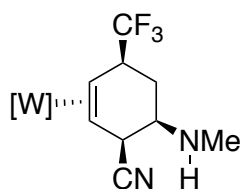
Compound 81. To a 4-dram vial charged with a stir pea were added **52** (200 mg, 0.308 mmol) followed by acetonitrile (2 mL, -30°C) and a 1M solution of HOTf in acetonitrile (0.46 mL, 0.46 mmol, -30°C), resulting in a homogeneous golden solution, which was allowed to sit for 20 min at -30°C . Morpholine (416 mg, 4.78 mmol) was added with stirring, and then the reaction solution was allowed to sit at -30°C for 17 h. While the reaction was still cold, 1M tBuOK in *tert*-butanol (1.23 mL, 1.23 mmol) was added.

Precipitation was then induced by adding H₂O (6 mL) to the reaction solution with stirring, and the resulting pale yellow solid was collected on a 15 mL fine porosity fritted disc, washed with H₂O (2 x 3 mL), acetonitrile (0.5 mL), and pentane (3 x 5 mL) then desiccated overnight, yielding **81** (193 mg, 0.262 mmol, 85% yield). IR: $\nu(\text{BH}) = 2487 \text{ cm}^{-1}$, $\nu(\text{NO}) = 1559 \text{ cm}^{-1}$. Anal. Calc'd for C₂₃H₃₃BF₃N₈O₂PW: C, 37.52; H, 4.52; N, 15.22. Found: C, 37.48; H, 4.60; N, 15.17. ³¹P NMR (d⁶-acetone, δ): -11.74 ($J_{\text{WP}} = 282$). ¹H NMR (d⁶-acetone, δ): 8.11 (d, 1H, PzB3), 8.06 (d, 1H, PzA3), 7.97 (d, 1H, PzC5), 7.95 (d, 1H, PzB5), 7.84 (d, 1H, PzA5), 7.71 (d, 1H, PzC3), 7.13 (m, 1H, H2), 6.40 (t, 1H, PzB4), 6.36 (t, 1H, PzC4), 6.30 (t, 1H, PzA4), 4.00 (d, $J = 7.7$, 1H, H5), 3.52 (t, $J = 4.5$, 4H, H2' & H6'), 3.04 (m, 1H, H3), 2.83 (buried, 1H, H6x), 2.80 (m, 2H, H3'/H5'), 2.51 (dt, $J = 11.3, 4.5$, 2H, H3'/H5'), 2.37 (d, $J = 17.5$, 1H, H6y), 1.32 (buried, 1H, H4), 1.30 (d, $J = 8.5$, 9H, PMe₃). ¹³C NMR (d⁶-acetone, δ): 144.5 (PzB3), 142.3 (PzA3), 142.0 (PzC3), 137.8 (PzC5), 137.2 (PzB5), 137.0 (PzA5), 136.6 (m, C2), 126.6 (q, $J = 269.5$, CF₃), 117.4 (q, $J = 29.0$, C1), 107.3 (PzB4), 107.1 (PzC4), 106.6 (PzA4), 68.2 (2C, C2' & C6'), 62.2 (C5), 52.6 (C4), 50.2 (2C, C3' & C5'), 49.6 (d, $J = 9.5$, C3), 22.5 (C6), 13.8 (d, $J = 28.6$, PMe₃).



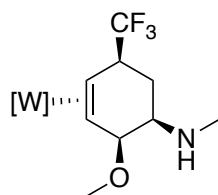
Compound 82. To a 4-dram vial charged with a stir pea were added **52** (50 mg, 0.077 mmol) followed by acetonitrile (0.5 mL, -30°C) and a 1M solution of HOTf in acetonitrile (0.11 mL, 0.11 mmol, -30°C), resulting in a homogeneous golden solution, which was allowed to sit for 15 min at -30°C. 2-Thiophenemethylamine (192 mg, 1.70 mmol) was

added with stirring, and then the reaction solution was allowed to sit at -30°C for 5 h. While the reaction was still cold, 1M tBuOK in *tert*-butanol (0.31 mL, 0.31 mmol) was added. Precipitation was then induced by adding H_2O (2 mL) to the reaction solution with stirring, and the resulting pale yellow solid was collected on a 15 mL fine porosity fritted disc, washed with H_2O (2 x 3 mL), and pentane (4 x 4 mL) then desiccated overnight, yielding **82** (50 mg, 0.066 mmol, 86% yield). IR: $\nu(\text{BH}) = 2486 \text{ cm}^{-1}$, $\nu(\text{NO}) = 1564 \text{ cm}^{-1}$. ^1H NMR (d^6 -DMSO, δ): 8.05 (bs, 3H, Pz3/5), 7.91 (d, 1H, Pz3/5), 7.80 (d, 1H, Pz3/5), 7.64 (d, 1H, Pz3/5), 7.30 (m, 1H, Ar-H), 7.16 (m, 1H, H2), 6.90 (bs, 1H, Ar-H), 6.85 (bs, 1H, Ar-H), 6.42 (t, 1H, Pz4), 6.36 (t, 1H, Pz4), 6.29 (t, 1H, Pz4), 3.91 (m, 2H, H5'), 3.74 (bs, 1H, H5), 2.87 (m, 1H, H3), 2.69 (m, 1H, H6x), 2.31 (m, 1H, H6y), 1.34 (m, 1H, H4), 1.19 (d, $J = 7.9$, 9H, PMe_3). ^{13}C NMR (d^6 -DMSO, δ): 145.9 (Ar-C), 143.4 (Pz3), 141.7 (Pz3), 141.2 (Pz3), 137.2 (Pz5), 136.5 (Pz5), 136.3 (m, C2), 136.1 (Pz5), 126.4 (Ar-C), 125.5 (q, $J = 269.0$, CF_3), 124.2 (Ar-C), 123.9 (Ar-C), 113.6 (q, $J = 29.8$, C1), 106.6 (Pz4), 106.4 (Pz4), 106.0 (Pz4), 59.1 (C4), 54.1 (C5), 46.3 (d, $J = 9.6$, C3), 45.7 (C5'), 25.2 (C6), 13.0 (d, $J = 28.6$, PMe_3).



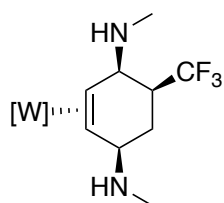
Compound 84. To a 4-dram vial charged with a stir pea were added **78** (30 mg, 0.044 mmol), acetonitrile (0.5 mL, -30°C), and a 1M solution of HOTf in acetonitrile (0.11 mL, 0.11 mmol, -30°C), resulting in a homogeneous yellow solution, which was allowed to sit for 15 min at -30°C . A solution of NaCN (14 mg, 0.29 mmol) and MeOH (0.5 mL, -30°C) was added to the reaction solution with stirring, and then the reaction was left at -30°C for 18 h. The

reaction was then evaporated *in vacuo* to dryness. The resulting solid was dissolved in d⁶-acetone to take ¹H, ¹³C and 2D NMR data. ¹H NMR (d⁶-acetone, δ): 8.11 (d, 1H, PzB3), 7.99 (d, 1H, PzC5), 7.96 (d, 1H, PzB5), 7.88 (d, 1H, PzA5), 7.65 (d, 1H, PzA3), 7.48 (d, 1H, PzC3), 6.40 (t, 1H, PzB4), 6.37 (t, 1H, PzC4), 6.35 (t, 1H, PzA4), 3.86 (m, 1H, H4), 3.84 (m, 1H, H1), 3.17 (m, 1H, H5), 2.80 (ddd, *J* = 13.6, 11.1, 2.4, 1H, H2), 1.95 (m, 1H, H6x), 1.53 (q, *J* = 12.0, 1H, H6y), 1.23 (d, *J* = 8.6, 9H, PMe₃) 1.18 (d, *J* = 11.1, 1H, H3). ¹³C NMR (d⁶-acetone, δ): 144.9 (PzB3), 143.2 (PzA3), 141.8 (PzC3), 137.8 (Pz5), 137.6 (2C, Pz5), 131.6 (q, *J* = 279.6, CF₃), 125.6 (CN), 107.3 (Pz4), 107.2 (Pz4), 107.1 (Pz4), 56.2 (C3) 53.0 (C5), 49.5 (NMe), 42.8 (m, C1), 39.5 (m, C2), 36.4 (C4), 28.3 (C6), 13.3 (d, *J* = 29.3, PMe₃).



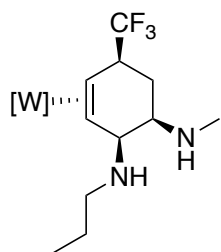
Compound 85. To a 4-dram vial charged with a stir pea were added **78** (30 mg, 0.044 mmol), followed by acetonitrile (0.6 mL, -30°C), and a 1M solution of HOTf in acetonitrile (0.11 mL, 0.11 mmol, -30°C), resulting in a homogeneous golden solution, which was allowed to sit for 20 min at -30°C. 1M Bu₄OH/MeOH (0.66 mL, 0.66 mmol, -30°C) was then added to the reaction vial with stirring, and the reaction was allowed to sit at -30°C for 19 h. The reaction was evaporated *in vacuo* to ~half volume then diluted with H₂O (10 mL) and extracted with Et₂O (10 mL). The organic layer was then dried over MgSO₄ and evaporated *in vacuo* to dryness. The film was redissolved in minimal THF and added to stirring pentane (15 mL, -30°C), which resulted in an oil. The solution was again evaporated *in vacuo* to dryness, redissolved in THF and added to pentane (15 mL, -30°C).

The resulting pale yellow solid was filtered on a 15 mL fine porosity fritted disc and discarded. The filtrate was cooled to -30°C overnight, resulting in the precipitation of a crystalline solid. The solid was collected on a 15 mL fine porosity fritted disc, rinsed with pentane (2 mL, -30°C) then desiccated overnight, yielding **85** (10 mg, 0.014 mmol, 32% yield). CV (DMAc) $E_{p,a} = +0.51$ V (NHE). IR: $\nu(\text{BH}) = 2493$ cm^{-1} , $\nu(\text{NO}) = 1549$ cm^{-1} . ^{31}P NMR (CD_3CN , δ): -11.82 ($J_{\text{WP}} = 283$). ^1H NMR (CD_3CN , δ): 8.05 (d, 1H, PzB3), 7.87 (d, 1H, PzC5), 7.86 (d, 1H, PzB5), 7.77 (d, 1H, PzA5), 7.72 (d, 1H, PzA3), 7.33 (d, 1H, PzC3), 6.36 (t, 1H, PzB4), 6.30 (t, 1H, PzC4), 6.29 (t, 1H, PzA4), 4.00 (m, 1H, H4), 3.72 (m, 1H, H1), 3.11 (s, 3H, OMe), 3.09 (ddd, $J = 12.3, 4.0, 2.6$, 1H, H5), 2.73 (ddd, $J = 13.6, 11.0, 2.3$, 1H, H2), 2.45 (s, 3H, NMe), 1.67 (ddd, $J = 11.8, 7.4, 4.0$, 1H, H6x), 1.51 (q, $J = 12.1$, 1H, H6y), 1.30 (d, $J = 11.0$, 1H, H3), 1.13 (d, $J = 8.5$, 9H, PMe_3). ^{13}C NMR (CD_3CN , δ): 145.0 (PzB3), 144.7 (PzA3), 142.2 (PzC3), 138.0 (PzC5), 137.7 (2C, PzA5 & PzB5), 132.4 (q, $J = 279.3$, CF_3), 107.6 (PzB4), 107.3 (PzA4/PzC4), 107.0 (PzA4/PzC4), 81.6 (C4), 56.9 (OMe), 55.9 (C3) 55.3 (C5), 43.6 (q, $J = 24.0$, C1), 42.9 (d, $J = 12.5$, C2), 34.0 (NMe), 26.2 (m, C6), 13.6 (d, $J = 28.8$, PMe_3).



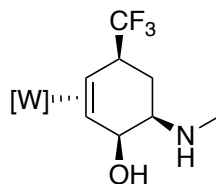
Compound 86. To a 4-dram vial charged with a stir pea were added **78** (30 mg, 0.044 mmol), followed by acetonitrile (0.5 mL, -30°C), and a 1M solution of HOTf in acetonitrile (0.11 mL, 0.11 mmol, -30°C), resulting in a homogeneous golden solution, which was allowed to sit for 15 min at -30°C . 2M $\text{H}_2\text{NMe}/\text{THF}$ (0.22 mL, 0.44 mmol, -30°C) was then added to the reaction vial with stirring, and it was allowed to sit at -30°C for 26 h. The

reaction solution was then evaporated *in vacuo* to dryness. The resulting solid was dissolved in CD₃CN to take ¹H and 2D NMR data. ¹H NMR (CD₃CN, δ): 8.14 (d, 1H, PzB3), 7.91 (overlapping d, 2H, PzB5 & PzC5), 7.79 (overlapping d, 2H, PzA3 & PzA5), 7.54 (d, 1H, PzC3), 6.42 (t, 1H, PzB4), 6.34 (t, 1H, PzC4), 6.31 (t, 1H, PzA4), 3.91 (m, 1H, H5), 3.83 (t, *J* = 3.3, 1H, H2), 2.97 (m, 1H, H1), 2.75 (td, *J* = 11.4, 2.7, 1H, H3), 2.67 (s, 3H, NMe), 2.55 (s, 3H, NMe), 2.34 (m, 1H, H6x), 1.94 (m, 1H, H6y), 1.23 (buried, 1H, H4), 1.21 (d, *J* = 8.7, 9H, PMe₃).



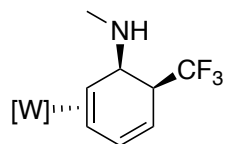
Compound 87A. To a 4-dram vial charged with a stir pea were added **78** (50 mg, 0.074 mmol) followed by acetonitrile (0.8 mL, -30°C) and a 1M solution of HOTf in acetonitrile (0.18 mL, 0.18 mmol, -30°C), resulting in a homogeneous golden solution, which was allowed to sit for 15 min at -30°C. Propylamine (61 mg, 1.0 mmol, -30°C) was added with stirring, and then the reaction solution was allowed to sit at -30°C for 17 h. While the reaction was still cold, 2M NaOtBu in THF (0.15 mL, 0.30 mmol) was added with stirring, and then the reaction was evaporated *in vacuo* to dryness. The resulting solid was dissolved in CD₃CN to take ¹H, ¹³C, and 2D NMR data. ³¹P NMR (CD₃CN, δ): -12.22 (*J*_{WP} = 283). ¹H NMR (CD₃CN, δ): 8.04 (d, 1H, PzB3), 7.87 (d, 1H, PzC5), 7.86 (d, 1H, PzB5), 7.77 (d, 1H, PzA5), 7.73 (d, 1H, PzA3), 7.29 (d, 1H, PzC3), 6.35 (t, 1H, PzB4), 6.29 (t, 1H, PzC4), 6.28 (t, 1H, PzA4), 3.71 (m, 1H, H1), 3.25 (bs, 1H, H4), 3.05 (dt, *J* = 12.2, 3.8, 1H, H5), 2.69 (m, 1H,

H2), 2.40 (s, 3H, NMe), 2.39 (buried, 1H, H7x), 2.18 (m, 1H, H7y), 1.64 (m, 1H, H6x), 1.38 (m, 1H, H6y), 1.34 (buried, 1H, H3), 1.31 (m, 1H, H8x), 1.25 (m, 1H, H8y), 1.13 (d, $J = 8.5$, 9H, PMe₃), 0.75 (t, $J = 7.4$, 3H, H9). ¹³C NMR (CD₃CN, δ): 144.8 (PzB3), 144.1 (PzA3), 141.9 (PzC3), 137.9 (Pz5), 137.6 (2C, Pz5), 132.5 (q, $J = 279.3$, CF₃), 107.5 (Pz4), 107.2 (Pz4), 106.9 (Pz4), 59.7 (C3), 56.9 (C4), 54.7 (C5), 51.2 (C7), 42.6 (m, C1), 41.2 (m, C2), 34.0 (NMe), 25.8 (C6), 13.4 (d, $J = 29.1$, PMe₃), 12.1 (C9).

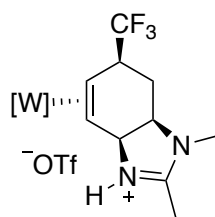


Compound 89. To a 4-dram vial charged with a stir pea were added **78** (22 mg, 0.032 mmol) followed by acetonitrile (0.7 mL, -30°C) and a 1M solution of HOTf in acetonitrile (0.1 mL, 0.1 mmol, -30°C), resulting in a homogeneous golden solution, which was allowed to sit for 15 min at -30°C. 1M KOtBu in *tert*-butanol (0.12 mL, 0.12 mmol, -30°C) was added with stirring, and then the reaction was left at -30°C for 26 h. Precipitation was then induced by adding H₂O (6 mL) to the reaction solution with stirring, and the resulting pale yellow solid was collected on a 15 mL fine porosity fritted disc, washed with pentane (2 mL) then desiccated overnight, yielding **89** (11 mg, 0.016 mmol, 50% yield). ¹H NMR (d⁶-acetone, δ): 8.11 (d, 1H, PzB3), 7.97 (d, 1H, PzC5), 7.94 (d, 1H, PzB5), 7.82 (d, 1H, PzA5), 7.75 (d, 1H, PzA3), 7.40 (d, 1H, PzC3), 6.38 (t, 1H, PzB4), 6.36 (t, 1H, PzC4), 6.29 (t, 1H, PzA4), 4.52 (bs, 1H, H4), 3.75 (m, 1H, H1), 3.09 (ddd, $J = 12.1, 3.6, 2.7$, 1H, H5), 2.79 (ddd, $J =$

13.8, 11.1, 2.7, 1H, H2), 2.48 (s, 3H, NMe), 1.70 (q, $J = 11.9$, 1H, H6x), 1.57 (m, 1H, H6y), 1.22 (d, $J = 8.5$, 9H, PMe₃), 1.21 (buried, 1H, H4).

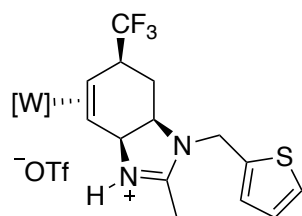


Compound 90. **89** (11 mg, 0.016 mmol) was dissolved in d⁶-acetone (0.7 mL) and monitored by ¹H NMR. Over time, the peaks for **89** decreased as a new product grew in. After 8 d, **89** had completely converted to **90**, and 2D NMR data was collected. ¹H NMR (d⁶-acetone, δ): 8.11 (overlapping d, 2H, PzA3 & PzB3), 7.98 (d, 1H, Pz5), 7.97 (d, 1H, Pz5), 7.80 (d, 1H, Pz5), 7.70 (d, 1H, PzC3), 6.82 (m, 1H, H3), 6.41 (t, 1H, Pz4), 6.35 (t, 1H, Pz4), 6.28 (t, 1H, Pz4), 4.88 (dt, $J = 9.6, 1.5$, 1H, H2), 3.69 (bs, 1H, H6), 3.67 (m, 1H, H1), 3.00 (m, 1H, H5), 2.64 (s, 3H, NMe), 1.59 (m, 1H, H4), 1.33 (d, $J = 8.4$, 9H, PMe₃).



Compound 91. To a 4-dram vial charged with a stir pea were added **78** (50 mg, 0.074 mmol), acetonitrile (1 mL, -30°C), and a 1M solution of HOTf in acetonitrile (0.18 mL, 0.18 mmol, -30°C) with stirring, resulting in a homogeneous golden/orange solution, which was allowed to sit for 15 min at -30°C. To this solution was added MMTP (107 mg, 0.614 mmol, -30°C). After 14 h at -30°C, Et₃N (72 mg, 0.71 mmol) was added to the reaction solution with stirring, then the reaction was left at -30°C for 6 h. The reaction was then warmed to

room temperature and monitored by ^{31}P NMR. After 24 h at room temperature, the reaction solution was removed from the glove box, diluted with H_2O (20 mL) and extracted with DCM (2 x 20 mL). The combined organic layer was dried over MgSO_4 and evaporated *in vacuo* to dryness. The film was redissolved in minimal DCM and added to stirring Et_2O (25 mL). The resulting pale solid was collected on a 15 mL fine porosity fritted disc, washed with pentane (2 x 3 mL) and desiccated overnight, yielding **91** (43 mg, 0.11 mmol, 66% yield). IR: $\nu(\text{BH}) = 2496 \text{ cm}^{-1}$, $\nu(\text{NO}) = 1548 \text{ cm}^{-1}$. ^{31}P NMR (d^6 -acetone, δ): -11.39 ($J_{\text{WP}} = 277$). ^1H NMR (d^6 -acetone, δ): 9.02 (bs, 1H, NH), 8.19 (d, 1H, PzB3), 8.08 (d, 1H, PzA3), 8.01 (d, 1H, PzC5), 7.99 (d, 1H, PzB5), 7.88 (d, 1H, PzA5), 7.65 (d, 1H, PzC3), 6.45 (t, 1H, PzB4), 6.39 (t, 1H, PzC4), 6.32 (t, 1H, PzA4), 5.62 (d, $J = 12.5$, 1H, H3a), 4.39 (dd, $J = 12.5, 7.2$, 1H, H7a), 3.49 (m, 1H, H6), 3.19 (s, 3H, NMe), 2.52 (m, 2H, H5 & H7x), 2.33 (s, 3H, C2-Me), 2.16 (d, $J = 17.1$, 1H, H7y), 1.24 (d, $J = 8.5$, 9H, PMe_3), 1.21 (buried, 1H, H4). ^{13}C NMR (d^6 -acetone, δ): 165.6 (CN), 144.5 (PzB3), 143.2 (PzA3), 142.1 (PzC3), 138.4 (PzC5), 137.7 (PzA5), 137.6 (PzB5), 132.0 (q, $J = 281.7$, CF_3), 107.6 (PzB4), 107.4 (PzC4), 107.1 (PzA4), 58.3 (C7a), 57.7 (C3a), 48.2 (C4), 44.0 (d, $J = 13.0$, C5), 41.6 (q, $J = 25.4$, C6), 30.5 (NMe), 19.0 (C7), 12.8 (d, $J = 28.6$, PMe_3), 12.1 (C2-Me).



Compound 93. To a 4-dram vial charged with a stir pea were added **82** (20 mg, 0.026 mmol), acetonitrile (0.5 mL, -30°C), and a 1M solution of HOTf in acetonitrile (0.07 mL, 0.07

mmol, -30°C) with stirring, resulting in a homogeneous golden solution, which was allowed to sit for 20 min at -30°C. To this solution was added MMTP (39 mg, 0.22 mmol, -30°C). After 22 h at -30°C, Et₃N (41 mg, 0.41 mmol) was added to the reaction solution with stirring, then the reaction was left at -30°C for 30 min. The reaction was then concentrated *in vacuo* to an oil. The oil was redissolved in minimal THF and added to stirring Et₂O (15 mL). The resulting tan solid was collected on a 15 mL fine porosity fritted disc, washed with Et₂O (3 mL) and desiccated overnight, yielding **93** (13 mg, 0.014 mmol, 54% yield).

¹H NMR (d⁶-acetone, δ): 9.36 (bs, 1H, NH), 8.18 (d, 1H, PzB3), 8.10 (d, 1H, PzA3), 8.02 (d, 1H, PzC5), 7.99 (d, 1H, PzB5), 7.88 (d, 1H, PzA5), 7.68 (d, 1H, PzC3), 7.55 (d, *J* = 5.1, 1H, Ar-H), 7.31 (d, *J* = 3.5, 1H, Ar-H), 7.08 (dd, *J* = 5.1, 3.5, 1H, Ar-H), 6.44 (t, 1H, PzB4), 6.40 (t, 1H, PzC4), 6.29 (t, 1H, PzA4), 5.69 (d, *J* = 12.4, 1H, H3a), 5.24 (d, *J* = 16.5, 1H, H8x), 4.93 (d, *J* = 16.5, 1H, H8y), 4.45 (dd, *J* = 12.4, 7.0, 1H, H7a), 3.53 (m, 1H, H6), 2.53 (s, 3H, C2-Me), 2.52 (buried, 2H, H5 & H7x), 2.32 (d, *J* = 16.3, 1H, H7y), 1.24 (d, *J* = 8.5, 9H, PMe₃), 1.22 (buried, 1H, H4).

4.5. References

- (1) Wilson, K. B.; Myers, J. T.; Nedzbala, H. S.; Combee, L. A.; Sabat, M.; Harman, W. D. *J. Am. Chem. Soc.* **2017**, *139*, 11401.
- (2) Blakemore, D. C.; Castro, L.; Churcher, I.; Rees, D. C.; Thomas, A. W.; Wilson, D. M.; Wood, A. *Nature Chemistry* **2018**, *10*, 383.
- (3) Vitaku, E.; Smith, D. T.; Njardarson, J. T. *Journal of Medicinal Chemistry* **2014**, *57*, 10257.
- (4) Ilardi, E. A.; Vitaku, E.; Njardarson, J. T. *Journal of Medicinal Chemistry* **2014**, *57*, 2832.
- (5) MacLeod, B. L.; Pienkos, J. A.; Wilson, K. B.; Sabat, M.; Myers, W. H.; Harman, W. D. *Organometallics* **2016**, *35*, 370.
- (6) Spande, T. F.; Garraffo, H. M.; Edwards, M. W.; Daly, J. W. *J. Am. Chem. Soc.* **1992**, *114*, 3475.
- (7) Badio, B.; Daly, J. W. *Molecular Pharmacology* **1994**, *45*, 563.
- (8) Gonzalez, J.; Koontz, J. I.; Myers, W. H.; Hodges, L. M.; Sabat, M.; Nilsson, K. R.; Neely, L. K.; Harman, W. D. *J. Am. Chem. Soc.* **1995**, *117*, 3405.
- (9) Ellis, J. L.; Harman, D.; Gonzalez, J.; Spera, M. L.; Liu, R.; Shen, T. Y.; Wypij, D. M.; Zuo, F. *J. Pharm. Expt. Ther.* **1999**, *288*, 1143.
- (10) Lis, E. C.; Delafuente, D. A.; Lin, Y.; Mocella, C. J.; Todd, M. A.; Liu, W.; Sabat, M.; Myers, W. H.; Harman, W. D. *Organometallics* **2006**, *25*, 5051.
- (11) Yanfeng, J.; Wenjing, H.; W., S. H.; Olivier, B.; Thomas, F.; Heinz, B. *European Journal of Inorganic Chemistry* **2014**, *2014*, 140.

(12) Handford, R. C.; Wakeham, R. J.; Patrick, B. O.; Legzdins, P. *Inorganic Chemistry* **2017**, *56*, 3612.

(13) Welch, K. D.; Harrison, D. P.; Lis, E. C.; Liu, W.; Salomon, R. J.; Harman, W. D.; Myers, W. H. *Organometallics* **2007**, *26*, 2791.

Chapter 5

Tungsten Dearomatization of Aniline Derivatives

5.1 Introduction

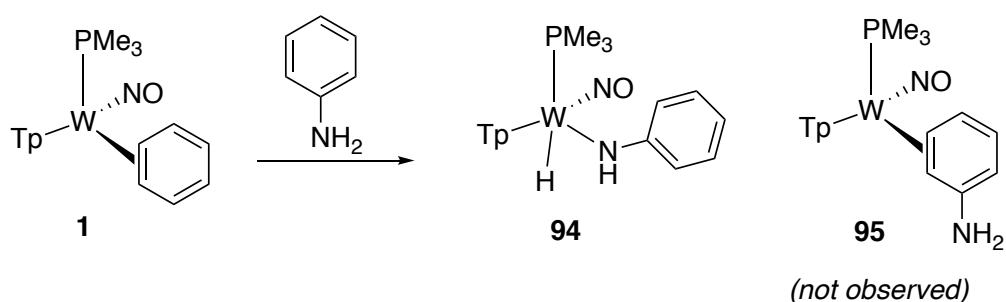
Chapter 3 discussed the impacts of electron-donating groups and electron-withdrawing groups on the coordination and subsequent reactivity of η^2 -coordinated substituted benzenes. Our group previously investigated the coordination chemistry of benzenes substituted with an electron-donating group (e.g., phenol, anisole, aniline)¹⁻³ when bound by the electron rich {TpW(NO)(PMe₃)} fragment; however, the recent findings with η^2 -benzene and η^2 -PhCF₃ provide the opportunity to revisit previous results from a different perspective. This chapter focuses on the coordination and reactivity of aniline derivatives.

5.2 Results and Discussion

5.2.1 Previous Investigations into the Coordination and Reactivity of η^2 -Aniline

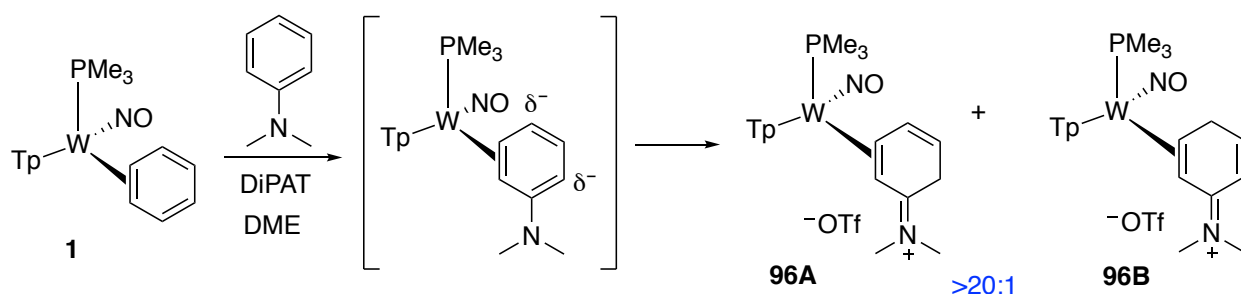
Initial efforts to isolate the parent η^2 -aniline complex (**95**) through a ligand substitution with **1** resulted predominately in the N-H oxidative addition product **94** (Scheme 5.1). **94** exhibits a ¹⁸³W-³¹P coupling constant of 165 Hz, which is more consistent with a W(II) 7-coordinate system (100-212 Hz) than a W(0) η^2 -arene complex (288-314 Hz).^{3,4} The increased back-donation of the tungsten system compared to Mo(0), Re(I), and Os(II) systems is consistent with the observed preference for the oxidative addition pathway.

Scheme 5.1: Dihapto-coordination of aniline



Attempts to coordinate a modified form of aniline, such as anilinium triflate, anilineborane, or *N,N*-dimethylaniline did not yield any appreciable amount of the desired η^2 -aromatic.³ An unfavorable interaction between the extremely π -basic tungsten system and the electron rich aniline ligand was invoked to explain the difficulty in isolating the η^2 -*N,N*-dimethylaniline complex. Fortunately, monitoring the ligand substitution reaction by cyclic voltammetry revealed a transient product peak with an $E_{p,a} = -0.40$ V (vs. NHE) consistent with an electron rich η^2 -arene species. For comparison, **1** has an $E_{p,a} = -0.13$ V, meaning the purported η^2 -*N,N*-dimethylaniline species is shifted ~ 0.27 V more negative.

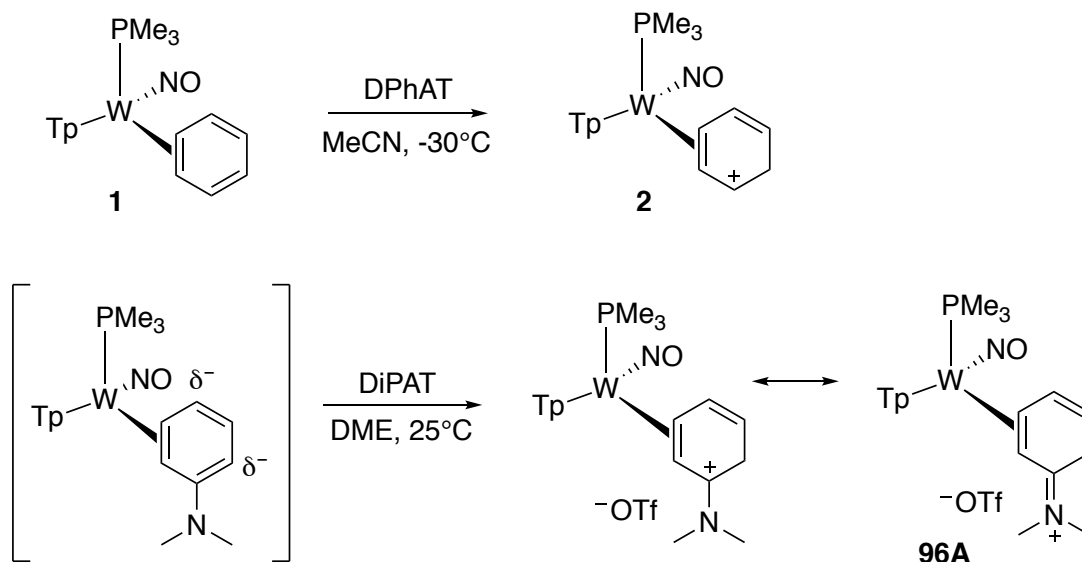
Scheme 5.2: In situ protonation of η^2 -*N,N*-dimethylaniline



To trap the η^2 -*N,N*-dimethylaniline species in a stable, isolable form, the substitution reaction was repeated in the presence of a relatively weak Brønsted acid, diisopropylammonium triflate (DiPAT, $pK_a = 11.5$). The strength of the acid was key in that it needed to be strong enough to protonate the neutral complex in situ, but not so strong that it would oxidize **1**, as was observed with anilinium triflate ($pK_a = 4.6$).³ The substitution reaction was run at room temperature for ~ 18 h at which point the ortho protonated isomer, **96A** had precipitated out of dimethoxyethane (DME) in a 57% yield (Scheme 5.2). We would expect the amino group to direct the protonation to the ortho or para position, but in this case only the ortho protonated species is observed. Initially, this regioselective

protonation was thought to be controlled by the amino group³; however, protonation at the same position on the ring is also observed with the η^2 -benzene complex (Chapter 2), which is solely metal controlled. In the case of benzene, we were able to demonstrate that the selective protonation occurs under thermodynamic control, favoring the allyl with the positive charge localized distal to the PMe_3 . Selective protonation of the η^2 -*N,N*-dimethylaniline system is likely a result of thermodynamic control as well, with the combined influence of the metal and the amino group; however, this has not been confirmed because we have been unable to establish an equilibrium.

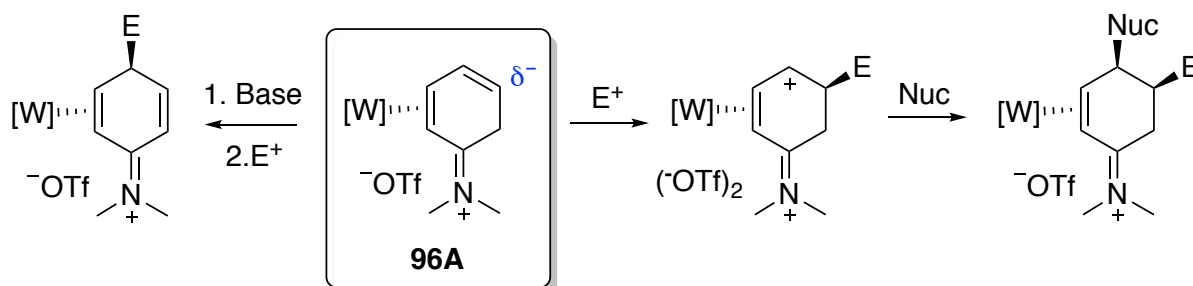
Regioselective protonation of both the benzene and dimethylaniline complexes results in allyl complexes with the positive charge localized distal to the PMe_3 ; however, in the case of **96A**, the resulting “allyl” species forms an extremely stabilized conjugated iminium system, with an $E_{p,a} = 1.04$ V (Scheme 5.3). As expected, the successful protonation of **1** requires a stronger acid (DPhAT, $\text{pK}_a = 0.8$), and fortunately reducing the temperature for the protonation to -30°C avoids the decomposition pathways that occur at room temperature. Utilizing a similar protonation procedure for the aniline system is not as feasible, because the process requires a substitution reaction from **1**, which would be drastically slowed at reduced temperatures. Additionally, we would expect excess aniline ligand to quench stronger acids in situ and are limited to non-coordinating solvents for the substitution reaction.

Scheme 5.3: Protonation comparison of η^2 -benzene and η^2 -*N,N*-dimethylaniline

Investigation into the reactivity of **96A** led to two divergent reaction schemes (Scheme 5.4). The $\{\text{TpW}(\text{NO})(\text{PMe}_3)\}$ fragment is simplified to $[\text{W}]$ in schemes and figures where the focus is organic transformations. The conjugated iminium system provides a good π -acid for the tungsten to back-donate electron density into, which is reflected by the decrease in the IR C=N stretch (1562 cm^{-1}) compared to the typical range of $1620\text{--}1660\text{ cm}^{-1}$.^{1,3} Although **96A** is positively charged, back-donation from the tungsten fragment renders it unreactive towards most nucleophiles. Remarkably, the cationic species **96A** is instead capable of undergoing a second electrophilic addition (Scheme 5.4, right). Also of note, the aniline ring is activated towards electrophilic addition at the meta position, giving a reversal of the reactivity that is typically observed with the free aromatic. Conveniently, the increased reduction potential of **96A** stabilizes the complex towards oxidative conditions and expands the range of compatible electrophilic sources to include relatively strong acids

(HOTf, DPhAT), electrophilic halogen sources (*N*-chlorosuccinimide (NCS), Selectfluor®), and heteroatom electrophiles (mCPBA).³

Scheme 5.4: Reactivity of η^2 -*N,N*-dimethylanilinium



After the addition of an electrophile, the resulting allyl complexes are reactive towards a range of nucleophiles including relatively weak aromatic nucleophiles, due to the increased electrophilicity of the dicationic species. For comparison, the monocationic allyl complexes discussed in Chapters 2 and 3 have not shown any appreciable reactivity with most aromatic nucleophiles. The successful reactions of **96A** with aromatic nucleophiles occur via a Friedel-Crafts type mechanism, resulting in a carbon-carbon bond formation between two rings. This reaction can be realized with aromatics as electron-rich as indole to less reactive aromatic nucleophiles like 2-methylfuran.^{3,5} In all cases, the tandem electrophilic/nucleophilic addition occurs regioselectively in a 1,2-fashion with the nucleophile adding stereoselectively anti to the metal (Scheme 5.4, right).

The high degree of regiocontrol observed with tandem additions to **96A** can be rationalized by considering the allyl complex that forms upon addition of a second electrophile to **96A**. When acid is used as the electrophilic source, the doubly cationic complex can be isolated and characterized.⁶ Figure 5.1 gives a comparison of the allyl complexes of **96A** and 1,3-dienes from **1** and **52**. The experimentally observed allyls are

shown in blue. The allyls stemming from η^2 -benzene and η^2 -PhCF₃ preferentially localize the positive charge distal to the PMe₃ due to the influence of the asymmetric tungsten center and the position of the destabilizing CF₃ group.^{7,8} In these cases, the terminal allyl protons are typically separated by 1.5-2 ppm, with the proton at the carbocation shown in blue shifted more downfield. The dicationic anilinium system however is even more distorted than these allyl complexes, with a difference of over 3 ppm between the terminal allyl protons. Additionally, the impact of the positively charged conjugated iminium system causes the favored allyl complex to localize the allylic positive charge proximal to the PMe₃ ("up"). This could be due to a variety of interrelated effects such as the stabilizing effect of the π -acidic conjugated iminium system increasing the kinetic barrier for the tungsten to shift, or due to the destabilization of a positive charge adjacent to the iminium system. The distortion of this allylic species was supported by X-ray structure determination, which reflected a greater distance between the tungsten and the carbocation carbon (~ 0.37 Å) than the tungsten and the other two allyl carbons.⁷ Additionally, DFT calculations for the two allylic species showed that the observed allyl is favored by >4 kcal/mol.⁷ Subsequent addition of nucleophiles to the dicationic anilinium allyl occurs predictably at the carbocation, giving solely the 1,2-addition products (Scheme 5.4, right).

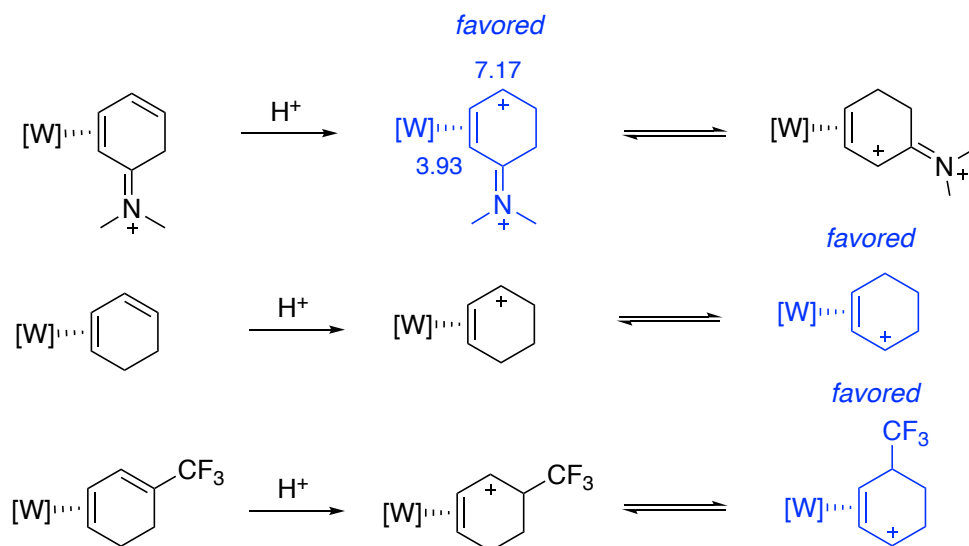
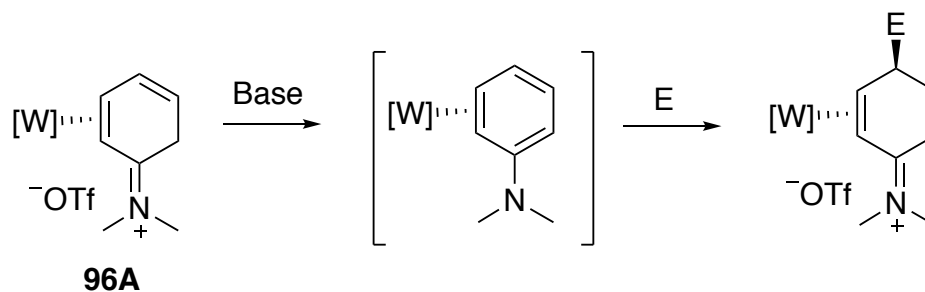


Figure 5.1: Comparison of allyl complexes from **1**, **52**, and **96A** (triflate omitted)

Another reaction pathway demonstrated with the η^2 -*N,N*-dimethylanilinium complex goes through the neutral aniline complex, which can be generated in situ with base (DBU).³ This transient η^2 -*N,N*-dimethylaniline species is activated towards electrophilic addition. Interestingly, when the electrophilic source is a carbon electrophile instead of a proton, addition occurs selectively at the para position, anti to the metal (Scheme 5.5). The back-donation from the metal, in tandem with the electron-donation from the amino group enables the addition of carbon electrophiles such as allyl bromide, benzyl bromide, and 1-bromo-2-butanone.³

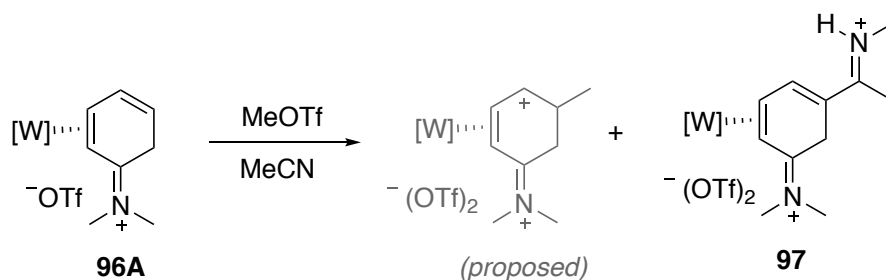
Scheme 5.5: Electrophilic addition at the para position of **96A**



5.2.2 New Reactivity of η^2 -Anilinium Derivatives

The reactivity of **96A** towards electrophilic addition with reagents such as acids and heteroatom electrophiles has been established; however, there has not been much success with the addition of carbon electrophiles at the meta position. Ideally, expansion of this chemistry would include carbon-carbon bond formation reactions, which would both set a stereocenter, and also be less prone to elimination than heteroatom electrophiles. Rebecca Salomon reported some preliminary success with the addition of acetals to the meta position of **96A** in her dissertation.⁶ With these results in mind, other carbon electrophiles, such as methyl triflate and Michael acceptors were investigated.

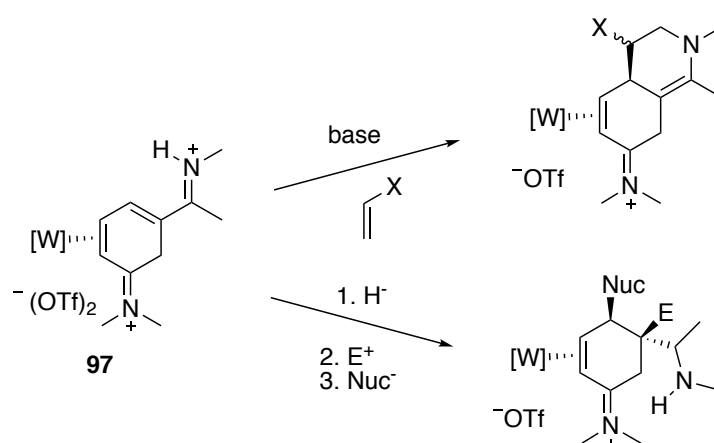
We found that the addition of methyl triflate (2 eq.) to **96A** in acetonitrile at room temperature initially resulted in the formation of more than 5 different products, as observed by ³¹P NMR. The reaction was monitored over 2 days, and during this time one major product grew in, giving a 9:1 ratio. The major product exhibited a ¹⁸³W-³¹P coupling constant of 277 Hz, which is slightly larger than what we would expect for the proposed methylated allyl (Scheme 5.6). When the reaction was repeated with the amount of methyl triflate reduced to one equivalent, the reaction again funneled to one major product over two days, this time giving a ratio of >20:1. The reaction solution was then evaporated to dryness, redissolved in DCM and precipitated from Et₂O. ¹H NMR data of the isolated solid showed one major complex, which was identified as **97** by 2D NMR analysis (Scheme 5.6).

Scheme 5.6: Addition of methyl triflate to **96A**

Formation of **97** is a result of methylated acetonitrile adding as the electrophile instead of a direct alkylation of the anilinium system. This addition is followed by an elimination, which leads to a favorable extended conjugated system. ¹H NMR of the isolated product revealed a proton peak at 8.08 ppm, which both coupled to the upbound proton and had an NOE correlation with the PMe₃. We assigned this proton as the alkene proton in the para position, and proposed that the downfield shift was due to the alkene being in conjugation with an electron-withdrawing group. In addition to the two methyl groups on the aniline nitrogen ($\delta = 3.62, 2.44$), two additional methyl groups were observed at 3.44 and 2.55 ppm. Furthermore, the signal at 3.44 ppm was split into a doublet by a broad resonance at 9.27 ppm, which was identified as an N-H proton. One of the most important features that enabled the identification of **97** was the presence of two signals around 180 ppm in the ¹³C NMR spectrum, one of which corresponded to the aniline iminium carbon. The other carbon at 180 ppm was identified as an iminium carbon with HMBC correlations to the two new methyl groups at 3.44 and 2.55 ppm. This analysis led to the identification of **97** as the product, with the two new methyl signals coming from the addition of methylated acetonitrile.

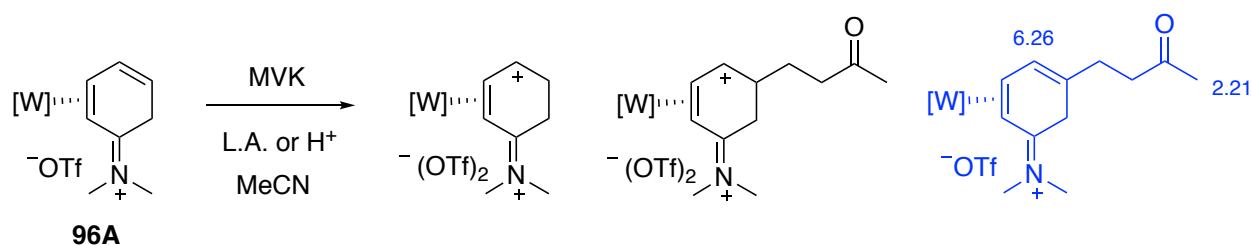
The conjugated system of **97** provides a number of potential reaction pathways that could be explored to further expand the reactivity accessible to η^2 -aniliniums. Scheme 5.7 outlines two potential reaction pathways for this complex. The top pathway is a proposed cycloaddition, which could be realized after deprotonation of the iminium nitrogen followed by the addition of a dienophile. This reaction would potentially allow for the stereoselective formation of a bicyclic system. Furthermore, the proposed ring system is a derivative of a tetrahydroisoquinoline core, which is one of the most common nitrogen heterocycles found in pharmaceuticals.⁹ An alternative pathway proposed for **97** is the selective reduction of the new iminium system, followed by a tandem electrophilic/nucleophilic addition to the uncoordinated alkene. Previous reports have shown that the iminium system in direct conjugation with the metal requires lithium aluminum hydride (LAH) to facilitate the reduction of the iminium (*vide infra*).¹⁰ Based on these reports we proposed that a weaker hydride source (NaBH_4 , NaCNBH_3) could be used to reduce the other iminium and enable a tandem addition to be enacted on the uncoordinated double bond (Scheme 5.7). These pathways would further increase the range of reactivity accessible for η^2 -aniliniums, and potentially enable the stereoselective formation of carbon-carbon bonds to build up more complex small molecules.

Scheme 5.7: Proposed reaction pathways for **97**



The next group of carbon electrophiles explored was Michael acceptors. When complex **96A** was treated with methyl vinyl ketone (MVK) no reaction was observed. Thus a series of experiments were performed using either a Lewis acid ($\text{BF}_3 \cdot \text{OEt}_2$) or a Brønsted acid (HOTf) to activate the Michael acceptor as an electrophile at -30°C . The experiments run with the Lewis acid were monitored by ^1H and ^{31}P NMR. Slightly over 1 equivalent of $\text{BF}_3 \cdot \text{OEt}_2$ was used and 1-5 equivalents of MVK were added. In most cases, three products were observed, with the major product believed to be the MVK elimination product (Scheme 5.8, blue). This assignment was based on a new methyl singlet at 2.21 ppm, as well as a single alkene resonance at 6.26 ppm in the ^1H NMR spectrum. This product was favored by $\sim 5:1$ over what we believed to be the proteo allyl complex, based on overlaying ^1H NMRs with the previously reported allyl complex. Failure to increase the ratio to better than 5:1 with $\text{BF}_3 \cdot \text{OEt}_2$ led us to explore the use of other activators with MVK.

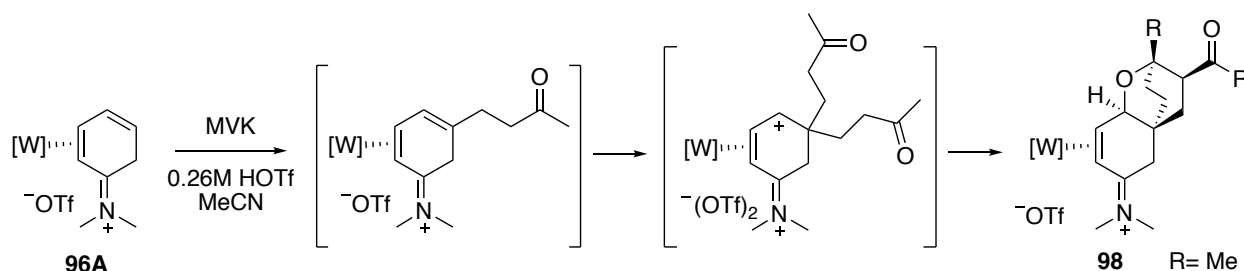
Scheme 5.8: Reactivity of η^2 -*N,N*-dimethylanilinium with Michael acceptors



Similar experiments were conducted using a Brønsted acid instead of a Lewis acid to activate MVK. The addition of acid could lead to a couple different complications, including the rapid polymerization of the MVK. Additionally, the anilinium complex could be protonated instead of the MVK, at which point the complex would no longer be reactive towards the carbon electrophile. In the first experiment, **96A** was dissolved in CD_3CN at -

30°C then excess MVK and a solution of HOTf in acetonitrile (-30°C) were added. An in situ ^1H NMR taken after 2 hours revealed the formation of one major product, which was believed to be the MVK elimination product. However, as the reaction was monitored over the course of a day, it funneled to one new major product **98** (Scheme 5.9). After a basic aqueous work-up, a sufficiently clean product was observed by ^1H NMR to allow for full 2D NMR analysis.

Scheme 5.9: Intramolecular cyclization with **96A** and MVK



2D NMR analysis, as well as CV and IR data led us to assign **98** as the structure shown in Scheme 5.9. A CV of the isolated product revealed an $E_{p,a} = 1.15$ V, consistent with the iminium system still being intact. The IR spectrum exhibited characteristic nitrosyl and iminium stretches at 1573 and 1591 cm^{-1} . Furthermore, a potential carbonyl stretch was observed at 1692 cm^{-1} . We propose that formation of complex **98** is a result of the double addition of MVK at the meta position of the aniline ring, followed by an intramolecular cyclization. This mechanism is supported by the observation of the MVK elimination product in situ, which would be activated towards a second electrophilic addition at the terminal position of the uncoordinated alkene.

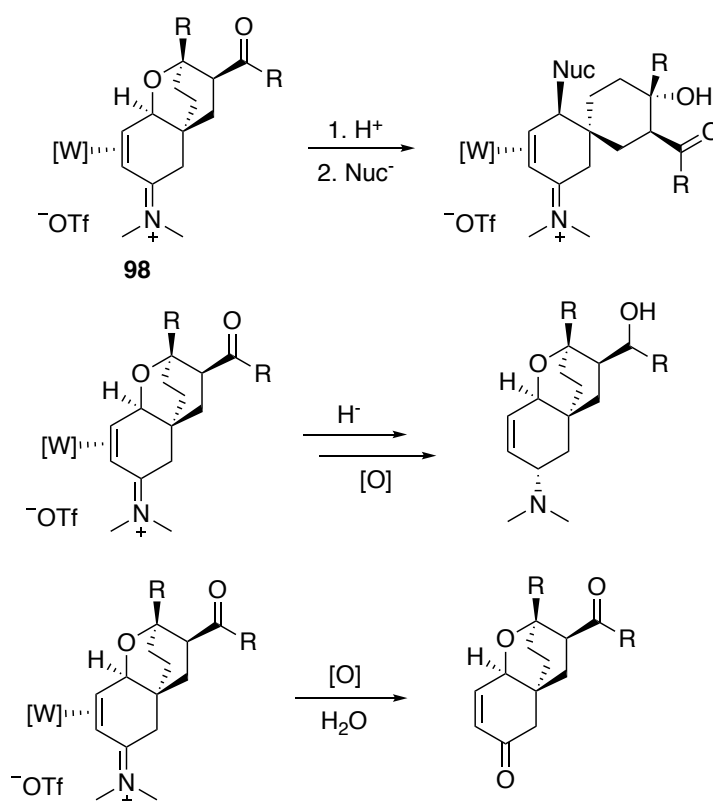
The subsequent cyclization could result from a ketone oxygen closing at the allyl carbon, followed by the enolate of the other MVK group closing on the carbonyl carbon. In this one step reaction, three new carbon-carbon bonds are formed, and in the process three stereocenters are set stereoselectively. Some of the key NMR data that enabled the identification of the structure and stereochemistry of **98** include a ^1H NMR signal at 5.05 ppm, which has an NOE correlation with the PMe_3 ligand. The downfield shift of this methine proton is consistent with being adjacent to an oxygen, and was assigned as the proton at the previously allylic position. Additionally, four different methyl peaks were observed, two of which corresponded to the methyls on the iminium nitrogen. A new methyl peak at 2.33 ppm with an HMBC correlation to a carbon at 211 ppm was identified as the methyl group adjacent to the ketone from one of the MVK additions. The fourth methyl signal was shifted further upfield than the rest (1.13 ppm), which would not be expected if the carbonyl from the second MVK addition was still intact. Instead, the methyl signal at 1.13 ppm is in a chemical shift range typical for a methyl that is beta to a heteroatom, which is consistent with the proposed cyclized structure of **98**.

Once the structure of **98** was identified, the conditions for its synthesis were optimized. We found that control of the concentration was crucial for the successful formation of the product. Specifically, using a more dilute HOTf/acetonitrile solution (0.26M) and adding the acid drop-wise with stirring was necessary to avoid substantial formation of the proteo allyl complex. Ultimately we found that 1 equivalent of acid and 5 equivalents of MVK were optimal, which yielded **98** in an 88% yield.

To support the incorporation of two Michael acceptors and to see if this reactivity could be expanded, ethyl vinyl ketone (EVK) was added under similar conditions, and the

reaction was monitored by ^1H NMR. The reaction seemed to progress similarly through the elimination product, as evidenced by the formation of an alkene peak at 6.31 ppm. This complex then slowly converted to the cyclized product (Scheme 5.9, R= Et). As seen with **98**, the EVK version has a signal at 5.05 ppm for the methine bridgehead proton. Additionally, two triplets each integrating for three protons were observed upfield (< 1 ppm), which we identified as the EVK methyl groups. The presence of these two methyl signals supports the incorporation of two EVK groups in the cyclized product.

Scheme 5.10: Proposed reaction pathways for **98**



With the optimized cyclization reaction in hand, several reaction pathways are proposed for the isolation of the free organic or for further functionalization of the aniline core (Scheme 5.10). One potential pathway involves the addition of acid, which could

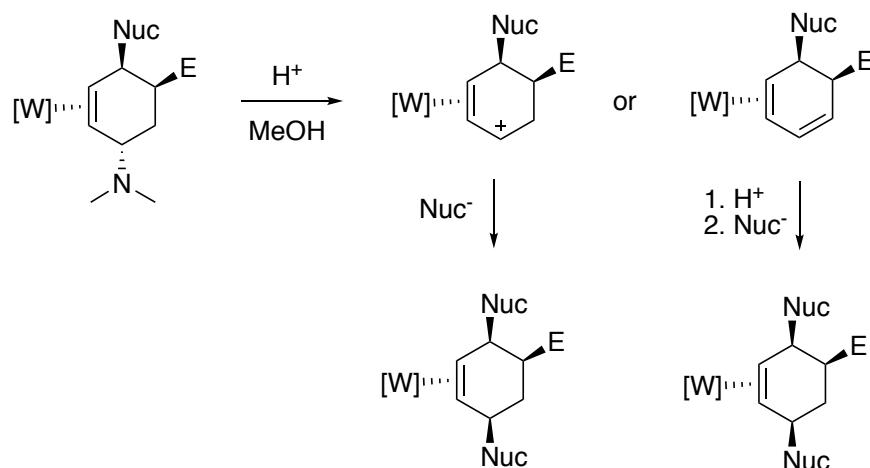
protonate the oxygen and cause the ring to open. Subsequent addition of a nucleophile at the allylic position would set an additional stereocenter and lead to a spiro[5.5] product with four stereocenters (Scheme 5.10, top). Another possible reaction pathway could be realized by the addition of a hydride source such as LAH, which would be strong enough to reduce the ketone, as well as the iminium. This would lead to two additional stereocenters, although it is uncertain whether reduction of the ketone would be stereoselective, as it is further removed from the metal center, and thus less controlled. The free organic could then be isolated via oxidation with a one electron oxidant like NOPF₆. Alternatively, direct oxidation of **98** with the iminium still intact can be achieved with stronger oxidants like ceric ammonium nitrate (CAN) to give the free enone organic, which has been demonstrated previously with the η^2 -*N,N*-dimethylanilinium system (Scheme 5.10, bottom).⁵

5.2.3 η^2 -Anilinium Complexes as Precursors to Cyclohexenes

As previously discussed, the conjugated iminium system of **96A** increases the reduction potential to over 1 V (vs. NHE) and stabilizes the complex towards oxidative conditions. Previously, optimal conditions were reported for the stereoselective reduction of the iminium system utilizing the relative strong hydride source LAH.¹⁰ Once the iminium is reduced, the reduction potential of the complex drops by almost a volt, which enables the use of more mild oxidants to liberate the transformed ligand. However, once the iminium group is reduced, a new reaction pathway becomes available. As Brianna MacLeod outlined in her thesis, addition of acid to the dimethylamino cyclohexene complexes results in the

protonation of the amino group, which can subsequently fall off to form the allyl in situ, or undergo an elimination to give an η^2 -1,3-diene species (Scheme 5.11).¹¹

Scheme 5.11: η^2 -Anilinium as precursor for functionalized cyclohexenes



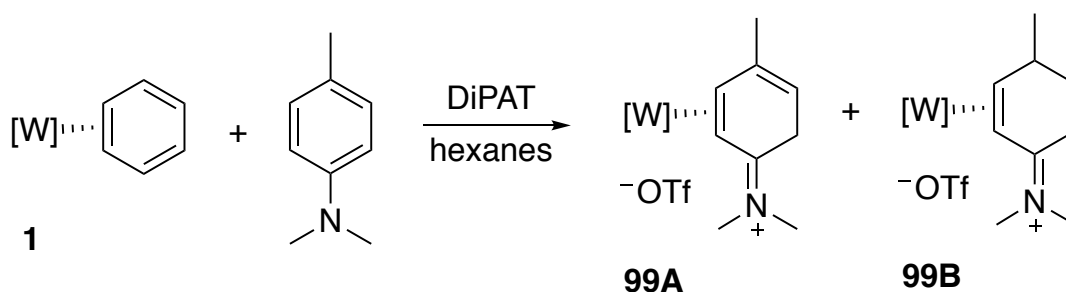
Theoretically, addition of a nucleophile to the allyl generated in situ, or addition of acid and then a nucleophile to the η^2 -1,3-diene species, would result in the products shown in Scheme 5.11. The regiochemistry expected for this reaction, based on the allyl distortion discussed in Chapter 2, would install the second nucleophile directly across from the initial nucleophile. These types of substituted cyclohexenes are similar to those described in Chapter 2, where the reactivity of η^2 -1,3-dienes originating from η^2 -benzene predominately led to the synthesis of disubstituted 3,6-cyclohexenes, with the two nucleophiles installed para to each other. However, starting from η^2 -*N,N*-dimethylanilinium provides some potential benefits in terms of expanding the range of accessible cyclohexenes. Because the iminium system stabilizes the complex towards oxidative conditions, a wider range of electrophiles have been added to aniline, including halogens and epoxides, as well as a cyclopropanation reaction.^{3,11} These reactions would lead to cyclohexenes with an additional stereocenter set. Furthermore, the allyl complexes that result after electrophilic

addition are more reactive than those described in Chapter 2, because in this case the system is dicationic. This increased reactivity enables the addition of relatively weak aromatic nucleophiles that have thus far not been successfully added to the benzene system allyls.⁵ With these potential benefits in mind, the anilinium system can be viewed as an activating group that expands our synthetic capabilities and then can be cleaved to provide another double bond to be functionalized.

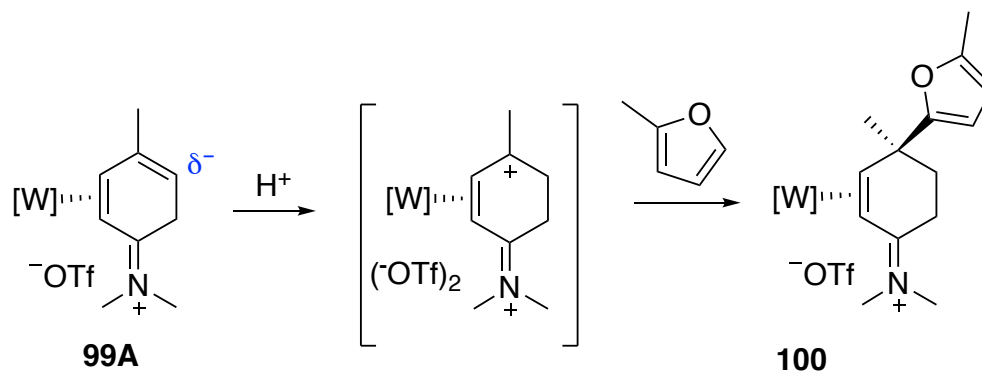
5.2.4 The Synthesis and Reactivity of η^2 -*N,N*,4-trimethylanilinium

The ability to coordinate and functionalize more substituted anilines was also investigated using *N,N*,4-trimethylaniline. This system was chosen to probe the effect of a para substituent on the regioselectivity of protonation. Additionally, the methyl group in this position would provide the opportunity to synthesize aminocyclohexenes with a quaternary carbon. In this case, the substitution reaction of **1** in DME in the presence of DiPAT and *N,N*,4-trimethylaniline did not result in the spontaneous precipitation of the anilinium complex. An alternative procedure was optimized in which the substitution reaction was stirred as a heterogeneous mixture in hexanes for 3 days yielding **99A** in a 68% yield on a ~2.5g scale (Scheme 5.12). As seen with *N,N*-dimethylaniline, protonation occurs selectively at the ortho position, yielding an uncoordinated double bond in conjugation with the metal.³

Scheme 5.12: In situ acid trapping of *N,N*,4-trimethylaniline



The ability of this system to undergo a tandem electrophilic/nucleophilic addition was investigated. The additional substituent on the aniline ring could potentially cause issues with the nucleophilic addition reaction, as was seen previously with the inability to add aromatic nucleophiles to the *p*-cresol complex.⁵ In the case of *p*-cresol, this lack of reactivity could be due to unfavorable steric interactions with the nucleophile adding to the same carbon as the methyl group. Nucleophilic attack at the allylic carbon would push the methyl group back towards the PMe_3 , which could also cause an unfavorable steric interaction. Further, the methyl group at the allylic position would act to further stabilize the carbocation, and thus make it less reactive towards nucleophiles. Similar reaction conditions were attempted with **99A** by adding a HOTf/MeCN solution to the complex at room temperature, followed by the addition of excess aromatic nucleophile (2-methylfuran). The reaction was monitored by ^{31}P NMR revealing one product peak with a ^{183}W - ^{31}P coupling constant of 281 Hz, which is consistent with an addition product to an anilinium complex.⁵ **100** was isolated by a basic aqueous work-up and precipitation from Et_2O in a 70% yield (Scheme 5.13). 2D NMR analysis supports the regio- and stereoselective addition of 2-methylfuran, with the nucleophile adding anti to the metal center. This assignment was supported by an NOE interaction between the para methyl group at 1.61 ppm and the PMe_3 ligand. Incorporation of 2-methylfuran in the product was supported by aromatic protons at 6.18 and 5.93 ppm, as well as an additional methyl singlet at 2.26 ppm. HMBC and NOE correlations were used to confirm that the reaction occurred at the alpha-carbon of the aromatic heterocycle, which is consistent with what was observed with the parent η^2 -*N,N*-dimethylanilinium system.⁵

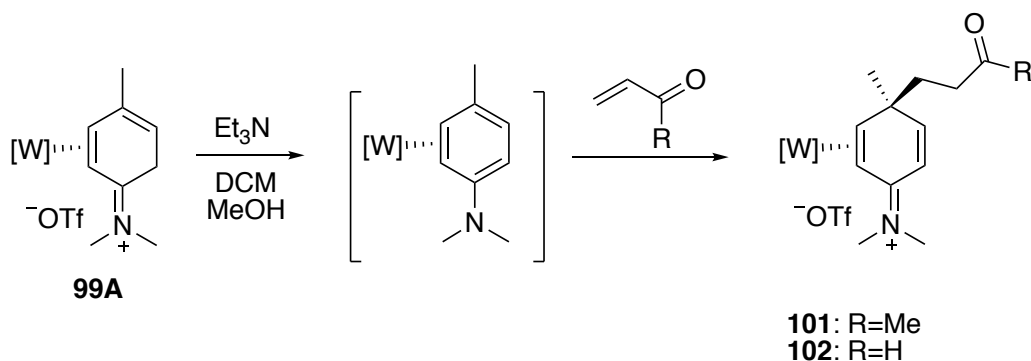
Scheme 5.13: Tandem electrophilic/nucleophilic addition to **99A**

A second reactivity scheme was investigated with the paramethylanilinium complex, which allows for the overall addition of an electrophile at the para position of the ring, as opposed to the meta position (Scheme 5.14). Similar reactivity was explored with **96A** by first treating the complex with base to access a transient neutral η^2 -aniline complex, which was reactive with benzyl and allyl bromide.³ This type of reaction pathway was explored with **99A** with Michael acceptors, including methyl vinyl ketone (MVK) and acrolein. For both reactions we found that addition of excess Michael acceptor (5 eq) followed by slightly less than 1 equivalent of Et_3N allowed for the isolation of the desired species (**101**, **102**), with the electrophile adding anti to the metal at the para position (Scheme 5.14).

Overall this reaction facilitates a stereoselective C-C bond formation, resulting in a quaternary center. Key features in the NMR data that support the assignment of these complexes include an NOE interaction between the para methyl group and the PMe_3 ligand, as well as an alkene proton resonance around 6.5 ppm indicative of an uncoordinated alkene. In the case of the acrolein addition, a minor product is observed that was tentatively identified as the ortho addition of acrolein based on the presence of a minor aldehyde peak and a single alkene proton at 4.73 ppm. The addition of electrophiles at the

ortho position has been reported previously with the Os(II) system for the addition of Michael acceptors to η^2 -*p*-cresol.¹²

Scheme 5.14: Addition of Michael acceptors to **99A**



The MVK addition to **99A** was scaled up to 2.5 g with the intention of isolating the free organic as the hydrolyzed hexadieneone **103** on a large scale (Figure 5.2, right). This compound was targeted for a collaboration with the Cobb group from the University of Reading in the UK, whose focus is the asymmetric synthesis of biologically important molecules. The synthesis of this small molecule was previously reported by our group starting from the η^2 -*p*-cresol complex with Os(II). The collaboration was initiated by the Cobb group because **103** is not easily made by traditional organic methods, and is potentially an important precursor for building steroid cores with a methyl group at the bridgehead position (Figure 5.2).

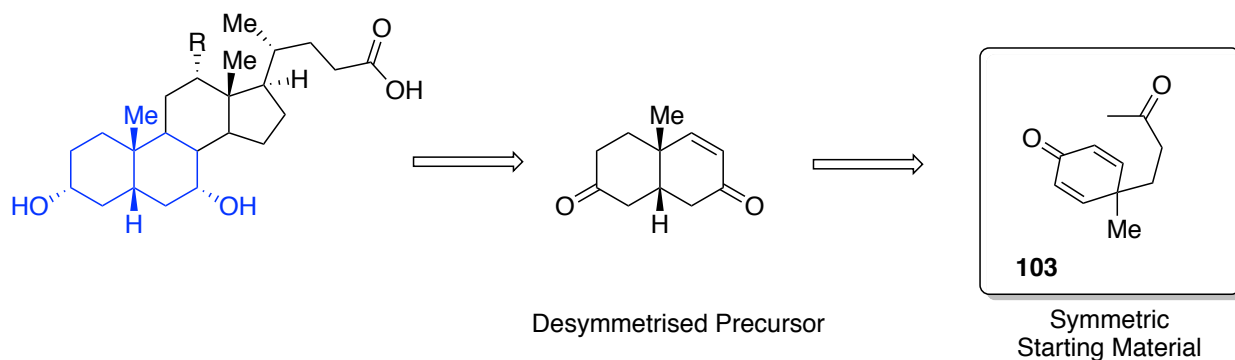
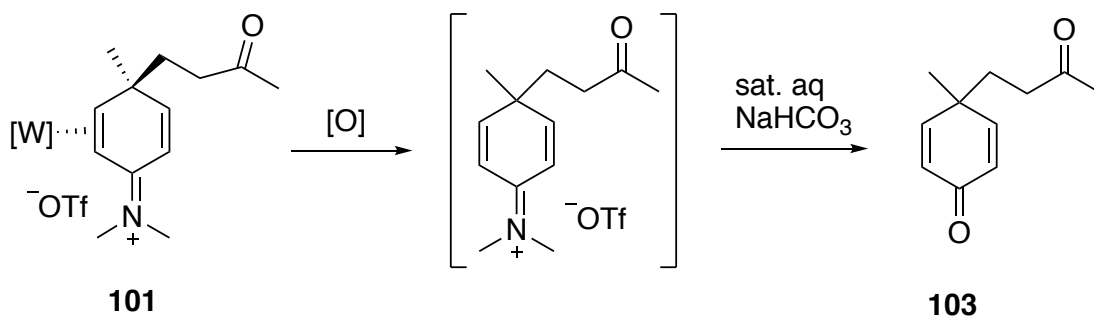


Figure 5.2: Retrosynthetic analysis of bile acid target

The oxidation of **101** was first attempted using CAN as the oxidant. We hypothesized that CAN would be strong enough to oxidize **101** ($E_{p,a} = 0.90$ V), and additionally it has been used previously to access the hydrolyzed organics of η^2 -*N,N*-dimethylanilinium complexes.⁵ An NMR scale experiment was conducted in d^6 -acetone to monitor the oxidation of **101** with 2 equivalents of CAN. After the addition of CAN, the proposed iminium intermediate was observed by ^1H NMR, with two peaks at 7.41 ppm and 7.31 ppm each integrating for two protons. The downfield shift of these signals is consistent with alkene protons in conjugation with an iminium. Furthermore, a singlet integrating for six protons was observed at 3.85 ppm, which is in the right range to be the iminium methyl groups. The reaction solution was then stirred with saturated aqueous NaHCO_3 , and the organic was extracted with Et_2O . A ^1H NMR spectrum of the resulting oil indicated the successful formation of **103**, based on the presence of alkene protons at 6.87 and 6.17 ppm, as well as a ketone methyl at 2.03 ppm, and the para methyl group at 1.28 ppm.

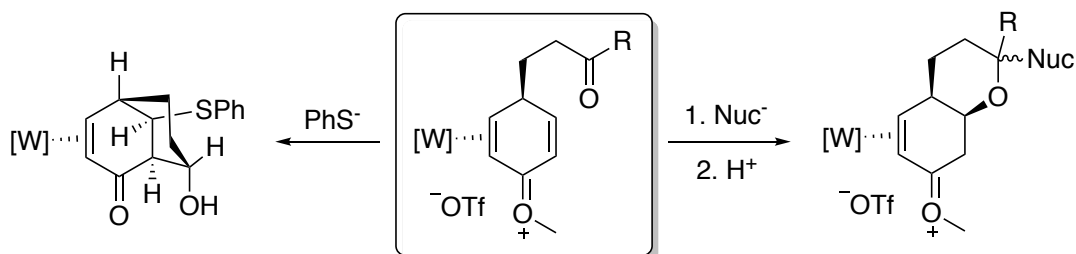
Scheme 5.15: Oxidation and hydrolysis of **101**

Unfortunately, when these conditions were scaled-up, the formation of other products was observed, including the rearomatized aniline ligand and a number of other unidentified compounds. We found that switching the oxidant to NOPF_6 allowed for a cleaner oxidation of **101**; however, additional products and some of the rearomatized ligand were still observed by ^1H NMR. One of the potential causes of this is the reversible MVK addition, which can lead to the regeneration of *N,N*,4-trimethylaniline under basic conditions. Unfortunately, aqueous base conditions could not be avoided, as they were needed to hydrolyze the iminium to a ketone. Thus, the concentration and time spent in the presence of base were varied in order to reduce undesirable side reactions. Keeping the concentration and equivalents of NOPF_6 (1.5) constant, and varying the time spent stirring with aqueous NaHCO_3 from 40 minutes to 10 minutes resulted in a change in ratio from 2.75:1 to 25:1 (**103**:*N,N*,4-trimethylaniline). Similarly, higher concentrations led to more rapid generation of the aromatic ligand.

Using these results, the reaction was scaled up to 1 g. After oxidation (stirring 4.5 hours) the iminium was hydrolyzed by stirring with 1:1 H_2O :saturated aqueous NaHCO_3 for 10 minutes, then the organic was extracted with Et_2O . The crude organic was purified by

eluting through a silica gel column with 60% HPLC EtOAc/hexanes, giving **103** in an 84% yield (Scheme 5.15).

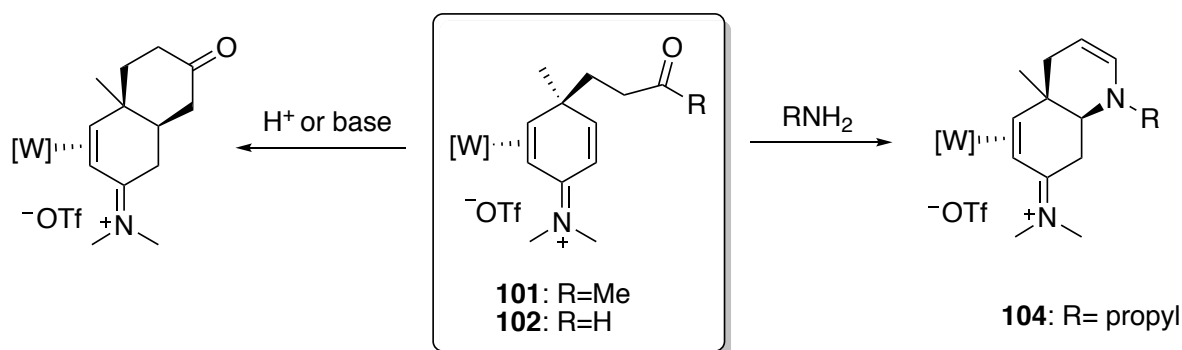
Scheme 5.16: Intramolecular cyclizations with η^2 -anisolium



The Michael additions to **99A** result in products with an uncoordinated double bond in conjugation with the iminium system (**101** and **102**). Theoretically, the β -carbon of the uncoordinated alkene should be electrophilic; however, the back-donation of electron density from the metal complex into this π -system could potentially render this position unreactive. Previously, our group reported the ability to add a nucleophile to this position with the η^2 -anisolium system, typically via an intramolecular cyclization (Scheme 5.16); however, this type of reactivity has not been shown with the anilinium system. Thus, we began investigating the ability of **101** and **102** to undergo cyclization reactions. We proposed that the desired intramolecular cyclization originally proposed by the Cobb group (Figure 5.2) could be facilitated by the metal under either acid or basic conditions, with the additional benefit of the metal center to help control the stereochemistry of the cyclization (Scheme 5.17). Unfortunately, no reaction was observed under acidic conditions with acid strengths ranging from relatively weak acids all the way to HOTf in DCM. Conversely, basic conditions typically resulted in the retro-Michael addition and

decomposition of the η^2 -anilinium species. Using stronger bases (KHDMS) at reduced temperature also did not lead to the desired cyclization product.

Scheme 5.17: Intramolecular cyclization reactions of **101** and **102**



A different type of cyclization pathway was attempted with **102** by adding a primary amine. We expected the addition of an amine to the aldehyde would form an imine in solution, which potentially could close on the electrophilic alkene through the nitrogen (Scheme 5.17, right). To test this, **102** was dissolved in CD_3CN and propylamine (4 equivalents) was added. The reaction was checked by 1H NMR after 45 minutes. Although some rearomatized ligand was observed, one major new product was formed. 2D NMR analysis of this reaction led to the assignment of the cyclized product **104** shown in Scheme 5.17.

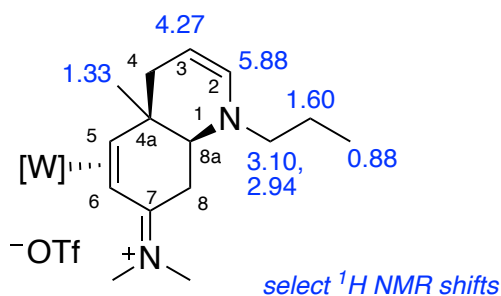


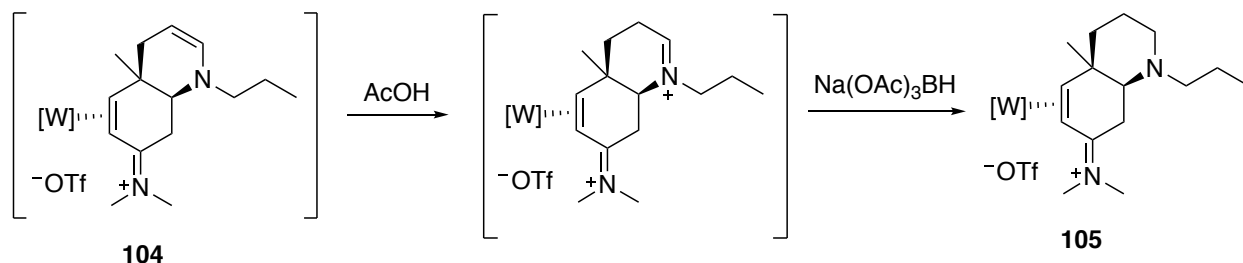
Figure 5.3: ¹H NMR assignments of **104**

The NMR data supported the incorporation of the propylamine group, with a characteristic triplet for the propyl methyl at 0.88 ppm (Figure 5.3). The enamine group in the newly formed 6-membered ring has alkene proton resonances at 5.88 and 4.27 ppm, with corresponding carbons at 131.8 and 92.2 ppm, which is consistent with a polarized alkene like an enamine. Furthermore, the methylene group of the propyl chain adjacent to the nitrogen has an NOE correlation with the alpha alkene proton of the enamine. The alkene proton at 4.27 ppm has an NOE correlation with an adjacent methylene group. The bridgehead proton H8a has an NOE correlation with the bridgehead methyl at 1.33 ppm, which supports the *cis* stereochemistry of the ring juncture.

Isolation of this complex was challenging due to the instability of the enamine group, so instead the enamine was reacted in situ. Starting from **102**, the reaction conditions were altered slightly to reduce the retro-Michael reaction that occurs in the presence of base, by reducing the temperature and reducing the amount of amine added to just over 1 equivalent. The formation of **104** was confirmed by ¹H NMR, and then acetic acid (AcOH) and Na(OAc)₃BH were added. After an hour ¹H NMR data revealed the disappearance of the enamine peaks associated with **104**, and the formation of a new major product. Full 2D NMR analysis enabled the identification of **105** as the desired

product (Scheme 5.18), with two new sets of methylene protons supporting the successful protonation and reduction of the enamine/iminium. Additionally, the reduction potential of **105** ($E_{p,a} = 1.05$ V) supports that the iminium system in conjugation with the metal is still intact, after selectively reducing the more reactive iminium.

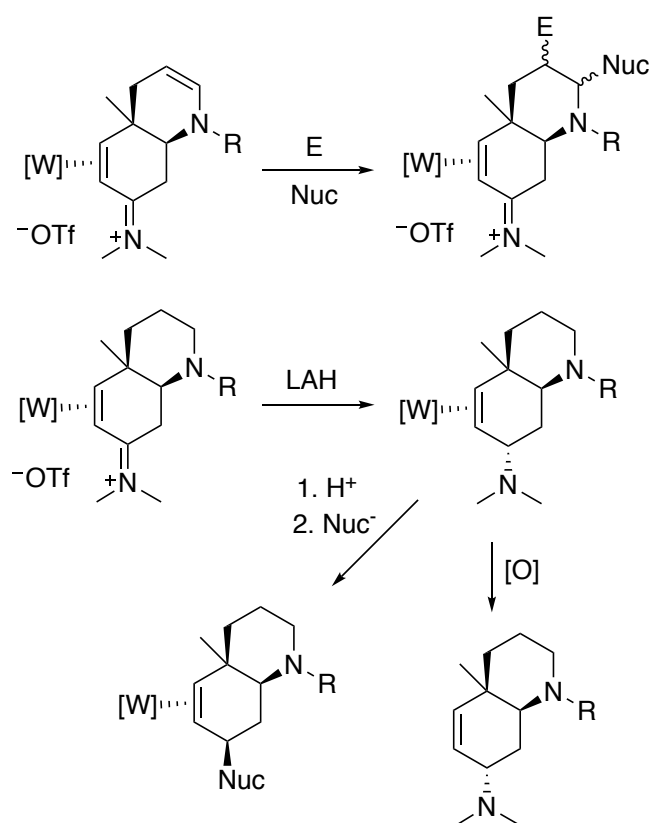
Scheme 5.18: In situ iminium reduction with **104**



Using this dihapto-dearomatization methodology, a saturated quinoline derivative with a bridgehead methyl group can be accessed in two steps from the paramethylanilinium complex, with control of the newly formed stereocenters. Quinolines and their saturated derivatives are an important class of nitrogen heterocycles found in natural products and pharmaceuticals.^{9,13,14} These types of alkaloids and their biological activity will be further discussed in Chapter 6. With this type of reactivity discovered with **102**, we can propose a number of different reaction pathways to further functionalize the quinoline core or to access the free organic (Scheme 5.19). The primary amine that is added in the cyclization step could be changed to provide different groups off of the nitrogen. Furthermore, the enamine could be reacted with electrophiles other than a proton, and the resulting iminium could be reacted with nucleophiles other than hydrides. Because the enamine group is further from the metal than the coordinated ring, it is unclear whether the metal would influence the stereoselectivity of these additions. Additionally, to access the free organic the iminium of the original anilinium system could be reduced with LAH to

lower the reduction potential of the complex and enable the oxidation and isolation of the octahydroquinoline organic. Finally, once the iminium is reduced, the newly formed amino group could theoretically be protonated and fall off, leaving an allyl that could be reacted in situ with a nucleophile. This proposed reaction is similar to the reactivity pathway that was outlined in Scheme 5.11 with η^2 -*N,N*-dimethylanilinium.

Scheme 5.19: Proposed reaction pathways for **104** and **105**



5.3 Conclusion

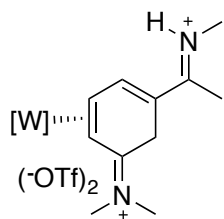
Our group has previously reported the dihapto-coordination of *N,N*-dimethylaniline by in situ protonation with a relatively weak Brønsted acid (DiPAT).³ The regioselective protonation at the ortho position is believed to be both nitrogen and metal controlled. The

resulting stabilized anilinium complex has been shown to be reactive towards a second electrophilic addition, followed by a nucleophilic addition with high regio- and stereocontrol.³ Furthermore, reactivity of the η^2 -*N,N*-dimethylanilinium system with carbon electrophiles was explored with some promising results. Most interestingly, the double addition of a Michael acceptor at the meta position and subsequent cyclization produced a bridged bicyclic chromen derivative.

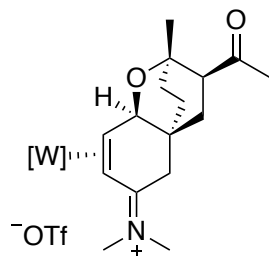
The coordination of *N,N*,4-dimethylaniline was achieved using a similar in situ protonation method, with protonation selectively occurring at the ortho position. This complex was shown to undergo a tandem addition with a proton and 2-methylfuran, with the relatively weak aromatic nucleophile successfully adding to form a quaternary carbon. Additionally, in the presence of base, η^2 -*N,N*,4-dimethylanilinium was reactive with carbon electrophiles at the para position. In one case, the addition of a primary amine to the anilinium complex with acrolein added led to an intramolecular cyclization, yielding a hexahydroquinoline system. In all cases, the influence of the asymmetric metal in tandem with the amino group of the anilinium allowed for high regio- and stereocontrol.

5.4 Experimental

General Methods: NMR spectra were obtained on Varian 500, 600 MHz and Bruker 600, 800 MHz spectrometers. Chemical shifts are referenced to tetramethylsilane (TMS) utilizing residual ^1H signals of the deuterated solvents as internal standards. Chemical shifts are reported in ppm and coupling constants (J) are reported in hertz (Hz). Phosphorus NMR signals are referenced to 85% H_3PO_4 ($\delta = 0.00$) using a triphenylphosphate external standard ($\delta = -16.58$). Infrared Spectra (IR) were recorded on a spectrometer as a glaze on a diamond anvil ATR assembly, with peaks reported in cm^{-1} . Electrochemical experiments were performed under a nitrogen atmosphere using a BAS Epsilon EC-2000 potentiostat. Cyclic voltammetric data were recorded at ambient temperature at 100 mV/s, unless otherwise noted, with a standard three electrode cell from +1.8 V to -1.8 V with a glassy carbon working electrode, *N,N*-dimethylacetamide (DMA) solvent, and tetrabutylammonium hexafluorophosphate (TBAH) electrolyte (~0.5 M). All potentials are reported versus the normal hydrogen electrode (NHE) using cobalticinium hexafluorophosphate ($E_{1/2} = -0.78$ V, -1.75 V) or ferrocene ($E_{1/2} = 0.55$ V) as an internal standard. Peak separation of all reversible couples was less than 100 mV. Unless otherwise noted, all synthetic reactions were performed in a glovebox under a dry nitrogen atmosphere. All solvents were purged with nitrogen prior to use. Deuterated solvents were used as received from Cambridge Isotopes. Triflate salts of amines were prepared by combining a triflic acid/ Et_2O solution with a solution of ether and the corresponding amine. **96A** was synthesized using a previously reported procedure.³

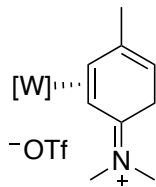


Compound 97. To a 4-dram vial were added **96** (300 mg, 0.387 mmol) followed by acetonitrile (4 mL), resulting in a homogeneous golden solution. MeOTf (74 mg, 0.451 mmol) was added and the reaction solution was stirred for 48 h. The reaction was checked by ^{31}P NMR, then more MeOTf (38 mg, 0.23 mmol) was added and stirred for 24 h. The reaction solution was then evaporated *in vacuo* to dryness. The film was redissolved in minimal DCM and added to stirring Et_2O (35 mL). The resulting precipitate was collected on a 15 mL fine porosity fritted disc, washed with hexanes (2 x 10 mL) and desiccated overnight, yielding **97** (284 mg, 0.290 mmol, 75% yield). CV (DMAc) $E_{\text{p,a}} = +1.42$ V (NHE). IR: $\nu(\text{BH}) = 2503$ cm^{-1} , $\nu(\text{NO})$ and $\nu(\text{iminium}) = 1616$ cm^{-1} , 1601 cm^{-1} and 1581 cm^{-1} . ^{31}P NMR (CD_3CN , δ): -10.22 ($J_{\text{WP}} = 277$). ^1H NMR (CD_3CN , δ): 9.27 (bs, 1H, NH), 8.08 (d, $J = 5.5$, 1H, H4), 8.05 (d, 1H, PzB3/PzC5), 8.04 (d, 1H, PzB3/PzC5), 7.94 (m, 2H, PzA5 and PzB5), 7.83 (d, 1H, PzC3), 7.17 (d, 1H, PzA3), 6.51 (t, 1H, PzC4), 6.43 (t, 1H, PzB4), 6.39 (t, 1H, PzA4), 4.13 (m, 1H, H3), 3.63 (d, $J = 21.7$ 1H, H6x), 3.62 (s, 3H, NMe), 3.44 (d, $J = 5.2$, 3H, HNMe), 3.14 (d, $J = 21.7$, 1H, H6y), 2.83 (d, $J = 7.2$, 1H, H2), 2.55 (s, 3H, Me), 2.44 (s, 3H, NMe), 1.26 (d, $J = 9.4$, 9H, PMe_3). ^{13}C NMR (CD_3CN , δ): 181.0 (C1), 177.6 (C-iminium) 152.6 (C4), 145.7 (PzB3), 142.9 (PzC3), 142.6 (PzA3), 139.6 (Pz5), 139.4 (Pz5), 139.3 (Pz5), 114.9 (C5), 108.7 (Pz4), 108.6 (Pz4), 108.1 (Pz4), 64.7 (d, $J = 8.1$, C3), 57.1 (C2), 43.6 (NMe), 42.2 (NMe), 33.7 (MeNH), 29.9 (C6), 16.3 (Me), 13.5 (d, $J = 31.7$, PMe_3).



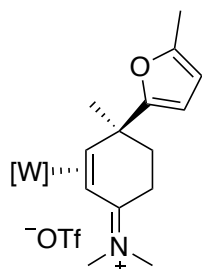
Compound 98. To a 4-dram vial were added **96** (100 mg, 0.129 mmol), acetonitrile (1.5 mL), and MVK (49 mg, 0.70 mmol), resulting in a homogeneous golden solution. A 0.26M solution of HOTf in acetonitrile (0.5 mL, 0.13 mmol) was added drop wise with stirring, and the reaction solution was stirred for 48 h. The reaction was monitored over 4 d by ^{31}P NMR, then the reaction solution was removed from the glove box, diluted with saturated aqueous Na_2CO_3 (20 mL), then extracted with DCM (2 x 20 mL). The combined organic layer was washed with H_2O (20 mL), then dried over MgSO_4 and concentrated *in vacuo* to an oil. The oil was redissolved in minimal DCM and added to stirring Et_2O (40 mL). The resulting tan precipitate was collected on a 15 mL medium porosity fritted disc and desiccated overnight, yielding **98** (104 mg, 0.114 mmol, 88% yield). CV (DMAc) $E_{\text{p,a}} = +1.15$ V (NHE). IR: $\nu(\text{BH}) = 2510$ cm^{-1} , $\nu(\text{CO}) = 1692$ cm^{-1} , $\nu(\text{NO})$ and $\nu(\text{iminium}) = 1591$ cm^{-1} and 1573 cm^{-1} . ^{31}P NMR (CD_3CN , δ): -8.53 ($J_{\text{WP}} = 281$). ^1H NMR (CD_3CN , δ): 8.09 (d, 1H, PzB3), 7.97 (d, 1H, PzC5), 7.91 (d, 1H, PzB5), 7.89 (d, 1H, PzA5), 7.63 (d, 1H, PzC3), 7.15 (d, 1H, PzA3), 6.45 (t, 1H, PzC4), 6.42 (t, 1H, PzB4), 6.35 (t, 1H, PzA4), 5.05 (bs, 1H, H4), 3.46 (s, 3H, NMe), 3.42 (m, 1H, H3), 2.68 (m, 2H, H6x & H8), 2.59 (d, $J = 16.5$, 1H, H6y), 2.40 (m, 1H, H7x), 2.33 (s, 3H, CO-Me), 2.32 (m, 1H, H2), 2.22 (s, 3H, NMe), 1.92 (m, 1H, H10x), 1.78 (m, 1H, H10y), 1.69 (m, 2H, H11), 1.39 (m, 1H, H7y), 1.30 (d, $J = 9.3$, 9H, PMe_3), 1.13 (s, 3H, C9-Me). ^{13}C NMR (CD_3CN , δ): 211.1 (CO), 184.9 (C1), 145.6 (PzB3), 144.3 (PzA3), 142.2 (PzC3), 139.0 (2C, Pz5), 138.7 (Pz5), 108.3 (PzB4/PzC4), 108.2 (PzB4/PzC4), 107.9 (PzA4), 79.3 (C4),

72.4 (C9), 68.8 (d, $J = 14.0$, C3), 55.7 (C2), 55.5 (C8), 43.3 (NMe), 41.4 (NMe), 37.5 (C5), 36.8 (C6), 34.7 (C10), 30.8 (C11), 29.9 (CO-Me), 29.3 (C7), 24.3 (C9-Me), 13.7 (d, $J = 30.9$, PMe_3).



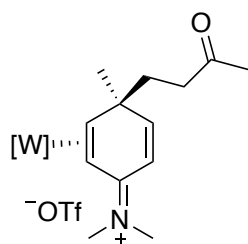
Compound 99A. 1 (2.68 g, 4.61 mmol) was combined with DiPAT (1.28 g, 5.09 mmol) in a 4-dram vial. *N,N*,4-trimethylaniline (5.62 g, 41.6 mmol) and hexanes (25 mL) were added to a 100 mL round bottom charged with a stir bar. The mixture of **1** and DiPAT was added to the round bottom flask with stirring. The 4-dram vial was then rinsed with hexanes (15 mL) and added to the reaction mixture. The resulting yellow heterogeneous mixture was stirred for 72 h. The reaction mixture was filtered through a 30 mL fine porosity fritted funnel, yielding a dark-yellow/brown solid. The solid was transferred to a 25 mL round bottom flask and triturated in DME (8 mL) for 10 min. The yellow solid was then collected on a 30 mL medium porosity fritted funnel, washed with DME (6 mL), 1:1 DME/Et₂O (3 x 10 mL) and hexanes (2 x 15 mL), yielding **99A** (2.46 g, 3.12 mmol, 68% yield). CV (DMA): $E_{p,a} = +0.98$ V. IR: $\nu(\text{BH}) = 2507 \text{ cm}^{-1}$, $\nu(\text{NO})$ and $\nu(\text{iminium}) = 1604 \text{ cm}^{-1}$ and 1577 cm^{-1} . ³¹P NMR (CD₃CN, δ): -10.29 ($J_{\text{WP}} = 288$). ¹H NMR (CD₃CN, δ): 8.08 (d, 1H, PzB3), 7.99 (d, 1H, PzC5), 7.92 (d, 1H, Pz5), 7.90 (d, 1H, Pz5), 7.67 (d, 1H, PzC3), 7.07 (d, 1H, PzA3), 6.47 (t, 1H, PzC4), 6.41 (t, 1H, PzB4), 6.36 (t, 1H, PzA4), 4.70 (bs, 1H, H5), 3.88 (m, 1H, H3), 3.52 (d, $J = 23.0$, 1H, H6x), 3.36 (s, 3H, NMe), 3.23 (d, $J = 23.0$, 1H, H6y), 2.34 (d, $J = 8.3$, 1H, H2), 2.10 (s, 3H, NMe), 1.90 (s, 3H, 4Me), 1.22 (d, $J = 8.9$, 9H, PMe_3). ¹³C NMR (CD₃CN, δ): 183.1 (C1), 145.5 (Pz3/Pz5), 142.4 (Pz3/Pz5), 142.3 (Pz3/Pz5), 139.3 (Pz3/Pz5), 139.0 (Pz3/Pz5),

138.8 (Pz3/Pz5), 136.6 (C4), 109.6 (C5), 108.4 (Pz4), 108.3 (Pz4), 107.6 (Pz4), 66.9 (d, $J = 13.0$, C3), 58.4 (C2), 42.6 (NMe), 40.8 (NMe), 31.4 (C6), 24.6 (C4-Me), 14.3 (d, $J = 31.0$, PMe₃).



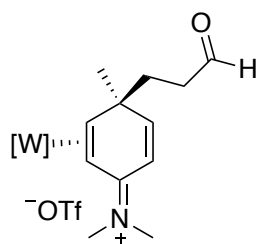
Compound 100. 99A (585 mg, 0.742 mmol) was combined with a 0.26M HOTf/MeCN solution (5.9 mL, 1.53 mmol), resulting in a dark red homogenous solution that was allowed to sit for 1 h. 2-methylfuran (637 mg, 7.42 mmol) was added to the reaction solution and allowed to react for 1.5 h. The reaction solution was then removed from the glove box, diluted with DCM (50 mL), and extracted with saturated aqueous Na₂CO₃ (2 x 50 mL). The combined aqueous layers were back extracted with DCM (50 mL). The combined organic layers were washed with H₂O (50 mL), dried over MgSO₄ and concentrated *in vacuo*. The resulting yellow oil was redissolved in minimal DCM and precipitated into stirring Et₂O (200 mL). The pale tan solid was collected on a 15 mL medium porosity fritted funnel and washed with Et₂O (5 mL) and pentane (10 mL), yielding **100** (496 mg, 0.570 mmol, 77% yield). IR: $\nu(\text{BH}) = 2512 \text{ cm}^{-1}$, $\nu(\text{NO})$ and $\nu(\text{iminium}) = 1560 \text{ cm}^{-1}$. ³¹P NMR (CD₃CN, δ): -10.52 ($J_{\text{WP}} = 281$). ¹H NMR (CD₃CN, δ): 8.09 (d, 1H, PzB3), 8.00 (d, 1H, PzB5/PzC5), 7.96 (d, 1H, PzB5/PzC5), 7.90 (d, 1H, PzA5), 7.63 (d, 1H, PzC3), 7.18 (d, 1H, PzA3), 6.46 (m, 2H, PzB4 and PzC4), 6.37 (t, 1H, PzA4), 6.18 (d, $J = 2.9$, 1H, H3'), 5.93 (bs, 1H, H4'), 3.89 (dd, $J = 13.6, 9.2$, 1H, H3), 3.27 (s, 3H, NMe), 2.67 (dd, $J = 18.8, 5.9$, 1H, H6x),

2.44 (m, 1H, H5x), 2.39 (m, 1H, H6y), 2.29 (d, $J = 9.2$, 1H, H2), 2.26 (s, 3H, 5'Me), 1.94 (buried, 1H, H5y), 1.91 (s, 3H, NMe), 1.61 (s, 3H, 4Me), 1.13 (d, $J = 8.8$, 9H, PMe₃). ¹³C NMR (CD₃CN, δ): 188.0 (C1), 165.1 (C2'), 151.3 (C5'), 144.6 (PzA3), 144.0 (PzB3), 142.0 (PzC3), 139.1 (Pz5), 138.9 (Pz5), 138.8 (Pz5), 108.7 (PzB4/PzC4), 108.5 (PzB4/PzC4), 108.0 (PzA4), 106.8 (C4'), 106.1 (C3'), 73.4 (d, $J = 13.2$, C3), 59.5 (C2), 42.1 (NMe), 41.2 (C4), 40.2 (NMe), 31.0 (C4Me), 30.9 (C5), 27.3 (C6), 14.0 (d, $J = 30.8$, PMe₃), 13.6 (C5'Me).



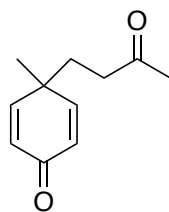
Compound 101. **99A** (2.50 g, 3.17 mmol), DCM (3 mL), and MVK (1.12 g, 16.0 mmol) were added to a 50 mL round bottom flask charged with a stir bar. In a 4-dram vial Et₃N (290 mg, 2.87 mmol) and MeOH (10 mL) were combined, then this solution was added to the round bottom flask with stirring. The reaction was monitored by ³¹P NMR, and after 5 d the reaction was removed from the glove box, diluted with saturated aqueous NaHCO₃ (50 mL) and H₂O (25 mL), then extracted with DCM (4 x 50 mL). The combined organic layer was washed with H₂O (40 mL), then this aqueous layer was back-extracted with DCM (50 mL). The combined organic layers were dried over MgSO₄ and concentrated *in vacuo* to an oil. DCM (10 mL) was added to the oil, and this solution was added to stirring Et₂O (500 mL). The resulting solid was collected on a 60 mL fine porosity fritted disc, washed with Et₂O (20 mL) and pentane (30 mL) then desiccated overnight, yielding **101** (1.73 g, 2.02 mmol, 64% yield). CV (DMAc) $E_{p,a} = +0.90$ V (NHE). IR: $\nu(\text{BH}) = 2499$ cm⁻¹, $\nu(\text{CO}) = 1706$ cm⁻¹,

$\nu(\text{NO})$ and $\nu(\text{iminium}) = 1586 \text{ cm}^{-1}$ and 1562 cm^{-1} . ^{31}P NMR (d^6 -acetone, δ): -10.71 ($J_{\text{WP}} = 284$). ^1H NMR (d^6 -acetone, δ): 8.15 (d, 1H, PzC5), 8.11 (d, 1H, PzB3), 8.09 (d, 1H, PzB5), 8.05 (d, 1H, PzA5), 7.89 (d, 1H, PzC3), 7.27 (d, 1H, PzA3), 6.67 (dd, $J = 10.4, 1.4$, 1H, H6), 6.53 (t, 1H, PzC4), 6.50 (t, 1H, PzB4), 6.47 (t, 1H, PzA4), 6.46 (buried, 1H, H5), 3.83 (ddd, $J = 13.9, 8.8, 1.1$, 1H, H3), 3.61 (s, 3H, NMe), 2.79 (m, 1H, H8x), 2.60 (m, 1H, H8y), 2.34 (dd, $J = 8.8, 1.1$, 1H, H2), 2.17 (s, 3H, NMe), 2.10 (s, 3H, CO-Me), 2.09 (buried, 2H, H7), 1.54 (s, 3H, C4-Me), 1.19 (d, $J = 8.5$, 9H, PMe_3). ^{13}C NMR (CDCl_3 , δ): 209.9 (CO), 174.6 (C1), 156.6 (C5), 143.6 (PzB3), 142.9 (PzA3), 141.6 (PzC3), 138.0 (Pz5), 137.9 (Pz5), 137.7 (Pz5), 114.7 (C6), 108.5 (Pz4), 107.8 (Pz4), 107.0 (Pz4), 69.2 (d, $J = 12.5$, C3), 57.7 (C2), 43.1 (C7), 42.5 (C4), 41.8 (NMe), 40.1 (NMe), 38.9 (C8), 30.9 (C4-Me), 30.5 (CO-Me), 14.5 (d, $J = 30.1$, PMe_3).

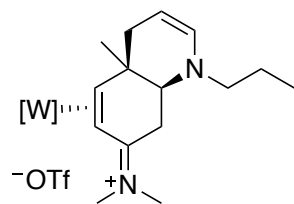


Compound 102. 99A (30 mg, 0.038 mmol), MeOH (0.6 mL) and acrolein (10 mg, 0.18 mmol) were added to a 4-dram vial charged with a stir pea. In a separate 4-dram vial Et_3N (4 mg, 0.04 mmol) and DCM (0.2 mL) were combined, and then this solution was added to the reaction vial with stirring. The reaction was monitored by ^{31}P NMR and after 3 d the reaction was removed from the glove box, diluted with saturated aqueous NaHCO_3 (10 mL), then extracted with DCM (3 x 10 mL). The combined organic layers were dried over MgSO_4 and concentrated *in vacuo* to dryness. The film was then redissolved in minimal DCM and added to stirring Et_2O (25 mL). The resulting solid was collected on a 15 mL fine porosity

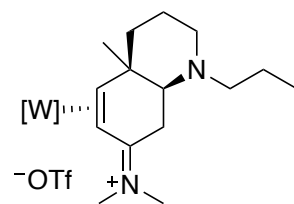
fritted disc and desiccated, yielding **102** (21 mg, 0.025 mmol, 66% yield). ^1H NMR (d_6 -acetone, δ): 9.78 (t, $J = 1.6$, 1H, CO-H), 8.15 (d, 1H, PzC5), 8.12 (d, 1H, PzB3), 8.10 (d, 1H, PzB5), 8.05 (d, 1H, PzA5), 7.91 (d, 1H, PzC3), 7.29 (d, 1H, PzA3), 6.70 (dd, $J = 10.4, 1.6$, 1H, H6), 6.53 (t, 1H, PzC4), 6.50 (t, 1H, PzB4), 6.47 (t, 1H, PzA4), 6.45 (buried, 1H, H5), 3.80 (ddd, $J = 13.8, 8.7, 1.5$, 1H, H3), 3.61 (s, 3H, NMe), 2.77 (m, 1H, H8x), 2.56 (m, 1H, H8y), 2.34 (dd, $J = 8.7, 1.4$, 1H, H2), 2.19 (m, 2H, H7), 2.16 (s, 3H, NMe), 1.57 (s, 3H, C4-Me), 1.19 (d, $J = 8.5, 9\text{H}$, PMe_3).



Compound 103. NOPF_6 (335 mg, 1.92 mmol) was added to a 4-dram vial charged with a stir pea. **101** (1.03 g, 1.20 mmol) was dissolved in acetone (14 mL) and added to the vial with NOPF_6 with stirring. The vial was rinsed acetone (6 mL) and added to the reaction solution. After 4.5 h the reaction solution was added to a 500 mL Erlenmeyer flask, diluted with acetone (172 mL), and 1:1 saturated aqueous $\text{NaHCO}_3/\text{H}_2\text{O}$ (172 mL), and stirred for 15 min. The solution was then diluted with H_2O (225 mL) and extracted with Et_2O (2 x 200 mL), then EtOAc (200 mL). The combined organic layers were washed with brine (100 mL), dried over MgSO_4 and evaporated *in vacuo*. The crude oil was redissolved in DCM and loaded onto a silica gel column set in 10% EtOAc /hexanes. The organic band was eluted with 60% EtOAc /hexanes and concentrated *in vacuo* to an oil, yielding **103** (179 mg, 1.00 mmol, 83% yield). ^1H NMR (CD_3Cl , δ): 6.70 (m, 2H, H3 & H5), 6.29 (m, 2H, H2 & H6), 2.22 (m, 2H, H8), 2.06 (s, 3H, CO-Me), 1.96 (m, 2H, H7), 1.30 (s, 3H, C4-Me).



Compound 104. Not isolated, see procedure below to generate **104** in situ. ^1H NMR (d^6 -acetone, δ): 8.19 (d, 1H, PzB3), 8.15 (d, 1H, PzC5), 8.09 (d, 1H, PzB5), 8.03 (d, 1H, PzA5), 7.87 (d, 1H, PzC3), 7.42 (d, 1H, PzA3), 6.54 (t, 1H, PzC4), 6.53 (t, 1H, PzB4), 6.44 (t, 1H, PzA4), 5.88 (dm, $J = 7.9$, 1H, H2), 4.27 (m, 1H, H3), 3.94 (dd, $J = 13.8, 9.0$, 1H, H5), 3.92 (buried, 1H, H8a), 3.52 (s, 3H, NMe), 3.16 (dd, $J = 19.2, 6.6$, 1H, H8x), 3.10 (m, 1H, H9x), 2.93 (dt, $J = 13.7, 7.3$, 1H, H9y), 2.32 (m, 2H, H4x & H8y), 2.25 (d, $J = 9.0$, 1H, H6), 2.06 (s, 3H, NMe), 1.94 (dm, $J = 17.2$, 1H, H4y), 1.59 (m, 2H, H10), 1.33 (s, 3H, C4a-Me), 1.24 (d, $J = 8.8$, 9H, PMe_3), 0.88 (t, $J = 7.4$, 3H, H11). ^{13}C NMR (CD_3CN , δ): 187.4 (C7), 144.6 (PzA3), 144.0 (PzB3), 141.9 (PzC3), 139.0 (Pz5), 138.8 (2C, Pz5), 132.7 (C2), 108.6 (Pz4), 108.5 (Pz4), 108.0 (Pz4), 93.1 (C3), 79.1 (C5), 57.8 (C6), 55.7 (C9), 54.9 (C8a), 42.1 (NMe), 41.0 (C4), 40.3 (NMe), 37.7 (C4a), 31.0 (C8), 27.6 (C4a-Me), 23.5 (C10), 14.1 (d, $J = 30.8$, PMe_3), 11.7 (C11).



Compound 105. **102** (27 mg, 0.032 mmol), CD_3CN (0.6 mL), and propylamine (8 mg, 0.14 mmol) were added to a 4-dram vial charged with a stir bar, forming **104** in situ. After 24 h acetic acid (13 mg, 0.22 mmol) was added with stirring, followed by $\text{NaBH}(\text{OAc})_3$ (38 mg, 0.18 mmol). The reaction was stirred for 1 h then removed from the glove box, diluted with

saturated aqueous NaHCO₃ (15 mL) and extracted with DCM (3 x 20 mL). The combined organic layer was washed with H₂O (20 mL), then dried over MgSO₄ and concentrated *in vacuo* to dryness. The film was redissolved in minimal DCM then added to stirring Et₂O (15 mL). The resulting solid was collected on a 15 mL fine porosity fritted disc and desiccated overnight, yielding **105** (13 mg, 0.015 mmol, 47% yield). CV (DMAc) $E_{p,a} = +1.05$ V (NHE). IR: $\nu(\text{BH}) = 2505$ cm⁻¹, $\nu(\text{NO})$ and $\nu(\text{iminium}) = 1585$ cm⁻¹ and 1560 cm⁻¹. ³¹P NMR (CD₃CN, δ): -10.28 ($J_{\text{WP}} = 286$). ¹H NMR (CD₃CN, δ): 8.06 (d, 1H, PzB3), 7.99 (d, 1H, PzC5), 7.94 (d, 1H, PzB5), 7.89 (d, 1H, PzA5), 7.62 (d, 1H, PzC3), 7.12 (d, 1H, PzA3), 6.45 (t, 1H, PzC4), 6.44 (t, 1H, PzB4), 6.37 (t, 1H, PzA4), 3.63 (dd, $J = 13.6, 9.3$, 1H, H5), 3.54 (t, $J = 8.0$, 1H, H8a), 3.35 (s, 3H, NMe), 2.61 (m, 1H, H8x), 2.55 (m, 2H, H2x & H8y), 2.49 (td, $J = 12.3, 3.1$, 1H, H9x), 2.36 (m, 1H, H9y), 2.19 (d, $J = 9.1$, 1H, H6), 1.93 (s, 3H, NMe), 1.80 (m, 1H, H3x), 1.68 (m, 1H, H4x), 1.55 (m, 1H, H4y), 1.53 (m, 3H, H3y & H10), 1.51 (s, 3H, C4a-Me), 1.09 (d, $J = 8.2$, 9H, PMe₃), 0.90 (t, $J = 7.4$, 3H, H11). ¹³C NMR (CD₃CN, δ): 186.6 (C7), 144.2 (PzA3), 144.1 (PzB3), 141.9 (PzC3), 139.0 (2C, Pz5), 138.8 (Pz5), 108.6 (Pz4), 108.4 (Pz4), 107.8 (Pz4), 80.5 (d, $J = 13.2$, C5), 58.5 (C6), 56.7 (C9), 56.6 (C8a), 45.9 (C2), 42.0 (NMe), 41.8 (C4), 40.4 (NMe), 39.7 (C4a), 27.8 (C4a-Me), 24.6 (C3), 23.2 (C8), 21.5 (C10), 14.2 (d, $J = 31.0$, PMe₃), 12.3 (C11).

5.5 References

- (1) Todd, M. A.; Grachan, M. L.; Sabat, M.; Myers, W. H.; Harman, W. D. *Organometallics* **2006**, *25*, 3948.
- (2) Lis, E. C.; Salomon, R. J.; Sabat, M.; Myers, W. H.; Harman, W. D. *J. Am. Chem. Soc.* **2008**, *130*, 12472.
- (3) Salomon, R. J.; Todd, M. A.; Sabat, M.; Myers, W. H.; Harman, W. D. *Organometallics* **2010**, *29*, 707.
- (4) Welch, K. D.; Harrison, D. P.; Lis, E. C.; Liu, W.; Salomon, R. J.; Harman, W. D.; Myers, W. H. *Organometallics* **2007**, *26*, 2791.
- (5) Pienkos, J. A.; Zottig, V. E.; Iovan, D. A.; Li, M.; Harrison, D. P.; Sabat, M.; Salomon, R. J.; Strausberg, L.; Teran, V. A.; Myers, W. H.; Harman, W. D. *Organometallics* **2013**, *32*, 691.
- (6) Salomon, R. J., University of Virginia, 2010.
- (7) Harrison, D. P.; Nichols-Nielander, A. C.; Zottig, V. E.; Strausberg, L.; Salomon, R. J.; Trindle, C. O.; Sabat, M.; Gunnoe, T. B.; Iovan, D. A.; Myers, W. H.; Harman, W. D. *Organometallics* **2011**, *30*, 2587.
- (8) Wilson, K. B.; Myers, J. T.; Nedzbala, H. S.; Combee, L. A.; Sabat, M.; Harman, W. D. *J. Am. Chem. Soc.* **2017**, *139*, 11401.
- (9) Vitaku, E.; Smith, D. T.; Njardarson, J. T. *Journal of Medicinal Chemistry* **2014**, *57*, 10257.
- (10) MacLeod, B. L.; Pienkos, J. A.; Wilson, K. B.; Sabat, M.; Myers, W. H.; Harman, W. D. *Organometallics* **2016**, *35*, 370.
- (11) MacLeod, B. L., University of Virginia, 2016.

- (12) Kopach, M. E.; Harman, W. D. *J. Am. Chem. Soc.* **1994**, *116*, 6581.
- (13) Sridharan, V.; Suryavanshi, P. A.; Menéndez, J. C. *Chem. Rev.* **2011**, *111*, 7157.
- (14) Daly, J. W.; Ware, N.; Saporito, R. A.; Spande, T. F.; Garraffo, H. M. *Journal of Natural Products* **2009**, *72*, 1110.

Chapter 6

Tungsten Dearomatization of Tetrahydroquinoline

Derivatives

6.1 Introduction

Chapter 5 outlined the successful η^2 -coordination of *N,N*-dimethylaniline to the {TpW(NO)(PMe₃)} fragment, and gave an overview of the novel synthetic pathways available for the nitrogen substituted arene through dearomatization. With the coordination and reactivity established with the parent aniline complex, we sought to expand this coordination chemistry to more complex multicyclic nitrogen heterocycles. Nitrogen heterocycles are prevalent in pharmaceuticals, as well as natural products, and thus methods to synthesize and functionalize these types of systems are of importance in synthetic chemistry.^{1,2}

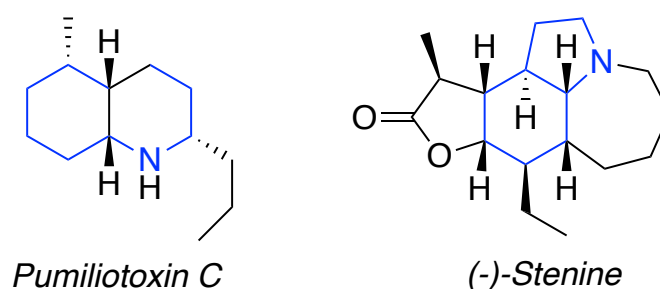


Figure 6.1: Alkaloid natural products

Specifically, natural products in the alkaloid family are common synthetic targets due to their impressive range of biological activity.^{3,4} The aromatic heterocycles quinoline and indole, in addition to their saturated forms, are common to a number of natural products, as illustrated by the structures shown in Figure 6.1.⁵ These types of compounds have been shown to exhibit antitumor and antimalarial activity, and find use in a variety of other medicinal and therapeutic applications.^{3,4} Although these types of synthetic targets can be reached via a total synthesis method, increasingly, methods to rapidly increase molecular complexity are being sought. To this end, dearomatization reactions facilitate the

rapid transformation of typically unreactive planar cyclic structures into relatively complex compounds with multiple sp^3 centers (Figure 6.2). In addition to enforcing stereocontrol, metal coordination also opens up novel reaction pathways, not typically accessible to the aromatic building blocks. With the objective of synthesizing novel, pharmaceutically relevant small molecules, the coordination and reactivity of tetrahydroquinoline derivatives is the focus of this chapter. We have previously reported the reactivity of the η^2 -*N,N*-dimethylanilinium (Chapter 5) and η^2 -*N*-ethylindolinium complexes, which share the same reactive core as the tetrahydroquinoline system (Figure 6.2, red).⁵⁻⁷

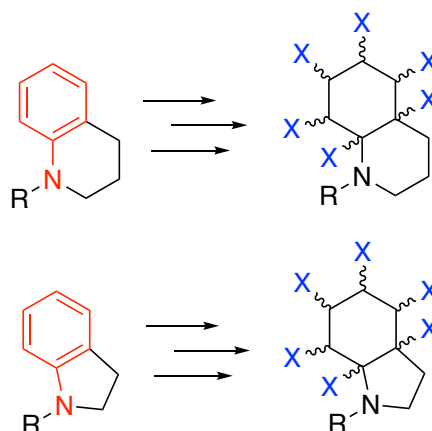
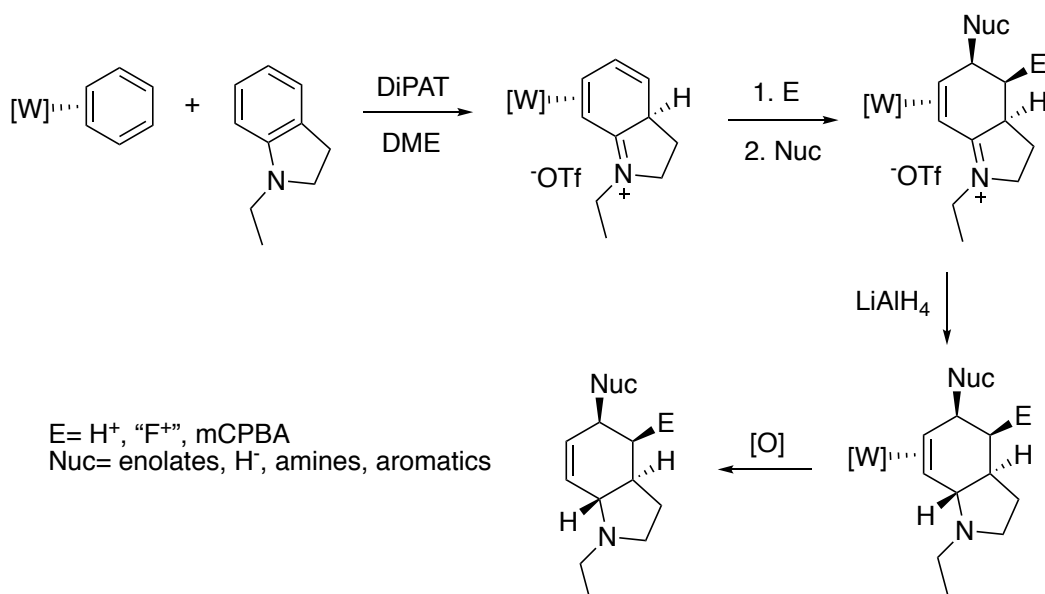


Figure 6.2: Functionalization of tetrahydroquinoline and indoline cores

The coordination and in situ protonation of *N*-ethylindoline to the tungsten fragment leads to the ortho protonated product, shown in Scheme 6.1. The reactivity of this complex has been previously explored with a range of electrophilic and nucleophilic sources similar to the range demonstrated with the η^2 -*N,N*-dimethylanilinium complex (Chapter 5).^{5,6,8,9} The tandem addition to the η^2 -*N*-ethylindolinium complex also results in a regioselective 1,2-addition across the uncoordinated alkene. Furthermore, conditions were found that allow for the stereoselective reduction of the iminium, with the hydride adding

anti to the metal (Scheme 6.1).⁶ The functionalized η^2 -ligand can then be liberated from the complex through oxidation with NOPF_6 , yielding novel hexahydroindole organics. With the reactivity of the indoline system established, we envisioned a similar reaction scheme for the tetrahydroquinoline system.

Scheme 6.1: Coordination and reactivity of *N*-ethylindoline



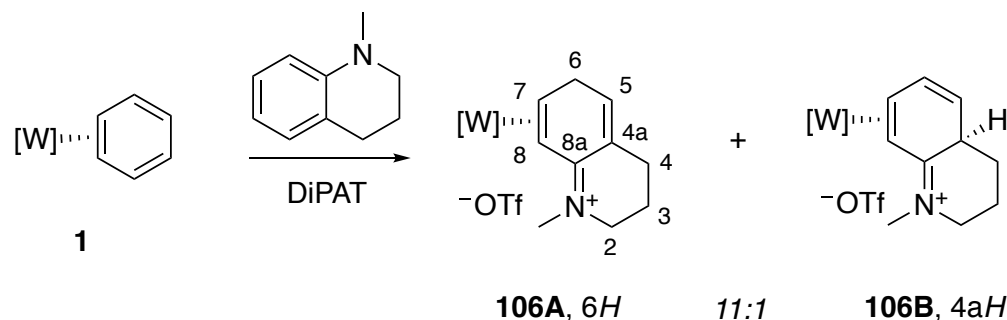
6.2 Results and Discussion

6.2.1 Coordination and Reactivity of *N*-methyl-1,2,3,4-tetrahydroquinoline

Previously, we reported the coordination of *N*-methyl-1,2,3,4-tetrahydroquinoline to the tungsten dearomatization agent via an exchange reaction from $\text{TpW}(\text{NO})(\text{PMe}_3)(\eta^2\text{-benzene})$.⁵ Isolation of a stable dihapto-coordinated complex was achieved by in situ protonation with diisopropylammonium triflate (DiPAT). Assuming that the tetrahydroquinoline system is similar to the aniline system, protonation would be expected to occur at the 4aH carbon (ortho position). However, in situ protonation in this case leads

to the formation of two η^2 -coordinated isomers in a ratio of 11:1, favoring the 6*H* protonated species over the expected 4*aH* protonated isomer (Scheme 6.2).⁵ The major isomer formed in the case of *N*-methyltetrahydroquinoline has an alkene bond that is not in direct conjugation with the metal, making a metal controlled reactivity pathway was less likely. In contrast, protonation at the 4*aH* position leaves the uncoordinated double bond still in conjugation with the metal, which would be expected to react similarly to the η^2 -*N,N*-dimethylanilium and η^2 -3*aH-N*-ethylindolinium complexes.

Interestingly, with η^2 -*N*-ethylindolinium and the minor isomer of η^2 -*N*-methyltetrahydroquinoline protonation leads to the formation of a stereocenter, with the protonation occurring selectively syn to the metal. Historically, our group has assumed that the addition of incoming reagents occurs anti to the metal, which has been supported by a multitude of data and crystal structures. However, less was known about the stereoselectivity of additions when the incoming electrophile is a proton, often because a stereocenter is not formed. The small steric profile of a proton could potentially enable the syn addition, which is not observed with bulkier electrophiles. Recently, deuterium-labeling experiments with η^2 -benzene and η^2 -PhCF₃ (Chapter 2 and Chapter 3) complexes supported a stereoselective syn protonation of the aromatic ligand. This could result from a tungsten hydride intermediate, or initial protonation of the nitrosyl and then delivery of the proton to the aromatic ligand.¹⁰ These results could shed some light on what is observed with the quinoline and indoline systems, where initially it was proposed that the size of the conjugate base of the acid influences the stereoselective syn protonation.

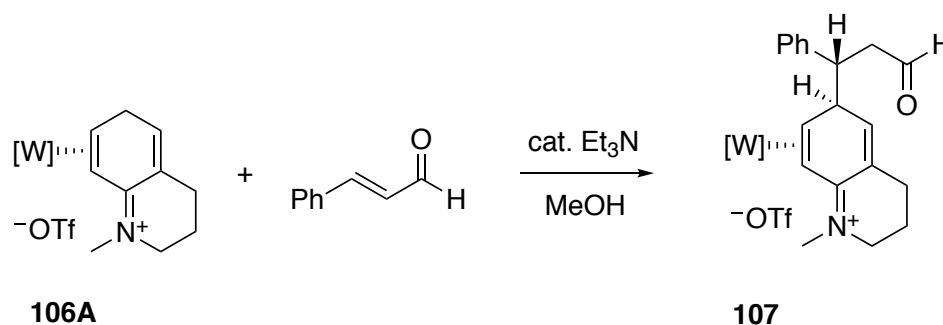
Scheme 6.2: Coordination of *N*-methyltetrahydroquinoline

Preferential formation of **106A** was unexpected based on the regioselective protonation at the ortho position of the η^2 -*N,N*-dimethylanilium system. To try to understand the selectivity in the case of quinoline, and determine if the *6H* isomer was being formed as the thermodynamic product, the ligand substitution reaction was monitored by ^{31}P NMR. After 30 minutes, the product ratio was 4:1 favoring the *6H* isomer. Over the course of the reaction, the ratio increased to >10:1, at which point no further change was observed. These results support the conclusion that the *6H* isomer is the thermodynamic product, but we were unable to make any definitive conclusions because of the inability to establish that an equilibrium was formed.⁵ Since this protonation method utilizes a relatively weak acid source, it has the potential to deprotonate and reprotonate to give a thermodynamic ratio. Using a stronger acid to potentially trap **106B** as the kinetic product was not viable due to the incompatibility of the η^2 -benzene complex with most acids ($\text{pK}_a > 8$). In order to test whether the ratio of **106A** to **106B** could be changed to establish an equilibrium ratio, Et_3N or DBU was added to a methanol solution of **106A** and **106B**; however, no change in the ratio of isomers was observed. Furthermore, treating the mixture with an equivalent of triflic acid leveled in acetonitrile (HOTf/MeCN) resulted in the protonation of **106B**, forming the allylic species, with no detectable change to **106A**.

One potential explanation for favored protonation at C6 over C4a is based on steric interactions within the bicyclic system of tetrahydroquinoline that are not present in the aniline system, causing the thermodynamic preference for **106A**.

Since we were unable to facilitate the conversion of **106A** to **106B**, the reactivity of **106A** was explored. We proposed that this system could potentially be deprotonated in the presence of an electrophile and react at the para position, as was demonstrated with the aniline system in Chapter 5.⁷ Initial investigation of the reactivity of 6*H*-quinolinium with a range of Michael acceptors in the presence of Et₃N in DMF led to the formation multiple products, as seen by ³¹P NMR. The Michael acceptors that were screened included *trans*-cinnamaldehyde, MVK, and methyl acrylate. In all cases, the reaction resulted in the formation of multiple products, with ¹⁸³W-³¹P coupling constants ~280 Hz, which is consistent with η²-anilinium products.⁵ To increase the selectivity of the reaction, the solvent, reagent concentration, base strength, and addition order were varied. The use of a protic solvent (MeOH) increased the selectivity of product formation; however, ultimately, only the addition of *trans*-cinnamaldehyde was optimized to access a single product (**107**) with a ratio >10:1 (Scheme 6.3).

Scheme 6.3: Michael additions to **106A**

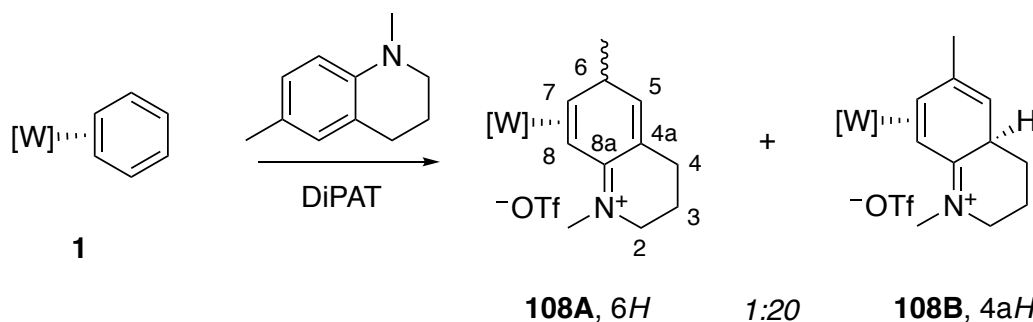


The greater product selectivity with *trans*-cinnamaldehyde in comparison to the other Michael acceptors could potentially be due to increased reactivity of the aldehyde, or steric constraints implemented by the phenyl at the β -position in cinnamaldehyde. 2D NMR analysis of **107** reveals the selective formation of a stereocenter as a result of Michael addition occurring *anti* to the metal, established by a NOE correlation between the H6 proton (3.74 ppm) and the PMe₃ ligand. Additionally, evidence for incorporation of *trans*-cinnamaldehyde into the product includes an aldehyde peak in the ¹H NMR spectrum at 9.88 ppm, as well as 5 aromatic protons. This conclusion is further supported by IR analysis, which exhibits a carbonyl stretch at 1720 cm⁻¹. The selective formation of one product in the case of cinnamaldehyde is especially interesting because a second stereocenter is established at the β -carbon of the Michael acceptor, adjacent to the phenyl group. The ability to control the stereochemistry at the benzylic carbon has been seen with the η^2 -anisole complex when reacted with Michael acceptors with a prochiral carbon.¹¹ This stereoselectivity is believed to be the result of an ordered transition state. In previous reports, this control was attributed to a Diels-Alder like transition state, with the rearomatized ligand favoring an *endo* orientation of the Michael acceptor.¹¹ The reaction then proceeds via ring opening and protonation, forming a product with two new stereocenters. Unfortunately, attempts to functionalize the remaining uncoordinated alkene were unsuccessful, potentially due to the stabilization of the conjugated system. Furthermore, oxidation of the complex to liberate the transformed quinoline ligand resulted in rearomatization.

6.2.2 Coordination and Reactivity of *N*,6-dimethyl-1,2,3,4-tetrahydroquinoline

With the limited success demonstrated for the functionalization of the 6*H* species of *N*-methyltetrahydroquinoline, we began investigating the impact of an additional substituent on the aromatic ring in terms of controlling the regioselectivity of the protonation. We proposed that protonation at 4*aH* could be favored by using a tetrahydroquinoline derivative with a methyl substituent at C6. Initially we suggested that the transition state for C6 protonation would be destabilized relative to C4*a* protonation, due to the unfavorable steric interaction forming between the methyl group and the metal complex, as the proton is delivered *anti* to the metal.¹² However, the recent results with the syn protonation of η^2 -benzene and η^2 -PhCF₃ suggest that this protonation might occur syn to the metal, which would negate the unfavorable transition state argument. Nevertheless, the selective formation of the C4*a* isomer could still be realized based on a thermodynamic preference.

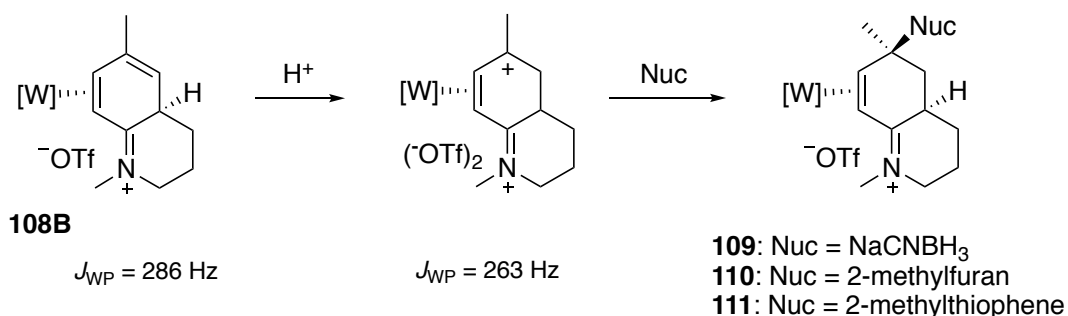
Scheme 6.4: In situ protonation of *N*,6-dimethyl-1,2,3,4-tetrahydroquinoline



In order to test the effect of a C6-substituent on the isomer ratio of the tetrahydroquinoline system, a homogenous ligand substitution reaction of *N*,6-dimethyl-1,2,3,4-tetrahydroquinoline with **1** in the presence of DiPAT was monitored by ³¹P NMR

(Scheme 6.4). The initial formation of a single product with a $J_{WP} = 287$ Hz was consistent with an η^2 -coordinated species. However, as the reaction progressed significant decomposition was observed along with a few minor unidentified peaks. In an effort to isolate and identify the first product observed in ^{31}P NMR, the reaction was repeated under heterogeneous reaction conditions in hexanes and allowed to react for 3 days. After isolation, a ^1H NMR spectrum revealed the formation of a single complex with a resonance at 4.55 ppm, corresponding to the alkene H5 proton of the uncoordinated double bond, consistent with formation of the desired *4aH* isomer of the tetrahydroquinolinium complex (Scheme 6.4). As seen with the *N*-ethylindolinium complex, protonation occurs *syn* to the metal, confirmed by a NOE interaction between H4a and the PzA3 proton of the Tp ligand.⁵ A final test to confirm the identification of **108B** was the treatment of the complex with triflic acid leveled in acetonitrile, which resulted in the formation of an allyl complex, as seen by ^{31}P NMR. The signal for the allyl species exhibits a $J_{WP} = 263$ Hz, consistent with previously reported allyl complexes of aniline derivatives (Scheme 6.5).^{5,7}

Scheme 6.5: Tandem electrophilic/nucleophilic addition to **108B**



Although a C6-methyl substituent allows access to the *4aH*-quinolinium isomer, the ability of this complex to undergo a tandem electrophilic/nucleophilic addition could be

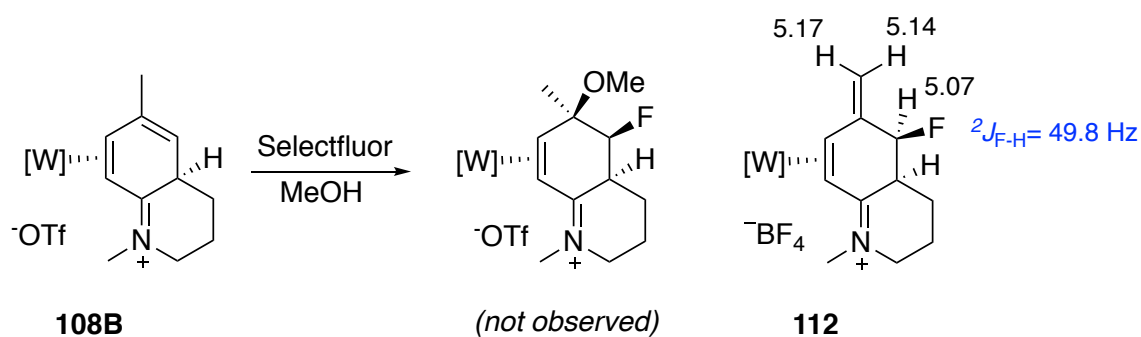
hindered by unfavorable steric interactions caused by the methyl group (Scheme 6.5). Previously, our group reported the inability of the η^2 -*p*-cresol complex to undergo nucleophilic additions with aromatic nucleophiles at the para position, potentially due to the effects of the para methyl substituent; however, in Chapter 5 the successful addition of 2-methylfuran to the tertiary allyl of the η^2 -*N,N*,4-dimethylanilinium complex was shown.⁹ With these results in mind, we sought to find conditions to effect a tandem addition across the uncoordinated double bond of **108B**.

A series of tandem addition reactions were run at room temperature, using a proton (HOTf/MeCN) as the electrophile and a range of nucleophiles including hydrides, protected enolates, amines, and electron rich aromatics. The addition of a proton and a hydride was successful, using NaCNBH₃ as the hydride source to yielding **109** (Scheme 6.5). Addition of (1-methoxy-2-methylprop-1-en-1-yl)trimethylsilane (MMTP) at room temperature and -30°C resulted in deprotonation and isolation of starting material. Lithium dimethylmalonlate (LiDMM) was added at -30°C instead of room temperature in order to favor the addition of the nucleophile over deprotonation. ¹H NMR of the product revealed a 1:1 mixture of starting material and the intended addition product. A further drop in temperature improved this ratio; however, starting material was still present. The successful addition of amines to a cationic system was demonstrated with the *N*-ethylindolinium complex; however, in this case amines preferentially acted as bases instead of adding to the tertiary allyl.⁶ Finally, the aromatic nucleophiles 2-methylfuran and 2-methylthiophene added cleanly as nucleophiles at room temperature, giving **110** and **111** respectively. In the case of successful addition, key features of the complexes included a NOE correlation between the para methyl group and the PMe₃ ligand. For complexes **110**

and **111**, the ^1H NMR spectra exhibited three new aromatic peaks and an additional methyl singlet, supported the successful addition of the aromatic nucleophiles.

The ability to expand the reactivity of the uncoordinated double bond of **108B** to other electrophilic reagents was also explored. **108B** is compatible with a wider range of reagents compared to the η^2 -1,3-dienes described in Chapter 2 and 3, which is in part due to the stability afforded by the protonated iminium system, giving the complex a reduction potential of 1.03 V. This relatively high reduction potential allows for increased metal stability under oxidative conditions, and increases the range of reagents that can be added to the dearomatized ligand. In addition to being stable towards HOTf/MeCN at room temperature, **108B** can be reacted with the electrophilic fluorination agent Selectfluor[®], in the presence of MeOH without oxidation of the metal.

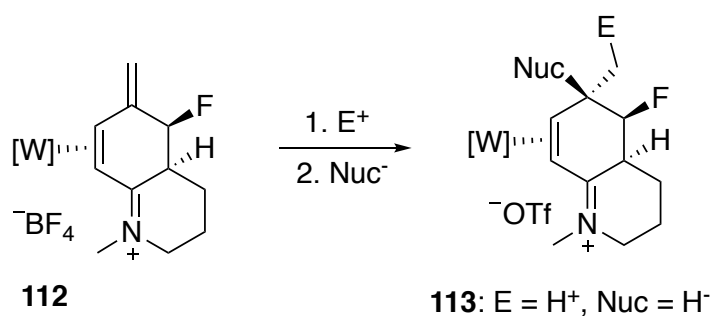
Scheme 6.6: Electrophilic fluorination of **108B**



The expected product for the addition of “F⁺” and a methoxy group across the double bond is shown in the top reaction of Scheme 6.6.⁶ When 1 equivalent of Selectfluor[®] was used, the ^1H NMR of the isolated solid showed the formation of a single product; however, the complex lacked signals expected for the desired product, such as a signal for the methoxy group. Additionally, the C6 methyl signal was absent and three new peaks,

each representing one proton in the 4-5 ppm region were present. One of these protons was determined to be the proton directly adjacent to the fluorine, as shown by a ^{19}F - ^1H coupling constant of 49.8 Hz. The two additional peaks in this region were determined to be alkene peaks with a corresponding carbon at 114.5 ppm, resulting from elimination at the C6 methyl group, giving complex **112** (Scheme 6.6, bottom). Increasing the equivalents of Selectfluor[®] did not result in the formation of the desired product, and instead led to a mix of products. However, we proposed a new reaction scheme for the elimination product, which would theoretically be activated towards a second tandem addition reaction across the exo-cyclic double bond (Scheme 6.7). Because the elimination product is isolated away from the Selectfluor[®], this tandem addition could potentially be achieved with a wider range of nucleophiles than previously accessible because of the incompatibility with the Selectfluor[®] present in situ.⁶

Scheme 6.7: Second tandem addition to fluorinated quinoline complex



The successful tandem addition of Selectfluor[®] and either H₂O, MeOH, pyrazole, or imidazole was demonstrated with the η^2 -*N*-ethylindolinium complex, but other nucleophiles were unsuccessful. The allyl complex resulting from addition of the electrophilic fluorine to the η^2 -*N*-ethylindolinium complex readily decomposed in the

absence of a nucleophile, thus the nucleophiles were added to the reaction solution prior to the addition of Selectfluor® and had to be compatible with the fluorination agent. In this case, the isolation of the elimination product with the quinoline system allows the potential to expand the range of nucleophiles accessible, while still installing the desired fluorine. This proposed reaction pathway was attempted using acid as the electrophile followed by NaCNBH₃ as the hydride source (Scheme 6.7). The reaction was monitored by ³¹P NMR, showing the clean conversion to a single new product with a ¹⁸³W-³¹P coupling constant of 278 Hz. After an aqueous basic work-up, full 2D NMR analysis (COSY, NOESY, HSQC, HMBC) of the product showed the disappearance of the alkene protons and appearance of a new methyl doublet, supporting the successful addition of a hydride at the tertiary center to give complex **113** (Scheme 6.7). Furthermore, the new methyl doublet exhibited a strong NOE correlation with a doublet at 4.74 ppm with a large ¹⁹F-¹H coupling constant of 48.6 Hz, which was identified as the methine at the fluorinated carbon. This observation, in addition to further NOE correlations were used to support the stereoselective addition of both the fluorine and the hydride anti to the metal. The successful regio- and stereoselective incorporation of a fluorine atom into this heterocyclic system is a significant transformation, as new synthetic methods are sought to incorporate fluorine atoms into small molecules due to the beneficial properties that fluorine has shown for biological activity.^{13,14}

To further test the reactivity of **108B** towards traditional alkene transformations, the Simmons-Smith cyclopropanation reaction was attempted. The heterogeneous reaction was allowed to stir for 20 hours, at which point a single product peak was observed with a ¹⁸³W-³¹P coupling constant of 280 Hz. ¹H NMR of the isolated product revealed the

successful cyclopropanation at the trisubstituted alkene, with the characteristic feature of an upfield diastereotopic methylene group of the cyclopropane ring at 0.76 ppm and 0.31 ppm (Scheme 6.8). This conclusion was confirmed by single-crystal molecular structure determination of **114**, which showed the successful formation of the cyclopropane ring oriented anti to the metal (Figure 6.3). Additionally, the crystal structure revealed that the counter ion was an iodide, presumably coming from the CH_2I_2 , instead of the expected triflate counterion.

Scheme 6.8: Simmons-Smith cyclopropanation of **108B**

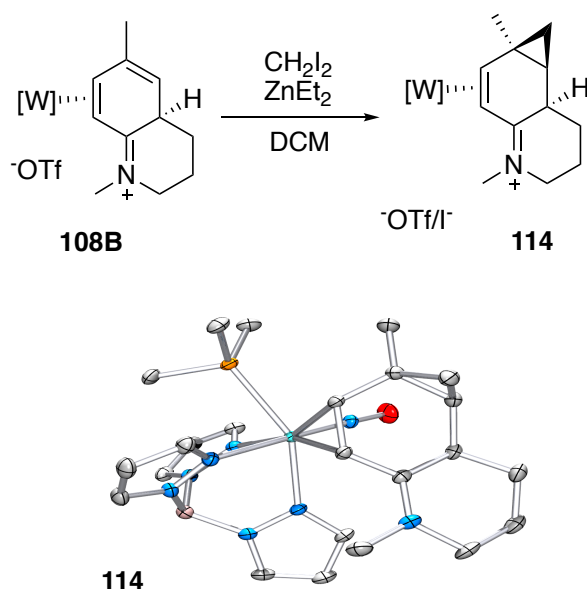


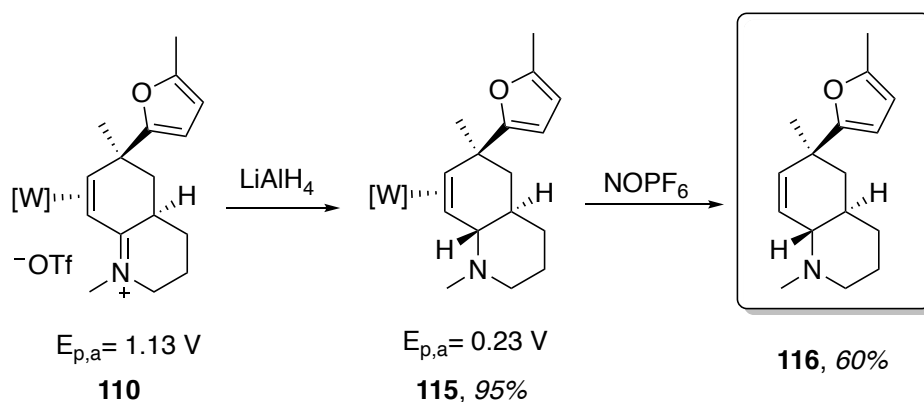
Figure 6.3: Crystal structure of complex **114**

6.2.3 Reduction of Iminium and Isolation of Octahydroquinoline Organics

In order to ultimately isolate the functionalized saturated quinoline organics from the reactions demonstrated in this chapter, the metal must first be oxidized with a one-electron oxidant. The reduction in electron density of the oxidized tungsten system reduces

its ability to back-donate into the π -system of the ligand, which weakens the η^2 -bond and allows the organic to fall off. In the case of the parent η^2 -*N,N*-dimethylanilinium complex, the functionalized complexes could be oxidized with ceric ammonium nitrate (CAN), which was a sufficiently strong oxidant to yield the free organics. Hydrolysis of the iminium system during the aqueous work-up yielded the α,β -unsaturated ketone form of the organics.⁹ Previous work with the η^2 -*N*-ethylindolinium system employed a reduction of the iminium prior to oxidation to enable the formation of an additional stereocenter, and also allow the use of weaker oxidants to yield the free hexahydroindole organics.⁶

Scheme 6.9: Iminium reduction and octahydroquinoline organic isolation



The stereoselective reduction of the quinoline iminium was attempted with **110** using LAH as the hydride source. The use of weaker hydride sources such as NaBH_4 and NaCNBH_3 , which would be expected to reduce typical organic iminiums, were unreactive with this conjugated iminium system. However, when **110** was stirred in dry DME with 4 equivalents of LAH a color change from yellow to almost clear was observed. After 10 minutes the reaction was checked with ^{31}P NMR, revealing a single product with a ^{183}W - ^{31}P coupling constant of 266 Hz (**110**: $J_{\text{WP}} = 283 \text{ Hz}$). The reaction was then quenched with H_2O ,

and after a basic work-up with saturated aqueous Na_2CO_3 , **115** was isolated in a 95% yield (Scheme 6.9). The stereoselective addition of the hydride anti to the metal was supported by a NOE correlation between the nitrogen methyl group and a proton on the pyrazole ring of the Tp ligand trans to the PMe_3 .^{5,6} Furthermore, the absence of an NOE interaction between the new bridgehead proton at 3.76 ppm and the adjacent bridgehead proton syn to the metal support the formation of a trans-fused bicyclic system. Further data also supported the reduction of the iminium, including the absence of an iminium stretch in the IR spectrum. Additionally, a CV of **115** reflected the loss of the conjugated iminium system with a decrease in the reduction potential by 0.90 V (Scheme 6.9).

The dramatic shift in reduction potential upon reduction of the iminium π -system allows for more mild oxidative conditions to recover the free organic.⁶ Previously, we found with the η^2 -*N*-ethylindolinium system that NOPF_6 gave a relatively clean oxidation reaction, leaving the hexahydroindole core intact. Similarly, when **115** was treated with NOPF_6 , the free organic was observed by ^1H NMR with characteristic free alkene peaks ~ 5.5 - 6.0 ppm. After an aqueous basic work-up, much of the metal decomposition can be separated from the organic by a precipitation from Et_2O . The organic left in the filtrate is purified through chromatography using basic alumina preparatory plates. Staining the preparatory plate with KMnO_4 enables the identification of the desired organic band. After sonication in HPLC EtOAc , **116** was isolated in a 60% yield (Scheme 6.9). This octahydroquinoline organic, along with other novel small molecules synthesized in our lab, are subsequently submitted to the open innovation program at Eli Lilly to be tested for biological activity.

6.3 Conclusions

Although amino-substituted arenes (e.g. aniline) were able to be η^2 -coordinated to the pentaammineosmium system¹⁵, incompatibility between the π -basic {TpW(NO)(PMe₃)} fragment and the electron rich arene prevented the isolation of a stable η^2 -complex with the tungsten dearomatization agent. Fortunately, in-situ protonation with a relatively weak Brønsted acid (DiPAT) enabled the isolation of a stable η^2 -anilinium complex.⁷ This acid trapping procedure has been successfully applied with other nitrogen containing aromatics in order to access more complex η^2 -coordinated nitrogen heterocycles, such as indoline and tetrahydroquinoline derivatives.⁵ Coordination and functionalization of these nitrogen heterocycles provides a valuable synthetic tool to rapidly build up structural complexity from these core structures, which are common in biologically active compounds including natural products.^{1,3,4,16} The reaction pathways accessible upon dearomatization of these heteroaromatics allow the synthesis of novel small molecules with increased saturation, which has been shown to be an important factor for the success of small molecule drug candidates.¹⁷

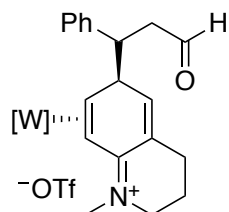
The dihapto-coordination of *N*-methyltetrahydroquinoline to the tungsten dearomatization agent in the presence of a weak acid predominantly resulted in the para protonated product (**106A**). Treating this complex with base in the presence of a carbon electrophile, specifically Michael acceptors, resulted in a stereoselective addition of the electrophile at the para position. In contrast, acid trapping of a paramethyl-substituted quinoline derivative (*N*,6-dimethyltetrahydroquinoline) enabled the isolation of the ortho protonated product **108B**, which was able to undergo tandem electrophilic/nucleophilic addition reactions at the uncoordinated double bond with high regio- and stereocontrol. As

typically seen with the tungsten system, the nucleophile selectively adds anti to the metal, and in this case, a quaternary carbon is formed due to the para methyl substituent. Subsequent reduction of the iminium and oxidation with a one-electron oxidant allowed for the isolation of a functionalized octahydroquinoline organic.

6.4 Experimental

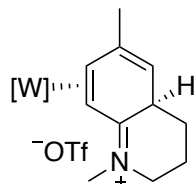
General Methods: NMR spectra were obtained on Varian 500, 600 MHz and Bruker 600, 800 MHz spectrometers. Chemical shifts are referenced to tetramethylsilane (TMS) utilizing residual ^1H signals of the deuterated solvents as internal standards. Chemical shifts are reported in ppm and coupling constants (J) are reported in hertz (Hz). Phosphorus NMR signals are referenced to 85% H_3PO_4 ($\delta = 0.00$) using a triphenylphosphate external standard ($\delta = -16.58$). Infrared Spectra (IR) were recorded on a spectrometer as a glaze on a diamond anvil ATR assembly, with peaks reported in cm^{-1} . Electrochemical experiments were performed under a nitrogen atmosphere using a BAS Epsilon EC-2000 potentiostat. Cyclic voltammetric data were recorded at ambient temperature at 100 mV/s, unless otherwise noted, with a standard three electrode cell from +1.8 V to -1.8 V with a glassy carbon working electrode, *N,N*-dimethylacetamide (DMA) solvent, and tetrabutylammonium hexafluorophosphate (TBAH) electrolyte (~0.5 M). All potentials are reported versus the normal hydrogen electrode (NHE) using cobalticinium hexafluorophosphate ($E_{1/2} = -0.78$ V, -1.75 V) or ferrocene ($E_{1/2} = 0.55$ V) as an internal standard. Peak separation of all reversible couples was less than 100 mV. Unless otherwise noted, all synthetic reactions were performed in a glovebox under a dry nitrogen atmosphere. All solvents were purged with nitrogen prior to use. Deuterated solvents were used as received from Cambridge Isotopes. Triflate salts of amines were prepared by combining a triflic acid/ether solution with a solution of ether and the corresponding amine. *N*-methyl-1,2,3,4-tetrahydroquinoline and *N*,6-dimethyl-1,2,3,4-tetrahydroquinoline organics were synthesized based off modified procedures from a previously reported method.¹⁸ **106** was synthesized using a previously reported method.⁵

Complex Characterization



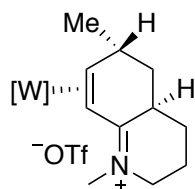
Compound 107. 106 (100 mg, 0.125 mmol) was dissolved in MeOH (2 mL) in a 4-dram vial. To this solution Et₃N (19 mg, 0.19 mmol) was added, followed immediately by *trans*-cinnamaldehyde (142 mg, 1.07 mmol). The resulting yellow homogenous solution was stirred for 6 h then removed from the glove box and concentrated *in vacuo*. The resulting yellow oil was redissolved in DCM (20 mL) and washed with H₂O (3 x 20 mL). The organic layer was dried over anhydrous MgSO₄, and concentrated *in vacuo*. The resulting yellow oil was redissolved in minimal DCM and precipitated from stirring Et₂O (100 mL). The bright yellow solid was collected on a 15 mL fine porosity fritted funnel and washed with hexanes (2 x 15 mL), yielding **107** (95 mg, 0.10 mmol, 80% yield). CV (DMA): E_{p,a} = +1.07 V. IR: $\nu(\text{BH}) = 2492 \text{ cm}^{-1}$, $\nu(\text{CO}) = 1720$, $\nu(\text{NO})$ and $\nu(\text{iminium}) = 1593 \text{ cm}^{-1}$ and 1574 cm^{-1} . ³¹P NMR (MeOH, δ): -8.94 ($J_{\text{WP}} = 282$). ¹H NMR (CD₃CN, δ): 9.74 (s, 1H, H3') 7.95 (d, 2H, PzB3, & PzC5), 7.87 (d, 1H, PzB5), 7.82 (d, 1H, PzA5), 7.74 (d, 1H, PzC3), 7.36 (m, 2H, H2''), 7.25 (t, $J = 7.0$, 2H, H3''), 7.20 (m, 1H, H4''), 7.18 (d, 1H, PzA3), 6.46 (t, 1H, PzC4), 6.38 (bd, $J = 6.0$, 1H, H5), 6.37 (t, 1H, PzB4), 6.28 (t, 1H, PzA4), 3.81 (m, 1H, H1'), 3.73 (bs, 1H, H6), 3.64 (m, 1H, H2x), 3.37 (dd, $J = 8.9, 13$, 1H, H7), 3.23 (m, 1H, H2y), 3.21 (dd, $J = 18.0, 7.3$, 1H, H2'x), 3.01 (ddd, $J = 18.0, 7.6, 1.6$, 1H, H2'y), 2.56 (dt, $J = 14.8, 4.7$, 1H, H4x), 2.47 (m, 1H, H4y), 1.97 (m, 1H, H3x), 1.93 (s, 3H, NMe), 1.90 (m, 1H, H3y), 1.65 (d, $J = 8.9$, 1H, H8), 1.18 (d, $J = 9.0$, 9H, PMe₃). ¹³C NMR (CD₃CN, δ): 202.9 (C3'), 174.5 (C8a), 145.0 (PzB3), 144.4 (PzA3), 142.1

(PzC3), 140.4 (C4a/C1''), 138.6 (3C, Pz5/C5), 137.8 (C5/Pz5), 131.0 (2C, C3''), 129.5 (C1''/C4a), 128.2 (2C, C2''), 127.7 (C4''), 108.1 (PzB4), 108.0 (PzC4), 107.6 (PzA4), 65.2 (d, $J = 13.2$, C7), 54.2 (C8), 53.6 (C2), 50.5 (C1'), 47.1 (C6), 46.3 (C2'), 39.9 (NMe), 26.8 (C4), 22.5 (C3), 12.9 (d, $J = 30.0$, PMe₃).



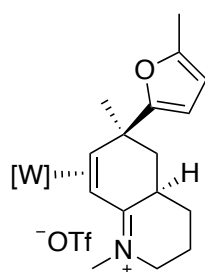
Compound 108B. 1 (1.00 g, 1.72 mmol) was combined with DiPAT (519 mg, 2.07 mmol) in a 4-dram vial charged with a stir pea. To this heterogeneous mixture was added a solution of hexanes (15 mL) and *N*,6-dimethyl-1,2,3,4-tetrahydroquinoline (2.22 g, 13.8 mmol). The pale-brown heterogeneous reaction mixture was stirred for 72 h. The reaction mixture was filtered through a 30 mL medium porosity fritted funnel, yielding a dark-yellow solid. The solid was removed from the frit and triturated with DME (0.8 mL) for 5 min. This bright-yellow solid was collected on a 15 mL medium porosity fritted funnel, washed with DME (1 x 1 mL), Et₂O (2 x 5 mL), and hexanes (2 x 10 mL), yielding **108B** (532 mg, 0.653 mmol, 40%). CV (DMA): $E_{p,a} = +1.03$ V. IR: $\nu(\text{BH}) = 2507$ cm⁻¹, $\nu(\text{NO})$ and $\nu(\text{iminium}) = 1601$ cm⁻¹ and 1577 cm⁻¹. ³¹P NMR (CDCl₃, δ): -10.07 ($J_{\text{WP}} = 286$). ¹H NMR (CD₃CN, δ): 8.06 (d, 1H, PzB3), 7.99 (d, 1H, PzC5), 7.93 (d, 1H, PzB5), 7.89 (d, 1H, PzA5), 7.69 (d, 1H, PzC3), 7.22 (d, 1H, PzA3), 6.46 (t, 1H, PzC4), 6.42 (t, 1H, PzB4), 6.36 (t, 1H, PzA4), 4.55 (bs, 1H, H5), 3.92 (m, 1H, H7), 3.69 (m, 2H, H2), 3.28 (bs, 1H, H4a), 2.27 (d, $J = 8.2$, 1H, H8), 2.17 (m, 1H, H3x), 2.14 (s, 3H, NMe), 2.10 (m, 1H, H4x), 2.06 (m, 1H, H3y), 1.92 (bs, 3H, 6Me), 1.60 (m, 1H, H4y), 1.24 (d, $J = 9.1$, 9H, PMe₃). ¹³C NMR (CD₃CN, δ): 185.9 (C8a), 145.5 (PzB3), 142.3

(PzC3), 141.4 (PzA3), 139.0 (2C, Pz5), 138.8 (Pz5), 137.8 (C6), 114.4 (C5), 108.4 (Pz4), 108.2 (Pz4), 107.8 (Pz4), 69.0 (d, $J = 11.8$, C7), 57.5 (C8), 55.0 (C2), 40.7 (NMe), 38.3 (C4a), 26.5 (C4), 24.5 (C6-Me), 22.7 (C3), 14.3 (d, $J = 31.0$, PMe₃).



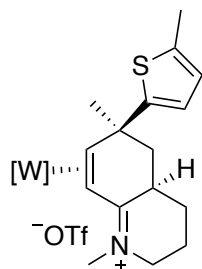
Compound 109. To a 4-dram vial were added **108B** (101 mg, 0.124 mmol) followed by acetonitrile (1.5 mL). A 1M solution of HOTf in acetonitrile (0.26 mL, 0.26 mmol) was then added, resulting in a homogeneous red solution, which was allowed to cool for 20 min at -30°C. The reaction solution was then added to a 4-dram vial containing NaCNBH₃ (62 mg, 0.99 mmol). After 3.5 h, the reaction solution was removed from the glove box, diluted with saturated aqueous Na₂CO₃ (2 mL), and extracted with DCM (1 x 40 mL, 2 x 20 mL). The combined organic layers were washed with H₂O (10 mL), dried over anhydrous MgSO₄, and concentrated *in vacuo*. The resulting yellow film was redissolved in minimal DCM and precipitated into stirring Et₂O (25 mL). This bright-yellow solid was collected on a 15 mL fine porosity fritted disc, washed with Et₂O (2 mL) and hexanes (5 mL), yielding **109** (39 mg, 0.048 mmol, 39% yield). CV (DMA): E_{p,a} = +1.10 V. IR: $\nu(\text{BH}) = 2505 \text{ cm}^{-1}$, $\nu(\text{NO})$ and $\nu(\text{iminium}) = 1592 \text{ cm}^{-1}$ and 1573 cm^{-1} . ³¹P NMR (CD₃CN, δ): -10.01 ($J_{\text{WP}} = 285$). ¹H NMR (CD₃CN, δ): 8.07 (d, 1H, PzB3), 7.98 (d, 1H, PzC5), 7.92 (d, 1H, PzB5), 7.90 (d, 1H, PzA5), 7.63 (d, 1H, PzC3), 7.17 (d, 1H, PzA3), 6.45 (t, 1H, PzC4), 6.43 (t, 1H, PzB4), 6.39 (t, 1H, PzA4), 3.90 (m, 1H, H7), 3.67 (m, 1H, H6), 3.61 (m, 2H, H2), 2.75 (m, 1H, H4a), 2.14 (d, $J =$

9.4, 1H, H8), 2.05 (s, 3H, NMe), 2.02 (m, 1H, H3x), 2.01 (buried, 1H, H4x), 1.89 (m, 1H, H3y), 1.79 (m, 2H, H5), 1.37 (m, 1H, H4y), 1.28 (d, $J = 7.2$, 3H, C6-Me), 1.15 (d, $J = 8.8$, 9H, PMe₃).
¹³C NMR (CD₃CN, δ): 188.0 (C8a), 144.7 (PzB3), 143.5 (PzA3), 141.7 (PzC3), 139.1 (Pz5), 139.0 (Pz5), 138.8 (Pz5), 108.5 (Pz4), 108.4 (Pz4), 108.1 (Pz4), 72.6 (d, $J = 13.2$, C7), 57.5 (C8), 54.5 (C2), 43.1 (C5), 40.3 (NMe), 33.6 (C4a), 31.7 (C6), 26.6 (C4), 25.4 (C6-Me), 22.4 (C3), 14.3 (d, $J = 30.8$, PMe₃).



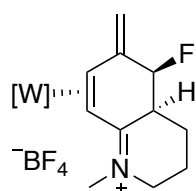
Compound 110. A 0.25M solution of HOTf/MeCN (5 mL, 1.25 mmol) was added to **108B** (200 mg, 0.245 mmol), resulting in a light orange homogenous solution. After 1 h, 2-methylfuran (376 mg, 4.57 mmol) was added, and the light yellow solution was stirred for 3 h. The reaction solution was then removed from the glove box, diluted with DCM (20 mL) and washed with saturated aqueous Na₂CO₃ (2 x 20 mL). The combined aqueous layer was back extracted with DCM (2 x 10 mL), and then the combined organic layer was washed with H₂O (30 mL) and brine (30 mL). The organic layer was then dried over MgSO₄ and concentrated *in vacuo*. The resulting yellow oil was redissolved in minimal DCM and added to stirring Et₂O (200 mL). The light-tan precipitate was collected on a 15 mL fine porosity fritted disc and washed with Et₂O (15 mL), yielding **110** (184 mg, 0.205 mmol, 84% yield).
¹H NMR (CD₃CN, δ): 8.09 (d, 1H, PzB3), 7.99 (d, 1H, Pz5), 7.93 (d, 1H, Pz5), 7.92 (d, 1H, Pz5), 7.58 (d, 1H, PzC3), 7.17 (d, 1H, PzA3), 6.44 (m, 2H, PzB4 & PzC4), 6.40 (t, 1H, PzA4),

6.17 (d, $J = 3.1$, 1H, H3'), 5.96 (m, 1H, H4'), 3.82 (dd, $J = 13.4, 9.8$, 1H, H7), 3.62 (m, 2H, H2), 2.85 (m, 1H, H4a), 2.30 (buried, 1H, H8), 2.29 (s, 3H, 5'-Me), 2.09 (s, 3H, N-Me), 2.03 (buried, 1H, H5x), 1.99 (buried, 1H, H3x), 1.98 (m, 1H, H5y), 1.97 (m, 1H, H4x), 1.89 (m, 1H, H3y), 1.66 (s, 3H, 6-Me), 1.24 (m, 1H, H4y), 1.08 (d, $J = 8.9$, 9H, PMe₃). ¹³C NMR (CD₃CN, δ): 187.6 (C8a), 165.3 (C2'), 151.8 (C5'), 144.8 (PzB3), 143.7 (PzA3), 142.1 (PzC3), 139.4 (Pz5), 139.2 (Pz5), 139.1 (Pz5), 108.8 (Pz4), 108.6 (Pz4), 108.3 (Pz4), 106.9 (C4'), 106.1 (C3'), 75.9 (d, $J = 13.4$, C7), 57.7 (C8), 54.6 (C2), 47.8 (C5), 41.6 (C6), 40.5 (N-Me), 34.0 (C4a), 29.8 (6-Me), 26.8 (C4), 22.5 (C3), 14.8 (d, $J = 31.0$, PMe₃), 13.8 (5'-Me). ³¹P NMR (CDCl₃, δ): -10.31 ($J_{WP} = 283$). CV (DMAc) $E_{p,a} = +1.17$ V (NHE). IR: $\nu(\text{BH}) = 2506$ cm⁻¹, $\nu(\text{NO})$ and $\nu(\text{iminium}) = 1593$ cm⁻¹ and 1573 cm⁻¹.



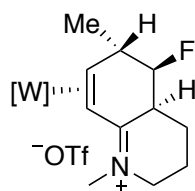
Compound 111. To a 4-dram vial were added **108B** (49 mg, 0.060 mmol) a 0.25M HOTf/MeCN solution (1 mL, 0.25 mmol), resulting in a dark red homogenous solution. The reaction was monitored by ³¹P NMR. After 21 h, 2-methylthiophene (51 mg, 0.52 mmol) was added to the reaction solution. After 4 d more 2-methylthiophene (41 mg, 0.50 mmol) was added. A week after the reaction started, excess 2-methylthiophene was added and allowed to react overnight. The reaction solution was then removed from the glove box, diluted with DCM (20 mL), and washed with saturated aqueous Na₂CO₃ (2 x 20 mL). The combined aqueous layers were back extracted with DCM (40 mL). The combined organic

layers were washed with H₂O (50 mL), dried over MgSO₄ and concentrated *in vacuo*. The resulting yellow oil was redissolved in minimal DCM and precipitated from stirring Et₂O (30 mL). The pale tan solid was collected on a 15 mL medium porosity fritted disc, yielding **111** (20 mg, 0.022 mmol, 37% yield). CV (DMA): E_{p,a} = +1.13 V. IR: $\nu(\text{BH}) = 2515 \text{ cm}^{-1}$, $\nu(\text{NO})$ and $\nu(\text{iminium}) = 1597 \text{ cm}^{-1}$ and 1581 cm^{-1} . ³¹P NMR (CDCl₃, δ): -8.91 ($J_{\text{WP}} = 282$). ¹H NMR (CD₃CN, δ): 8.08 (d, 1H, PzB3), 8.00 (d, 1H, PzC5), 7.93 (m, 2H, PzB5, PzA5), 7.55 (d, 1H, PzC3), 7.17 (d, 1H, PzA3), 6.92 (d, $J = 3.5$, 1H, H3'), 6.66 (m, 1H, H4'), 6.46 (t, 1H, PzC4), 6.44 (t, 1H, PzB4), 6.41 (t, 1H, PzA4), 3.92 (dd, $J = 13.8, 9.7$, 1H, H7), 3.63 (m, 2H, H2), 2.87 (m, 1H, H4a), 2.47 (d, $J = 1.2$, 3H, 5'Me), 2.38 (d, $J = 9.7$, 1H, H8), 2.13 (s, 3H, NMe), 2.10 (dd, $J = 13.6, 4.3$, 1H, H5x), 2.00 (m, 1H, H3x), 1.98 (m, 1H, H5y), 1.96 (m, 1H, H4x), 1.89 (m, 1H, H3y), 1.79 (s, 3H, 6Me), 1.25 (m, 1H, H4y), 1.06 (d, $J = 8.8$, 9H, PMe₃). ¹³C NMR (CD₃CN, δ): 186.6 (C8a), 160.5 (C2'/C5'), 144.7 (PzB3), 143.5 (PzA3), 141.7 (PzC3), 139.0 (4C, PzA5, PzB5, PzC5, C2'/C5'), 125.6 (C4'), 124.0 (C3'), 108.6 (Pz4), 108.5 (Pz4), 108.2 (Pz4), 79.2 (d, $J = 13.2$, C7), 57.0 (C8), 54.5 (C2), 53.8 (C5), 43.1 (C6), 40.4 (NMe), 34.3 (C4a), 31.6 (C6Me) 26.3 (C4), 22.3 (C3), 15.3 (C5'Me), 14.6 (d, $J = 30.8$, PMe₃).



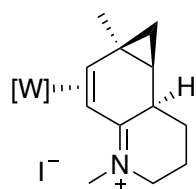
Compound 112. Selectfluor® (39 mg, 0.12 mmol) and acetonitrile (3.3 mL) were added to a 4-dram vial charged with a stir pea and stirred. **108B** (100 mg, 0.123 mmol) was dissolved in MeOH (3.3 mL), and this solution was added to the Selectfluor® with stirring.

The golden homogeneous solution was stirred for 5 d, then removed from the glove box, diluted with saturated aqueous Na₂CO₃ (30 mL), and extracted with DCM (2 x 30 mL). The combined organic layer was washed with H₂O (20 mL), then dried over MgSO₄ and evaporated *in vacuo* to dryness. The film was redissolved in minimal DCM and precipitated into stirring Et₂O (20 mL). The pale yellow solid was collected on a 15 mL fine porosity fritted disc, washed with Et₂O (2 x 5 mL) and pentane (5 mL), then desiccated overnight, yielding **112** (64 mg, 0.083 mmol, 67% yield). ¹H NMR (CD₃CN, δ): 8.06 (d, 1H, PzB3), 8.00 (d, 1H, PzC5), 7.93 (d, 1H, PzB5), 7.91 (d, 1H, PzA5), 7.70 (d, 1H, PzC3), 7.14 (d, 1H, PzA3), 6.47 (t, 1H, PzC4), 6.43 (t, 1H, PzB4), 6.40 (t, 1H, PzA4), 5.17 (dd, *J* = 4.1, 1.2, 1H, C6'-H), 5.14 (dd, *J* = 6.5, 1.2, 1H, C6'-H), 5.07 (dd, *J* = 49.9, 2.9, 1H, H5), 4.31 (m, 1H, H7), 3.74 (m, 1H, H2x), 3.67 (m, 1H, H2y), 3.18 (dm, *J* = 32.1, 1H, H4a), 2.36 (d, *J* = 8.5, 1H, H8), 2.13 (s, 3H, NMe), 2.12 (buried, 2H, H3x & H4x), 2.03 (m, 1H, H3y), 1.84 (m, 1H, H4y), 1.25 (d, *J* = 9.1, 9H, PMe₃). ¹³C NMR (CD₃CN, δ): 182.5 (C8a), 145.6 (PzB3), 145.1 (C6), 143.2 (PzA3), 142.4 (PzC3), 139.3 (Pz5), 139.2 (Pz5), 139.0 (Pz5), 115.5 (d, *J* = 12.5, C6'), 108.6 (Pz4), 108.4 (Pz4), 108.1 (Pz4), 97.2 (d, *J* = 171.4, C5), 61.9 (d, *J* = 12.3, C7), 55.9 (C8), 54.8 (C2), 40.8 (NMe), 40.4 (d, *J* = 22.5, C4a), 22.0 (C3), 21.4 (d, *J* = 5.4, C4), 13.9 (d, *J* = 31.1, PMe₃).



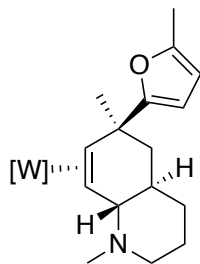
Compound 113. **112** (22 mg, 0.029 mmol) was dissolved in CD₃CN (0.7 mL), added to an NMR tube and cooled to -30°C. NaCNBH₃ (14 mg, 0.22 mmol) was weighed out in a 4-dram

vial. A 1M solution of HOTf/MeCN (0.06 mL, 0.06 mmol, -30°C) was added the NMR tube, and the NMR tube was shaken. This reaction solution was then added to the vial with NaCNBH₃, and the reaction was allowed to sit at -30°C for 1 d. The reaction was then removed from the glove box, diluted with DCM (20 mL), and washed with saturated aqueous Na₂CO₃ (2 x 20 mL). The combined aqueous layer was back-extracted with DCM (20 mL). The combined organic layer was washed with H₂O (20 mL), then dried over MgSO₄ and evaporated *in vacuo* to dryness. The resulting film was redissolved in minimal DCM and added to stirring Et₂O (15 mL); however, no precipitation occurred. The cloudy Et₂O solution was evaporated *in vacuo* to dryness, then redissolved in minimal DCM and added to stirring pentane (15 mL). This resulted in some precipitation of solid, which clumped on the sides of the flask. The liquid was decanted off and the residual solid was desiccated overnight, yielding **113**. ³¹P NMR (d⁶-acetone, δ): -9.83 (*J*_{WP} = 278). ¹H NMR (d⁶-acetone, δ): 8.23 (d, 1H, PzB3), 8.17 (d, 1H, PzC5), 8.09 (overlapping d, 2H, PzA5 & PzB5), 7.97 (d, 1H, PzC3), 7.32 (d, 1H, PzA3), 6.56 (t, 1H, PzC4), 6.53 (t, 1H, PzB4), 6.51 (t, 1H, PzA4), 4.74 (d, *J* = 48.6, 1H, H5), 3.92 (dt, *J* = 14.0, 9.1, 1H, H7), 3.86 (m, 2H, H2), 3.81 (dm, *J* = 24.6, 1H, H6), 3.10 (ddd, *J* = 33.9, 11.0, 6.6, 1H, H4a), 2.47 (d, *J* = 9.4, 1H, H8), 2.27 (s, 3H, NMe), 2.24 (m, 1H, H3x), 2.18 (m, 1H, H4x), 2.04 (buried, 1H, H3y), 1.86 (m, 1H, H4y), 1.34 (dd, *J* = 7.6, 0.8, 3H, C6-Me), 1.29 (d, *J* = 8.8, 9H, PMe₃). ¹³C NMR (d⁶-acetone, δ): 182.9 (C8a), 145.1 (PzB3), 143.5 (PzA3), 141.8 (PzC3), 139.3 (Pz5), 139.1 (Pz5), 138.9 (Pz5), 108.6 (Pz4), 108.5 (Pz4), 108.2 (Pz4), 102.2 (d, *J* = 175.5, C5), 67.2 (d, *J* = 14.3, C7), 57.4 (C8), 54.7 (C2), 40.5 (NMe), 38.2 (d, *J* = 20.1, C6), 37.9 (d, *J* = 20.6, C4a), 22.6 (C4), 22.2 (C3), 21.9 (d, *J* = 13.9, C6-Me), 14.1 (d, *J* = 30.8, PMe₃).



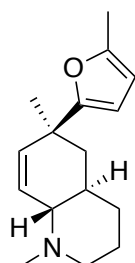
Compound 114. CH_2I_2 (373 mg, 1.39 mmol) and DCM (2.5 mL) were added to a flame-dried 25 mL round-bottom flask charged with a stir bar and stirred. A solution of ZnEt_2 (61 mg, 0.49 mmol) in DCM (3.7 mL) was added drop-wise to the $\text{CH}_2\text{I}_2/\text{DCM}$ solution, creating a milky white solution. A solution of **108B** (51 mg, 0.063 mmol) in DCM (1.2 mL) was added to the reaction solution and stirred for 2 d. The reaction mixture was removed from the glove box and diluted with DCM (20 mL). This was treated with saturated aqueous NH_4Cl (2×20 mL). The aqueous layer was back-extracted with DCM (2×20 mL), and then the combined organic layer was washed with H_2O (40 mL). The organic layer was dried over MgSO_4 and evaporated *in vacuo* to dryness. The resulting film was redissolved in minimal DCM and precipitated into stirring Et_2O (40 mL). The pale yellow solid was collected on a 15 mL fine porosity fritted disc, washed with Et_2O (5 mL), and desiccated overnight, yielding **114** (30 mg, 0.037 mmol, 59% yield). CV (DMAc) $E_{p,a} = +1.11$ V (NHE). IR: $\nu(\text{BH}) = 2509$ cm^{-1} , $\nu(\text{NO})$ and $\nu(\text{iminium}) = 1589$ cm^{-1} and 1571 cm^{-1} . ^{31}P NMR (CD_3CN , δ): -10.32 ($J_{\text{WP}} = 286$). ^1H NMR (CD_3CN , δ): 8.09 (d, 1H, PzB3), 7.96 (d, 1H, PzC5), 7.95 (d, 1H, PzB5), 7.88 (d, 1H, PzA5), 7.57 (d, 1H, PzC3), 7.20 (d, 1H, PzA3), 6.46 (t, 1H, PzB4), 6.44 (t, 1H, PzC4), 6.38 (t, 1H, PzA4), 4.24 (dd, $J = 13.3, 9.2$, 1H, H7), 3.63 (m, 1H, H2x), 3.57 (dd, $J = 14.7, 6.8$, 1H, H2y), 3.02 (m, 1H, H4a), 2.13 (m, 1H, H3x), 2.08 (m, 1H, H3y), 2.03 (d, $J = 9.1$, 1H, H8), 2.00 (buried, 1H, H4x), 1.91 (s, 3H, N-Me), 1.61 (q of m, $J = 13.2$, 1H, H4y), 1.36 (s, 3H, C6-Me), 1.10 (d, $J = 8.4$, 9H, PMe_3) 1.07 (buried, 1H, H5), 0.76 (dd, $J = 8.5, 4.0$, 1H, H9x), 0.31 (broad t, $J = 4.7$, 1H, H9y). ^{13}C NMR (CD_3CN , δ): 185.5 (C8a), 145.0 (PzB3), 142.6

(PzA3), 141.9 (PzC3), 139.1 (Pz5), 139.1 (Pz5), 138.6 (Pz5), 108.7 (Pz4), 108.4 (Pz4), 107.7 (Pz4), 75.2 (d, $J = 12.8$, C7), 58.6 (C8), 54.8 (C2), 40.0 (*N*-Me), 36.1 (C4a), 28.0 (C5) 27.7 (C6-Me), 26.1 (C4), 22.5 (C3), 22.5 (C9), 22.1 (C6) 13.9 (d, $J = 31.1$, PMe₃).



Compound 115. DME (35 mL) was added to a flame-dried 100 mL round-bottom flask charged with a stir bar. A solution of **110** (173 mg, 0.193 mmol) in DCM (3 mL) was added to the DME. The resulting solution was stirred vigorously as LiAlH₄ (31 mg, 0.82 mmol) was added, and then the mixture was stirred for 40 min. The reaction was quenched with H₂O until gas was no longer evolved, and then the solution was removed from the glove box and diluted with DCM (100 mL). This was treated with saturated aqueous Na₂CO₃ (2 x 50 mL). The combined aqueous layer was back-extracted with DCM (2 x 50 mL), and then the combined organic layer was washed with H₂O (50 mL) and brine (50 mL). The organic layer was dried over MgSO₄ and evaporated *in vacuo* to dryness. The resulting film was redissolved in minimal chloroform, then added to a tared 4-dram vial and evaporated *in vacuo* to dryness, yielding **115** (137 mg, 0.183 mmol, 95% yield). CV (DMAc) E_{p,a} = +0.23 V (NHE). IR: $\nu(\text{BH}) = 2479 \text{ cm}^{-1}$, $\nu(\text{NO}) = 1539 \text{ cm}^{-1}$. ³¹P NMR (d⁶-acetone, δ): -13.24 ($J_{\text{WP}} = 266$). ¹H NMR (d⁶-acetone, δ): 8.97 (d, 1H, PzA3), 8.12 (d, 1H, PzB3), 7.97 (d, 1H, PzC5), 7.91 (d, 1H, PzB5), 7.68 (d, 1H, PzA5), 7.44 (d, 1H, PzC3), 6.39 (t, 1H, PzB4), 6.36 (t, 1H,

PzC4), 6.13 (d, $J = 3.0$, 1H, H3'), 6.04 (t, 1H, PzA4), 5.89 (dq, $J = 3.0, 1.1$, 1H, H4'), 3.76 (d, $J = 8.6$, 1H, H8a), 3.56 (dd, $J = 16.0, 12.3$, 1H, H7), 2.66 (dm, $J = 10.8$, 1H, H2x), 2.30 (d, $J = 1.0$, 3H, C5'-Me), 2.07 (buried, 2H, H4a & H5x), 1.79 (ddd, $J = 12.4, 3.2, 1.3$, 1H, H8) 1.74 (buried, 1H, H2y), 1.70 (buried, 1H, H3x), 1.69 (buried, 1H, H4x), 1.65 (buried, 1H, H5y), 1.55 (buried, 1H, H3y), 1.55 (s, 3H, C6-Me), 1.42 (s, 3H, NMe), 1.24 (m, 1H, H4y), 0.98 (d, $J = 7.9$, 9H, PMe₃). ¹³C NMR (d⁶-acetone, δ): 169.0 (C2'), 150.2 (PzA3), 149.5 (C5'), 142.9 (PzB3), 141.0 (PzC3), 137.5 (PzC5), 136.8 (PzB5), 136.6 (PzA5), 107.3 (PzB4/PzC4), 107.2 (PzB4/PzC4), 106.5 (C4'), 104.6 (PzA4), 104.4 (C3'), 72.7 (C8a), 62.8 (d, $J = 11.7$, C7), 59.0 (C2), 58.5 (C8), 44.0 (C5), 42.9 (NMe), 42.3 (C6), 36.2 (C4a), 35.1 (C4), 34.8 (C6-Me), 27.4 (C3), 13.9 (C5'-Me), 13.8 (d, $J = 27.8$, PMe₃).



Compound 116. (Outside of glovebox) To a 4-dram vial charged with a stir pea was added NOPF₆ (41 mg, 0.23 mmol). In a separate 4-dram vial, **115** (112 mg, 0.150 mmol) was dissolved in acetone (4 mL) and added to the vial with NOPF₆ while stirring, resulting in an immediate color change from yellow to brown. The first vial was rinsed with acetone (1 mL), and this solution was added to the reaction vial. The reaction was stirred for 1.5 h then diluted with DCM (40 mL). This was treated with saturated aqueous Na₂CO₃ (2 x 40 mL). The combined aqueous layer was back-extracted with DCM (2 x 40 mL), and then the combined organic layer was washed with H₂O (40 mL) and brine (40 mL). The organic

layer was dried over MgSO_4 and concentrated *in vacuo* to an oil. The oil was redissolved in DCM (5 mL), and then this solution was added to stirring Et_2O (50 mL). The resulting precipitate was filtered over a 15 mL fine porosity fritted disc and discarded. The yellow filtrate was concentrated *in vacuo* to an oil. The oil was loaded onto a 250 μm basic alumina preparatory plate with DCM (3 x 0.3 mL) and eluted with 25% EtOAc /hexanes (HPLC grade, 200 mL). A KMnO_4 active band at R_f 0.099-0.362 was collected and sonicated in EtOAc (HPLC grade, 50 mL) for 15 min. The silica was filtered off on a 30 mL fine porosity fritted disc and washed with EtOAc (HPLC grade, 2 x 20 mL). The filtrate was evaporated *in vacuo* yielding **116** (22 mg, 0.090 mmol, 60% yield). ^1H NMR (d^6 -acetone, δ): 5.90 (d, J = 3.0, 1H, $\text{H}4'$), 5.87 (m, 2H, $\text{H}3'$ and $\text{H}8$), 5.58 (dt, J = 10.2, 2.1, 1H, $\text{H}7$), 2.86 (m, 1H, $\text{H}2\text{x}$), 2.25 (s, 3H, NMe), 2.21 (d, J = 1.0, 3H, $\text{C}2'\text{Me}$), 2.17 (dm, J = 8.9, 1H, $\text{H}8\text{a}$), 2.09 (td, J = 12.1, 3.0, 1H, $\text{H}2\text{y}$), 1.76 (t, J = 12.7, 1H, $\text{H}5\text{x}$), 1.68 (m, 2H, $\text{H}3\text{x}$ & $\text{H}4\text{a}$), 1.60 (m, 3H, $\text{H}3\text{y}$, $\text{H}4\text{x}$ & $\text{H}5\text{y}$), 1.32 (d, J = 0.6, 3H, $\text{C}6\text{-Me}$), 1.09 (qd, J = 12.1, 3.9, 1H, $\text{H}4\text{y}$). ^{13}C NMR (d^6 -acetone, δ): 161.3 ($\text{C}5'$), 151.0 ($\text{C}2'$), 135.0 ($\text{C}7$), 127.0 ($\text{C}8$), 106.6 ($\text{C}3'$), 104.3 ($\text{C}4'$), 68.3 ($\text{C}8\text{a}$), 58.7 ($\text{C}2$), 42.0 (NMe), 41.7 ($\text{C}5$), 38.9 ($\text{C}6$), 35.6 ($\text{C}4\text{a}$), 32.3 ($\text{C}4$), 26.8 ($\text{C}6\text{-Me}$), 25.8 ($\text{C}3$), 13.5 ($\text{C}2'\text{-Me}$).

6.5 References

- (1) Vitaku, E.; Smith, D. T.; Njardarson, J. T. *Journal of Medicinal Chemistry* **2014**, *57*, 10257.
- (2) Blakemore, D. C.; Castro, L.; Churcher, I.; Rees, D. C.; Thomas, A. W.; Wilson, D. M.; Wood, A. *Nature Chemistry* **2018**, *10*, 383.
- (3) Daly, J. W.; Ware, N.; Saporito, R. A.; Spande, T. F.; Garraffo, H. M. *Journal of Natural Products* **2009**, *72*, 1110.
- (4) Sridharan, V.; Suryavanshi, P. A.; Menéndez, J. C. *Chem. Rev.* **2011**, *111*, 7157.
- (5) MacLeod, B. L.; Pienkos, J. A.; Myers, J. T.; Sabat, M.; Myers, W. H.; Harman, W. D. *Organometallics* **2014**, *33*, 6286.
- (6) MacLeod, B. L.; Pienkos, J. A.; Wilson, K. B.; Sabat, M.; Myers, W. H.; Harman, W. D. *Organometallics* **2016**, *35*, 370.
- (7) Salomon, R. J.; Todd, M. A.; Sabat, M.; Myers, W. H.; Harman, W. D. *Organometallics* **2010**, *29*, 707.
- (8) Salomon, R. J.; Todd, M. A.; Sabat, M.; Myers, W. H.; Harman, W. D. *Organometallics* **2010**, *29*, 707.
- (9) Pienkos, J. A.; Zottig, V. E.; Iovan, D. A.; Li, M.; Harrison, D. P.; Sabat, M.; Salomon, R. J.; Strausberg, L.; Teran, V. A.; Myers, W. H.; Harman, W. D. *Organometallics* **2013**, *32*, 691.
- (10) Wilson, K. B.; Myers, J. T.; Nedzbala, H. S.; Combee, L. A.; Sabat, M.; Harman, W. D. *J. Am. Chem. Soc.* **2017**, *139*, 11401.
- (11) Smith, P. L.; Keane, J. M.; Shankman, S. E.; Chordia, M. D.; Harman, W. D. *J. Am. Chem. Soc.* **2004**, *126*, 15543.

- (12) Kolis, S. P.; Gonzalez, J.; Bright, L. M.; Harman, W. D. *Organometallics* **1996**, *15*, 245.
- (13) Wang, J.; Sánchez-Roselló, M.; Aceña, J. L.; del Pozo, C.; Sorochinsky, A. E.; Fustero, S.; Soloshonok, V. A.; Liu, H. *Chem. Rev.* **2014**, *114*, 2432.
- (14) Ilardi, E. A.; Vitaku, E.; Njardarson, J. T. *Journal of Medicinal Chemistry* **2014**, *57*, 2832.
- (15) Kolis, S. P.; Gonzalez, J.; Bright, L. M.; Harman, W. D. *Organometallics* **1996**, *15*, 245.
- (16) Mazurais, M.; Lescot, C.; Retailleau, P.; Dauban, P. *European Journal of Organic Chemistry* **2014**, *2014*, 66.
- (17) Lovering, F.; Bikker, J.; Humblet, C. *Journal of Medicinal Chemistry* **2009**, *52*, 6752.
- (18) Rauckman, B. S.; Tidwell, M. Y.; Johnson, J. V.; Roth, B. *Journal of Medicinal Chemistry* **1989**, *32*, 1927.

Chapter 7

The Development and Application of an Enantioenriched Tungsten Dearomatization Agent

7.1 Introduction

The dearomatization chemistry developed utilizing π -basic metal fragments has enabled the rapid transformation of planar aromatic compounds into more complex 3D molecules with multiple stereocenters. These novel transformations provide a valuable alternative to conventional synthetic methods; however, the ability to control the absolute stereochemistry of these reactions is critical for the utility of this synthetic methodology. The diverse range of dearomatization chemistry that was demonstrated with the initial achiral $\{\text{Os}(\text{NH}_3)_5\}^{2+}$ system was typically limited to racemic mixtures of organic products.¹ Although the η^2 -coordination of a prochiral aromatic ligand resulted in the formation of a chiral complex, the complex was formed as a racemic mixture.² Attempts to modify the ligand set to introduce chirality at the metal center were unsuccessful due to the inability of the modified system to coordinate aromatics in a dihapto-fashion.³ In one case, a chiral auxiliary was shown to enable enantioselective chemistry with dihapto-coordinated anisole complexes;² however, a universal method was sought with a chiral-at-metal system.

Investigations into alternatives to the osmium system led to the development of the $\{\text{TpRe}(\text{CO})(\text{L})\}$ (Tp = hydridotris(pyrazolyl)borate) system, where L can be a range of σ donor ligands, including ^tBuNC, pyridine, 1-methylimidazole (MeIm), NH_3 , or PMe_3 .⁴⁻⁷ Importantly, this ligand set established chirality at the metal center, and thus offered the potential to control absolute stereochemistry. The lack of stereocontrol in the synthetic step that establishes chirality at the metal center affords the complex as a racemic mixture.⁸ However, a method was established to separate the enantiomers of the metal utilizing a chiral tri-substituted alkene (*(R)*- α -pinene) starting from the racemic $\text{TpRe}(\text{CO})(\text{MeIm})(\eta^2\text{-benzene})$ complex.⁹

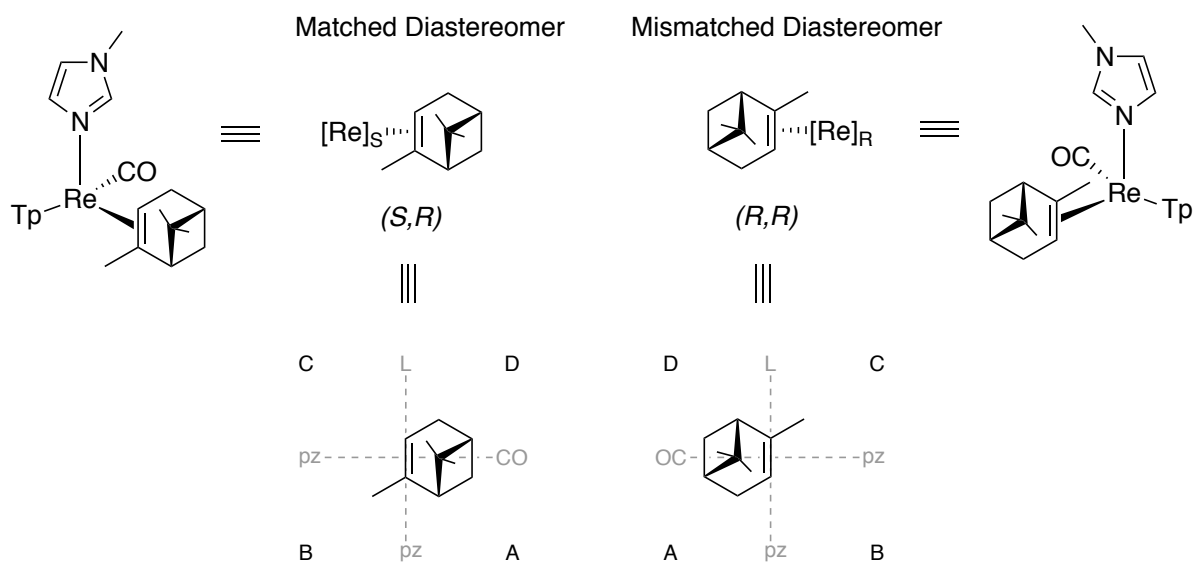
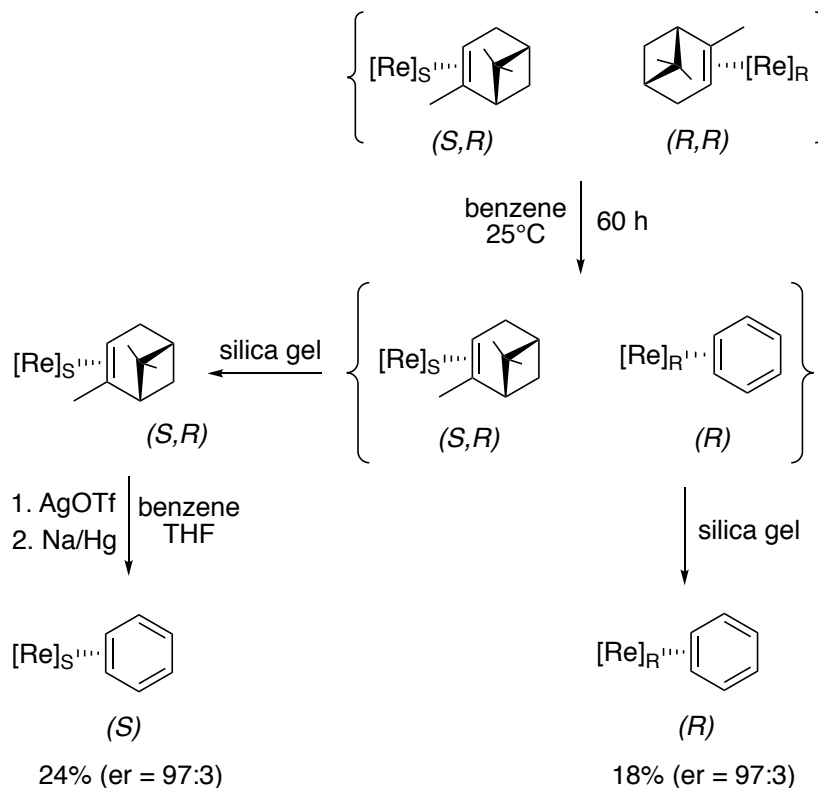


Figure 7.1: Matched and mismatched diastereomers of Re-*(R)*- α -pinene complex

Although at least 8 coordination orientations are theoretically possible for α -pinene, a ligand substitution reaction of $\text{TpRe}(\text{CO})(\text{MeIm})(\eta^2\text{-benzene})$ for *(R)*- α -pinene results in only two observed complexes (Figure 7.1). This chiral trisubstituted alkene has a single hindered face, which disfavors any complexes where the alkene is coordinated such that the bulky geminal dimethyl bridge is pointed towards the metal. Furthermore, a quadrant analysis of the rhenium system revealed that the C quadrant was the most sterically congested.¹⁰ Thus, the η^2 -complexes of *(R)*- α -pinene that placed the steric bulk of the ligand in the C quadrant were disfavored. In one of the observed complexes deemed the “matched” diastereomer, the *(R)*- α -pinene coordinates to the *S* enantiomer of the rhenium fragment such that no alkyl groups are placed in the sterically congested C quadrant (Figure 7.1). The other complex that is observed results from the coordination of *(R)*- α -pinene to the *R* enantiomer of the metal and places the methyl group in quadrant C, giving the “mismatched” diastereomer.

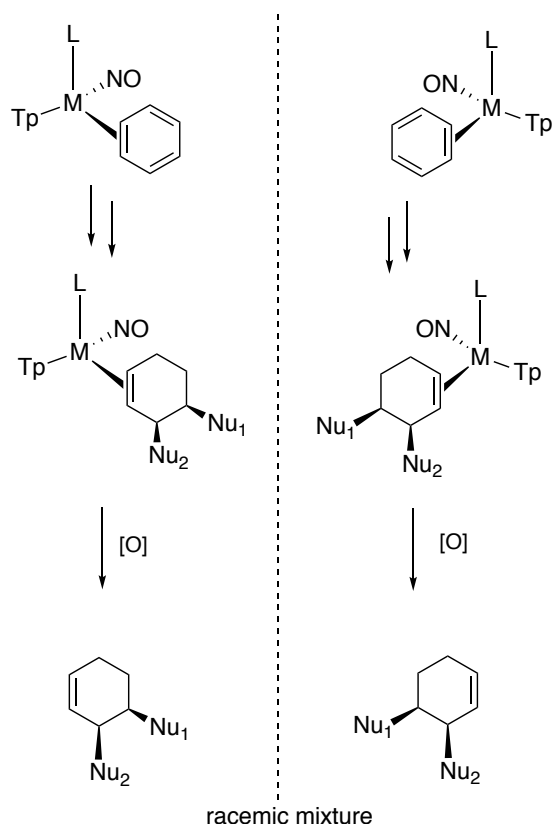
Scheme 7.1: Resolution of $\text{TpRe}(\text{CO})(\text{MeIm})(\eta^2\text{-benzene})$ 

The unfavorable steric interaction in the “mismatched” diastereomer destabilizes the complex relative to the “matched” diastereomer. This difference in stability is reflected in different substitution half-lives for the two diastereomers, with the alkene of the mismatched complex being more labile towards substitution. Thus, the two diastereomers can be stirred in benzene, with only the mismatched $\text{Re}(R,R)\text{-}\alpha$ -pinene undergoing ligand substitution with benzene, giving the enantioenriched $(R)\text{-TpRe}(\text{CO})(\text{MeIm})(\eta^2\text{-benzene})$ complex with an enantiomeric ratio (er) of 97:3 (Scheme 7.1).⁹ It is important to note in this substitution step, that the metal stereocenter does not epimerize, and the enantioenrichment is maintained through the substitution. The matched diastereomer,

once separated via chromatography, can be oxidized then reduced to access the enantioenriched (*S*)-TpRe(CO)(MeIm)(η^2 -benzene) complex with an er = 97:3.

Due to cost and difficulties with large-scale synthesis of the rhenium dearomatization agent, alternative metal systems were investigated, which resulted in the group six dearomatization agents {TpW(NO)(PMe₃)} and {TpMo(NO)(L)} (L = MeIm, 4-dimethylaminopyridine (4-DMAP)). The similar ligand sets of these systems also provide chiral-at-metal complexes that are synthesized in a racemic mixture. Subsequent transformations of the dihapto-coordinated aromatic ligand typically occur with a high degree of relative stereocontrol (reagents add selectively anti to the metal center), but due to the racemic metal system, a racemic mixture of the organic product results upon removal from the metal (Scheme 7.2).

Scheme 7.2: Synthesis of racemic organics with W(0) and Mo(0)



Methods for the enantioenrichment of both the tungsten and molybdenum complexes have been investigated^{11,12}. The α -pinene method for resolution was attempted with the molybdenum system, resulting in the formation of only a single “matched” complex with one enantiomer of the metal. Unfortunately, this method has been complicated due to the tendency of the second row transition metal to epimerize upon substitution of the α -pinene ligand for an aromatic ligand. This problem is circumvented by oxidation of the enantioenriched molybdenum complex, followed by a reduction with Na⁰ at 15°C in the presence of TFT, yielding enantioenriched TpMo(NO)(DMAP)(η^2 -PhCF₃).¹² This complex has been elaborated into a diene, and HPLC analysis of the free organic reflected an er = 99:1. Work is currently being done to generalize this enantioenrichment method to allow access to a wide range of η^2 -aromatic complexes. The focus of this chapter will be the enantioenrichment of the tungsten dearomatization agent and the application of this method to access enantioenriched organics.

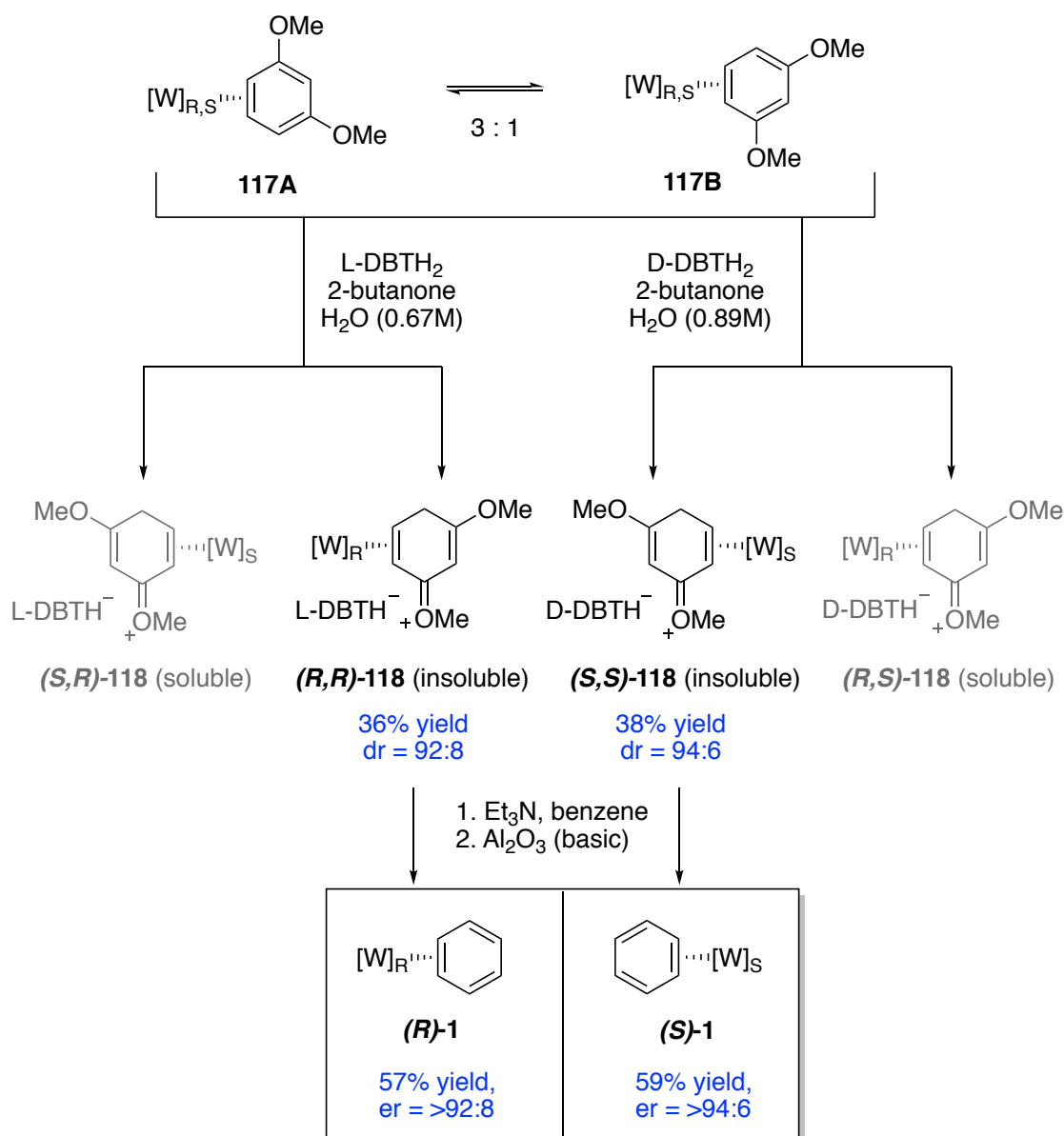
7.2 Results and Discussion

7.2.1 Enantioenrichment through Protonation with a Chiral Acid

In initial studies, the α -pinene method of enantioenrichment was investigated with the {TpW(NO)(PMe₃)} fragment and was used to access an enantioenriched pyridine derivative (er = 90:10).¹³ However, the increased π -back-donation of W(0) compared to Re(I) resulted in stronger coordination of the (*R*)- α -pinene ligand, resulting in low yields and difficulties accessing η^2 -aromatic complexes via substitution.¹³ An alternative method to separate the enantiomers of the metal was proposed, which utilized a chiral acid to protonate TpW(NO)(PMe₃)(η^2 -1,3-dimethoxybenzene). Stemming from this work, our

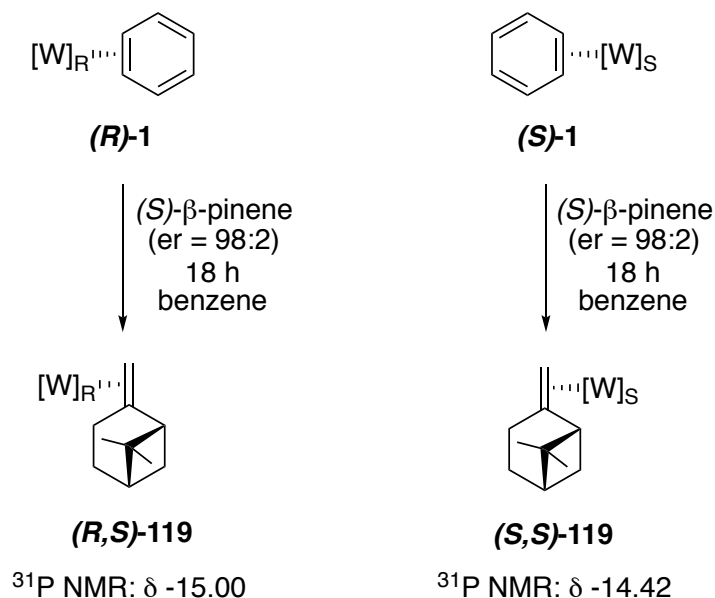
group recently reported a procedure to enantioenrich the $\{\text{TpW}(\text{NO})(\text{PMe}_3)\}$ fragment by exploiting disparate solubility of the diastereomeric salts that form upon protonation with L-dibenzoyl tartaric acid (L-DBTAH₂) (Scheme 7.3).¹¹

Scheme 7.3: Synthesis of enantioenriched tungsten benzene complex



Stirring **117** in wet 2-butanone, in the presence of L-DBTH₂ for 24-48 h enables the isolation of [W_R-η²-1,3-dimethoxybenzene][L-DBTH] with a diastereomeric ratio (dr) of 92:8 (Scheme 7.3).¹¹ The presence of H₂O in the 2-butanone solution was found to be crucial for the selective precipitation of the matched diastereomer (**(R,R)-118**), leaving the mismatched diastereomer (**(S,R)-118**) in solution. Unfortunately, the W_S diastereomer that remains in solution decomposes and is unable to be recovered in an enriched form. To access the *S* hand of the metal, a similar protonation procedure was employed with the other enantiomer of the chiral acid (D-DBTH₂), which facilitated the selective precipitation of **(S,S)-118** with a dr = 94:6 (Scheme 7.3, right). **(R,R)-118** and **(S,S)-118** can then be deprotonated in the presence of benzene to access **(R)-1** and **(S)-1**, respectively.

Importantly, the enantioenrichment of the metal center is maintained through the ligand substitution without epimerization of the metal center, in contrast to what was observed with the molybdenum system (vide supra). In order to determine the enantiomer ratio of the enriched benzene complexes, the η²-ligand was exchanged for the chiral alkene reporter ligand, (*S*)-β-pinene. Exchange of the aromatic ligand for (*S*)-β-pinene results in two diastereomers of the metal complex with distinct ³¹P NMR resonances (Scheme 7.4, **(R,S)-119** and **(S,S)-119**). Relative integration of the signals in the NMR spectra allows for an estimate of the enantiomeric ratio of **(R)-1** and **(S)-1**.

Scheme 7.4: β -Pinene test for determination of enantioenrichment

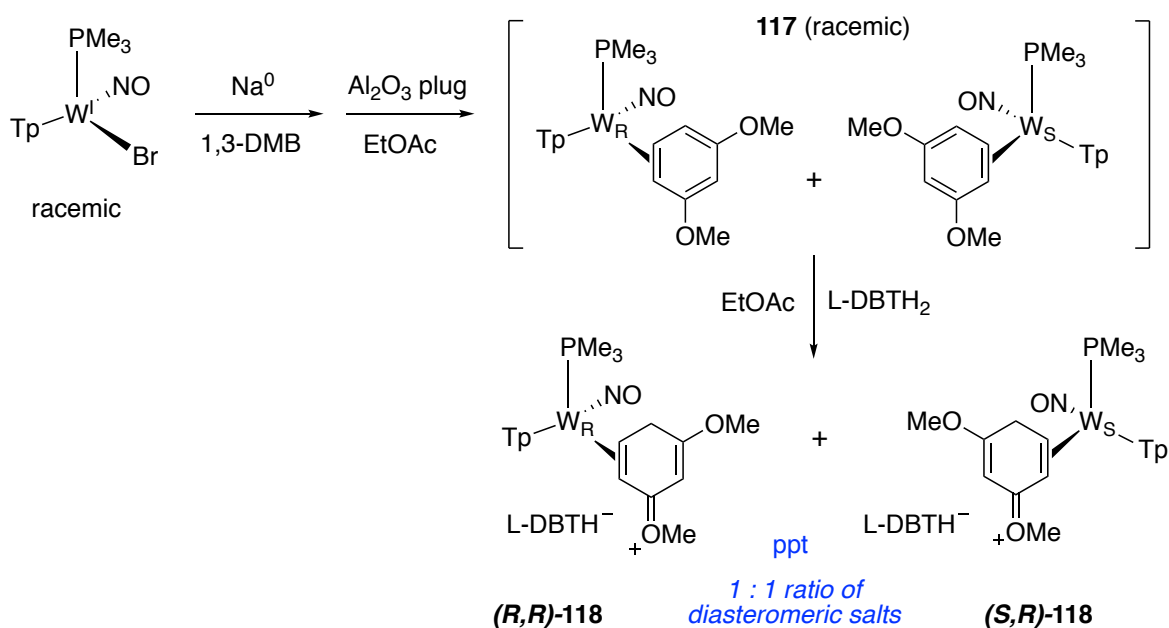
7.2.2 Optimization of Tungsten Enantioenrichment Procedure

Once a method for the enantioenrichment of the $\{\text{TpW}(\text{NO})(\text{PMe}_3)\}$ fragment was discovered, the next step was to optimize the synthesis on a large scale and employ this method to access enantioenriched organic products. A few potential drawbacks of this procedure include low yields for the synthesis of the initial $\eta^2\text{-1,3-DMB}$ complex (**117**, racemic), and the stoichiometric loss of half of the racemic complex in the enantioenrichment step. The reported synthesis for the starting material for this enantioenrichment procedure (**117**) began with the reduction of $\text{TpW}(\text{NO})(\text{PMe}_3)(\text{Br})$ (15 g) with Na^0 dispersion in the presence of 1,3-dimethoxybenzene. The reaction solution was then loaded on a basic alumina column in the glove box and eluted with ethyl acetate (EtOAc). Isolation of the neutral $\eta^2\text{-1,3-DMB}$ complex required the lengthy process of evaporating EtOAc and typically resulted in low yields ($\sim 15\text{-}30\%$), potentially due to incomplete precipitation or decomposition of the complex in the presence of a coordinating

solvent. In the resolution step, the protonation and subsequent selective precipitation required a stir time of 24-48 h to achieve high levels of enrichment. Under these conditions, the soluble diastereomer of the metal decomposed and was unable to be isolated.

To address the low yield and inconvenience of the synthesis of **117**, we sought to isolate the dimethoxybenzene complex in its protonated form instead. A procedure for isolation of the protonated form of **117** using triflic acid was previously reported by our group.¹⁴ Instead of triflic acid however, we proposed to use L-DBTH₂ to protonate **117** in situ after the reduction step (Scheme 7.5). Previously, it was shown that protonation of **117** with L-DBTH₂ in EtOAc resulted in the precipitation of (*R,R*)-**118** and (*S,R*)-**118** in a 1:1 ratio (as determined by a (*S*)- β -pinene test).¹¹ At the time, this result was not desirable due to the lack of separation of the diastereomers; however, applying this to the Na⁰ reduction step could simplify the procedure and increase the yield. The only question was whether the precipitation procedure could be applied to a large-scale protonation of **117** in situ after elution with EtOAc.

Scheme 7.5: Precipitation of 1:1 diastereomeric salts out of EtOAc



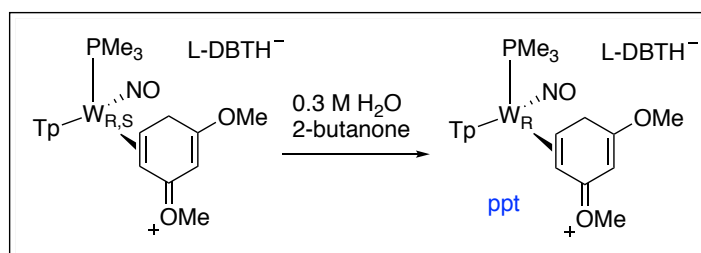
The optimization of the in-situ protonation procedure began with small-scale experiments with isolated η^2 -1,3-DMB complex to determine how the equivalents of acid used affects the yield. These control reactions were not run with the in situ reaction solution from the Na^0 reduction because of our inability to determine the yield from the reduction step, which would impede our ability to make direct conclusions about how the amount of acid affected the yield. We proposed that an increased concentration of acid would push the equilibrium towards the protonated species, leaving less of the neutral form in solution and increasing the yield. Furthermore, we expect the protonated form to be more stable than the neutral species towards both oxidative conditions and substitution. This increased stability could also increase the yield. Experimentally we found that protonation of **117** using 1.2 equivalents of L-DBTH₂ in EtOAc resulted in a 71% yield. Increasing to 2-3 equivalents of L-DBTH₂ resulted in an increased yield, ranging from 92-96%. Increasing the acid equivalents up to 5 resulted in a 91% yield, reflecting no improvement in yield compared to 2-3 equivalents of acid. Ultimately, slightly over 2 equivalents was taken as the optimized amount of acid based on maximizing yield and minimizing excess acid.

The optimized conditions for the protonation of **117** in EtOAc were then applied on a large scale (10-20 g) with the reduction of $\text{TpW}(\text{NO})(\text{PMe}_3)(\text{Br})$ to **117**. The published procedure for the synthesis of **117** was modified slightly¹⁵, and upon elution of the neutral η^2 -1,3-dimethoxybenzene with EtOAc, L-DBTH₂ was added to the filtrate, resulting in the successful precipitation and isolation of **118** as a 1:1 mixture of diastereomers (Scheme 7.5). The amount of L-DBTH₂ needed was estimated based on an assumed 50% yield for the

reduction. Under these conditions the optimized yield for the reduction step was 51%, a large improvement from the yield of the neutral η^2 -1,3-DMB complex (15-40%).

Another important aspect of the adapted procedure that needed to be addressed was the ability to enrich the 1:1 mixture of diastereomers by stirring in wet 2-butanone. To test this, the 1:1 mixture of **(R,R)-118** and **(S,R)-118** was fully dissolved in 2-butanone and then a H₂O/2-butanone solution was added (overall 0.3M H₂O/2-butanone solution). The stirring orange solution remained homogenous for a few minutes, then a yellow precipitate began to form, which was consistent with the selective precipitation of **(R,R)-118**. Once this proof of concept was demonstrated, experiments were performed to determine the yield and degree of enrichment based on the stir time (Table 7.1). Additional experiments were conducted to test other solvents and concentrations of H₂O, but ultimately we found that the conditions reported previously for enrichment were optimal.¹¹

Table 7.1: Effect of stir time on resolution of **(R,R)-118**



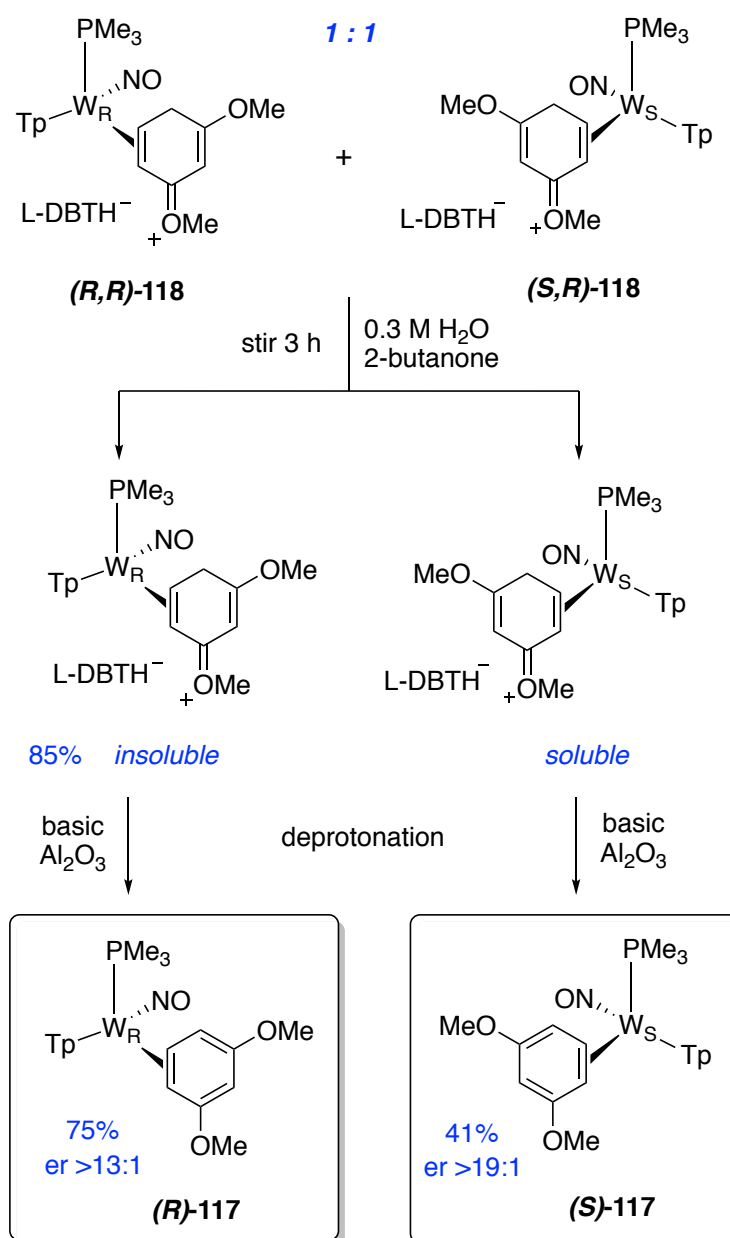
Stir Time (h)	Yield (%)	dr
1	47	6:1
1.5	66	7:1
2	84	7:1
2	80	9:1
2.5	79	10:1
3	73	11:1
3	75	13:1

There are several potential benefits of undergoing the enantioenrichment step starting from the diastereomeric salts of **118**, including increased stability in solution (compared to the neutral form), and potentially reduced time needed to get enantioenrichment. Table 7.1 provides a summary of the experimental results of the effect of stir time on the enantioenrichment and yield of **(R,R)-118**. Overall we observed that a high degree of enrichment could be achieved in a much shorter time frame (3 h vs. 24 h) by starting from the diastereomeric salts. The % yield shown represents the yield of **(R,R)-118**, with 100% yield considered as 50% of the possible total yield (from the 1:1 diastereomers). Stirring for <1 h resulted in both a lower yield and lower dr. The lower enrichment was expected with shorter time frames and the lower yield could result from more time needed to allow for precipitation of **(R,R)-118**. The experiments that were stirred for two hours seemed to be optimal for the yield (~82% average), with an average dr = 8:1. To improve the degree of enrichment without decreasing the yield substantially, the enrichment step was allowed to stir 3 hours, improving the dr to ~12:1. We also discovered that washing the collected complex with 2-butanone further increases the dr (with a slight loss of yield) from 13:1 to 17:1.

Achieving separation of the diastereomers in a shorter time frame opened up the possible recovery of the *S* enantiomer of the metal complex that remains in solution. To explore this possibility, once the insoluble $[W]_R$ diastereomer was collected, the filtrate containing potentially enriched $[W]_S$ complex was loaded on a basic alumina plug, in order to deprotonate the complex, then eluted with THF. The other enantiomer of the chiral acid (D-DBTH₂, 2 eq) was added to the filtrate and **(S,S)-118** was isolated. Significantly, we observed that **(S,S)-118** could be recovered in ~ 52% yield with a dr = 86:14. Once the

ability to recover the previously lost complex in enriched forms was demonstrated, we set out to optimize the procedure. To save time and combine synthetic steps, after eluting the *S* hand of the metal with THF, the neutral (*S*)-117 complex was isolated instead of protonating with D-DBTH₂. The overall procedure to access (*R*)-117 and (*S*)-117 is shown in Scheme 7.6.

Scheme 7.6: Isolation of enriched (*R*)-117 and (*S*)-117



The optimized conditions were scaled to 7.5 g of **118** (1:1 salt), which was stirred for 3 h in 0.3M H₂O/2-butanone. **(R,R)**-**118** was recovered in an 85% yield and **(S)**-**117** was recovered in 41% yield, with a er = 19:1. The combined overall yield from the enantioenrichment step was 63%. **(R,R)**-**118** (3 g) was taken through a subsequent deprotonation step using basic alumina and isolated as the neutral η^2 -1,3-dimethoxybenzene (**(S)**-**117**) in a 75% yield, with an er = 13:1.

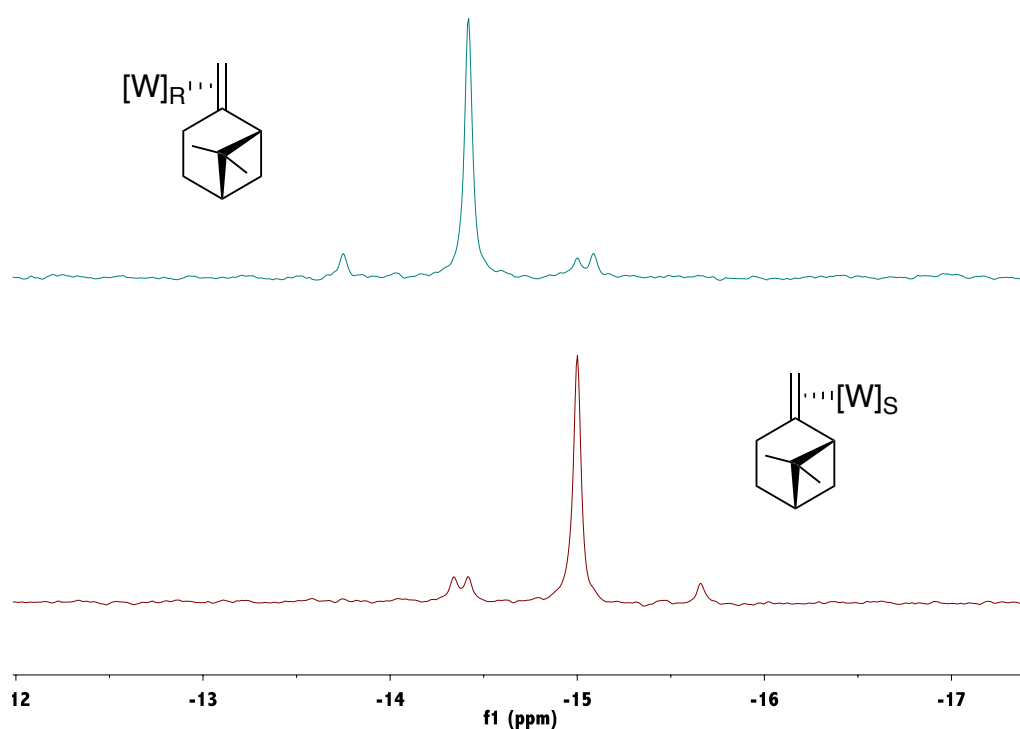


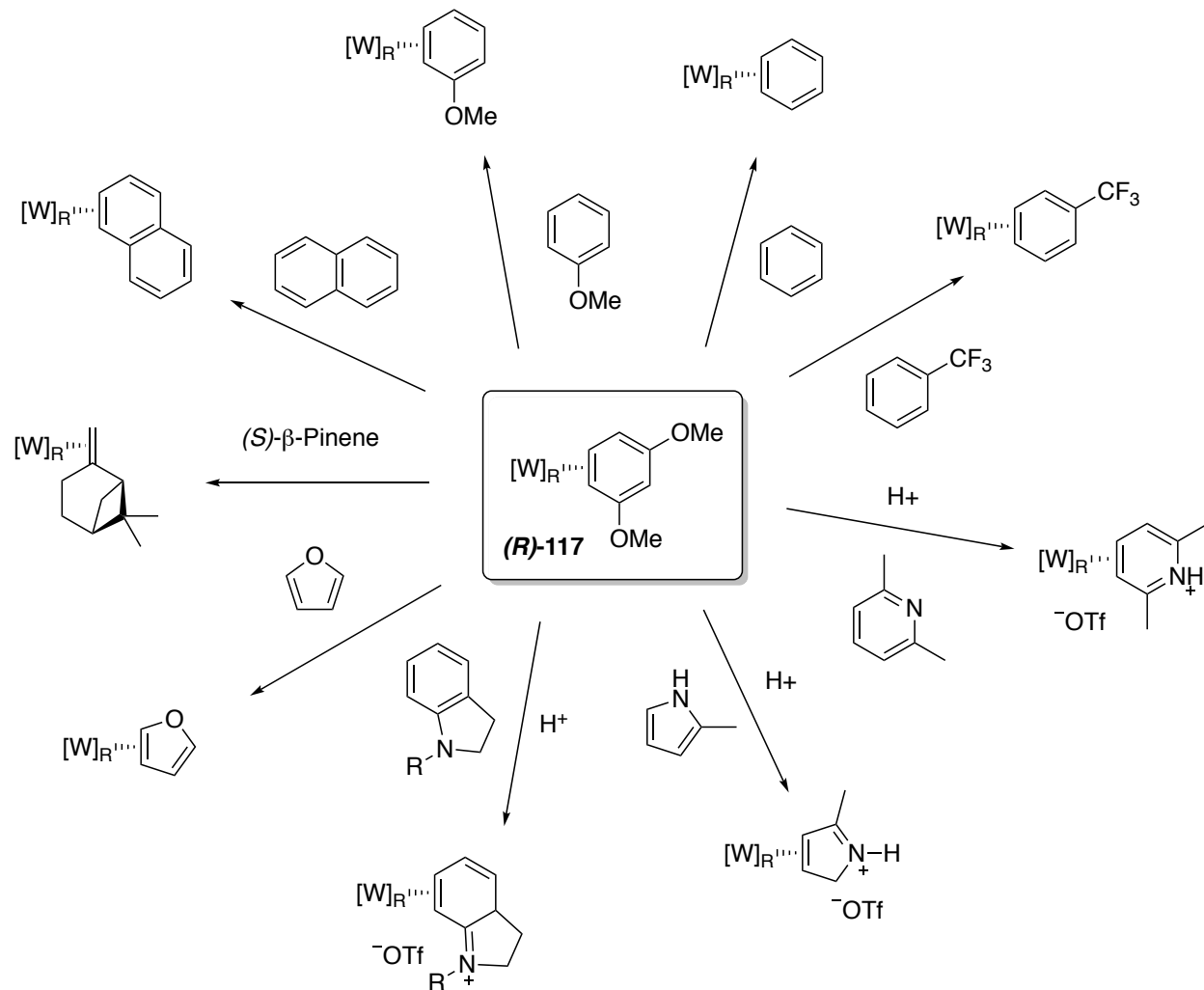
Figure 7.2: ³¹P NMR of *(S)*- β -pinene test

Overall, this enantioenrichment method provides a faster synthetic procedure, and more importantly, the ability to recover both enantiomers of the metal from the racemic mixture in enantioenriched forms. In all these experiments, the degree of enrichment was determined by the “*(S)*- β -pinene test”, described previously (Scheme 7.4), which relies on

relative integration of the peaks for the diastereomers of the (*S*)- β -pinene complex in the ^{31}P NMR spectrum. Figure 7.2 displays ^{31}P NMR spectra of (*R,S*)-**119** and (*S,S*)-**119**, which result from substitution reactions from enriched forms of both enantiomers of the η^2 -1,3-dimethoxybenzene complex.

7.2.3 η^2 -1,3-Dimethoxybenzene as Synthetic Precursor

The previously published procedure for enantioenrichment of the {TpW(NO)(PMe₃)} fragment reported the isolation of (*R*)-**1** and (*S*)-**1** by deprotonation of (*R,R*)-**118** and (*S,S*)-**118**, followed by a ligand substitution reaction with benzene (Scheme 7.3).¹¹ (*R*)-**1** and (*S*)-**1** were recovered in a 57% and 59% yield, respectively, with enantioenrichment maintained during the substitution; however, to simplify the procedure and avoid losing yield in the substitution reaction, we proposed to use neutral η^2 -1,3-dimethoxybenzene as the synthetic precursor to other aromatics. Although **117** has a slightly longer $t_{1/2}$ than **1** (4.3 h vs. 1.1 h)¹⁴, the dimethoxybenzene complex successfully undergoes ligand substitution reactions with a range of aromatic ligands (Scheme 7.7). These substitution reactions were monitored by ^{31}P NMR, and control reactions using **1** were monitored simultaneously. The substitution reactions using **117** progressed at a slightly slower rate than those with **1** as expected; however, the overall substitutions were still successful, the formation of the desired η^2 -aromatics and comparable amounts of decomposition to the control reactions.

Scheme 7.7: Substitution reactions from *(R)*-117

7.2.4 Synthesis of Enantioenriched Organic Compounds

The final stage of this enantioenrichment process was to demonstrate the ability to control absolute stereochemistry in the final organic products. This would also serve to confirm retention of stereochemistry throughout the process and give us a better idea of the degree of enantioenrichment. Although the *(S)*- β -pinene test gives an estimate of the enantioenrichment of the complex, this method is limited by the er of the *(S)*- β -pinene itself

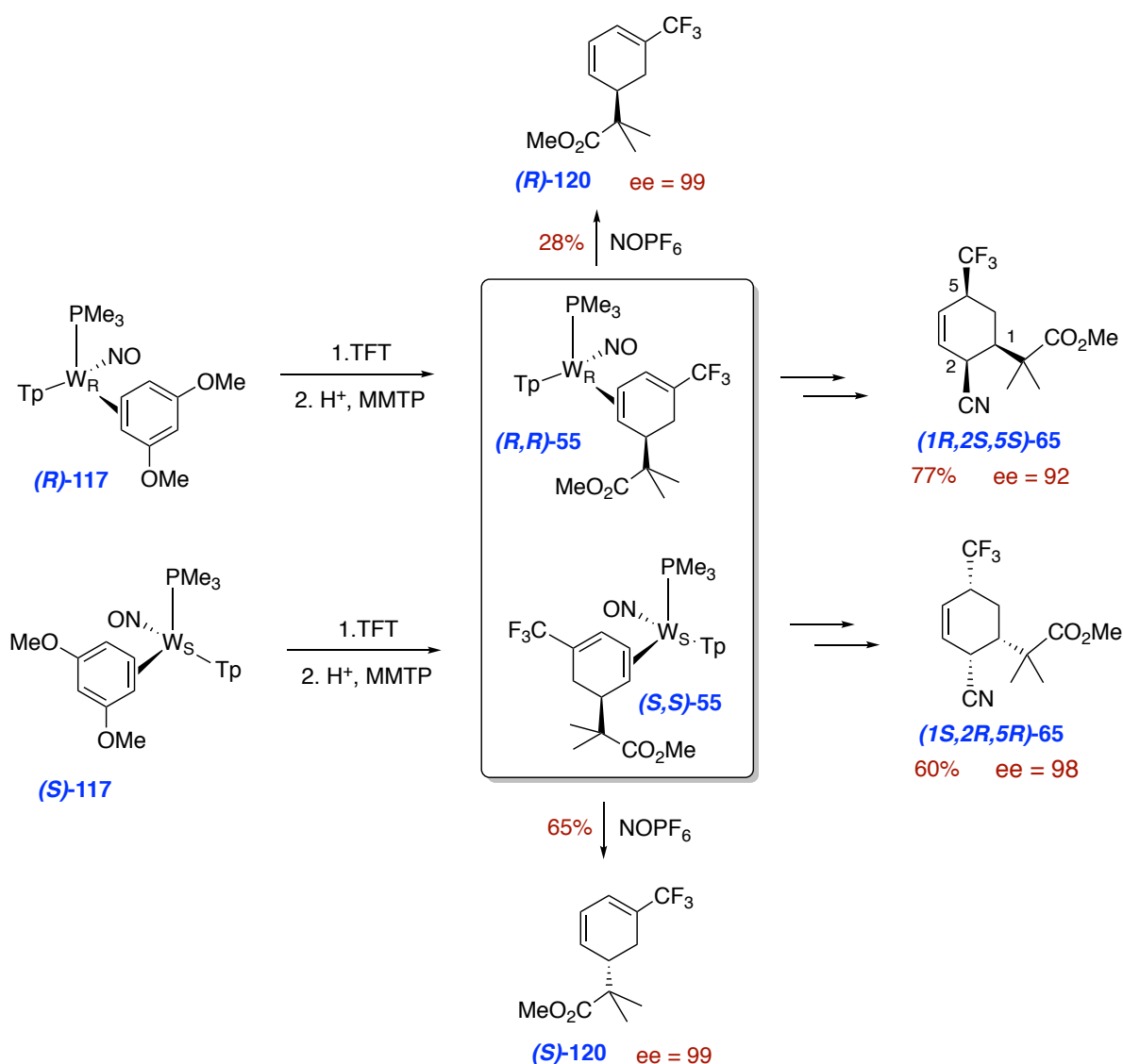
(98:2) and the integration of the relative peaks on ^{31}P NMR. We chose to first apply the enantioenrichment method with the η^2 -TFT complex, due to the newly developed chemistry of this system (Chapter 3).¹⁵

To access enantioenriched $\text{TpW}(\text{NO})(\text{PMe}_3)(\eta^2\text{-PhCF}_3)$, **(R)-117** and **(S)-117** were each stirred in neat TFT to undergo a ligand substitution, resulting in resolved forms of the trifluorotoluene complex, **(R)-52** and **(S)-52**. Completion of the substitution reaction was confirmed by ^{31}P NMR. **(R)-52** and **(S)-52** where each reacted in-situ with acid and a masked enolate at -30°C to give **(R,R)-55** and **(S,S)-55** (42% and 41% respectively, from **117**)(Scheme 7.8). Oxidation of both enantiomers of the η^2 -1,3-diene complex with NOPF_6 enabled the isolation of the organic dienes **(R)-120** (65%) and **(S)-120** (28%) as shown in Scheme 7.8. HPLC analysis with a Chiralpak IC-3 column was used to determined that **(R)-120** and **(S)-120** were each prepared with an ee = 99%.¹⁵ This process was also used to synthesize enantioenriched forms of the cyclohexene organic **65** with the metal influencing the selective formation of three new stereocenters. **(1R,2S,5S)-65** and **(1S,2R,5R)-65** were isolated in fair yields (77% and 60%), with similar ee's (>92% and 98%). Variations in the enantiomeric excess between enantiomers of the isolated organic compounds are due to differences in the enantioenrichment of the initial **(R)-117** and **(S)-117** complexes. After the isolation of enriched forms of **(R)-117** and **(S)-117**, we have typically observed that the *S* enantiomer of the metal is slightly more enriched, which we believe is a result of the isolation process.

The enantioenriched synthesis of cyclohexenes elaborated from **1** was recently explored to further support the general application of this enantioenrichment method. Similar to the procedure shown in Scheme 7.8, **(R)-117** and **(S)-117** were each stirred in

benzene to access **(R)**-1 and **(S)**-1. Each enantiomer of the benzene complex was then reacted in situ with DPhAT and dimethylmalonate at -60°C . The resulting η^2 -1,3-diene complexes (**(R)**-11 and **(S)**-11) were taken through a second addition with acid and NaCN, as described in Chapter 2. Oxidation of the resulting complexes enabled the isolation of both enantiomers of **42** in comparable yields (48% and 45%, Figure 7.3).

Scheme 7.8: Synthesis of enantioenriched trifluoromethylated cyclohexenes



HPLC analysis using a Chiralpak IC-3 column gave enantiomeric ratios of 13:1 and 18:1 for **(1*R*,2*S*)-42** and **(1*S*,2*R*)-42** (Figure 7.3). The retention time of **(1*R*,2*S*)-42** was 2.93 min in the racemic sample and 2.93 min in the enriched sample. The retention time of **(1*S*,2*R*)-42** was 3.28 min in the racemic sample and 3.28 min in the enriched sample as well. Combining the two enriched samples of **42** and observing the overlapping peaks at the expected retention times provided further confirmation of the correct assignments of enantiomers based on retention time.

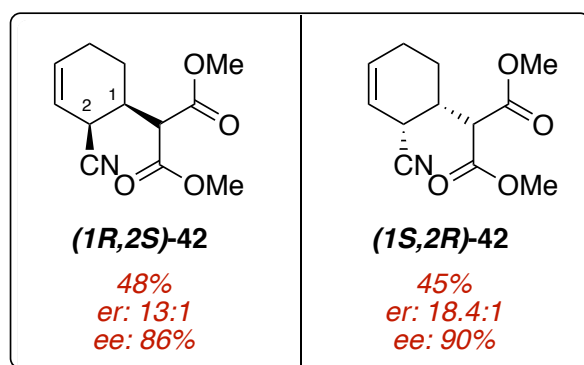


Figure 7.3: Synthesis of enantioenriched cyclohexenes from η^2 -benzene

7.3 Conclusions

A method to enantioenrich the $\{\text{TpW}(\text{NO})(\text{PMe}_3)\}$ fragment through the formation of diastereomeric salts prepared from L-dibenzoyltartaric acid (L-DBTH₂) was discovered.¹¹ The modification and optimization of this procedure enabled the separation and recovery of both enantiomers of the metal complex on a large scale (15 g). Both complexes are recovered in enantioenriched forms of the neutral η^2 -dimethoxybenzene complex (**(*R*)-117** er>13:1, **(*S*)-117** er>19:1). **(*R*)-117** was shown to undergo a ligand substitution reaction with a range of aromatic ligands with retention of the metal

stereocenter. The transfer of asymmetry from the metal to transformed organic products was demonstrated starting from enantioenriched forms of **1** and **52**, with HPLC analysis showing ee's ranging from 86-99% for the functionalized cyclohexenes.¹⁵ The successful synthesis of these enantioenriched organic compounds illustrates the power and synthetic utility of dihapto-dearomatization chemistry, wherein flat aromatics can be controllably transformed into single enantiomers of more complex 3D molecules.

7.4 Experimental

General Methods: NMR spectra were obtained on 500, 600 or 800 MHz spectrometers. Chemical shifts are referenced to tetramethylsilane (TMS) utilizing residual ^1H or ^{13}C signals of the deuterated solvents as internal standards. Chemical shifts are reported in ppm and coupling constants (J) are reported in hertz (Hz). Infrared Spectra (IR) were recorded on a spectrometer as a glaze on a diamond anvil ATR assembly, with peaks reported in cm^{-1} . All synthetic reactions were performed in a glovebox under a dry nitrogen atmosphere unless otherwise noted. All solvents were purged with nitrogen prior to use. Deuterated solvents were used as received from Cambridge Isotopes. Characterization of **55**, **65**, **117**, (*R,R*)-**118**, (*S,R*)-**118**, (*S,S*)-**118**, (*R,S*)-**119**, and (*S,S*)-**119** have been previously reported.^{11,14,15} The synthetic procedure and characterization of **42** is provided in Chapter 2.

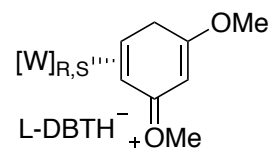
General Procedure for Substitution Reactions from **1** and **117**

1 or **117** (25 mg) was dissolved in THF (1 mL) in a 4-dram. To this homogenous solution was added 8 equivalents of the aromatic ligand. The reaction was monitored by ^{31}P NMR until the reaction was complete (based on the disappearance of the starting material peak). The relative amount of decomposition was based off of the presence of a free PMe_3 peak in the ^{31}P NMR spectrum, which is observed upon decomposition of the tungsten system.

General Enantioenrichment Procedure: Enantioenriched forms of the η^2 -dimethoxybenzene complex ((*R*)-**117** and (*S*)-**117**) were synthesized by modifying the

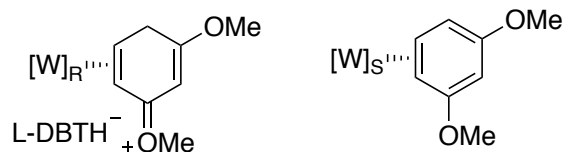
procedures for the reduction and enantioenrichment steps from previous publications.^{11,14}

The modified procedures are shown below.



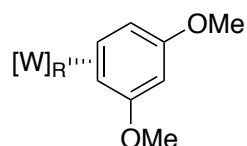
Synthesis of 1:1 (*R,R*)-118 + (*S,R*)-118

Sodium dispersion (30-35% in paraffin wax) (9.39 g, 123 mmol) was added to a flame dried 500 mL roundbottom flask and stirred with hexanes. The hexanes wax mixture was decanted and more hexanes was added to the round bottom flask and stirred. This process was repeated until all the wax appeared to be gone from the Na⁰. 1,3-dimethoxybenzene (425 mL, 3.25 mol) and TpW(NO)(PMe₃)(Br) (10.0 g, 17.2 mmol) were then added to the round bottom flask and the reaction was stirred for 16 h. The dark golden mixture was filtered through a Celite plug in a 350 mL medium porosity fritted disc and then the plug was rinsed with 100 mL 1,3-dimethoxybenzene. The filtrate was diluted with Et₂O (750 mL) and then loaded onto a basic alumina column (350 mL medium porosity fritted disc) packed with Et₂O. The desired yellow band was eluted with EtOAc (~550 mL), then the filtrate was evaporated under reduced pressure until the volume was decreased by ~100 mL. L-DBTA (6.18 g, 17.2 mmol) was added to the golden solution with stirring, causing the immediate precipitation of an orange solid. Et₂O (100 mL) was added to further induce precipitation, and the solid was collected on a 150 mL medium porosity fritted disc, washed with Et₂O (3 x 30 mL) and hexanes (2 x 50 mL), then desiccated, yielding (*R,R*)-118 + (*S,R*)-118 (8.26 g, 8.39 mmol, 49% yield).



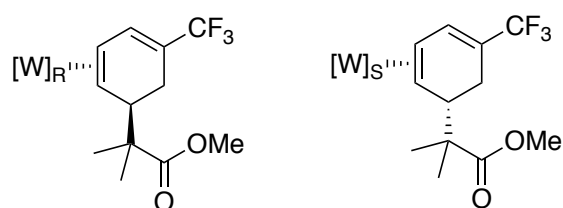
Synthesis of *(R,R)*-118 and *(S)*-117

***(R,R)*-118 + *(S,R)*-118** (7.5 g, 7.5 mmol) was dissolved in 2-butanone (80 mL) in a 100 mL round bottom flask charged with a stir egg. 2-butanone (14 mL) and H₂O (514 mg, 28.6 mmol) were combined in a 4-dram vial, then this solution was added to the round bottom flask with stirring. After stirring approximately 1 minute, the orange homogeneous solution started to turn heterogeneous as a yellow solid began precipitating out. The mixture was vigorously stirred for 3 h and then the yellow solid was collected on a 150 mL medium porosity fritted disc. The solid was washed with 2-butanone (15 mL), Et₂O (2 x 40 mL), and hexanes (2 x 40 mL) then desiccated yielding ***(R,R)*-118** (3.17 g, 3.17 mmol, 85 % yield). The initial filtrate, containing ***(S,R)*-118** in 2-butanone was stirred with basic alumina (40 mL) for 5 min, then filtered through a 60 mL medium porosity fritted disc. The alumina plug was rinsed with THF (~110 mL), and then the resulting golden filtrate was evaporated *in vacuo*. At ~40 mL, hexanes was added (100 mL) and then the solution was concentrated further. When the volume of the mixture was around 25 mL, hexanes (100 mL) was added again, causing a precipitate to form. The yellow solid was then collected on a 30 mL fine porosity fritted disc, washed with hexanes (2 x 15 mL), and desiccated yielding ***(S)*-117** (991 mg, 1.55 mmol, 41% yield).



Synthesis of **(R)**-117

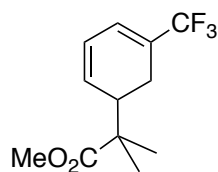
(R,R)-118 (3.17 g, 3.17 mmol) and THF (200 mL) were added to a 200 mL Erlenmeyer flask charged with a stir bar, then basic alumina (45 mL) was added and the mixture was stirred for 5 min. The reaction mixture was pulled through a 1 cm basic alumina plug in a 150 mL fine porosity fritted disc. The plug was rinsed with THF (100 mL) and then the yellow filtrate was concentrated *in vacuo*. When the volume was reduced to roughly 50 mL, hexanes (100 mL) were added and the evaporation was continued. With approximately 75 mL left, hexanes (50 mL) were added again, and then the yellow solid was collected on a 60 mL medium porosity fritted disc. The yellow precipitate was washed with hexanes (3 x 15 mL), then desiccated yielding **(R)**-117 (1.53 g, 2.39 mmol, 75% yield).



Synthesis of **(R,R)**-55 and **(S,S)**-55

(R)-117 (1.00 g, 1.56 mmol) and TFT (7 mL) were added to a 4-dram vial charged with a stir pea, and the resulting mixture was stirred for 52 h. Completion of the substitution reaction was monitored by ³¹P NMR and then the homogeneous dark golden solution was cooled to -30°C. The reaction solution was diluted with MeCN (1 mL, -30°C), then a 1M solution of HOTf in acetonitrile (2.88 mL, 2.88 mmol, -30°C) was added, resulting in a

homogeneous dark golden/red solution, which was allowed to sit for 15 min at -30°C . To this solution was added MMTP (1.45 mL, 7.14 mmol, -30°C). After 20 h at -30°C , Et_3N was added to the reaction solution (2.00 mL, 14.3 mmol). A 60 mL medium porosity fritted disc was filled $\frac{3}{4}$ full of silica gel and set in Et_2O . The reaction solution was loaded on the column and a pale yellow band was eluted with Et_2O (75 mL). The filtrate was evaporated to dryness *in vacuo*, then redissolved in minimal DCM and added to stirring hexanes (40 mL). The resulting pale yellow solid was collected on a 15 mL medium porosity fritted disc, washed with hexanes (2 x 5 mL) and desiccated overnight, yielding **(R,R)-55** (489 mg, 0.651 mmol, 42% yield). A similar procedure was used to synthesize **(S,S)-55** starting from **(S)-117** (500 mg, 0.780 mmol), giving the desired product (240 mg, 0.319 mmol, 41% yield).



Synthesis of Compound 120. (Outside of glovebox, racemic) NOPF_6 (39 mg, 0.22 mmol) was added to a 4-dram vial charged with a stir pea. In a separate 4-dram vial, **55** (110 mg, 0.146 mmol) was dissolved in acetone (3 mL) and added to the vial with NOPF_6 , resulting in an immediate color change from pale yellow to brown. This solution was stirred for 1 h, and then evaporated *in vacuo* to a film. This film was redissolved in DCM (1 mL) and precipitated into stirring hexanes (25 mL). The vial was rinsed with DCM (0.3 mL), followed by hexanes (2 mL) and added to the stirring mixture. The resulting precipitate was filtered off using a 15 mL fine porosity fritted disc and was washed with hexanes (2 x 5

mL). The pale yellow filtrate was evaporated *in vacuo* and the resulting oil was loaded (3 x 0.3 mL DCM) onto a 250 μ m silica preparatory plate and eluted with 10% EtOAc/hexanes (HPLC grade, 200 mL). A UV active band with an R_f of 0.55-0.73 was collected and sonicated in EtOAc (HPLC grade, 30 mL) for 15 min. The silica was filtered off on a 30 mL medium porosity fritted disc and washed with EtOAc (HPLC grade, 3 x 20 mL). The filtrate was evaporated *in vacuo* and dried under N_2 for 30 min, yielding **120** (15 mg, 0.059 mmol, 40% yield). IR: $\nu(\text{CO}) = 1731 \text{ cm}^{-1}$. EA: Calculated for $6\text{C}_{12}\text{H}_{15}\text{F}_3\text{O}_2 \cdot \text{hexanes}$: C, 59.46; H, 6.65. Found: C, 59.25; H, 6.62. ^1H NMR (d^6 -acetone, δ): 6.36 (1H, m, H2), 6.04 (1H, m, H3), 5.83 (1H, dd, $J = 9.6$ & 3.9 , H4), 3.69 (3H, s, OMe), 2.86 (1H, m, H6), 2.32 (1H, m, H5), 2.21 (1H, m, H6), 1.19 (3H, s, Me), 1.18 (3H, s, Me). ^{13}C NMR (CDCl_3 , d): 177.4 (CO), 131.4 (C4), 125.6 (q, $J = 30.9$, C1), 124.8 (q, $J = 6.5$, C2), 124.0 (q, $J = 270.0$, CF_3), 123.5 (C3), 52.2 (OMe), 45.7 (C7), 40.6 (C5), 22.4 (Me), 22.2 (Me), 21.2 (C6).

7.5 References

- (1) Harman, W. D. *Chem. Rev.* **1997**, *97*, 1953.
- (2) Chordia, M. D.; Harman, W. D. *J. Am. Chem. Soc.* **1998**, *120*, 5637.
- (3) Barrera, J.; Orth, S. D.; Harman, W. D. *J. Am. Chem. Soc.* **1992**, *114*, 7316.
- (4) Gunnoe, T. B.; Sabat, M.; Harman, W. D. *J. Am. Chem. Soc.* **1999**, *121*, 6499.
- (5) Gunnoe, T. B.; Sabat, M.; Harman, W. D. *Organometallics* **2000**, 728.
- (6) Brooks, B. C.; Gunnoe, T. B.; Harman, W. D. *Coord. Chem. Rev.* **2000**, 3.
- (7) Meiere, S. H.; Brooks, B. C.; Gunnoe, T. B.; Sabat, M.; Harman, W. D. *Organometallics* **2001**, *20*, 1038.
- (8) Meiere, S. H.; Brooks, B. C.; Gunnoe, T. B.; Carrig, E. H.; Sabat, M.; Harman, W. D. *Organometallics* **2001**, *20*, 3661.
- (9) Meiere, S. H.; Valahovic, M. T.; Harman, W. D. *J. Am. Chem. Soc.* **2002**, *124*, 15099.
- (10) Meiere, S. H.; Harman, W. D. *Organometallics* **2001**, *20*, 3876.
- (11) Lankenau, A. W.; Iovan, D. A.; Pienkos, J. A.; Salomon, R. J.; Wang, S.; Harrison, D. P.; Myers, W. H.; Harman, W. D. *J. Am. Chem. Soc.* **2015**, *137*, 3649.
- (12) Shivokevich, P. J.; Myers, J. T.; Smith, J. A.; Pienkos, J. A.; Dakermanji, S. J.; Pert, E. K.; Welch, K. D.; Trindle, C. O.; Harman, W. D. *Organometallics* **2018**.
- (13) Graham, P. M.; Delafuente, D. A.; Liu, W.; Myers, W. H.; Sabat, M.; Harman, W. D. *J. Am. Chem. Soc.* **2005**, *127*, 10568.
- (14) Welch, K. D.; Harrison, D. P.; Lis, E. C.; Liu, W.; Salomon, R. J.; Harman, W. D.; Myers, W. H. *Organometallics* **2007**, *26*, 2791.

- (15) Wilson, K. B.; Myers, J. T.; Nedzbala, H. S.; Combee, L. A.; Sabat, M.; Harman, W. D. *J. Am. Chem. Soc.* **2017**, *139*, 11401.

Concluding Remarks

The dihapto-coordination of aromatic compounds to π -basic transition metals (Os(II), Re(I), W(0), and Mo(0)) has been investigated for over 30 years since the η^2 -benzene complex of {Os(NH₃)₅} was first reported in 1987. Each of these metal systems has facilitated novel synthetic transformations with aromatics by breaking the aromaticity and unlocking the latent alkene functionality within the cyclic systems. The ability to rapidly and stereoselectively convert planar aromatic compounds into more complex alicyclic systems has become an increasingly important transformation for the synthetic and medicinal chemistry fields.

The dearomatization chemistry afforded by the potent π -basic {TpW(NO)(PMe₃)} fragment has facilitated the synthesis of a range of novel alicyclic small molecules starting from simple aromatic precursors such as aniline, phenol, anisole, pyridines, naphthalene, furan, and pyrroles. After 15 years of investigation into tungsten dearomatization chemistry, novel reactivity has continued to proliferate. Only recently, conditions were found to more thoroughly investigate the reactivity of the parent TpW(NO)(PMe₃)(η^2 -benzene) complex. In Chapter 2, the ability to effect a regio- and stereoselective addition across an uncoordinated double bond of the benzene was demonstrated with a range of nucleophiles. The resulting η^2 -1,3-dienes, with a π -system still in conjugation with the metal, are activated towards a second tandem electrophilic/nucleophilic reaction, leading to functionalized cis 3,4 cyclohexene and cis 3,6-cyclohexene organics. Recently, our group has shown the use of an oxidant to catalyze ligand substitution reactions. As discussed in Chapter 2, we have demonstrated a catalyzed intramolecular alkene isomerization with the η^2 -1,3-diene **55**. The utility of this newly established facet of our chemistry was demonstrated in the regiocontrolled synthesis of cis-3,5 cyclohexenes, giving us access to

three different substitution patterns for chiral cyclohexenes starting from simple benzene. These recent advances with catalytic substitutions and alkene isomerizations provide further opportunities to expand this synthetic methodology.

The effect of an electron-withdrawing group on the chemistry of an η^2 -aromatic was explored in Chapters 3 and 4 with the η^2 -TFT complex. This work is the first investigation into the reactivity of a benzene substituted with an electron-withdrawing group with the tungsten system. We were able to show that the CF_3 group, in tandem with the tungsten fragment, enables a regio- and stereoselective 1,2-addition of a proton and a nucleophile across an uncoordinated alkene in the ring. A second protonation at the terminal alkene carbon of the η^2 -1,3-diene leads to a highly distorted allyl, due to the combined influence of the asymmetric tungsten fragment and the electron-withdrawing CF_3 group. Subsequent nucleophilic addition to this allylic species gives a regiocontrolled 1,4-addition reaction. Liberation of the transformed ligand gives trisubstituted cis-trifluoromethylated cyclohexenes, with the two nucleophiles installed adjacent to one another.

The ability to add a range of primary and secondary amines as nucleophiles was also demonstrated with the TFT complex. This synthetically challenging transformation enables the stereo- and regioselective incorporation of functional groups that have been shown to be important in biologically active small molecules. Furthermore, within this investigation, a novel cyclization reaction was discovered, giving a benzimidazole type core structure. In this reaction, we believe the reversible coordination of a Lewis acid (TMS) to the nitrosyl ligand activates the complex towards nucleophilic addition. The potential ability to modulate the reactivity of the tungsten system through nitrosyl coordination is another

new facet of our dearomatization chemistry and could further expand the novel reaction pathways accessible through dihapto-dearomatization.

The chemistry demonstrated with the benzene and TFT (Chapters 2-4) complexes represents the first examples of dihapto-dearomatization where a total of four metal controlled addition reactions were realized. Furthermore, understanding the coordination chemistry of the unsubstituted benzene ring, as well as a benzene ring substituted with an electron-withdrawing group, has dramatically increased our understanding of the regioselectivity of other systems. In Chapter 5, we discuss the regioselectivity of the η^2 -*N,N*-dimethylanilinium system in the context of what we have learned from the chemistry of the η^2 -benzene and η^2 -TFT complexes. Furthermore, we were able to demonstrate novel reactivity for the anilinium system with carbon electrophiles, generating more complex multicyclic systems through intramolecular cyclization reactions. The chemistry observed for the parent η^2 -*N,N*-dimethylanilinium has also provided a guide for the reactivity of more complex nitrogen heterocycles, such as quinoline and indoline derivatives. The η^2 -coordination and functionalization of these systems enables the synthesis of complex nitrogen heterocycles with multiple new stereocenters set by the metal (Chapter 6).

One of the major synthetic hurdles of this transition metal mediated dearomatization methodology is the ability to control the absolute stereochemistry of the addition reactions. Within the last few years, the enantioenrichment of the tungsten fragment was reported, utilizing a chiral acid to form diastereomers of the dimethoxybenzene complex, which were separated based on disparate solubilities. This enrichment method was optimized to allow access to both enantiomers of the tungsten complex starting from the racemic η^2 -1,3-dimethoxybenzene complex (Chapter 7).

Furthermore, we have demonstrated the stereocontrolled synthesis of chiral cyclohexenes originating from benzene and α,α,α -trifluorotoluene with ee's ranging from 86-99% (Chapter 7) using this enrichment procedure.

Hexahapto-coordination of aromatics to electron-deficient complexes provides a complementary transition-metal mediated dearomatization methodology to the electron-rich dearomatization described in this work. The development and application of this chemistry has yielded a range of substituted aromatic products, as well as disubstituted 1,3-cyclohexadienes, typically with a trans stereochemical relationship. In comparison to this, one of the strengths of η^2 -dearomatization chemistry is the ability to activate the coordinated ligand towards up to four addition reactions, which typically leads to cyclohexene products. In these functionalized cyclohexene products, the substituents on the ring typically have a syn relationship, in contrast to the hexahapto products. An additional advantage of dihapto-dearomatization is the wide range of nucleophiles that are reactive towards the η^2 -allyls that result from the initial electrophilic addition. The addition of nucleophiles to these η^2 -allyl complexes has been demonstrated with nucleophiles ranging from Grignard reagents, hydrides, enolates, cyanide, to amines, and even relatively weak aromatic nucleophiles. In contrast, electron-deficient η^6 -arene systems typically require relatively strong nucleophiles to react with the coordinated ligand (organo lithium reagents). However, η^6 -dearomatization facilitates the stereoselective formation of C-C bonds with the addition of carbon electrophiles to the intermediate cyclohexadienyl complexes. Although the successful addition of carbon electrophiles was demonstrated with the $\{\text{Os}(\text{NH}_3)_5\}^{2+}$ system, the addition of these reagents to $\text{TpW}(\text{NO})(\text{PMe}_3)(\eta^2\text{-aromatics})$ has thus far shown limited success. Both of these transition-metal mediated

dearomatization methodologies have enabled the asymmetric synthesis of chiral dearomatized organics and provide powerful synthetic tools to access functionalized alicyclic systems.

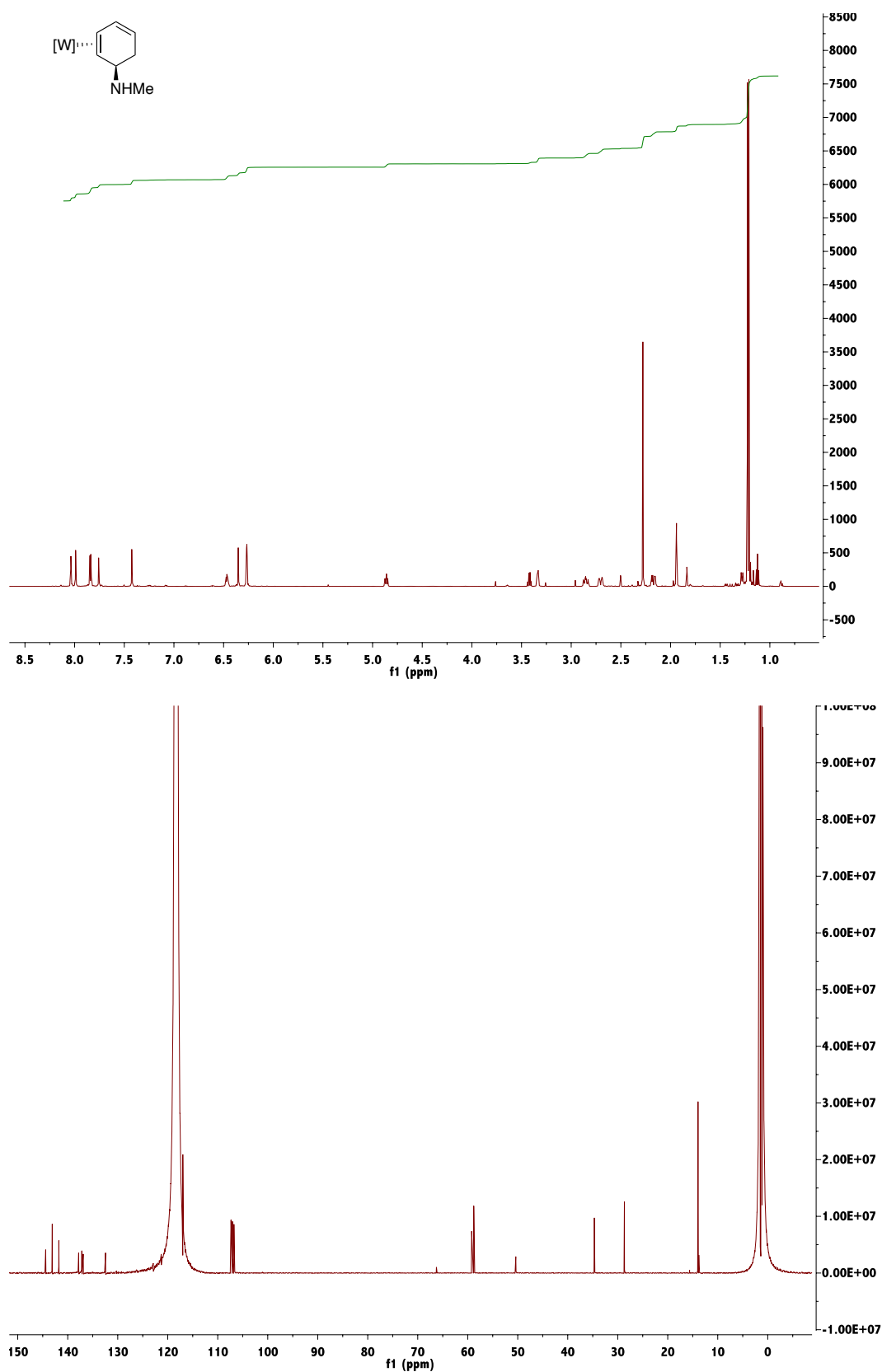
In addition to transition-metal dearomatization methods, alternative approaches for dearomatization have been explored including photochemical/thermal, radical and enzymatic dearomatization, which yield cyclic dienes and alkenes. These techniques are useful for the synthesis of alicyclic synthetic scaffolds, as each method typically results in a specific type of functionalized dearomatized product. For example, the radical dearomatization methods described in Chapter 1 yield 1,4-cyclohexadiene products, and the microbial dearomatization of benzene with *Pseudomonas putida* gives cis-cyclohexadienol products. These methods have been exploited to access specific dearomatized and desymmetrized products, which often provide the crucial framework for subsequent functionalization into more complex compounds, including natural products.

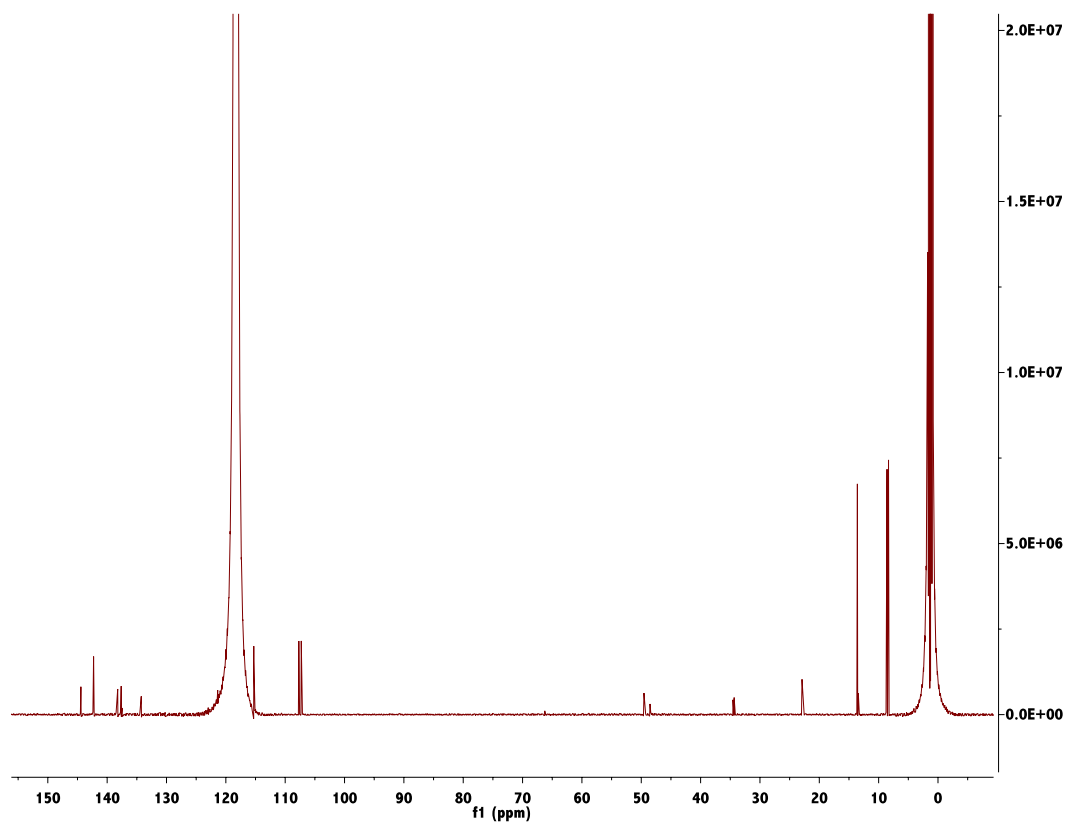
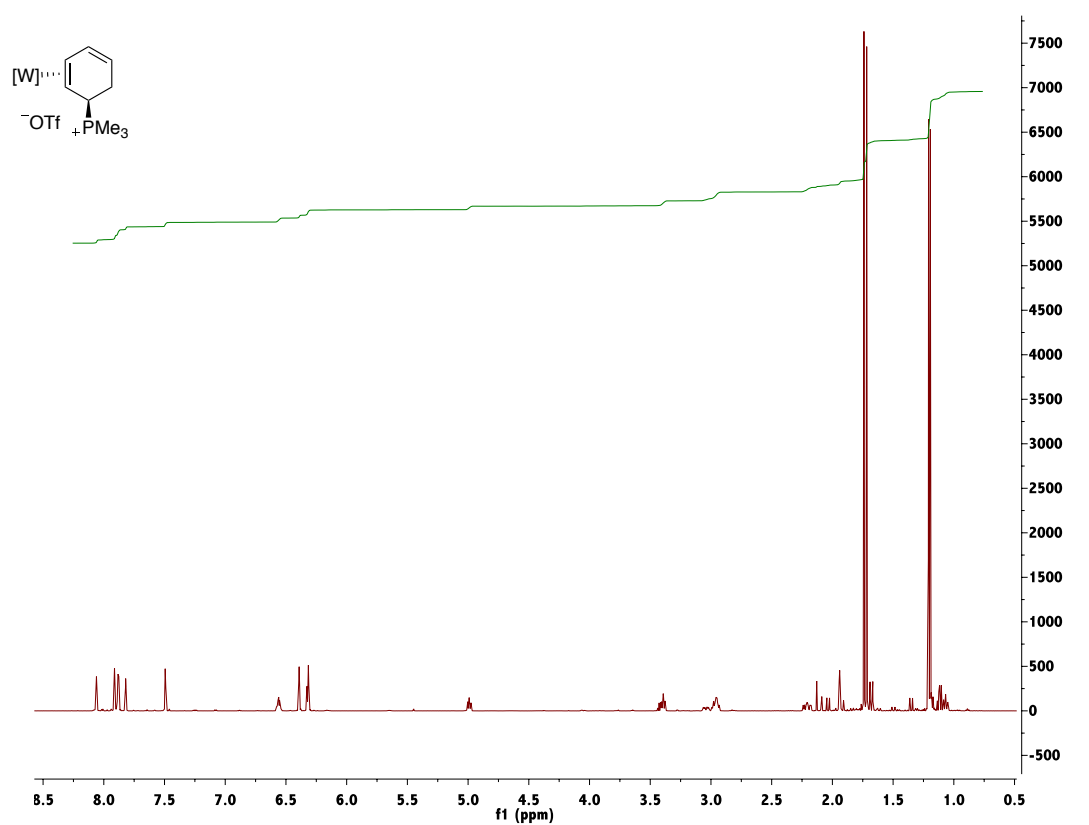
The dihapto-dearomatization methodology differs from most of these types of synthetic strategies in a few subtle but significant ways. The dearomatization of the aromatic system occurs upon coordination to the π -basic metal, without any coinciding functionalization of the ring. This coordination has been demonstrated with an extensive range of aromatics and primes the cyclic alkene system towards novel addition reactions with a diverse range of reagents. This chemistry could find synthetic use as a means of accessing desymmetrized compounds with absolute stereochemistry defined, to be used as important precursors for further organic elaborations. But in addition to this function, our chemistry provides a unique opportunity to access novel molecular frameworks and expand chemical space. Coordination of the aromatic to the asymmetric metal system not

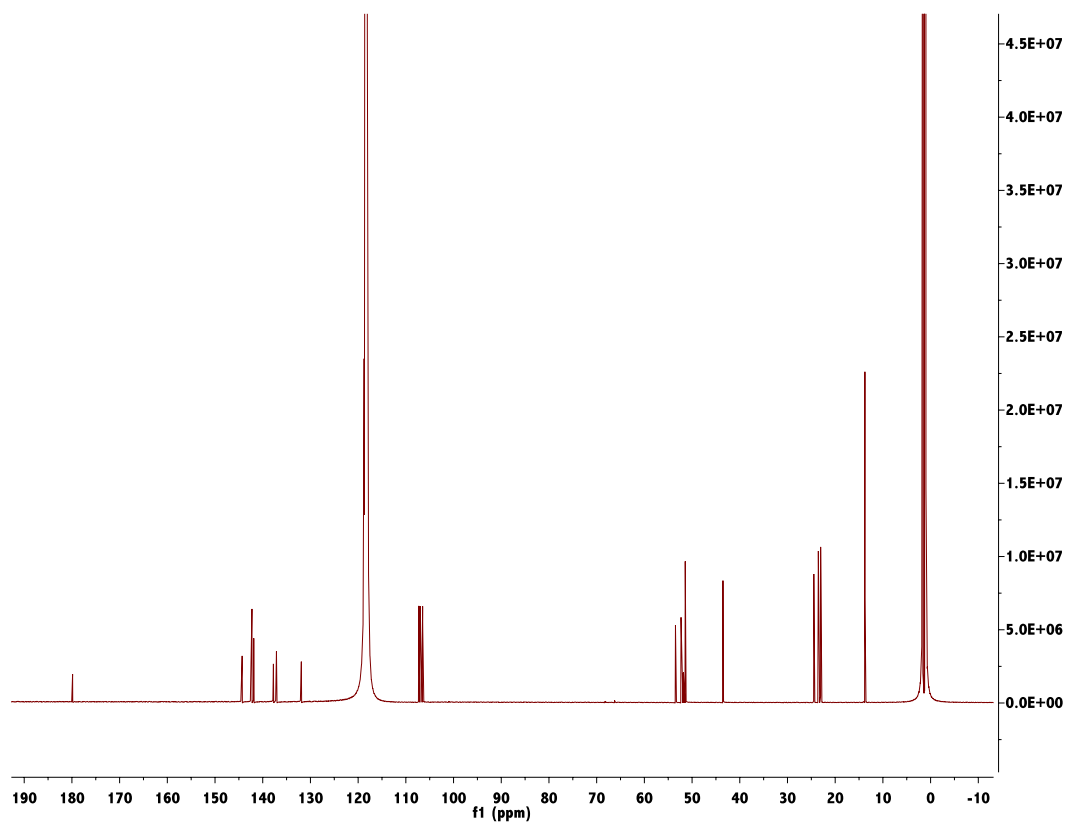
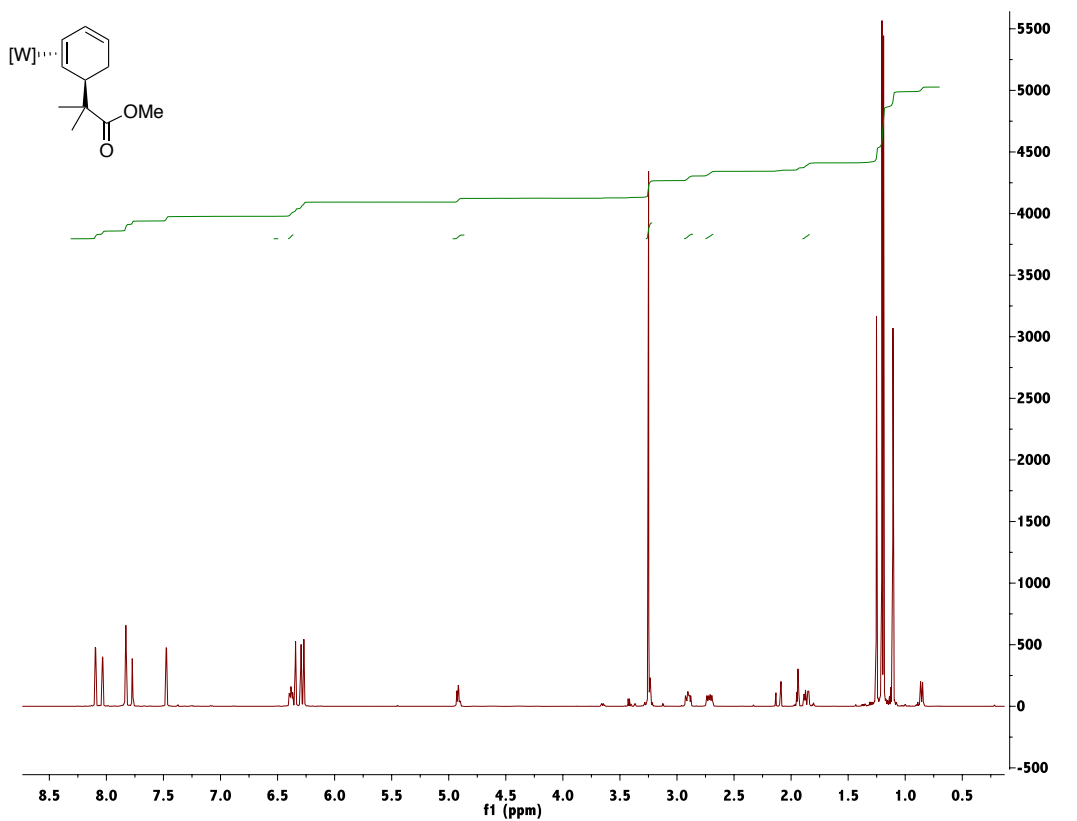
only dearomatizes the ligand, but also fundamentally changes its reactivity, often giving a reversal of the inherent reactivity of the free aromatic. Furthermore, this chemistry enables multiple sequential additions to the coordinated ligand that are typically regio- and stereoselective, with the capability of absolute stereocontrol in the formation of new stereocenters. Despite these capabilities, our chemistry has found limited use by synthetic chemists potentially due to air sensitivity, quantitative use of the metal, or perceived learning curve. To advance this methodology we must focus on bridging the gap between the synthetic transformations we can achieve and what is valued in the synthetic and medicinal chemistry fields.

As our understanding of the reactivity and regiochemistry of $\text{TpW}(\text{NO})(\text{PMe}_3)(\eta^2\text{-aromatic})$ systems increases, we are better able to predict new reactivity and expand our synthetic schemes to incorporate more complex reagents, known to be important for pharmaceutical applications. Predictable reactivity, high regioselectivity, and the ability to control absolute stereochemistry are crucial features for the synthetic utility of dearomatization chemistry and its application towards drug discovery. With these advances, we can more effectively utilize dearomatization chemistry to access novel molecular scaffolds, to be tested for biological activity in fragment libraries where topological diversity is key. As we demonstrate the powerful synthetic potential of this method, hopefully others will begin to incorporate this methodology to access important molecular scaffolds, as the synthetic potential of dearomatization chemistry through dihapto-coordination is only limited but the limited number of those researching it.

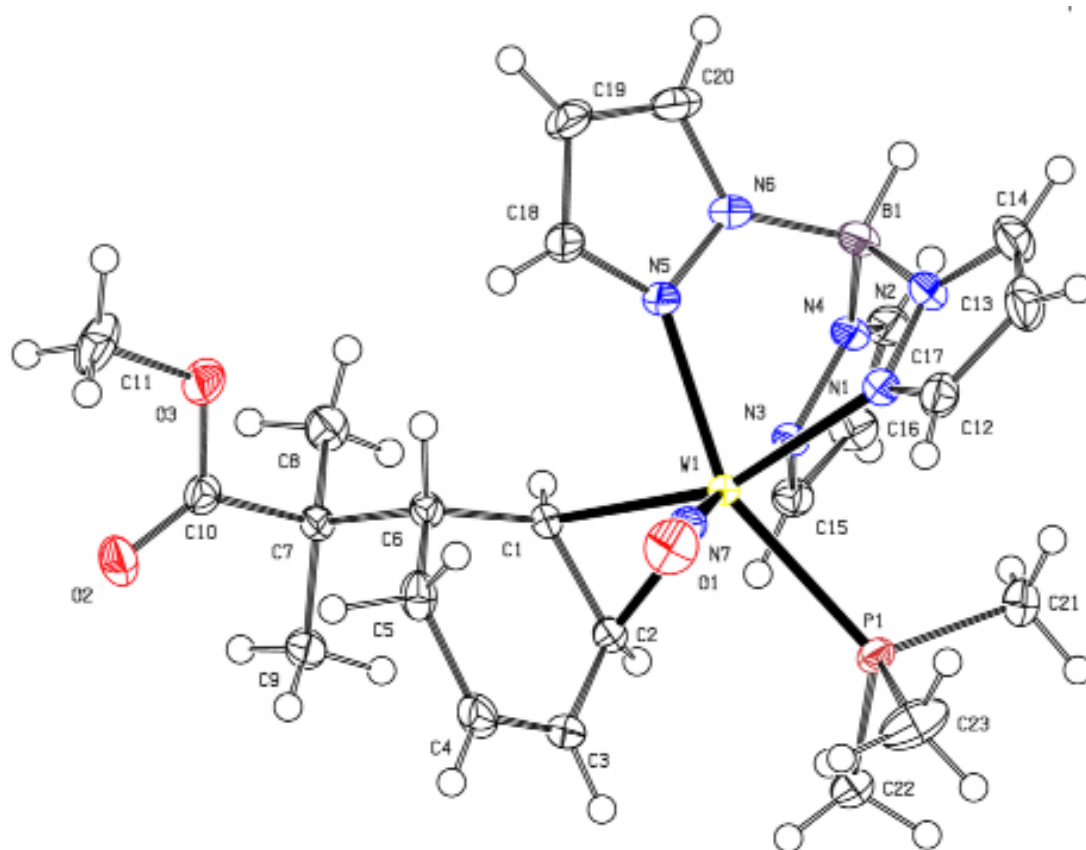
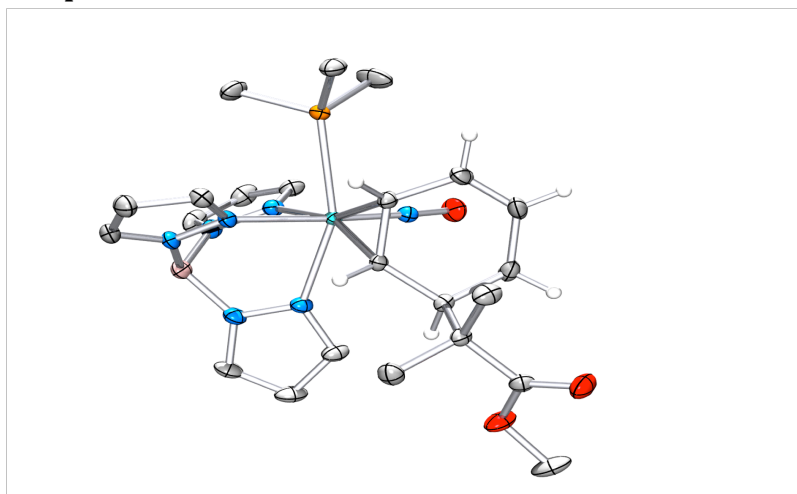
Appendix

$^1\text{H-NMR}$ (CD_3CN) and $^{13}\text{C-NMR}$ (CD_3CN) of Compound 4A:

$^1\text{H-NMR}$ (CD_3CN) and $^{13}\text{C-NMR}$ (CD_3CN) of Compound 5A:

$^1\text{H-NMR}$ (CD_3CN) and $^{13}\text{C-NMR}$ (CD_3CN) of Compound 6A:

Compound 6A



Compound 6ATable 1. Sample and crystal data for C₂₃H₃₅BN₇O₃PW

Chemical formula	C ₂₃ H ₃₅ BN ₇ O ₃ PW	
Formula weight	683.21 g/mol	
Temperature	150(2) K	
Wavelength	0.71073 Å	
Crystal size	0.156 x 0.204 x 0.394 mm	
Crystal habit	yellow rod	
Crystal system	monoclinic	
Space group	P 2 ₁ /c	
Unit cell dimensions	a = 12.1006(15) Å	α = 90°
	b = 11.2249(14) Å	β = 99.526(4)°
	c = 20.340(3) Å	γ = 90°
Volume	2724.6(6) Å ³	
Z	4	
Density (calculated)	1.666 g/cm ³	
Absorption coefficient	4.336 mm ⁻¹	
F(000)	1360	

Table 2. Data collection and structure refinement for C₂₃H₃₅BN₇O₃PW

Diffractometer	Bruker Kappa APEXII Duo
Radiation source	fine focus sealed-tube, Mo K _α
Theta range for data collection	1.71 to 29.62°
Index ranges	-15 ≤ h ≤ 16, -15 ≤ k ≤ 15, -28 ≤ l ≤ 24
Reflections collected	34138
Independent reflections	7660 [R(int) = 0.0164]
Coverage of independent reflections	99.7%
Absorption correction	Multi-Scan

Max. and min. transmission	0.5510 and 0.2800
Structure solution technique	direct methods
Structure solution program	SHELXT 2014/5 (Sheldrick, 2014)
Refinement method	Full-matrix least-squares on F^2
Refinement program	SHELXL-2016/6 (Sheldrick, 2016)
Function minimized	$\Sigma w(F_o^2 - F_c^2)^2$
Data / restraints / parameters	7660 / 0 / 335
Goodness-of-fit on F^2	1.060
Δ/σ_{\max}	0.006
Final R indices	7001 data; $I > 2\sigma(I)$ R1 = 0.0138, wR2 = 0.0317 all data R1 = 0.0168, wR2 = 0.0328
Weighting scheme	$w = 1/[\sigma^2(F_o^2) + (0.0130P)^2 + 1.4628P]$ where $P = (F_o^2 + 2F_c^2)/3$
Largest diff. peak and hole	0.538 and -0.894 $e\text{\AA}^{-3}$
R.M.S. deviation from mean	0.067 $e\text{\AA}^{-3}$

Table 3. Atomic coordinates and equivalent isotropic atomic displacement parameters (\AA^2) for $C_{23}H_{35}BN_7O_3PW$

U(eq) is defined as one third of the trace of the orthogonalized U_{ij} tensor.

	x/a	y/b	z/c	U(eq)
W1	0.22854(2)	0.75778(2)	0.38405(2)	0.01337(2)
P1	0.05465(3)	0.71126(3)	0.30328(2)	0.01763(7)
O1	0.18151(10)	0.02052(10)	0.37716(7)	0.0310(3)

	x/a	y/b	z/c	U(eq)
O2	0.71431(10)	0.96575(11)	0.30345(6)	0.0315(3)
O3	0.69189(10)	0.93772(11)	0.40884(6)	0.0301(3)
N1	0.11151(11)	0.74755(11)	0.45668(7)	0.0193(2)
N2	0.11977(11)	0.66380(12)	0.50550(7)	0.0221(3)
N3	0.24101(10)	0.55804(11)	0.39599(6)	0.0171(2)
N4	0.22959(10)	0.50678(11)	0.45540(6)	0.0192(2)
N5	0.34116(10)	0.75214(11)	0.48254(6)	0.0188(2)
N6	0.32617(11)	0.66699(12)	0.52848(6)	0.0215(3)
N7	0.20509(10)	0.91354(11)	0.37867(6)	0.0183(2)
C1	0.38890(11)	0.75059(12)	0.34685(7)	0.0149(2)
C2	0.30121(12)	0.74087(12)	0.28957(7)	0.0171(3)
C3	0.28508(12)	0.84168(15)	0.24260(8)	0.0231(3)
C4	0.34091(13)	0.94378(15)	0.25386(9)	0.0261(3)
C5	0.42255(12)	0.96592(13)	0.31649(8)	0.0224(3)
C6	0.47341(11)	0.85193(12)	0.35186(7)	0.0161(3)
C7	0.58507(11)	0.81273(13)	0.32821(7)	0.0169(3)
C8	0.63540(13)	0.70408(15)	0.36915(9)	0.0247(3)
C9	0.57012(13)	0.78410(16)	0.25394(8)	0.0246(3)
C10	0.66945(12)	0.91366(13)	0.34344(8)	0.0194(3)
C11	0.77429(14)	0.02912(18)	0.42864(11)	0.0367(4)
C12	0.03126(12)	0.82334(15)	0.46735(8)	0.0237(3)
C13	0.98651(14)	0.78971(17)	0.52339(9)	0.0299(4)
C14	0.04529(14)	0.68849(16)	0.54624(9)	0.0292(4)
C15	0.25085(12)	0.46805(13)	0.35392(8)	0.0204(3)
C16	0.24588(13)	0.35870(14)	0.38590(8)	0.0251(3)
C17	0.23312(13)	0.38733(14)	0.44984(8)	0.0234(3)
C18	0.42692(13)	0.81912(15)	0.51118(8)	0.0240(3)
C19	0.46943(14)	0.77701(17)	0.57477(8)	0.0294(4)
C20	0.40302(14)	0.68126(16)	0.58384(8)	0.0273(3)

	x/a	y/b	z/c	U(eq)
C21	0.96679(14)	0.60049(17)	0.33543(9)	0.0312(4)
C22	0.05865(14)	0.65296(15)	0.22037(8)	0.0261(3)
C23	0.96142(17)	0.83716(17)	0.28415(11)	0.0406(5)
B1	0.22438(15)	0.58269(16)	0.51746(9)	0.0222(3)

Table 4. Bond lengths (Å) for C₂₃H₃₅BN₇O₃PW

W1-N7	1.7718(13)	W1-C1	2.1978(14)
W1-N1	2.2121(13)	W1-N5	2.2296(13)
W1-C2	2.2498(15)	W1-N3	2.2575(13)
W1-P1	2.5010(4)	P1-C23	1.8100(17)
P1-C22	1.8170(17)	P1-C21	1.8260(17)
O1-N7	1.2335(17)	O2-C10	1.2018(19)
O3-C10	1.3405(19)	O3-C11	1.441(2)
N1-C12	1.335(2)	N1-N2	1.3590(18)
N2-C14	1.350(2)	N2-B1	1.546(2)
N3-C15	1.3418(19)	N3-N4	1.3659(17)
N4-C17	1.3468(19)	N4-B1	1.533(2)
N5-C18	1.3347(19)	N5-N6	1.3695(18)
N6-C20	1.3460(19)	N6-B1	1.540(2)
C1-C2	1.444(2)	C1-C6	1.5218(18)
C1-H1	1.0	C2-C3	1.473(2)
C2-H2	1.0	C3-C4	1.331(2)
C3-H3	0.95	C4-C5	1.498(2)
C4-H4	0.95	C5-C6	1.545(2)
C5-H5A	0.99	C5-H5B	0.99
C6-C7	1.5703(19)	C6-H6	1.0
C7-C10	1.522(2)	C7-C9	1.526(2)
C7-C8	1.544(2)	C8-H8A	0.98
C8-H8B	0.98	C8-H8C	0.98
C9-H9A	0.98	C9-H9B	0.98
C9-H9C	0.98	C11-H11A	0.98
C11-H11B	0.98	C11-H11C	0.98
C12-C13	1.393(2)	C12-H12	0.95

C13-C14	1.380(3)	C13-H13	0.95
C14-H14	0.95	C15-C16	1.395(2)
C15-H15	0.95	C16-C17	1.373(2)
C16-H16	0.95	C17-H17	0.95
C18-C19	1.393(2)	C18-H18	0.95
C19-C20	1.373(3)	C19-H19	0.95
C20-H20	0.95	C21-H21A	0.98
C21-H21B	0.98	C21-H21C	0.98
C22-H22A	0.98	C22-H22B	0.98
C22-H22C	0.98	C23-H23A	0.98
C23-H23B	0.98	C23-H23C	0.98
B1-H1A	1.106(18)		

Table 5. Bond angles (°) for C₂₃H₃₅BN₇O₃PW.

N7-W1-C1	99.00(5)	N7-W1-N1	88.79(5)
C1-W1-N1	158.01(5)	N7-W1-N5	98.71(5)
C1-W1-N5	82.25(5)	N1-W1-N5	76.24(5)
N7-W1-C2	96.41(5)	C1-W1-C2	37.88(5)
N1-W1-C2	161.80(5)	N5-W1-C2	119.86(5)
N7-W1-N3	173.66(5)	C1-W1-N3	87.33(5)
N1-W1-N3	85.15(4)	N5-W1-N3	81.67(4)
C2-W1-N3	88.82(5)	N7-W1-P1	93.25(4)
C1-W1-P1	117.45(4)	N1-W1-P1	82.29(4)
N5-W1-P1	155.10(3)	C2-W1-P1	80.01(4)
N3-W1-P1	84.11(3)	C23-P1-C22	101.13(9)
C23-P1-C21	103.26(10)	C22-P1-C21	101.17(8)
C23-P1-W1	113.89(6)	C22-P1-W1	122.42(5)
C21-P1-W1	112.54(6)	C10-O3-C11	115.98(14)
C12-N1-N2	106.83(13)	C12-N1-W1	129.68(11)
N2-N1-W1	123.10(9)	C14-N2-N1	109.31(14)
C14-N2-B1	129.56(14)	N1-N2-B1	118.80(12)
C15-N3-N4	106.24(12)	C15-N3-W1	133.67(10)
N4-N3-W1	119.92(9)	C17-N4-N3	109.63(13)
C17-N4-B1	128.95(13)	N3-N4-B1	121.22(12)
C18-N5-N6	106.06(12)	C18-N5-W1	133.76(11)
N6-N5-W1	120.17(9)	C20-N6-N5	109.66(13)
C20-N6-B1	128.32(14)	N5-N6-B1	121.51(12)

O1-N7-W1	175.04(12)	C2-C1-C6	120.42(12)
C2-C1-W1	73.01(8)	C6-C1-W1	124.85(9)
C2-C1-H1	111.1	C6-C1-H1	111.1
W1-C1-H1	111.1	C1-C2-C3	117.77(12)
C1-C2-W1	69.11(8)	C3-C2-W1	117.42(10)
C1-C2-H2	115.0	C3-C2-H2	115.0
W1-C2-H2	115.0	C4-C3-C2	122.75(14)
C4-C3-H3	118.6	C2-C3-H3	118.6
C3-C4-C5	122.26(14)	C3-C4-H4	118.9
C5-C4-H4	118.9	C4-C5-C6	114.48(13)
C4-C5-H5A	108.6	C6-C5-H5A	108.6
C4-C5-H5B	108.6	C6-C5-H5B	108.6
H5A-C5-H5B	107.6	C1-C6-C5	112.11(11)
C1-C6-C7	111.89(11)	C5-C6-C7	112.71(12)
C1-C6-H6	106.5	C5-C6-H6	106.5
C7-C6-H6	106.5	C10-C7-C9	108.90(12)
C10-C7-C8	106.66(12)	C9-C7-C8	109.83(13)
C10-C7-C6	108.13(11)	C9-C7-C6	113.29(12)
C8-C7-C6	109.80(12)	C7-C8-H8A	109.5
C7-C8-H8B	109.5	H8A-C8-H8B	109.5
C7-C8-H8C	109.5	H8A-C8-H8C	109.5
H8B-C8-H8C	109.5	C7-C9-H9A	109.5
C7-C9-H9B	109.5	H9A-C9-H9B	109.5
C7-C9-H9C	109.5	H9A-C9-H9C	109.5
H9B-C9-H9C	109.5	O2-C10-O3	122.25(14)
O2-C10-C7	125.96(14)	O3-C10-C7	111.77(13)
O3-C11-H11A	109.5	O3-C11-H11B	109.5
H11A-C11-H11B	109.5	O3-C11-H11C	109.5
H11A-C11-H11C	109.5	H11B-C11-H11C	109.5
N1-C12-C13	110.61(15)	N1-C12-H12	124.7
C13-C12-H12	124.7	C14-C13-C12	104.49(15)
C14-C13-H13	127.8	C12-C13-H13	127.8
N2-C14-C13	108.76(15)	N2-C14-H14	125.6
C13-C14-H14	125.6	N3-C15-C16	110.47(14)
N3-C15-H15	124.8	C16-C15-H15	124.8
C17-C16-C15	104.84(14)	C17-C16-H16	127.6
C15-C16-H16	127.6	N4-C17-C16	108.82(14)

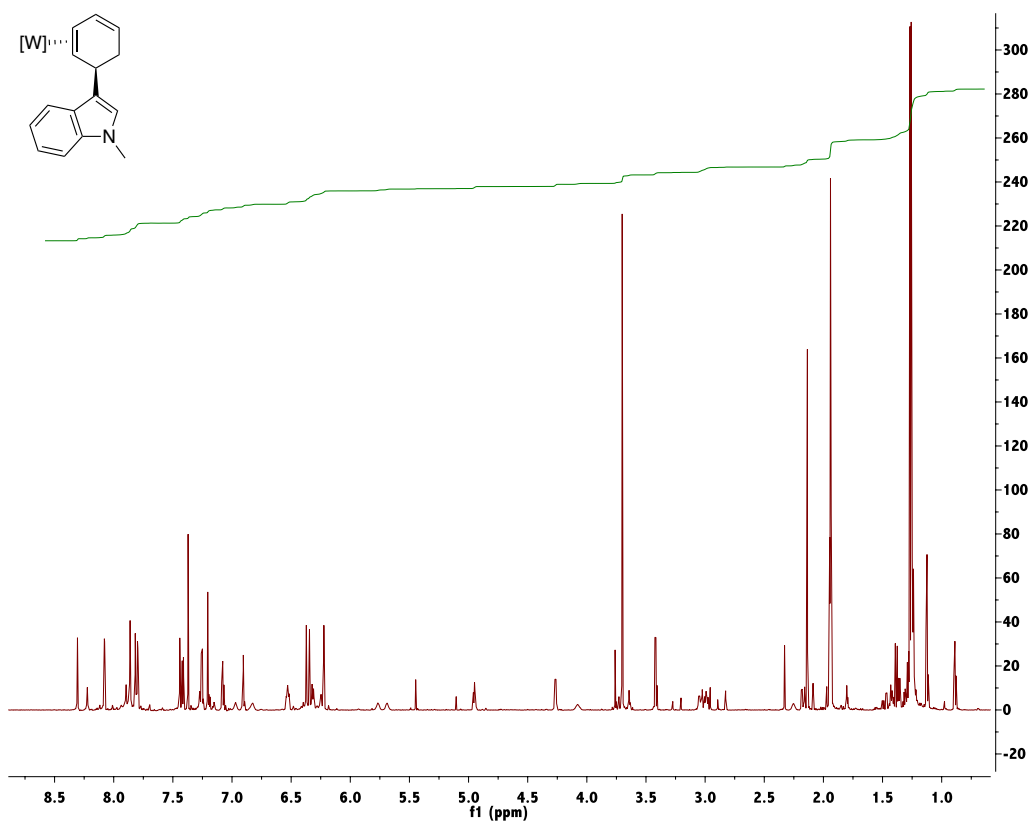
N4-C17-H17	125.6	C16-C17-H17	125.6
N5-C18-C19	110.79(15)	N5-C18-H18	124.6
C19-C18-H18	124.6	C20-C19-C18	104.83(14)
C20-C19-H19	127.6	C18-C19-H19	127.6
N6-C20-C19	108.64(15)	N6-C20-H20	125.7
C19-C20-H20	125.7	P1-C21-H21A	109.5
P1-C21-H21B	109.5	H21A-C21-H21B	109.5
P1-C21-H21C	109.5	H21A-C21-H21C	109.5
H21B-C21-H21C	109.5	P1-C22-H22A	109.5
P1-C22-H22B	109.5	H22A-C22-H22B	109.5
P1-C22-H22C	109.5	H22A-C22-H22C	109.5
H22B-C22-H22C	109.5	P1-C23-H23A	109.5
P1-C23-H23B	109.5	H23A-C23-H23B	109.5
P1-C23-H23C	109.5	H23A-C23-H23C	109.5
H23B-C23-H23C	109.5	N4-B1-N6	108.69(13)
N4-B1-N2	110.01(13)	N6-B1-N2	105.99(13)
N4-B1-H1A	111.0(9)	N6-B1-H1A	110.6(9)
N2-B1-H1A	110.4(9)		

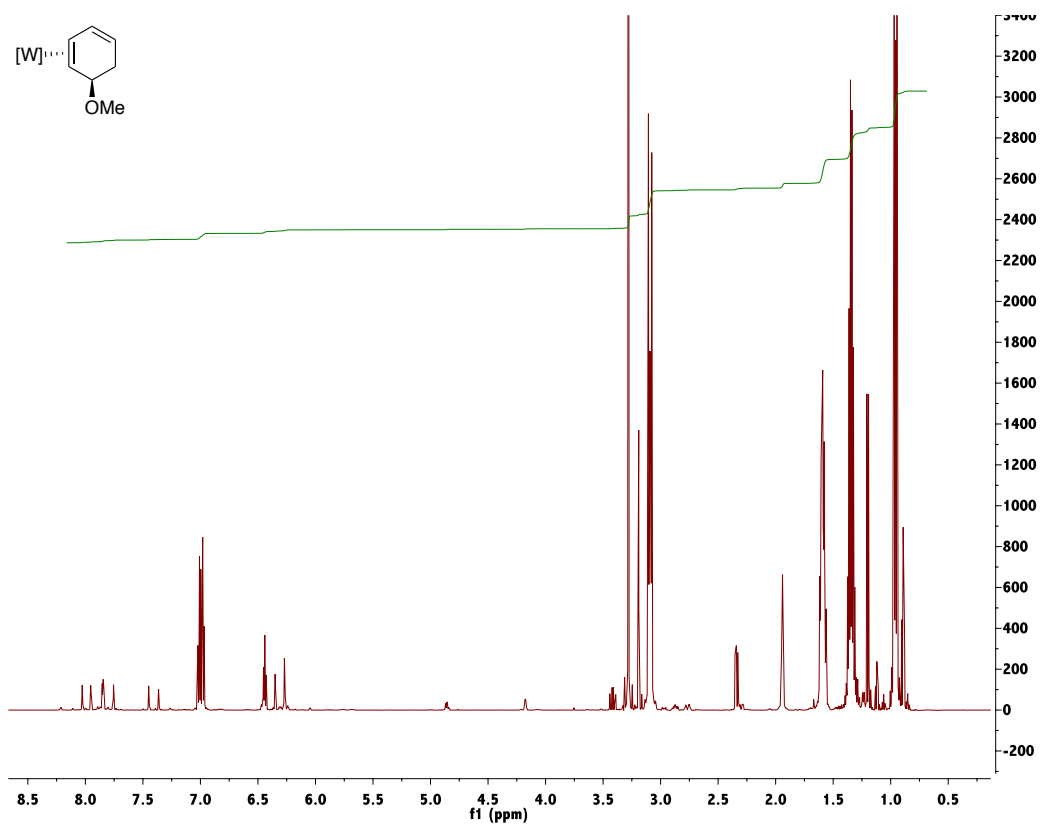
Table 6. Anisotropic atomic displacement parameters (\AA^2) for $\text{C}_{23}\text{H}_{35}\text{BN}_7\text{O}_3\text{PW}$.

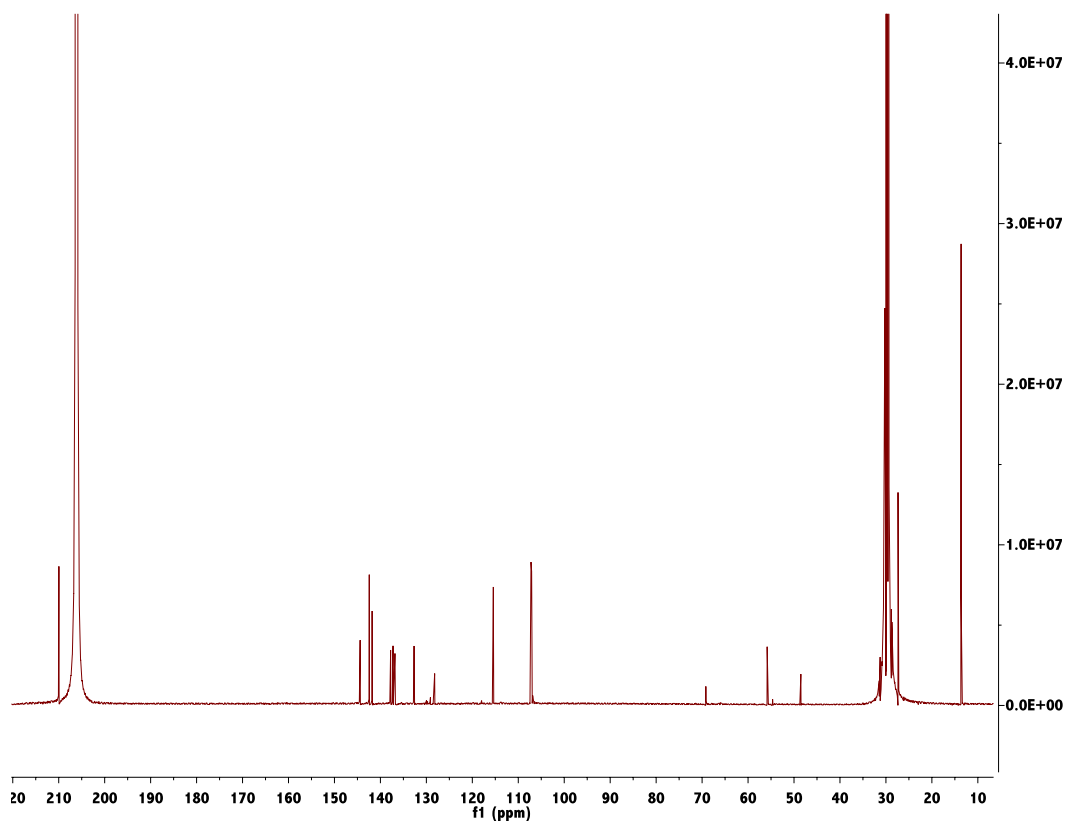
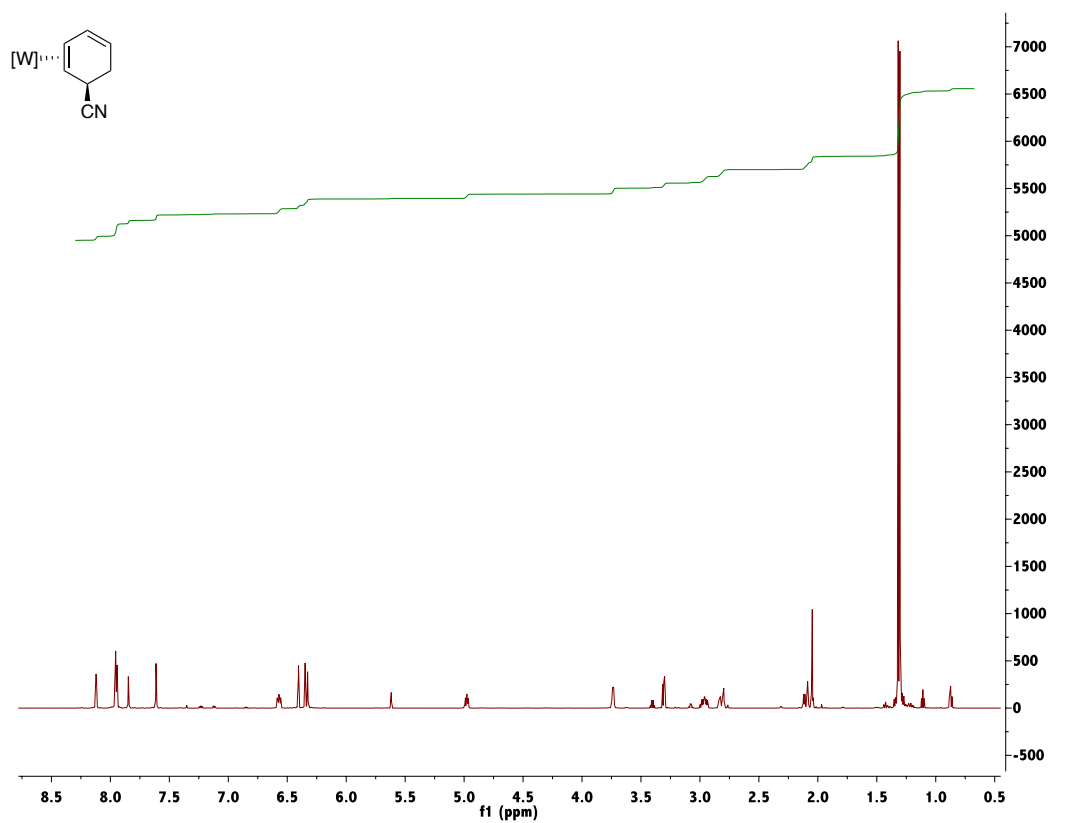
The anisotropic atomic displacement factor exponent takes the form: $-2\pi^2 [h^2 a^{*2} U_{11} + \dots + 2 h k a^* b^* U_{12}]$

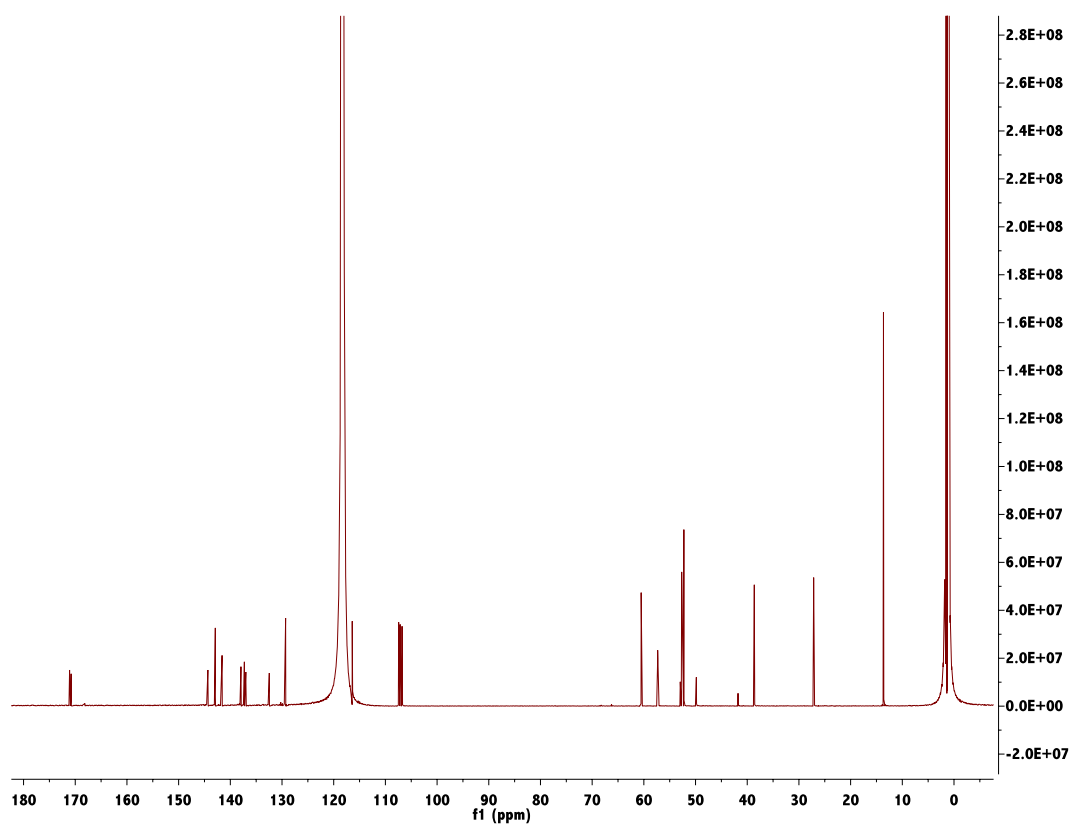
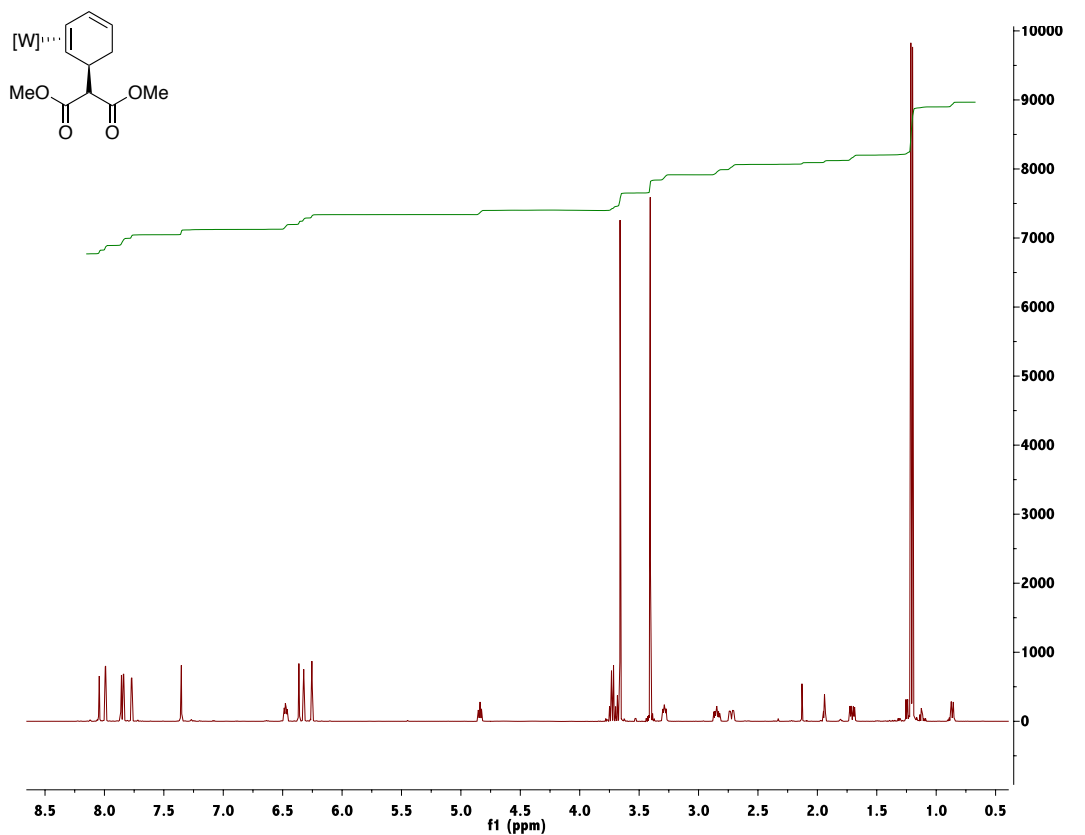
	U_{11}	U_{22}	U_{33}	U_{23}	U_{13}	U_{12}
W1	0.01304(3)	0.01559(3)	0.01123(3)	0.00091(2)	0.00124(2)	-0.00115(2)
P1	0.01586(16)	0.01833(16)	0.01730(17)	0.00146(14)	-0.00139(13)	-0.00023(13)
O1	0.0339(6)	0.0184(5)	0.0401(8)	-0.0003(5)	0.0046(5)	0.0054(5)
O2	0.0298(6)	0.0370(7)	0.0295(7)	0.0009(5)	0.0100(5)	-0.0129(5)
O3	0.0274(6)	0.0396(7)	0.0230(6)	-0.0112(5)	0.0035(5)	-0.0131(5)
N1	0.0173(6)	0.0244(6)	0.0164(6)	0.0002(5)	0.0032(4)	-0.0013(5)
N2	0.0230(6)	0.0275(7)	0.0168(6)	0.0017(5)	0.0064(5)	-0.0041(5)
N3	0.0185(6)	0.0188(6)	0.0137(6)	0.0035(4)	0.0022(4)	-0.0014(4)
N4	0.0213(6)	0.0206(6)	0.0153(6)	0.0053(5)	0.0016(4)	-0.0018(5)
N5	0.0175(6)	0.0252(6)	0.0134(6)	-0.0004(5)	0.0020(4)	-0.0013(5)

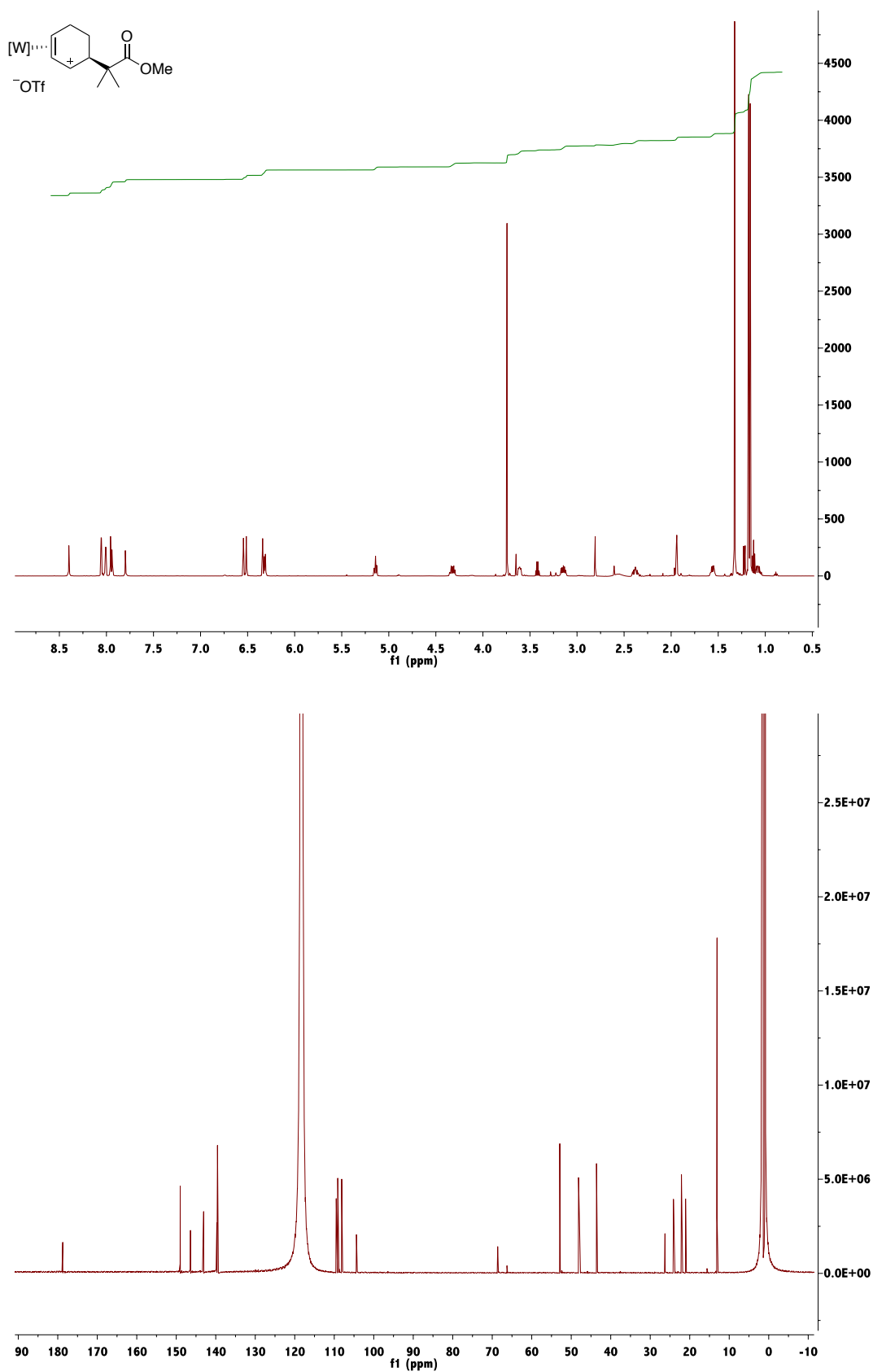
	U ₁₁	U ₂₂	U ₃₃	U ₂₃	U ₁₃	U ₁₂
N6	0.0229(6)	0.0268(7)	0.0140(6)	0.0017(5)	0.0002(5)	-0.0003(5)
N7	0.0181(6)	0.0197(6)	0.0167(6)	-0.0002(5)	0.0019(4)	0.0002(4)
C1	0.0141(6)	0.0162(6)	0.0149(6)	0.0010(5)	0.0037(5)	-0.0011(5)
C2	0.0175(6)	0.0193(7)	0.0149(6)	-0.0003(5)	0.0035(5)	-0.0035(5)
C3	0.0201(7)	0.0326(8)	0.0161(7)	0.0061(6)	0.0016(5)	-0.0024(6)
C4	0.0228(7)	0.0270(8)	0.0285(9)	0.0135(6)	0.0048(6)	0.0002(6)
C5	0.0196(7)	0.0164(7)	0.0320(9)	0.0028(6)	0.0066(6)	-0.0019(5)
C6	0.0161(6)	0.0173(6)	0.0154(7)	-0.0018(5)	0.0043(5)	-0.0015(5)
C7	0.0166(6)	0.0197(7)	0.0149(7)	-0.0009(5)	0.0040(5)	-0.0022(5)
C8	0.0210(7)	0.0255(8)	0.0280(8)	0.0034(6)	0.0054(6)	0.0049(6)
C9	0.0236(7)	0.0334(8)	0.0177(7)	-0.0059(6)	0.0064(6)	-0.0050(6)
C10	0.0148(6)	0.0224(7)	0.0212(7)	-0.0016(6)	0.0034(5)	0.0007(5)
C11	0.0218(8)	0.0414(10)	0.0456(12)	-0.0218(9)	0.0016(7)	-0.0087(7)
C12	0.0178(7)	0.0285(8)	0.0252(8)	-0.0041(6)	0.0043(6)	-0.0019(6)
C13	0.0249(8)	0.0354(9)	0.0327(9)	-0.0070(7)	0.0146(7)	-0.0051(7)
C14	0.0310(8)	0.0357(9)	0.0240(8)	-0.0021(7)	0.0138(7)	-0.0084(7)
C15	0.0209(7)	0.0207(7)	0.0195(7)	0.0008(6)	0.0029(5)	0.0017(5)
C16	0.0285(8)	0.0190(7)	0.0269(8)	0.0017(6)	0.0015(6)	0.0022(6)
C17	0.0242(7)	0.0204(7)	0.0239(8)	0.0069(6)	-0.0006(6)	-0.0018(6)
C18	0.0213(7)	0.0340(8)	0.0169(7)	-0.0058(6)	0.0039(5)	-0.0062(6)
C19	0.0222(7)	0.0458(10)	0.0184(8)	-0.0083(7)	-0.0016(6)	-0.0033(7)
C20	0.0286(8)	0.0364(9)	0.0148(7)	-0.0001(6)	-0.0028(6)	0.0040(7)
C21	0.0240(8)	0.0408(10)	0.0286(9)	0.0011(7)	0.0039(6)	-0.0137(7)
C22	0.0257(8)	0.0318(8)	0.0193(8)	-0.0027(6)	-0.0005(6)	-0.0079(6)
C23	0.0383(10)	0.0349(10)	0.0416(11)	-0.0043(8)	-0.0141(8)	0.0168(8)
B1	0.0261(8)	0.0254(8)	0.0149(8)	0.0034(6)	0.0031(6)	-0.0035(7)

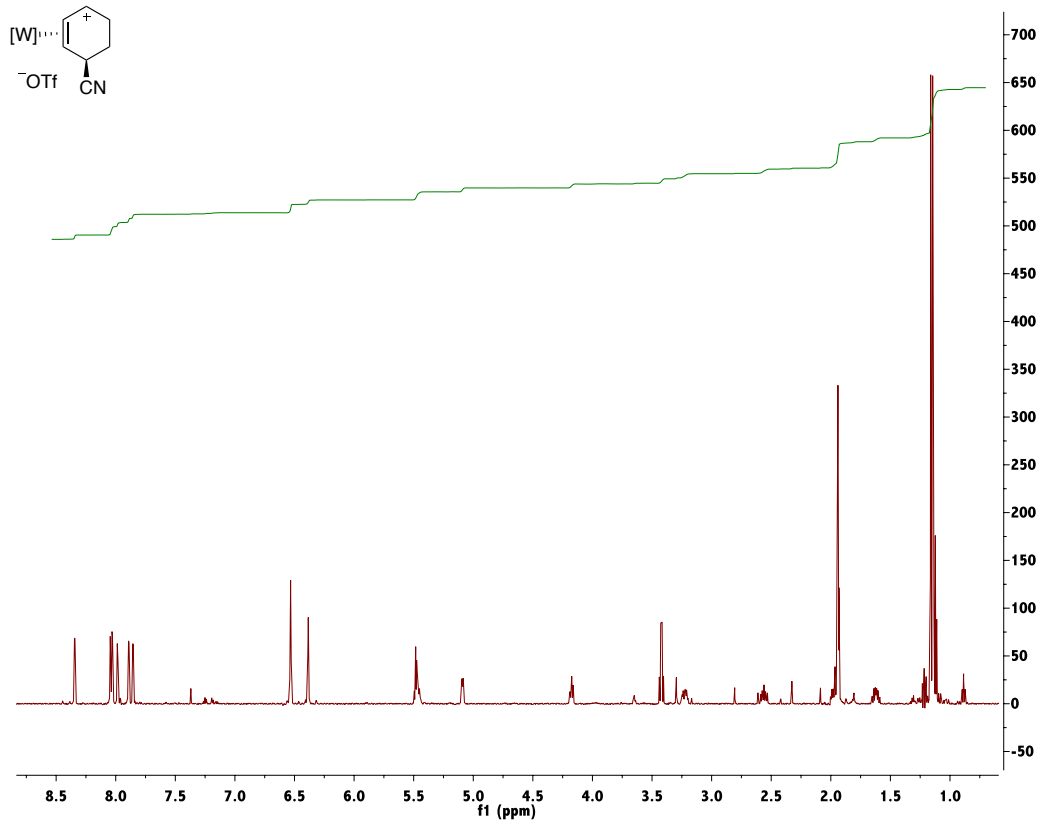
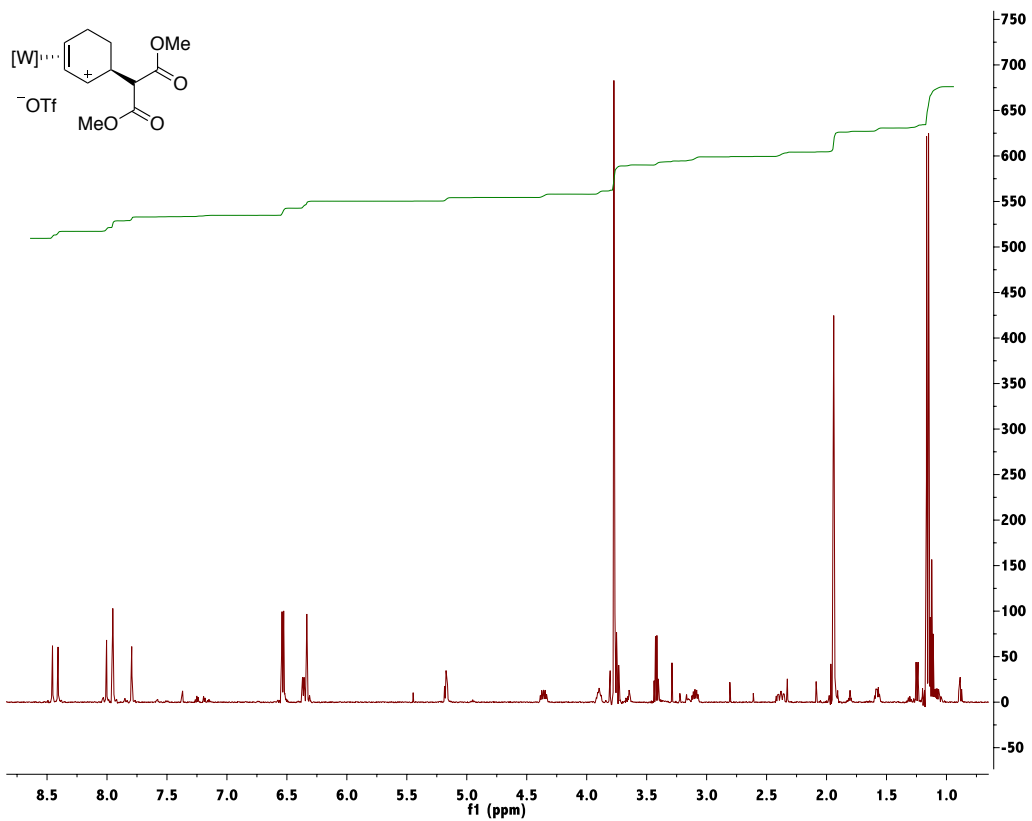
$^1\text{H-NMR}$ (CD_3CN) of Compound 7:

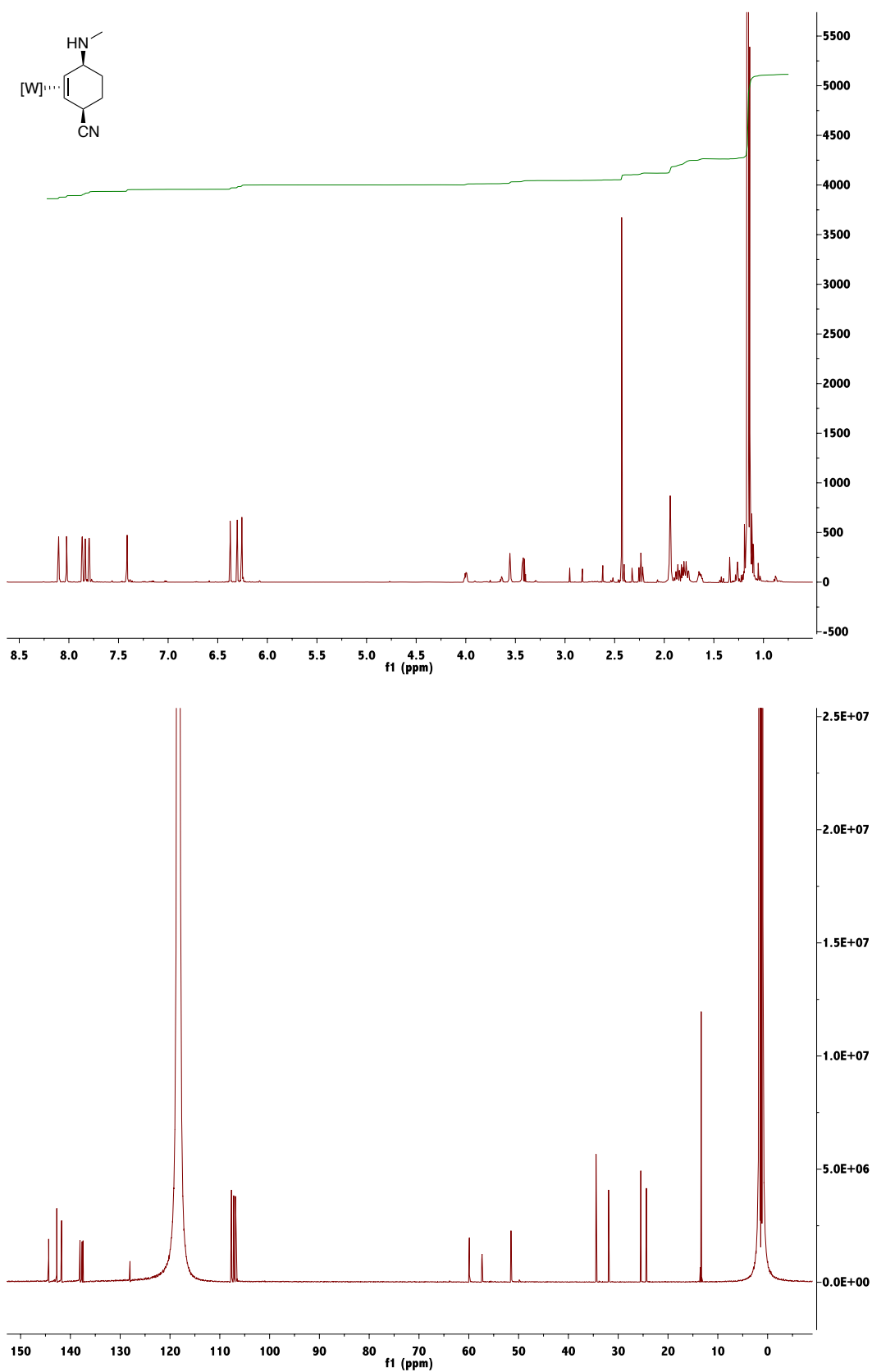
$^1\text{H-NMR}$ (CD_3CN) of Compound 9A:

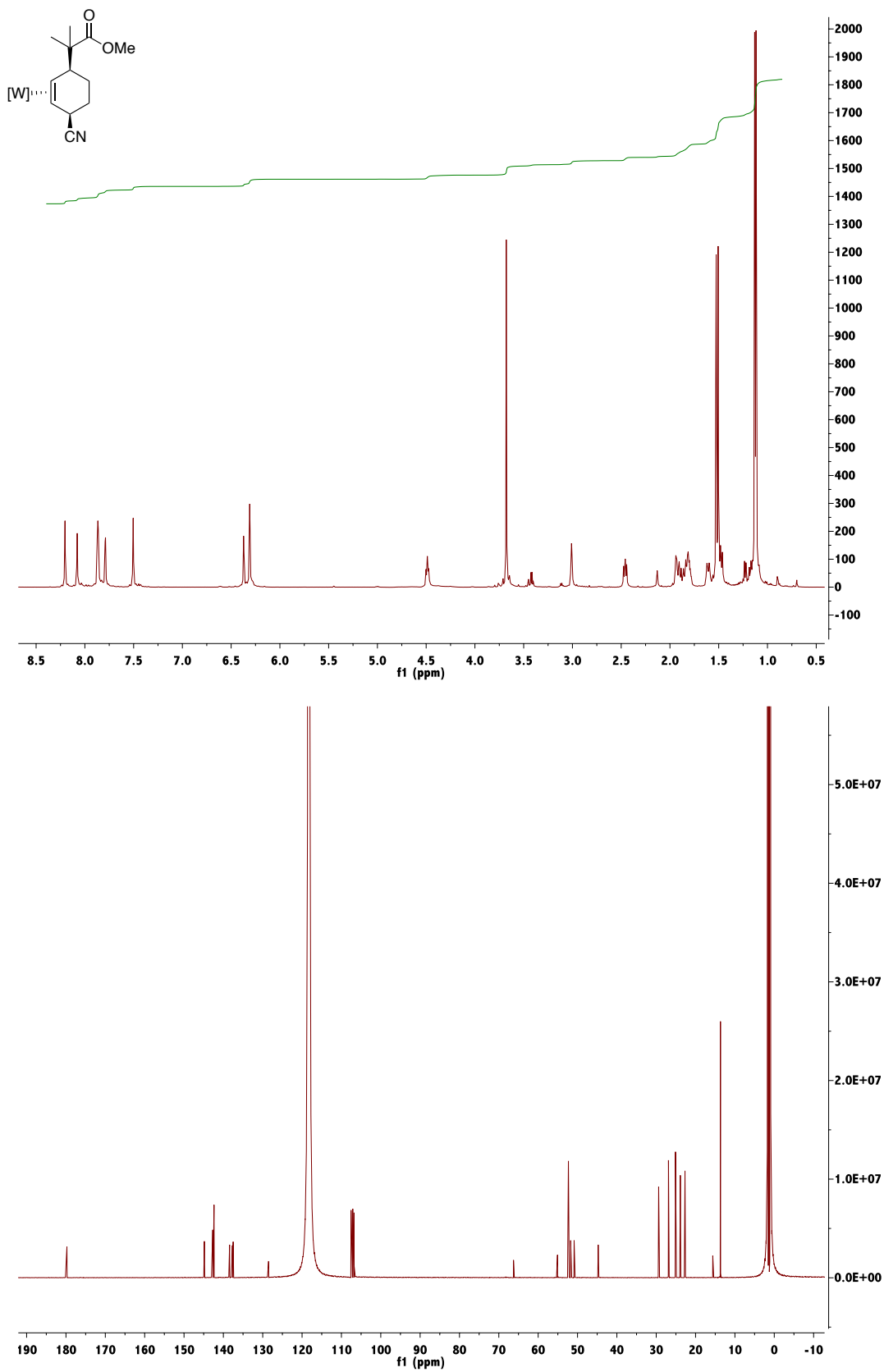
$^1\text{H-NMR}$ ($\text{d}^6\text{-acetone}$) and $^{13}\text{C-NMR}$ ($\text{d}^6\text{-acetone}$) of Compound 10A:

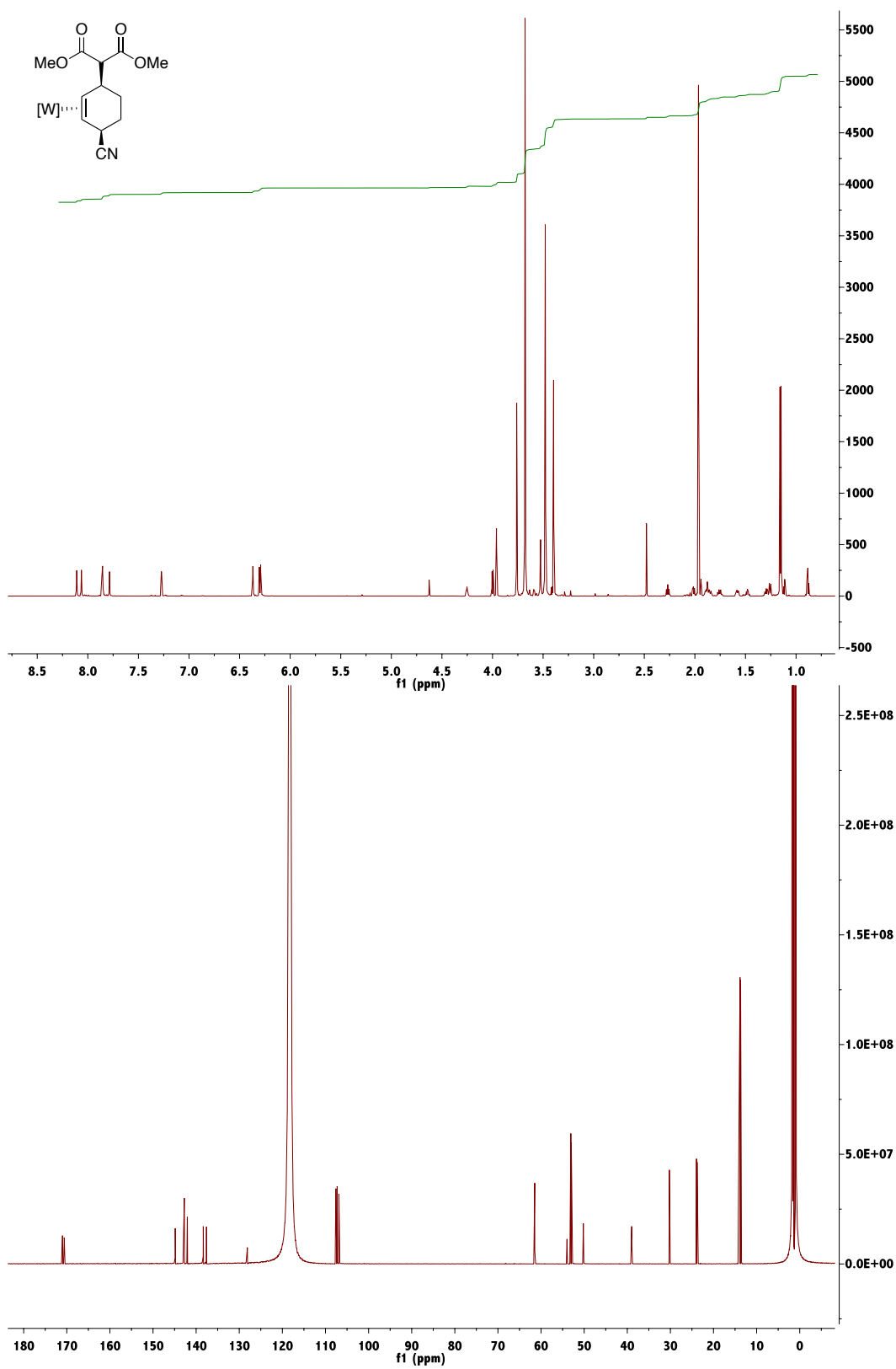
$^1\text{H-NMR}$ (CD_3CN) and $^{13}\text{C-NMR}$ (CD_3CN) of Compound 11A:

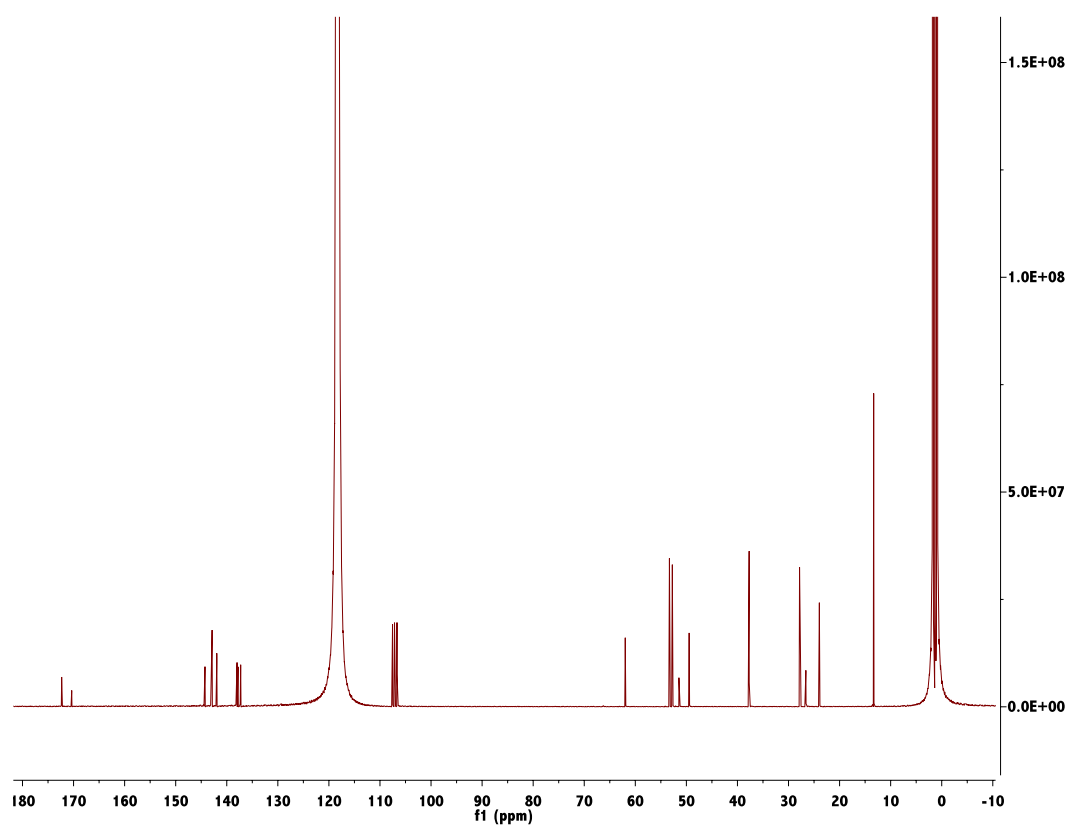
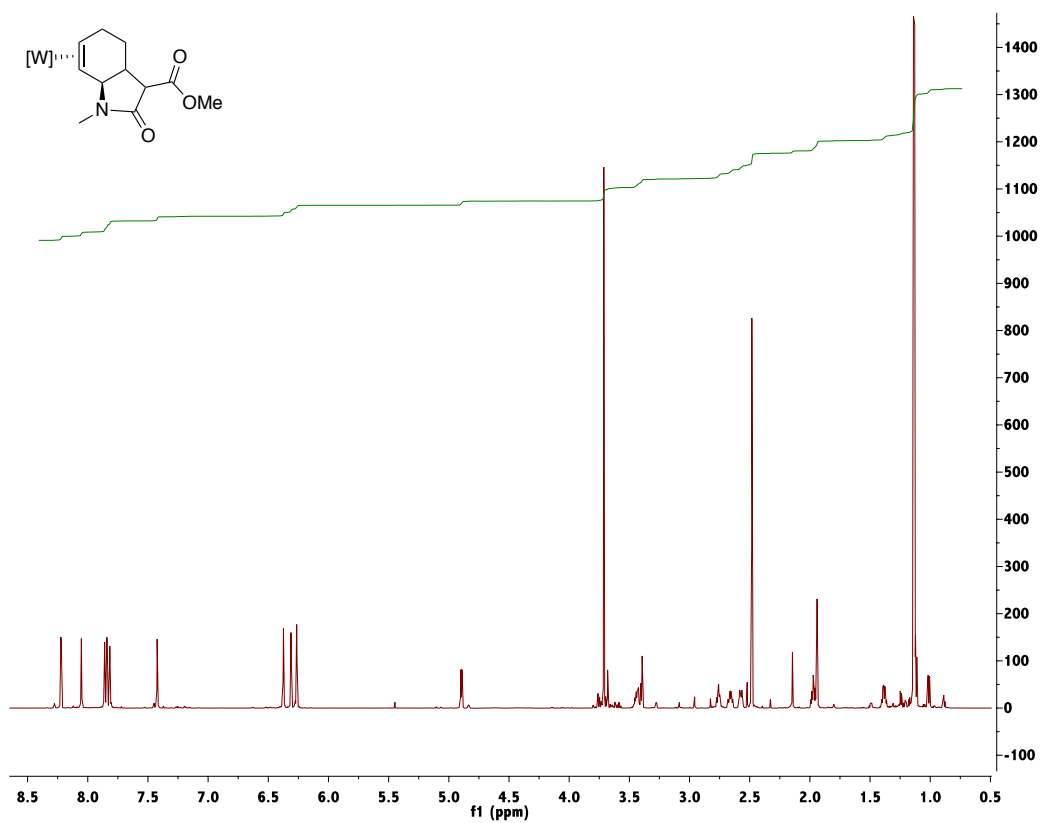
$^1\text{H-NMR}$ (CD_3CN) and $^{13}\text{C-NMR}$ (CD_3CN) of Compound 12:

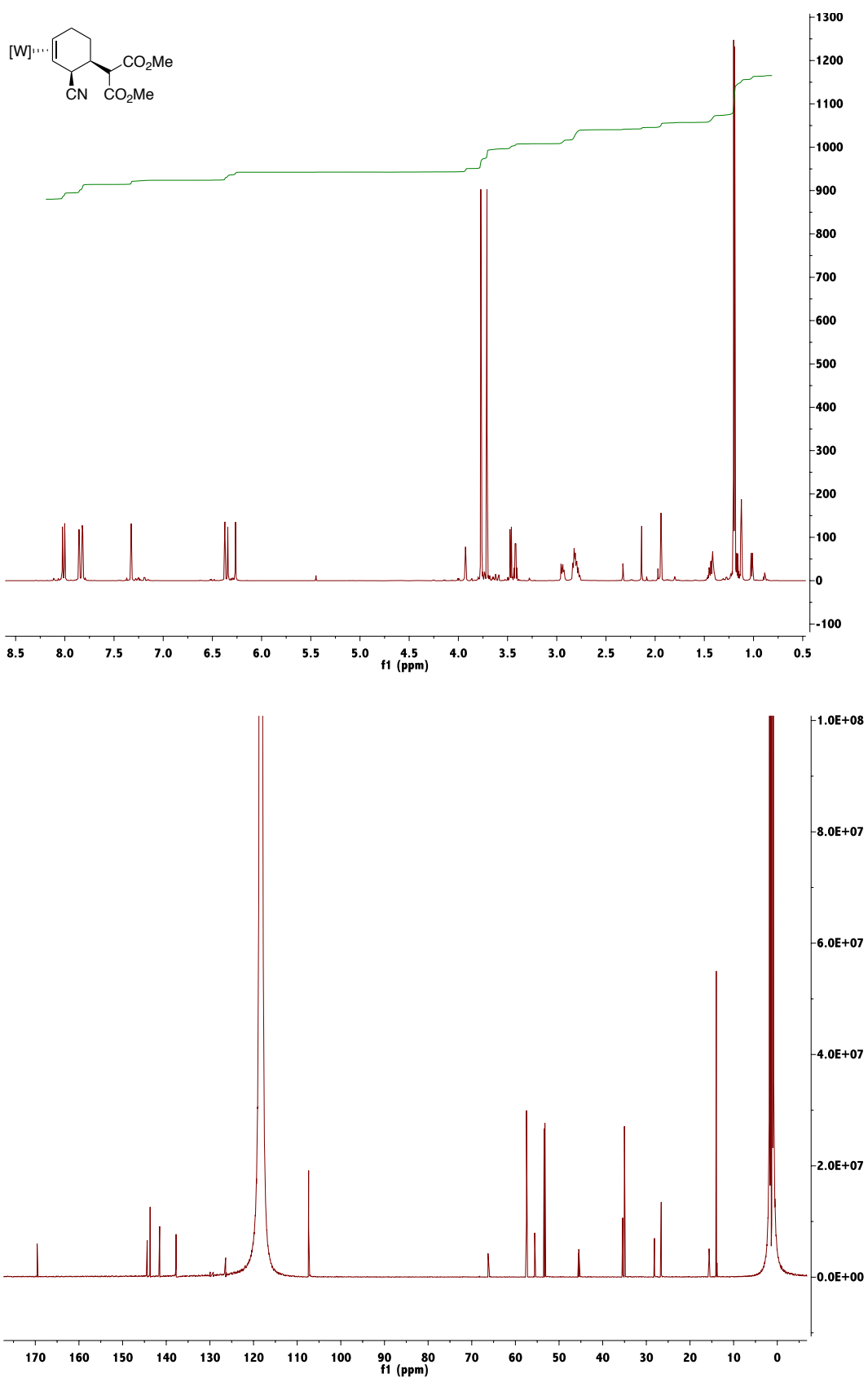
¹H-NMR (CD₃CN) of Compound 13:**¹H-NMR (CD₃CN) of Compound 14:**

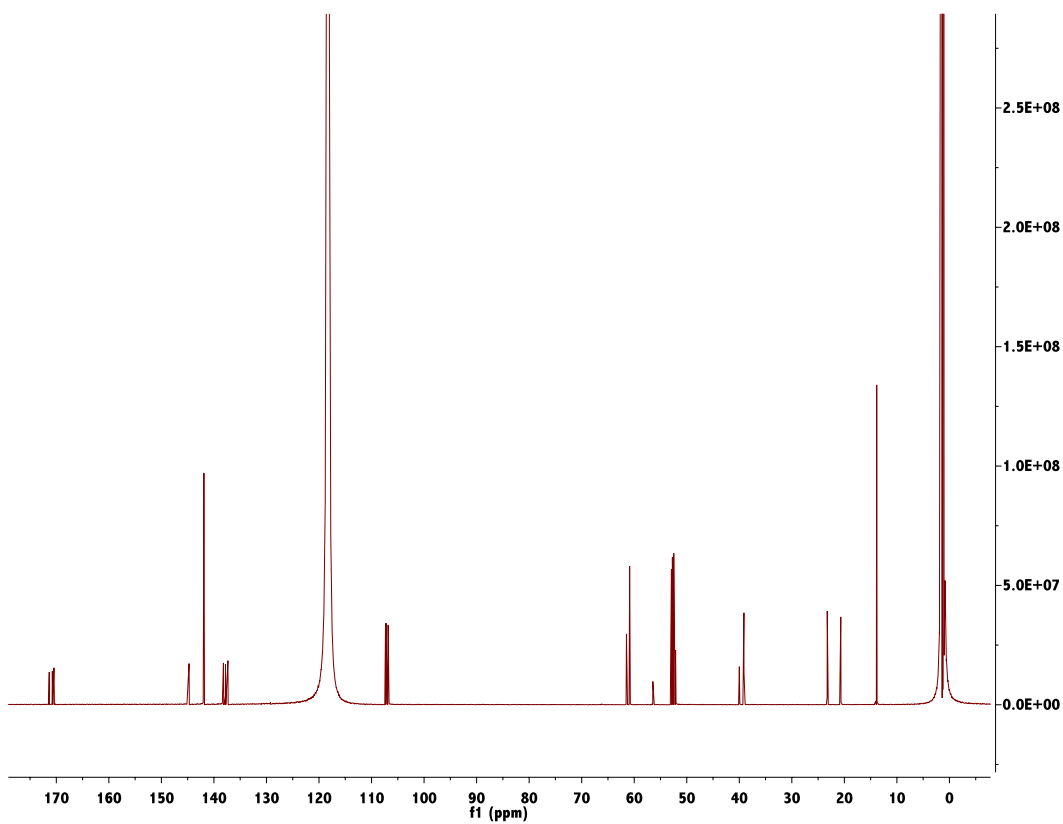
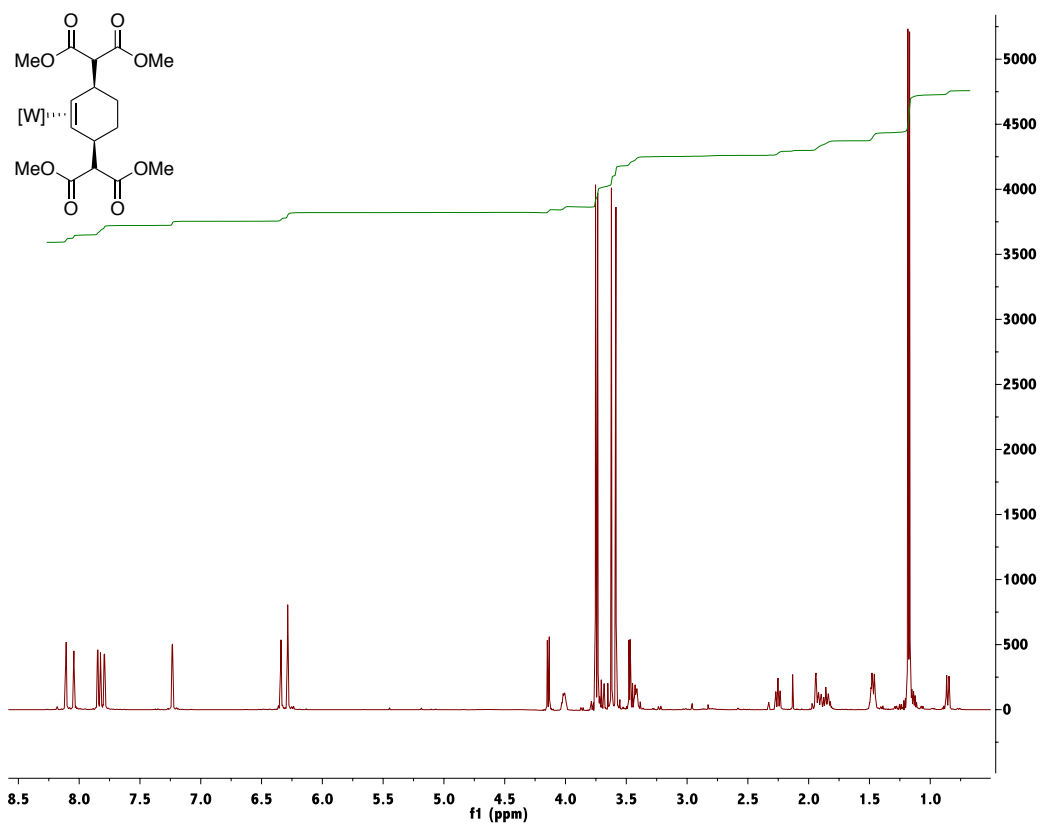
$^1\text{H-NMR}$ (CD_3CN) and $^{13}\text{C-NMR}$ (CD_3CN) of Compound 15A:

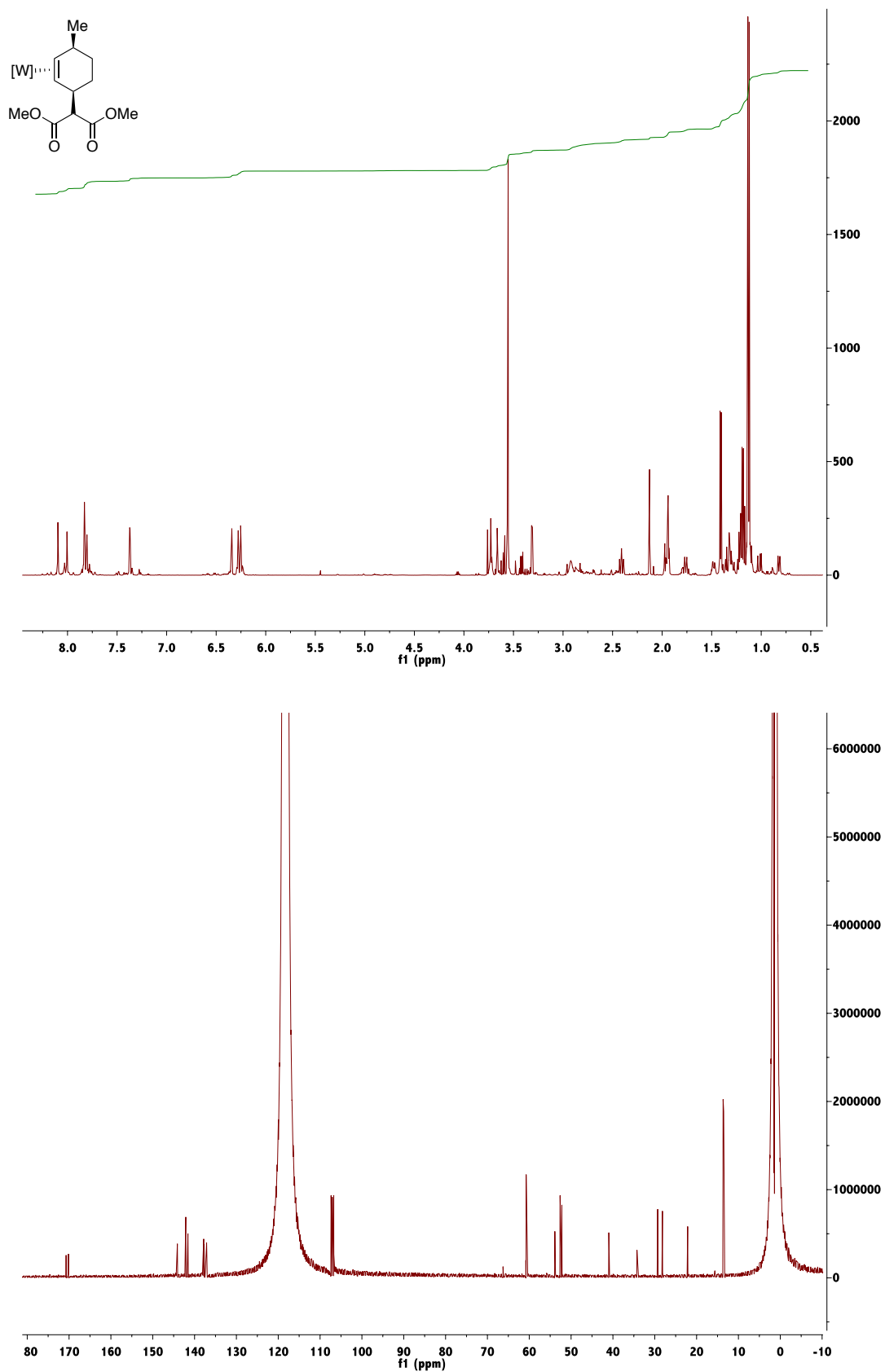
$^1\text{H-NMR}$ (CD_3CN) and $^{13}\text{C-NMR}$ (CD_3CN) of Compound 16A:

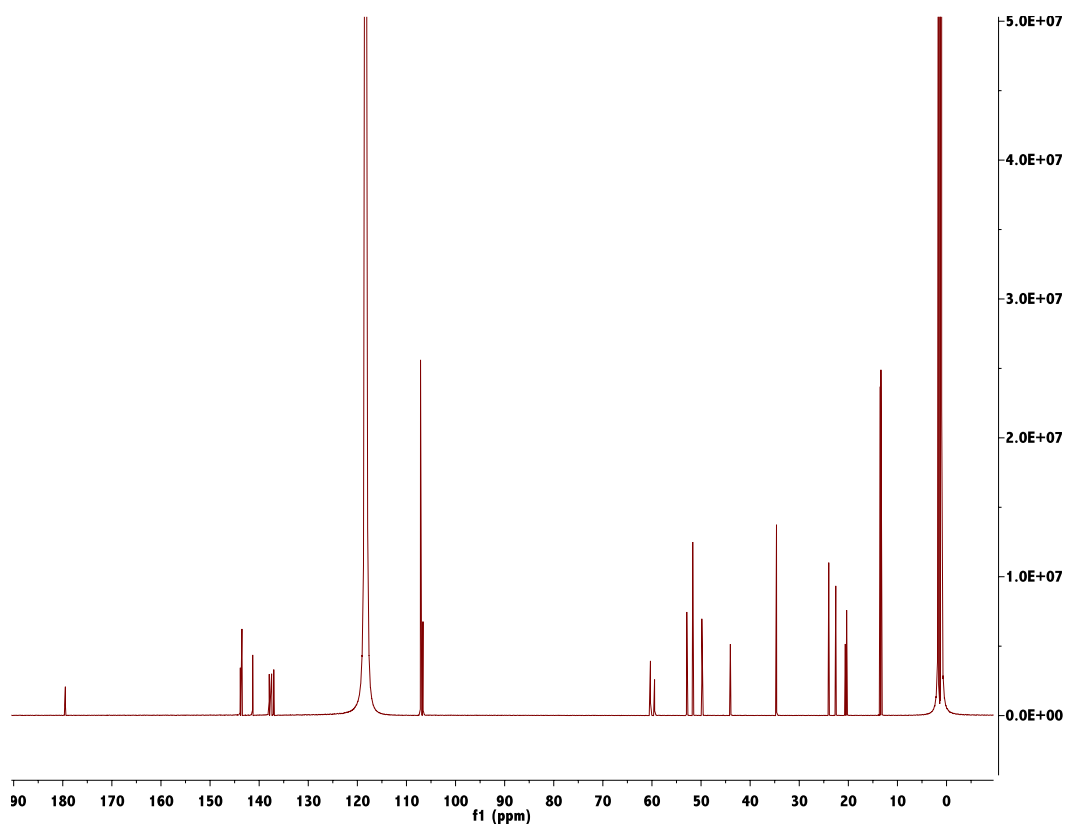
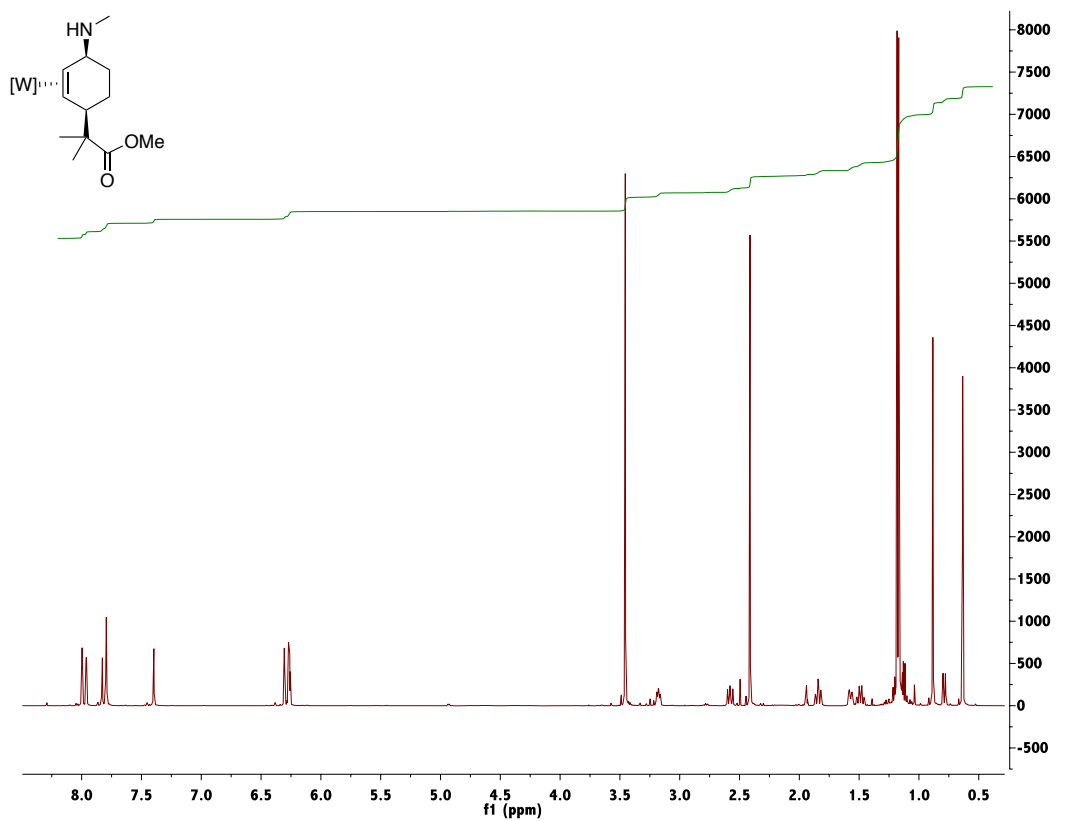
$^1\text{H-NMR}$ (CD_3CN) and $^{13}\text{C-NMR}$ (CD_3CN) of Compound 18A:

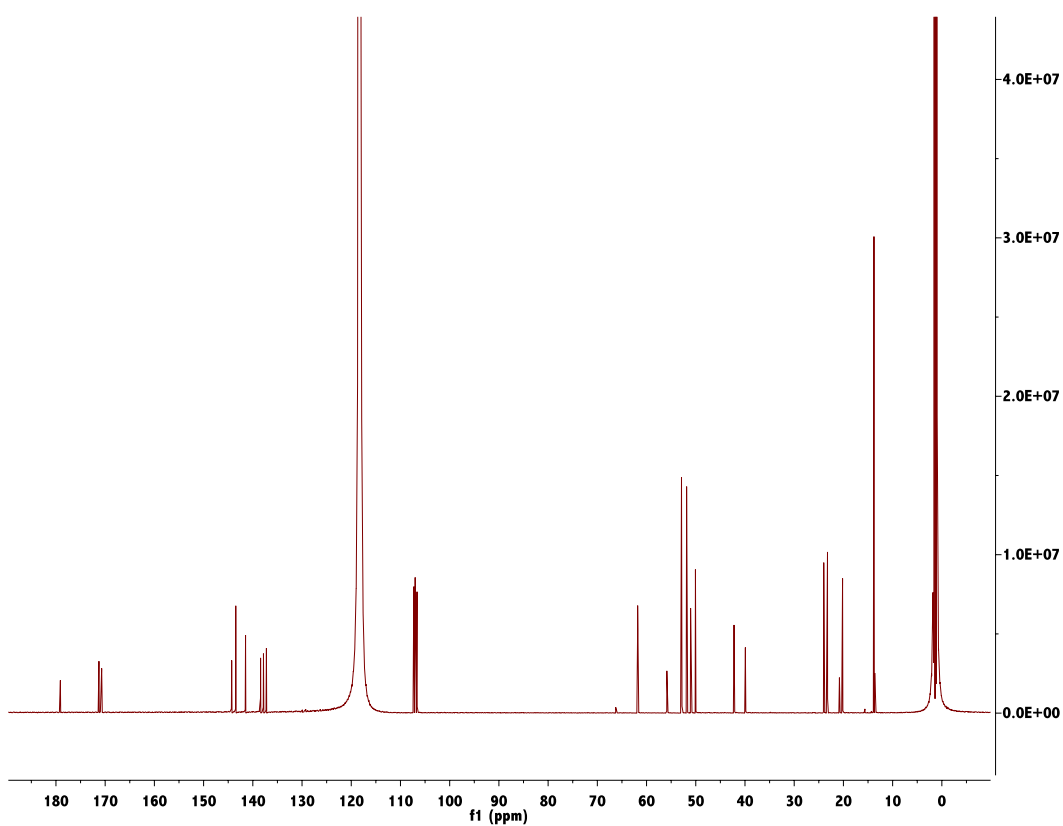
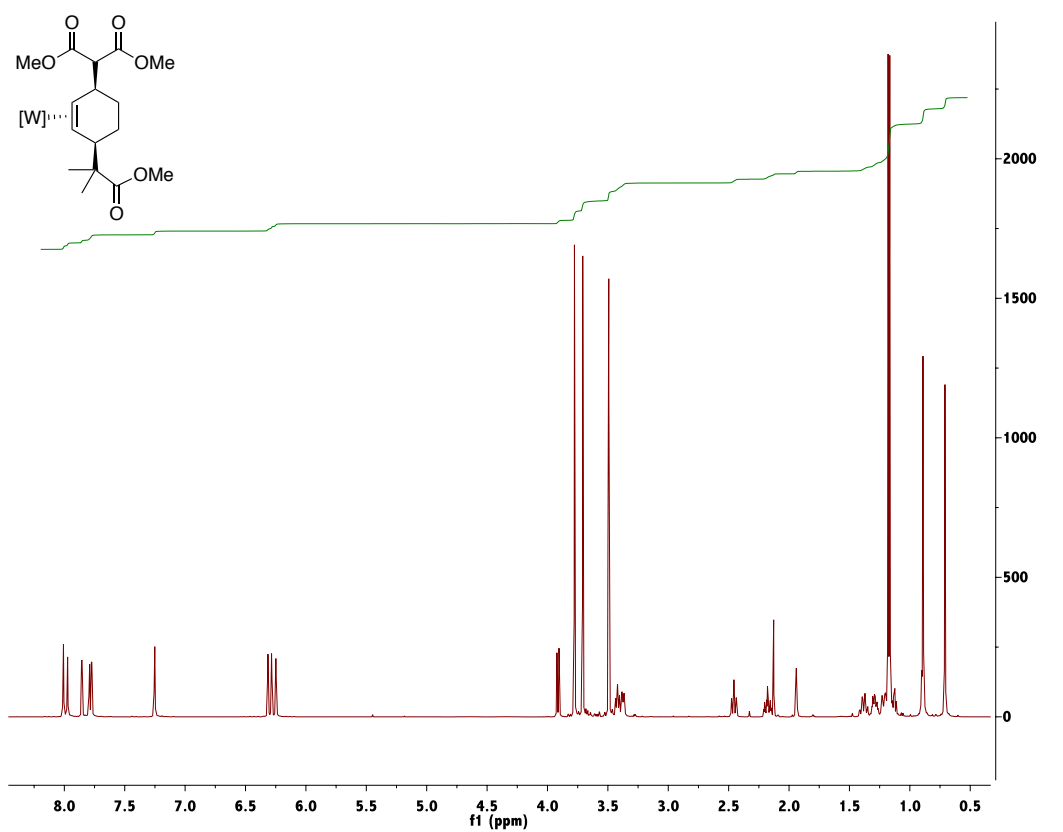
$^1\text{H-NMR}$ (CD_3CN) and $^{13}\text{C-NMR}$ (CD_3CN) of Compound 20B:

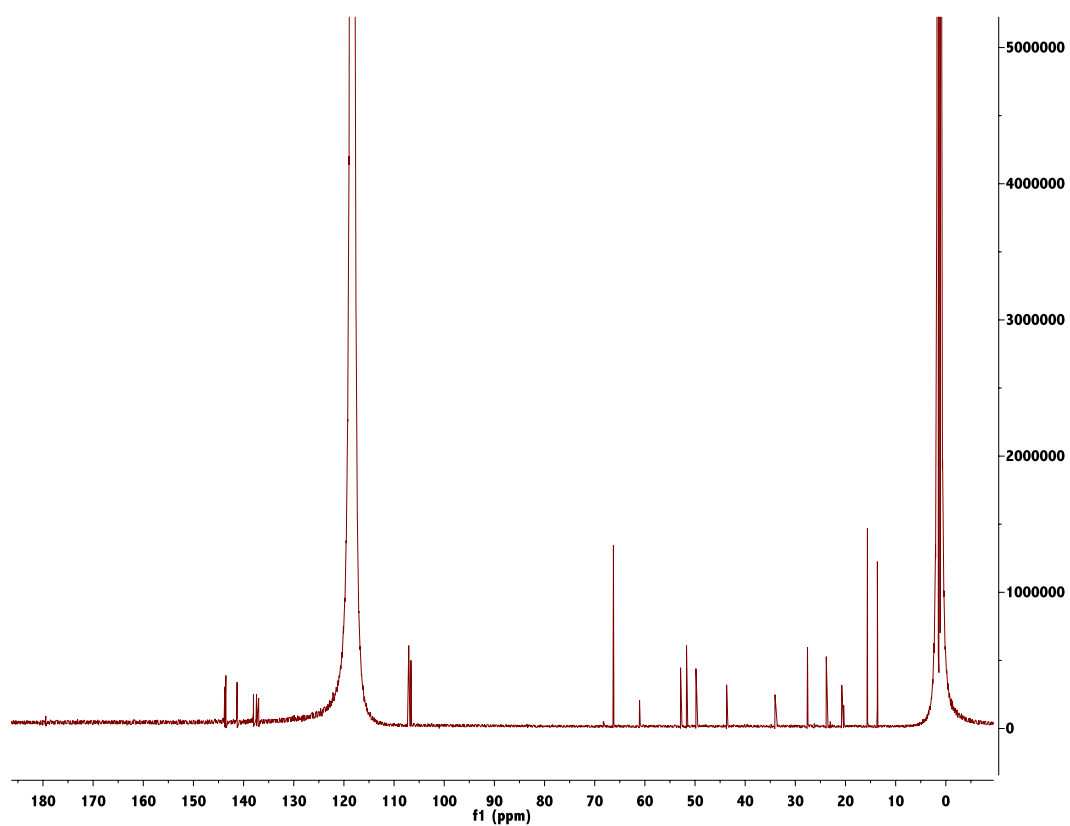
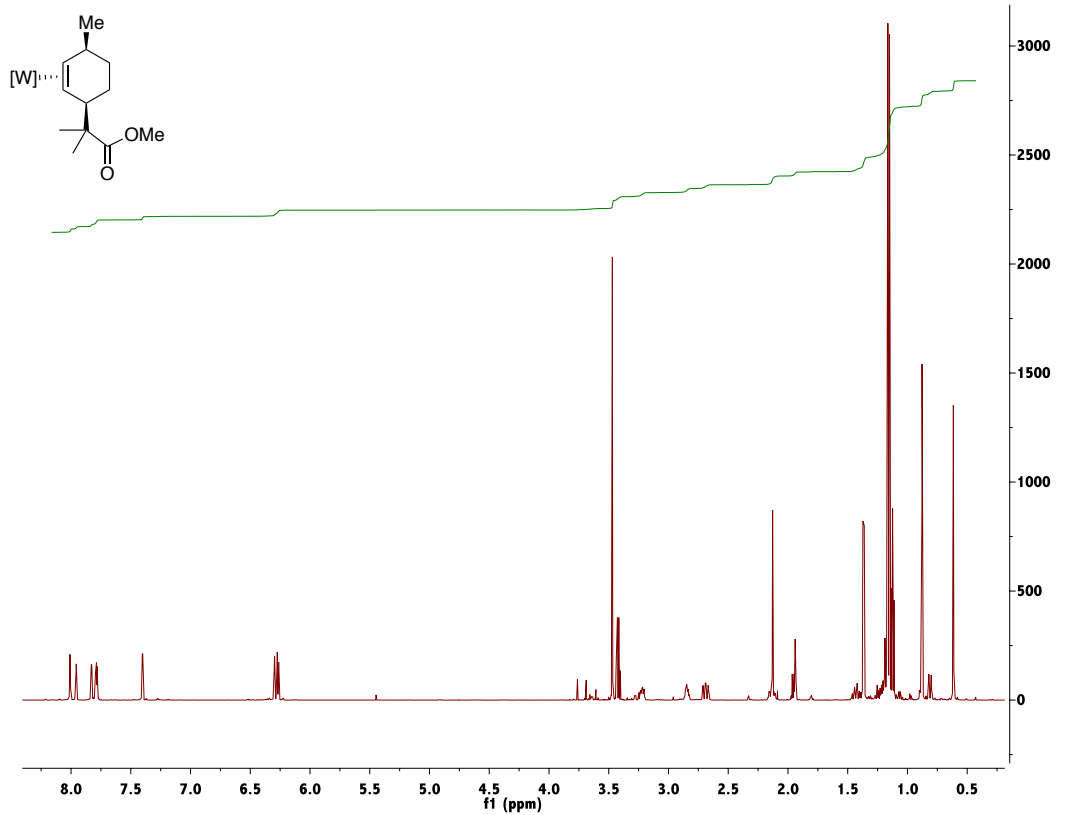
$^1\text{H-NMR}$ (CD_3CN) and $^{13}\text{C-NMR}$ (CD_3CN) of Compound 22B:

$^1\text{H-NMR}$ (CD_3CN) and $^{13}\text{C-NMR}$ (CD_3CN) of Compound 23A:

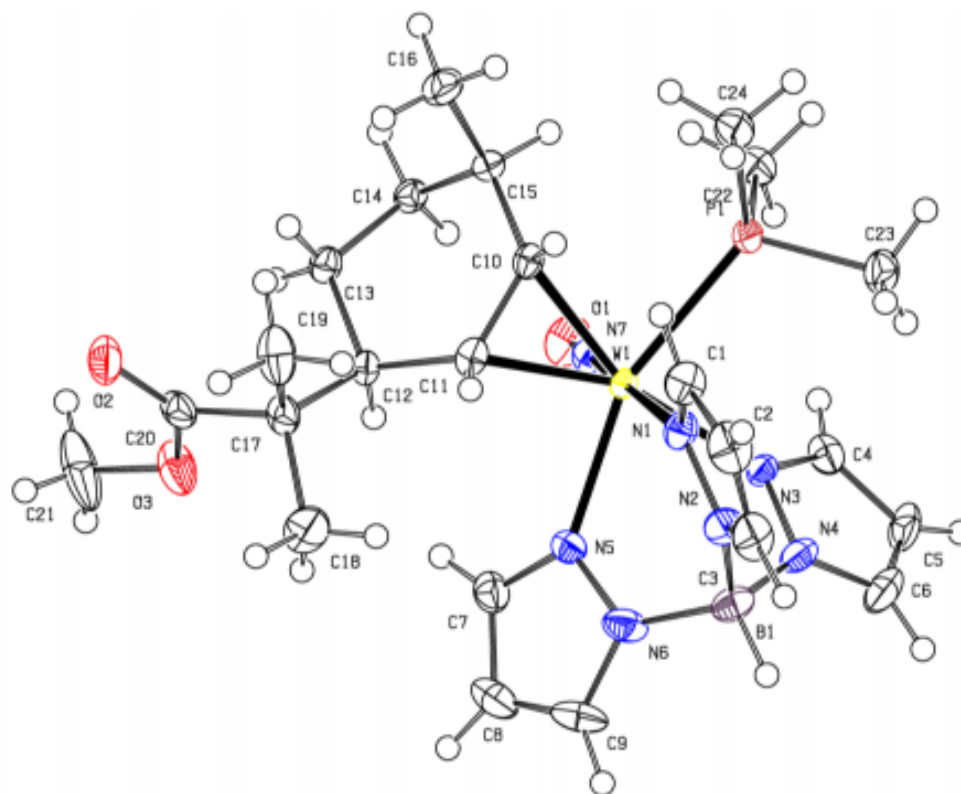
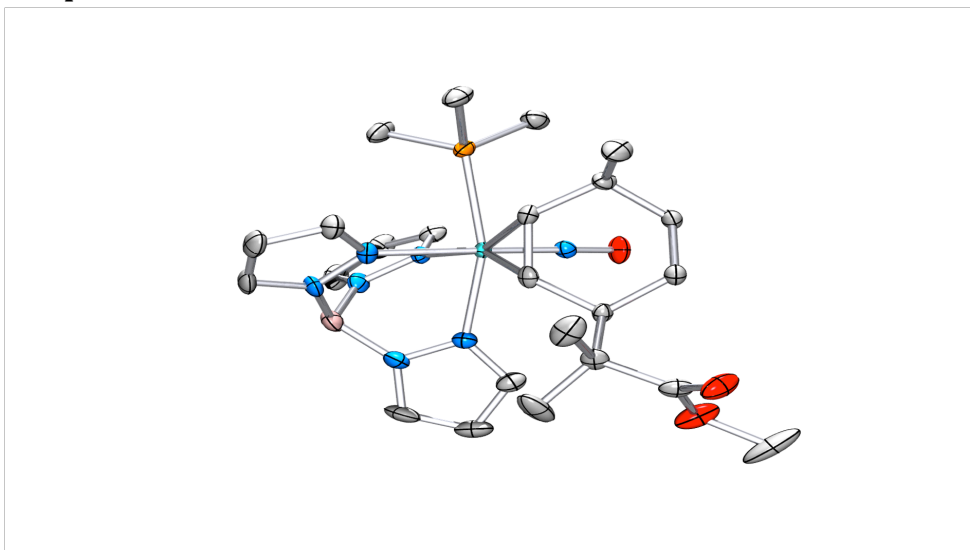
$^1\text{H-NMR}$ (CD_3CN) and $^{13}\text{C-NMR}$ (CD_3CN) of Compound 24A:

$^1\text{H-NMR}$ (CD_3CN) and $^{13}\text{C-NMR}$ (CD_3CN) of Compound 25A:

$^1\text{H-NMR}$ (CD_3CN) and $^{13}\text{C-NMR}$ (CD_3CN) of Compound 28A:

$^1\text{H-NMR}$ (CD_3CN) and $^{13}\text{C-NMR}$ (CD_3CN) of Compound 29A:

Compound 29A



Compound 29ATable 1. Sample and crystal data for C₂₄H₃₉BN₇O₃PW.

Chemical formula	C ₂₄ H ₃₉ BN ₇ O ₃ PW	
Formula weight	699.25 g/mol	
Temperature	150(2) K	
Wavelength	0.71073 Å	
Crystal size	0.142 x 0.173 x 0.228 mm	
Crystal habit	yellow block	
Crystal system	monoclinic	
Space group	P 2 ₁ /n	
Unit cell dimensions	a = 10.5223(8) Å	α = 90°
	b = 22.0818(17) Å	β = 94.7150(10)°
	c = 12.5260(9) Å	γ = 90°
Volume	2900.6(4) Å ³	
Z	4	
Density (calculated)	1.601 g/cm ³	
Absorption coefficient	4.075 mm ⁻¹	
F(000)	1400	

Table 2. Data collection and structure refinement for C₂₄H₃₉BN₇O₃PW.

Diffractometer	Bruker Kappa APEXII CCD
Radiation source	fine-focus sealed tube, Mo K _α
Theta range for data collection	1.84 to 29.59°
Index ranges	-14 ≤ h ≤ 14, -30 ≤ k ≤ 30, -17 ≤ l ≤ 17
Reflections collected	34614
Independent reflections	8162 [R(int) = 0.0481]
Coverage of independent reflections	100.0%
Absorption correction	Multi-Scan

Max. and min. transmission	0.5950 and 0.4570
Structure solution technique	direct methods
Structure solution program	SHELXT 2014/5 (Sheldrick, 2014)
Refinement method	Full-matrix least-squares on F^2
Refinement program	SHELXL-2016/6 (Sheldrick, 2016)
Function minimized	$\Sigma w(F_o^2 - F_c^2)^2$
Data / restraints / parameters	8162 / 0 / 344
Goodness-of-fit on F^2	1.009
Δ/σ_{\max}	0.001
Final R indices	6552 data; $I > 2\sigma(I)$ R1 = 0.0274, wR2 = 0.0458 all data R1 = 0.0425, wR2 = 0.0493
Weighting scheme	$w = 1/[\sigma^2(F_o^2) + (0.0119P)^2 + 1.5873P]$ where $P = (F_o^2 + 2F_c^2)/3$
Largest diff. peak and hole	0.761 and -0.823 $e\text{\AA}^{-3}$
R.M.S. deviation from mean	0.116 $e\text{\AA}^{-3}$

Table 3. Atomic coordinates and equivalent isotropic atomic displacement parameters (\AA^2) for $C_{24}H_{39}BN_7O_3PW$.

$U(\text{eq})$ is defined as one third of the trace of the orthogonalized U_{ij} tensor.

	x/a	y/b	z/c	$U(\text{eq})$
W1	0.19442(2)	0.60886(2)	0.25814(2)	0.01430(3)
P1	0.17281(7)	0.67449(3)	0.09510(6)	0.02055(16)
O1	0.91639(19)	0.57663(10)	0.23703(18)	0.0324(5)
O2	0.0725(2)	0.68860(10)	0.76198(17)	0.0351(6)
O3	0.0301(2)	0.59636(10)	0.69648(17)	0.0394(6)

	x/a	y/b	z/c	U(eq)
N1	0.4076(2)	0.62231(11)	0.26167(19)	0.0216(5)
N2	0.4869(2)	0.57304(12)	0.2551(2)	0.0242(6)
N3	0.2308(2)	0.53747(10)	0.13943(18)	0.0174(5)
N4	0.3394(2)	0.50390(11)	0.1452(2)	0.0241(5)
N5	0.2488(2)	0.52873(11)	0.35966(19)	0.0206(5)
N6	0.3553(2)	0.49532(12)	0.3431(2)	0.0280(6)
N7	0.0300(2)	0.59181(10)	0.24764(18)	0.0184(5)
C1	0.4840(3)	0.67053(15)	0.2677(2)	0.0273(7)
C2	0.6115(3)	0.65349(17)	0.2658(3)	0.0337(8)
C3	0.6087(3)	0.59184(16)	0.2581(3)	0.0320(8)
C4	0.1604(3)	0.51817(13)	0.0519(2)	0.0240(7)
C5	0.2229(3)	0.47314(14)	0.0000(3)	0.0315(8)
C6	0.3356(3)	0.46519(14)	0.0626(3)	0.0335(8)
C7	0.1885(3)	0.49920(14)	0.4334(2)	0.0266(7)
C8	0.2556(3)	0.44796(15)	0.4672(3)	0.0353(8)
C9	0.3596(3)	0.44672(15)	0.4091(3)	0.0375(9)
C10	0.1818(3)	0.70100(12)	0.3307(2)	0.0183(6)
C11	0.2063(2)	0.65674(13)	0.4139(2)	0.0189(6)
C12	0.1170(2)	0.64697(12)	0.5037(2)	0.0168(6)
C13	0.0042(3)	0.69149(13)	0.4970(2)	0.0201(6)
C14	0.9552(2)	0.70724(13)	0.3829(2)	0.0193(6)
C15	0.0579(3)	0.73794(12)	0.3225(2)	0.0197(6)
C16	0.0840(3)	0.80300(13)	0.3621(3)	0.0315(7)
C17	0.1911(3)	0.65081(14)	0.6171(2)	0.0232(6)
C18	0.2813(3)	0.59615(17)	0.6377(3)	0.0448(10)
C19	0.2682(3)	0.70912(16)	0.6322(3)	0.0363(8)
C20	0.0934(3)	0.64886(13)	0.7000(2)	0.0249(7)
C21	0.9369(4)	0.5890(2)	0.7734(3)	0.0641(14)
C22	0.0114(3)	0.67641(15)	0.0314(2)	0.0289(7)
C23	0.2698(3)	0.65140(15)	0.9876(3)	0.0329(8)
C24	0.2137(3)	0.75511(13)	0.0994(3)	0.0313(7)
B1	0.4334(3)	0.50871(17)	0.2469(3)	0.0279(8)

Table 4. Bond lengths (Å) for C₂₄H₃₉BN₇O₃PW.

W1-N7	1.765(2)	W1-C11	2.214(3)
W1-N3	2.222(2)	W1-N5	2.226(2)
W1-C10	2.237(3)	W1-N1	2.260(2)
W1-P1	2.4992(8)	P1-C22	1.817(3)
P1-C23	1.827(3)	P1-C24	1.831(3)
O1-N7	1.238(3)	O2-C20	1.204(3)
O3-C20	1.336(4)	O3-C21	1.440(4)
N1-C1	1.333(4)	N1-N2	1.378(3)
N2-C3	1.345(4)	N2-B1	1.528(4)
N3-C4	1.341(3)	N3-N4	1.359(3)
N4-C6	1.341(4)	N4-B1	1.550(4)
N5-C7	1.333(4)	N5-N6	1.371(3)
N6-C9	1.353(4)	N6-B1	1.543(5)
C1-C2	1.395(4)	C1-H1	0.95
C2-C3	1.365(5)	C2-H2	0.95
C3-H3	0.95	C4-C5	1.384(4)
C4-H4	0.95	C5-C6	1.378(5)
C5-H5	0.95	C6-H6	0.95
C7-C8	1.381(4)	C7-H7	0.95
C8-C9	1.364(5)	C8-H8	0.95
C9-H9	0.95	C10-C11	1.436(4)
C10-C15	1.535(4)	C10-H10	1.0
C11-C12	1.539(4)	C11-H11	1.0
C12-C13	1.538(4)	C12-C17	1.566(4)
C12-H12	1.0	C13-C14	1.519(4)
C13-H13A	0.99	C13-H13B	0.99
C14-C15	1.528(4)	C14-H14A	0.99
C14-H14B	0.99	C15-C16	1.537(4)
C15-H15	1.0	C16-H16A	0.98
C16-H16B	0.98	C16-H16C	0.98
C17-C20	1.520(4)	C17-C19	1.526(4)
C17-C18	1.544(4)	C18-H18A	0.98
C18-H18B	0.98	C18-H18C	0.98
C19-H19A	0.98	C19-H19B	0.98
C19-H19C	0.98	C21-H21A	0.98
C21-H21B	0.98	C21-H21C	0.98

C22-H22A	0.98	C22-H22B	0.98
C22-H22C	0.98	C23-H23A	0.98
C23-H23B	0.98	C23-H23C	0.98
C24-H24A	0.98	C24-H24B	0.98
C24-H24C	0.98	B1-H1A	1.07(3)

Table 5. Bond angles ($^{\circ}$) for $C_{24}H_{39}BN_7O_3PW$.

N7-W1-C11	98.72(10)	N7-W1-N3	91.18(9)
C11-W1-N3	158.19(9)	N7-W1-N5	94.45(9)
C11-W1-N5	83.28(9)	N3-W1-N5	76.58(8)
N7-W1-C10	97.70(10)	C11-W1-C10	37.65(10)
N3-W1-C10	159.49(9)	N5-W1-C10	120.78(9)
N7-W1-N1	174.27(9)	C11-W1-N1	86.32(9)
N3-W1-N1	83.17(8)	N5-W1-N1	83.40(9)
C10-W1-N1	87.95(9)	N7-W1-P1	92.29(7)
C11-W1-P1	115.98(8)	N3-W1-P1	82.74(6)
N5-W1-P1	158.35(7)	C10-W1-P1	78.48(7)
N1-W1-P1	87.90(6)	C22-P1-C23	103.98(15)
C22-P1-C24	101.49(15)	C23-P1-C24	98.54(15)
C22-P1-W1	113.04(10)	C23-P1-W1	114.92(11)
C24-P1-W1	122.30(11)	C20-O3-C21	116.2(3)
C1-N1-N2	105.6(2)	C1-N1-W1	134.4(2)
N2-N1-W1	120.00(17)	C3-N2-N1	109.6(3)
C3-N2-B1	129.3(3)	N1-N2-B1	121.1(2)
C4-N3-N4	106.0(2)	C4-N3-W1	131.18(19)
N4-N3-W1	122.78(17)	C6-N4-N3	109.5(2)
C6-N4-B1	130.9(3)	N3-N4-B1	118.9(2)
C7-N5-N6	106.4(2)	C7-N5-W1	132.0(2)
N6-N5-W1	121.08(18)	C9-N6-N5	108.7(3)
C9-N6-B1	129.5(3)	N5-N6-B1	120.6(2)
O1-N7-W1	176.1(2)	N1-C1-C2	111.1(3)
N1-C1-H1	124.5	C2-C1-H1	124.5
C3-C2-C1	104.8(3)	C3-C2-H2	127.6
C1-C2-H2	127.6	N2-C3-C2	108.9(3)
N2-C3-H3	125.5	C2-C3-H3	125.5
N3-C4-C5	111.1(3)	N3-C4-H4	124.4
C5-C4-H4	124.4	C6-C5-C4	104.1(3)

C6-C5-H5	127.9	C4-C5-H5	127.9
N4-C6-C5	109.2(3)	N4-C6-H6	125.4
C5-C6-H6	125.4	N5-C7-C8	110.7(3)
N5-C7-H7	124.7	C8-C7-H7	124.7
C9-C8-C7	105.4(3)	C9-C8-H8	127.3
C7-C8-H8	127.3	N6-C9-C8	108.8(3)
N6-C9-H9	125.6	C8-C9-H9	125.6
C11-C10-C15	120.7(2)	C11-C10-W1	70.30(15)
C15-C10-W1	122.31(18)	C11-C10-H10	112.4
C15-C10-H10	112.4	W1-C10-H10	112.4
C10-C11-C12	122.8(2)	C10-C11-W1	72.05(15)
C12-C11-W1	125.68(18)	C10-C11-H11	110.4
C12-C11-H11	110.4	W1-C11-H11	110.4
C13-C12-C11	112.7(2)	C13-C12-C17	109.8(2)
C11-C12-C17	111.5(2)	C13-C12-H12	107.5
C11-C12-H12	107.5	C17-C12-H12	107.5
C14-C13-C12	113.5(2)	C14-C13-H13A	108.9
C12-C13-H13A	108.9	C14-C13-H13B	108.9
C12-C13-H13B	108.9	H13A-C13-H13B	107.7
C13-C14-C15	111.6(2)	C13-C14-H14A	109.3
C15-C14-H14A	109.3	C13-C14-H14B	109.3
C15-C14-H14B	109.3	H14A-C14-H14B	108.0
C14-C15-C10	111.3(2)	C14-C15-C16	111.7(2)
C10-C15-C16	110.3(2)	C14-C15-H15	107.8
C10-C15-H15	107.8	C16-C15-H15	107.8
C15-C16-H16A	109.5	C15-C16-H16B	109.5
H16A-C16-H16B	109.5	C15-C16-H16C	109.5
H16A-C16-H16C	109.5	H16B-C16-H16C	109.5
C20-C17-C19	108.8(2)	C20-C17-C18	107.7(3)
C19-C17-C18	109.0(3)	C20-C17-C12	107.7(2)
C19-C17-C12	112.2(2)	C18-C17-C12	111.3(2)
C17-C18-H18A	109.5	C17-C18-H18B	109.5
H18A-C18-H18B	109.5	C17-C18-H18C	109.5
H18A-C18-H18C	109.5	H18B-C18-H18C	109.5
C17-C19-H19A	109.5	C17-C19-H19B	109.5
H19A-C19-H19B	109.5	C17-C19-H19C	109.5
H19A-C19-H19C	109.5	H19B-C19-H19C	109.5

O2-C20-O3	122.5(3)	O2-C20-C17	126.1(3)
O3-C20-C17	111.4(3)	O3-C21-H21A	109.5
O3-C21-H21B	109.5	H21A-C21-H21B	109.5
O3-C21-H21C	109.5	H21A-C21-H21C	109.5
H21B-C21-H21C	109.5	P1-C22-H22A	109.5
P1-C22-H22B	109.5	H22A-C22-H22B	109.5
P1-C22-H22C	109.5	H22A-C22-H22C	109.5
H22B-C22-H22C	109.5	P1-C23-H23A	109.5
P1-C23-H23B	109.5	H23A-C23-H23B	109.5
P1-C23-H23C	109.5	H23A-C23-H23C	109.5
H23B-C23-H23C	109.5	P1-C24-H24A	109.5
P1-C24-H24B	109.5	H24A-C24-H24B	109.5
P1-C24-H24C	109.5	H24A-C24-H24C	109.5
H24B-C24-H24C	109.5	N2-B1-N6	110.0(3)
N2-B1-N4	109.0(3)	N6-B1-N4	106.5(3)
N2-B1-H1A	111.1(17)	N6-B1-H1A	109.9(17)
N4-B1-H1A	110.2(16)		

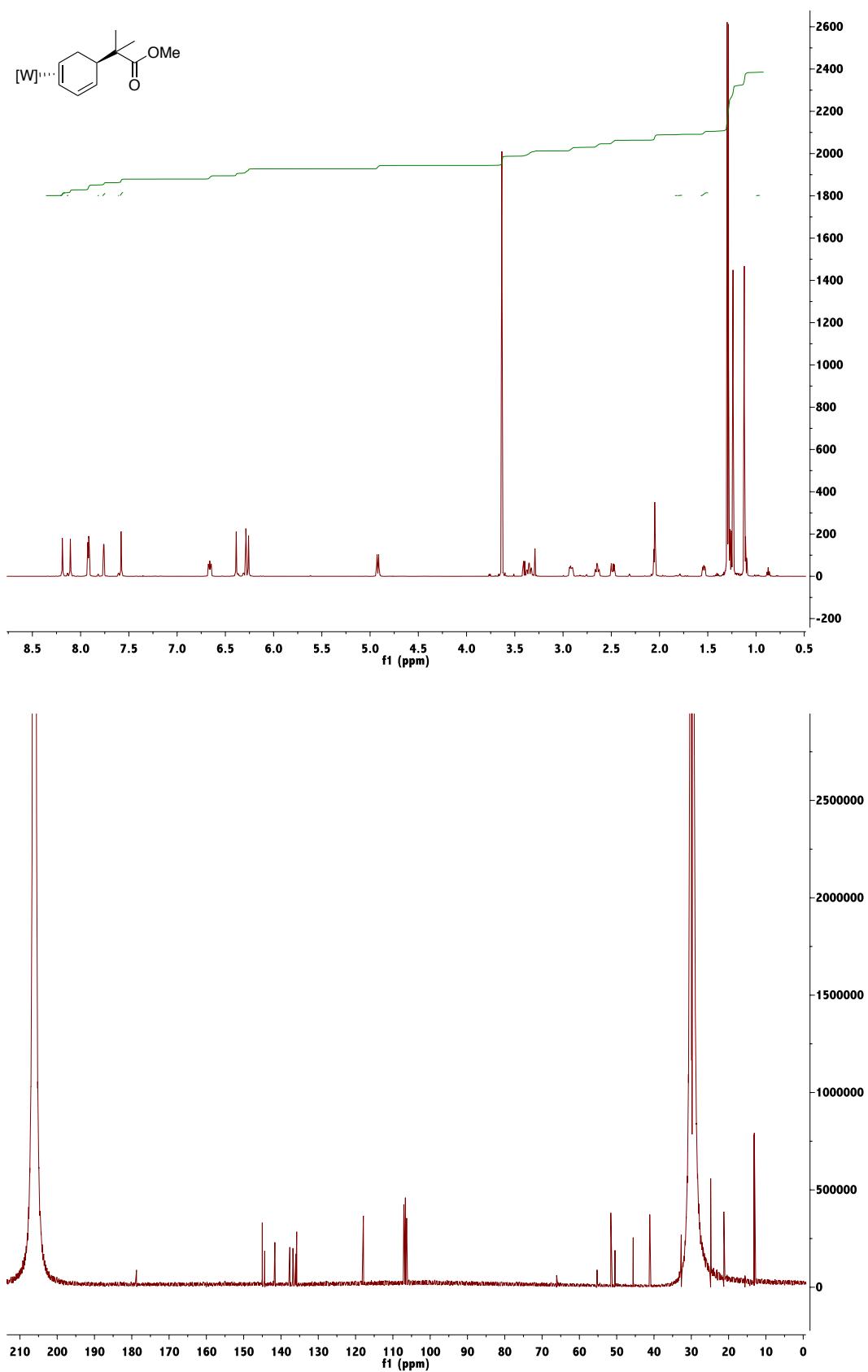
Table 6. Anisotropic atomic displacement parameters (\AA^2) for $\text{C}_{24}\text{H}_{39}\text{BN}_7\text{O}_3\text{PW}$.

The anisotropic atomic displacement factor exponent takes the form: $-2\pi^2 [h^2 a^{*2} U_{11} + \dots + 2 h k a^* b^* U_{12}]$

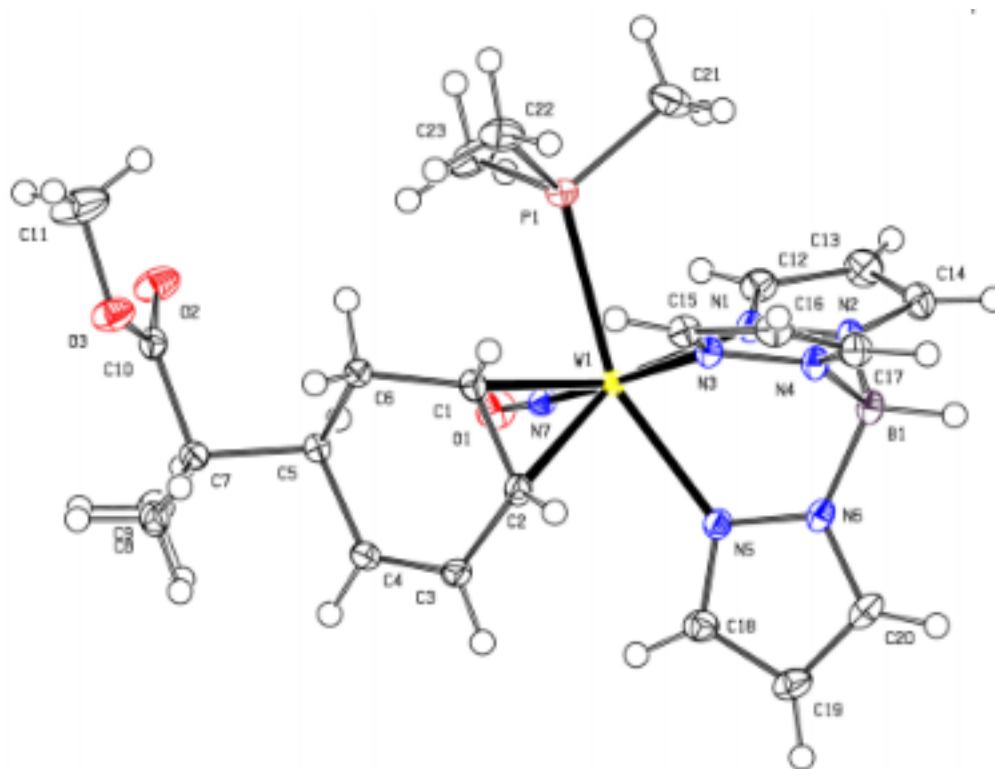
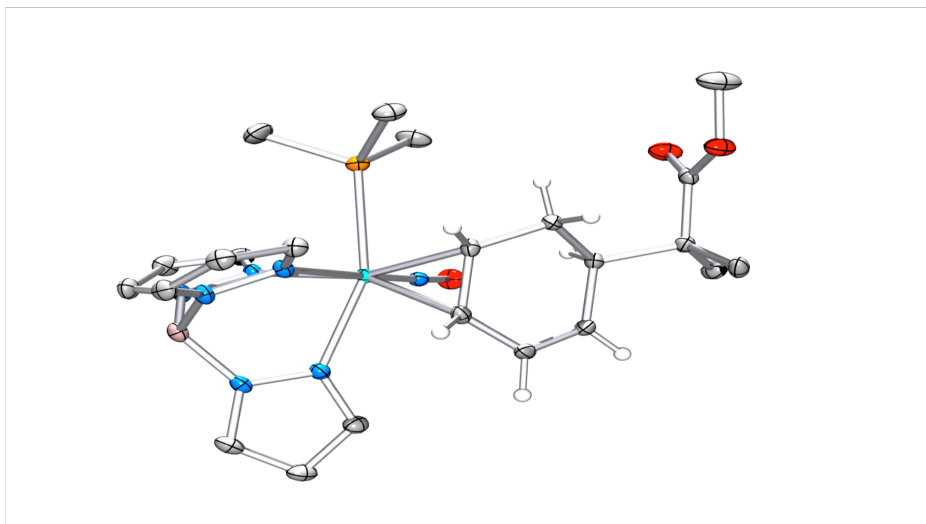
	U_{11}	U_{22}	U_{33}	U_{23}	U_{13}	U_{12}
W1	0.01135(5)	0.01611(5)	0.01562(5)	-0.00029(5)	0.00230(4)	-0.00002(5)
P1	0.0229(4)	0.0201(4)	0.0196(4)	0.0024(3)	0.0077(3)	0.0006(3)
O1	0.0152(10)	0.0404(13)	0.0420(14)	-0.0071(11)	0.0040(10)	-0.0062(10)
O2	0.0549(15)	0.0281(12)	0.0241(12)	-0.0051(10)	0.0148(11)	-0.0070(11)
O3	0.0656(17)	0.0301(13)	0.0231(12)	-0.0045(10)	0.0079(11)	-0.0196(12)
N1	0.0164(12)	0.0259(14)	0.0229(13)	-0.0027(10)	0.0042(10)	0.0002(10)
N2	0.0122(12)	0.0315(14)	0.0286(14)	0.0022(11)	0.0004(10)	0.0051(10)
N3	0.0170(12)	0.0169(11)	0.0188(12)	-0.0015(10)	0.0041(9)	0.0022(9)
N4	0.0235(13)	0.0187(12)	0.0310(14)	-0.0021(11)	0.0083(11)	0.0041(10)

	U ₁₁	U ₂₂	U ₃₃	U ₂₃	U ₁₃	U ₁₂
N5	0.0219(13)	0.0205(12)	0.0192(12)	0.0020(10)	-0.0003(10)	0.0005(10)
N6	0.0227(13)	0.0280(14)	0.0327(15)	0.0095(12)	-0.0009(11)	0.0052(11)
N7	0.0173(12)	0.0209(12)	0.0167(12)	-0.0013(9)	-0.0006(10)	0.0010(9)
C1	0.0190(15)	0.0315(17)	0.0318(17)	-0.0006(15)	0.0039(13)	-0.0030(13)
C2	0.0149(15)	0.051(2)	0.0356(19)	0.0021(16)	0.0025(14)	-0.0076(14)
C3	0.0116(14)	0.053(2)	0.0316(18)	0.0046(16)	0.0043(13)	0.0037(13)
C4	0.0286(16)	0.0230(15)	0.0204(15)	0.0001(12)	0.0012(13)	-0.0065(13)
C5	0.044(2)	0.0262(17)	0.0264(17)	-0.0128(14)	0.0133(15)	-0.0057(15)
C6	0.0368(19)	0.0263(17)	0.040(2)	-0.0103(15)	0.0165(16)	0.0023(15)
C7	0.0342(17)	0.0245(16)	0.0213(15)	-0.0012(13)	0.0038(13)	-0.0046(13)
C8	0.048(2)	0.0295(18)	0.0268(18)	0.0100(14)	-0.0053(16)	-0.0041(16)
C9	0.038(2)	0.0278(17)	0.044(2)	0.0149(16)	-0.0108(17)	0.0062(15)
C10	0.0164(13)	0.0201(14)	0.0190(14)	-0.0022(11)	0.0047(11)	-0.0017(11)
C11	0.0115(13)	0.0252(15)	0.0195(14)	-0.0061(12)	-0.0013(11)	-0.0016(11)
C12	0.0150(13)	0.0211(14)	0.0144(13)	-0.0023(11)	0.0016(11)	-0.0003(11)
C13	0.0162(13)	0.0236(15)	0.0208(14)	-0.0019(12)	0.0030(11)	0.0006(11)
C14	0.0154(13)	0.0222(14)	0.0203(14)	-0.0009(12)	0.0014(11)	0.0031(11)
C15	0.0238(15)	0.0159(13)	0.0197(14)	-0.0002(11)	0.0035(12)	0.0025(11)
C16	0.041(2)	0.0189(15)	0.0365(19)	-0.0009(14)	0.0126(15)	0.0036(14)
C17	0.0223(15)	0.0313(16)	0.0151(14)	-0.0032(12)	-0.0035(12)	0.0004(13)
C18	0.042(2)	0.062(3)	0.0276(18)	-0.0074(17)	-0.0146(16)	0.0275(19)
C19	0.0329(18)	0.052(2)	0.0237(17)	-0.0100(16)	0.0006(14)	-0.0162(16)
C20	0.0348(17)	0.0234(15)	0.0153(14)	0.0001(12)	-0.0042(13)	-0.0013(13)
C21	0.102(4)	0.067(3)	0.026(2)	-0.0064(19)	0.022(2)	-0.058(3)

	U ₁₁	U ₂₂	U ₃₃	U ₂₃	U ₁₃	U ₁₂
C22	0.0323(17)	0.0316(17)	0.0227(16)	0.0028(14)	0.0007(13)	0.0056(14)
C23	0.041(2)	0.0300(18)	0.0300(18)	0.0015(14)	0.0187(15)	0.0000(15)
C24	0.041(2)	0.0222(16)	0.0322(18)	0.0029(14)	0.0136(15)	-0.0038(14)
B1	0.0211(17)	0.0274(19)	0.035(2)	-0.0002(16)	0.0027(16)	0.0085(15)

$^1\text{H-NMR}$ ($\text{d}^6\text{-acetone}$) and $^{13}\text{C-NMR}$ ($\text{d}^6\text{-acetone}$) of Compound 30:

Compound 30



Compound 30Table 1. Sample and crystal data for C₂₃H₃₅BN₇O₃PW

Chemical formula	C ₂₃ H ₃₅ BN ₇ O ₃ PW
Formula weight	683.21 g/mol
Temperature	150(2) K
Wavelength	0.71073 Å
Crystal size	0.162 x 0.189 x 0.389 mm
Crystal habit	yellow plate
Crystal system	triclinic
Space group	P -1
Unit cell dimensions	a = 8.9012(6) Å α = 103.8490(10)° b = 11.0642(7) Å β = 104.7460(10)° c = 15.1042(10) Å γ = 99.213(2)°
Volume	1357.47(15) Å ³
Z	2
Density (calculated)	1.671 g/cm ³
Absorption coefficient	4.352 mm ⁻¹
F(000)	680

Table 2. Data collection and structure refinement for C₂₃H₃₅BN₇O₃PW

Diffractometer	Bruker Kappa APEXII Duo
Radiation source	fine-focus sealed tube, Mo K _α
Theta range for data collection	1.46 to 29.61°
Index ranges	-12 ≤ h ≤ 12, -15 ≤ k ≤ 15, -20 ≤ l ≤ 20
Reflections collected	31956
Independent reflections	7627 [R(int) = 0.0217]
Coverage of independent reflections	99.9%
Absorption correction	Multi-Scan

Max. and min. transmission	0.5390 and 0.2820
Structure solution technique	direct methods
Structure solution program	SHELXT 2014/5 (Sheldrick, 2014)
Refinement method	Full-matrix least-squares on F^2
Refinement program	SHELXL-2016/6 (Sheldrick, 2016)
Function minimized	$\Sigma w(F_o^2 - F_c^2)^2$
Data / restraints / parameters	7627 / 0 / 335
Goodness-of-fit on F^2	1.050
Δ/σ_{\max}	0.005
Final R indices	7224 data; $I > 2\sigma(I)$ R1 = 0.0131, wR2 = 0.0298 all data R1 = 0.0151, wR2 = 0.0303
Weighting scheme	$w = 1/[\sigma^2(F_o^2) + (0.0114P)^2 + 0.6791P]$ where $P = (F_o^2 + 2F_c^2)/3$
Largest diff. peak and hole	0.531 and -0.992 $e\text{\AA}^{-3}$
R.M.S. deviation from mean	0.068 $e\text{\AA}^{-3}$

Table 3. Atomic coordinates and equivalent isotropic atomic displacement parameters (\AA^2) for $C_{23}H_{35}BN_7O_3PW$

$U(\text{eq})$ is defined as one third of the trace of the orthogonalized U_{ij} tensor.

	x/a	y/b	z/c	$U(\text{eq})$
W1	0.16310(2)	0.46628(2)	0.74709(2)	0.01064(2)
P1	0.30578(5)	0.37118(4)	0.63497(3)	0.01536(7)
O1	0.07062(14)	0.63664(11)	0.62562(8)	0.0213(2)
O2	0.60515(14)	0.83870(13)	0.63958(8)	0.0250(3)
O3	0.80396(13)	0.86900(12)	0.77382(8)	0.0233(2)

	x/a	y/b	z/c	U(eq)
N1	0.95776(15)	0.31118(12)	0.65071(8)	0.0144(2)
N2	0.88629(15)	0.21685(12)	0.68070(9)	0.0153(2)
N3	0.22272(14)	0.32273(12)	0.82831(9)	0.0140(2)
N4	0.10288(15)	0.23115(12)	0.83106(9)	0.0153(2)
N5	0.97958(14)	0.47359(12)	0.82496(9)	0.0144(2)
N6	0.90378(14)	0.36421(12)	0.83737(9)	0.0147(2)
N7	0.10932(14)	0.57013(12)	0.67790(8)	0.0135(2)
C1	0.41305(17)	0.57835(14)	0.82402(10)	0.0143(3)
C2	0.31006(17)	0.61498(14)	0.88091(10)	0.0151(3)
C3	0.28578(18)	0.74532(15)	0.89697(10)	0.0171(3)
C4	0.34010(18)	0.82834(15)	0.85442(11)	0.0170(3)
C5	0.43206(17)	0.79535(14)	0.78444(10)	0.0143(3)
C6	0.51040(17)	0.68381(14)	0.79813(11)	0.0153(3)
C7	0.55852(18)	0.91674(14)	0.79167(10)	0.0152(3)
C8	0.6643(2)	0.98296(15)	0.89544(11)	0.0207(3)
C9	0.4723(2)	0.01148(15)	0.75246(12)	0.0217(3)
C10	0.65593(18)	0.87146(14)	0.72618(10)	0.0159(3)
C11	0.8971(2)	0.8176(2)	0.71482(14)	0.0383(5)
C12	0.87293(18)	0.29213(16)	0.55955(10)	0.0187(3)
C13	0.7459(2)	0.18497(17)	0.52971(11)	0.0229(3)
C14	0.75831(19)	0.14014(15)	0.60835(11)	0.0207(3)
C15	0.35807(18)	0.31019(15)	0.88585(10)	0.0164(3)
C16	0.32656(19)	0.21198(15)	0.92634(11)	0.0188(3)
C17	0.16361(19)	0.16441(15)	0.88965(11)	0.0183(3)
C18	0.92892(18)	0.56955(16)	0.87232(11)	0.0184(3)
C19	0.82269(18)	0.52331(17)	0.91701(11)	0.0210(3)
C20	0.81083(18)	0.39344(16)	0.89329(10)	0.0189(3)
C21	0.2177(2)	0.20392(18)	0.56467(15)	0.0348(4)
C22	0.5119(2)	0.36162(17)	0.68152(12)	0.0247(3)
C23	0.3127(2)	0.45091(19)	0.54354(12)	0.0269(4)
B1	0.9269(2)	0.23183(17)	0.78853(12)	0.0158(3)

Table 4. Bond lengths (Å) for C₂₃H₃₅BN₇O₃PW

W1-N7	1.7714(12)	W1-N1	2.2023(12)
W1-C2	2.2082(14)	W1-C1	2.2245(14)
W1-N5	2.2435(12)	W1-N3	2.2760(12)
W1-P1	2.5015(4)	P1-C23	1.8161(17)
P1-C22	1.8198(17)	P1-C21	1.8269(18)
O1-N7	1.2267(16)	O2-C10	1.2109(18)
O3-C10	1.3390(18)	O3-C11	1.446(2)
N1-C12	1.3383(18)	N1-N2	1.3637(17)
N2-C14	1.3509(19)	N2-B1	1.537(2)
N3-C15	1.3433(18)	N3-N4	1.3649(17)
N4-C17	1.3483(18)	N4-B1	1.537(2)
N5-C18	1.340(2)	N5-N6	1.3662(17)
N6-C20	1.3465(19)	N6-B1	1.545(2)
C1-C2	1.448(2)	C1-C6	1.5273(19)
C1-H1	1.0	C2-C3	1.464(2)
C2-H2	1.0	C3-C4	1.338(2)
C3-H3	0.95	C4-C5	1.507(2)
C4-H4	0.95	C5-C6	1.542(2)
C5-C7	1.570(2)	C5-H5	1.0
C6-H6A	0.99	C6-H6B	0.99
C7-C10	1.523(2)	C7-C8	1.536(2)
C7-C9	1.537(2)	C8-H8A	0.98
C8-H8B	0.98	C8-H8C	0.98
C9-H9A	0.98	C9-H9B	0.98
C9-H9C	0.98	C11-H11A	0.98
C11-H11B	0.98	C11-H11C	0.98
C12-C13	1.394(2)	C12-H12	0.95
C13-C14	1.379(2)	C13-H13	0.95
C14-H14	0.95	C15-C16	1.393(2)
C15-H15	0.95	C16-C17	1.376(2)
C16-H16	0.95	C17-H17	0.95
C18-C19	1.395(2)	C18-H18	0.95
C19-C20	1.375(2)	C19-H19	0.95
C20-H20	0.95	C21-H21A	0.98
C21-H21B	0.98	C21-H21C	0.98

C22-H22A	0.98	C22-H22B	0.98
C22-H22C	0.98	C23-H23A	0.98
C23-H23B	0.98	C23-H23C	0.98
B1-H1A	1.092(18)		

Table 5. Bond angles (°) for C₂₃H₃₅BN₇O₃PW

N7-W1-N1	90.93(5)	N7-W1-C2	97.53(6)
N1-W1-C2	157.33(5)	N7-W1-C1	96.48(5)
N1-W1-C1	161.19(5)	C2-W1-C1	38.13(5)
N7-W1-N5	99.30(5)	N1-W1-N5	76.39(5)
C2-W1-N5	81.49(5)	C1-W1-N5	119.09(5)
N7-W1-N3	176.54(5)	N1-W1-N3	85.78(4)
C2-W1-N3	85.93(5)	C1-W1-N3	86.34(5)
N5-W1-N3	80.99(4)	N7-W1-P1	90.35(4)
N1-W1-P1	83.63(3)	C2-W1-P1	117.15(4)
C1-W1-P1	79.08(4)	N5-W1-P1	157.86(3)
N3-W1-P1	88.21(3)	C23-P1-C22	103.27(8)
C23-P1-C21	102.74(10)	C22-P1-C21	99.32(9)
C23-P1-W1	113.38(6)	C22-P1-W1	120.03(6)
C21-P1-W1	115.69(6)	C10-O3-C11	115.39(13)
C12-N1-N2	106.82(12)	C12-N1-W1	130.59(10)
N2-N1-W1	122.45(9)	C14-N2-N1	109.40(12)
C14-N2-B1	128.97(13)	N1-N2-B1	119.22(12)
C15-N3-N4	105.87(12)	C15-N3-W1	133.95(10)
N4-N3-W1	119.92(9)	C17-N4-N3	109.90(12)
C17-N4-B1	128.18(13)	N3-N4-B1	120.69(12)
C18-N5-N6	106.35(12)	C18-N5-W1	133.42(10)
N6-N5-W1	120.03(9)	C20-N6-N5	109.51(13)
C20-N6-B1	129.30(13)	N5-N6-B1	121.17(12)
O1-N7-W1	176.53(11)	C2-C1-C6	117.62(13)
C2-C1-W1	70.33(8)	C6-C1-W1	127.95(10)
C2-C1-H1	111.5	C6-C1-H1	111.5
W1-C1-H1	111.5	C1-C2-C3	118.16(13)
C1-C2-W1	71.55(8)	C3-C2-W1	119.10(10)
C1-C2-H2	113.9	C3-C2-H2	113.9
W1-C2-H2	113.9	C4-C3-C2	123.73(14)
C4-C3-H3	118.1	C2-C3-H3	118.1

C3-C4-C5	122.66(14)	C3-C4-H4	118.7
C5-C4-H4	118.7	C4-C5-C6	111.61(12)
C4-C5-C7	110.65(12)	C6-C5-C7	111.58(12)
C4-C5-H5	107.6	C6-C5-H5	107.6
C7-C5-H5	107.6	C1-C6-C5	115.81(12)
C1-C6-H6A	108.3	C5-C6-H6A	108.3
C1-C6-H6B	108.3	C5-C6-H6B	108.3
H6A-C6-H6B	107.4	C10-C7-C8	111.96(13)
C10-C7-C9	107.34(12)	C8-C7-C9	109.61(13)
C10-C7-C5	106.75(12)	C8-C7-C5	111.46(12)
C9-C7-C5	109.59(12)	C7-C8-H8A	109.5
C7-C8-H8B	109.5	H8A-C8-H8B	109.5
C7-C8-H8C	109.5	H8A-C8-H8C	109.5
H8B-C8-H8C	109.5	C7-C9-H9A	109.5
C7-C9-H9B	109.5	H9A-C9-H9B	109.5
C7-C9-H9C	109.5	H9A-C9-H9C	109.5
H9B-C9-H9C	109.5	O2-C10-O3	122.75(14)
O2-C10-C7	123.94(14)	O3-C10-C7	113.30(12)
O3-C11-H11A	109.5	O3-C11-H11B	109.5
H11A-C11-H11B	109.5	O3-C11-H11C	109.5
H11A-C11-H11C	109.5	H11B-C11-H11C	109.5
N1-C12-C13	110.28(14)	N1-C12-H12	124.9
C13-C12-H12	124.9	C14-C13-C12	104.99(13)
C14-C13-H13	127.5	C12-C13-H13	127.5
N2-C14-C13	108.51(14)	N2-C14-H14	125.7
C13-C14-H14	125.7	N3-C15-C16	110.93(14)
N3-C15-H15	124.5	C16-C15-H15	124.5
C17-C16-C15	104.59(13)	C17-C16-H16	127.7
C15-C16-H16	127.7	N4-C17-C16	108.70(13)
N4-C17-H17	125.6	C16-C17-H17	125.6
N5-C18-C19	110.51(14)	N5-C18-H18	124.7
C19-C18-H18	124.7	C20-C19-C18	104.72(14)
C20-C19-H19	127.6	C18-C19-H19	127.6
N6-C20-C19	108.89(14)	N6-C20-H20	125.6
C19-C20-H20	125.6	P1-C21-H21A	109.5
P1-C21-H21B	109.5	H21A-C21-H21B	109.5
P1-C21-H21C	109.5	H21A-C21-H21C	109.5

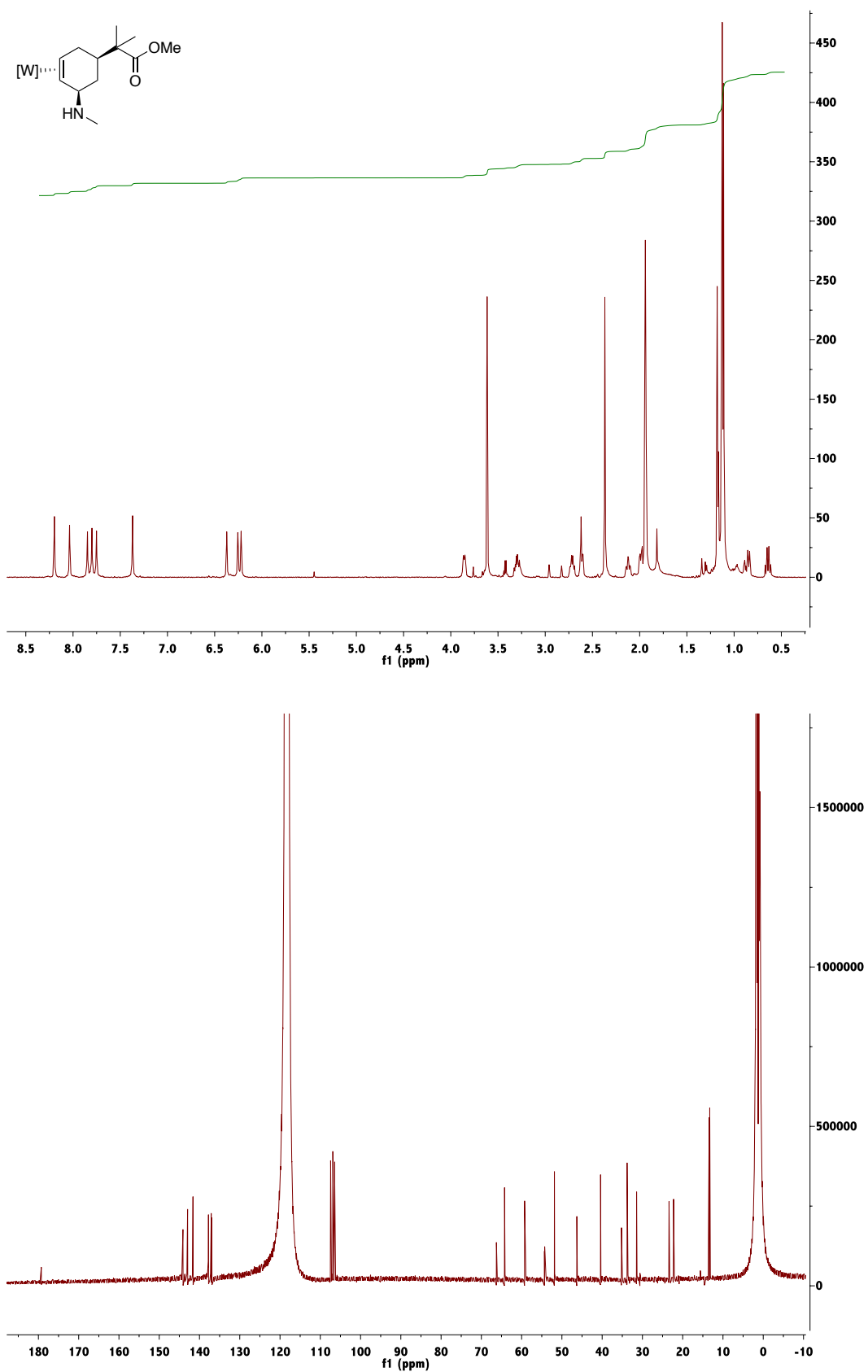
H21B-C21-H21C	109.5	P1-C22-H22A	109.5
P1-C22-H22B	109.5	H22A-C22-H22B	109.5
P1-C22-H22C	109.5	H22A-C22-H22C	109.5
H22B-C22-H22C	109.5	P1-C23-H23A	109.5
P1-C23-H23B	109.5	H23A-C23-H23B	109.5
P1-C23-H23C	109.5	H23A-C23-H23C	109.5
H23B-C23-H23C	109.5	N4-B1-N2	110.80(12)
N4-B1-N6	107.43(12)	N2-B1-N6	107.34(12)
N4-B1-H1A	109.9(9)	N2-B1-H1A	110.8(9)
N6-B1-H1A	110.5(10)		

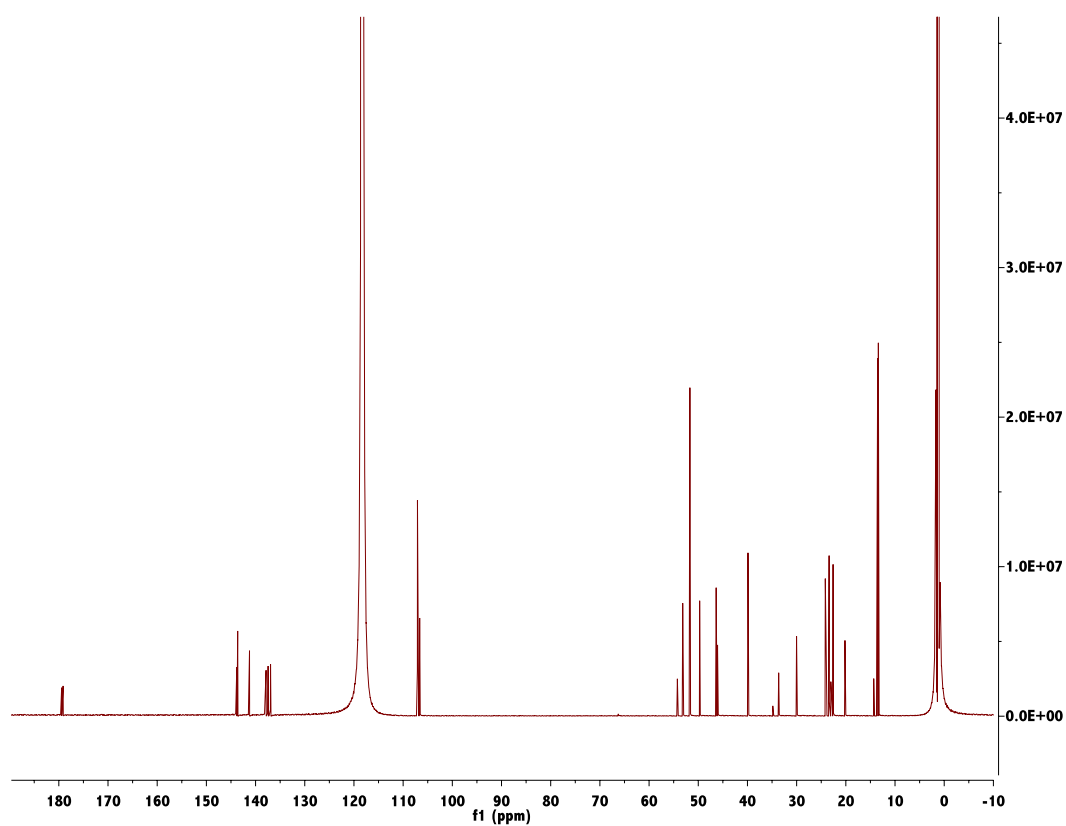
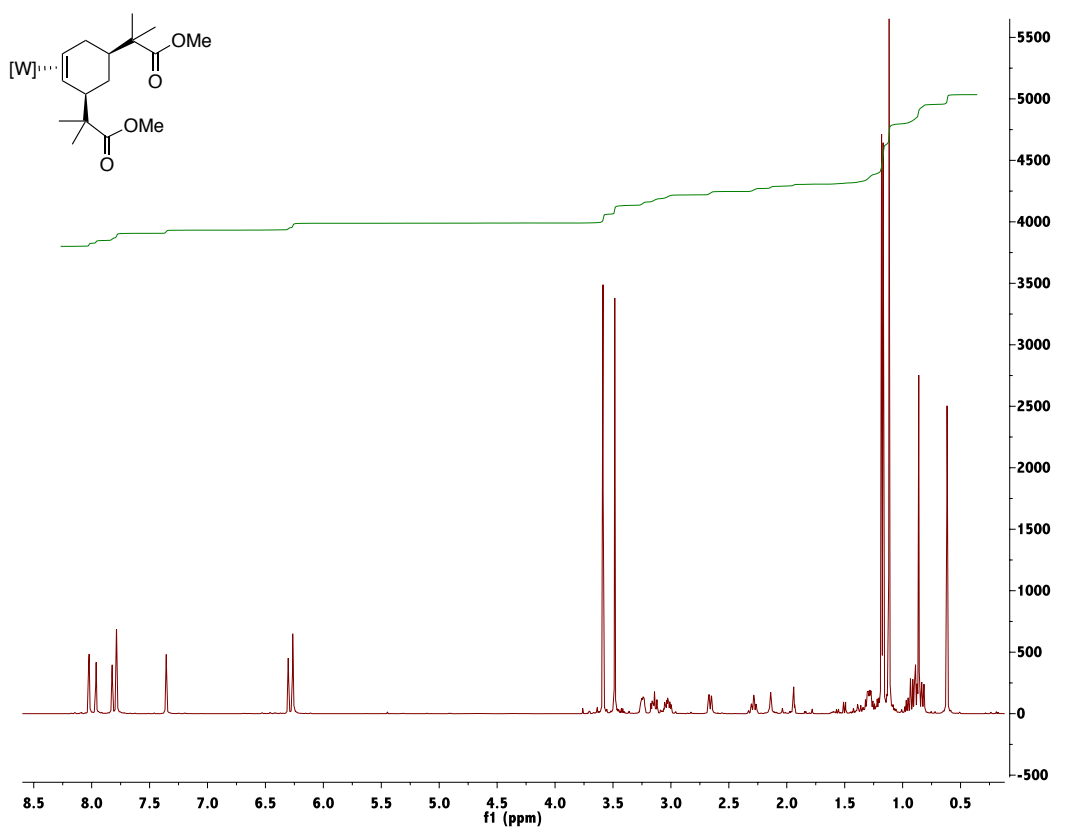
Table 6. Anisotropic atomic displacement parameters (\AA^2) for $\text{C}_{23}\text{H}_{35}\text{BN}_7\text{O}_3\text{PW}$

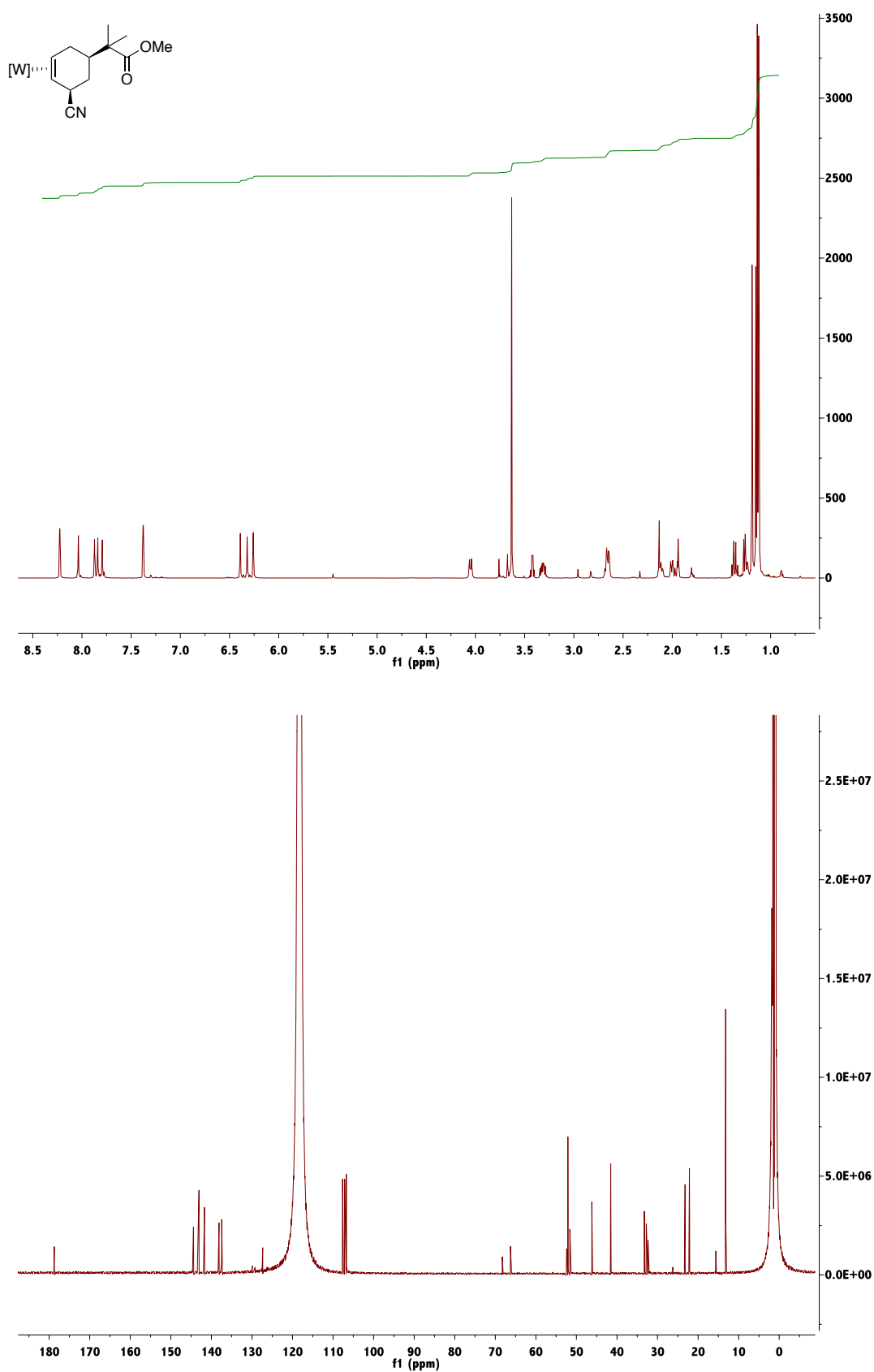
The anisotropic atomic displacement factor exponent takes the form: $-2\pi^2 [h^2 a^{*2} U_{11} + \dots + 2 h k a^* b^* U_{12}]$

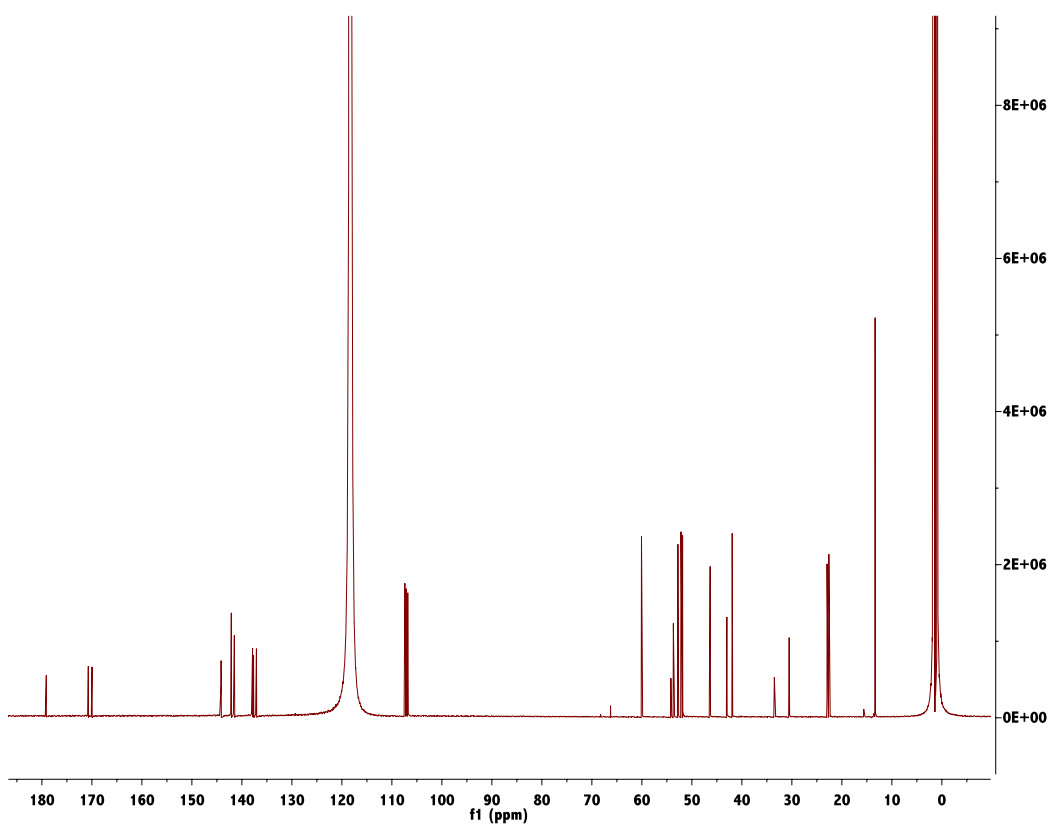
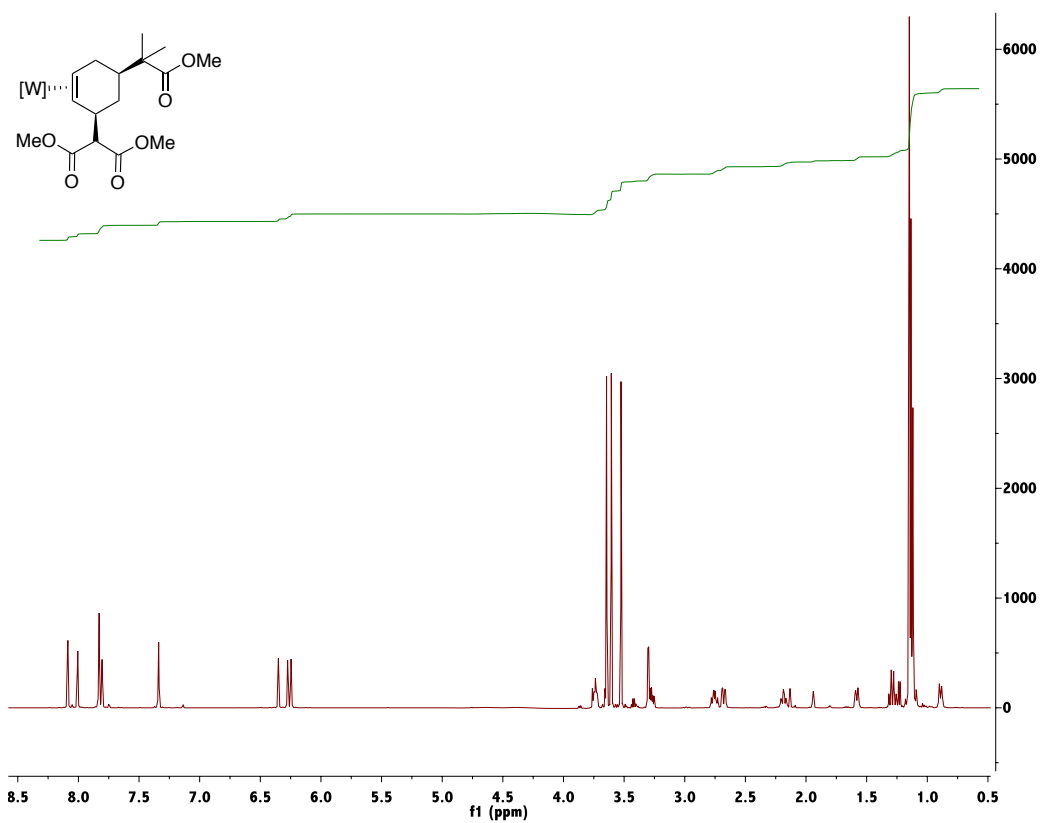
	U_{11}	U_{22}	U_{33}	U_{23}	U_{13}	U_{12}
W1	0.01145(3)	0.01083(3)	0.01016(3)	0.00391(2)	0.00378(2)	0.00196(2)
P1	0.01607(17)	0.01618(18)	0.01479(17)	0.00361(14)	0.00648(14)	0.00502(14)
O1	0.0259(6)	0.0239(6)	0.0207(5)	0.0141(5)	0.0077(5)	0.0117(5)
O2	0.0235(6)	0.0375(7)	0.0147(5)	0.0061(5)	0.0071(4)	0.0100(5)
O3	0.0176(5)	0.0317(7)	0.0192(5)	0.0036(5)	0.0057(4)	0.0080(5)
N1	0.0148(6)	0.0149(6)	0.0129(5)	0.0048(5)	0.0042(4)	0.0007(5)
N2	0.0155(6)	0.0142(6)	0.0152(6)	0.0051(5)	0.0045(5)	-0.0001(5)
N3	0.0138(5)	0.0142(6)	0.0144(5)	0.0055(5)	0.0044(4)	0.0023(5)
N4	0.0161(6)	0.0148(6)	0.0161(6)	0.0073(5)	0.0053(5)	0.0020(5)
N5	0.0143(6)	0.0150(6)	0.0142(6)	0.0046(5)	0.0052(5)	0.0020(5)
N6	0.0134(5)	0.0182(6)	0.0137(5)	0.0070(5)	0.0049(4)	0.0023(5)
N7	0.0139(5)	0.0147(6)	0.0120(5)	0.0030(5)	0.0055(4)	0.0028(5)
C1	0.0128(6)	0.0125(6)	0.0160(6)	0.0040(5)	0.0028(5)	0.0012(5)
C2	0.0152(6)	0.0157(7)	0.0119(6)	0.0033(5)	0.0032(5)	-0.0006(5)
C3	0.0154(7)	0.0170(7)	0.0154(7)	-0.0011(5)	0.0065(5)	0.0001(6)
C4	0.0160(7)	0.0130(7)	0.0205(7)	0.0006(6)	0.0073(6)	0.0025(5)
C5	0.0143(6)	0.0123(6)	0.0152(6)	0.0025(5)	0.0051(5)	0.0014(5)
C6	0.0140(6)	0.0134(7)	0.0193(7)	0.0038(5)	0.0074(5)	0.0029(5)
C7	0.0178(7)	0.0132(7)	0.0144(6)	0.0032(5)	0.0064(5)	0.0020(5)
C8	0.0242(8)	0.0173(7)	0.0157(7)	0.0008(6)	0.0071(6)	-0.0040(6)
C9	0.0291(8)	0.0171(7)	0.0243(8)	0.0083(6)	0.0135(7)	0.0085(6)

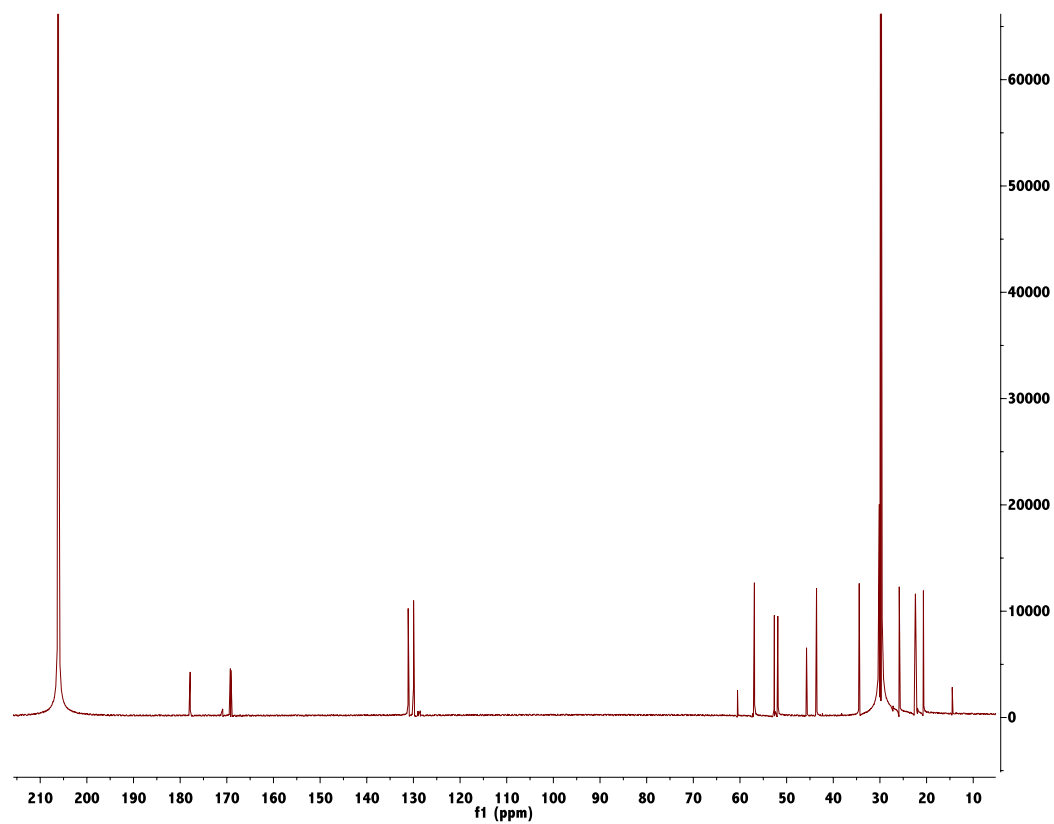
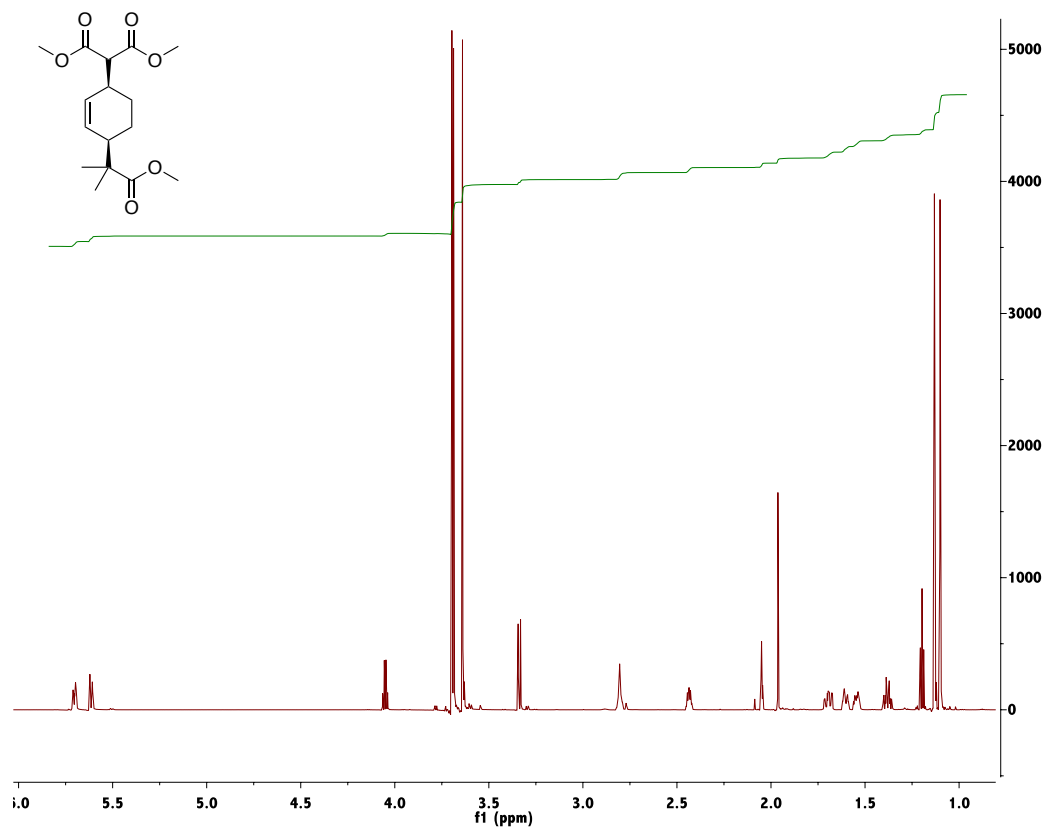
	U ₁₁	U ₂₂	U ₃₃	U ₂₃	U ₁₃	U ₁₂
C10	0.0167(7)	0.0138(7)	0.0173(7)	0.0054(5)	0.0060(5)	0.0014(5)
C11	0.0243(9)	0.0618(14)	0.0294(9)	0.0053(9)	0.0106(8)	0.0197(9)
C12	0.0204(7)	0.0225(8)	0.0127(6)	0.0051(6)	0.0044(6)	0.0050(6)
C13	0.0203(7)	0.0263(8)	0.0148(7)	0.0009(6)	0.0008(6)	0.0007(6)
C14	0.0178(7)	0.0182(7)	0.0208(7)	0.0021(6)	0.0037(6)	-0.0015(6)
C15	0.0166(7)	0.0174(7)	0.0161(7)	0.0063(6)	0.0043(5)	0.0054(6)
C16	0.0227(7)	0.0204(8)	0.0167(7)	0.0088(6)	0.0058(6)	0.0098(6)
C17	0.0240(7)	0.0171(7)	0.0186(7)	0.0099(6)	0.0088(6)	0.0072(6)
C18	0.0152(7)	0.0197(7)	0.0187(7)	0.0030(6)	0.0043(6)	0.0050(6)
C19	0.0152(7)	0.0292(9)	0.0174(7)	0.0031(6)	0.0058(6)	0.0065(6)
C20	0.0134(6)	0.0297(8)	0.0152(7)	0.0084(6)	0.0058(5)	0.0041(6)
C21	0.0330(10)	0.0227(9)	0.0406(11)	-0.0082(8)	0.0161(8)	0.0027(8)
C22	0.0217(8)	0.0285(9)	0.0246(8)	0.0048(7)	0.0069(6)	0.0131(7)
C23	0.0288(9)	0.0405(10)	0.0207(8)	0.0151(7)	0.0141(7)	0.0139(8)
B1	0.0151(7)	0.0166(8)	0.0162(7)	0.0075(6)	0.0047(6)	0.0017(6)

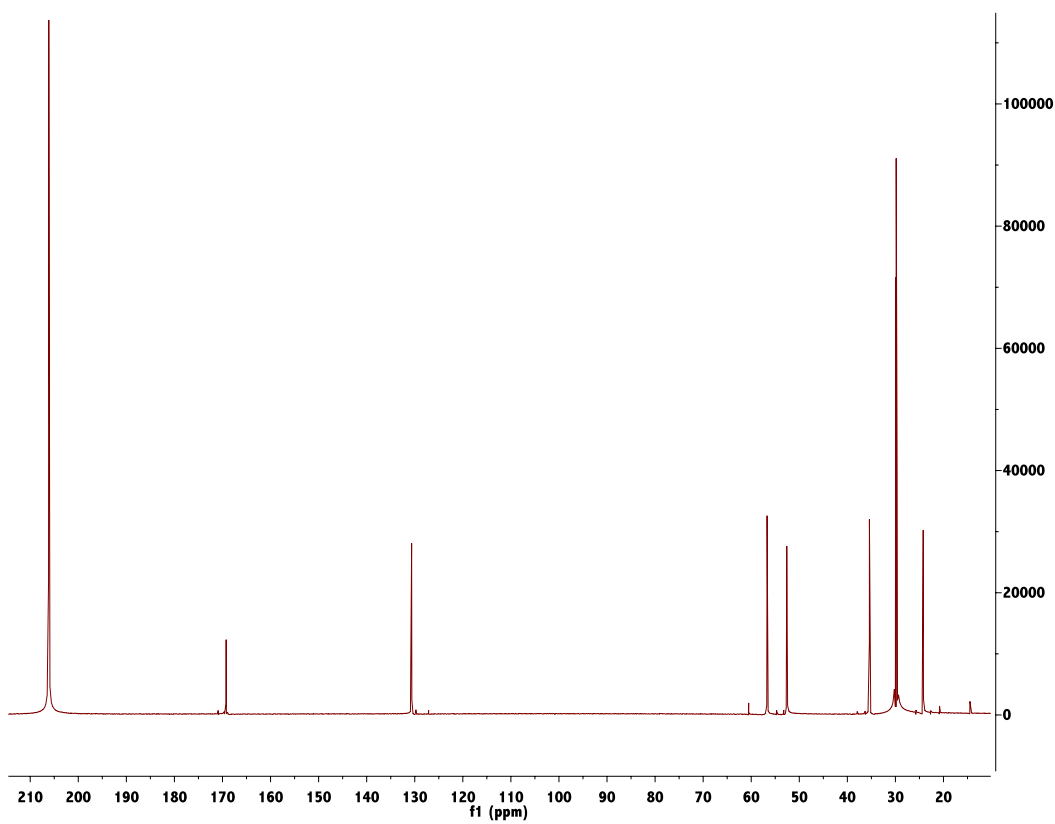
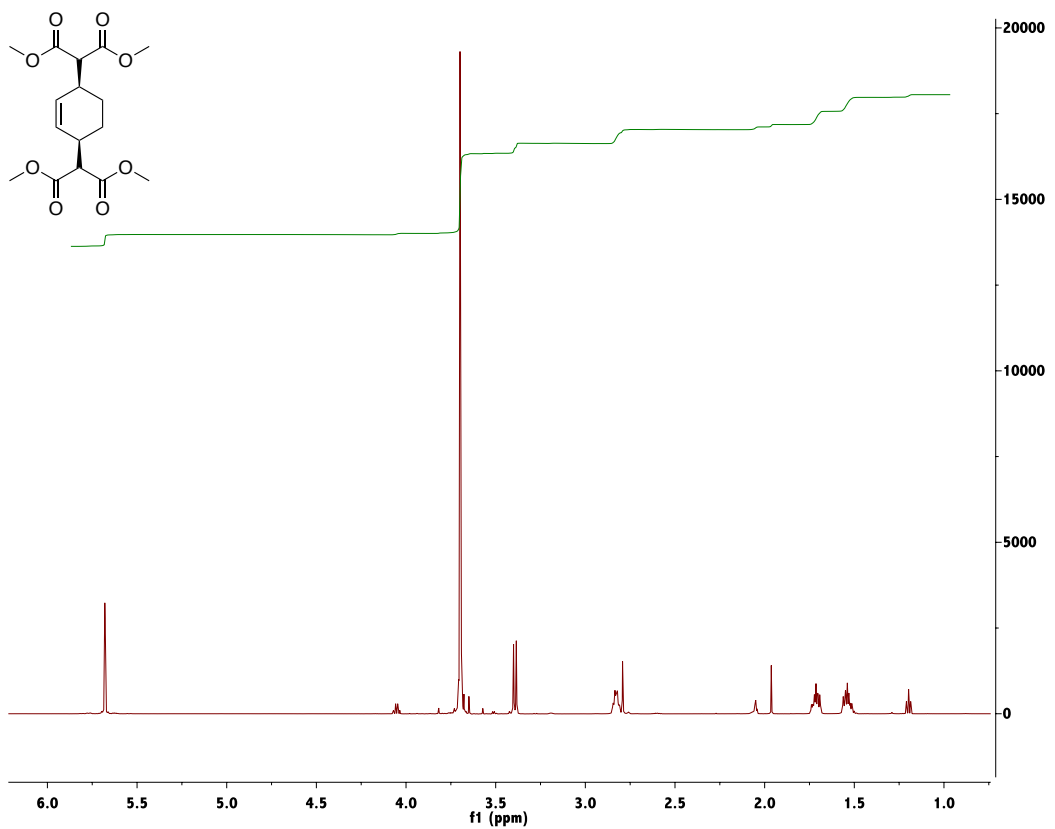
$^1\text{H-NMR}$ (CD_3CN) and $^{13}\text{C-NMR}$ (CD_3CN) of Compound 31A:

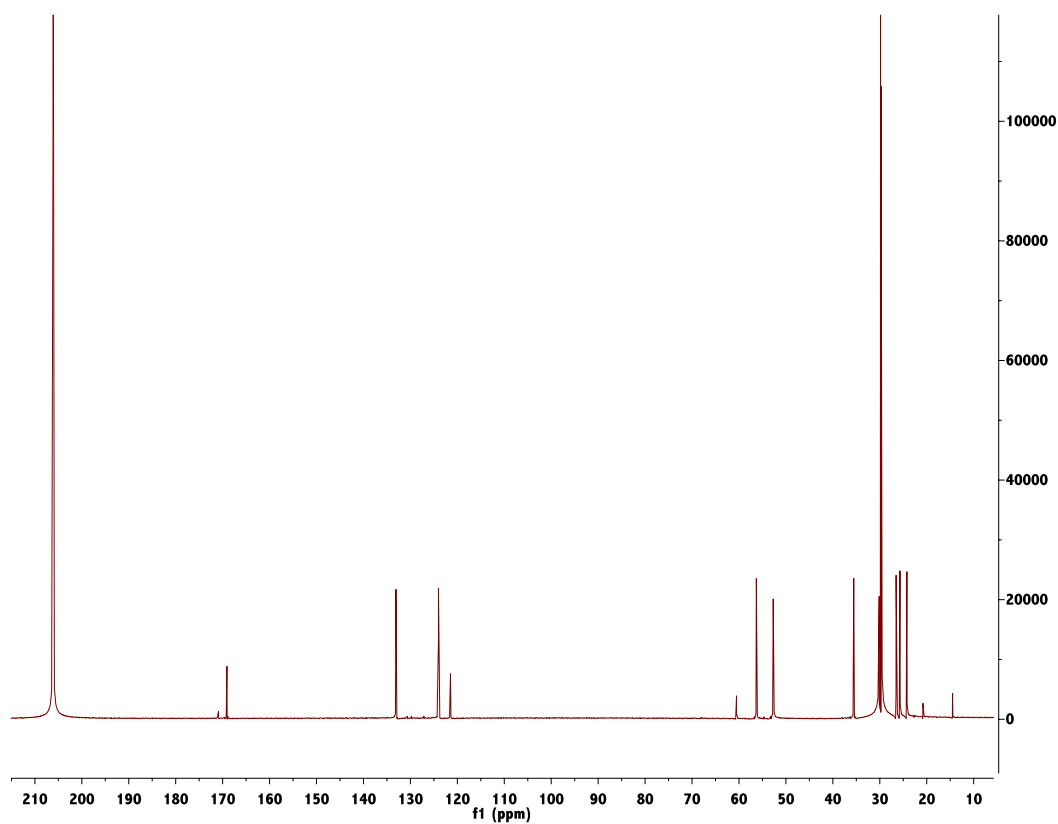
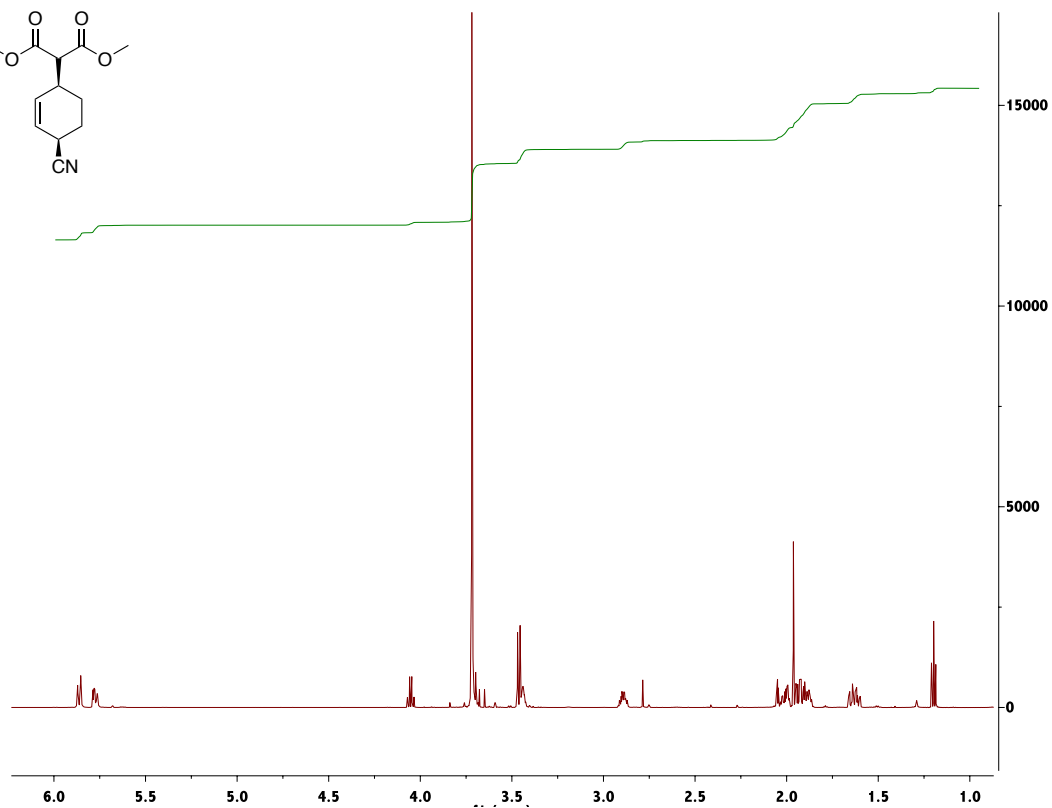
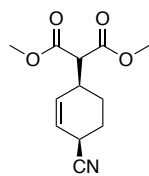
$^1\text{H-NMR}$ (CD_3CN) and $^{13}\text{C-NMR}$ (CD_3CN) of Compound 32A:

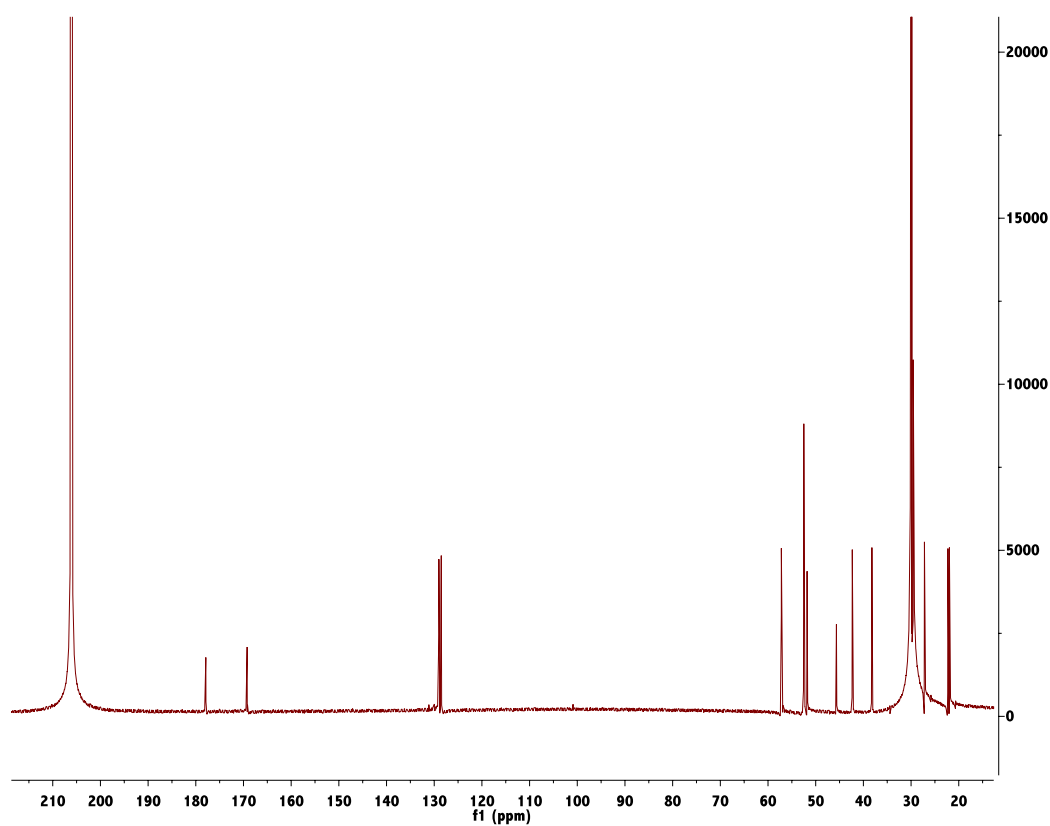
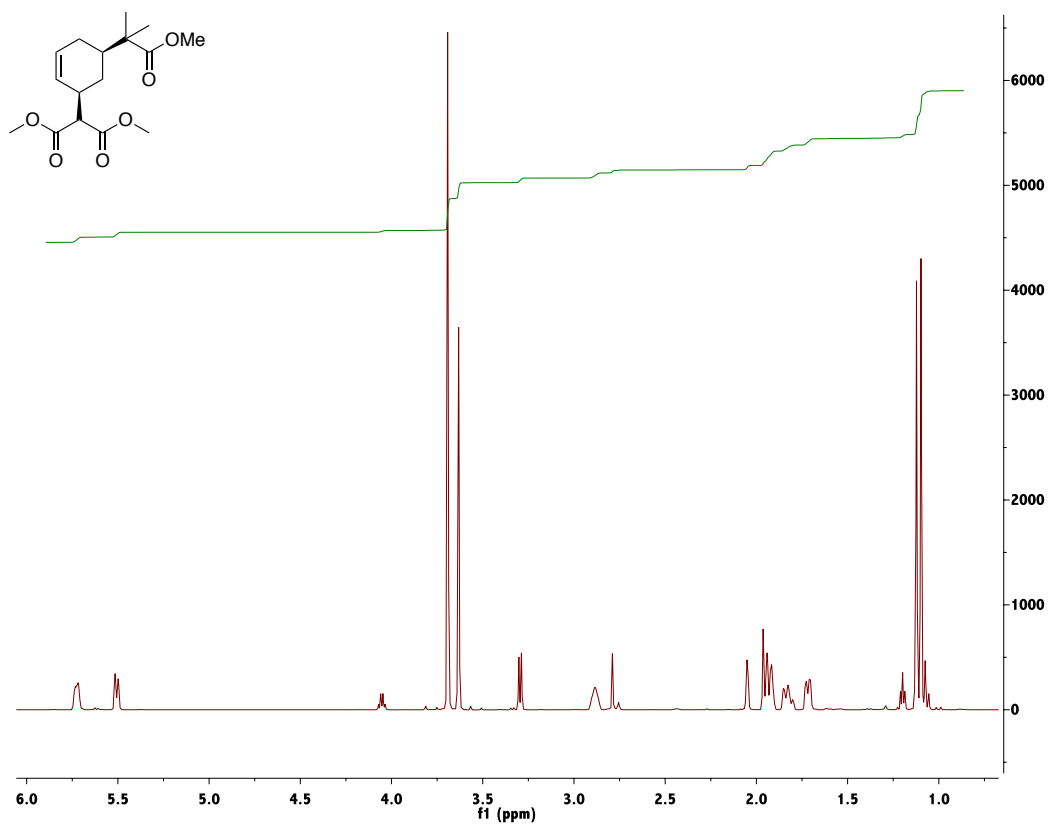
$^1\text{H-NMR}$ (CD_3CN) and $^{13}\text{C-NMR}$ (CD_3CN) of Compound 33A:

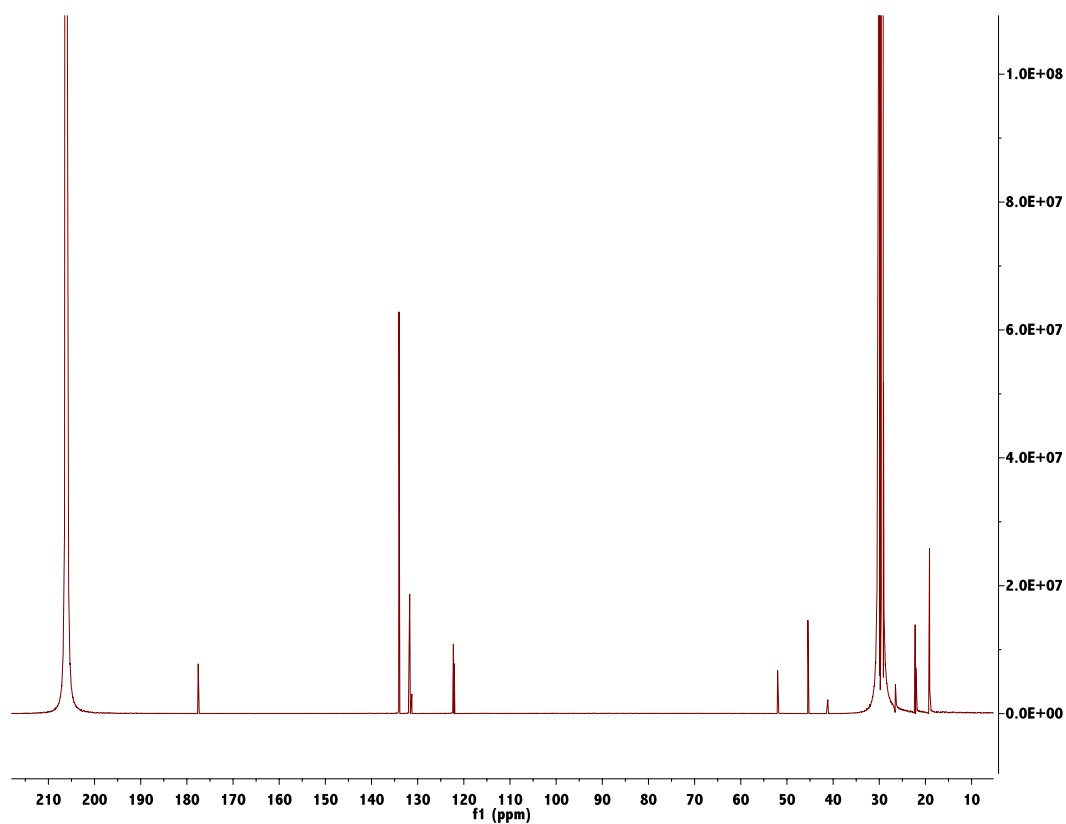
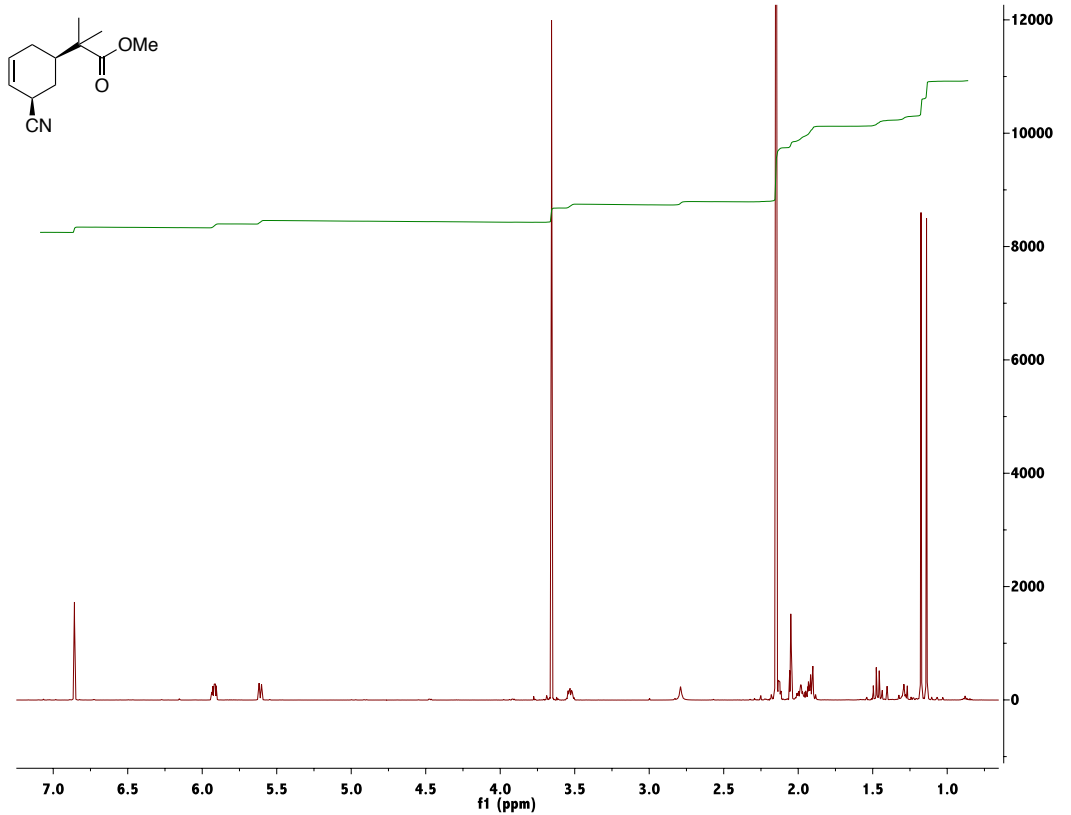
$^1\text{H-NMR}$ (CD_3CN) and $^{13}\text{C-NMR}$ (CD_3CN) of Compound 34A:

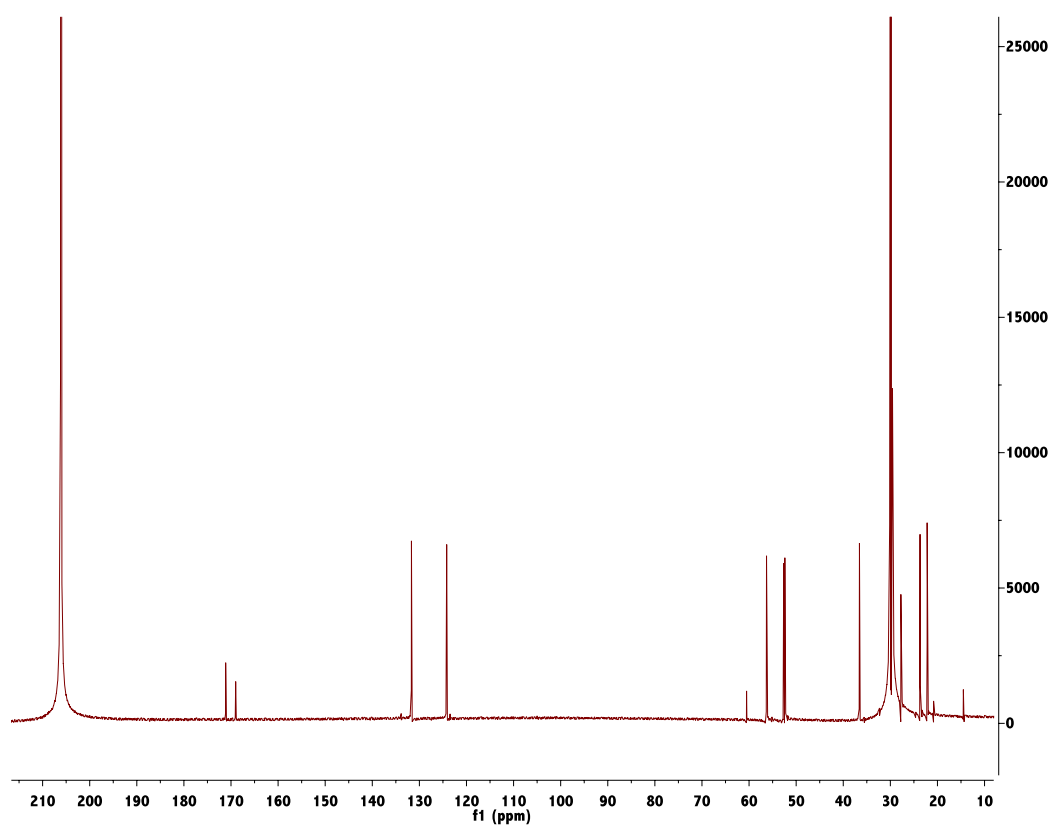
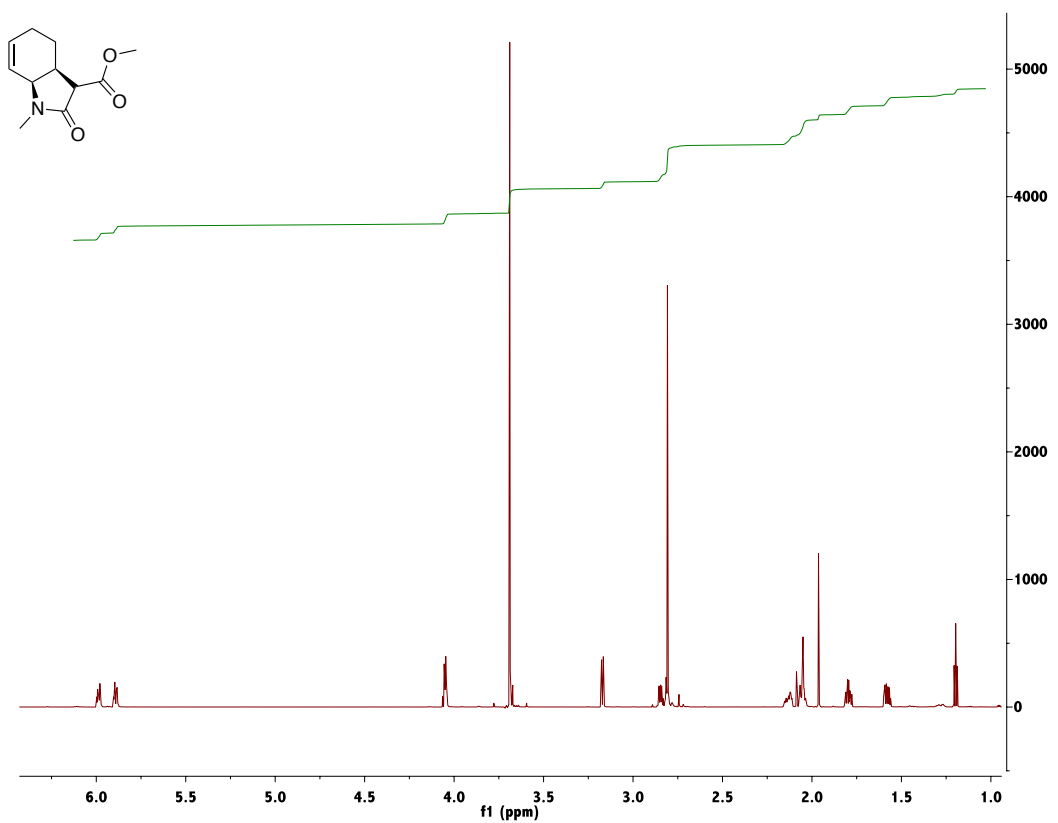
$^1\text{H-NMR}$ ($\text{d}^6\text{-acetone}$) and $^{13}\text{C-NMR}$ ($\text{d}^6\text{-acetone}$) of Compound 36:

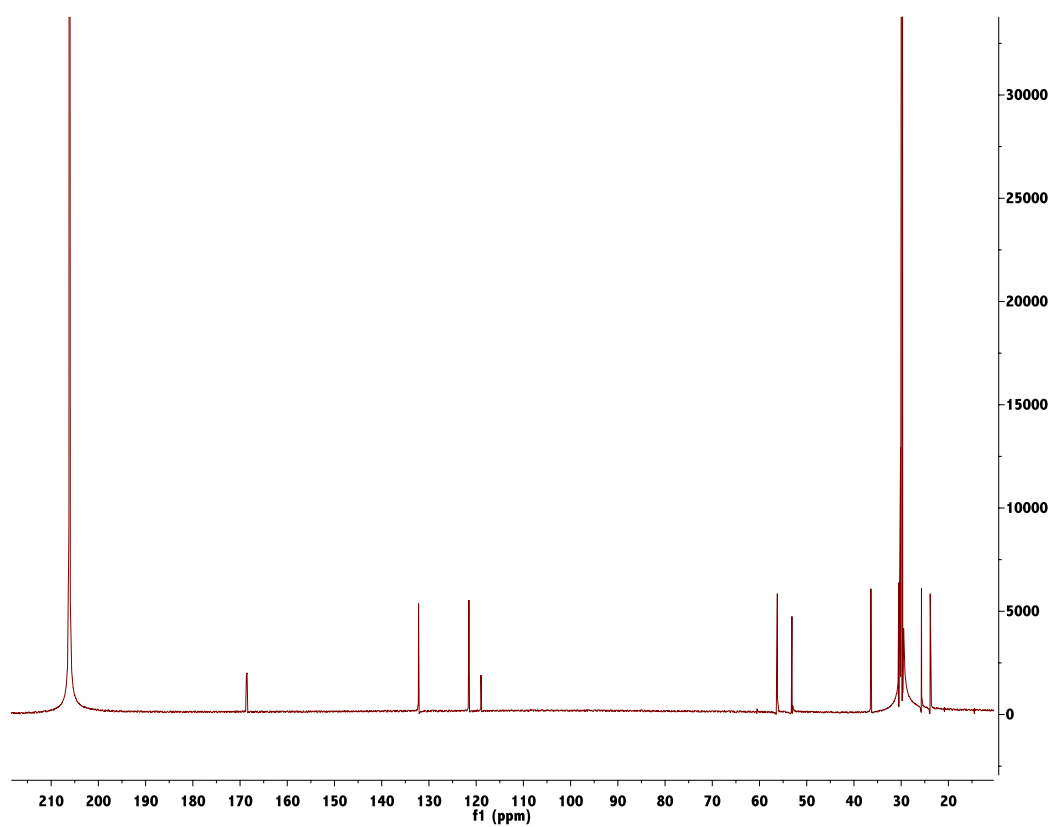
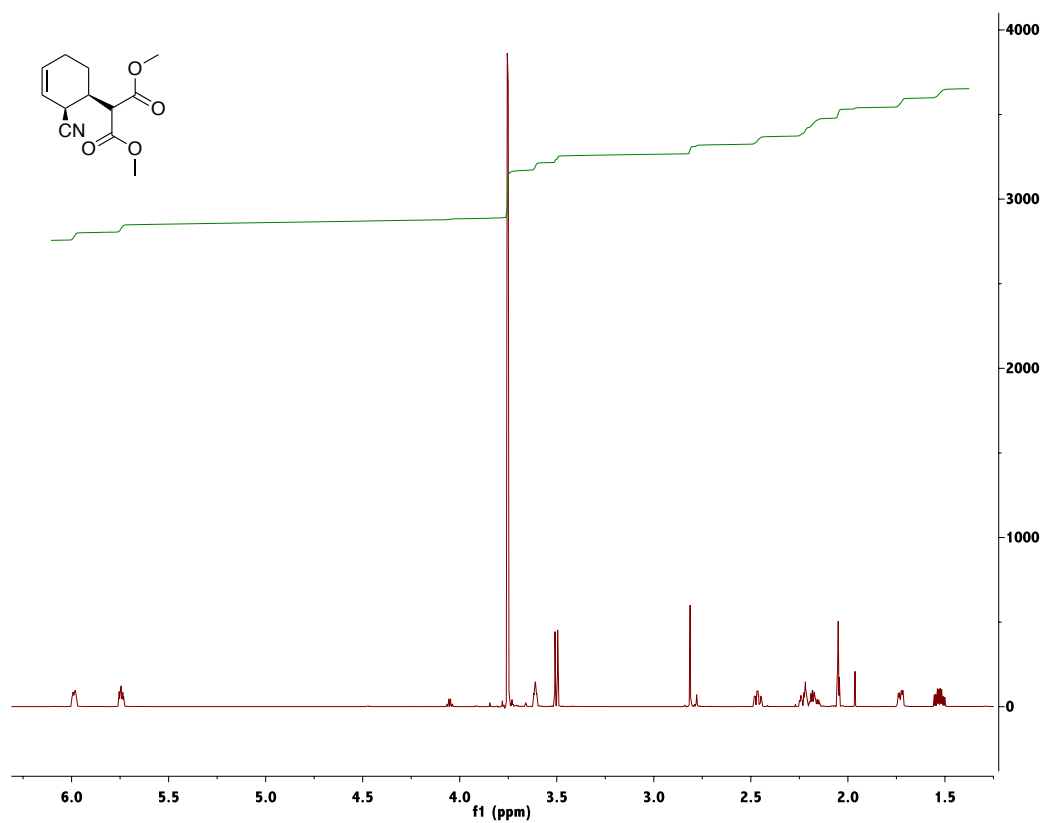
$^1\text{H-NMR}$ ($\text{d}^6\text{-acetone}$) and $^{13}\text{C-NMR}$ ($\text{d}^6\text{-acetone}$) of Compound 37:

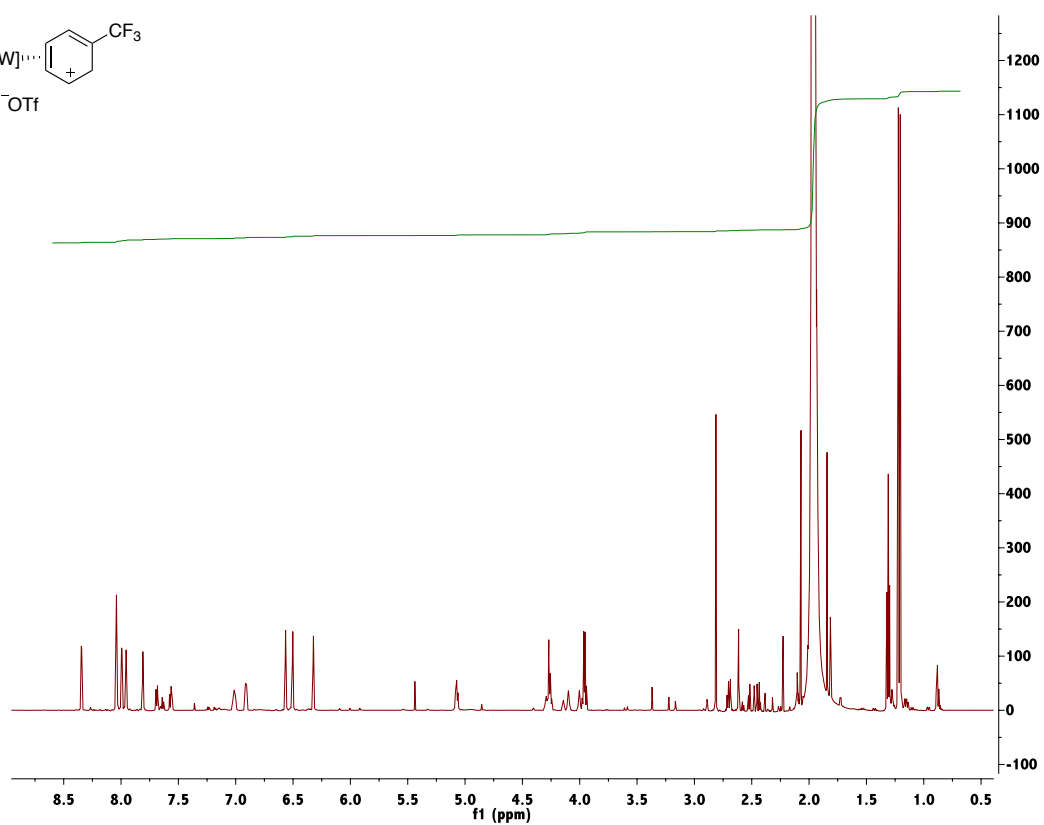
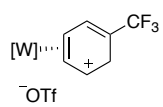
$^1\text{H-NMR}$ ($\text{d}^6\text{-acetone}$) and $^{13}\text{C-NMR}$ ($\text{d}^6\text{-acetone}$) of Compound 38:

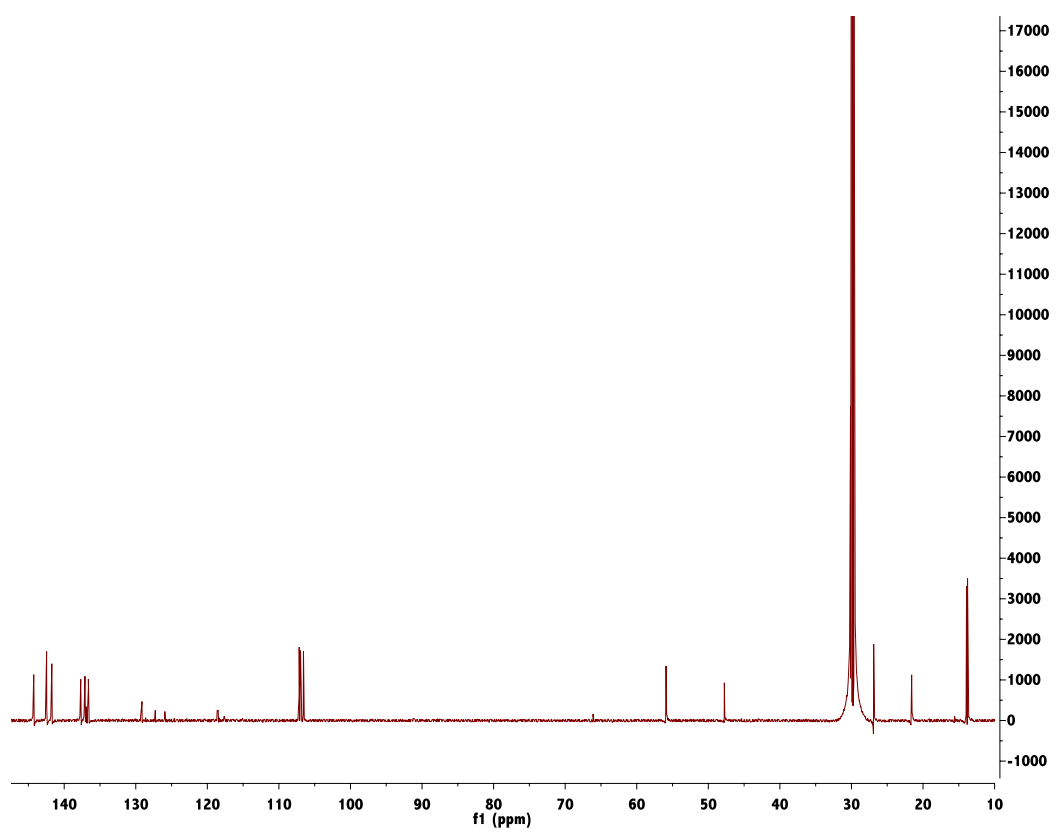
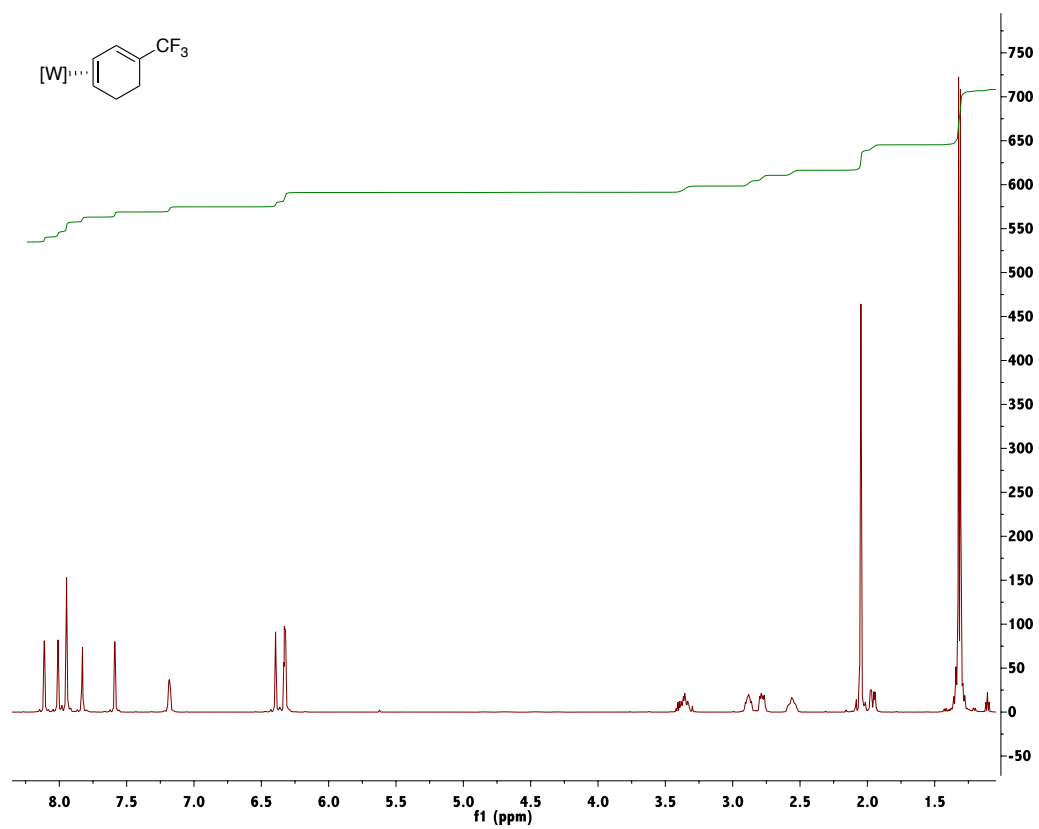
$^1\text{H-NMR}$ ($\text{d}^6\text{-acetone}$) and $^{13}\text{C-NMR}$ ($\text{d}^6\text{-acetone}$) of Compound 39:

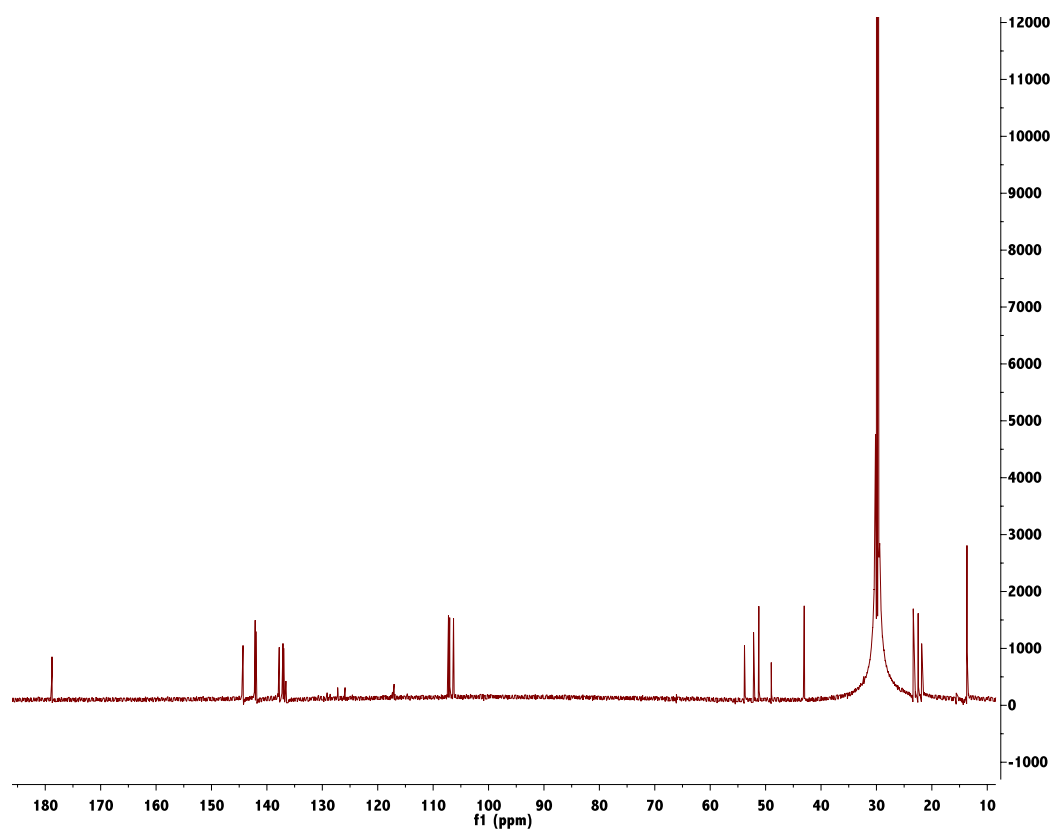
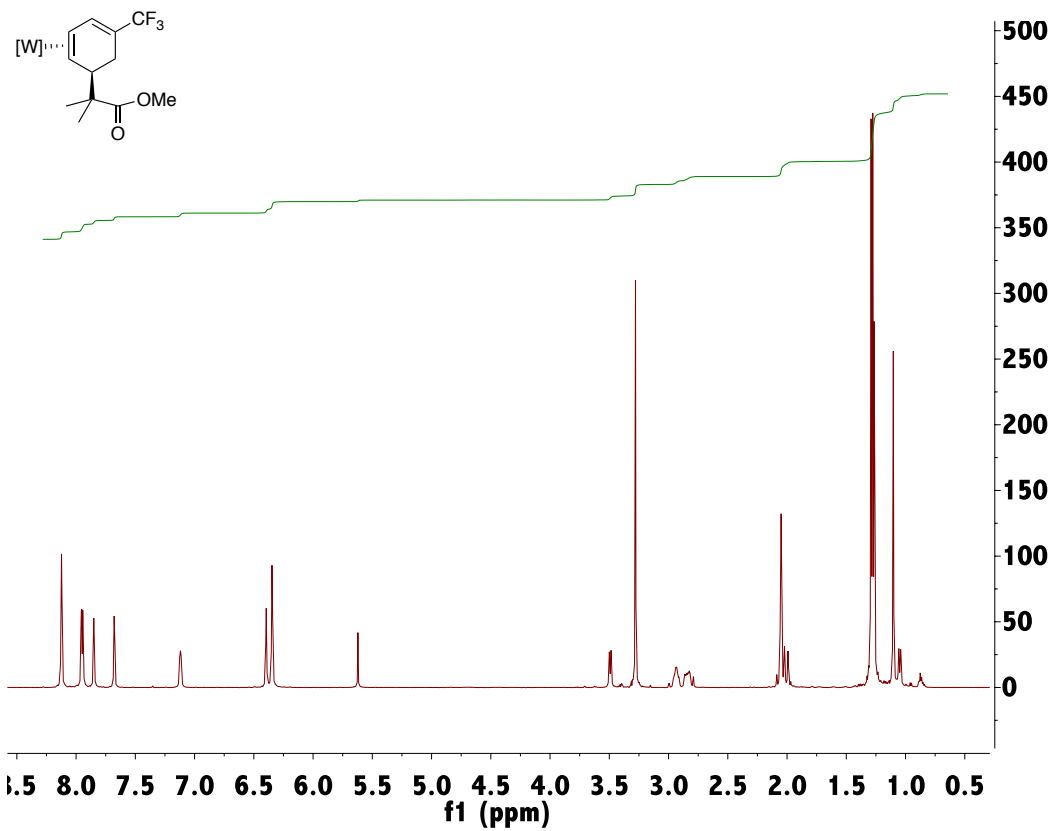
$^1\text{H-NMR}$ ($\text{d}^6\text{-acetone}$) and $^{13}\text{C-NMR}$ ($\text{d}^6\text{-acetone}$) of Compound 40

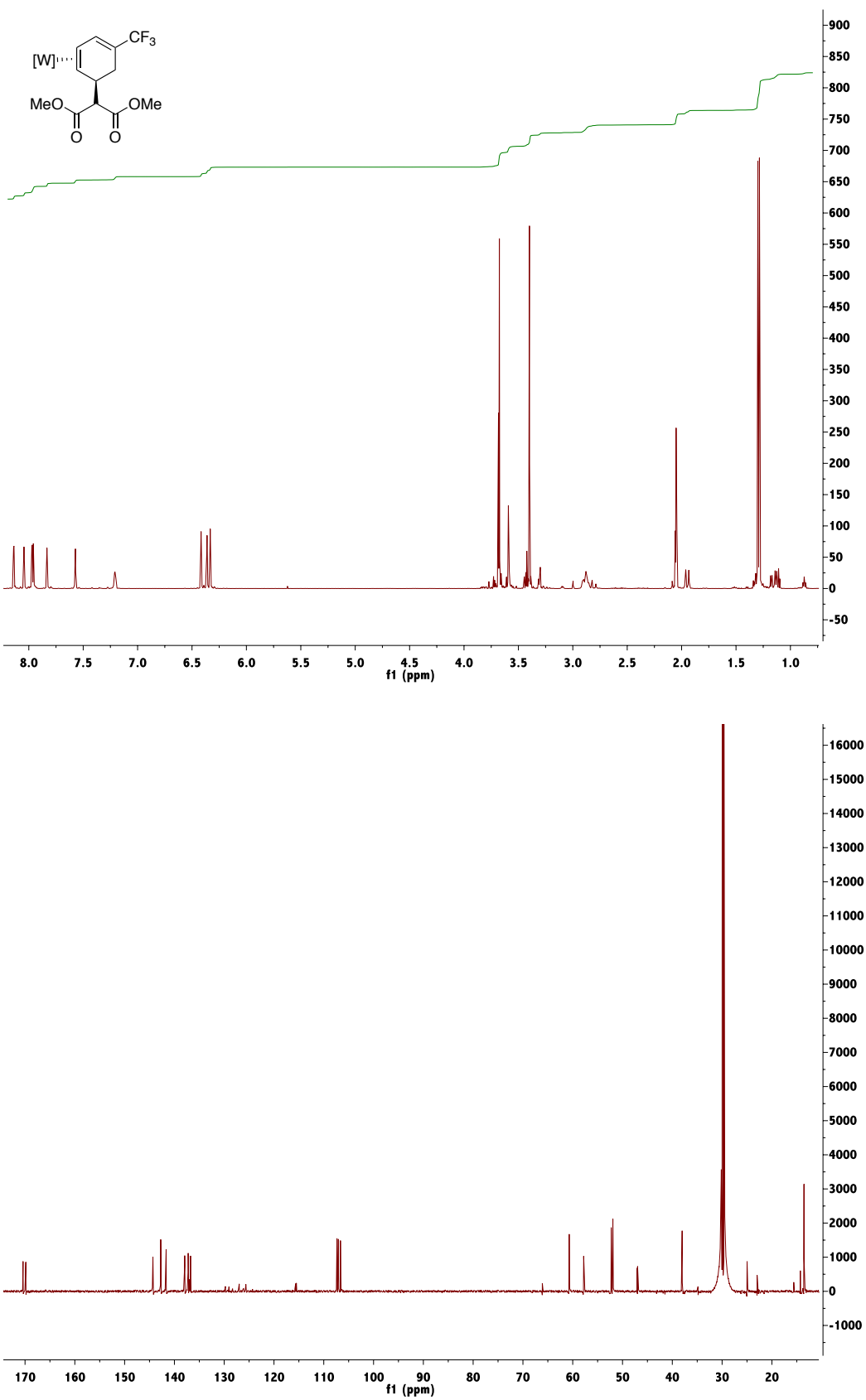
$^1\text{H-NMR}$ ($\text{d}^6\text{-acetone}$) and $^{13}\text{C-NMR}$ ($\text{d}^6\text{-acetone}$) of Compound 41:

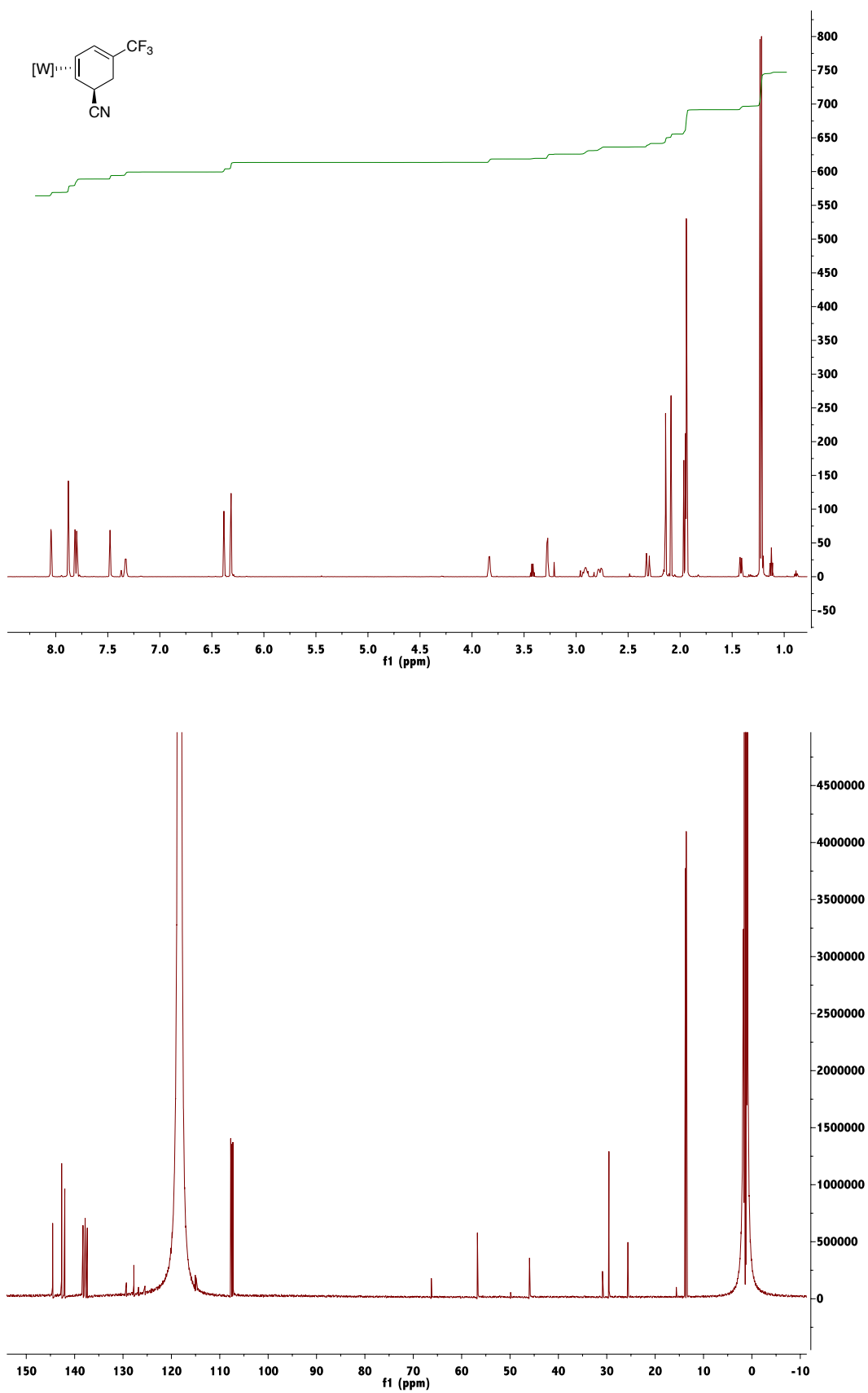
$^1\text{H-NMR}$ ($\text{d}^6\text{-acetone}$) and $^{13}\text{C-NMR}$ ($\text{d}^6\text{-acetone}$) of Compound 42:

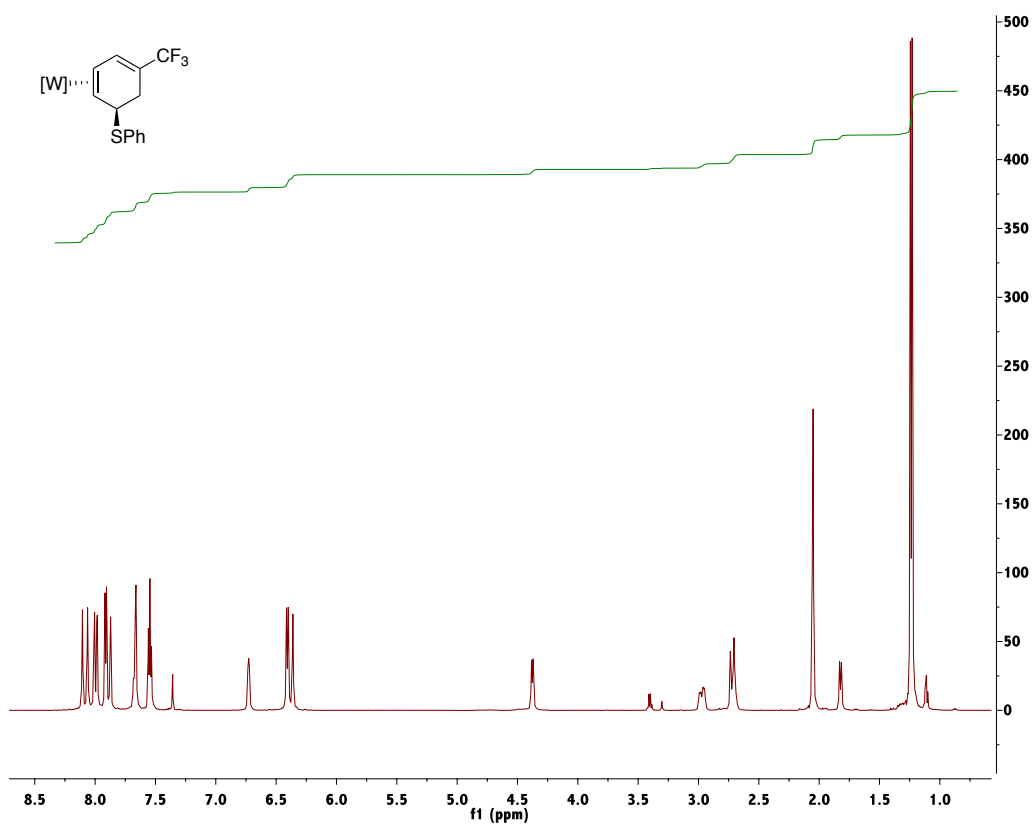
$^1\text{H-NMR}$ (CD_3CN) of Compound 53:

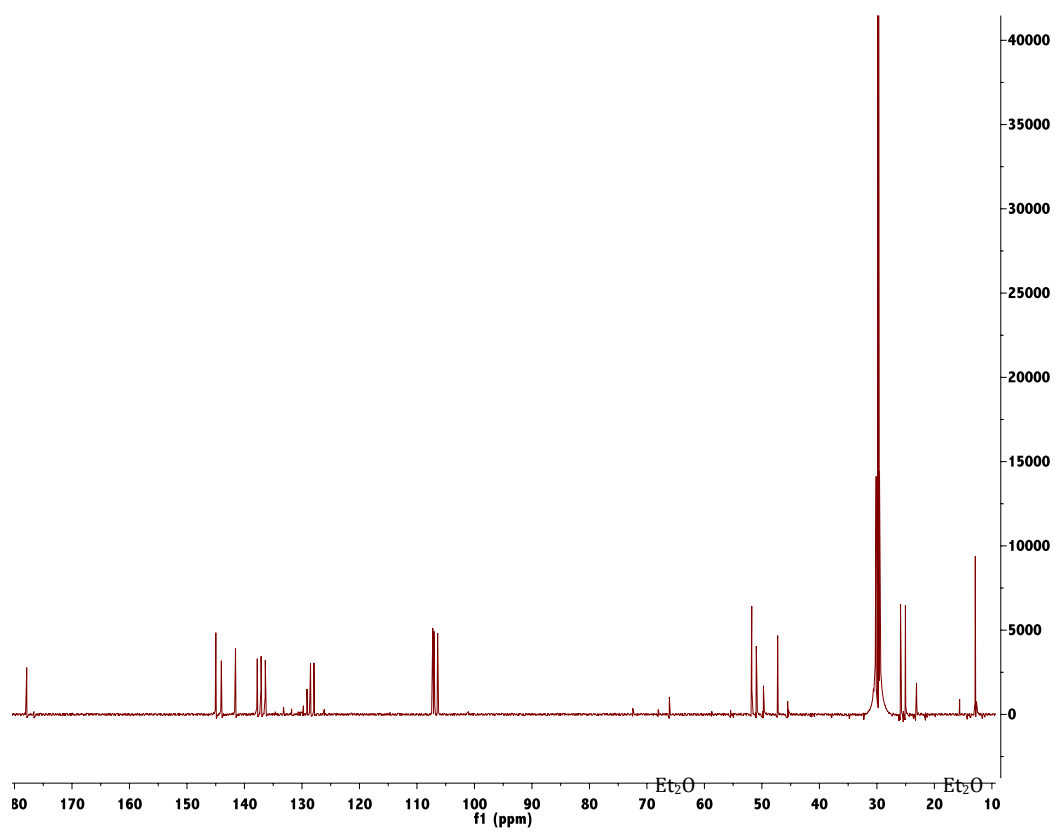
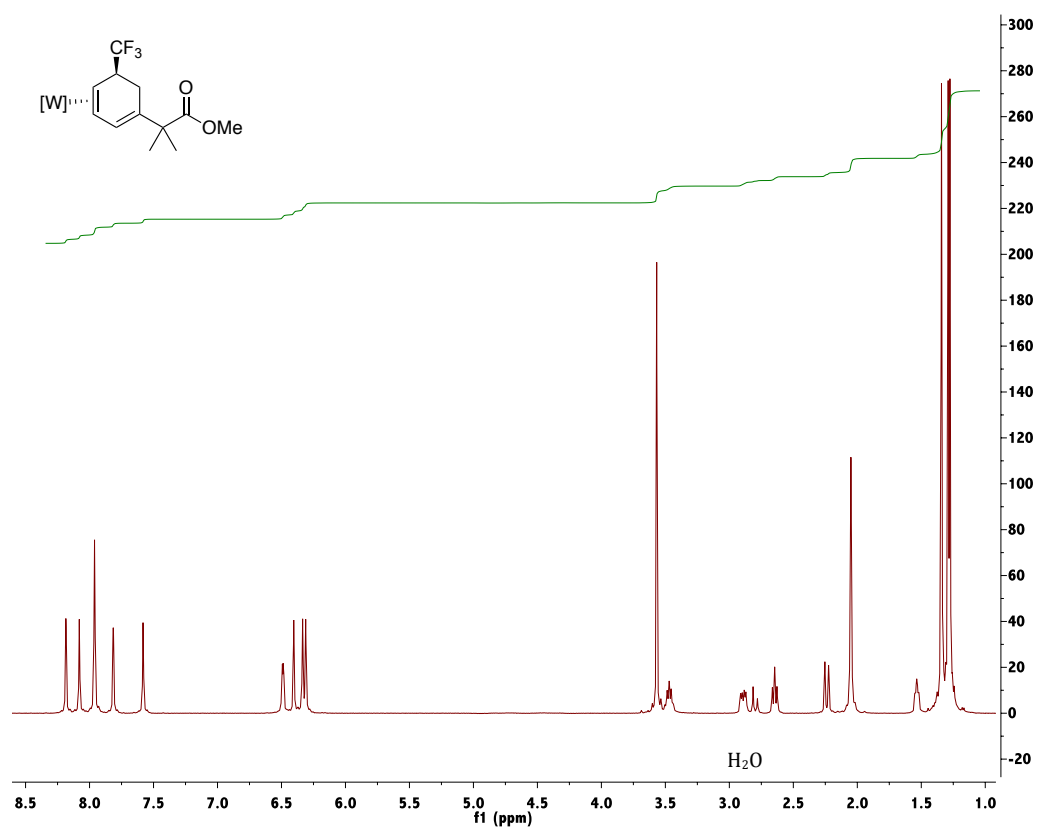
$^1\text{H-NMR}$ (d^6 -acetone) and $^{13}\text{C-NMR}$ (d^6 -acetone) of Compound 54:

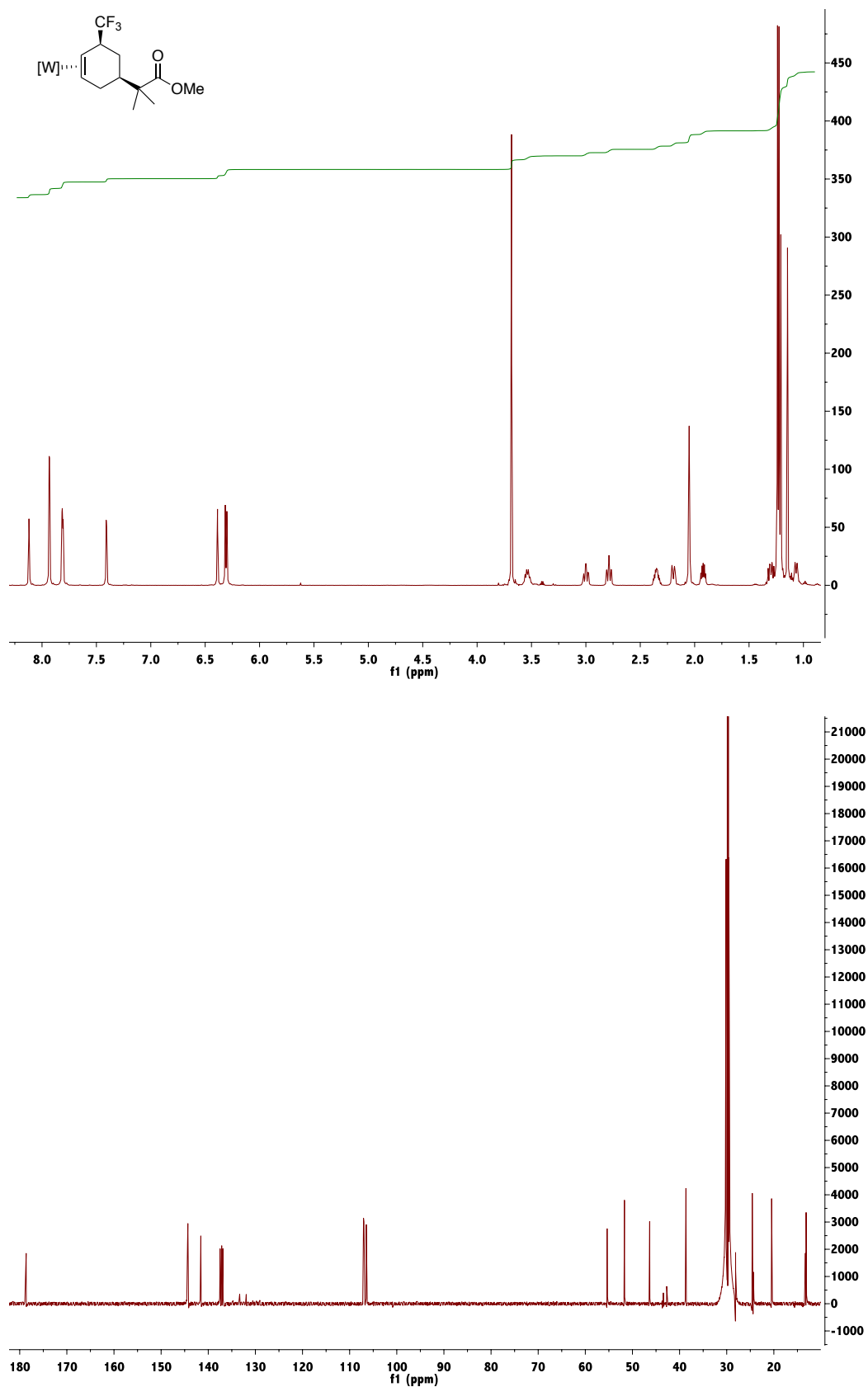
$^1\text{H-NMR}$ (CD_3CN) and $^{13}\text{C-NMR}$ (CD_3CN) of Compound 55:

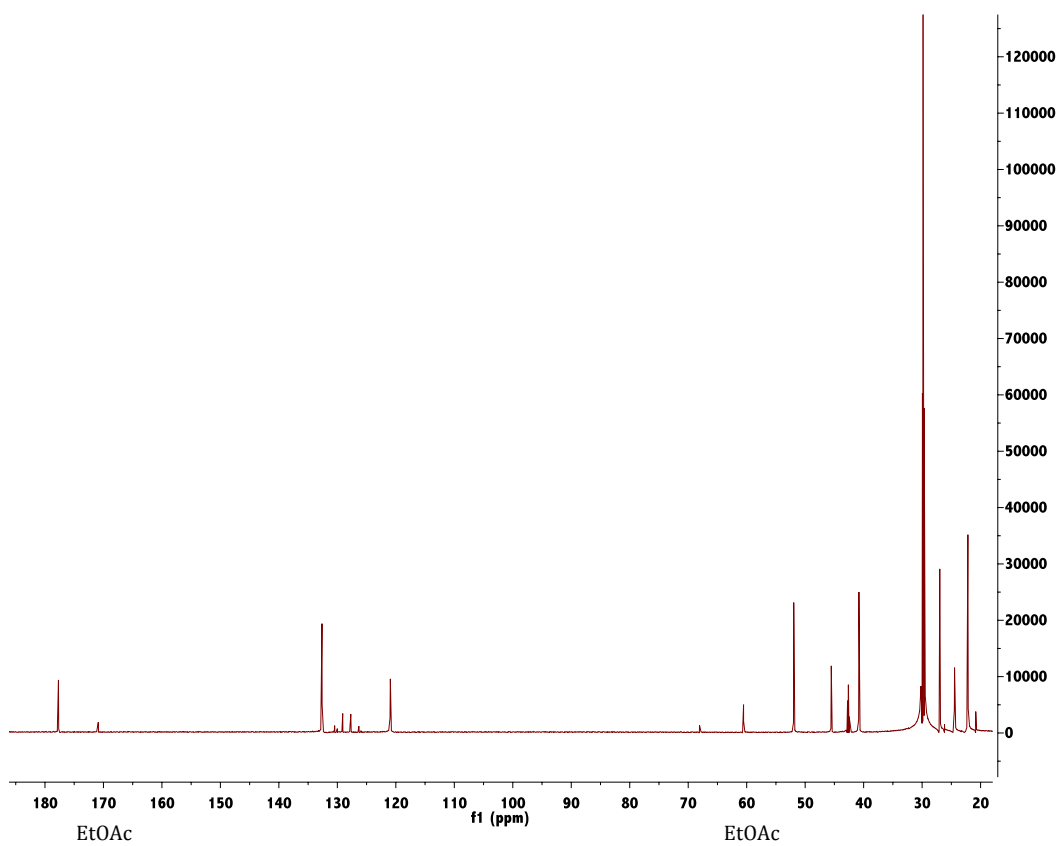
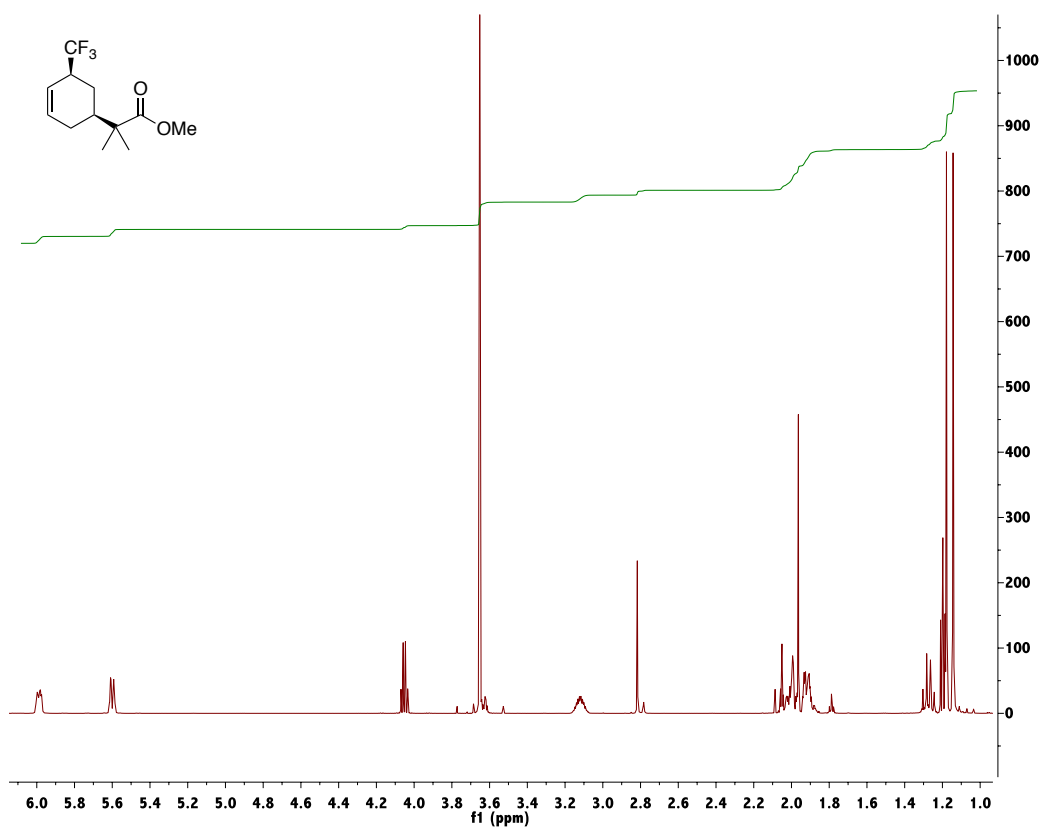
$^1\text{H-NMR}$ ($\text{d}^6\text{-acetone}$) and $^{13}\text{C-NMR}$ ($\text{d}^6\text{-acetone}$) of Compound 56:

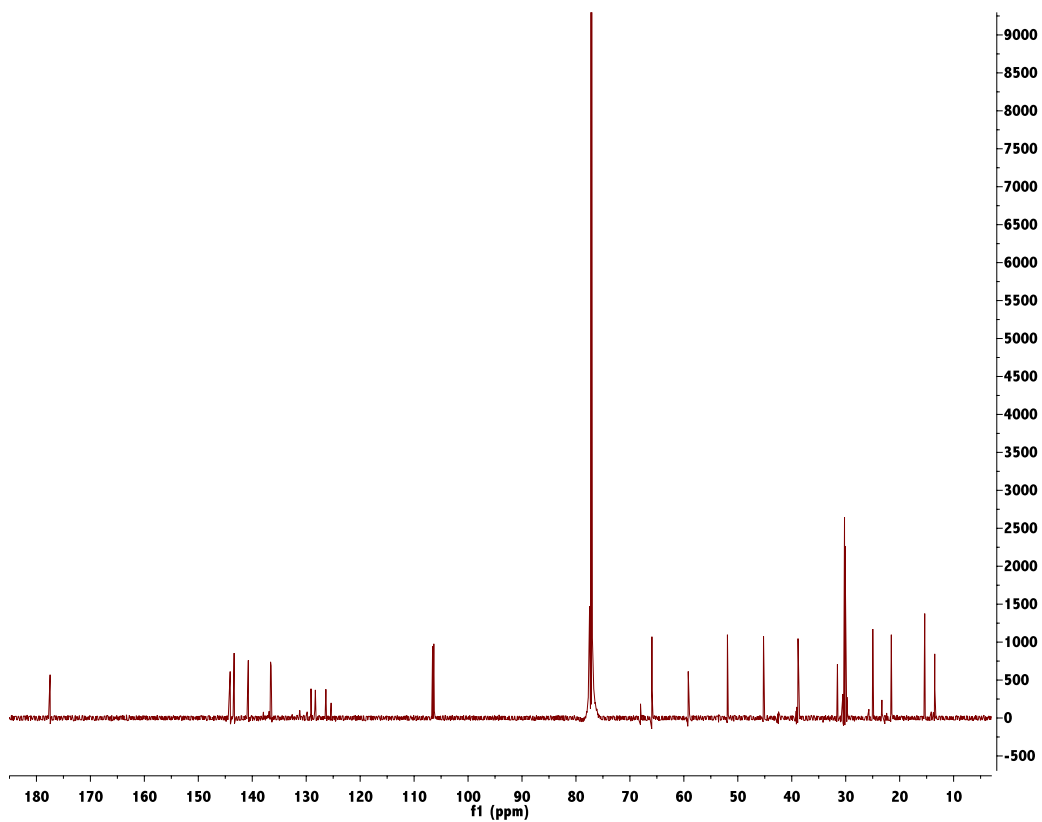
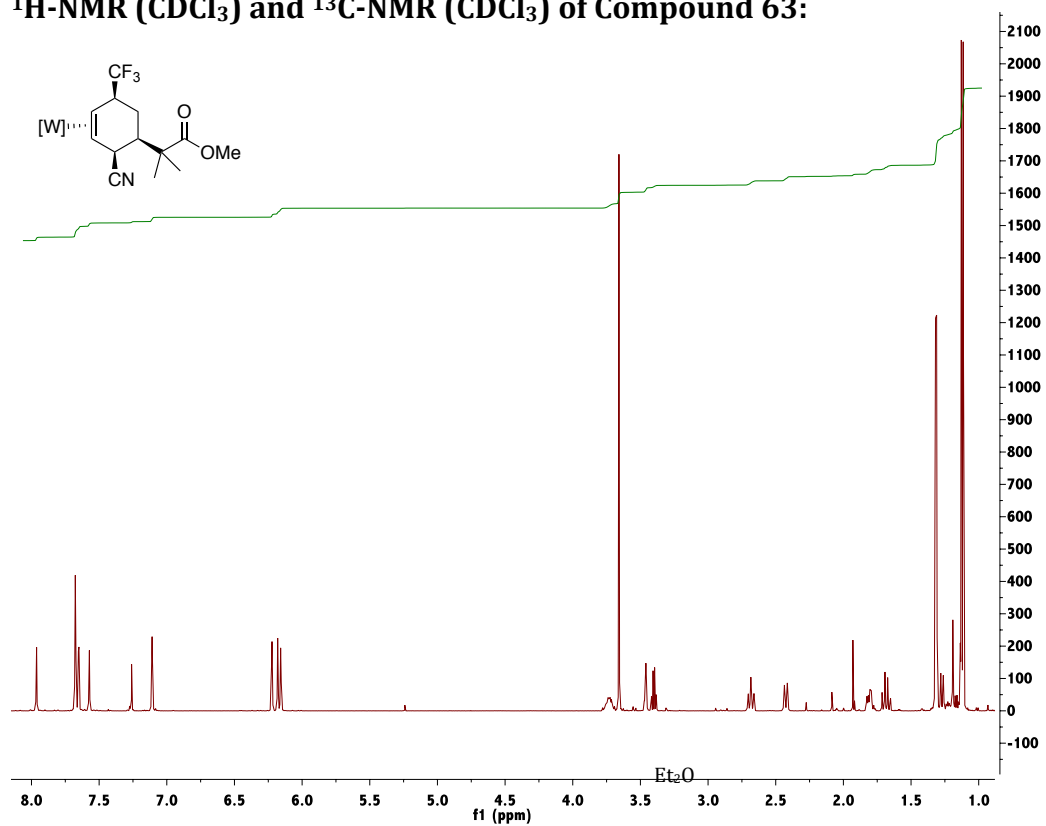
$^1\text{H-NMR}$ (CD_3CN) and $^{13}\text{C-NMR}$ (CD_3CN) of Compound 57:

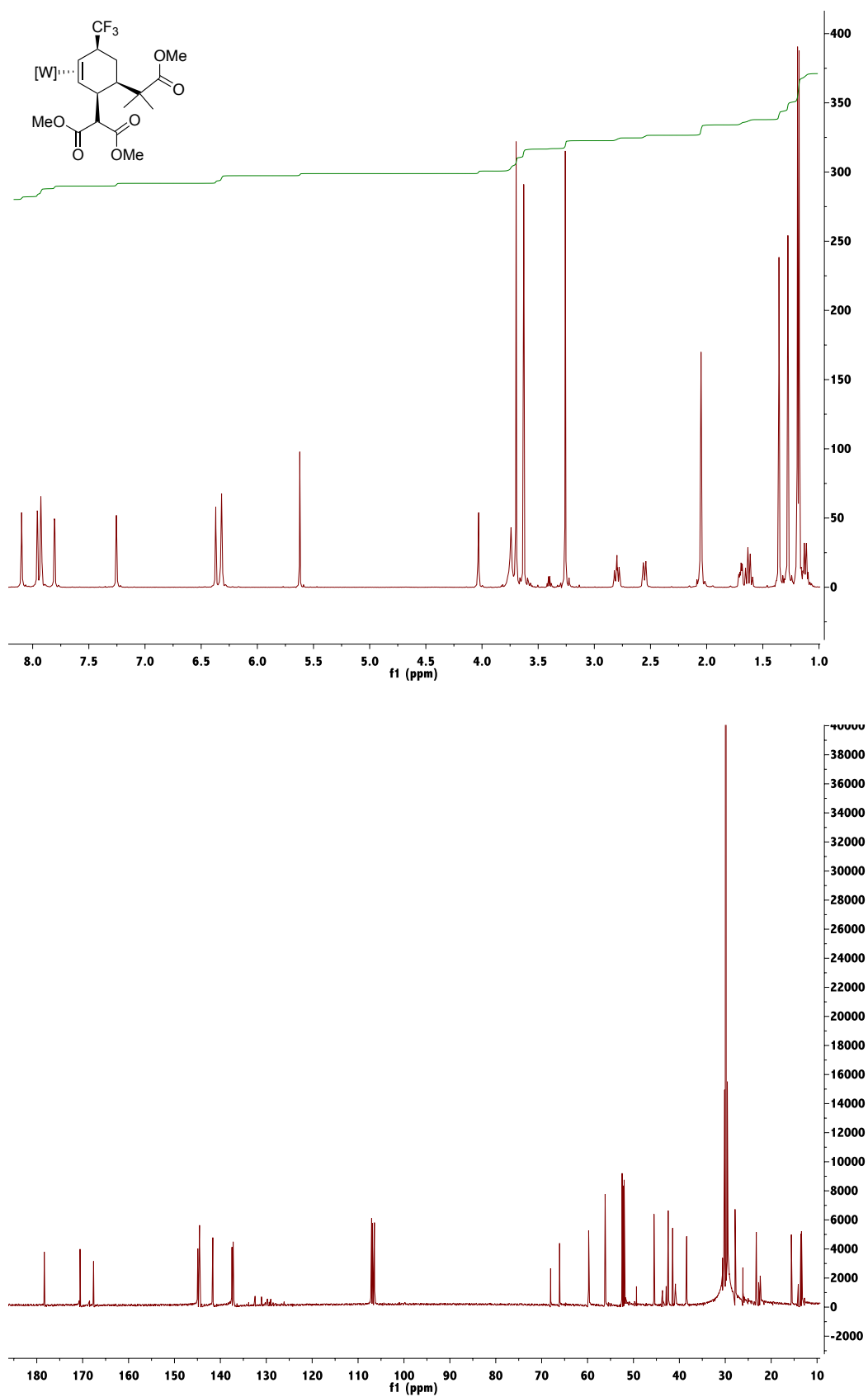
$^1\text{H-NMR}$ ($\text{d}^6\text{-acetone}$) of Compound 58:

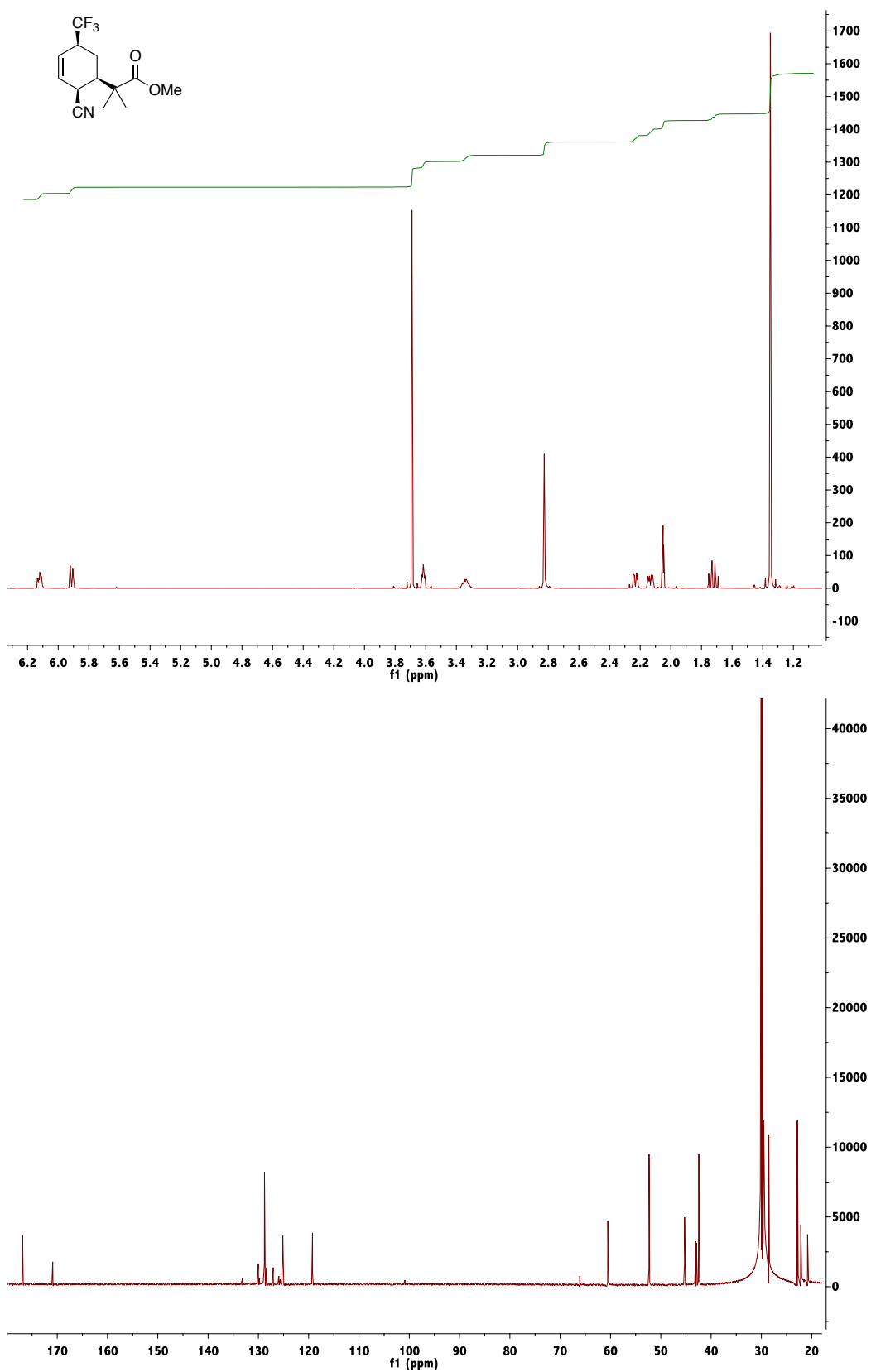
$^1\text{H-NMR}$ ($\text{d}^6\text{-acetone}$) and $^{13}\text{C-NMR}$ ($\text{d}^6\text{-acetone}$) of Compound 60:

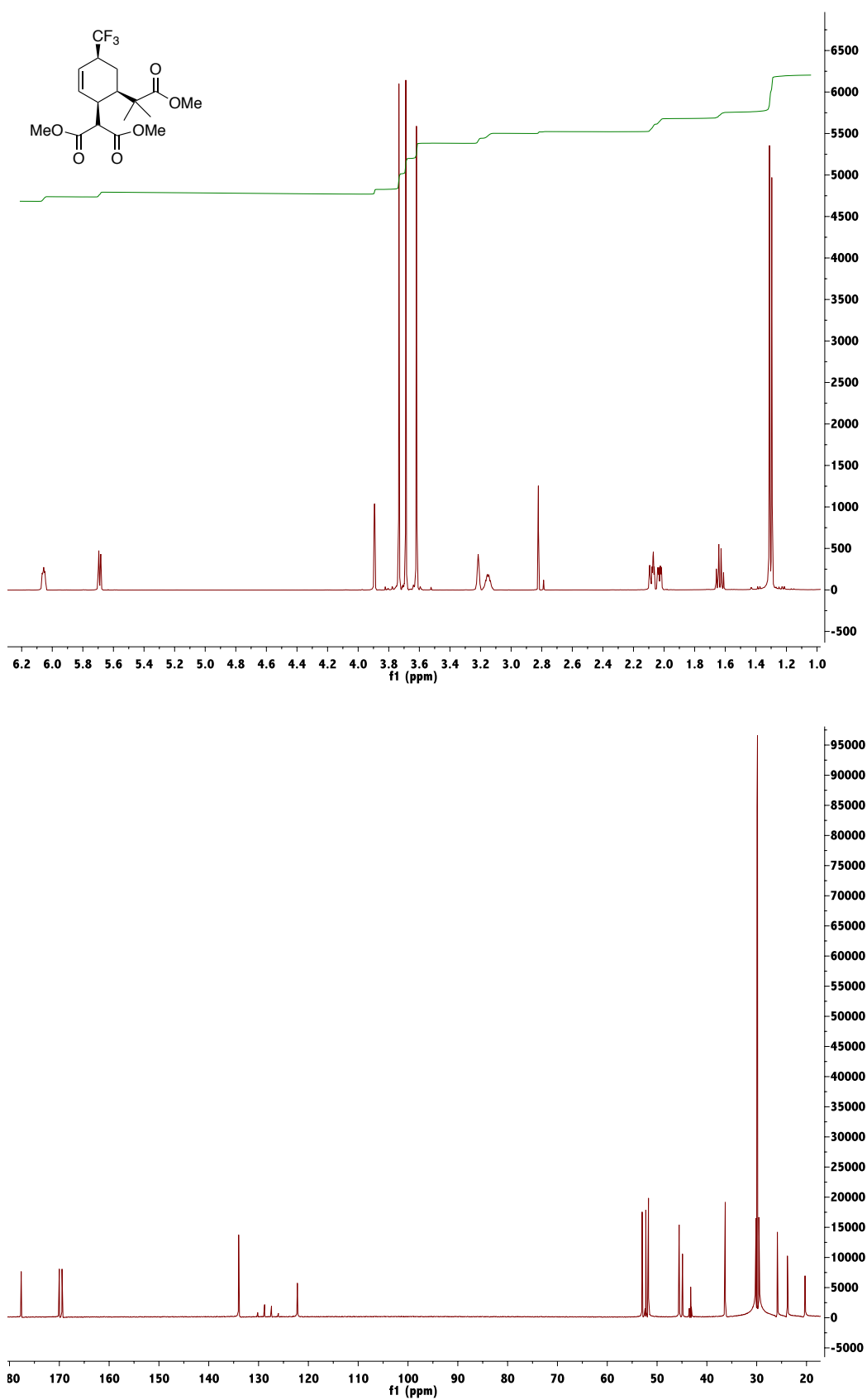
$^1\text{H-NMR}$ ($\text{d}^6\text{-acetone}$) and $^{13}\text{C-NMR}$ ($\text{d}^6\text{-acetone}$) of Compound 61:

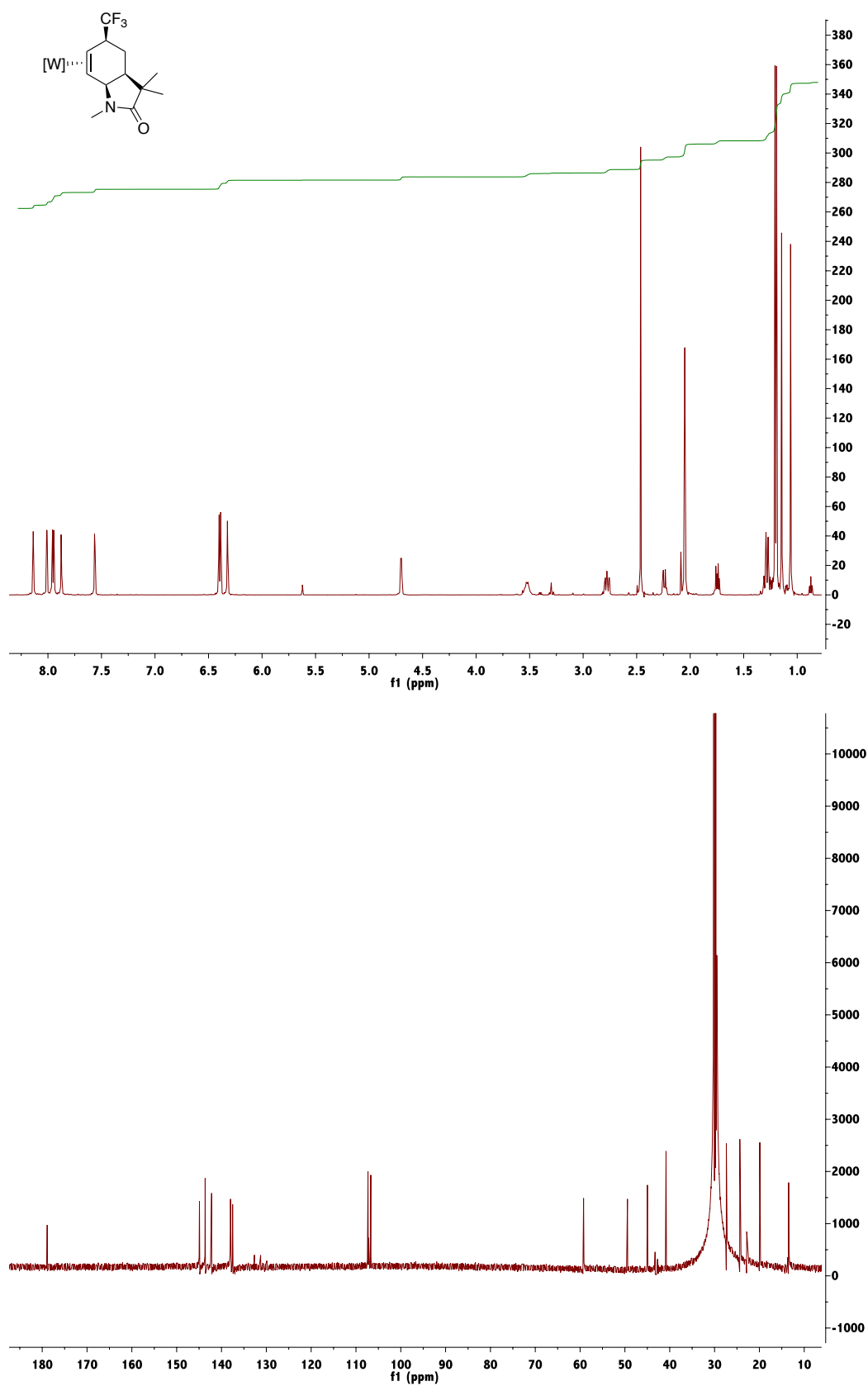
$^1\text{H-NMR}$ ($\text{d}^6\text{-acetone}$) and $^{13}\text{C-NMR}$ ($\text{d}^6\text{-acetone}$) of Compound 62:

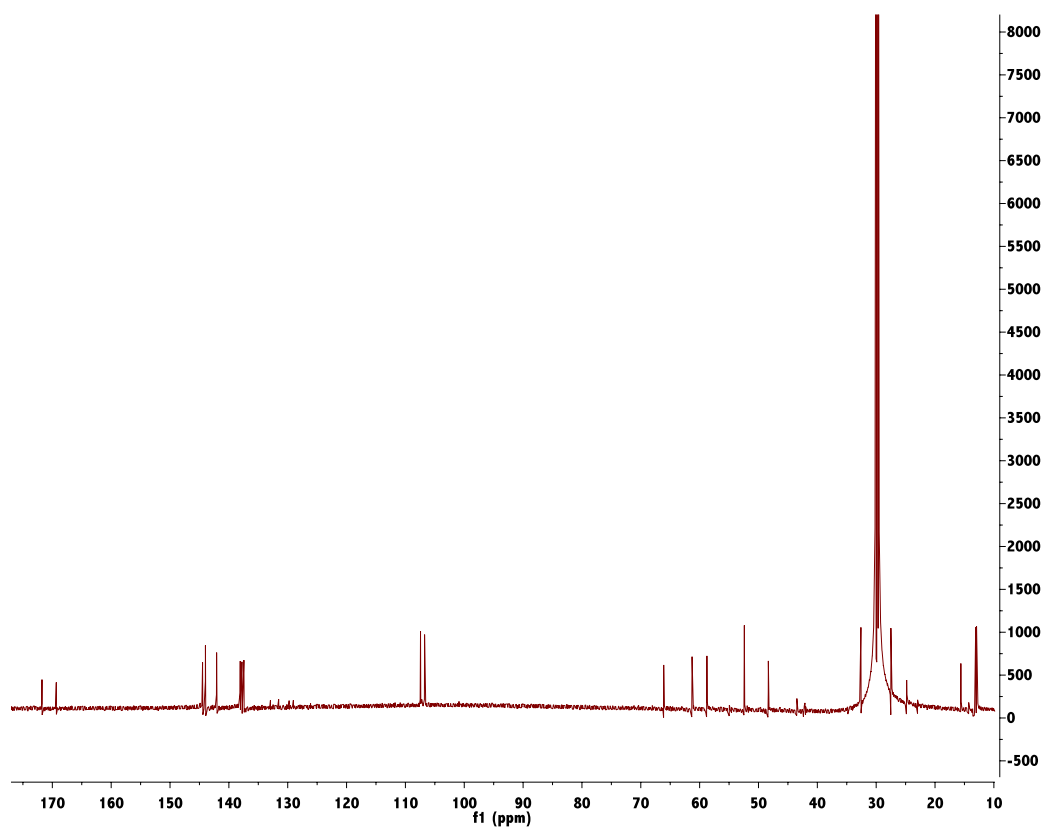
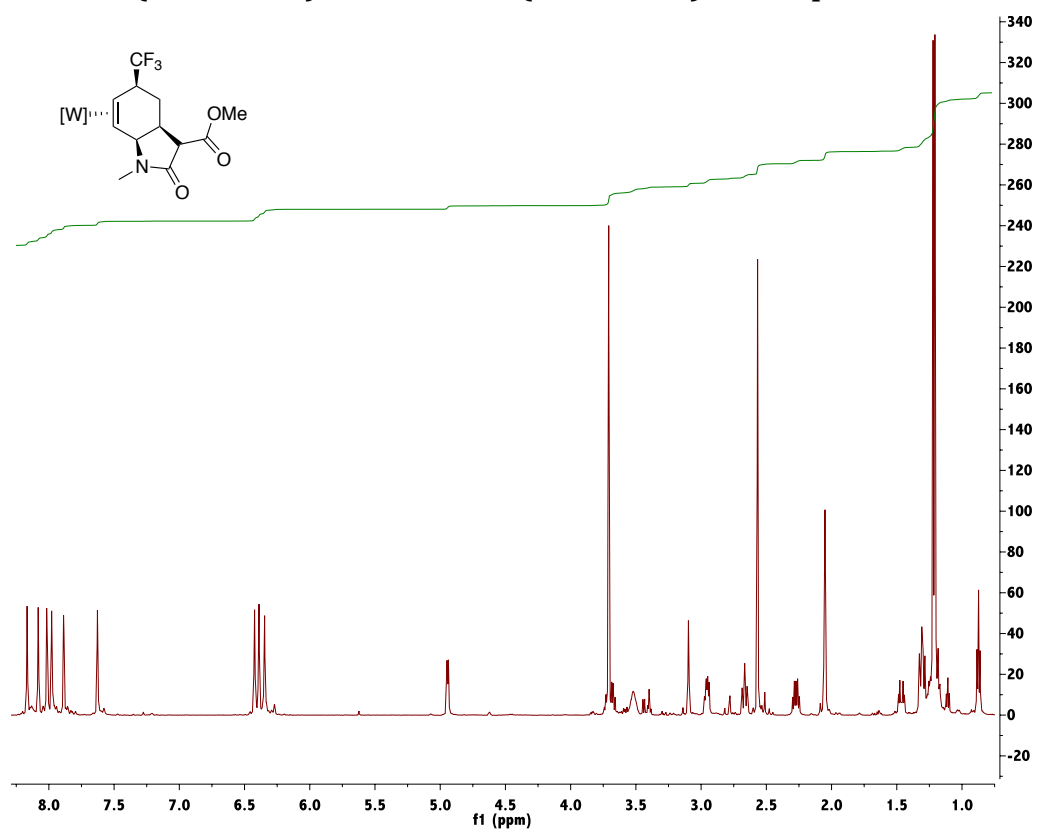
$^1\text{H-NMR}$ (CDCl_3) and $^{13}\text{C-NMR}$ (CDCl_3) of Compound 63:

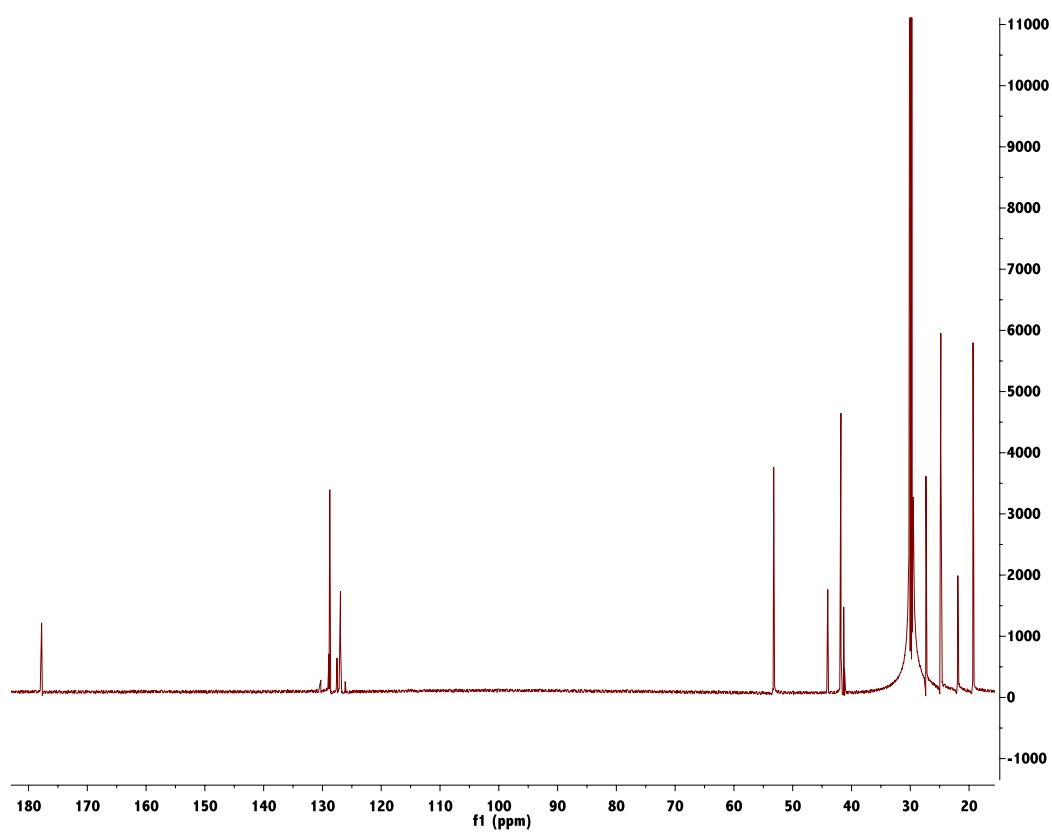
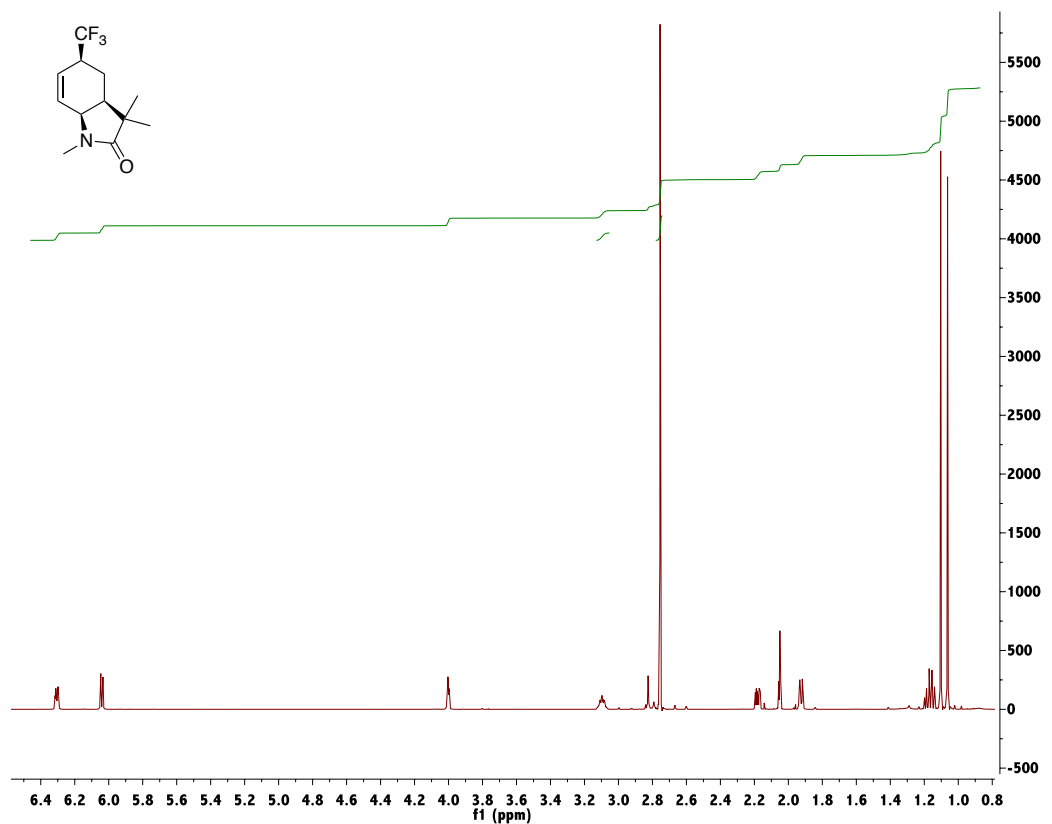
$^1\text{H-NMR}$ ($\text{d}^6\text{-acetone}$) and $^{13}\text{C-NMR}$ ($\text{d}^6\text{-acetone}$) of Compound 64:

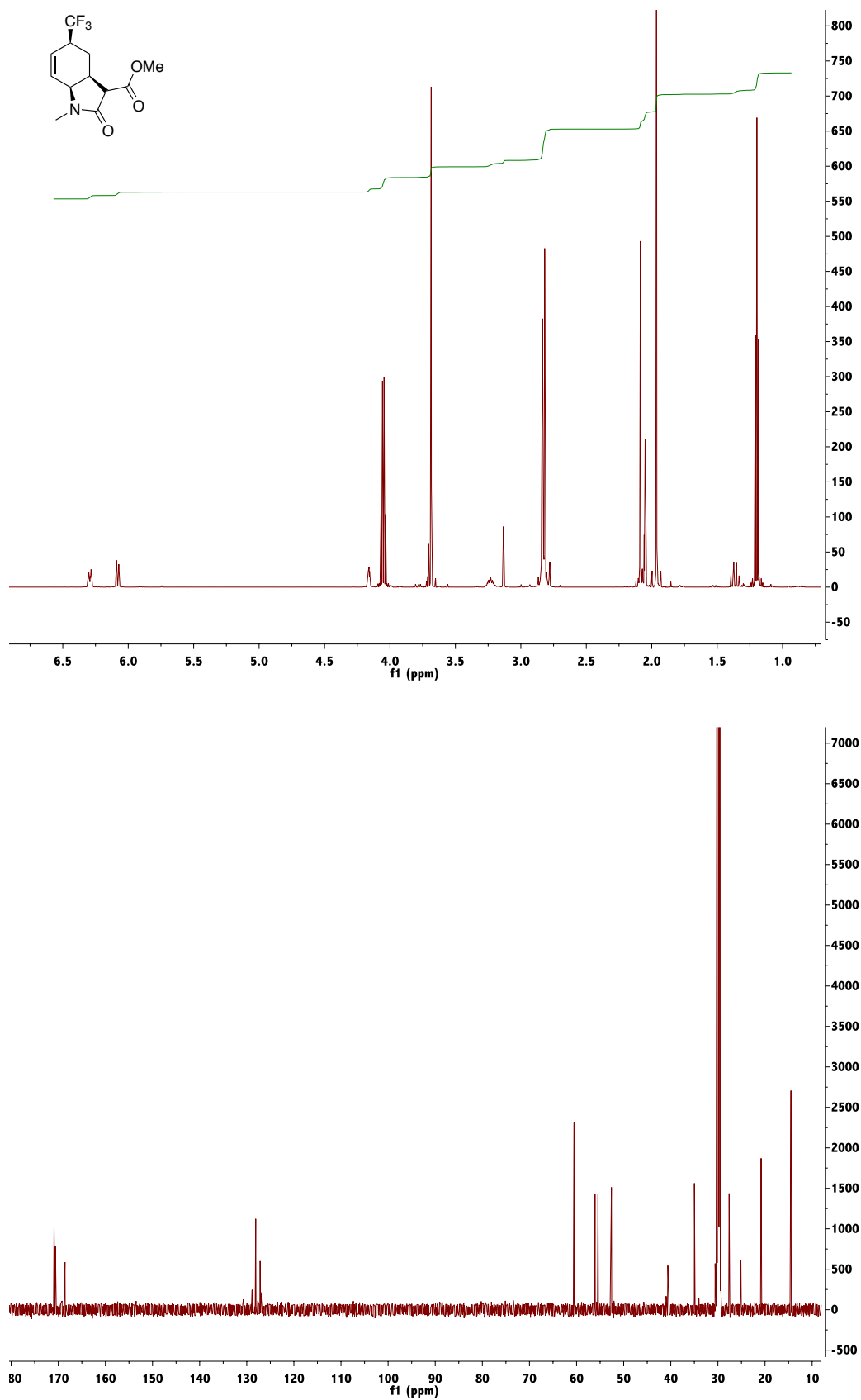
$^1\text{H-NMR}$ ($\text{d}^6\text{-acetone}$) and $^{13}\text{C-NMR}$ ($\text{d}^6\text{-acetone}$) of Compound 65:

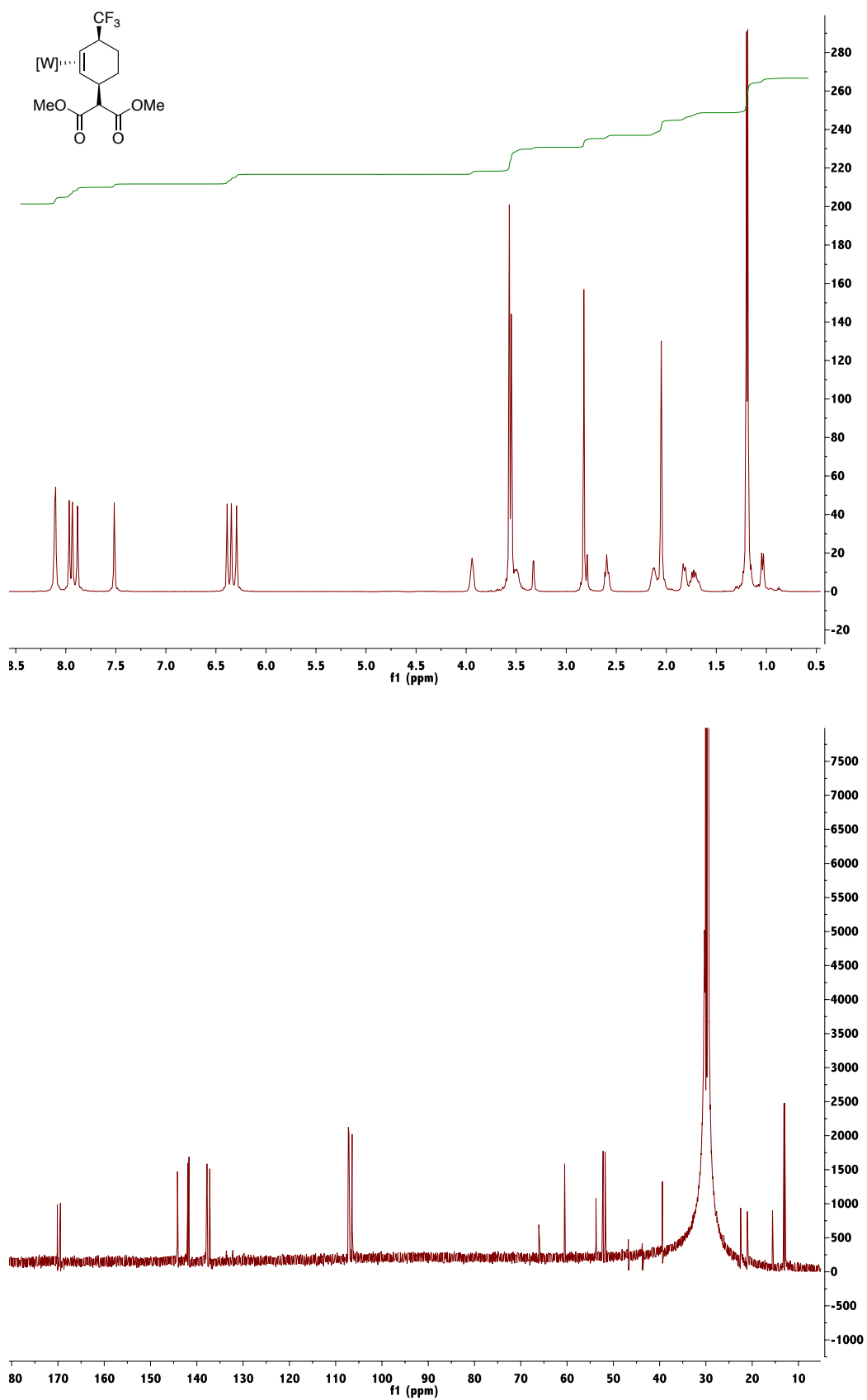
$^1\text{H-NMR}$ ($\text{d}^6\text{-acetone}$) and $^{13}\text{C-NMR}$ ($\text{d}^6\text{-acetone}$) of Compound 66:

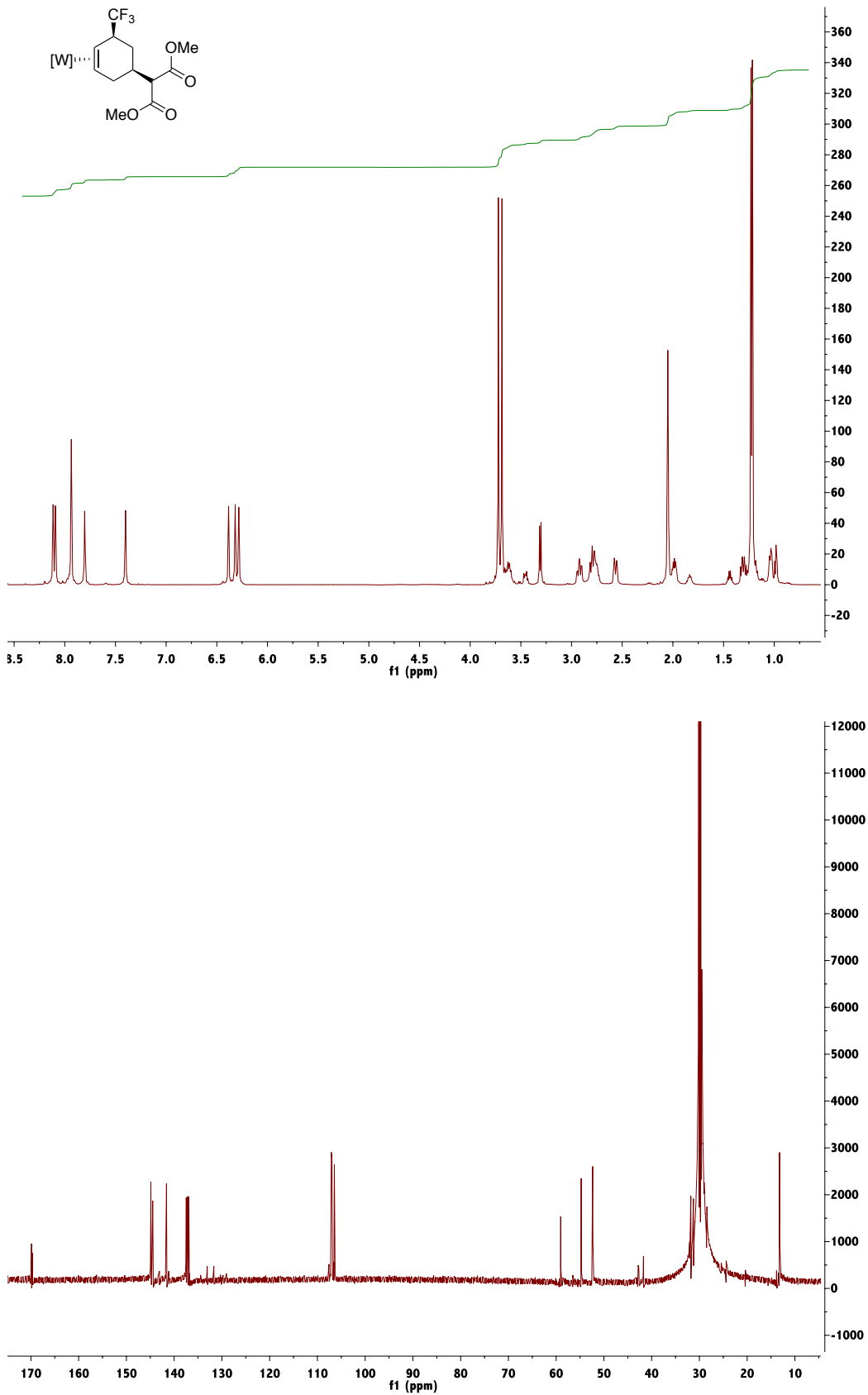
$^1\text{H-NMR}$ ($\text{d}^6\text{-acetone}$) and $^{13}\text{C-NMR}$ ($\text{d}^6\text{-acetone}$) of Compound 67:

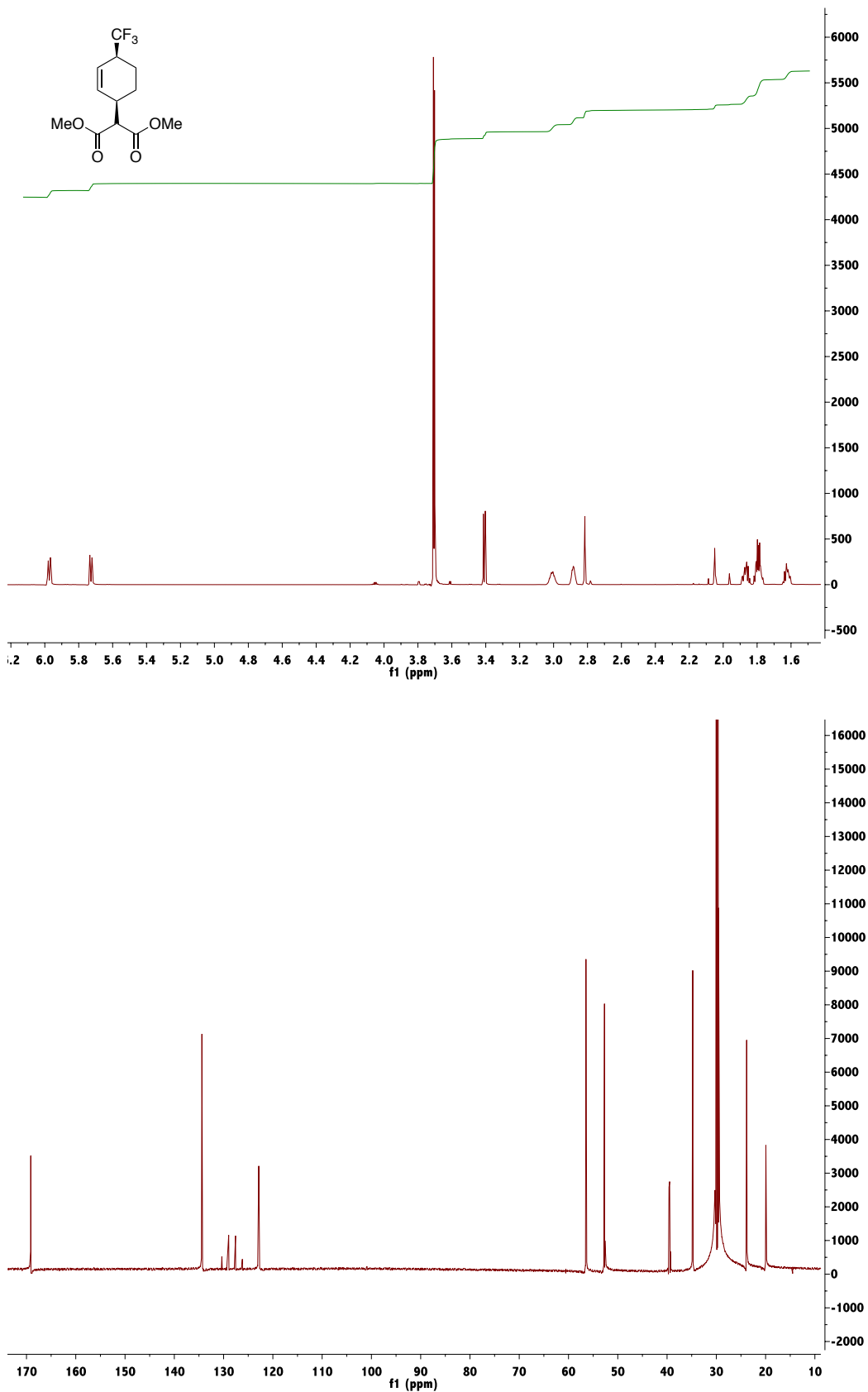
$^1\text{H-NMR}$ ($\text{d}^6\text{-acetone}$) and $^{13}\text{C-NMR}$ ($\text{d}^6\text{-acetone}$) of Compound 68:

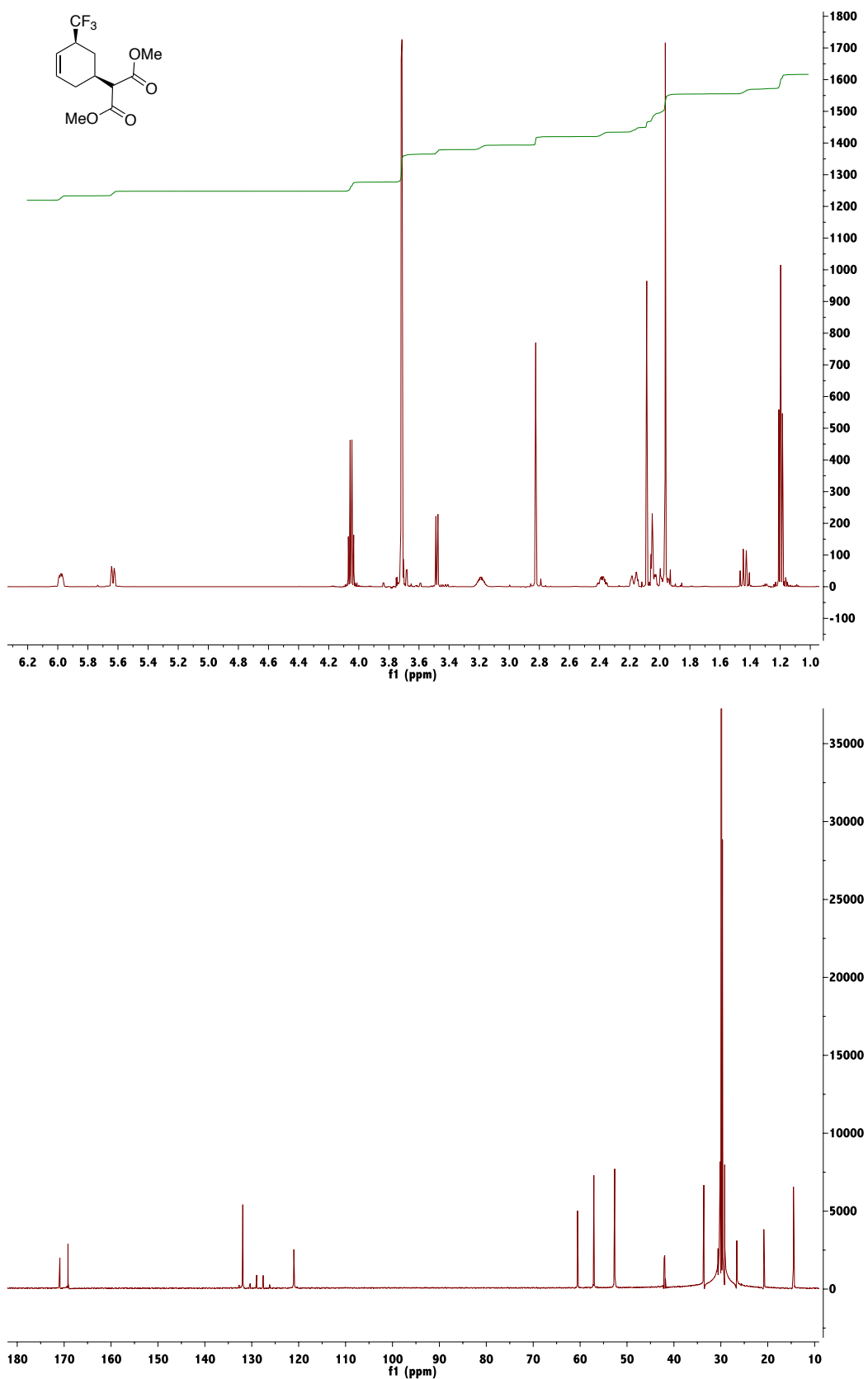
$^1\text{H-NMR}$ ($\text{d}^6\text{-acetone}$) and $^{13}\text{C-NMR}$ ($\text{d}^6\text{-acetone}$) of Compound 69:

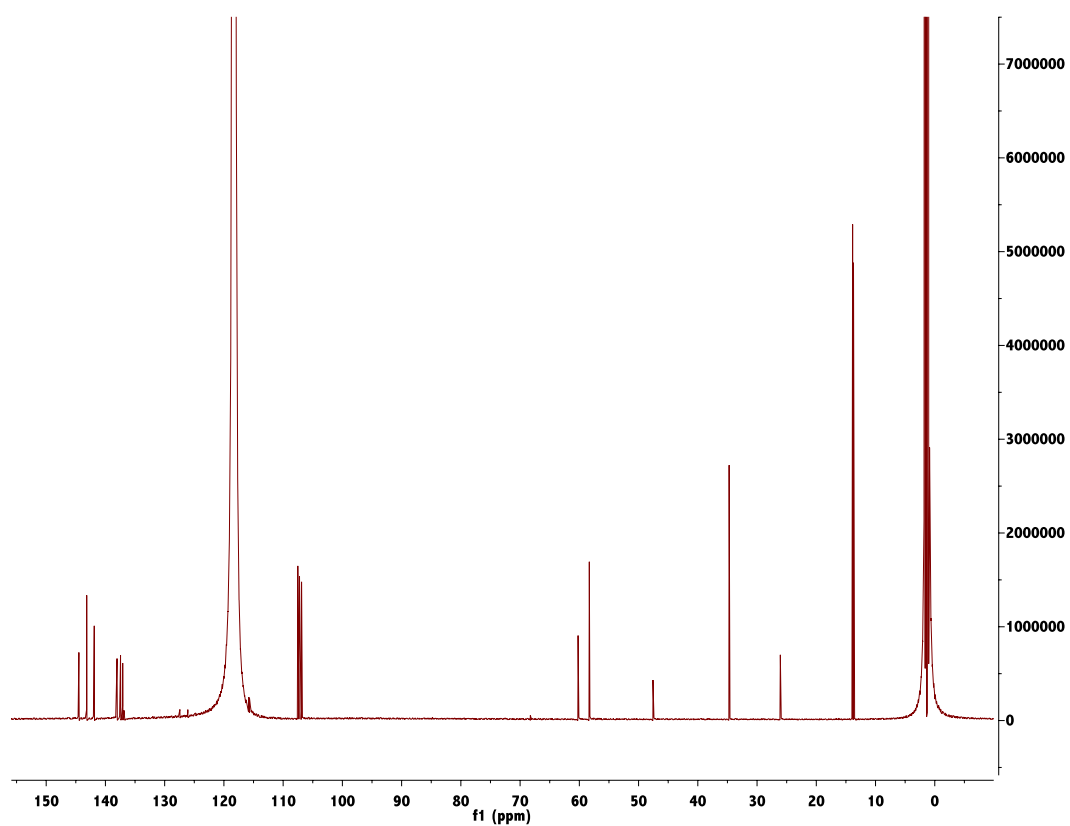
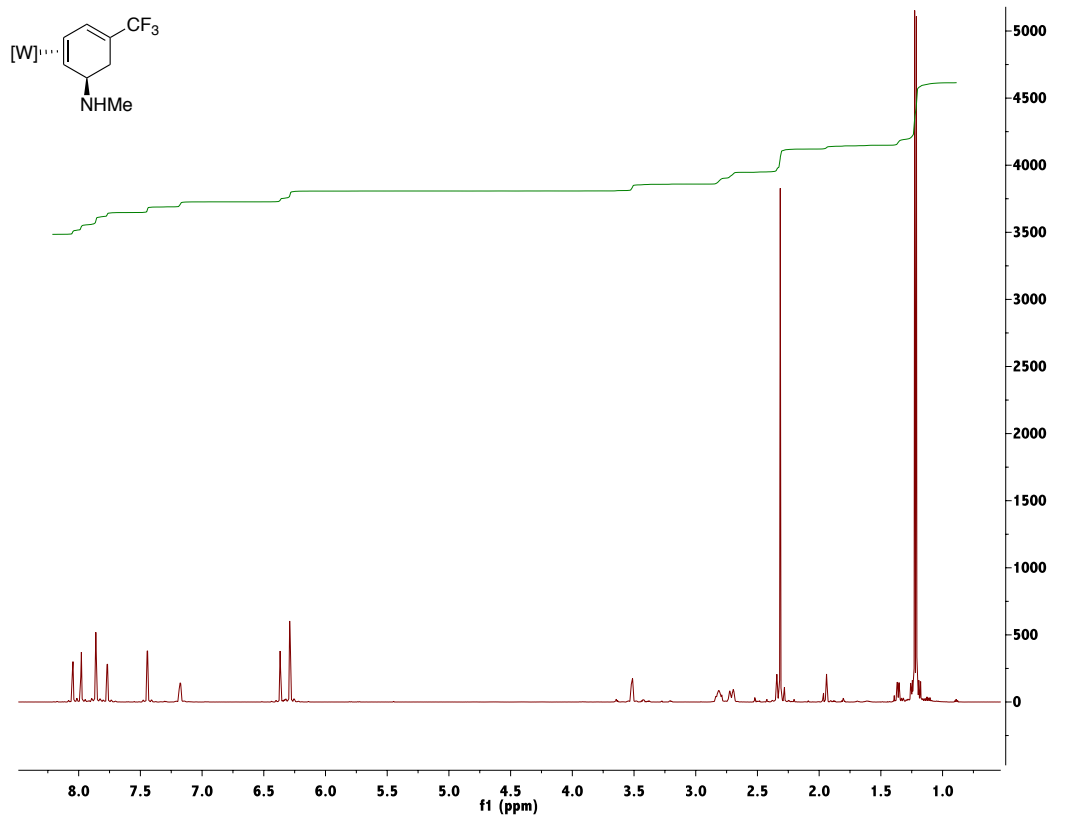
$^1\text{H-NMR}$ ($\text{d}^6\text{-acetone}$) and $^{13}\text{C-NMR}$ ($\text{d}^6\text{-acetone}$) of Compound 70:

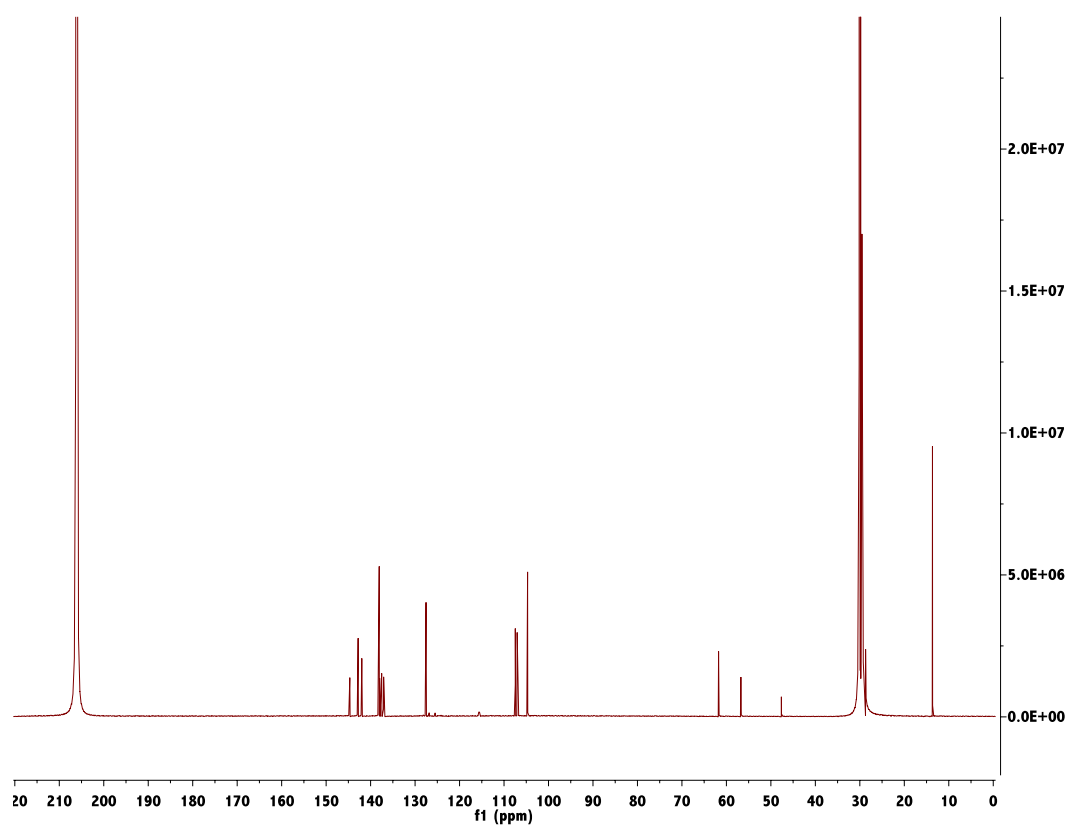
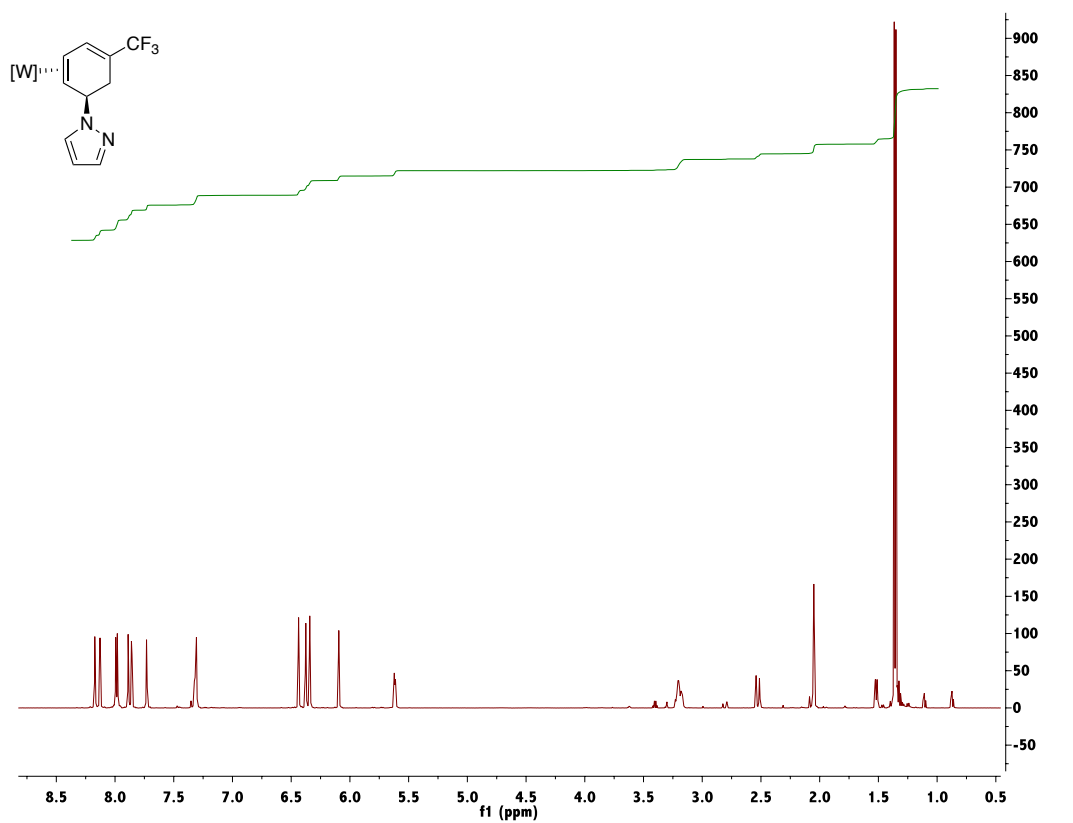
$^1\text{H-NMR}$ ($\text{d}^6\text{-acetone}$) and $^{13}\text{C-NMR}$ ($\text{d}^6\text{-acetone}$) of Compound 71:

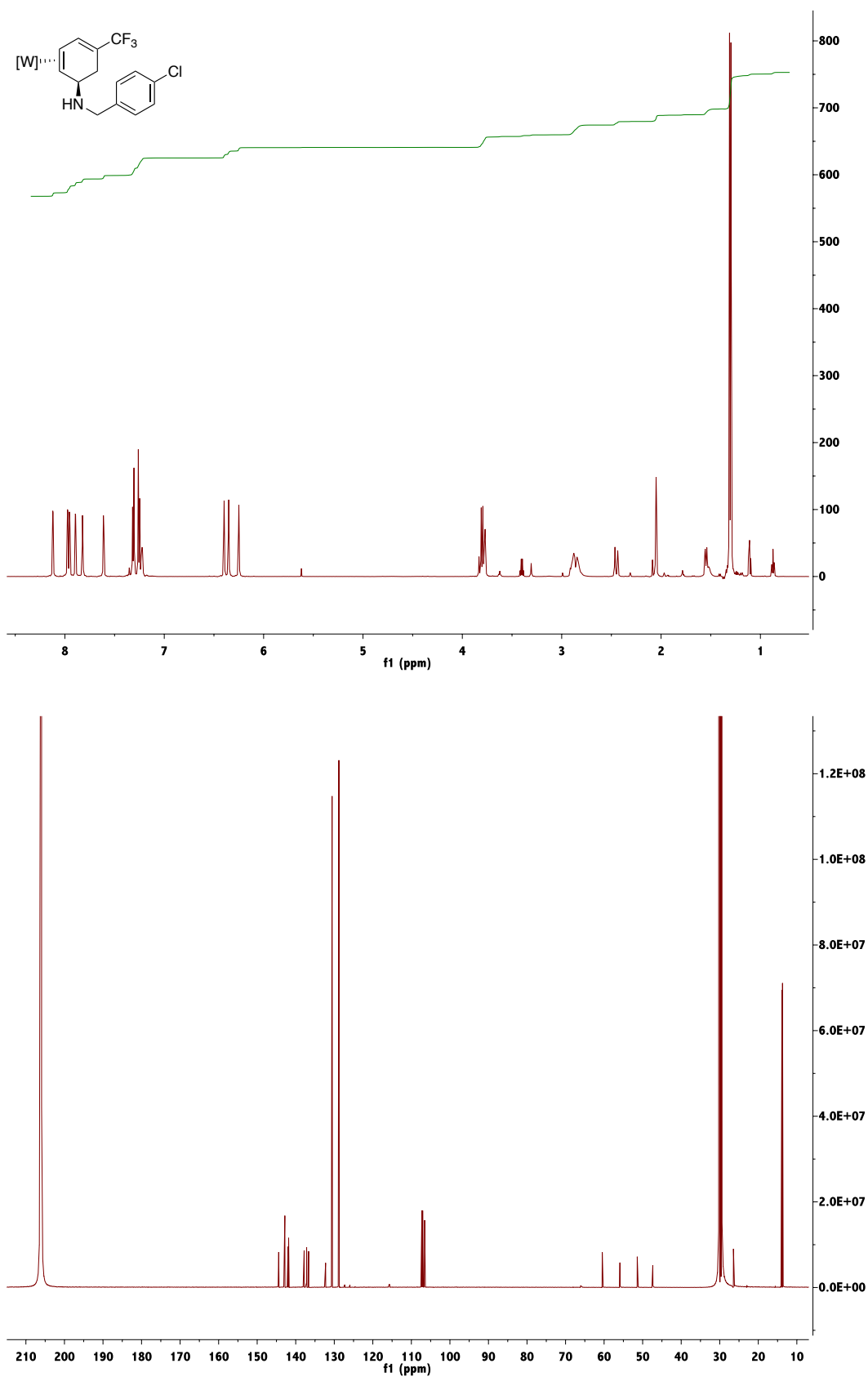
$^1\text{H-NMR}$ ($\text{d}^6\text{-acetone}$) and $^{13}\text{C-NMR}$ ($\text{d}^6\text{-acetone}$) of Compound 72:

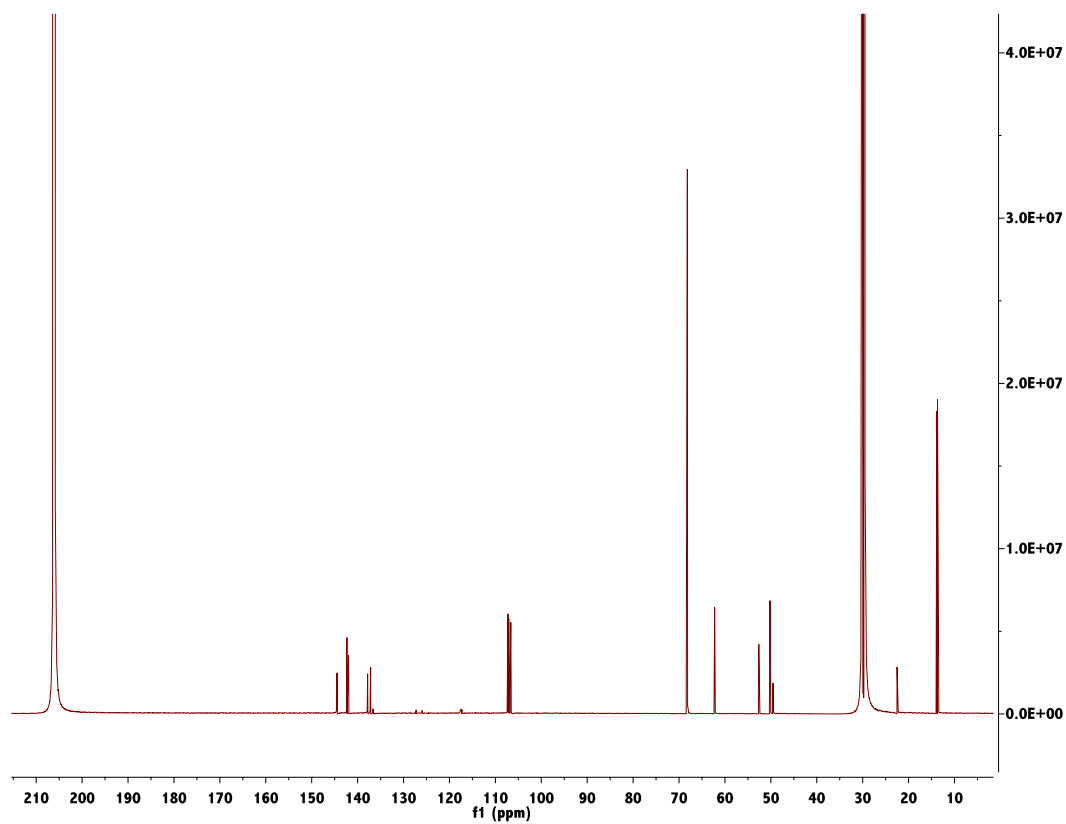
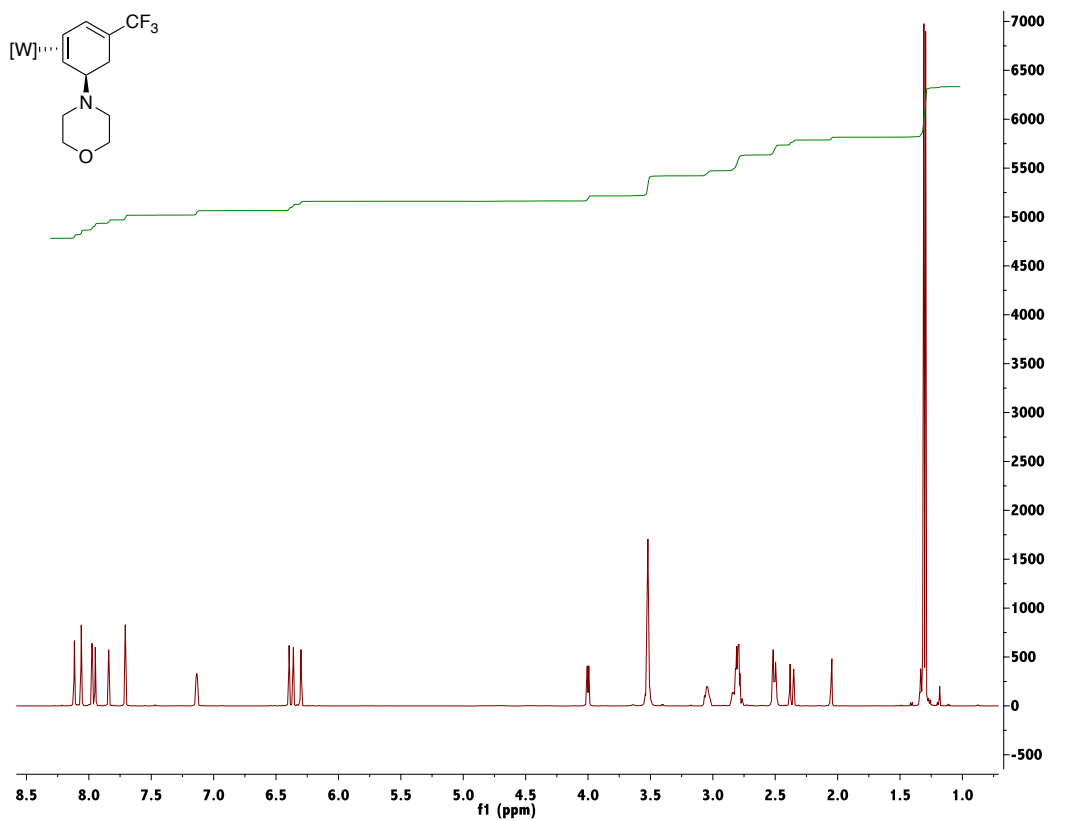
$^1\text{H-NMR}$ ($\text{d}^6\text{-acetone}$) and $^{13}\text{C-NMR}$ ($\text{d}^6\text{-acetone}$) of Compound 73:

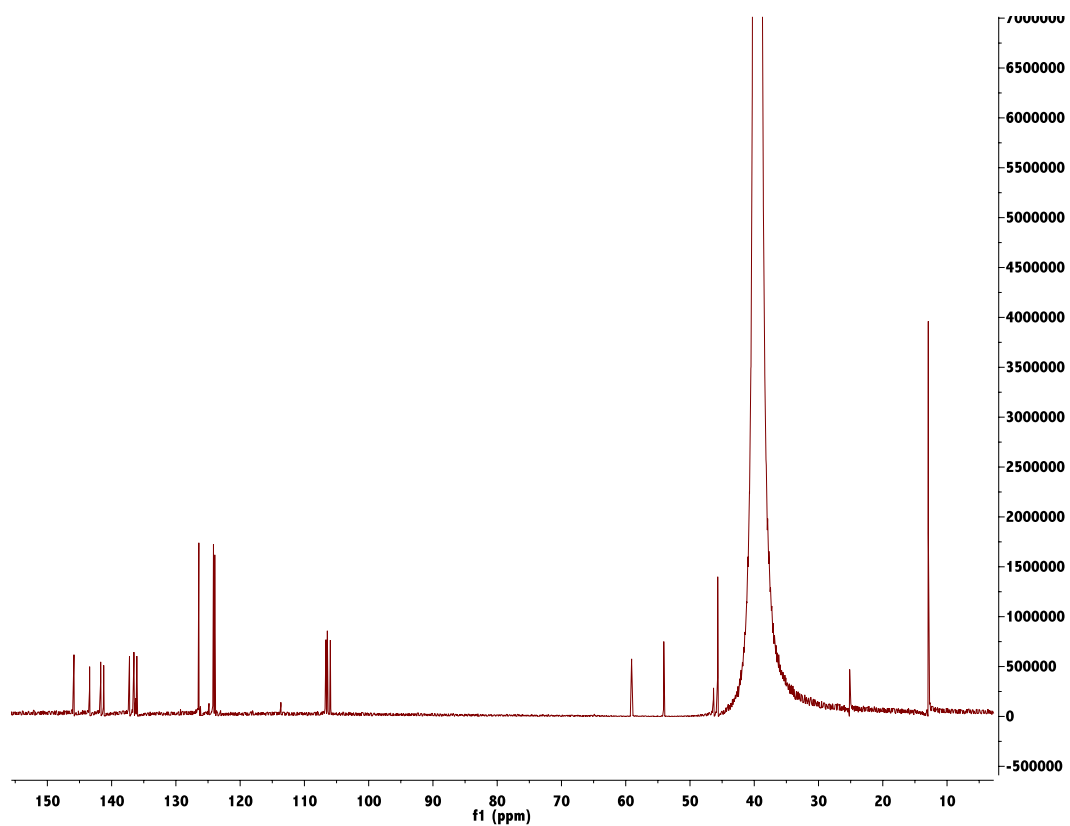
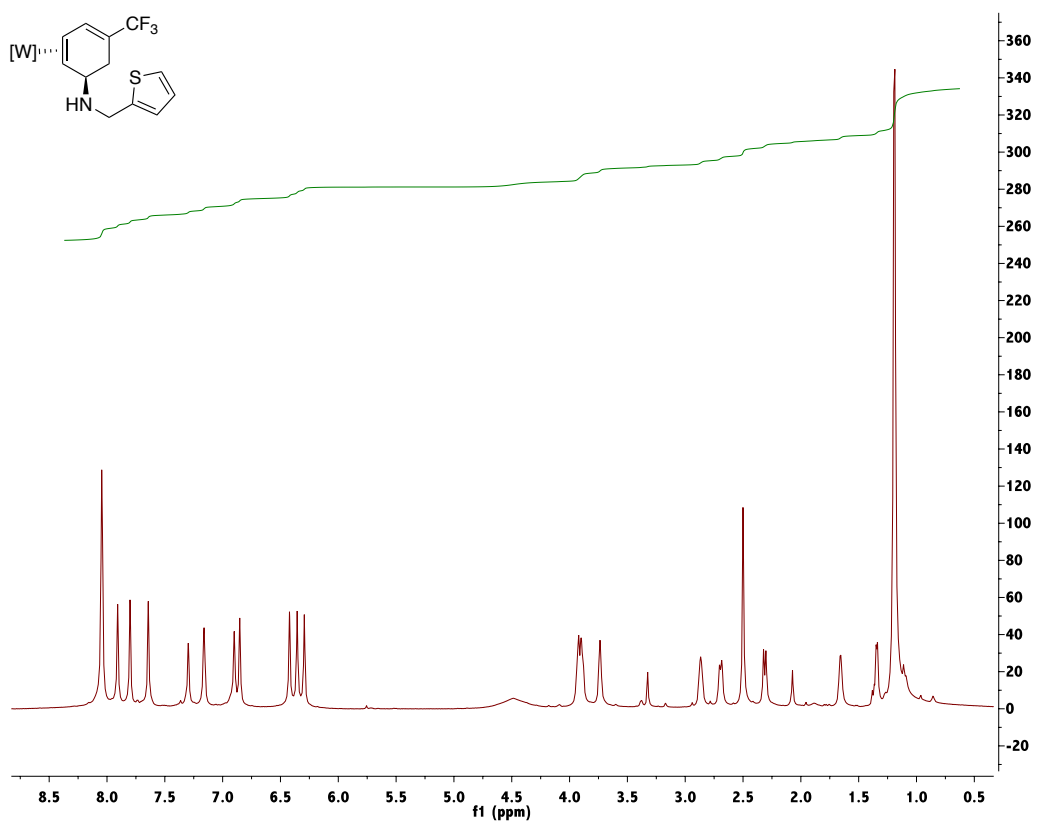
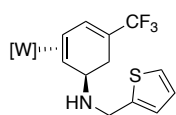
$^1\text{H-NMR}$ ($\text{d}^6\text{-acetone}$) and $^{13}\text{C-NMR}$ ($\text{d}^6\text{-acetone}$) of Compound 74:

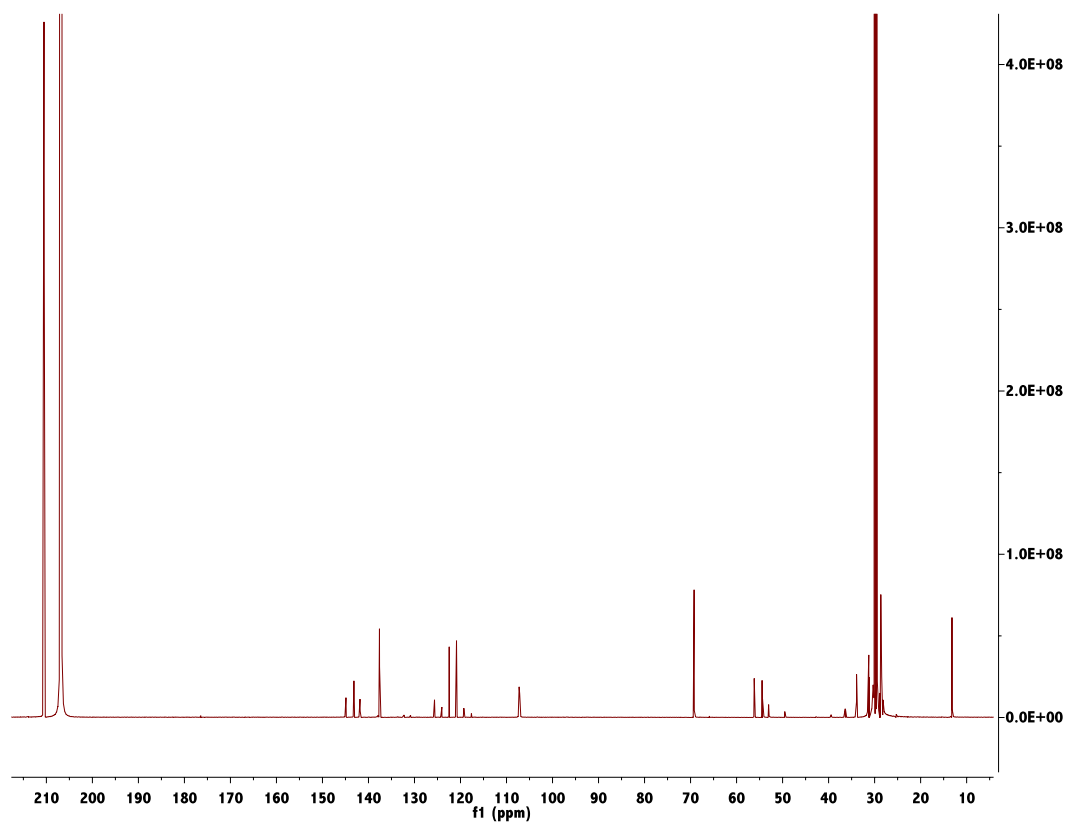
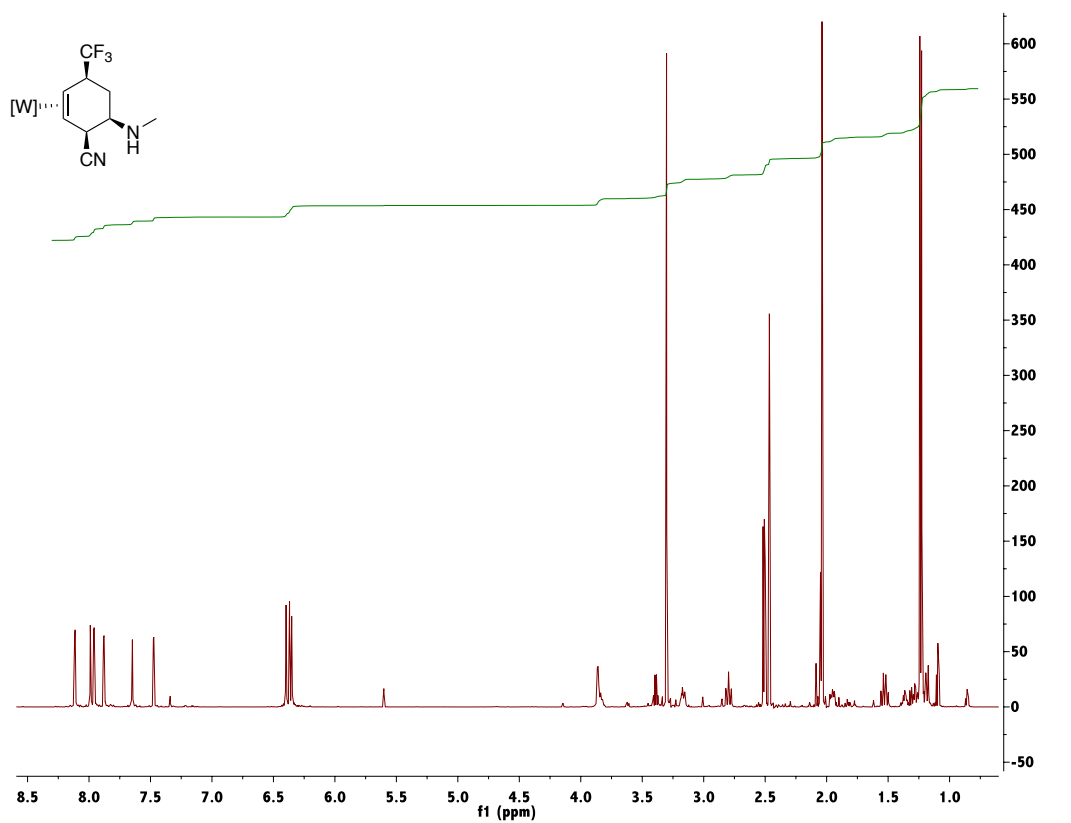
$^1\text{H-NMR}$ (CD_3CN) and $^{13}\text{C-NMR}$ (CD_3CN) of Compound 78:

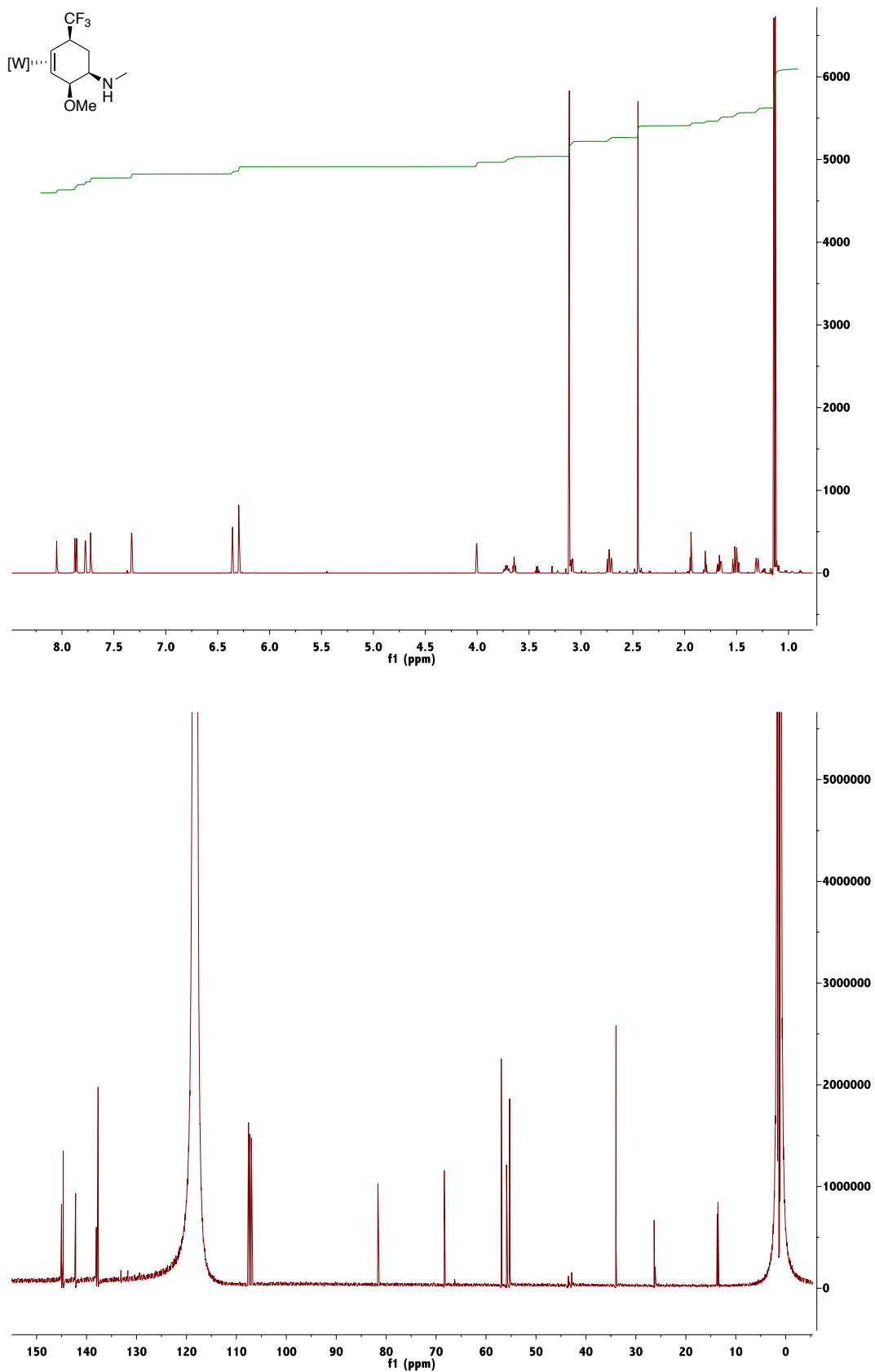
$^1\text{H-NMR}$ ($\text{d}^6\text{-acetone}$) and $^{13}\text{C-NMR}$ ($\text{d}^6\text{-acetone}$) of Compound 79:

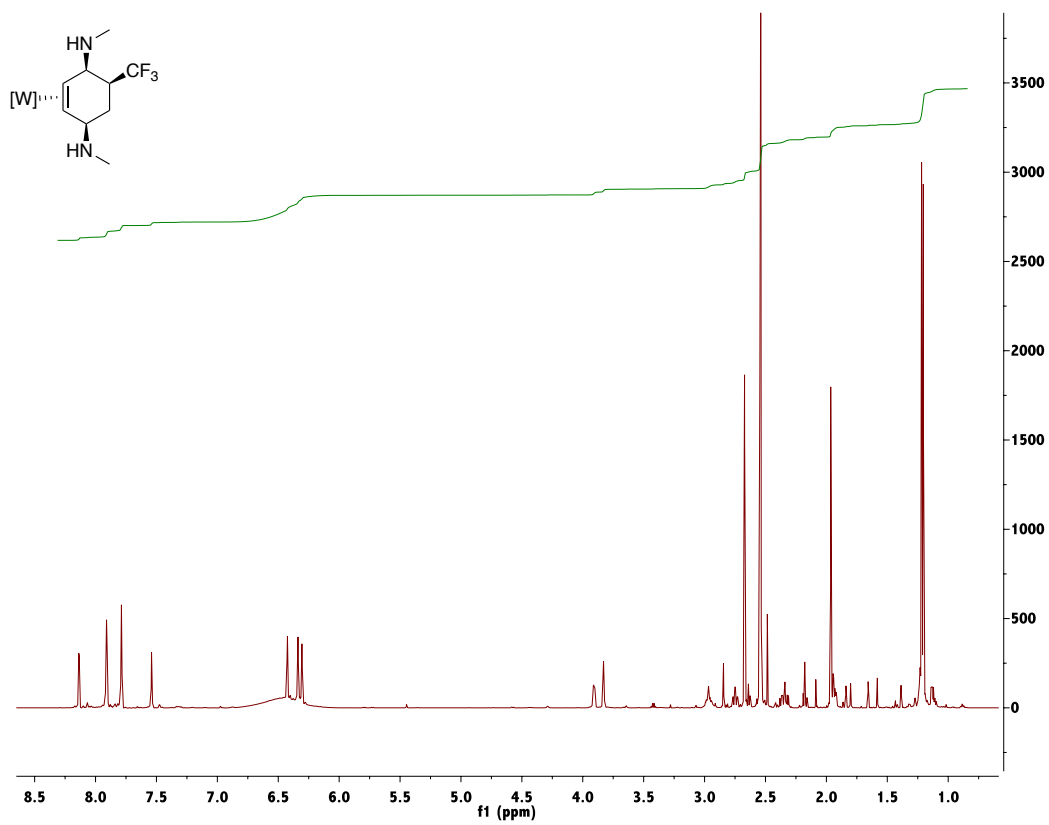
$^1\text{H-NMR}$ ($\text{d}^6\text{-acetone}$) and $^{13}\text{C-NMR}$ ($\text{d}^6\text{-acetone}$) of Compound 80:

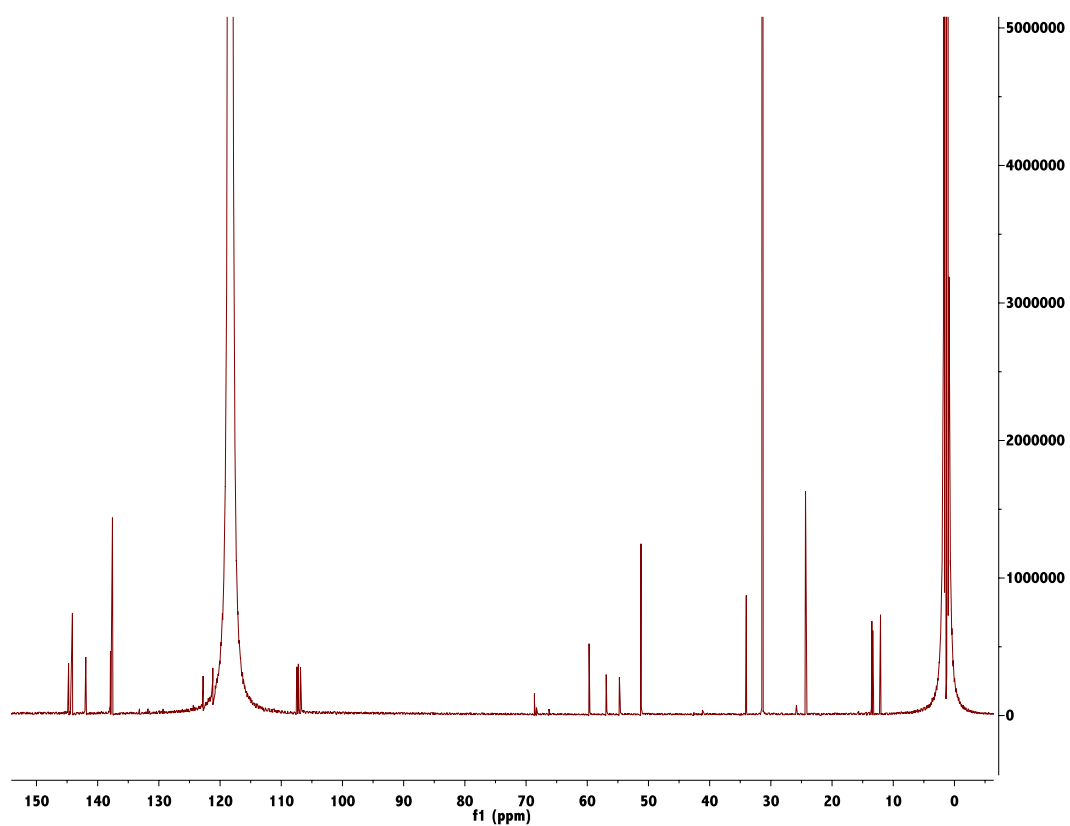
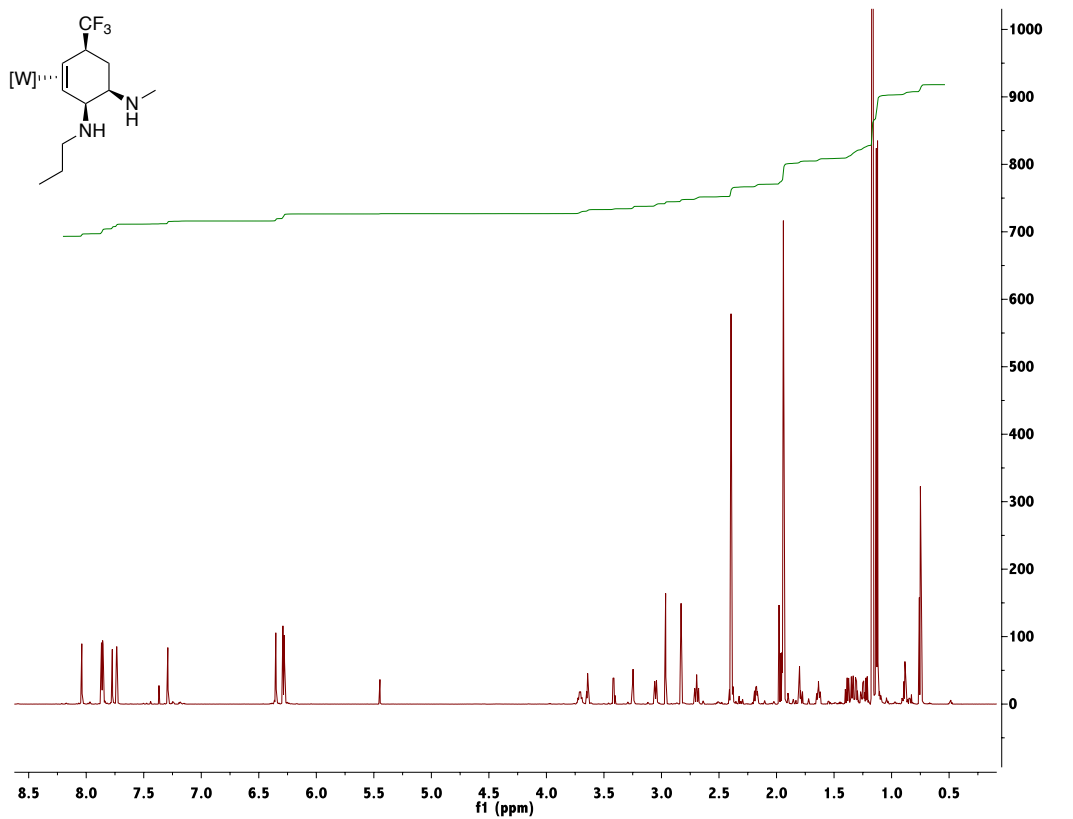
$^1\text{H-NMR}$ ($\text{d}^6\text{-acetone}$) and $^{13}\text{C-NMR}$ ($\text{d}^6\text{-acetone}$) of Compound 81:

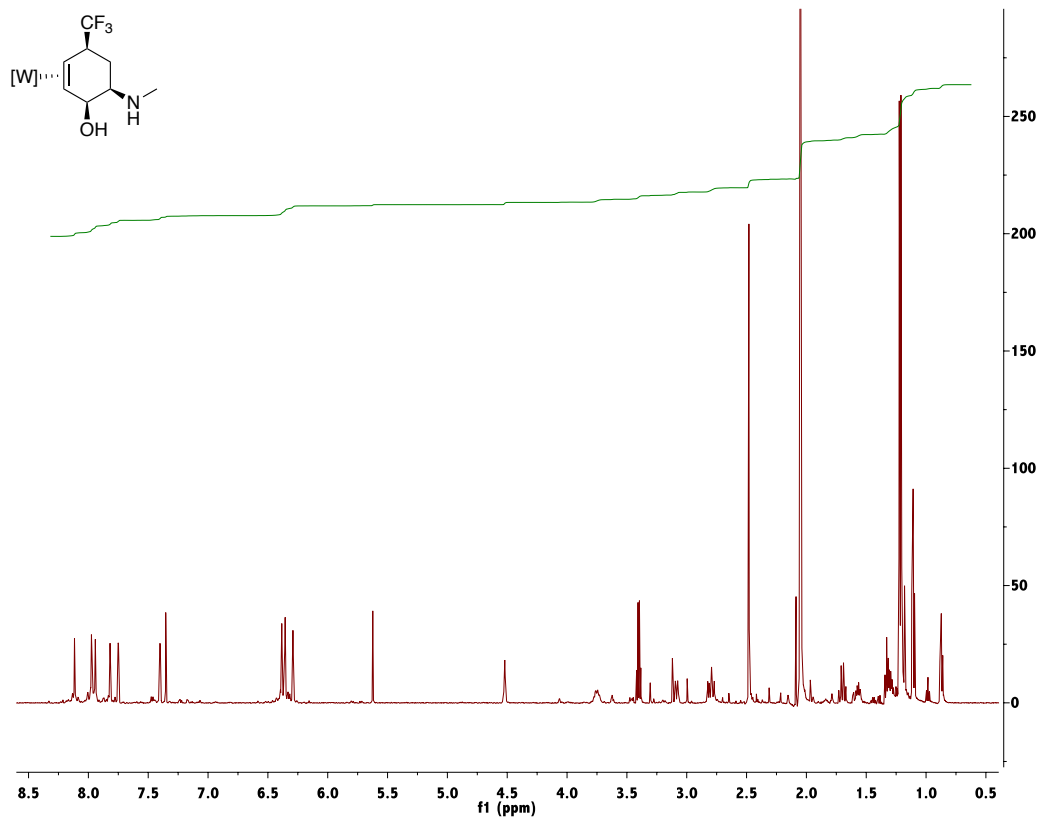
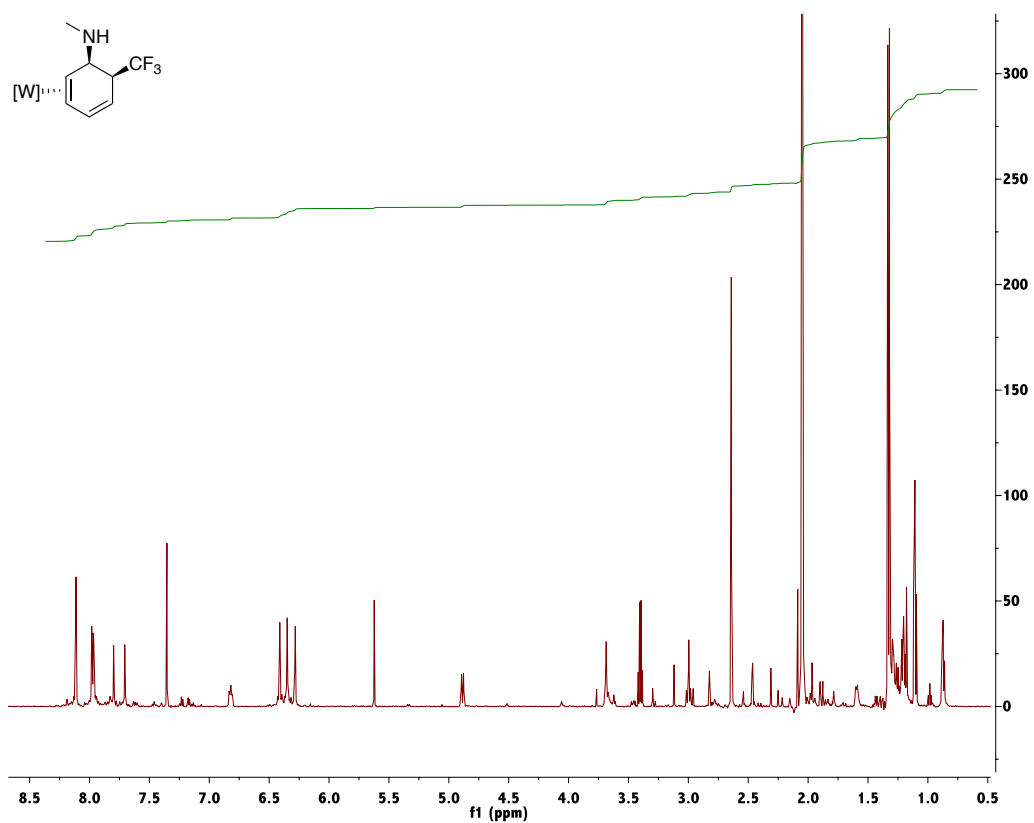
$^1\text{H-NMR}$ ($\text{d}^6\text{-DMSO}$) and $^{13}\text{C-NMR}$ ($\text{d}^6\text{-DMSO}$) of Compound 82:

$^1\text{H-NMR}$ (d^6 -acetone) and $^{13}\text{C-NMR}$ (d^6 -acetone) of Compound 84:

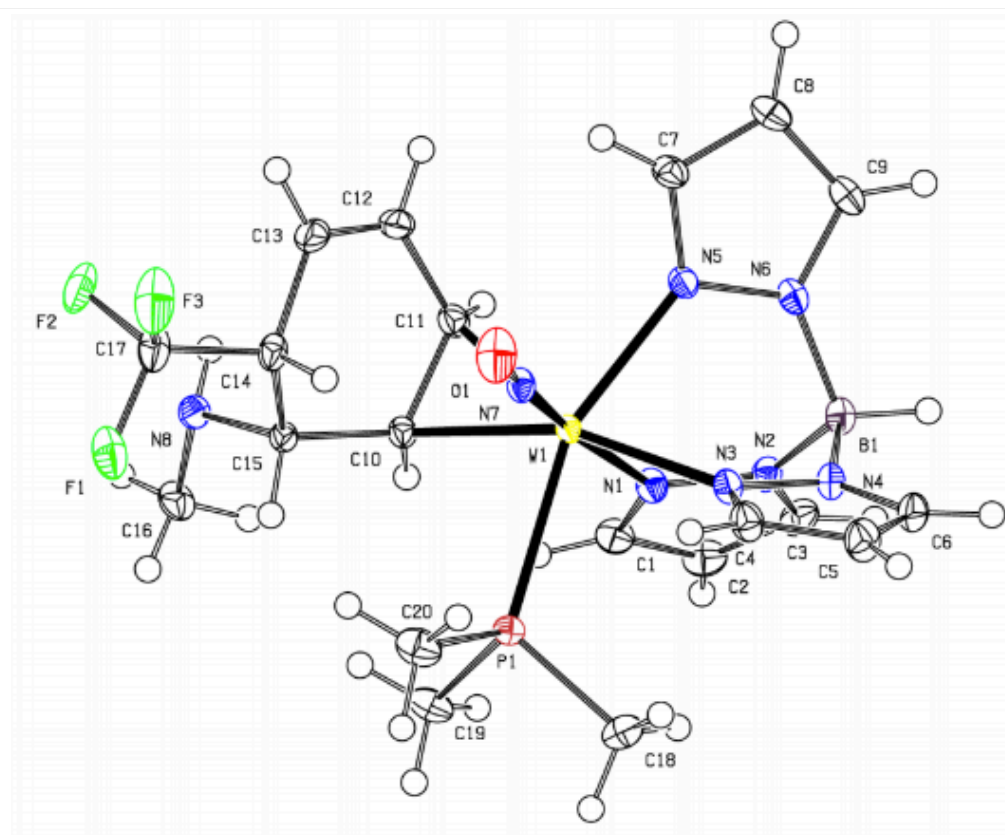
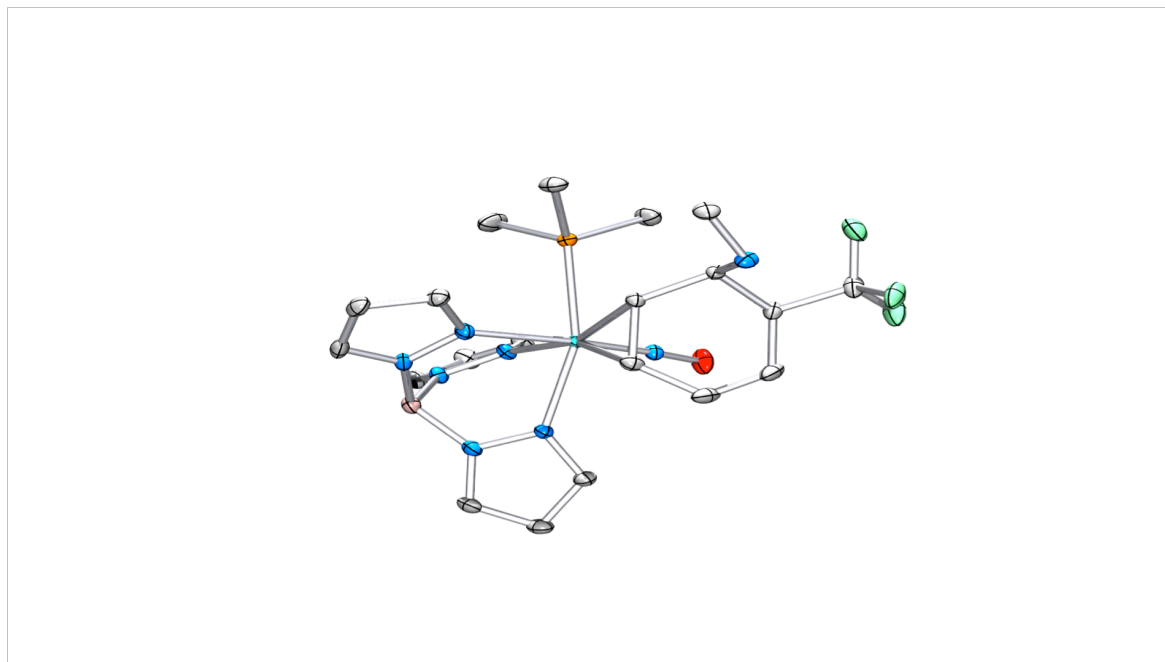
$^1\text{H-NMR}$ (CD_3CN) and $^{13}\text{C-NMR}$ (CD_3CN) of Compound 85:

$^1\text{H-NMR}$ (CD_3CN) of Compound 86:

$^1\text{H-NMR}$ (CD_3CN) and $^{13}\text{C-NMR}$ (CD_3CN) of Compound 87A:

¹H-NMR (d⁶-acetone) of Compound 89:**¹H-NMR (d⁶-acetone) of Compound 90:**

Compound 90



Compound 90Table 1. Sample and crystal data for C₂₀H₂₉BF₃N₈OPW.

Chemical formula	C ₂₀ H ₂₉ BF ₃ N ₈ OPW
Formula weight	680.14 g/mol
Temperature	150(2) K
Wavelength	0.71073 Å
Crystal size	0.275 x 0.341 x 0.374 mm
Crystal habit	yellow block
Crystal system	triclinic
Space group	P -1
Unit cell dimensions	a = 8.1339(8) Å α = 69.2530(10)° b = 12.1299(12) Å β = 77.0650(10)° c = 14.5476(15) Å γ = 74.1330(10)°
Volume	1278.2(2) Å ³
Z	2
Density (calculated)	1.767 g/cm ³
Absorption coefficient	4.633 mm ⁻¹
F(000)	668

Table 2. Data collection and structure refinement for C₂₀H₂₉BF₃N₈OPW.

Diffractometer	Bruker Kappa APEXII Duo
Radiation source	fine-focus sealed tube, Mo K _α
Theta range for data collection	1.84 to 31.52°
Index ranges	-11 ≤ h ≤ 11, -16 ≤ k ≤ 17, -21 ≤ l ≤ 21
Reflections collected	33029
Independent reflections	8508 [R(int) = 0.0169]
Coverage of independent reflections	99.8%
Absorption correction	Multi-Scan

Max. and min. transmission	0.3620 and 0.2760
Structure solution technique	direct methods
Structure solution program	SHELXT 2014/5 (Sheldrick, 2014)
Refinement method	Full-matrix least-squares on F ²
Refinement program	SHELXL-2016/6 (Sheldrick, 2016)
Function minimized	$\Sigma w(F_o^2 - F_c^2)^2$
Data / restraints / parameters	8508 / 0 / 328
Goodness-of-fit on F ²	1.107
Δ/σ_{\max}	0.002
Final R indices	8266 data; I>2 σ (I) R1 = 0.0132, wR2 = 0.0322
	all data R1 = 0.0140, wR2 = 0.0324
Weighting scheme	$w=1/[\sigma^2(F_o^2)+(0.0131P)^2+0.7403P]$ where $P=(F_o^2+2F_c^2)/3$
Largest diff. peak and hole	0.469 and -1.274 eÅ ⁻³
R.M.S. deviation from mean	0.074 eÅ ⁻³

Table 3. Atomic coordinates and equivalent isotropic atomic displacement parameters (Å²) for C₂₀H₂₉BF₃N₈OPW.

U(eq) is defined as one third of the trace of the orthogonalized U_{ij} tensor.

	x/a	y/b	z/c	U(eq)
W1	0.67679(2)	0.62051(2)	0.25902(2)	0.01083(2)
P1	0.61048(4)	0.66591(3)	0.08779(3)	0.01462(6)
F1	0.91647(13)	0.21004(9)	0.13207(8)	0.0290(2)
F2	0.91396(13)	0.09503(8)	0.28499(9)	0.0297(2)
F3	0.12443(12)	0.18430(10)	0.21231(10)	0.0375(3)

	x/a	y/b	z/c	U(eq)
O1	0.05729(14)	0.53388(11)	0.20463(10)	0.0276(2)
N1	0.40241(15)	0.71424(10)	0.29704(9)	0.0153(2)
N2	0.37191(15)	0.81565(10)	0.32455(9)	0.0158(2)
N3	0.72791(15)	0.80472(10)	0.19975(8)	0.0154(2)
N4	0.64036(15)	0.89521(10)	0.23840(9)	0.0161(2)
N5	0.70546(14)	0.65407(10)	0.39425(8)	0.01421(19)
N6	0.63021(15)	0.76153(11)	0.41160(9)	0.0159(2)
N7	0.90045(14)	0.56441(10)	0.22710(9)	0.01428(19)
N8	0.58297(15)	0.25097(11)	0.27959(9)	0.0160(2)
C1	0.24598(17)	0.69714(13)	0.29600(10)	0.0180(2)
C2	0.11528(18)	0.78707(14)	0.32210(11)	0.0213(3)
C3	0.20041(18)	0.85989(13)	0.33973(11)	0.0202(3)
C4	0.85303(19)	0.84817(13)	0.12933(11)	0.0194(3)
C5	0.8454(2)	0.96714(14)	0.12196(11)	0.0230(3)
C6	0.71023(19)	0.99312(13)	0.19322(11)	0.0196(3)
C7	0.80278(17)	0.58883(13)	0.46640(10)	0.0174(2)
C8	0.79281(19)	0.65354(14)	0.53074(11)	0.0203(3)
C9	0.68262(18)	0.76243(14)	0.49303(10)	0.0190(3)
C10	0.57940(16)	0.45902(11)	0.27537(9)	0.0131(2)
C11	0.61819(18)	0.45137(12)	0.37075(10)	0.0160(2)
C12	0.7606(2)	0.35401(13)	0.41305(11)	0.0214(3)
C13	0.8727(2)	0.28599(13)	0.36192(12)	0.0228(3)
C14	0.85970(17)	0.30929(12)	0.25447(11)	0.0169(2)
C15	0.66984(16)	0.35352(11)	0.23526(10)	0.0130(2)
C16	0.41707(18)	0.27169(14)	0.24718(11)	0.0202(3)
C17	0.95044(18)	0.19932(13)	0.22194(13)	0.0225(3)
C18	0.5650(3)	0.82490(15)	0.01431(14)	0.0330(4)
C19	0.42519(19)	0.62112(15)	0.07061(11)	0.0225(3)
C20	0.7899(2)	0.59895(16)	0.01032(11)	0.0238(3)
B1	0.5191(2)	0.86327(14)	0.33777(12)	0.0167(3)

Table 4. Bond lengths (Å) for C₂₀H₂₉BF₃N₈OPW.

W1-N7	1.7767(11)	W1-N3	2.2118(12)
W1-C11	2.2144(13)	W1-N5	2.2170(11)
W1-C10	2.2261(13)	W1-N1	2.2550(11)
W1-P1	2.5033(4)	P1-C20	1.8232(15)
P1-C18	1.8235(17)	P1-C19	1.8280(15)
F1-C17	1.351(2)	F2-C17	1.3382(18)
F3-C17	1.3580(17)	O1-N7	1.2298(15)
N1-C1	1.3481(17)	N1-N2	1.3684(16)
N2-C3	1.3488(17)	N2-B1	1.537(2)
N3-C4	1.3443(18)	N3-N4	1.3632(16)
N4-C6	1.3470(18)	N4-B1	1.5449(19)
N5-C7	1.3400(17)	N5-N6	1.3657(16)
N6-C9	1.3501(17)	N6-B1	1.542(2)
N8-C16	1.4567(18)	N8-C15	1.4733(17)
N8-H8	0.86(2)	C1-C2	1.394(2)
C1-H1	0.95	C2-C3	1.378(2)
C2-H2	0.95	C3-H3	0.95
C4-C5	1.394(2)	C4-H4	0.95
C5-C6	1.384(2)	C5-H5	0.95
C6-H6	0.95	C7-C8	1.3965(19)
C7-H7	0.95	C8-C9	1.381(2)
C8-H8A	0.95	C9-H9	0.95
C10-C11	1.4568(18)	C10-C15	1.5302(18)
C10-H10	1.0	C11-C12	1.473(2)
C11-H11	1.0	C12-C13	1.336(2)
C12-H12	0.95	C13-C14	1.510(2)
C13-H13	0.95	C14-C17	1.517(2)
C14-C15	1.5443(18)	C14-H14	1.0
C15-H15	1.0	C16-H16A	0.98
C16-H16B	0.98	C16-H16C	0.98
C18-H18A	0.98	C18-H18B	0.98
C18-H18C	0.98	C19-H19A	0.98
C19-H19B	0.98	C19-H19C	0.98
C20-H20A	0.98	C20-H20B	0.98
C20-H20C	0.98	B1-H1A	1.08(2)

Table 5. Bond angles (°) for C₂₀H₂₉BF₃N₈OPW.

N7-W1-N3	88.30(5)	N7-W1-C11	97.31(5)
N3-W1-C11	158.34(5)	N7-W1-N5	95.41(5)
N3-W1-N5	77.39(4)	C11-W1-N5	81.25(5)
N7-W1-C10	98.75(5)	N3-W1-C10	161.05(5)
C11-W1-C10	38.30(5)	N5-W1-C10	119.03(4)
N7-W1-N1	172.58(5)	N3-W1-N1	84.54(4)
C11-W1-N1	88.67(5)	N5-W1-N1	81.11(4)
C10-W1-N1	88.67(4)	N7-W1-P1	93.53(4)
N3-W1-P1	83.57(3)	C11-W1-P1	116.74(4)
N5-W1-P1	158.68(3)	C10-W1-P1	78.47(3)
N1-W1-P1	87.66(3)	C20-P1-C18	103.36(9)
C20-P1-C19	103.38(7)	C18-P1-C19	99.44(8)
C20-P1-W1	112.30(5)	C18-P1-W1	116.12(6)
C19-P1-W1	120.04(5)	C1-N1-N2	106.01(11)
C1-N1-W1	134.47(10)	N2-N1-W1	119.46(8)
C3-N2-N1	109.76(12)	C3-N2-B1	128.16(12)
N1-N2-B1	122.04(11)	C4-N3-N4	106.53(11)
C4-N3-W1	129.77(10)	N4-N3-W1	123.43(9)
C6-N4-N3	109.93(11)	C6-N4-B1	129.51(12)
N3-N4-B1	118.34(11)	C7-N5-N6	106.57(11)
C7-N5-W1	131.50(9)	N6-N5-W1	121.63(8)
C9-N6-N5	109.39(11)	C9-N6-B1	129.75(12)
N5-N6-B1	120.61(11)	O1-N7-W1	175.13(10)
C16-N8-C15	114.56(11)	C16-N8-H8	109.5(15)
C15-N8-H8	109.1(15)	N1-C1-C2	110.67(13)
N1-C1-H1	124.7	C2-C1-H1	124.7
C3-C2-C1	104.79(12)	C3-C2-H2	127.6
C1-C2-H2	127.6	N2-C3-C2	108.78(13)
N2-C3-H3	125.6	C2-C3-H3	125.6
N3-C4-C5	110.18(13)	N3-C4-H4	124.9

C5-C4-H4	124.9	C6-C5-C4	105.10(13)
C6-C5-H5	127.4	C4-C5-H5	127.4
N4-C6-C5	108.25(13)	N4-C6-H6	125.9
C5-C6-H6	125.9	N5-C7-C8	110.68(13)
N5-C7-H7	124.7	C8-C7-H7	124.7
C9-C8-C7	104.46(12)	C9-C8-H8A	127.8
C7-C8-H8A	127.8	N6-C9-C8	108.90(12)
N6-C9-H9	125.5	C8-C9-H9	125.5
C11-C10-C15	116.95(11)	C11-C10-W1	70.41(7)
C15-C10-W1	128.24(9)	C11-C10-H10	111.5
C15-C10-H10	111.5	W1-C10-H10	111.5
C10-C11-C12	117.77(12)	C10-C11-W1	71.28(7)
C12-C11-W1	119.44(10)	C10-C11-H11	113.9
C12-C11-H11	113.9	W1-C11-H11	113.9
C13-C12-C11	123.30(13)	C13-C12-H12	118.4
C11-C12-H12	118.4	C12-C13-C14	120.01(13)
C12-C13-H13	120.0	C14-C13-H13	120.0
C13-C14-C17	111.11(12)	C13-C14-C15	111.08(12)
C17-C14-C15	112.39(11)	C13-C14-H14	107.3
C17-C14-H14	107.3	C15-C14-H14	107.3
N8-C15-C10	112.31(11)	N8-C15-C14	108.77(10)
C10-C15-C14	110.82(10)	N8-C15-H15	108.3
C10-C15-H15	108.3	C14-C15-H15	108.3
N8-C16-H16A	109.5	N8-C16-H16B	109.5
H16A-C16-H16B	109.5	N8-C16-H16C	109.5
H16A-C16-H16C	109.5	H16B-C16-H16C	109.5
F2-C17-F1	107.33(12)	F2-C17-F3	105.62(12)
F1-C17-F3	105.66(13)	F2-C17-C14	114.73(14)
F1-C17-C14	112.31(12)	F3-C17-C14	110.59(12)
P1-C18-H18A	109.5	P1-C18-H18B	109.5
H18A-C18-H18B	109.5	P1-C18-H18C	109.5

H18A-C18-H18C	109.5	H18B-C18-H18C	109.5
P1-C19-H19A	109.5	P1-C19-H19B	109.5
H19A-C19-H19B	109.5	P1-C19-H19C	109.5
H19A-C19-H19C	109.5	H19B-C19-H19C	109.5
P1-C20-H20A	109.5	P1-C20-H20B	109.5
H20A-C20-H20B	109.5	P1-C20-H20C	109.5
H20A-C20-H20C	109.5	H20B-C20-H20C	109.5
N2-B1-N6	109.13(11)	N2-B1-N4	109.55(11)
N6-B1-N4	105.89(11)	N2-B1-H1A	112.1(11)
N6-B1-H1A	110.1(11)	N4-B1-H1A	109.8(10)

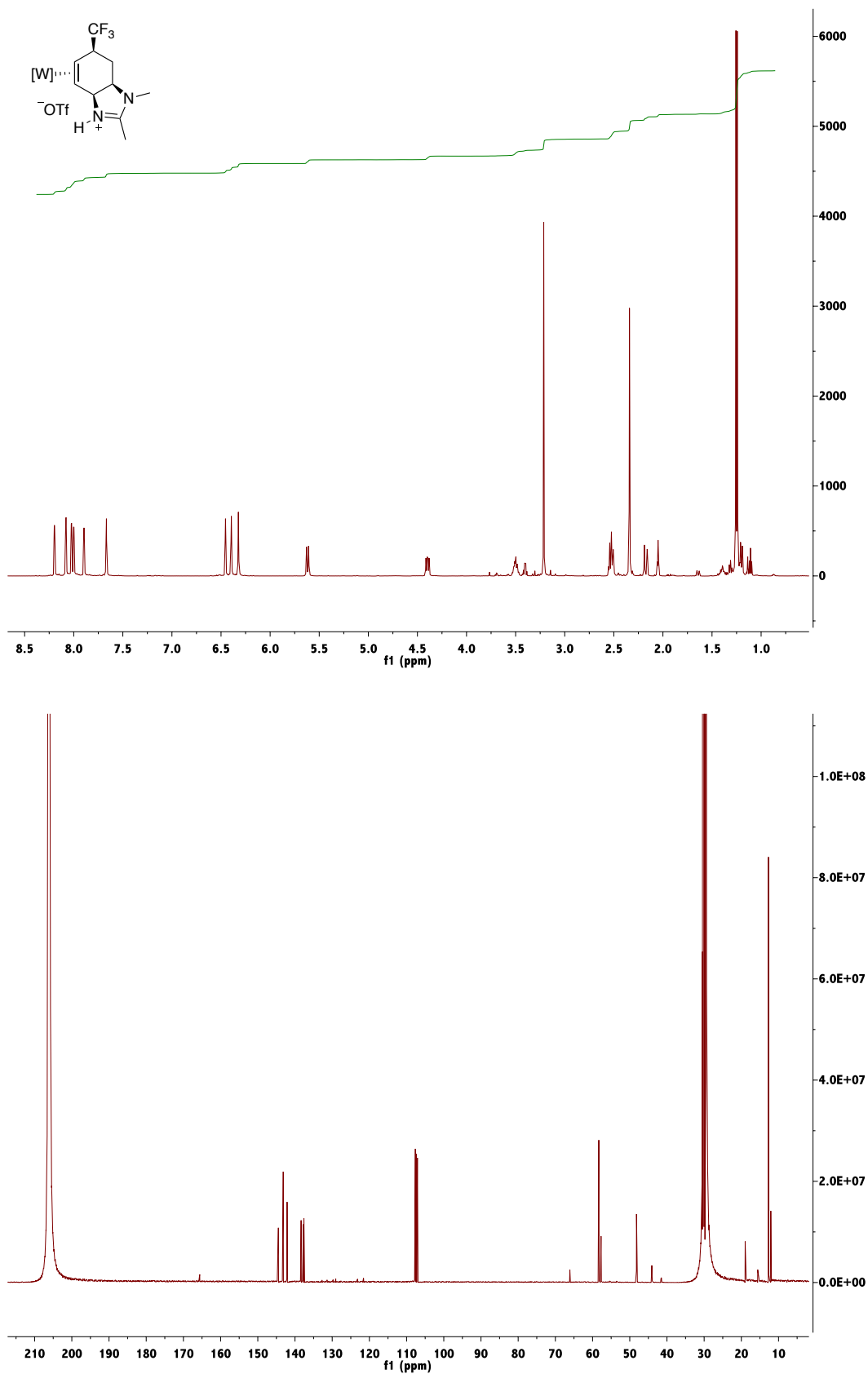
Table 6. Anisotropic atomic displacement parameters (\AA^2) for $\text{C}_{20}\text{H}_{29}\text{BF}_3\text{N}_8\text{OPW}$.

The anisotropic atomic displacement factor exponent takes the form: -

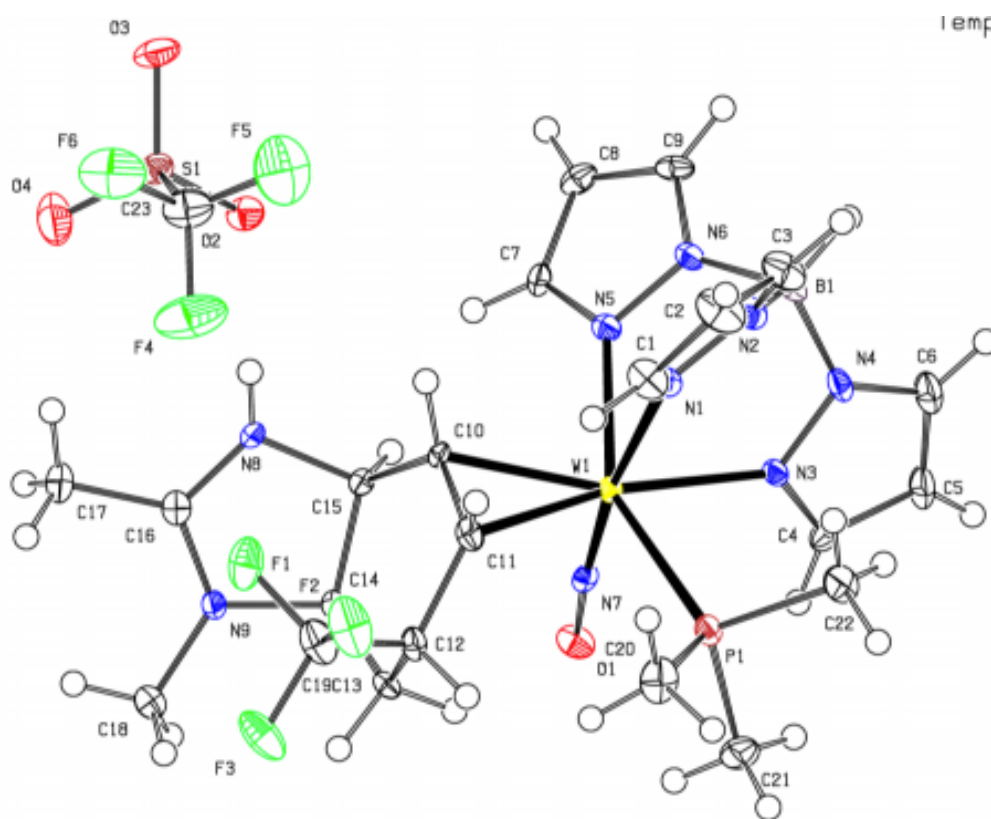
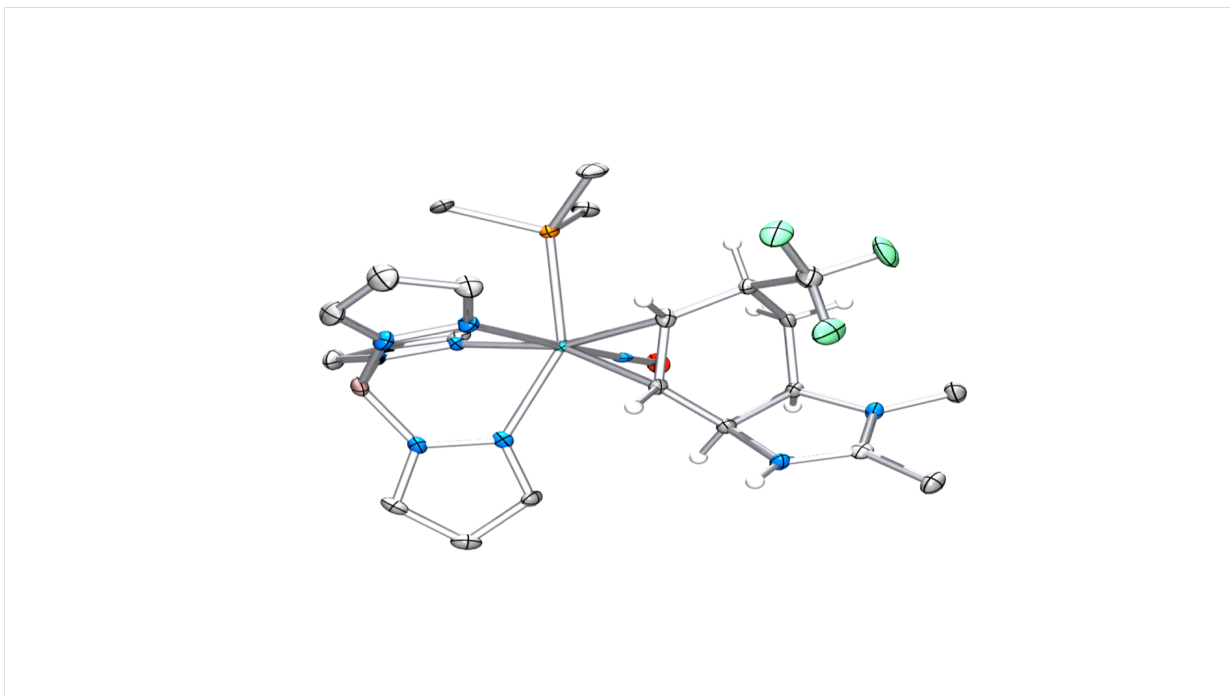
$$2\pi^2 [h^2 a^{*2} U_{11} + \dots + 2 h k a^* b^* U_{12}]$$

	U_{11}	U_{22}	U_{33}	U_{23}	U_{13}	U_{12}
W1	0.01040(2)	0.01108(2)	0.01236(2)	-0.00513(2)	-0.00196(2)	-0.00221(2)
P1	0.01558(14)	0.01460(14)	0.01415(14)	0.00455(11)	0.00430(11)	0.00211(11)
F1	0.0265(5)	0.0272(5)	0.0403(6)	-0.0218(4)	-0.0025(4)	-0.0037(4)
F2	0.0260(5)	0.0121(4)	0.0529(6)	-0.0085(4)	-0.0158(4)	-0.0007(3)
F3	0.0128(4)	0.0307(5)	0.0773(9)	-0.0296(6)	-0.0077(5)	0.0002(4)
O1	0.0107(4)	0.0273(6)	0.0479(7)	-0.0190(5)	-0.0001(4)	-0.0027(4)
N1	0.0130(5)	0.0161(5)	0.0181(5)	-0.0076(4)	-0.0018(4)	-0.0023(4)
N2	0.0142(5)	0.0136(5)	0.0192(5)	-0.0068(4)	-0.0021(4)	-0.0001(4)
N3	0.0173(5)	0.0145(5)	0.0161(5)	-0.0072(4)	-0.0011(4)	-0.0042(4)
N4	0.0180(5)	0.0130(5)	0.0187(5)	-0.0068(4)	-0.0019(4)	-0.0039(4)
N5	0.0139(5)	0.0150(5)	0.0155(5)	-0.0071(4)	-0.0030(4)	-0.0021(4)
N6	0.0161(5)	0.0174(5)	0.0169(5)	-0.0092(4)	-0.0014(4)	-0.0035(4)
N7	0.0128(5)	0.0136(5)	0.0186(5)	-0.0068(4)	-0.0025(4)	-0.0036(4)
N8	0.0163(5)	0.0147(5)	0.0194(5)	-0.0039(4)	-0.0055(4)	-0.0065(4)
C1	0.0133(6)	0.0216(6)	0.0195(6)	-0.0065(5)	-0.0028(5)	-0.0038(5)
C2	0.0123(6)	0.0257(7)	0.0228(6)	-0.0062(5)	-0.0038(5)	0.0000(5)

	U ₁₁	U ₂₂	U ₃₃	U ₂₃	U ₁₃	U ₁₂
C3	0.0158(6)	0.0180(6)	0.0224(6)	-0.0058(5)	-0.0033(5)	0.0032(5)
C4	0.0219(6)	0.0193(6)	0.0188(6)	-0.0078(5)	0.0013(5)	-0.0082(5)
C5	0.0282(7)	0.0202(7)	0.0224(7)	-0.0059(5)	0.0009(5)	-0.0124(6)
C6	0.0234(7)	0.0142(6)	0.0233(6)	-0.0057(5)	-0.0046(5)	-0.0064(5)
C7	0.0148(6)	0.0211(6)	0.0187(6)	-0.0076(5)	-0.0056(5)	-0.0031(5)
C8	0.0181(6)	0.0286(7)	0.0187(6)	-0.0103(5)	-0.0051(5)	-0.0063(5)
C9	0.0188(6)	0.0252(7)	0.0179(6)	-0.0125(5)	-0.0001(5)	-0.0068(5)
C10	0.0125(5)	0.0128(5)	0.0155(5)	-0.0055(4)	-0.0026(4)	-0.0030(4)
C11	0.0199(6)	0.0162(6)	0.0140(5)	-0.0047(4)	-0.0019(4)	-0.0076(5)
C12	0.0317(8)	0.0169(6)	0.0186(6)	-0.0003(5)	-0.0130(5)	-0.0097(5)
C13	0.0263(7)	0.0150(6)	0.0300(7)	-0.0033(5)	-0.0180(6)	-0.0030(5)
C14	0.0132(5)	0.0127(5)	0.0273(7)	-0.0073(5)	-0.0068(5)	-0.0023(4)
C15	0.0127(5)	0.0116(5)	0.0159(5)	-0.0045(4)	-0.0041(4)	-0.0027(4)
C16	0.0163(6)	0.0233(7)	0.0265(7)	-0.0107(5)	-0.0061(5)	-0.0066(5)
C17	0.0131(6)	0.0174(6)	0.0417(9)	-0.0136(6)	-0.0070(6)	-0.0021(5)
C18	0.0505(11)	0.0186(7)	0.0310(8)	-0.0006(6)	-0.0238(8)	-0.0041(7)
C19	0.0196(6)	0.0321(8)	0.0195(6)	-0.0092(6)	-0.0060(5)	-0.0072(6)
C20	0.0208(7)	0.0330(8)	0.0171(6)	-0.0103(6)	0.0010(5)	-0.0047(6)
B1	0.0170(6)	0.0150(6)	0.0193(7)	-0.0079(5)	-0.0014(5)	-0.0027(5)

$^1\text{H-NMR}$ ($\text{d}^6\text{-acetone}$) and $^{13}\text{C-NMR}$ ($\text{d}^6\text{-acetone}$) of Compound 91:

Compound 91



Compound 91Table 1. Sample and crystal data for C₂₃H₃₃BF₆N₉O₄PSW.

Chemical formula	C ₂₃ H ₃₃ BF ₆ N ₉ O ₄ PSW	
Formula weight	871.27 g/mol	
Temperature	100(2) K	
Wavelength	0.71073 Å	
Crystal size	0.138 x 0.163 x 0.173 mm	
Crystal habit	yellow block	
Crystal system	monoclinic	
Space group	P 1 21/c 1	
Unit cell dimensions	a = 9.1275(9) Å	α = 90°
	b = 24.928(2) Å	β = 90.643(3)°
	c = 14.0897(15) Å	γ = 90°
Volume	3205.6(6) Å ³	
Z	4	
Density (calculated)	1.805 g/cm ³	
Absorption coefficient	3.800 mm ⁻¹	
F(000)	1720	

Table 2. Data collection and structure refinement for C₂₃H₃₃BF₆N₉O₄PSW.

Diffractometer	Bruker Kappa APEXII Duo
Radiation source	fine-focus sealed tube (Mo K _α , λ = 0.71073 Å)
Theta range for data collection	1.63 to 27.54°
Index ranges	-10 ≤ h ≤ 11, -31 ≤ k ≤ 32, -18 ≤ l ≤ 18
Reflections collected	30769
Independent reflections	7370 [R(int) = 0.0517]
Coverage of independent reflections	97.9%
Absorption correction	Multi-Scan

Max. and min. transmission	0.6220 and 0.5590
Structure solution technique	direct methods
Structure solution program	SHELXT 2014/5 (Sheldrick, 2014)
Refinement method	Full-matrix least-squares on F^2
Refinement program	SHELXL-2017/1 (Sheldrick, 2017)
Function minimized	$\Sigma w(F_o^2 - F_c^2)^2$
Data / restraints / parameters	7370 / 0 / 427
Goodness-of-fit on F^2	1.025
Δ/σ_{\max}	0.002
Final R indices	6113 data; $I > 2\sigma(I)$ R1 = 0.0292, wR2 = 0.0487
	all data R1 = 0.0416, wR2 = 0.0521
Weighting scheme	$w = 1/[\sigma^2(F_o^2) + (0.0117P)^2 + 3.5815P]$ where $P = (F_o^2 + 2F_c^2)/3$
Largest diff. peak and hole	0.557 and -0.801 $e\text{\AA}^{-3}$
R.M.S. deviation from mean	0.124 $e\text{\AA}^{-3}$

Table 3. Atomic coordinates and equivalent isotropic atomic displacement parameters (\AA^2) for $C_{23}H_{33}BF_6N_9O_4PSW$.

$U(\text{eq})$ is defined as one third of the trace of the orthogonalized U_{ij} tensor.

	x/a	y/b	z/c	$U(\text{eq})$
W1	0.57157(2)	0.32884(2)	0.29472(2)	0.00951(4)
P1	0.47143(10)	0.29500(4)	0.44868(7)	0.01306(19)
F1	0.3302(3)	0.50958(8)	0.31167(16)	0.0281(5)
F2	0.3323(3)	0.48660(9)	0.45856(16)	0.0330(6)
F3	0.1303(2)	0.48494(10)	0.37796(18)	0.0354(6)

	x/a	y/b	z/c	U(eq)
O1	0.3247(3)	0.27994(10)	0.18141(18)	0.0176(6)
N1	0.7628(3)	0.35166(12)	0.3896(2)	0.0145(6)
N2	0.8878(3)	0.32083(12)	0.3868(2)	0.0167(7)
N3	0.6617(3)	0.24621(11)	0.2959(2)	0.0120(6)
N4	0.8067(3)	0.23443(11)	0.3075(2)	0.0143(6)
N5	0.7522(3)	0.33275(11)	0.1896(2)	0.0125(6)
N6	0.8860(3)	0.31058(11)	0.2105(2)	0.0139(6)
N7	0.4252(3)	0.30237(10)	0.22674(19)	0.0105(6)
N8	0.4466(3)	0.47471(11)	0.1215(2)	0.0132(6)
N9	0.2114(3)	0.46269(11)	0.1331(2)	0.0126(6)
C1	0.7809(4)	0.38453(15)	0.4639(3)	0.0212(9)
C2	0.9140(4)	0.37503(17)	0.5100(3)	0.0289(10)
C3	0.9770(4)	0.33457(16)	0.4589(3)	0.0244(9)
C4	0.5934(4)	0.20053(13)	0.2744(2)	0.0149(8)
C5	0.6947(4)	0.15840(14)	0.2707(3)	0.0213(9)
C6	0.8280(4)	0.18162(14)	0.2922(3)	0.0207(9)
C7	0.7621(4)	0.35084(13)	0.1008(3)	0.0136(7)
C8	0.8992(4)	0.33986(13)	0.0631(3)	0.0176(8)
C9	0.9739(4)	0.31386(14)	0.1347(3)	0.0157(8)
C10	0.5332(4)	0.41090(12)	0.2453(2)	0.0103(7)
C11	0.4676(4)	0.40617(13)	0.3375(3)	0.0136(8)
C12	0.3040(4)	0.41572(13)	0.3484(3)	0.0137(7)
C13	0.2143(4)	0.39515(14)	0.2639(3)	0.0144(8)
C14	0.2701(4)	0.41021(13)	0.1661(3)	0.0122(7)
C15	0.4397(4)	0.41839(13)	0.1563(2)	0.0114(7)
C16	0.3166(4)	0.49591(13)	0.1104(2)	0.0131(7)
C17	0.2915(4)	0.55112(13)	0.0735(3)	0.0181(8)
C18	0.0546(4)	0.47286(14)	0.1245(3)	0.0193(8)
C19	0.2746(4)	0.47357(16)	0.3727(3)	0.0236(9)
C20	0.4128(5)	0.33931(15)	0.5432(3)	0.0238(9)
C21	0.3191(4)	0.24848(15)	0.4355(3)	0.0220(9)
C22	0.6052(4)	0.25531(17)	0.5141(3)	0.0255(9)
B1	0.9155(4)	0.28124(18)	0.3054(3)	0.0175(9)
S1	0.75595(10)	0.57976(4)	0.11592(7)	0.0162(2)
F4	0.6223(3)	0.58034(11)	0.2780(2)	0.0493(8)
F5	0.8551(3)	0.56674(12)	0.28859(19)	0.0532(8)

	x/a	y/b	z/c	U(eq)
F6	0.7732(3)	0.64593(10)	0.25892(19)	0.0441(7)
O2	0.7318(3)	0.52247(9)	0.11164(18)	0.0187(6)
O3	0.9009(3)	0.59634(10)	0.0904(2)	0.0262(7)
O4	0.6370(3)	0.61092(11)	0.0780(2)	0.0333(7)
C23	0.7527(5)	0.59361(17)	0.2419(3)	0.0281(10)

Table 4. Bond lengths (Å) for C₂₃H₃₃BF₆N₉O₄PSW.

W1-N7	1.763(3)	W1-C10	2.188(3)
W1-N3	2.218(3)	W1-N5	2.231(3)
W1-C11	2.234(3)	W1-N1	2.260(3)
W1-P1	2.5094(10)	P1-C22	1.815(4)
P1-C20	1.816(4)	P1-C21	1.818(4)
F1-C19	1.347(5)	F2-C19	1.353(4)
F3-C19	1.350(4)	O1-N7	1.245(3)
N1-C1	1.338(5)	N1-N2	1.376(4)
N2-C3	1.340(5)	N2-B1	1.537(5)
N3-C4	1.331(4)	N3-N4	1.364(4)
N4-C6	1.348(4)	N4-B1	1.533(5)
N5-C7	1.334(4)	N5-N6	1.369(4)
N6-C9	1.344(4)	N6-B1	1.545(5)
N8-C16	1.307(4)	N8-C15	1.488(4)
N8-H8	0.83(4)	N9-C16	1.311(4)
N9-C18	1.457(4)	N9-C14	1.487(4)
C1-C2	1.392(5)	C1-H1	0.95
C2-C3	1.370(5)	C2-H2	0.95
C3-H3	0.95	C4-C5	1.401(5)
C4-H4	0.95	C5-C6	1.378(5)
C5-H5	0.95	C6-H6	0.95
C7-C8	1.392(5)	C7-H7	0.95
C8-C9	1.374(5)	C8-H8A	0.95
C9-H9	0.95	C10-C11	1.441(5)
C10-C15	1.522(5)	C10-H10	1.0
C11-C12	1.522(5)	C11-H11	1.0
C12-C19	1.507(5)	C12-C13	1.526(5)
C12-H12	1.0	C13-C14	1.521(5)

C13-H13A	0.99	C13-H13B	0.99
C14-C15	1.568(4)	C14-H14	1.0
C15-H15	1.0	C16-C17	1.488(5)
C17-H17A	0.98	C17-H17B	0.98
C17-H17C	0.98	C18-H18A	0.98
C18-H18B	0.98	C18-H18C	0.98
C20-H20A	0.98	C20-H20B	0.98
C20-H20C	0.98	C21-H21A	0.98
C21-H21B	0.98	C21-H21C	0.98
C22-H22A	0.98	C22-H22B	0.98
C22-H22C	0.98	B1-H1A	1.11(4)
S1-O4	1.433(3)	S1-O3	1.436(3)
S1-O2	1.446(2)	S1-C23	1.808(4)
F4-C23	1.341(5)	F5-C23	1.320(5)
F6-C23	1.339(5)		

Table 5. Bond angles (°) for C₂₃H₃₃BF₆N₉O₄PSW.

N7-W1-C10	93.43(12)	N7-W1-N3	86.26(11)
C10-W1-N3	158.24(12)	N7-W1-N5	102.52(11)
C10-W1-N5	82.23(11)	N3-W1-N5	76.62(10)
N7-W1-C11	98.53(12)	C10-W1-C11	38.03(12)
N3-W1-C11	163.28(12)	N5-W1-C11	117.44(12)
N7-W1-N1	172.40(11)	C10-W1-N1	94.15(12)
N3-W1-N1	86.88(10)	N5-W1-N1	79.04(10)
C11-W1-N1	87.16(12)	N7-W1-P1	93.60(9)
C10-W1-P1	122.05(9)	N3-W1-P1	79.64(8)
N5-W1-P1	150.19(8)	C11-W1-P1	84.07(9)
N1-W1-P1	81.93(8)	C22-P1-C20	99.27(19)
C22-P1-C21	102.33(19)	C20-P1-C21	103.39(18)
C22-P1-W1	111.89(13)	C20-P1-W1	122.89(13)
C21-P1-W1	114.31(13)	C1-N1-N2	105.6(3)
C1-N1-W1	134.8(2)	N2-N1-W1	118.5(2)
C3-N2-N1	109.4(3)	C3-N2-B1	128.8(3)

N1-N2-B1	121.6(3)	C4-N3-N4	107.1(3)
C4-N3-W1	128.3(2)	N4-N3-W1	124.0(2)
C6-N4-N3	109.4(3)	C6-N4-B1	130.2(3)
N3-N4-B1	117.5(3)	C7-N5-N6	105.6(3)
C7-N5-W1	134.1(2)	N6-N5-W1	120.3(2)
C9-N6-N5	110.1(3)	C9-N6-B1	128.0(3)
N5-N6-B1	121.5(3)	O1-N7-W1	175.2(2)
C16-N8-C15	112.3(3)	C16-N8-H8	130.(3)
C15-N8-H8	117.(3)	C16-N9-C18	126.3(3)
C16-N9-C14	111.7(3)	C18-N9-C14	122.0(3)
N1-C1-C2	111.1(3)	N1-C1-H1	124.4
C2-C1-H1	124.4	C3-C2-C1	104.4(3)
C3-C2-H2	127.8	C1-C2-H2	127.8
N2-C3-C2	109.4(3)	N2-C3-H3	125.3
C2-C3-H3	125.3	N3-C4-C5	110.0(3)
N3-C4-H4	125.0	C5-C4-H4	125.0
C6-C5-C4	105.0(3)	C6-C5-H5	127.5
C4-C5-H5	127.5	N4-C6-C5	108.5(3)
N4-C6-H6	125.8	C5-C6-H6	125.8
N5-C7-C8	111.2(3)	N5-C7-H7	124.4
C8-C7-H7	124.4	C9-C8-C7	104.7(3)
C9-C8-H8A	127.7	C7-C8-H8A	127.7
N6-C9-C8	108.4(3)	N6-C9-H9	125.8
C8-C9-H9	125.8	C11-C10-C15	121.2(3)
C11-C10-W1	72.75(18)	C15-C10-W1	117.6(2)
C11-C10-H10	113.1	C15-C10-H10	113.1
W1-C10-H10	113.1	C10-C11-C12	119.7(3)
C10-C11-W1	69.22(18)	C12-C11-W1	125.6(2)
C10-C11-H11	111.9	C12-C11-H11	111.9

W1-C11-H11	111.9	C19-C12-C11	110.5(3)
C19-C12-C13	113.8(3)	C11-C12-C13	112.8(3)
C19-C12-H12	106.4	C11-C12-H12	106.4
C13-C12-H12	106.4	C14-C13-C12	116.2(3)
C14-C13-H13A	108.2	C12-C13-H13A	108.2
C14-C13-H13B	108.2	C12-C13-H13B	108.2
H13A-C13-H13B	107.4	N9-C14-C13	112.2(3)
N9-C14-C15	102.2(3)	C13-C14-C15	117.0(3)
N9-C14-H14	108.4	C13-C14-H14	108.4
C15-C14-H14	108.4	N8-C15-C10	111.2(3)
N8-C15-C14	101.4(3)	C10-C15-C14	117.1(3)
N8-C15-H15	108.9	C10-C15-H15	108.9
C14-C15-H15	108.9	N8-C16-N9	112.5(3)
N8-C16-C17	123.5(3)	N9-C16-C17	124.0(3)
C16-C17-H17A	109.5	C16-C17-H17B	109.5
H17A-C17-H17B	109.5	C16-C17-H17C	109.5
H17A-C17-H17C	109.5	H17B-C17-H17C	109.5
N9-C18-H18A	109.5	N9-C18-H18B	109.5
H18A-C18-H18B	109.5	N9-C18-H18C	109.5
H18A-C18-H18C	109.5	H18B-C18-H18C	109.5
F1-C19-F3	105.7(3)	F1-C19-F2	105.4(3)
F3-C19-F2	105.7(3)	F1-C19-C12	115.0(3)
F3-C19-C12	112.9(3)	F2-C19-C12	111.4(3)
P1-C20-H20A	109.5	P1-C20-H20B	109.5
H20A-C20-H20B	109.5	P1-C20-H20C	109.5
H20A-C20-H20C	109.5	H20B-C20-H20C	109.5
P1-C21-H21A	109.5	P1-C21-H21B	109.5
H21A-C21-H21B	109.5	P1-C21-H21C	109.5
H21A-C21-H21C	109.5	H21B-C21-H21C	109.5

P1-C22-H22A	109.5	P1-C22-H22B	109.5
H22A-C22-H22B	109.5	P1-C22-H22C	109.5
H22A-C22-H22C	109.5	H22B-C22-H22C	109.5
N4-B1-N2	111.3(3)	N4-B1-N6	105.7(3)
N2-B1-N6	108.3(3)	N4-B1-H1A	108.8(19)
N2-B1-H1A	113.(2)	N6-B1-H1A	109.(2)
O4-S1-O3	116.59(18)	O4-S1-O2	113.88(16)
O3-S1-O2	114.48(15)	O4-S1-C23	103.9(2)
O3-S1-C23	102.47(18)	O2-S1-C23	103.02(18)
F5-C23-F6	107.9(4)	F5-C23-F4	108.2(4)
F6-C23-F4	107.2(3)	F5-C23-S1	111.9(3)
F6-C23-S1	111.0(3)	F4-C23-S1	110.5(3)

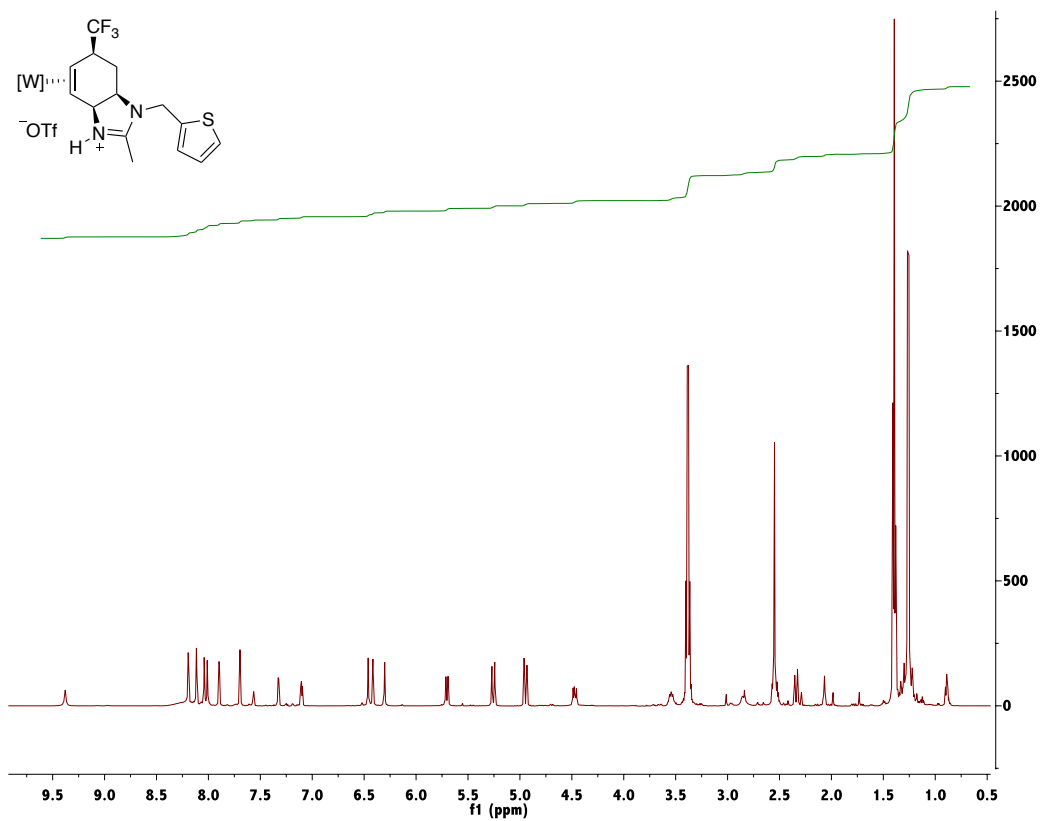
Table 7. Anisotropic atomic displacement parameters (\AA^2) for $\text{C}_{23}\text{H}_{33}\text{BF}_6\text{N}_9\text{O}_4\text{PSW}$.

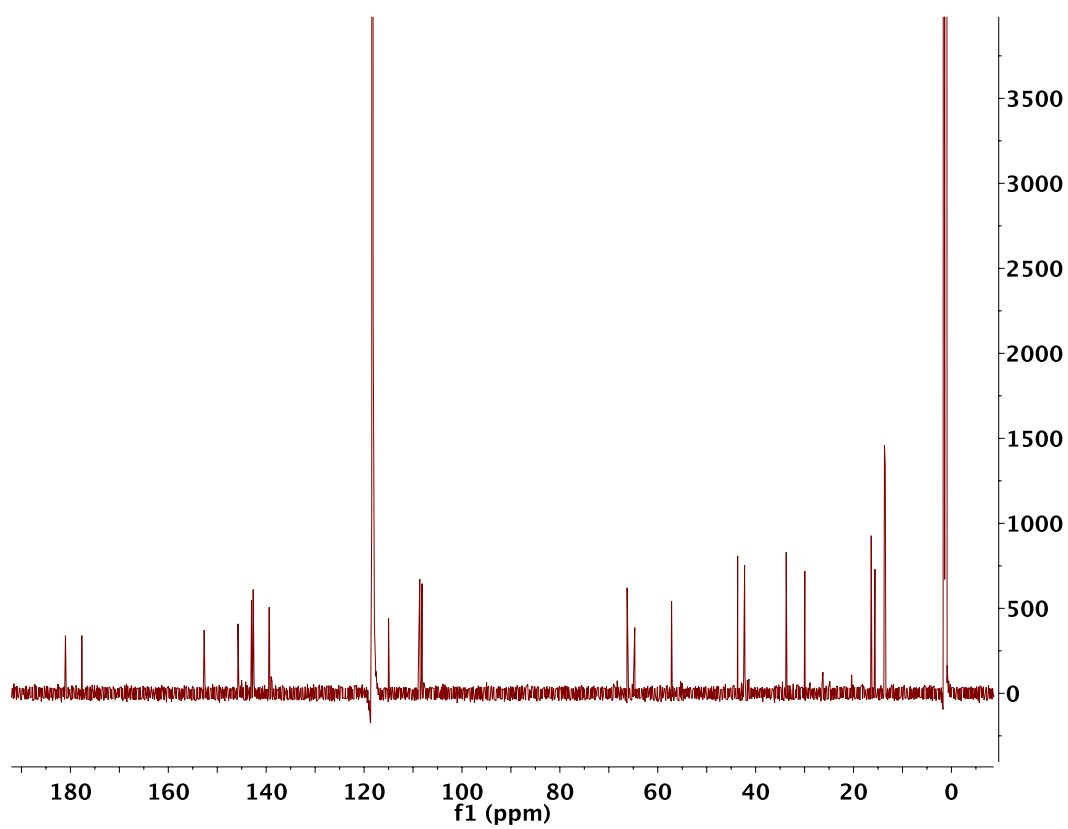
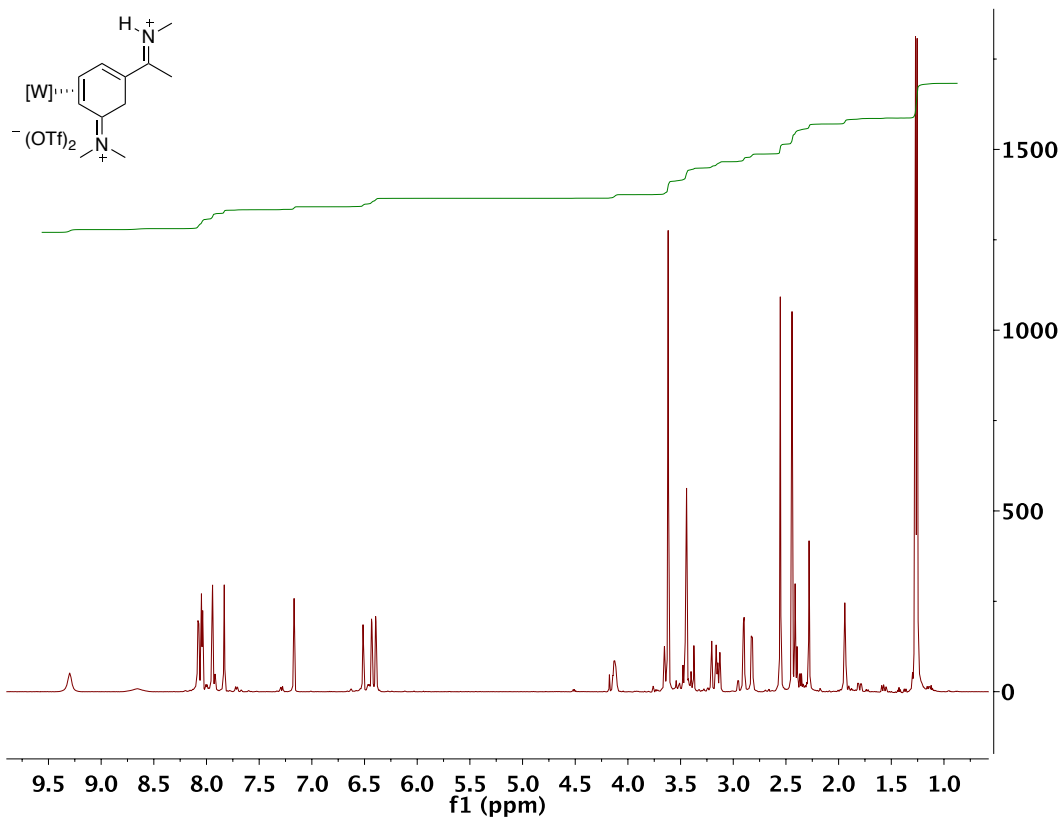
The anisotropic atomic displacement factor exponent takes the form: $-2\pi^2 [h^2 a^{*2} U_{11} + \dots + 2 h k a^* b^* U_{12}]$

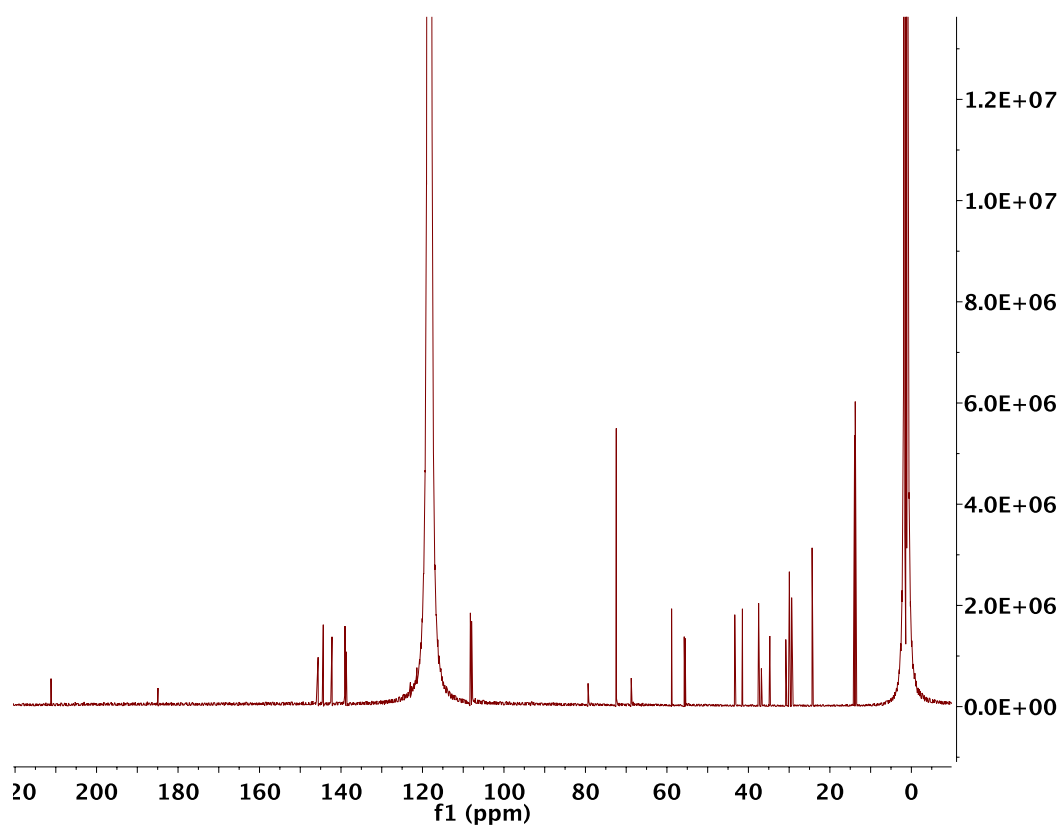
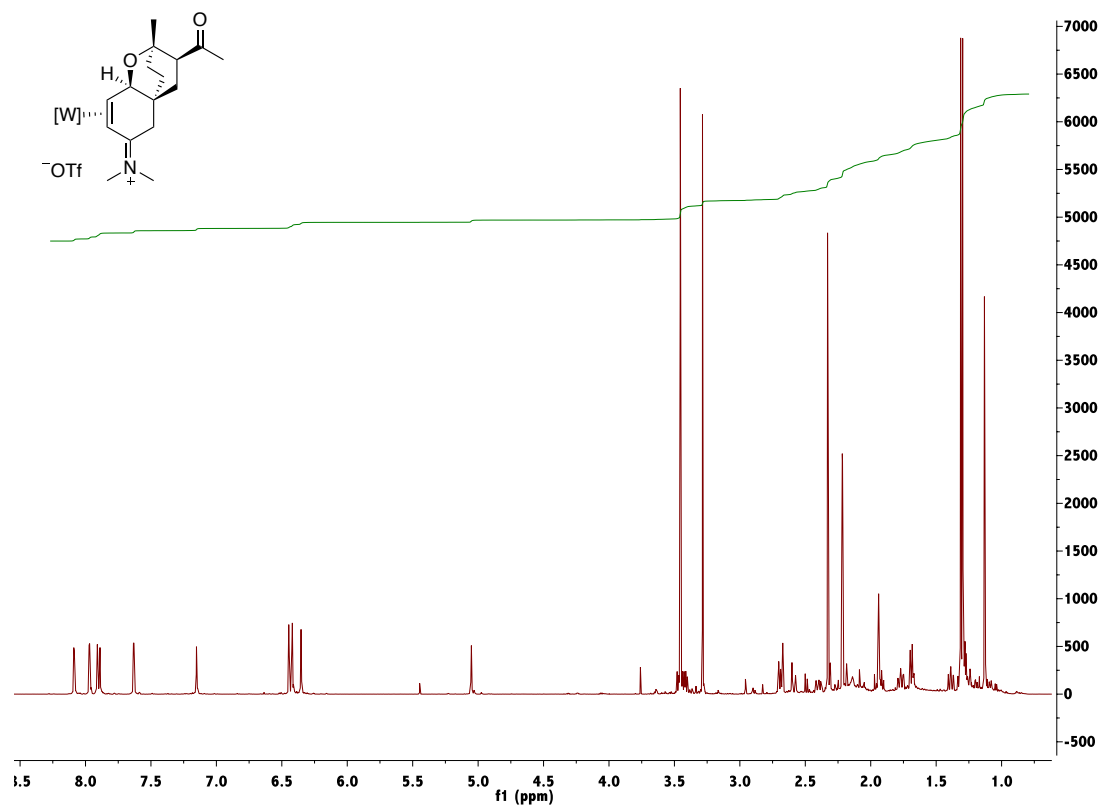
	U_{11}	U_{22}	U_{33}	U_{23}	U_{13}	U_{12}
W1	0.01024(7)	0.01063(6)	0.00764(7)	0.00094(6)	-0.00025(5)	0.00100(6)
P1	0.0140(5)	0.0161(5)	0.0091(5)	0.0016(4)	0.0007(4)	0.0034(4)
F1	0.0444(15)	0.0150(11)	0.0248(14)	-0.0032(10)	-0.0010(11)	0.0054(10)
F2	0.0474(16)	0.0351(13)	0.0163(13)	-0.0125(11)	-0.0076(11)	0.0167(12)
F3	0.0271(13)	0.0381(14)	0.0411(16)	-0.0116(13)	0.0036(12)	0.0189(11)
O1	0.0145(13)	0.0201(13)	0.0183(15)	-0.0065(11)	-0.0024(11)	-0.0008(11)
N1	0.0127(15)	0.0190(15)	0.0118(16)	0.0004(13)	-0.0016(12)	-0.0001(12)
N2	0.0139(15)	0.0215(17)	0.0145(16)	0.0016(13)	-0.0036(12)	0.0013(13)
N3	0.0104(15)	0.0147(15)	0.0110(16)	0.0026(12)	0.0022(12)	0.0033(12)

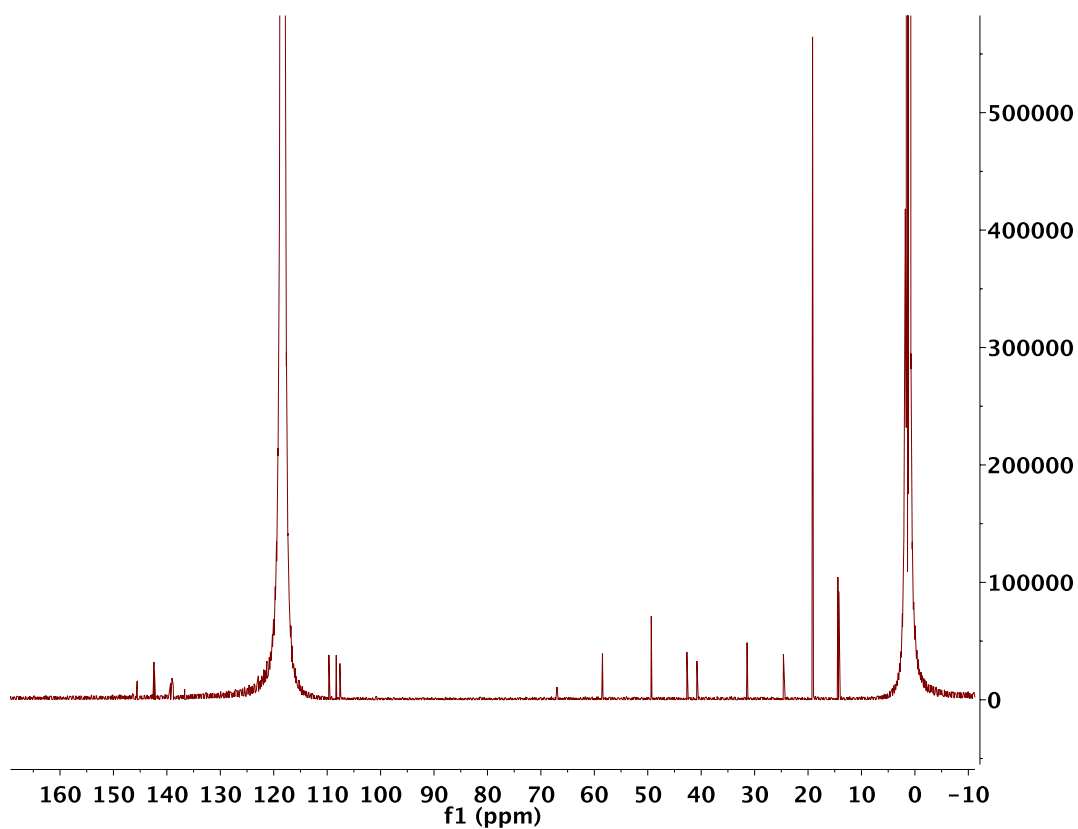
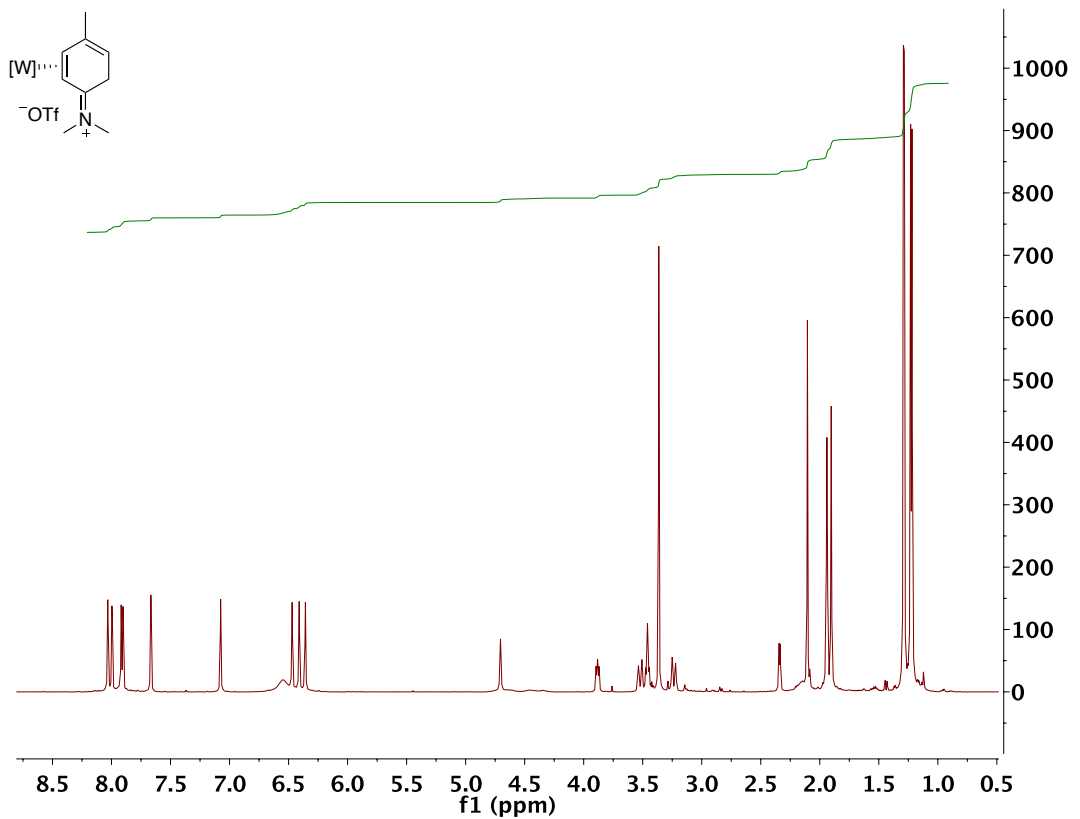
	U ₁₁	U ₂₂	U ₃₃	U ₂₃	U ₁₃	U ₁₂
N4	0.0145(15)	0.0179(15)	0.0106(16)	0.0027(13)	0.0001(12)	0.0073(12)
N5	0.0111(14)	0.0128(14)	0.0138(15)	-0.0012(13)	0.0007(11)	0.0002(12)
N6	0.0101(15)	0.0159(14)	0.0157(17)	0.0006(13)	0.0011(13)	0.0021(11)
N7	0.0149(15)	0.0105(13)	0.0062(16)	0.0007(11)	0.0041(12)	0.0011(12)
N8	0.0112(15)	0.0119(15)	0.0164(17)	0.0060(13)	0.0008(13)	-0.0009(12)
N9	0.0114(15)	0.0111(14)	0.0153(17)	0.0021(12)	-0.0019(12)	0.0009(12)
C1	0.022(2)	0.024(2)	0.017(2)	-0.0080(17)	-0.0025(17)	0.0021(17)
C2	0.024(2)	0.039(2)	0.023(2)	-0.011(2)	-0.0080(18)	0.0010(19)
C3	0.0171(19)	0.037(2)	0.019(2)	-0.0023(19)	-0.0086(16)	0.0011(18)
C4	0.0185(19)	0.0163(18)	0.010(2)	0.0035(14)	-0.0009(15)	-0.0021(15)
C5	0.027(2)	0.0139(19)	0.023(2)	0.0023(16)	0.0000(17)	0.0084(16)
C6	0.025(2)	0.018(2)	0.019(2)	0.0011(16)	0.0012(17)	0.0102(16)
C7	0.0171(19)	0.0112(16)	0.0126(19)	0.0033(15)	-0.0004(15)	0.0016(14)
C8	0.022(2)	0.0169(19)	0.0143(19)	0.0002(15)	0.0057(15)	-0.0042(15)
C9	0.0124(18)	0.0180(18)	0.017(2)	-0.0059(15)	0.0061(15)	-0.0030(14)
C10	0.0109(17)	0.0065(16)	0.0137(19)	0.0021(14)	-0.0002(14)	-0.0011(13)
C11	0.0145(18)	0.0117(17)	0.0145(19)	-0.0033(15)	-0.0023(15)	0.0021(14)
C12	0.0170(19)	0.0130(17)	0.0111(19)	0.0004(15)	0.0007(15)	0.0050(15)
C13	0.0098(17)	0.0154(17)	0.018(2)	0.0017(15)	0.0022(15)	0.0042(14)
C14	0.0121(18)	0.0116(17)	0.0130(19)	0.0027(14)	0.0004(14)	0.0019(14)
C15	0.0118(17)	0.0105(16)	0.0118(19)	0.0014(14)	0.0008(14)	0.0000(14)
C16	0.0179(19)	0.0126(17)	0.0087(18)	-0.0031(14)	-0.0012(15)	0.0015(14)

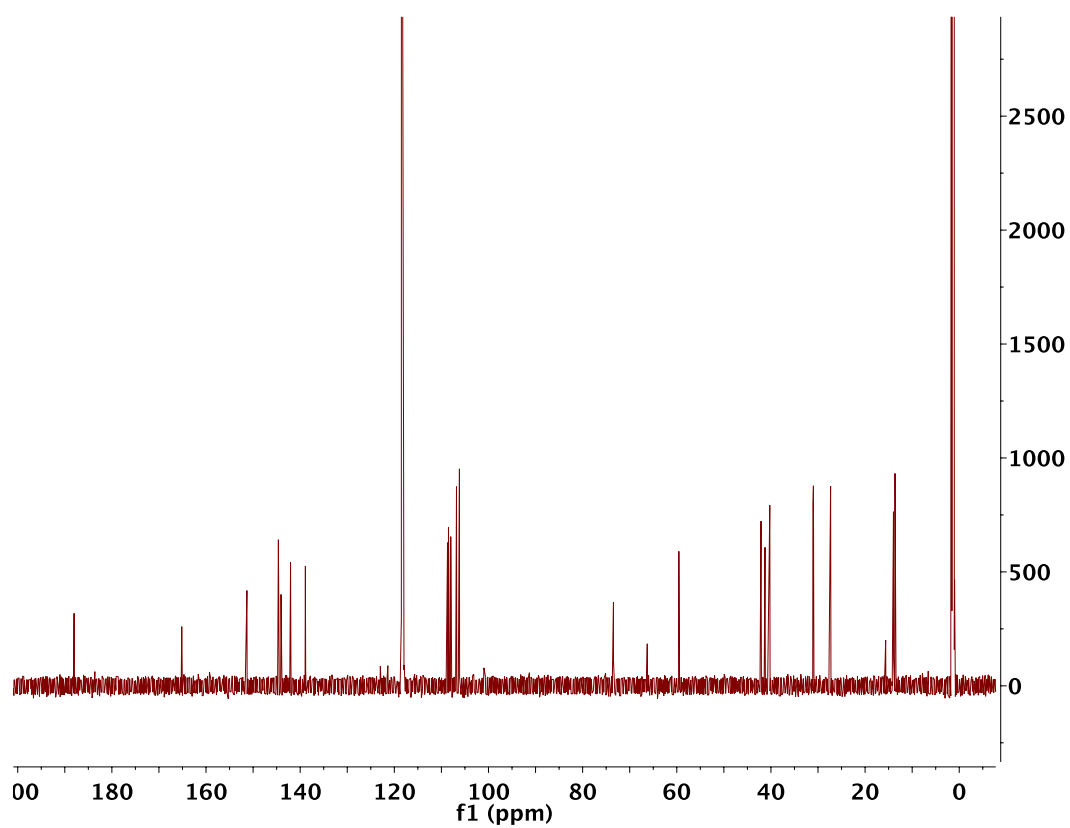
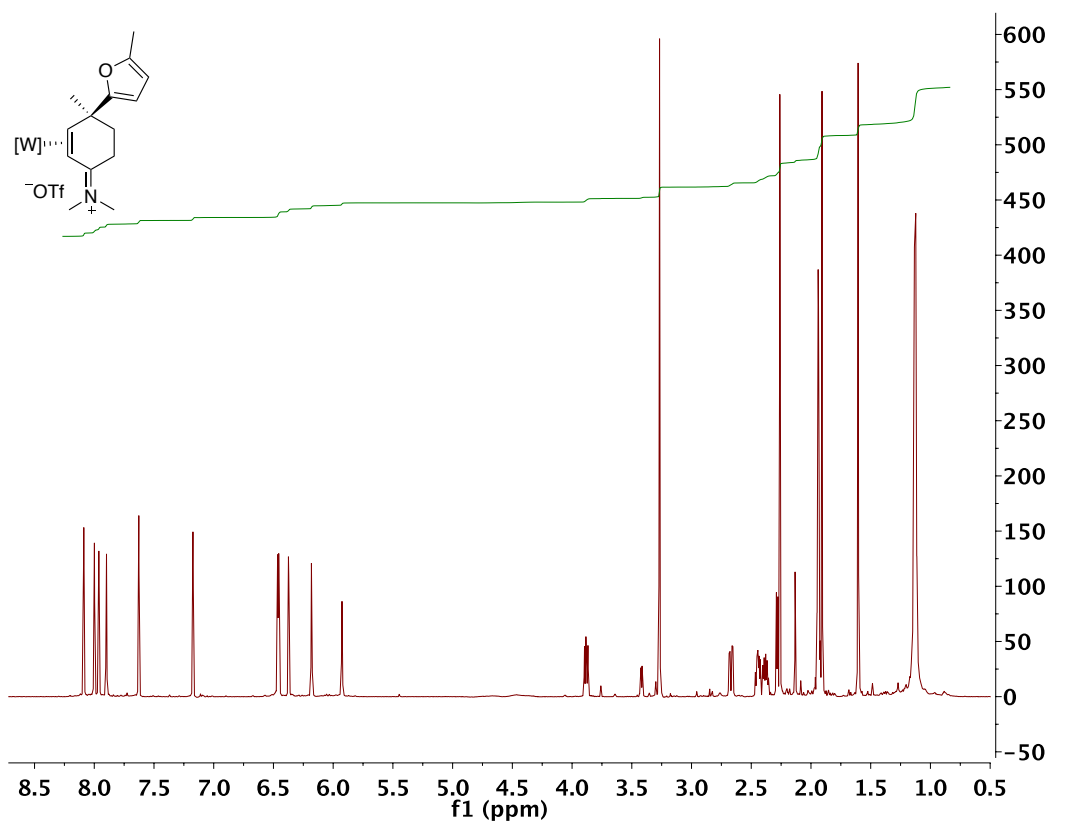
	U ₁₁	U ₂₂	U ₃₃	U ₂₃	U ₁₃	U ₁₂
C17	0.024(2)	0.0129(17)	0.018(2)	0.0011(16)	-0.0038(16)	0.0025(15)
C18	0.0162(19)	0.0178(19)	0.024(2)	0.0018(16)	0.0024(16)	0.0038(15)
C19	0.027(2)	0.025(2)	0.018(2)	-0.0065(18)	-0.0011(17)	0.0090(18)
C20	0.036(2)	0.026(2)	0.0091(19)	-0.0010(16)	0.0038(17)	0.0064(18)
C21	0.021(2)	0.027(2)	0.017(2)	0.0038(17)	0.0062(17)	-0.0009(17)
C22	0.022(2)	0.041(2)	0.014(2)	0.0156(19)	0.0038(16)	0.0089(18)
B1	0.010(2)	0.026(2)	0.017(2)	-0.0007(19)	-0.0011(17)	0.0052(18)
S1	0.0174(5)	0.0143(4)	0.0170(5)	-0.0014(4)	0.0029(4)	-0.0017(4)
F4	0.0534(18)	0.0571(18)	0.0382(18)	-0.0180(14)	0.0284(14)	-0.0191(14)
F5	0.066(2)	0.067(2)	0.0265(16)	0.0011(15)	-0.0202(15)	0.0065(16)
F6	0.0446(16)	0.0418(15)	0.0461(18)	-0.0306(14)	0.0102(13)	-0.0099(13)
O2	0.0198(14)	0.0158(13)	0.0204(15)	-0.0047(11)	0.0025(11)	-0.0029(11)
O3	0.0235(15)	0.0223(14)	0.0332(18)	-0.0024(13)	0.0149(13)	-0.0071(12)
O4	0.0343(17)	0.0238(15)	0.042(2)	0.0041(14)	-0.0120(15)	0.0049(13)
C23	0.029(2)	0.033(2)	0.023(2)	-0.0077(19)	0.0079(19)	-0.0047(19)

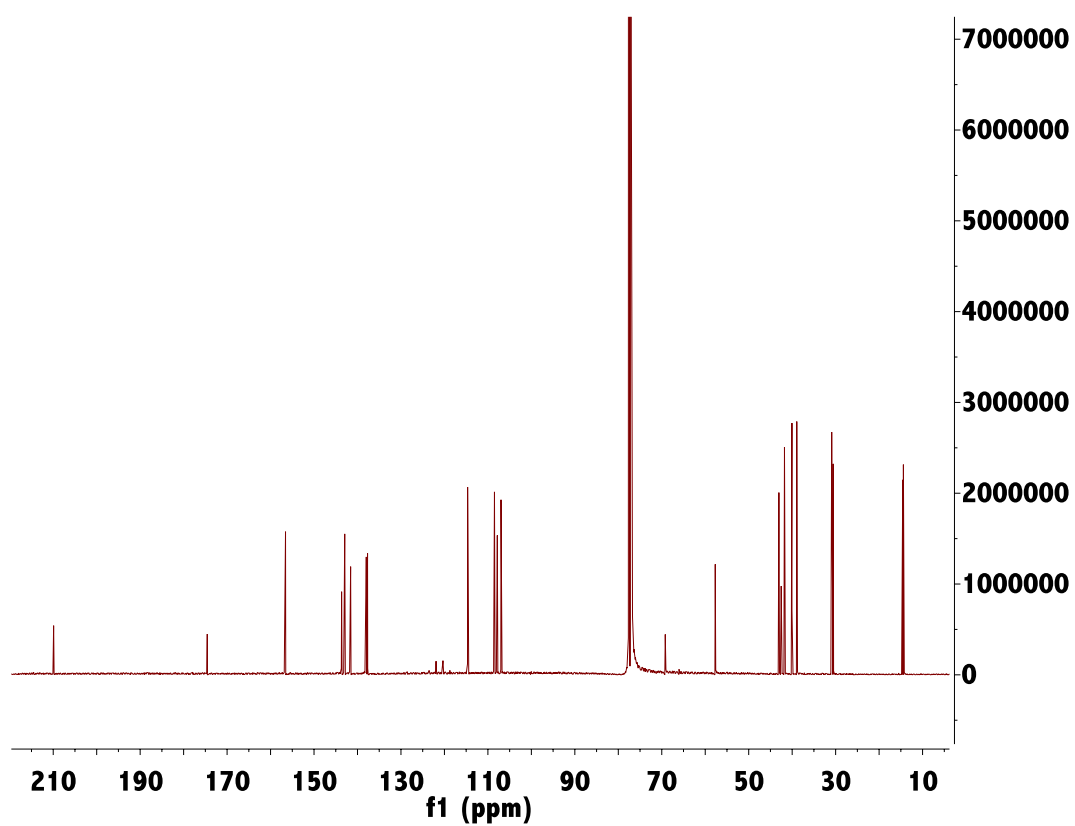
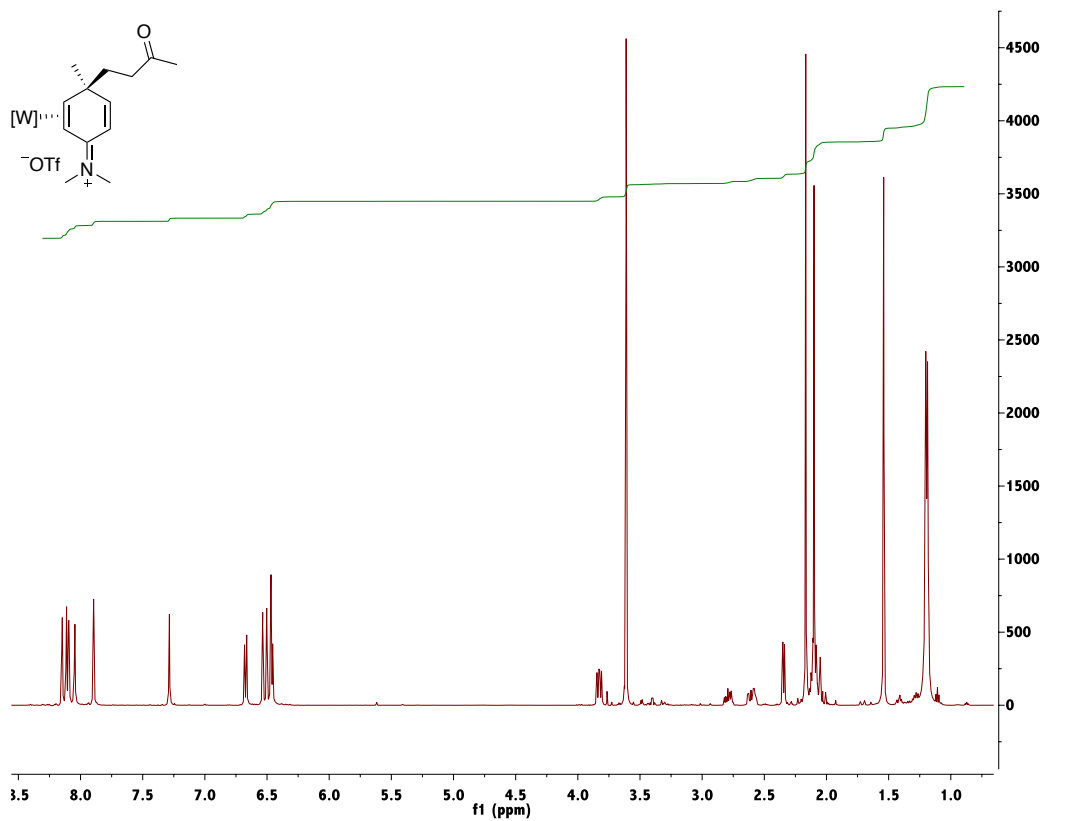
¹H-NMR (d⁶-acetone) of Compound 93:

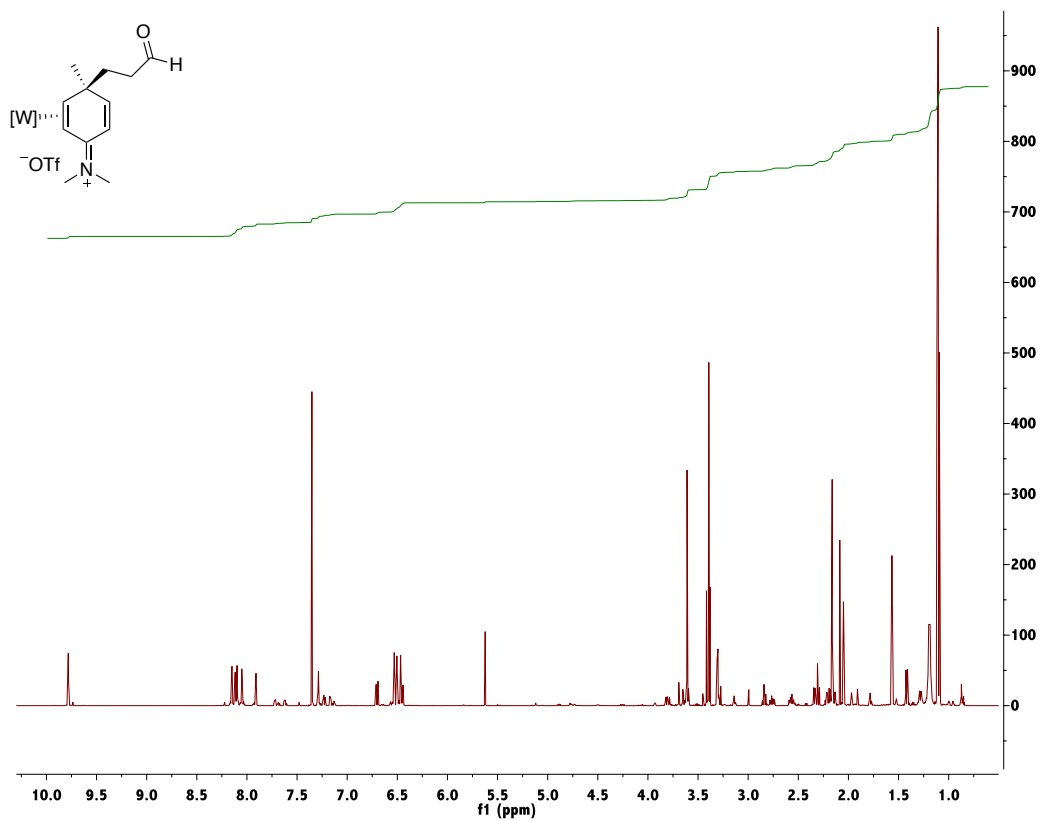
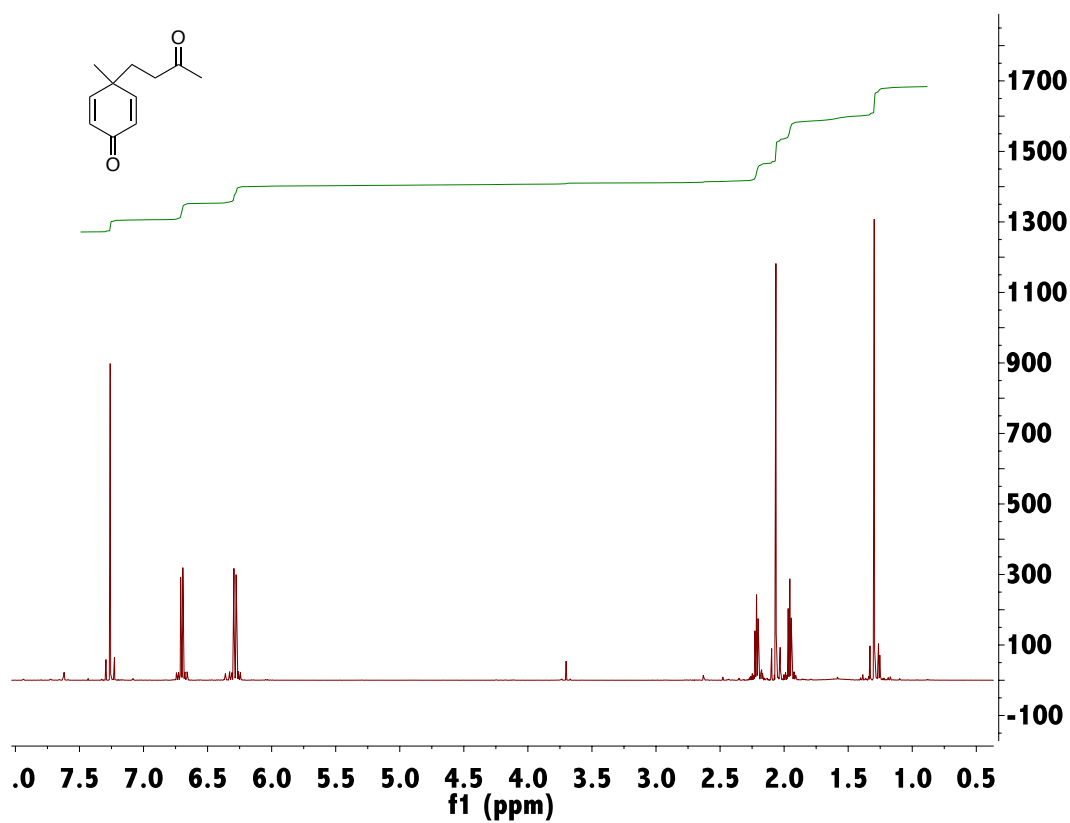
$^1\text{H-NMR}$ (CD_3CN) and $^{13}\text{C-NMR}$ (CD_3CN) of Compound 97:

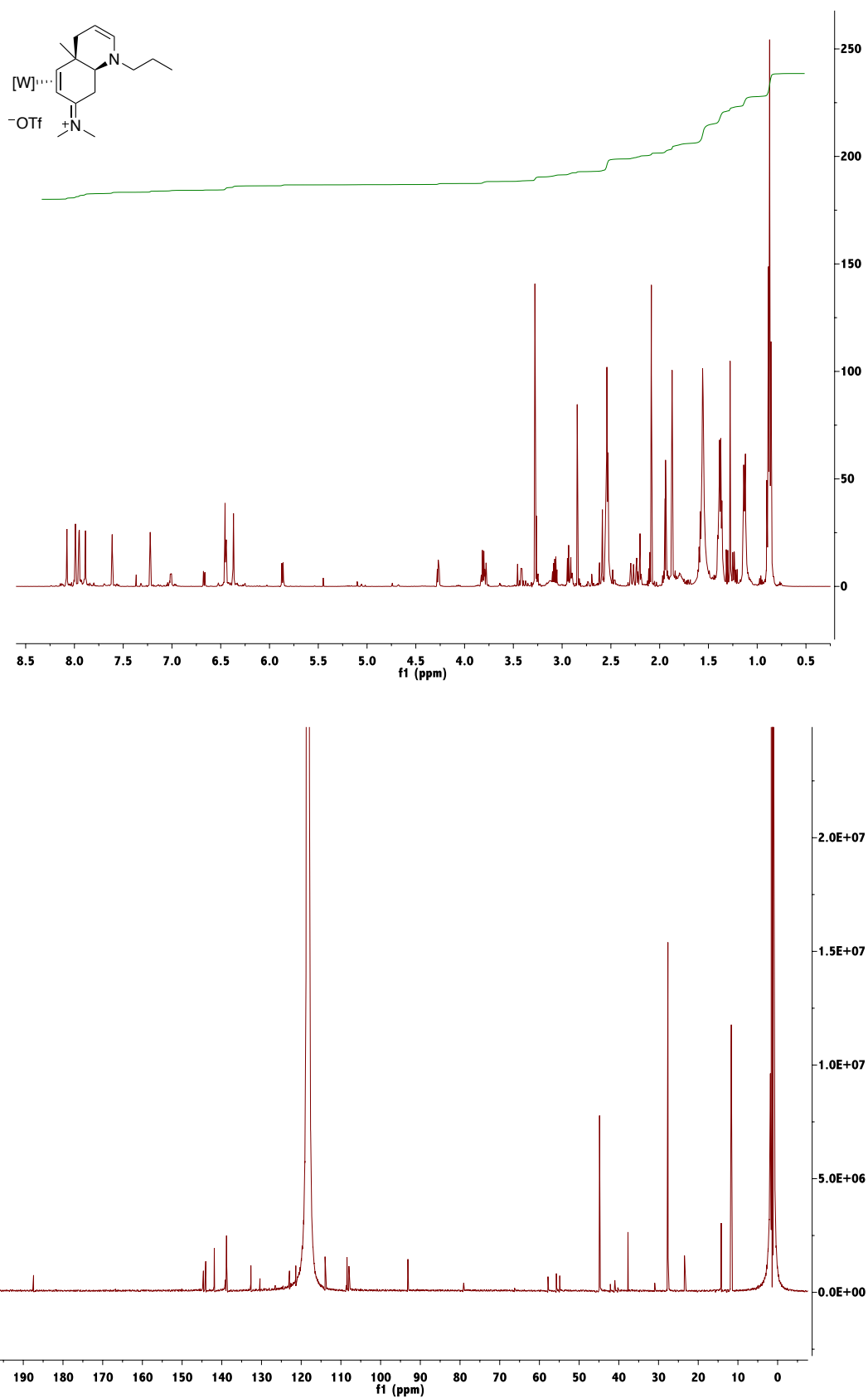
$^1\text{H-NMR}$ (CD_3CN) and $^{13}\text{C-NMR}$ (CD_3CN) of Compound 98:

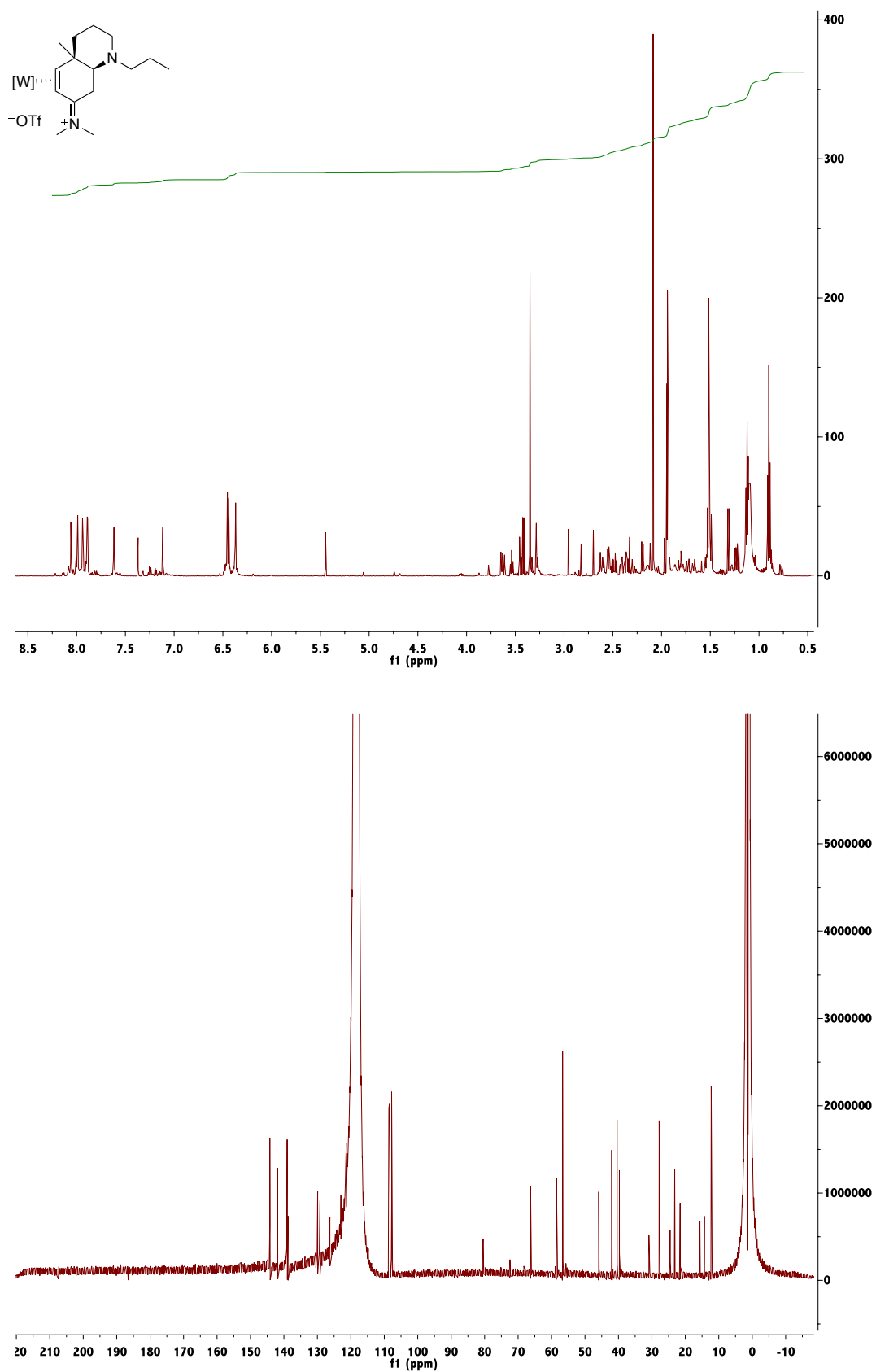
$^1\text{H-NMR}$ (CD_3CN) and $^{13}\text{C-NMR}$ (CD_3CN) of Compound 99A:

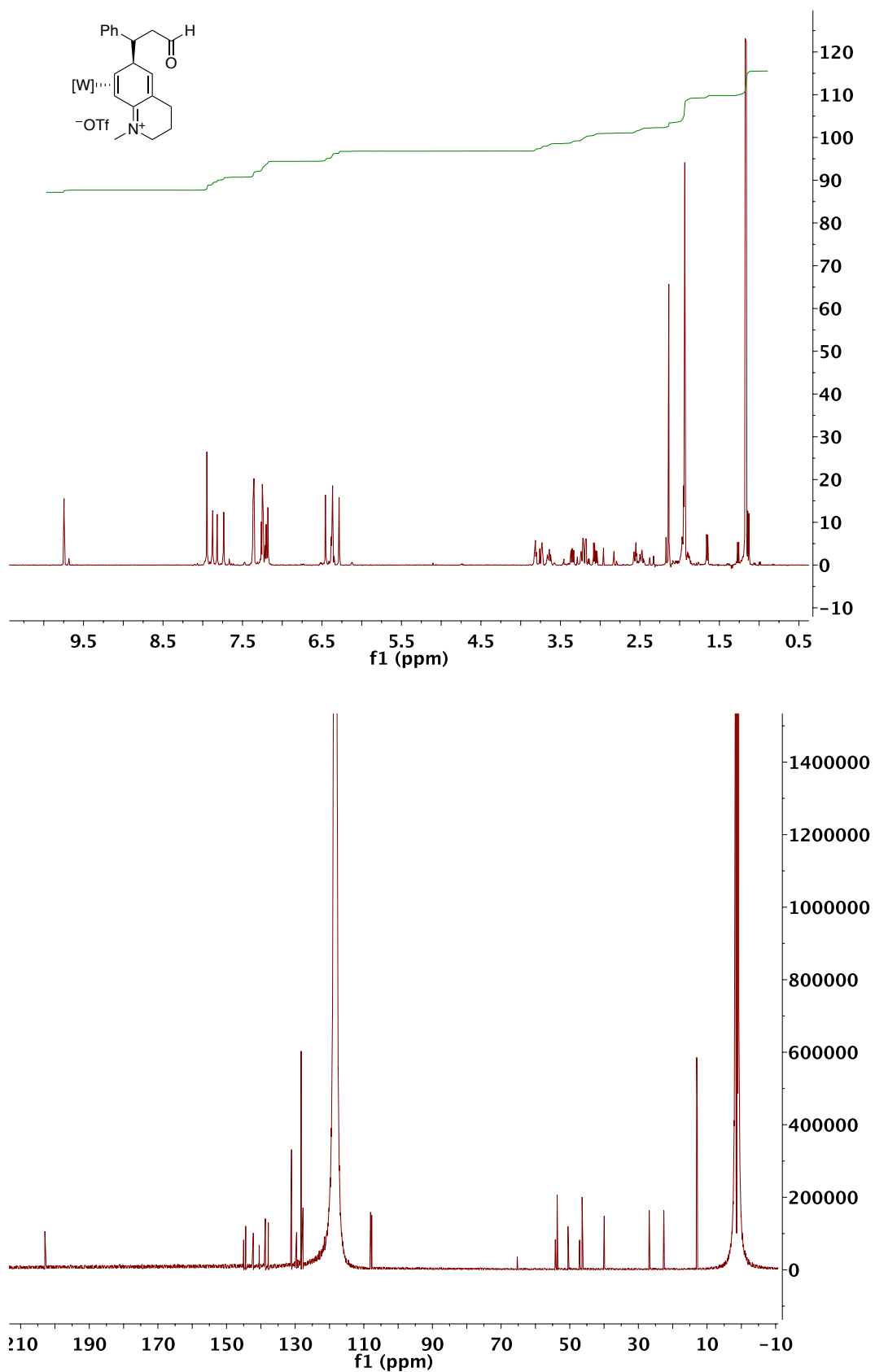
$^1\text{H-NMR}$ (CD_3CN) and $^{13}\text{C-NMR}$ (CD_3CN) of Compound 100:

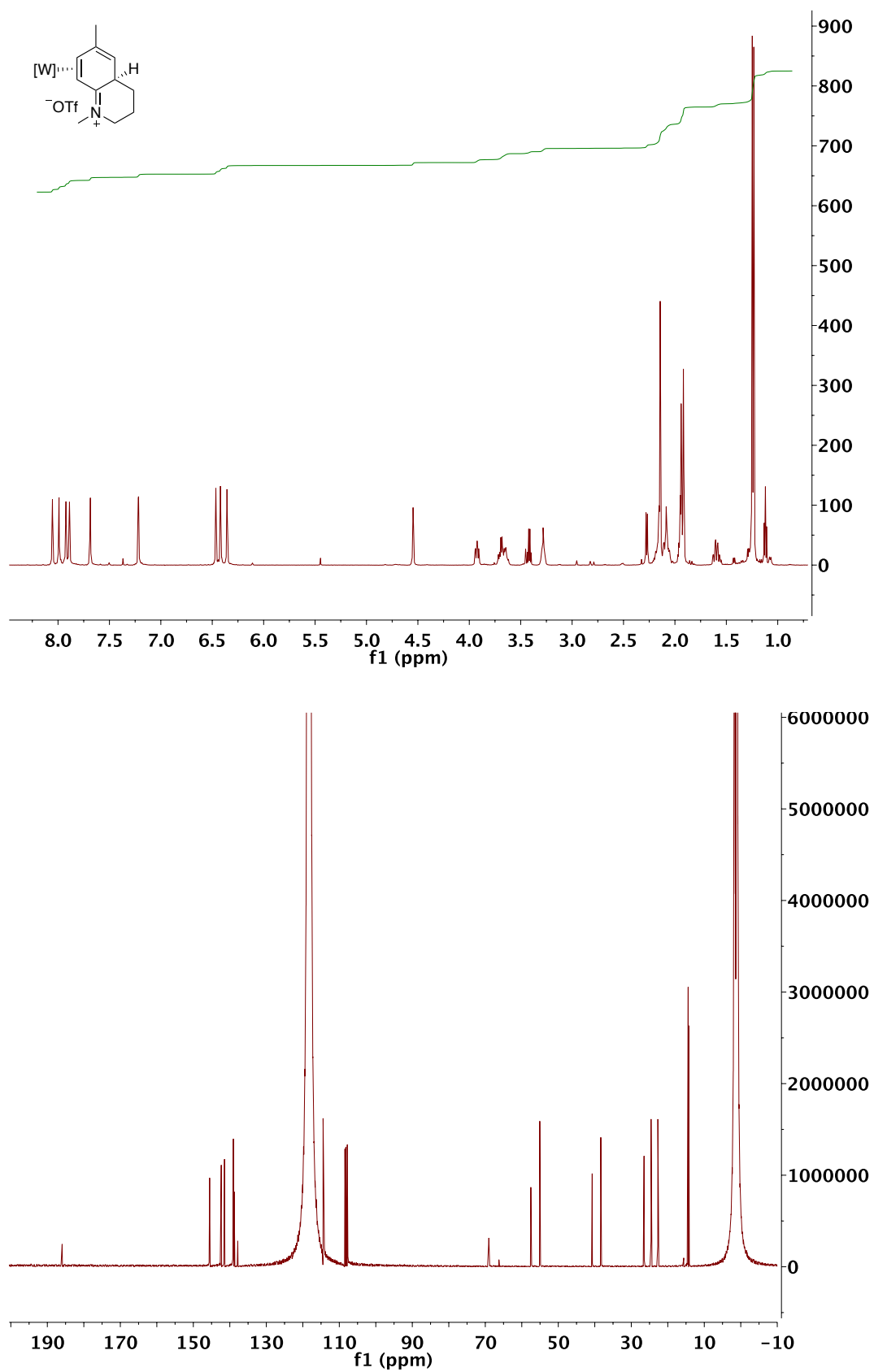
$^1\text{H-NMR}$ ($\text{d}^6\text{-acetone}$) and $^{13}\text{C-NMR}$ (CDCl_3) of Compound 101:

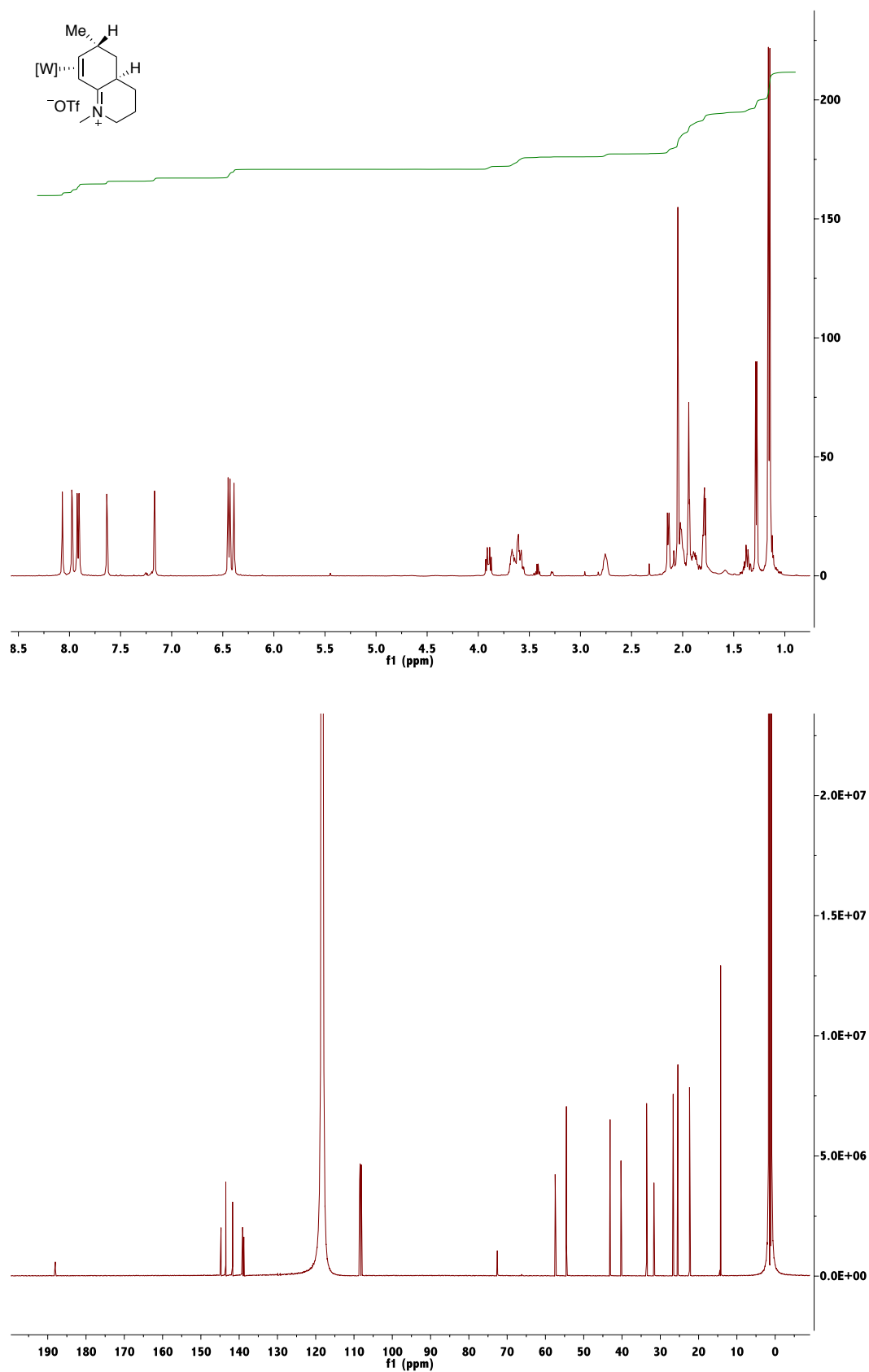
¹H-NMR (d⁶-acetone) of Compound 102:**¹H-NMR (CDCl₃) of Compound 103:**

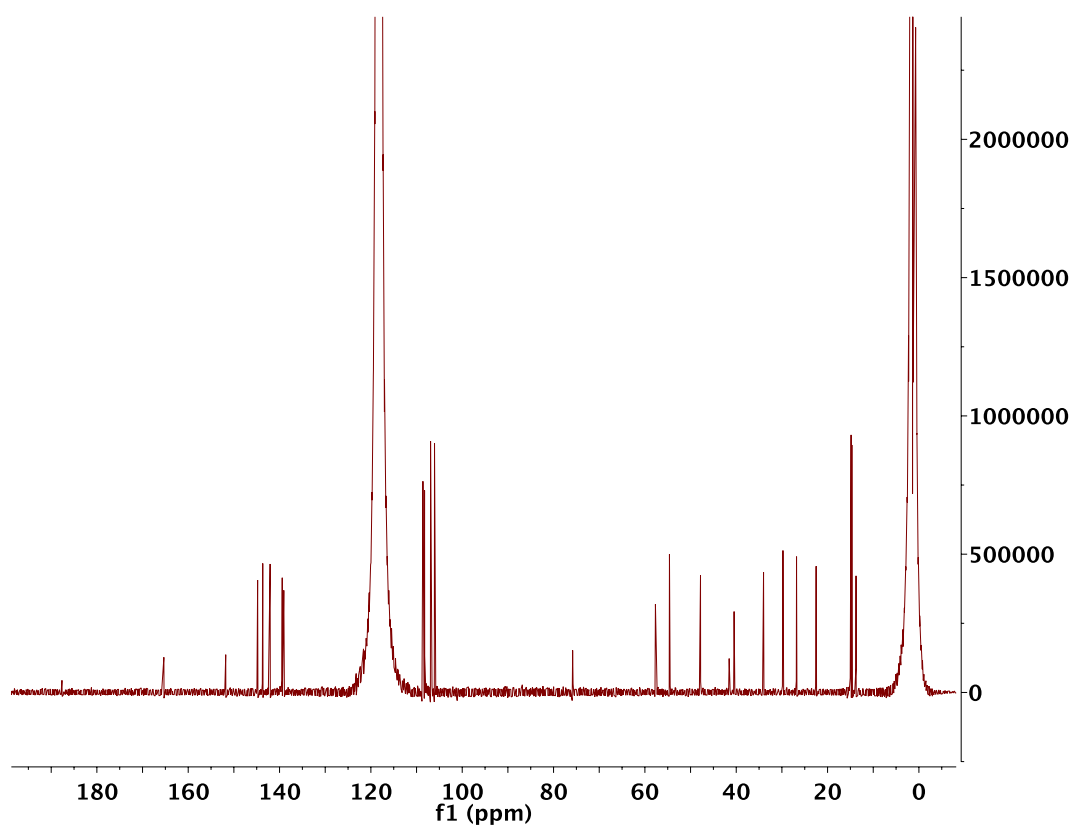
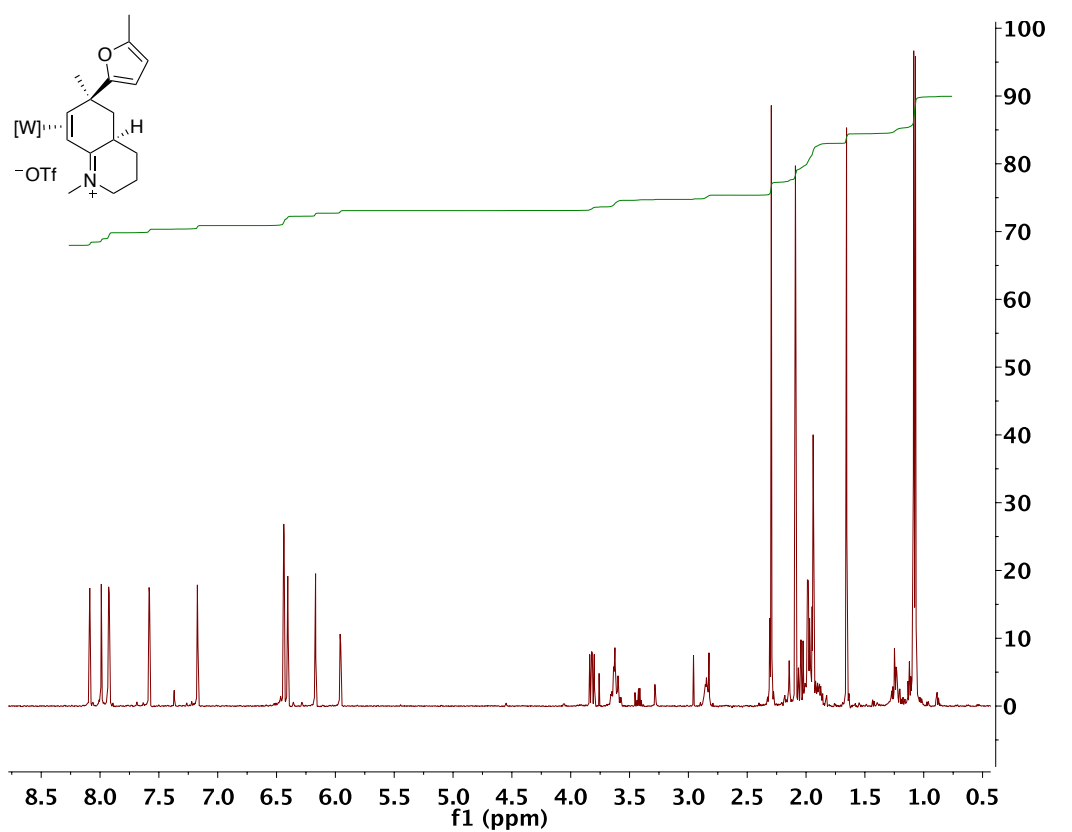
$^1\text{H-NMR}$ ($\text{d}^6\text{-acetone}$) and $^{13}\text{C-NMR}$ (CD_3CN) of Compound 104:

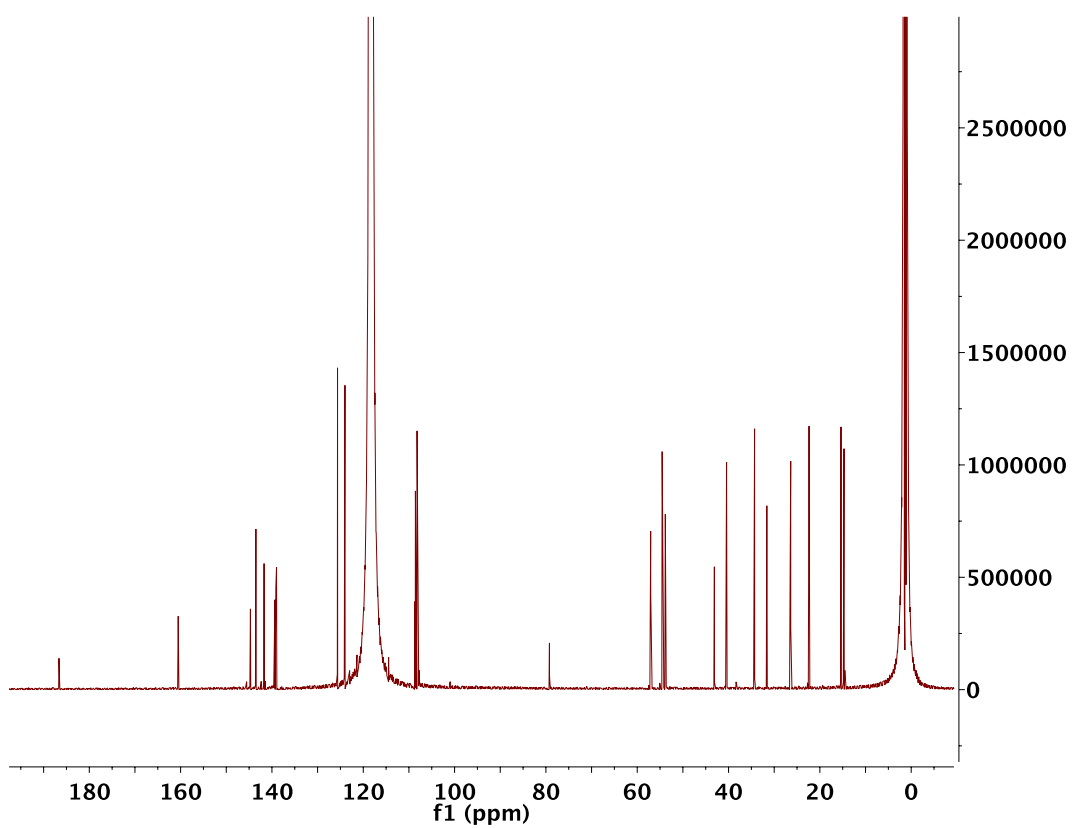
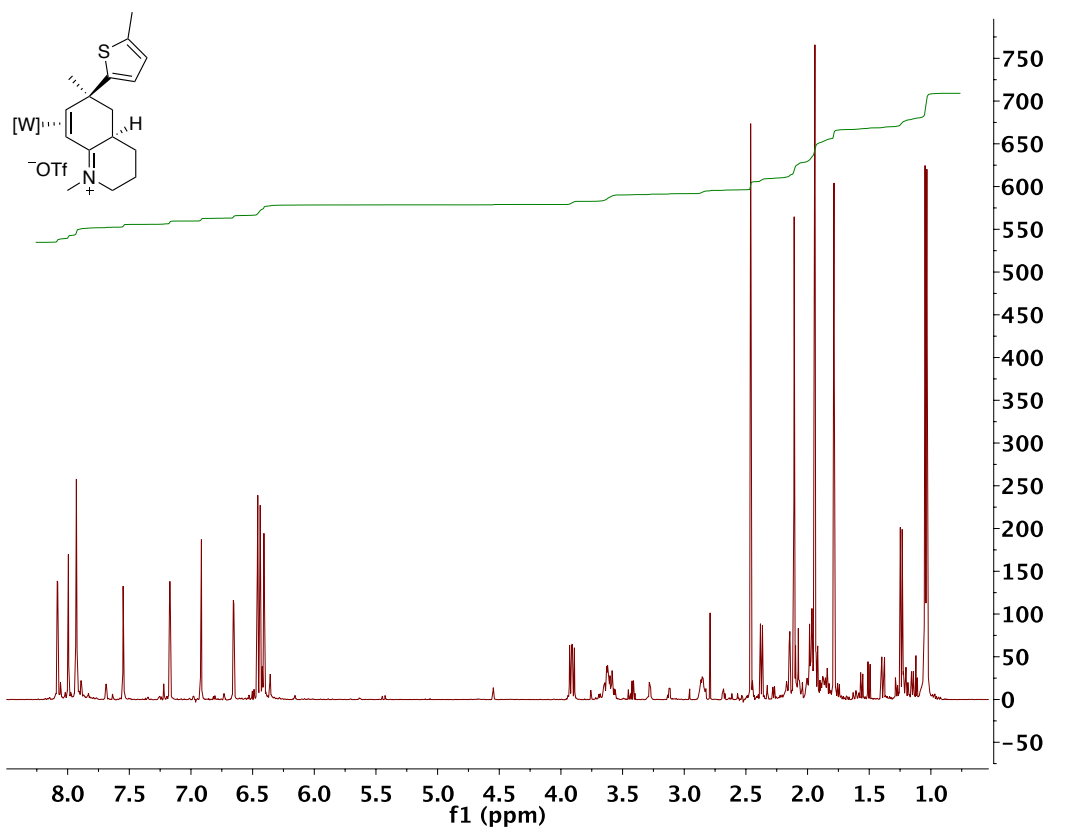
$^1\text{H-NMR}$ (CD_3CN) and $^{13}\text{C-NMR}$ (CD_3CN) of Compound 105:

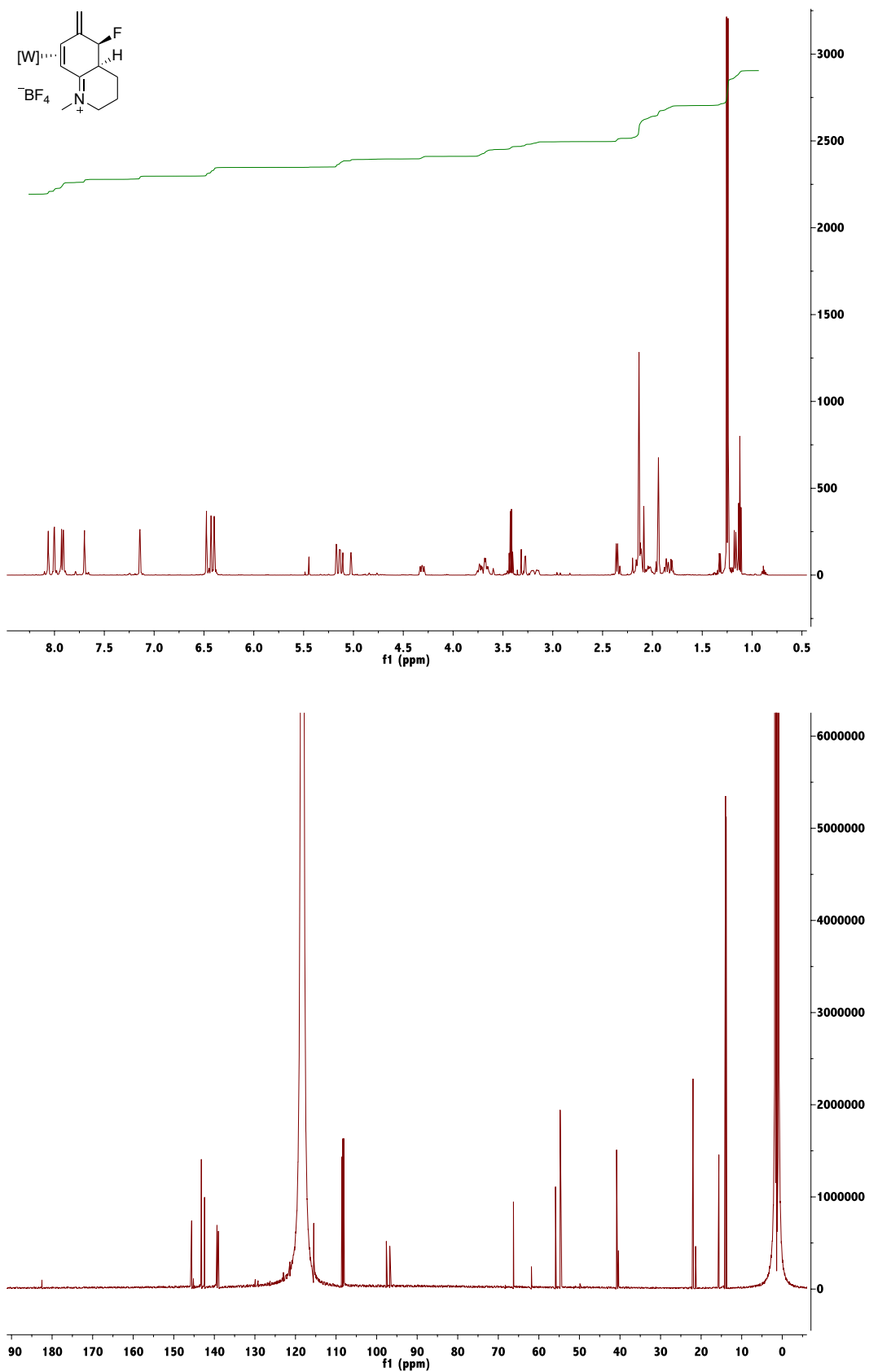
$^1\text{H-NMR}$ (CD_3CN) and $^{13}\text{C-NMR}$ (CD_3CN) of Compound 107:

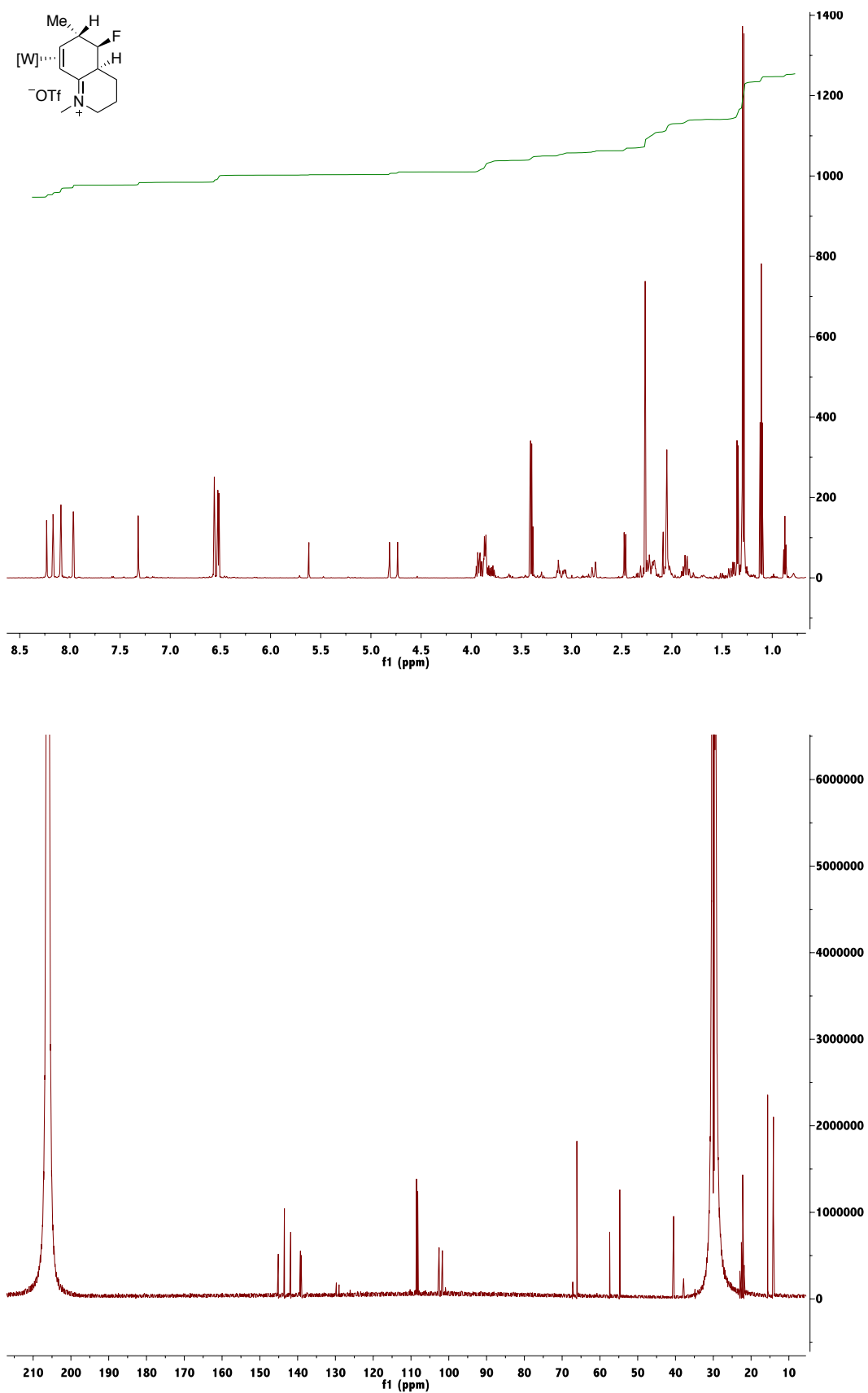
$^1\text{H-NMR}$ (CD_3CN) and $^{13}\text{C-NMR}$ (CD_3CN) of Compound 108B:

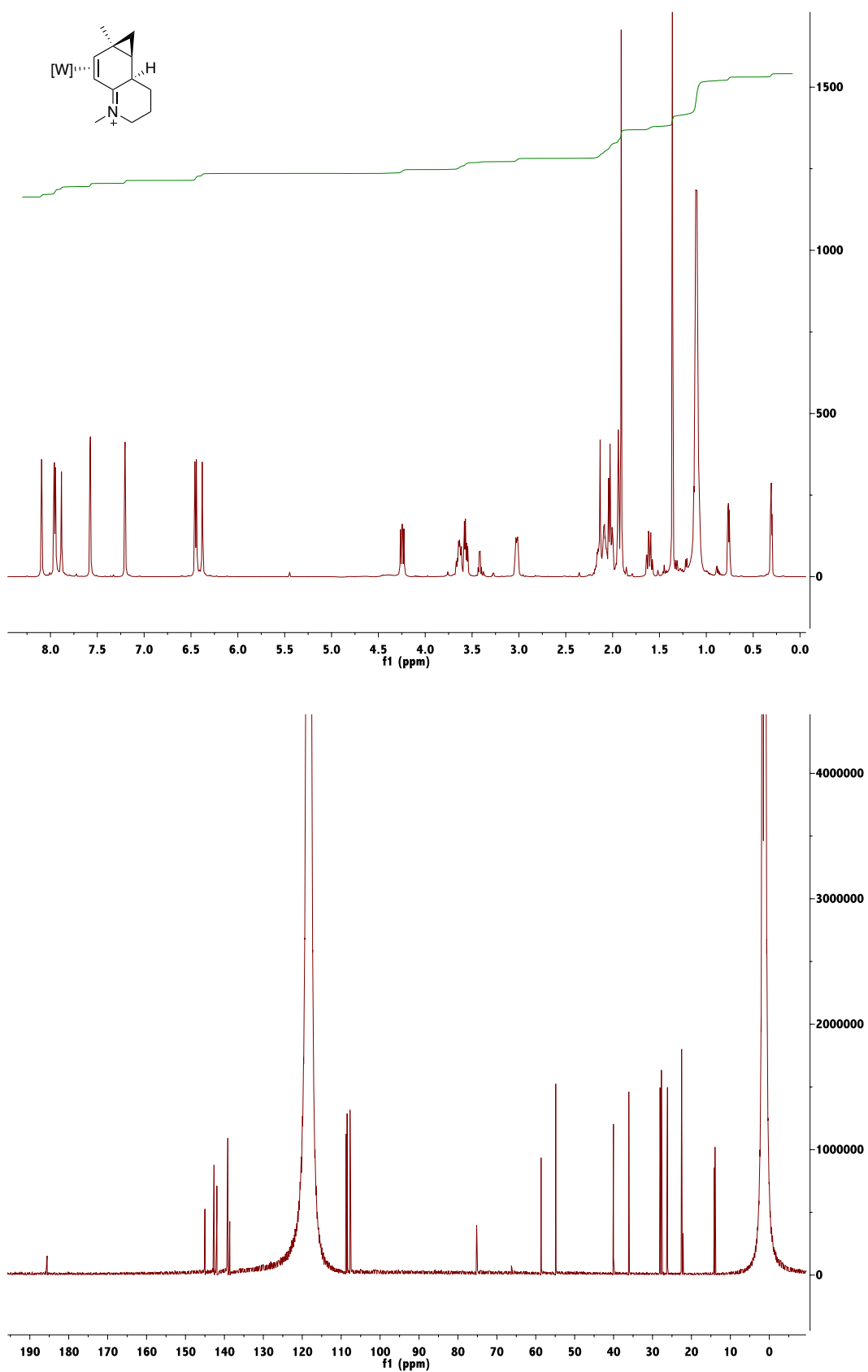
$^1\text{H-NMR}$ (CD_3CN) and $^{13}\text{C-NMR}$ (CD_3CN) of Compound 109:

$^1\text{H-NMR}$ (CD_3CN) and $^{13}\text{C-NMR}$ (CD_3CN) of Compound 110:

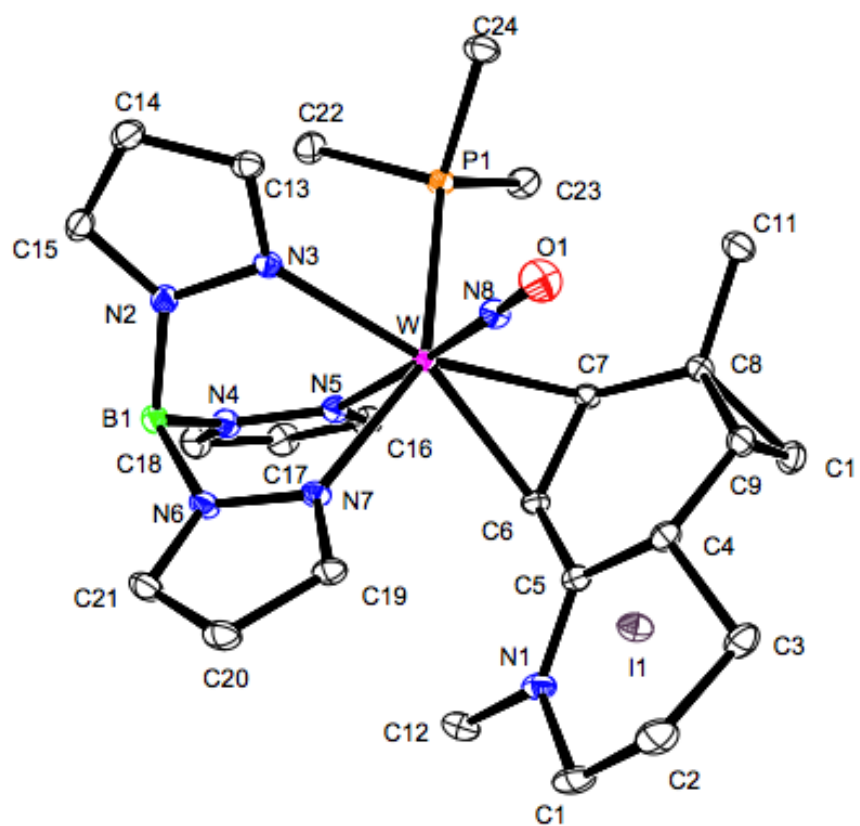
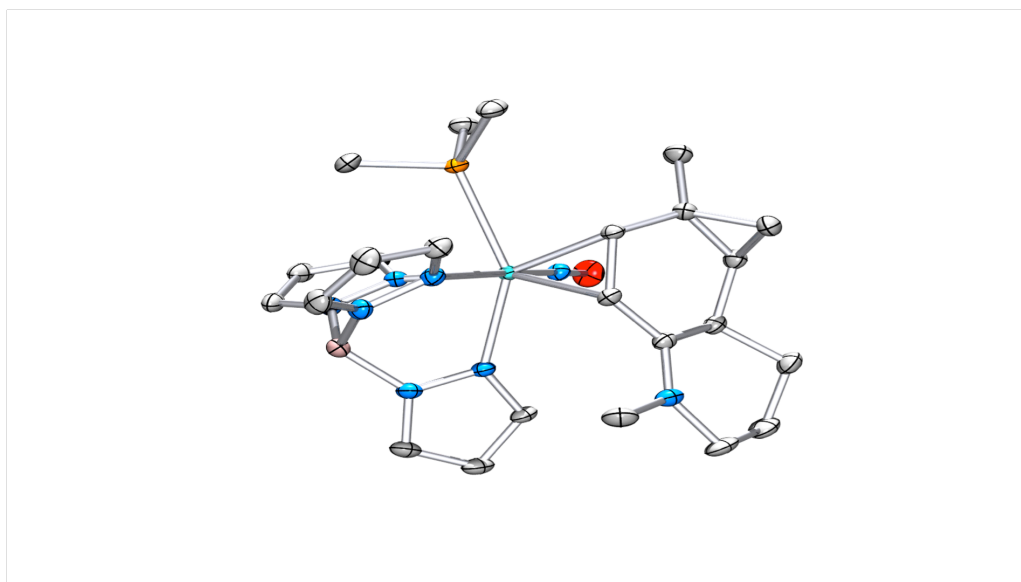
$^1\text{H-NMR}$ (CD_3CN) and $^{13}\text{C-NMR}$ (CD_3CN) of Compound 111:

$^1\text{H-NMR}$ (CD_3CN) and $^{13}\text{C-NMR}$ (CD_3CN) of Compound 112:

$^1\text{H-NMR}$ ($\text{d}^6\text{-acetone}$) and $^{13}\text{C-NMR}$ ($\text{d}^6\text{-acetone}$) of Compound 113:

$^1\text{H-NMR}$ (CD_3CN) and $^{13}\text{C-NMR}$ (CD_3CN) of Compound 114:

Compound 114



Compound 114Table 1. Crystal data and structure refinement for C₂₄H₃₇BN₈OPIW.

Empirical formula	C ₂₄ H ₃₇ B I N ₈ O P W	
Formula weight	806.14	
Temperature	153(2) K	
Wavelength	0.71073 \approx	
Crystal system	Orthorhombic	
Space group	Pbca	
Unit cell dimensions	a = 12.9737(9) \approx	a = 90 ∞ .
	b = 15.5354(11) \approx	b = 90 ∞ .
	c = 28.672(2) \approx	g = 90 ∞ .
Volume	5778.9(7) \approx^3	
Z	8	
Density (calculated)	1.853 Mg/m ³	
Absorption coefficient	5.155 mm ⁻¹	
F(000)	3136	
Crystal size	0.390 x 0.380 x 0.140 mm ³	
Theta range for data collection	3.138 to 37.230 ∞ .	
Index ranges	-20 \leq h \leq 21, -26 \leq k \leq 25, -48 \leq l \leq 47	
Reflections collected	139442	
Independent reflections	14229 [R(int) = 0.0285]	
Completeness to theta = 25.242 ∞	99.7 %	
Absorption correction	None	
Refinement method	Full-matrix least-squares on F ²	
Data / restraints / parameters	14229 / 0 / 351	
Goodness-of-fit on F ²	1.050	
Final R indices [I > 2 σ (I)]	R1 = 0.0315, wR2 = 0.0725	
R indices (all data)	R1 = 0.0401, wR2 = 0.0781	
Extinction coefficient	n/a	
Largest diff. peak and hole	2.707 and -1.941 e. \approx^3	

Table 2. Atomic coordinates ($\times 10^4$) and equivalent isotropic displacement parameters ($\approx^2 \times 10^3$) for $C_{24}H_{37}BN_8OPIW$. $U(eq)$ is defined as one third of the trace of the orthogonalized U^{ij} tensor.

	x	y	z	U(eq)
W	5271(1)	7474(1)	3716(1)	13(1)
I(1)	823(1)	7383(1)	3768(1)	26(1)
P(1)	5492(1)	7220(1)	2845(1)	18(1)
O(1)	6565(2)	6042(2)	4100(1)	31(1)
N(1)	3378(2)	7357(2)	4838(1)	21(1)
N(2)	6718(2)	9063(1)	3550(1)	19(1)
N(3)	6694(2)	8186(1)	3553(1)	17(1)
N(4)	4831(2)	9424(1)	3490(1)	20(1)
N(5)	4426(2)	8622(1)	3444(1)	18(1)
N(6)	5677(2)	9168(1)	4268(1)	19(1)
N(7)	5486(2)	8310(1)	4327(1)	17(1)
N(8)	6020(2)	6606(1)	3939(1)	17(1)
C(1)	3397(3)	7110(2)	5339(1)	28(1)
C(2)	3946(3)	6270(2)	5435(1)	31(1)
C(3)	3755(2)	5631(2)	5046(1)	26(1)
C(4)	4194(2)	6005(2)	4595(1)	19(1)
C(5)	3738(2)	6880(2)	4491(1)	17(1)
C(6)	3714(2)	7190(2)	4024(1)	16(1)
C(7)	3894(2)	6646(2)	3617(1)	16(1)
C(8)	3952(2)	5688(2)	3697(1)	18(1)
C(9)	4065(2)	5390(2)	4192(1)	20(1)
C(10)	3037(2)	5289(2)	3952(1)	23(1)
C(11)	4462(3)	5136(2)	3330(1)	26(1)
C(12)	2902(2)	8200(2)	4750(1)	27(1)
C(13)	7647(2)	7921(2)	3441(1)	20(1)
C(14)	8283(2)	8624(2)	3352(1)	24(1)
C(15)	7671(2)	9334(2)	3432(1)	22(1)
C(16)	3558(2)	8710(2)	3192(1)	22(1)
C(17)	3417(2)	9567(2)	3069(1)	27(1)

C(18)	4233(2)	10001(2)	3269(1)	25(1)
C(19)	5591(2)	8146(2)	4783(1)	19(1)
C(20)	5842(2)	8897(2)	5024(1)	25(1)
C(21)	5898(2)	9525(2)	4684(1)	24(1)
C(22)	5892(3)	8206(2)	2548(1)	26(1)
C(23)	4392(2)	6916(2)	2484(1)	25(1)
C(24)	6473(2)	6456(2)	2656(1)	26(1)
B(1)	5819(3)	9567(2)	3776(1)	20(1)

Table 3. Bond lengths [\AA] and angles [$^\circ$] for $\text{C}_{24}\text{H}_{37}\text{BN}_8\text{OPIW}$.

W-N(8)	1.782(2)
W-N(7)	2.197(2)
W-N(3)	2.203(2)
W-C(7)	2.219(3)
W-N(5)	2.233(2)
W-C(6)	2.247(2)
W-P(1)	2.5460(7)
P(1)-C(24)	1.822(3)
P(1)-C(23)	1.824(3)
P(1)-C(22)	1.827(3)
O(1)-N(8)	1.217(3)
N(1)-C(5)	1.327(3)
N(1)-C(12)	1.469(4)
N(1)-C(1)	1.486(4)
N(2)-C(15)	1.349(4)
N(2)-N(3)	1.362(3)
N(2)-B(1)	1.548(4)
N(3)-C(13)	1.342(3)
N(4)-C(18)	1.344(3)
N(4)-N(5)	1.359(3)
N(4)-B(1)	1.539(4)
N(5)-C(16)	1.345(3)

N(6)-C(21)	1.346(3)
N(6)-N(7)	1.366(3)
N(6)-B(1)	1.552(4)
N(7)-C(19)	1.339(3)
C(1)-C(2)	1.512(5)
C(1)-H(1A)	0.9900
C(1)-H(1B)	0.9900
C(2)-C(3)	1.515(5)
C(2)-H(2A)	0.9900
C(2)-H(2B)	0.9900
C(3)-C(4)	1.526(4)
C(3)-H(3A)	0.9900
C(3)-H(3B)	0.9900
C(4)-C(9)	1.510(4)
C(4)-C(5)	1.511(4)
C(4)-H(4)	1.0000
C(5)-C(6)	1.425(3)
C(6)-C(7)	1.459(3)
C(6)-H(6)	0.92(4)
C(7)-C(8)	1.507(4)
C(7)-H(7)	0.99(4)
C(8)-C(9)	1.500(4)
C(8)-C(11)	1.509(4)
C(8)-C(10)	1.527(4)
C(9)-C(10)	1.508(4)
C(9)-H(9)	1.0000
C(10)-H(10A)	0.9900
C(10)-H(10B)	0.9900
C(11)-H(11A)	0.9800
C(11)-H(11B)	0.9800
C(11)-H(11C)	0.9800
C(12)-H(12A)	0.9800
C(12)-H(12B)	0.9800
C(12)-H(12C)	0.9800
C(13)-C(14)	1.393(4)
C(13)-H(13)	0.9500

C(14)-C(15)	1.379(4)
C(14)-H(14)	0.9500
C(15)-H(15)	0.9500
C(16)-C(17)	1.389(4)
C(16)-H(16)	0.9500
C(17)-C(18)	1.380(5)
C(17)-H(17)	0.9500
C(18)-H(18)	0.9500
C(19)-C(20)	1.396(4)
C(19)-H(19)	0.9500
C(20)-C(21)	1.381(4)
C(20)-H(20)	0.9500
C(21)-H(21)	0.9500
C(22)-H(22A)	0.9800
C(22)-H(22B)	0.9800
C(22)-H(22C)	0.9800
C(23)-H(23A)	0.9800
C(23)-H(23B)	0.9800
C(23)-H(23C)	0.9800
C(24)-H(24A)	0.9800
C(24)-H(24B)	0.9800
C(24)-H(24C)	0.9800
B(1)-H(1BB)	1.06(4)
N(8)-W-N(7)	95.29(9)
N(8)-W-N(3)	89.91(9)
N(7)-W-N(3)	76.48(8)
N(8)-W-C(7)	92.61(10)
N(7)-W-C(7)	123.16(8)
N(3)-W-C(7)	159.79(8)
N(8)-W-N(5)	176.03(9)
N(7)-W-N(5)	82.52(8)
N(3)-W-N(5)	86.36(8)
C(7)-W-N(5)	91.36(9)
N(8)-W-C(6)	101.60(9)
N(7)-W-C(6)	85.28(9)

N(3)-W-C(6)	159.30(8)
C(7)-W-C(6)	38.13(9)
N(5)-W-C(6)	81.57(8)
N(8)-W-P(1)	99.95(7)
N(7)-W-P(1)	149.26(6)
N(3)-W-P(1)	77.00(6)
C(7)-W-P(1)	82.82(6)
N(5)-W-P(1)	80.54(6)
C(6)-W-P(1)	117.11(6)
C(24)-P(1)-C(23)	102.06(14)
C(24)-P(1)-C(22)	102.07(15)
C(23)-P(1)-C(22)	100.13(14)
C(24)-P(1)-W	118.14(10)
C(23)-P(1)-W	120.56(10)
C(22)-P(1)-W	110.99(9)
C(5)-N(1)-C(12)	121.2(2)
C(5)-N(1)-C(1)	125.1(3)
C(12)-N(1)-C(1)	113.8(2)
C(15)-N(2)-N(3)	109.6(2)
C(15)-N(2)-B(1)	129.6(2)
N(3)-N(2)-B(1)	119.1(2)
C(13)-N(3)-N(2)	106.5(2)
C(13)-N(3)-W	132.01(18)
N(2)-N(3)-W	121.47(17)
C(18)-N(4)-N(5)	110.1(2)
C(18)-N(4)-B(1)	129.5(2)
N(5)-N(4)-B(1)	120.4(2)
C(16)-N(5)-N(4)	106.4(2)
C(16)-N(5)-W	132.85(19)
N(4)-N(5)-W	120.58(17)
C(21)-N(6)-N(7)	109.4(2)
C(21)-N(6)-B(1)	128.0(2)
N(7)-N(6)-B(1)	121.6(2)
C(19)-N(7)-N(6)	106.7(2)
C(19)-N(7)-W	132.72(18)
N(6)-N(7)-W	120.06(15)

O(1)-N(8)-W	176.8(2)
N(1)-C(1)-C(2)	114.0(2)
N(1)-C(1)-H(1A)	108.7
C(2)-C(1)-H(1A)	108.7
N(1)-C(1)-H(1B)	108.7
C(2)-C(1)-H(1B)	108.7
H(1A)-C(1)-H(1B)	107.6
C(1)-C(2)-C(3)	110.7(3)
C(1)-C(2)-H(2A)	109.5
C(3)-C(2)-H(2A)	109.5
C(1)-C(2)-H(2B)	109.5
C(3)-C(2)-H(2B)	109.5
H(2A)-C(2)-H(2B)	108.1
C(2)-C(3)-C(4)	108.2(2)
C(2)-C(3)-H(3A)	110.0
C(4)-C(3)-H(3A)	110.0
C(2)-C(3)-H(3B)	110.0
C(4)-C(3)-H(3B)	110.0
H(3A)-C(3)-H(3B)	108.4
C(9)-C(4)-C(5)	111.9(2)
C(9)-C(4)-C(3)	111.5(2)
C(5)-C(4)-C(3)	111.3(2)
C(9)-C(4)-H(4)	107.3
C(5)-C(4)-H(4)	107.3
C(3)-C(4)-H(4)	107.3
N(1)-C(5)-C(6)	120.6(2)
N(1)-C(5)-C(4)	119.5(2)
C(6)-C(5)-C(4)	119.9(2)
C(5)-C(6)-C(7)	123.5(2)
C(5)-C(6)-W	114.55(17)
C(7)-C(6)-W	69.91(14)
C(5)-C(6)-H(6)	114(2)
C(7)-C(6)-H(6)	117(2)
W-C(6)-H(6)	107(2)
C(6)-C(7)-C(8)	117.4(2)
C(6)-C(7)-W	71.97(14)

C(8)-C(7)-W	120.91(18)
C(6)-C(7)-H(7)	116(2)
C(8)-C(7)-H(7)	110(2)
W-C(7)-H(7)	116(2)
C(9)-C(8)-C(7)	116.9(2)
C(9)-C(8)-C(11)	116.2(2)
C(7)-C(8)-C(11)	118.5(2)
C(9)-C(8)-C(10)	59.76(18)
C(7)-C(8)-C(10)	115.8(2)
C(11)-C(8)-C(10)	116.4(2)
C(8)-C(9)-C(10)	60.99(18)
C(8)-C(9)-C(4)	122.8(2)
C(10)-C(9)-C(4)	120.9(2)
C(8)-C(9)-H(9)	114.0
C(10)-C(9)-H(9)	114.0
C(4)-C(9)-H(9)	114.0
C(9)-C(10)-C(8)	59.25(17)
C(9)-C(10)-H(10A)	117.8
C(8)-C(10)-H(10A)	117.8
C(9)-C(10)-H(10B)	117.8
C(8)-C(10)-H(10B)	117.8
H(10A)-C(10)-H(10B)	115.0
C(8)-C(11)-H(11A)	109.5
C(8)-C(11)-H(11B)	109.5
H(11A)-C(11)-H(11B)	109.5
C(8)-C(11)-H(11C)	109.5
H(11A)-C(11)-H(11C)	109.5
H(11B)-C(11)-H(11C)	109.5
N(1)-C(12)-H(12A)	109.5
N(1)-C(12)-H(12B)	109.5
H(12A)-C(12)-H(12B)	109.5
N(1)-C(12)-H(12C)	109.5
H(12A)-C(12)-H(12C)	109.5
H(12B)-C(12)-H(12C)	109.5
N(3)-C(13)-C(14)	110.5(2)
N(3)-C(13)-H(13)	124.8

C(14)-C(13)-H(13)	124.8
C(15)-C(14)-C(13)	104.8(2)
C(15)-C(14)-H(14)	127.6
C(13)-C(14)-H(14)	127.6
N(2)-C(15)-C(14)	108.7(2)
N(2)-C(15)-H(15)	125.7
C(14)-C(15)-H(15)	125.7
N(5)-C(16)-C(17)	110.1(3)
N(5)-C(16)-H(16)	124.9
C(17)-C(16)-H(16)	124.9
C(18)-C(17)-C(16)	105.2(3)
C(18)-C(17)-H(17)	127.4
C(16)-C(17)-H(17)	127.4
N(4)-C(18)-C(17)	108.2(2)
N(4)-C(18)-H(18)	125.9
C(17)-C(18)-H(18)	125.9
N(7)-C(19)-C(20)	110.4(2)
N(7)-C(19)-H(19)	124.8
C(20)-C(19)-H(19)	124.8
C(21)-C(20)-C(19)	104.6(2)
C(21)-C(20)-H(20)	127.7
C(19)-C(20)-H(20)	127.7
N(6)-C(21)-C(20)	108.9(2)
N(6)-C(21)-H(21)	125.6
C(20)-C(21)-H(21)	125.6
P(1)-C(22)-H(22A)	109.5
P(1)-C(22)-H(22B)	109.5
H(22A)-C(22)-H(22B)	109.5
P(1)-C(22)-H(22C)	109.5
H(22A)-C(22)-H(22C)	109.5
H(22B)-C(22)-H(22C)	109.5
P(1)-C(23)-H(23A)	109.5
P(1)-C(23)-H(23B)	109.5
H(23A)-C(23)-H(23B)	109.5
P(1)-C(23)-H(23C)	109.5
H(23A)-C(23)-H(23C)	109.5

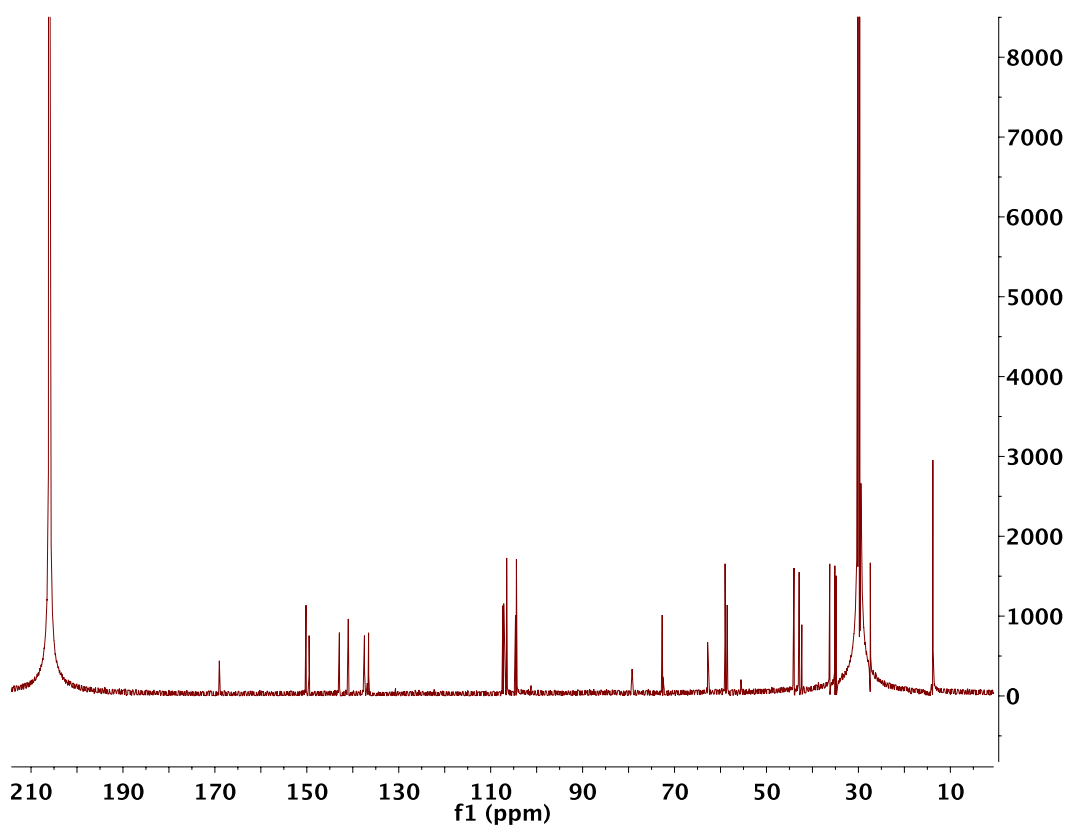
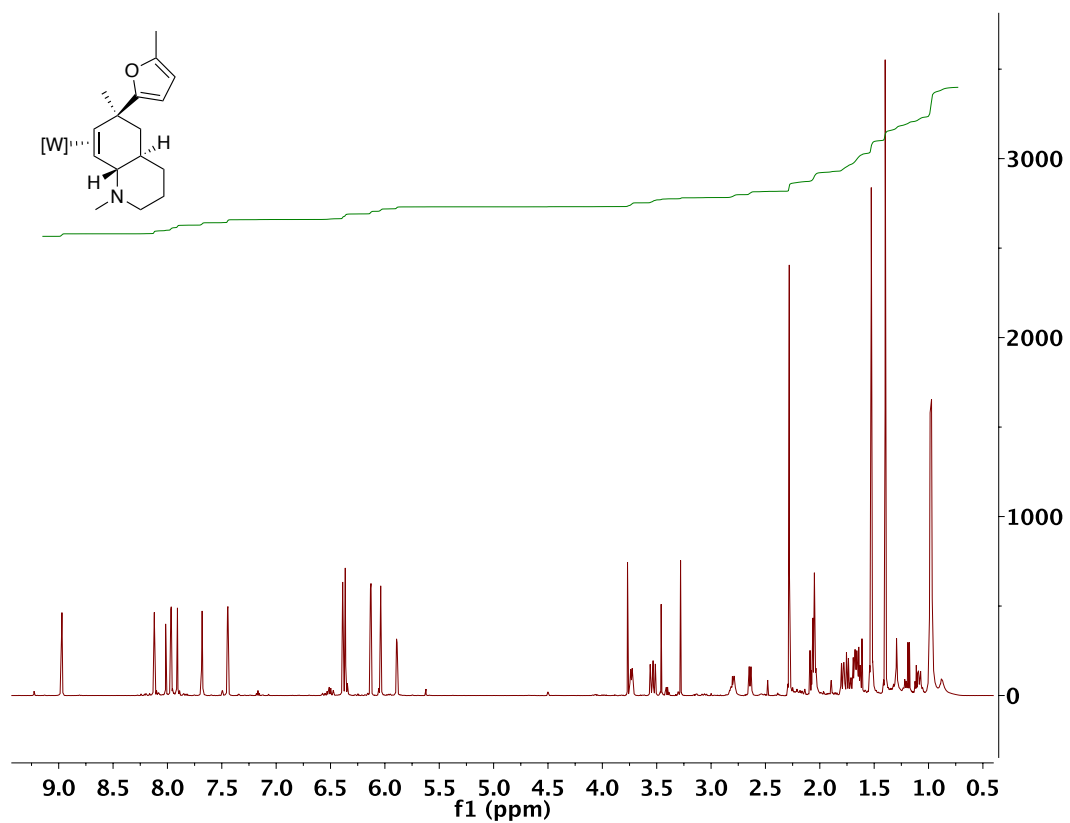
H(23B)-C(23)-H(23C)	109.5
P(1)-C(24)-H(24A)	109.5
P(1)-C(24)-H(24B)	109.5
H(24A)-C(24)-H(24B)	109.5
P(1)-C(24)-H(24C)	109.5
H(24A)-C(24)-H(24C)	109.5
H(24B)-C(24)-H(24C)	109.5
N(4)-B(1)-N(2)	109.3(2)
N(4)-B(1)-N(6)	109.3(2)
N(2)-B(1)-N(6)	105.6(2)
N(4)-B(1)-H(1BB)	112(2)
N(2)-B(1)-H(1BB)	110(2)
N(6)-B(1)-H(1BB)	111(2)

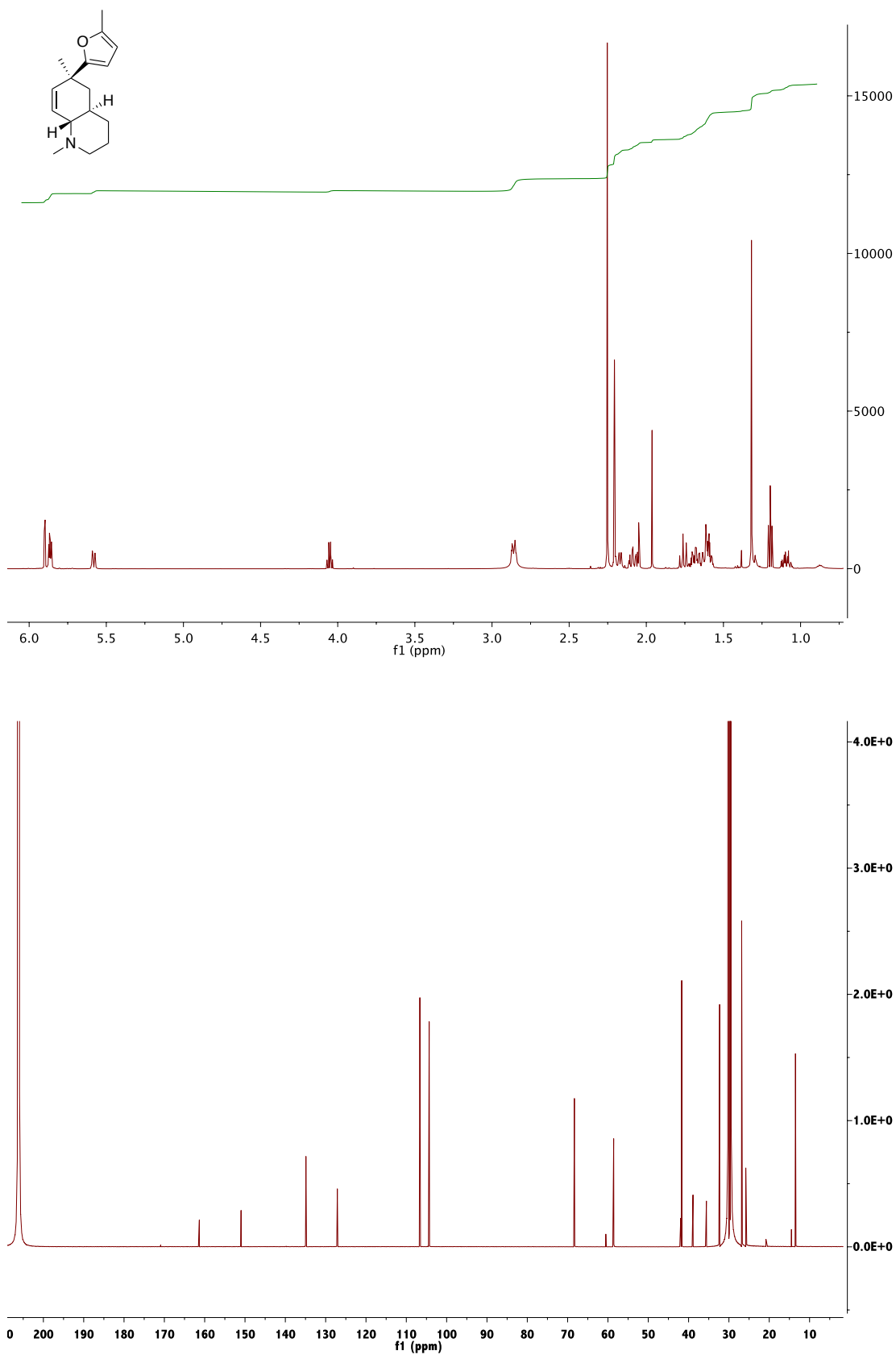
Symmetry transformations used to generate equivalent atoms:

Table 4. Anisotropic displacement parameters ($\approx 2 \times 10^3$) for $C_{24}H_{37}BN_8OPIW$. The anisotropic displacement factor exponent takes the form: $-2p^2 [h^2 a^*2U_{11} + \dots + 2 h k a^* b^* U_{12}]$

	U ₁₁	U ₂₂	U ₃₃	U ₂₃	U ₁₃	U ₁₂
W	15(1)	13(1)	11(1)	0(1)	0(1)	1(1)
I(1)	28(1)	32(1)	19(1)	-1(1)	-3(1)	6(1)
P(1)	21(1)	21(1)	11(1)	-1(1)	0(1)	-1(1)
O(1)	30(1)	28(1)	37(1)	8(1)	-4(1)	12(1)
N(1)	20(1)	27(1)	15(1)	-3(1)	1(1)	0(1)
N(2)	21(1)	18(1)	17(1)	1(1)	1(1)	-3(1)
N(3)	19(1)	18(1)	14(1)	-2(1)	0(1)	0(1)
N(4)	24(1)	16(1)	18(1)	2(1)	1(1)	2(1)
N(5)	20(1)	18(1)	15(1)	2(1)	0(1)	2(1)
N(6)	24(1)	19(1)	15(1)	-3(1)	0(1)	1(1)
N(7)	20(1)	20(1)	12(1)	-1(1)	0(1)	1(1)
N(8)	19(1)	17(1)	15(1)	2(1)	-1(1)	3(1)

C(1)	29(1)	44(2)	11(1)	-1(1)	2(1)	-1(1)
C(2)	37(2)	40(2)	15(1)	4(1)	0(1)	-1(1)
C(3)	29(1)	30(1)	19(1)	7(1)	2(1)	-3(1)
C(4)	19(1)	22(1)	15(1)	4(1)	0(1)	0(1)
C(5)	15(1)	22(1)	15(1)	0(1)	0(1)	-1(1)
C(6)	17(1)	18(1)	13(1)	1(1)	2(1)	2(1)
C(7)	19(1)	18(1)	11(1)	0(1)	0(1)	1(1)
C(8)	20(1)	18(1)	17(1)	-2(1)	1(1)	-1(1)
C(9)	25(1)	18(1)	18(1)	2(1)	0(1)	0(1)
C(10)	24(1)	24(1)	22(1)	0(1)	0(1)	-6(1)
C(11)	34(2)	21(1)	23(1)	-3(1)	4(1)	2(1)
C(12)	28(1)	30(1)	23(1)	-7(1)	2(1)	6(1)
C(13)	18(1)	25(1)	17(1)	-4(1)	1(1)	0(1)
C(14)	19(1)	32(1)	21(1)	-3(1)	3(1)	-5(1)
C(15)	23(1)	26(1)	18(1)	0(1)	2(1)	-8(1)
C(16)	21(1)	25(1)	20(1)	3(1)	-1(1)	3(1)
C(17)	27(1)	26(1)	29(1)	8(1)	-1(1)	7(1)
C(18)	31(1)	19(1)	26(1)	6(1)	1(1)	5(1)
C(19)	19(1)	27(1)	11(1)	0(1)	0(1)	0(1)
C(20)	25(1)	34(1)	16(1)	-7(1)	-1(1)	-1(1)
C(21)	26(1)	25(1)	21(1)	-9(1)	1(1)	0(1)
C(22)	35(2)	28(1)	15(1)	2(1)	3(1)	-6(1)
C(23)	25(1)	34(1)	15(1)	-1(1)	-4(1)	-3(1)
C(24)	25(1)	30(1)	22(1)	-8(1)	3(1)	2(1)
B(1)	24(1)	16(1)	19(1)	-1(1)	1(1)	-1(1)

$^1\text{H-NMR}$ ($\text{d}^6\text{-acetone}$) and $^{13}\text{C-NMR}$ ($\text{d}^6\text{-acetone}$) of Compound 115:

$^1\text{H-NMR}$ ($\text{d}^6\text{-acetone}$) and $^{13}\text{C-NMR}$ ($\text{d}^6\text{-acetone}$) of Compound 116:

$^1\text{H-NMR}$ ($\text{d}^6\text{-acetone}$) and $^{13}\text{C-NMR}$ (CDCl_3) of Compound 120: